Springer Series on Atomic, Optical, and Plasma Physics 93

Evgeny G. Drukarev
Aleksandr I. Mikhailov

High-Energy Atomic Physics

Springer

Springer Series on Atomic, Optical, and Plasma Physics

Volume 93

The Springer Series on Atomic, Optical, and Plasma Physics covers in a comprehensive manner theory and experiment in the entire field of atoms and molecules and their interaction with electromagnetic radiation. Books in the series provide a rich source of new ideas and techniques with wide applications in fields such as chemistry, materials science, astrophysics, surface science, plasma technology, advanced optics, aeronomy, and engineering. Laser physics is a particular connecting theme that has provided much of the continuing impetus for new developments in the field, such as quantum computation and Bose-Einstein condensation. The purpose of the series is to cover the gap between standard undergraduate textbooks and the research literature with emphasis on the fundamental ideas, methods, techniques, and results in the field.

More information about this series at http://www.springer.com/series/411

Evgeny G. Drukarev · Aleksandr I. Mikhailov

High-Energy Atomic Physics

Springer

Evgeny G. Drukarev
Petersburg Nuclear Physics Institute
Saint Petersburg
Russia

Aleksandr I. Mikhailov
Petersburg Nuclear Physics Institute
Saint Petersburg
Russia

ISSN 1615-5653 ISSN 2197-6791 (electronic)
Springer Series on Atomic, Optical, and Plasma Physics
ISBN 978-3-319-32734-1 ISBN 978-3-319-32736-5 (eBook)
DOI 10.1007/978-3-319-32736-5

Library of Congress Control Number: 2016939386

Printed on acid-free paper

This Springer imprint is published by Springer Nature
The registered company is Springer International Publishing AG Switzerland

Preface

In the atomic processes connected with the absorption of energy that is much larger than binding energies of the involved atoms, there are at least two energy scales. There are correspondingly two scales of momenta. This book is devoted to the theory of such processes. The presented approach based on analysis of the two regions of the recoil momenta does not always enable one to achieve high accuracy. However, it makes it possible to clarify the mechanisms of the processes and also to avoid the mistakes that are sometimes made in purely numerical computations.

The specifics of the experimental physics at such energies is beyond the scope of this book, and we present the results of experiments only as an illustration of the theory.

We assume that our reader knows the quantum mechanics and is familiar at least with fundamental points of quantum electrodynamics. We assume also that the reader has taken a standard course in atomic physics.

We hope that this book will be useful to the atomic physics community. We expect also that this book will help in overcoming the prejudice that "theoretical atomic physics is the science of precise computations."

This book is to a large extent based on the works of the authors. We thank our colleagues and coauthors for decades of fruitful cooperation. We are especially grateful to Mrs. Galina Stepanova for her assistance in preparation of the manuscript.

Saint Petersburg, Russia

Evgeny G. Drukarev
Aleksandr I. Mikhailov

Contents

Acronyms

CFHH	Correlation function hyperspherical harmonic (method)
FS	Fullerene shell
FSI	Final state interactions
FSM	Furry–Sommerfeld–Maue (functions)
HF	Hartree–Fock approximation
HFT	Hellmann–Feynman theorem
ICC	Internal conversion coefficient
IPA	Independent particle approximation
ISI	Initial state interactions
LHS	Left-hand side of equation
LSE	Lippmann–Schwinger equation
NEET	Nuclear–electron excitation transition
QED	Quantum electrodynamics
QFM	Quasifree mechanism
RDEC	Radiative double electron capture
RHS	Right-hand side of equation
RPAE	Random phase approximation with exchange
RRPA	Relativistic random phase approximation
SO	Shakeoff
SU	Shakeup
VAM	Vacuum-assisted mechanism
ZRPM	Zero-range potential model

Chapter 1
Introduction: What Is This Book About?

Abstract We present the main ideas of the book and describe the contents of the book in detail.

1.1 Main Ideas

Many recent publications devoted to the interaction of photons and electrons with atoms and molecules have the same structure. In the first step, a general quantum-mechanical formula for the cross section is given. In the next step, the most "accurate" numerical functions for the bound-state electrons are employed. Since the binding energies can be measured with high accuracy, the wave functions pass the test for reproducing the binding energies with a good accuracy. In the last step, the computer is put to work. Sometimes, attempts are made to include interactions between the electrons in the final state.

About thirty years ago such an approach was justified to some extent. Most calculations were connected with characteristics that could be detected experimentally. In such experiments energies of the order of the electron binding energies were transferred to the targets. There was no small parameter, and thus there was no possibility to evaluate the equations determined by the original formalism of quantum mechanics. The theoretical atomic physics was indeed becoming a science of precise computations. The near-threshold behavior of processes in which one could find a small parameter was rather an exception.

The situation changed at the end of 1980s, when new synchrotron sources of photons became available. Experiments involving photon energies of order about 10 keV were carried out. For light atoms, such energies are much larger than the binding energies. Some of theoretical calculations which could be of practical importance now contained a small parameter.

In the early years of quantum mechanics, Bethe [1, 2] described the main features of high-energy electron–atomic scattering; see also [3]. Here "high energy" means that the energy greatly exceeds the binding energy of the system. Thus, for example, an energy of 1 keV can be considered a "high energy" for an atom of hydrogen, but not for the K electrons of a neon atom. The main principles of high-energy

E.G. Drukarev and A.I. Mikhailov, *High-Energy Atomic Physics*,
Springer Series on Atomic, Optical, and Plasma Physics 93,
DOI 10.1007/978-3-319-32736-5_1

atomic physics were developed and employed later in the papers of our teacher V.G. Gorshkov and his collaborators (references will be given throughout the text). These principles can be extended to the analysis of any interaction between high-energy charged particles or photons with bound systems. They are as follows:

- The differential cross section of a high-energy process is enchased in the kinematic region, where the same process on the free electrons is allowed.
- Each act of exchange by large momentum q strongly exceeding the characteristic momentum μ_b of a bound system leads to a parametrically small factor.
- The interactions between the fast and slow participants of the process can be treated as a perturbation.
- The cross sections can be expressed in terms of certain parameters of the bound systems.

1.2 Subject Matter

In this book we show how these ideas work. In addition to the standard techniques of quantum mechanics, we employ the Lipmann–Schwinger equation (LSE) [4], which allows us to find the Fourier transforms of wave functions in terms of the wave functions at small distances. We use also Feynman diagrams, which can be viewed as graphical illustrations of the LSE. Employing Feynman diagrams for describing the bound electrons became possible due to the work of Furry [5]. The kinematic region where the momentum transferred to the nucleus, known also as the recoil momentum, can be made small ($q \sim \mu_b$) is called the *Bethe ridge*. In many cases the Bethe ridge provides the main contribution to the cross section. The characteristics of a process on the bound electrons at the Bethe ridge can be expressed in terms of those for the same process on free electrons. This makes the investigation of a process on free electrons a necessary step of theoretical analysis. Such an analysis carried out before beginning computations helps to avoid numerous possible mistakes. Unfortunately some of the latter can be found in published papers. These points are the subject of Chap. 2.

In Chap. 3, we show how the perturbative treatment of fast electrons should be carried out. Although looking to be simple, the perturbative approach was not always carried out properly. Validity of the perturbation expansion does not necessarily mean that the lowest-order approximation is sufficient even for a qualitative description of a process. We demonstrate that in processes with large momentum q transferred to the nucleus, the lowest-order term of perturbative series should contain the plane wave and the first-order Coulomb correction. We also develop the perturbative approach to the final state interaction (FSI) of a fast ejected electron with the atomic shell [6]. We demonstrate that the lowest-order FSI correction should include the terms describing one and two interactions between the fast electron and the atomic shell. The amplitude of the process contains infrared divergent terms that cancel in the expressions for the differential and total cross sections.

In Chap. 4, we demonstrate that $2 \to 3$ processes with large recoil momenta are described by triangle diagrams , with the main contributions determined by the anomalous singularities of the latter [7]. This enables us to obtain analytical expressions for the differential distributions and for the cross sections. The transfer of large momentum between the electron and the nucleus or between electrons is related to the small values of the corresponding distances, where the shape of the wave functions is determined by the Kato cusp conditions [8]. We explain the importance of the latter and construct the electron wave functions on the coalescence lines.

In Chap. 5, we consider processes in the Coulomb field in the framework of nonrelativistic approximation. We introduce a technique that simplifies the calculations in the Coulomb field [9]. We apply it to calculation of the first- and second-order processes. In other words, we calculate the differential distributions and the total cross sections for the photoeffect and also for the Rayleigh scattering, for the Raman scattering, and for the Compton effect.

In Chap. 6, we find the relativistic electron Coulomb functions as power series in $(\alpha Z)^2$ with the Furry–Sommerfeld–Maue functions as the lowest-order approximation [10]. The results are employed for calculation of the photoionization angular distribution and the cross section with inclusion of the terms of order $\alpha^3 Z^3$. We consider also second-order processes. We study the role of various mechanisms for photon elastic scattering on atoms. We present the characteristics of the Compton scattering on the Bethe ridge with inclusion of the $\alpha^2 Z^2$ terms. Employing the results of Chap. 4, we calculate the differential distributions for the Compton scattering outside the Bethe ridge.

In Chap. 7, we analyze the photoionization of atoms. We show the possibility of nonrelativistic asymptotic analysis. We demonstrate that the variety of forms of the electron–photon interactions is connected with the gauge invariance of quantum electrodynamics. We show that the asymptotics for photoionization of s states can be calculated in the velocity form by employing plane waves. In the length form one should include also the lowest nonvanishing term of interaction between the photoelectron and the nucleus. The latter should be included in calculations of the asymptotics for ionization of states with $\ell \neq 0$ in both forms. We analyze the Thomas–Reiche–Kuhn sum rules for the case of a nonlocal field. We carry out asymptotic analysis also for the relativistic case. We present a method for inclusion of the screening corrections for the relativistic case near the threshold and far away from it, as worked out in [11]. We demonstrate that inclusion of the correlations beyond the independent particle approximation (IPA) in the framework of the perturbative approach developed in Chap. 3 enables us to remove the discrepancy between the experimental data and the results of the IPA calculations. We show also how inclusion of the IPA breaking effects changes the asymptotic behavior of the photoionization cross sections [12].

Since the nonrelativistic photoionization cross section drops rapidly with an increase of the photon energy, the higher-order processes dominate in the formation of ions at larger values of the photon energy. In Chap. 8, we carry out relativistic analysis of the second-order and third-order processes. If the photon energy is large enough, the Compton scattering becomes the dominant mechanism of ionization.

We show that the seagull term of the nonrelativistic Compton scattering amplitude can be viewed as the contribution of the negative-energy intermediate states in the relativistic amplitude. We find the general equations for the characteristics of the Compton scattering on the Bethe ridge and show their connection with equations of the impulse approximation. Employing the results obtained in Chap. 4, we find the differential distributions outside the Bethe ridge. We demonstrate the infrared stability of the sum of the contribution to the Compton scattering cross section coming from soft scattered photons and the photoionization cross section, which includes the radiative corrections. At still larger photon energies $\omega > \omega_0$, the ions are produced mainly with the creation of electron–positron pairs. We obtain the energy distribution of the electrons ejected due to this mechanism. We calculate the dependence of ω_0 on the value of the nuclear charge Z for the single-electron ions and for the atoms containing Z electrons [13]. We find also the photon energy region where this mechanism dominates in the creation of excited atoms.

In Chap. 9, we consider mainly the double photoionization of the helium atom and of heliumlike ions. We analyze three mechanisms of the process. They are the shake off (SO), final-state interactions (FSI), and the quasifree mechanism (QFM). We study their role in the distribution of photoelectrons and their contribution to the double-to-single cross section ratio $R_0(\omega) = \sigma^{++}(\omega)/\sigma^{+}(\omega)$, analyzing their dependence on the nuclear charge. We suggest the perturbative model for the desctiption of correlations between the bound electrons in which the electron interactions are treated perturbatively, while their interactions with the nucleus are included exactly [14]. Special attention is devoted to the quasifree mechanism, which was also first considered in [14]. The QFM is at work only beyond the dipole approximation. It manifested itself in experiments on the recoil momentum distribution at photon energies $\omega \approx 800$ eV [15]. It modifies the shape of the spectral curve at energies of several keV. We demonstrate that the approximate wave functions employed in computations of the spectrum at these energies should satisfy the second Kato cusp condition. Otherwise, they can yield a qualitatively incorrect result. At energies of several hundred keV, the QFM dominates in large part of the energy distribution of the photoelectrons. It is also the main mechanism of breaking the nonrelativistic high-energy asymptotics of the ratio $R_0(\omega)$.

In Chap. 10, we study photoionization of fullerenes and of fullerenes with encapsulated atoms. We present the calculation for the photoionization cross section of negative ions C_{60}^{-}, describing the field of the fullerene shell by the Dirac bubble potential. Investigation of dependence of the high-energy asymptotics on the shape of the model potential is carried out. We analyze the photoionization of atom encapsulated into the fullerene. The energy-dependence of the cross section may differ fundamentally from that for an isolated atom due to interference of the outgoing electron wave with that reflected by the fullerene shell [16]. We analyze the inelastic processes in the fullerene shell that accompany the photoionization of the encapsulated atom. It appears to be possible to sum the perturbative series for photoelectron interaction with the fullerene shell [17]. The probability of inelastic processes was found to be close to unity in the large interval of the photon energies.

Since electron and positron scattering on atoms is analyzed in detail in numerous books, we do not consider those processes in our book (although some aspects of electron scattering by atoms are touched on). In Chap. 11, we analyze various channels for annihilation of positrons with atomic electrons. Since in the annihilation process a large energy exceeding 1 MeV is released, relativistic analysis is required even in the case of slow positrons. Employing the results of Chap. 6, we study the dominative two-photon annihilation process on the Bethe ridge including the contributions of order $\alpha^2 Z^2$. Using the results of Chap. 4, we investigate this process outside the Bethe ridge. We calculate the characteristics of single-quantum annihilation and of annihilation followed by the knockout of a bound electron to the continuum. In the latter case, the role of the QFM mechanism described in Chap. 9 is important [18]. We consider also annihilation followed by creation of $\mu^+\mu^-$ pair and annihilation accompanied by the creation of mesoatom.

In Chap. 12, we consider the mutual influence of nuclear and electronic transitions. We investigate the influence of the electronic shell on the energy distribution of electrons ejected in nuclear β decay, employing the approach presented in Chap. 3. We demonstrate how the considered effects manifest themselves in experiments on detection of the neutrino mass. We show how the analysis of interactions between the beta electron and the bound electron in the decay of tritium helped to solve the "heavy neutrino" problem. We present the results for probabilities of the creation of vacancies in the atomic shell in β^- and β^+ nuclear decays [19]. For the case of nuclear γ decays, we analyze the calculations of probabilities of internal nuclear conversion. Using the perturbative model developed in Chap. 9, we calculate the probability for ejection of two electrons from the electronic shell during the same nuclear γ transition. Employing the results obtained in Chap. 4, we clarify the mechanism and calculate the cross section for the nonresonant photoexcitation of the nucleus. We also present an analysis of the less-explored influence of the electronic shell on the probability of α decay.

References

1. H. Bethe, Ann. Phys. **5**, 325 (1930)
2. H. Bethe, in *Handbook der Physik*, vol. 24/1 (Springer, Berlin, 1933), p. 273
3. M. Inokuti, Rev. Mod. Phys. **43**, 297 (1971)
4. R. Newton, *Scattering Theory of Waves and Particles* (Springer, New York, 1982)
5. J.D. Bjorken, S.D. Drell, *Relativistic Quantum Mechanics* (McGraw-Hill Book Company, 1964)
6. E.G. Drukarev, M.I. Strikman, Phys. Lett. B **186**, 1 (1987)
7. V.G. Gorshkov, S.G. Sherman, Sov. Phys. JETP Lett. **17**, 374 (1973)
8. T. Kato, Commun. Pure Appl. Math. **10**, 151 (1957)
9. V.G. Gorshkov, A.I. Mikhailov, ZhETF **44**, 2142 (1963)
10. V.G. Gorshkov, Sov. Phys. JETP **20**, 1331 (1965)
11. A.I. Mikhailov, Sov. Phys. JETP **71**, 465 (1990)
12. E.G. Drukarev, N.B. Avdonina, J. Phys. B. **36**, 2033 (2003)
13. E.G. Drukarev, A.I. Mikhailov, I.A. Mikhailov, K.Y. Rakhimov, W. Scheid, Phys. Rev. A **75**, 032717 (2007)

14. M.Y. Amusia, E.G. Drukarev, V.G. Gorshkov, M.P. Kazachkov, J. Phys. B **8**, 1248 (1975)
15. M.S. Schöffler et al., Phys. Rev. Lett. **111**, 0132003 (2013)
16. M.Y. Amusia, A.S. Baltenkov, L.V. Chernysheva, Z. Felfli, A.Z. Msezane, J. Phys. B **38**, L169 (2005)
17. E.G. Drukarev, M.Y. Amusia, JETP Lett. **98**, 471 (2013)
18. A.I. Mikhailov, I.A. Mikhailov, JETP **86**, 429 (1998)
19. E.G. Drukarev, M.B. Trzhaskovskaya, Nucl. Phys. A **518**, 513 (1990)

Chapter 2
Box of Tools

Abstract Here we introduce the system of units. We recall the main equations of nonrelativistic quantum mechanics and quantum electrodynamics that we employ in this book. We single out two regions for the values of the recoil momentum. In the region of small recoil momentum called the "Bethe ridge," the characteristics of a process with participation of the bound electrons are expressed in terms of the process on the free electrons. The electron functions at large recoil momenta are calculated using the Lippmann–Schwinger equation.

2.1 Wave Functions and Propagators

2.1.1 System of Units

We employ a system of units that is convenient for both nonrelativistic and relativistic problems. We put $\hbar = 1$ and also measure velocities in units of the velocity of light c, putting $c = 1$. The fine-structure constant is $\alpha = 1/137$, and the square of the electron charge is $e^2 = \alpha$. In this system of units, the nonrelativistic binding energy of the ground state of a hydrogen atom is

$$I = \frac{m\alpha^2}{2}, \tag{2.1}$$

with $m \approx 511$ keV standing for the electron mass. The energy I is 1 Rydberg (Ry) $\approx 13.6\,\mathrm{eV}$. The atomic unit of energy (one Hartree) is thus $2I$.

The nonrelativistic binding energy for the ground state of a single-electron ion with the nucleus of charge Z is thus

$$I_Z = \frac{\eta^2}{2m}, \quad I_1 = I, \tag{2.2}$$

with

$$\eta = m\alpha Z. \tag{2.3}$$

E.G. Drukarev and A.I. Mikhailov, *High-Energy Atomic Physics*,
Springer Series on Atomic, Optical, and Plasma Physics 93,
DOI 10.1007/978-3-319-32736-5_2

Hence, η has the meaning of the average linear momentum of the $1s$ electron.

The three-dimensional momentum k of the photon carrying the energy ω is just

$$k = \omega. \tag{2.4}$$

For any four-vectors $a = (a_0, \mathbf{a})$ and $b = (b_0, \mathbf{b})$, we define the scalar product as $a \cdot b = a_0 b_0 - \mathbf{a} \cdot \mathbf{b}$. A free electron is described by the four-momentum $p = (E, \mathbf{p})$ with $E^2 - \mathbf{p}^2 = m^2$. The kinetic energy is $\hat{\varepsilon} = (m^2 + p^2)^{1/2} - m$. Its lowest-order nonvanishing term of expansion in powers of p^2/m^2 is the nonrelativistic energy $\varepsilon = p^2/2m$.

2.1.2 *Some Aspects of Quantum Electrodynamics*

Here we recall some points of quantum electrodynamics (QED) that will be employed in this book. We do not give detailed derivations, since they are contained in a number of books on QED [1–3].

We denote the single-particle wave function of the electron in the state with the set of quantum numbers x in position space by $\psi_x(\mathbf{r})$. Its Fourier transform

$$\tilde{\psi}_x(\mathbf{f}) = \int d^3 r \psi_x(\mathbf{r}) e^{-i\mathbf{f}\cdot\mathbf{r}} \tag{2.5}$$

can be viewed as the wave function of the same state in momentum space. Unless it is needed to avoid a misunderstanding, we omit the tilde for wave functions in momentum space.

In the nonrelativistic case, the bound-state wave functions are normalized by the condition

$$\int d^3 r |\psi_b(\mathbf{r})|^2 = 1, \tag{2.6}$$

and thus

$$\int \frac{d^3 f}{(2\pi)^3} |\psi_b(\mathbf{f})|^2 = 1. \tag{2.7}$$

The functions of the continuum states with the asymptotic momenta $\mathbf{p}, \mathbf{p}'$ are normalized by the condition

$$\int d^3 r \psi^*_{\mathbf{p}}(\mathbf{r}) \psi_{\mathbf{p}'}(\mathbf{r}) = (2\pi)^3 \delta(\mathbf{p} - \mathbf{p}'), \tag{2.8}$$

and thus

$$\int \frac{d^3 f}{(2\pi)^3} \psi^*_{\mathbf{p}}(\mathbf{f}) \psi_{\mathbf{p}'}(\mathbf{f}) = (2\pi)^3 \delta(\mathbf{p} - \mathbf{p}'). \tag{2.9}$$

For the free dynamics, we have

$$\psi_{\mathbf{p}}(\mathbf{r}) = \psi_{\mathbf{p}}^{(0)}(\mathbf{r}) = e^{i(\mathbf{p}\cdot\mathbf{r})}\zeta; \quad \psi_{\mathbf{p}}^{(0)}(\mathbf{f}) = (2\pi)^3\delta(\mathbf{p}-\mathbf{f})\zeta. \tag{2.10}$$

Here ζ is the two-component spinor χ, $\chi^*\chi = 1$. The spinors $\chi_+ = \begin{pmatrix}1\\0\end{pmatrix}$ and $\chi_- = \begin{pmatrix}0\\1\end{pmatrix}$ describe two possible projections of the electron spin $\pm 1/2$ on a chosen axis. We also use the notation

$$|\psi_{\mathbf{p}}^{(0)}\rangle = |\mathbf{p}\rangle\zeta. \tag{2.11}$$

It is employed for both the nonrelativistic and relativistic cases.

In the relativistic case, the wave functions ψ are the four-component spinors. For these functions, we have (2.6)–(2.9) with complex conjugation changed to Hermitian conjugation. The free motion is described by the function given by (2.10) with $\zeta = u/(2E)^{1/2}$, where u is the Dirac bispinor. The explicit form of the bispinor u depends on the form of the presentation of the Dirac 4×4 γ matrices. We employ the "standard" presentation

$$\gamma_0 = \begin{pmatrix} I & 0 \\ 0 & -I \end{pmatrix}; \quad \boldsymbol{\gamma} = \begin{pmatrix} 0 & \boldsymbol{\sigma} \\ -\boldsymbol{\sigma} & 0 \end{pmatrix}, \tag{2.12}$$

where I and $\boldsymbol{\sigma}$ are the 2×2 unit matrix and the Pauli matrices

$$I = \begin{pmatrix} 1 & 0 \\ 0 & 1 \end{pmatrix}, \quad \sigma_x = \begin{pmatrix} 0 & 1 \\ 1 & 0 \end{pmatrix}, \quad \sigma_y = \begin{pmatrix} 0 & -i \\ i & 0 \end{pmatrix}, \quad \sigma_z = \begin{pmatrix} 1 & 0 \\ 0 & -1 \end{pmatrix}. \tag{2.13}$$

The products of the γ matrices can be evaluated by employing the commutation relation

$$\gamma_\mu\gamma_\nu + \gamma_\nu\gamma_\mu = 2g_{\mu\nu}, \tag{2.14}$$

with $g_{\mu\nu} = 0$ for $\mu \neq \nu$, $g_{00} = 1$, $g_{ij} = -\delta_{ij}$ for $i, j = 1, 2, 3$. We shall need one more matrix, namely

$$\gamma_5 = \begin{pmatrix} 0 & -I \\ -I & 0 \end{pmatrix}. \tag{2.15}$$

Note that sometimes γ_5 is defined with the opposite sign.

We use also the 4×4 matrices

$$\beta = \gamma_0; \quad \boldsymbol{\alpha} = \gamma_0\boldsymbol{\gamma} = \begin{pmatrix} 0 & \boldsymbol{\sigma} \\ \boldsymbol{\sigma} & 0 \end{pmatrix}. \tag{2.16}$$

In the standard presentation the Dirac bispinor $u(p) = u(E, \mathbf{p})$ for the free motion and its Dirac conjugated partner $\bar{u} = u^+\gamma_0$ are

$$u(E,\mathbf{p}) = c_E \begin{pmatrix} \chi \\ \frac{\boldsymbol{\sigma}\cdot\mathbf{p}}{E+m}\chi \end{pmatrix}, \quad \bar{u}(E,\mathbf{p}) = c_E \left(\chi^*, -\chi^* \frac{\boldsymbol{\sigma}\cdot\mathbf{p}}{E+m}\right). \tag{2.17}$$

The coefficient c_E is determined by the normalization condition for the bispinor u. The relativistic-invariant condition

$$\bar{u}u \;=\; 2m \tag{2.18}$$

corresponds to normalization of the wave function to one particle per unit of volume. It leads to $c_E = \sqrt{E+m}$.

The bispinors u and $\bar{u}$ at $p = (E, \mathbf{p})$ can be expressed in terms of the bispinors describing the electron at rest. Introducing

$$\hat{p} \equiv \sum_\mu p^\mu \gamma_\mu = \sum_\mu p_\mu \gamma^\mu, \tag{2.19}$$

we write the Dirac equations for the free electron

$$(\hat{p} - m)u = 0; \quad \bar{u}(\hat{p} - m) = 0, \tag{2.20}$$

or

$$\Big(\boldsymbol{\alpha}\cdot\mathbf{p} + \beta m\Big)u = Eu; \quad \bar{u}\Big(-\boldsymbol{\alpha}\cdot\mathbf{p} + \beta m\Big) = \bar{u}E. \tag{2.21}$$

Note that these equations for $\bar{u}$ are written for real components of the four-vector p. We obtain also

$$u(E,\mathbf{p}) = \sqrt{\frac{E+m}{2m}}\Big(1 + \frac{\boldsymbol{\alpha}\cdot\mathbf{p}}{E+m}\Big)u_0; \quad \bar{u}(E,\mathbf{p}) = \sqrt{\frac{E+m}{2m}}\bar{u}_0\Big(1 - \frac{\boldsymbol{\alpha}\cdot\mathbf{p}}{E+m}\Big), \tag{2.22}$$

with $u_0 = u(m, 0)$ describing the electron at rest.

We shall analyze the interaction of the bound systems with external electromagnetic fields, which can be treated as a system of photons. The electric and magnetic fields can be expressed in terms of the four-dimensional vector potential A_μ. In the electromagnetic wave we can put $A_0 = 0$ and $\mathbf{A}\cdot\mathbf{k} = 0$, since the electric and magnetic fields are orthogonal to the direction of propagation of the wave. Thus a photon carrying momentum $\mathbf{k}$ and energy $\omega = |\mathbf{k}|$ can be described by the "wave function"

$$A_i(\mathbf{r}) = \frac{\sqrt{4\pi}}{\sqrt{2\omega}} e_i e^{i\mathbf{kr}}; \quad i = 1, 2, 3; \quad \mathbf{e}\cdot\mathbf{k} = 0 \tag{2.23}$$

with the polarization vector $\mathbf{e}$ directed along the electric field in the wave. In momentum representation, we have

$$A_i(\mathbf{f}) = \frac{\sqrt{4\pi}}{\sqrt{2\omega}} e_i \delta(\mathbf{f} - \mathbf{k}); \quad i = 1, 2, 3; \quad \mathbf{e}\cdot\mathbf{k} = 0. \tag{2.24}$$

Now we present the equations for the electron propagator, starting with the non-relativistic case. The wave equation in the field $V(\mathbf{r})$ can be written as

$$H\psi = \varepsilon\psi, \tag{2.25}$$

with

$$H = H^{(0)}(\mathbf{r}) + V(\mathbf{r}), \tag{2.26}$$

while $H^{(0)}(\mathbf{r}) = -\Delta_r^2/2m$ is the Hamiltonian of the free particle. The Green function, which is determined as

$$G = (\varepsilon - H)^{-1}, \tag{2.27}$$

satisfies the equation

$$(H^{(0)}(\mathbf{r}) + V(\mathbf{r}) - \varepsilon)G(\varepsilon; \mathbf{r}, \mathbf{r}') = -\delta(\mathbf{r} - \mathbf{r}'). \tag{2.28}$$

We employ also the notation $G(p)$, where $p = (2m\varepsilon)^{1/2}$ will be referred to as the momentum of the Green function.

In the case of free motion, when $V = 0$, the matrix element of the Green function G_0 takes a very simple form in momentum representation:

$$\langle \mathbf{f_1}|G_0(p)|\mathbf{f_2}\rangle = G_0(p, \mathbf{f_1})\delta(\mathbf{f_1} - \mathbf{f_2}); \quad G_0(p, \mathbf{f_1}) = \frac{1}{\varepsilon - f_1^2/2m + i\delta} = \tag{2.29}$$

$$= \frac{2m}{p^2 - f_1^2 + i\delta}; \quad \varepsilon = \frac{p^2}{2m}; \quad \delta \to 0.$$

The solutions of (2.25), i.e., the functions ψ_k for which $H\psi_k = \varepsilon_k\psi_k$, form a complete set. They describe the states of a discrete spectrum with $\varepsilon_k < 0$ and the continuum states with $\varepsilon \geq 0$. The Green function of (2.25) can be represented in terms of its eigenfunctions

$$G = \mathscr{S}_k \frac{|\psi_k\rangle\langle\psi_k|}{\varepsilon - \varepsilon_k + i\delta}; \quad \delta \to 0. \tag{2.30}$$

Here $\mathscr{S}_k$ denotes the sum and integration over the eigenstates of (2.25) of the discrete and continuum spectra correspondingle.

In the relativistic case, the wave equation (the Dirac equation) of the free motion in momentum representation is

$$(\hat{p} - m)\psi(p) = 0. \tag{2.31}$$

In the spatial representation, it is

$$(\hat{p} - m)\psi(x) = 0, \tag{2.32}$$

with

$$p_0 = i\frac{\partial}{\partial x_0}; \quad p_i = -i\nabla_i. \tag{2.33}$$

The Green function is the solution of the equation

$$(\hat{p} - m)G^{(0)}(x, x') = -\delta^{(4)}(x - x'). \tag{2.34}$$

In momentum representation,

$$G^{(0)}(p) \; = \; \frac{1}{\hat{p} - m}\,, \tag{2.35}$$

and

$$\langle \mathbf{f_1}|G^{(0)}(E)|\mathbf{f_2}\rangle = \frac{\hat{p} + m}{p^2 - m^2 + i\delta}\delta(\mathbf{f_1} - \mathbf{f_2}), \quad \delta \to 0, \tag{2.36}$$

with the four-momentum $p = (E, \mathbf{f}_1)$. While in the nonrelativistic case we did not need to clarify the origin of the external field V, in the relativistic case the electromagnetic external field can be expressed in terms of a four-vector potential $A_\mu(x)$. The Dirac equations describing the wave functions and the propagator of a fermion with charge e (for an electron, $e = -|e|$) in an external electromagnetic field can be obtained by replacing $p_\mu \to p_\mu - eA_\mu$ in the corresponding equations of the free motion.

The spectrum of the Dirac equation is more complicated than that of the Schrödinger equation. Besides the solutions $\psi_k^{(+)}$ corresponding to the eigenvalues $E^+ > 0$ (the states of the discrete spectrum with $E^+ < m$ and those of the continuum with $E^+ \geq m$), there are solutions $\psi_k^{(-)}$ with eigenvalues $E_k^- < 0$. The states $\psi_k^{(+)}$ and $\psi_k^{(-)}$ form a complete set. The relativistic propagator in an external electromagnetic field takes the form

$$G = \mathscr{S}_k \frac{|\psi_k^{(+)}\rangle\langle\psi_k^{(+)}|}{E - E_k^+ + i\delta} + \mathscr{S}_k \frac{|\psi_k^{(-)}\rangle\langle\psi_k^{(-)}|}{E - E_k^- - i\delta}; \quad \delta \to 0. \tag{2.37}$$

The electron interaction with the electromagnetic field is described by the amplitude

$$F = e\int d^3x A_\mu(x) j^\mu(x), \tag{2.38}$$

with the matrix element of the current

$$j^\mu(x) = \bar{\psi}_f(x)\gamma^\mu\psi_i(x). \tag{2.39}$$

The current is conserved, and it satisfies the equation

$$\partial_\mu j^\mu(x) = 0. \tag{2.40}$$

Employing (2.24), we find that in momentum representation,

$$F = -N(\omega)e_k \int \frac{d^3 f}{(2\pi)^3} \bar{\psi}_f(\mathbf{f})\gamma^k \psi_i(\mathbf{f} - \mathbf{k}), \tag{2.41}$$

with

$$N(\omega) = \sqrt{\frac{4\pi\alpha}{2\omega}}. \tag{2.42}$$

The interaction of two free electrons in which their four-momenta p_1 and p_2 change to p_1' and p_2' ($p_1 + p_2 = p_1' + p_2'$) is described by the amplitude

$$F = \frac{1}{\sqrt{2}}[j^\mu(p_1, p_1')D_{\mu\nu}(Q)j^\nu(p_2, p_2') - (p_2 \leftrightarrow p_2')]; \quad Q = p_1 - p_1' = p_2' - p_2. \tag{2.43}$$

One can check the conservation laws $Q_\mu j^\mu(p_1, p_1') = 0$ and $Q_\mu j^\mu(p_2, p_2') = 0$. The general form of the photon propagator $D_{\mu\nu}(Q)$ is

$$D_{\mu\nu}(Q) = g_{\mu\nu}D(Q^2) + \frac{Q_\mu Q_\nu}{Q^2} D^{(\ell)}(Q^2). \tag{2.44}$$

The function $D(Q^2)$ is the Fourier transform of the function $D(x)$ that satisfies the equation

$$\frac{\partial}{\partial x^\alpha}\frac{\partial}{\partial x_\alpha} D(x - x') = -4\pi\delta^{(4)}(x - x'), \tag{2.45}$$

i.e.,

$$D(Q^2) = -\frac{4\pi}{Q^2 + i\delta}; \quad \delta \to 0, \tag{2.46}$$

while $D^{(\ell)}$ can be any scalar function of Q^2. Due to the conservation of the current j, the second term on the right-hand side (RHS) of (2.44) does not contribute to the amplitude F.

Thus we can put

$$D_{\mu\nu}(Q) = D^F_{\mu\nu}(Q) = -g_{\mu\nu}\frac{4\pi}{Q^2 + i\delta}, \tag{2.47}$$

corresponding to the Feynman gauge.

Due to conservation of the current, any function of the form

$$D_{\mu\nu}(Q) = D^F_{\mu\nu}(Q) + Q_\mu \chi_\nu(Q) + \chi_\mu(Q)Q_\nu \tag{2.48}$$

can be employed as the photon propagator. We demonstrated this, taking the scattering of the plane waves as an example. However, this can be shown in the general case in which the electrons are moving in an external field. If $\chi_\nu(Q)$ on the RHS of (2.48) is a four-vector, the propagator $D_{\mu\nu}$ has a relativistic-invariant form. Otherwise, it does not. The form (2.47) is known as the Feynman gauge (this explains the upper index F). Setting $Q = (\omega, \mathbf{q})$, $q = |\mathbf{q}|$, and putting

$$\chi_0 = \frac{2\pi\omega}{Q^2q^2}; \quad \chi_i = \frac{2\pi q_i}{Q^2q^2}; \quad \chi_\mu = \frac{2\pi Q_\mu}{Q^2q^2} \quad Q^2 = \omega^2 - q^2, \tag{2.49}$$

we obtain the Coulomb gauge

$$D^C_{00} = \frac{4\pi}{q^2}; \quad D^C_{ij} = \frac{4\pi}{Q^2 + i\delta}(\delta_{ij} - \frac{q_iq_j}{q^2}); \quad D^C_{0i} = D^C_{i0} = 0; \quad i, j = 1, 2, 3. \tag{2.50}$$

A number of other gauges are often used in applications. Choosing

$$\chi_0 = \frac{2\pi}{\omega Q^2}; \quad \chi_i = -\frac{2\pi q_i}{\omega^2 q^2},$$

we obtain the propagator with

$$D_{00} = D_{0i} = D_{i0} = 0; \quad D_{ij} = \frac{4\pi}{Q^2 + i\delta}(\delta_{ij} - \frac{q_iq_j}{\omega^2}), \tag{2.51}$$

corresponding to the condition $A_0 = 0$. Note also that the equations for the current hold for any charged fermion.

If the initial-state wave functions ψ_i and the final-state wave functions ψ_f in (2.39) for the current are taken in the nonrelativistic limit, only the time component of the current j^0 obtains a nonvanishing value. Thus if at least one of the colliding fermions can be treated in nonrelativistic approximation and the Coulomb gauge is used for the photon propagator, only the time component D^C_{00} contributes to the amplitude of a process. In particular, only the component D^C_{00} should be included in interactions between the electrons and the nucleus, which we assume to be infinitely heavy.

Note that the invariance of the amplitude under transformation expressed by (2.48) is based on the fundamental feature of quantum electrodynamics (QED) known as the local gauge symmetry. The density of the QED Lagrangian (usually called just the Lagrangian) can be written as the sum of the Lagrangian of free electrons L_e, the Lagrangian of the electromagnetic field L_{em}, and the Lagrangian of their interaction

$$L \; = \; L_e + L_{em} + L_{int} \, . \tag{2.52}$$

Writing

$$L_e = \bar{\psi}(x)(i\gamma^\mu \partial_\mu - m)\psi(x); \quad L_{em} = -\frac{1}{4}F_{\mu\nu}^2; \quad L_{int} = -e\bar{\psi}(x)\gamma^\mu A_\mu(x)\psi(x) \tag{2.53}$$

($F_{\mu\nu} = \partial_\mu A^\nu - \partial_\nu A^\mu$), one can see that the Lagrangian is invariant under the simultaneous transformations

$$\psi(x) \to e^{ie\lambda(x)}\psi(x); \quad \bar{\psi}(x) \to e^{-ie\lambda(x)}\bar{\psi}(x); \quad A_\mu(x) \to A_\mu(x) - \partial_\mu\lambda(x). \tag{2.54}$$

Note that the terms L_e and L_{em} treated separately change after this transformation. One can begin with the Lagrangian of free electrons, requiring, however, local gauge invariance. This will lead to the necessity to introduce the electromagnetic field [4].

2.1.3 The Lippmann–Schwinger Equation

Along with the standard methods of atomic physics, we shall use the Lippmann–Schwinger equation (LSE); see, e.g., [5]. We show that the LSE is a good tool for analysis of high-energy processes.

In the nonrelativistic case, the LSE connects the solutions of the Schrödinger equations

$$H_0\psi_0 = \varepsilon\psi_0 \tag{2.55}$$

and

$$(H_0 + V)\psi = \varepsilon\psi\,. \tag{2.56}$$

Here H_0 is not necessarily the Hamiltonian of the free motion. It can include certain interactions, but not V. The LSE for the wave function can be obtained in a straightforward way:

$$\psi = \psi_0 + G_0(\varepsilon)V\psi. \tag{2.57}$$

It can also be written in the form

$$\psi = \psi_0 + G(\varepsilon)V\psi_0, \tag{2.58}$$

with G the Green function of (2.56). On the other hand, the LSEs for G are

$$G(\varepsilon) = G_0(\varepsilon) + G_0(\varepsilon)VG(\varepsilon); \quad G(\varepsilon) = G_0(\varepsilon) + G(\varepsilon)VG_0(\varepsilon). \tag{2.59}$$

The LSE is illustrated by Fig. 2.1.

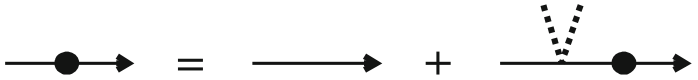

Fig. 2.1 Illustration of the Lippmann–Schwinger equation. The *solid lines* represents the electron. The dark blob denotes the external field. *Dashed lines* are for the external field in the lowest order.

One can write analogues of (2.57)–(2.59) for a light relativistic fermion moving in the field of an infinitely heavy nucleus. In the Coulomb gauge, only the time component of the current and the interaction $A_\mu j^\mu = \bar{\psi}_f \gamma_0 \psi_i A_0$ contribute. Thus the Dirac equation takes the form

$$(\hat{p} - \hat{V} - m)\psi = 0; \quad G = \frac{1}{\hat{p} - \hat{V} - m}; \quad \hat{V} = \gamma_0 V. \tag{2.60}$$

Employing (2.35), we obtain the LSE equations

$$\psi = \psi^{(0)} + G^{(0)}(E)\hat{V}\psi; \quad \psi = \psi^{(0)}(E) + G(E)\hat{V}\psi^{(0)}, \tag{2.61}$$

and

$$G(E) = G^{(0)}(E) + G^{(0)}(E)\hat{V}G(E); \quad G(E) = G^{(0)}(E) + G(E)\hat{V}G^{(0)}(E). \tag{2.62}$$

Note that calculations in the nonrelativistic approximation are usually simpler than in the relativistic case. The main simplification consists in separation of the spin variables. Indeed, in the relativistic Hamiltonian

$$H = \boldsymbol{\alpha} \cdot (\mathbf{p} - e\mathbf{A}) + \beta m + eA_0, \tag{2.63}$$

the space and spin variables are mixed. The corresponding nonrelativistic Hamiltonian

$$H_{nr} = \frac{(\mathbf{p} - e\mathbf{A})^2}{2m} + eA_0 \tag{2.64}$$

does not involve the spin variables. Thus, in the nonrelativistic approximation for the continuum electron, i.e., in the lowest nonvanishing terms of the expansion in powers of $v^2 = p^2/E^2$, the spin variables are separated. In the many-electron wave function, they form a symmetric or antisymmetric factor, ensuring the total antisymmetry of the state. The nonrelativistic description of the bound electrons is justified if the average momentum of the bound state μ_b is small enough. The average momentum is defined as

$$\mu_b = (2mI_b)^{1/2}, \tag{2.65}$$

where $I_b = -\varepsilon_b$, while $\varepsilon_b < 0$ is the single-particle energy of the bound state. The nonrelativistic approach is possible if $\mu_b \ll m$. In fact, usually the condition is $I_b \ll m$. Note that for the electrons of the $1s$ state of the hydrogenlike ions, this means that

$$(\alpha Z)^2 \ll 1. \tag{2.66}$$

Thus the processes that involve the $1s$ states of heavy atoms require additional analysis.

2.2 Two Scales of Momenta

We start this subsection with the analysis of Compton scattering on a bound electron. However, we shall come to more general conclusions at the end.

2.2.1 Differential Cross Sections for Bound and Free Electrons

The photon carrying momentum $\mathbf{k_1}$ and energy $\omega_1 = |\mathbf{k_1}|$ is scattered by atom with the charge of the nucleus Z. A bound electron is knocked out into the continuum, obtaining asymptotic momentum $\mathbf{p}$ and energy E, while the kinetic energy is $\hat{\varepsilon} = E - m$. The ejected photon carries momentum $\mathbf{k_2}$ and energy $\omega_2 = |\mathbf{k_2}|$.

The cross section of the process can be written as

$$d\sigma = 2\pi |F(\mathbf{k_1}, \mathbf{k_2}, \mathbf{p})|^2 \delta(\omega_1 + E_b - E - \omega_2) \frac{d^3p}{(2\pi)^3} \frac{d^3k_2}{(2\pi)^3}. \tag{2.67}$$

Here F is the amplitude of the process (it includes the normalization factors of the wave functions), averaging and summation over the initial- and final-state polarizations are assumed, and $E_b = m + \varepsilon_b (\varepsilon_b < 0)$ is the energy of the bound state. The atom is assumed to be initially at rest. We assume its nucleus to be infinitely heavy and thus neglect its recoil kinetic energy.

It is instructive to compare this cross section with that for Compton scattering on a free electron. In the rest frame of the latter,

$$d\sigma_0 = 2\pi |F_0(\mathbf{k_1}, \mathbf{k_2})|^2 \delta(\omega_1 + m - E - \omega_2) \delta(\mathbf{k_1} - \mathbf{k_2} - \mathbf{p}) \frac{d^3p}{(2\pi)^3} \frac{d^3k_2}{(2\pi)^3}, \tag{2.68}$$

where $F_0(\mathbf{k_1}, \mathbf{k_2}) = F_0(\mathbf{k_1}, \mathbf{k_2}, \mathbf{p} = \mathbf{k_1} - \mathbf{k_2})$ is the amplitude of the Compton scattering on the free electron.

We denote

$$\mathbf{q} = \mathbf{p} + \mathbf{k_2} - \mathbf{k_1}. \tag{2.69}$$

A momentum $\mathbf{q}$ is transferred from the nucleus. It is often called the recoil momentum. In the process with free electrons, $\mathbf{q} = 0$.

Compton scattering on the free electron can take place in a limited region of the phase volume. For example, in the case $\omega_1 \ll m$, the scattered photon carries the largest part of the energy ω_1. Conservation of energy and of momentum

$$\omega_1 = \omega_2 + \varepsilon; \quad \mathbf{k_1} = \mathbf{k_2} + \mathbf{p},$$

with $\varepsilon = p^2/2m$ requires that $\omega_1 - \omega_2 \leq \omega_1 \cdot \omega_1/m \ll \omega_1$. In the general case,

$$\omega_1 \geq \omega_2 \geq \frac{\omega_1}{1 + 2\omega_1/m}. \tag{2.70}$$

Otherwise, the condition $\mathbf{q} = 0$ cannot be satisfied.

Now we focus on the case $\omega_1 \ll m$, when nonrelativistic description of the electrons is possible. The results can be easily generalized for the case of larger energies. Let us write (2.67) in another way:

$$d\sigma = 2\pi |F(\mathbf{k_1}, \mathbf{k_2}, \mathbf{q})|^2 \delta(\omega_1 - \varepsilon_b - (\mathbf{k_1} - \mathbf{k_2} + \mathbf{q})^2/2m - \omega_2) \frac{d^3q}{(2\pi)^3} \frac{d^3k_2}{(2\pi)^3}. \tag{2.71}$$

We consider the case in which the energies of both the incoming and ejected photons $\omega_{1,2}$ and the energy of the outgoing electron ε are much larger than the ionization potential I_Z of the K-shell electron in a hydrogenlike atom with the same nuclear charge Z; (2.2).

$$\omega_{1,2} \gg I_Z; \quad \varepsilon \gg I_Z\,. \tag{2.72}$$

This ensures that

$$\omega_{1,2} \gg I_b; \quad \varepsilon \gg I_b\,. \tag{2.73}$$

We shall calculate the characteristics of the process in the lowest order of expansion in powers of $(I_Z/\omega_{1,2})^{1/2} \ll 1$.

The average momentum of the bound electron (2.65) is thus a natural scale for the electron momenta. For $1s$ electron in the Coulomb field,

$$\mu_b = \eta, \tag{2.74}$$

with η defined by (2.3).

Now we consider two regions of the values of the recoil momenta $q = |\mathbf{q}|$. These are $q \lesssim \mu_b$ and $q \gg \mu_b$.

2.2.2 The Bethe Ridge

In the region of small recoil momenta $q \lesssim \mu_b$, we keep q only in the wave function of the bound electron, putting $q = 0$ in the continuum electron wave function and propagators. This is possible, since the amplitude F contains the continuum electron wave function with momentum p and the electron propagators with momenta $p_1 = (2m\omega_1)^{1/2}$, $p_2 = i(2m\omega_2)^{1/2}$. We can put $q = 0$ also in the argument of the δ function in (2.71). (The region $\omega_1 - \omega_2 \sim I_b$ requires a special analysis.)

In the Coulomb field, the electron continuum wave functions and the propagators can be expanded in powers of η/p and $\eta/|p_i|$, $i = 1, 2$. The lowest-order terms of these expansions describe the free motion. The accuracy of this approximation will be discussed in Chap. 3. In the many-electron atom, the field is still long-range, just being weaker due to the screening. Thus the approximation becomes better in this case. Hence, assuming that the bound electrons are described by single-particle wave functions ψ, we can write

$$F(\mathbf{k_1}, \mathbf{k_2}, \mathbf{q}) = \psi(\mathbf{q}) F_0(\mathbf{k_1}, \mathbf{k_2}), \tag{2.75}$$

where F_0 is the amplitude of the process on the free electron. Thus for $q \lesssim \mu_b$, we obtain [6]

$$\frac{d\sigma}{d\Omega_2 d^3q} = \psi^2(\mathbf{q}) \frac{d\sigma_0}{d\Omega_2}, \tag{2.76}$$

where the last factor stands for the angular distribution of the free process. Similarly,

$$\frac{d\sigma}{d\omega_2 d^3q} = \psi^2(\mathbf{q}) \frac{d\sigma_0}{d\omega_2}. \tag{2.77}$$

Hence

$$\frac{d\sigma}{d\Omega_2} = \frac{d\sigma_0}{d\Omega_2} \int \frac{d^3q}{(2\pi)^3} \psi^2(\mathbf{q}), \quad \frac{d\sigma}{d\omega_2} = \frac{d\sigma_0}{d\omega_2} \int \frac{d^3q}{(2\pi)^3} \psi^2(\mathbf{q}), \tag{2.78}$$

with the integration over q carried out in the region $q \lesssim \mu_b$. As we shall see, the integrals over all possible q, which are determined by the normalization condition (2.7), are saturated by $q \lesssim \mu_b$:

$$\int\limits_{q \lesssim \mu_b} \frac{d^3q}{(2\pi)^3} \psi^2(\mathbf{q}) = \int\limits_{0<q<\infty} \frac{d^3q}{(2\pi)^3} \psi^2(\mathbf{q}) = 1. \tag{2.79}$$

One can see that (2.75)–(2.79) hold for every process in which the transferred momentum can be made small if the amplitude of the free process F_0 has no singularities in the physical region. Otherwise, expansion in powers of q is impossible in the vicinity of the singularity. The case of singular amplitudes will be analyzed in Chap. 4.

Employing (2.79), we can write

$$\frac{d\sigma}{d\Omega_2} = \frac{d\sigma_0}{d\Omega_2}, \quad \frac{d\sigma}{d\omega_2} = \frac{d\sigma_0}{d\omega_2}, \tag{2.80}$$

for the photon energies determined by (2.73) [6].

Thus in the region where transfer of small momentum q is possible, the differential cross sections for the Compton scattering on the bound electron are equal to those on the free electrons. This is true for every process that is allowed on a *single* bound electron. If a process is impossible for a single free electron but is possible for two of them, the differential cross sections take a more complicated form, yielding additional factors; see Chap. 9. In this region, the differential cross sections are determined by small momenta transferred to the recoil atom. We shall call this a *quasifree mechanism* (QFM). The amplitude of a process considered as a function of the kinematic variables reaches its largest values in the region where $q \lesssim \mu_b$. This region will be referred to as the *Bethe ridge* [7]. It peaks at $q = 0$. This condition corresponds to the free kinematics.

Consider, for example, the Compton scattering of photons on the ground state of the hydrogen atom. The photon energy ω_1 is assumed to be high, but the wavelength is much larger than the characteristic size of the $1s$ state. This means that $I = \eta^2/2m \ll \omega_1 \ll \eta$ with $\eta = m\alpha$. In other words, $10\,\text{eV} \ll \omega_1 \ll 4\,\text{keV}$. The Bethe ridge condition $q \lesssim \eta$ requires that $p \lesssim \eta$, i.e., the electron energy $\varepsilon \lesssim I = 13.6\,\text{eV}$.

The electron distributions do not always obtain their largest values at the Bethe ridge. Those values can be local maxima, since there can be other mechanisms of enhancement. The most instructive examples will be given in Chap. 9.

For a single-particle process, the contribution of the QFM to the total cross section coincides with the cross section of the process for a free electron,

$$\sigma^{QFM}(\omega) = \sigma^0(\omega)\,. \tag{2.81}$$

What is the role of the QFM in Compton scattering, which we consider as an example? The answer depends on an accurate definition of the value that we wish to calculate. According to Low's theorem [8], the distribution $d\sigma/d\omega_2$ behaves as $1/\omega_2$ at $\omega_2 \to 0$. Hence, in the soft photon part of the spectrum, far away from the Bethe ridge, the cross section is also enhanced. The cross section is that

$$\sigma = \int_0 d\omega_2 \frac{d\sigma}{d\omega_2}$$

diverges. We can calculate the value

$$\sigma(\omega_0) = \int_{\omega_0} d\omega_2 \frac{d\sigma}{d\omega_2}$$

for every finite value of ω_0. The contribution of the soft photon part of the spectrum thus contains the "large logarithm" $\ln(\omega_1/\omega_0)$. The relative importance of the QFM and soft photon emission thus depends on the value of ω_0.

The value $\omega_0 = 0$ corresponds to the situation in which no photons are emitted. It is demonstrated in Chap. 7 of the book [1] (using the example of electron–electron scattering) that the sum of the cross sections of the process with no photon emitted, but with inclusion of the lowest-order radiative correction and the same process with emission of the soft photon (in the general case one can consider arbitrary number of the soft photons) yields a finite value, and there is no "large logarithm." In the same way, for Compton scattering, the sum of the photoionization cross section with inclusion of the radiative correction and the cross section of the soft photon emission yields a finite value.

In similar way, we expect the QFM to provide the leading contribution to the processes that can take place for a single free electron. We shall see in Chap. 9 that, e.g., in double photoionization, the situation is more complicated. The relative role of the QFM depends on the value of the photon energy.

2.2.3 Transfer of Large Momenta

Large momentum q can be transferred to the nucleus by any electron participating in the process. We begin with calculation of the wave function of a bound state $\psi(\mathbf{q})$ for $q \gg \mu_b$.

In the case $q \ll m$, we can employ a nonrelativistic approximation. Using the LSE equation (2.57) with $\psi^{(0)} = 0$, we obtain

$$\psi(\mathbf{q}) = \int \frac{d^3f}{(2\pi)^3}\frac{d^3f_1}{(2\pi)^3}\langle \mathbf{q}|G_0(\varepsilon_b)|\mathbf{f}\rangle\langle \mathbf{f}|V|\mathbf{f_1}\rangle\psi(\mathbf{f_1}). \tag{2.82}$$

Here V is the sum of interactions of the electron with the nucleus and with the electrons of the atomic shell:

$$V = V_{eN} + V_{ee}\,. \tag{2.83}$$

Carrying out integration over $\mathbf{f}$, we obtain

$$\psi(\mathbf{q}) = -\frac{2m}{q^2}\int \frac{d^3f_1}{(2\pi)^3}\langle \mathbf{q}|V|\mathbf{f_1}\rangle\psi(\mathbf{f_1}) \tag{2.84}$$

for $q \gg \mu_b$.

Consider first the interaction with the nucleus, i.e., put $V = V_{eN}$ on the RHS of (2.84). Its matrix elements are

$$\langle \mathbf{r}|V_{eN}|\mathbf{r_1}\rangle = -\frac{\alpha Z\delta(\mathbf{r}-\mathbf{r_1})}{r}, \quad \langle \mathbf{q}|V_{eN}|\mathbf{f_1}\rangle = \frac{-4\pi\alpha Z}{(\mathbf{q}-\mathbf{f_1})^2}. \tag{2.85}$$

Since the integral on the right-hand side is saturated at $f_1 \sim \mu_b$, the matrix element $\langle \mathbf{q}|V_{eN}|\mathbf{f_1}\rangle$ is approximately equal to $\langle \mathbf{q}|V_{eN}|0\rangle = -4\pi\alpha Z/q^2$. Thus the contribution of the electron–nucleus interaction V_{eN} to the wave function $\psi(\mathbf{q})$ decreases at least as q^{-4} at large q. If a large momentum $\mathbf{q}$ is transferred to the electrons of the atomic shell, the wave function of the latter at $q \gg \mu_b$ will be involved, causing additional powers of q^{-2}. Hence, if large momentum q is transferred to the atom, it is transferred to the nucleus. In other words, if the electron is close to the nucleus, it interacts mainly with the nucleus. Thus for calculation of the leading terms of order q^{-2} of the function $\psi(\mathbf{q})$, it is sufficient to put $V = V_{eN}$ on the RHS of (2.82) and (2.84).

Thus for bound s electrons, we can put $\langle \mathbf{q}|V|\mathbf{f_1}\rangle = -4\pi\alpha Z/q^2$. This provides

$$\tilde{\psi}(q \gg \mu_b) = \frac{8\pi\eta}{q^4}\int \frac{d^3f}{(2\pi)^3}\tilde{\psi}(\mathbf{f}) = \frac{8\pi\eta}{q^4}\psi(\mathbf{r}=0). \tag{2.86}$$

For the electrons with a nonzero orbital momentum, we have $\psi(r=0)=0$, and one cannot neglect $\mathbf{f_1}$ in the matrix element $\langle \mathbf{q}|V|\mathbf{f_1}\rangle$. We can evaluate

$$\int \frac{d^3f_1}{(2\pi)^3}\langle \mathbf{q}|V_{eN}|\mathbf{f_1}\rangle\psi(\mathbf{f_1}) = -\alpha Z\int d^3r\frac{\psi(\mathbf{r})}{r}e^{-i\mathbf{q}\cdot\mathbf{r}}. \tag{2.87}$$

Thus the general expression, valid for every value of the orbital momentum ℓ, is

$$\tilde{\psi}_{n\ell m}(q \gg \mu_b) = \frac{2\eta}{q^2}\kappa_{n\ell m}(\mathbf{q}), \tag{2.88}$$

where

$$\kappa_{n\ell m}(\mathbf{q}) = \int d^3r\frac{\psi_{n\ell m}(\mathbf{r})}{r}e^{-i\mathbf{q}\cdot\mathbf{r}}. \tag{2.89}$$

Since the integral on the RHS of (2.89) is saturated at $r \sim 1/q \ll 1/\mu_b$, we can calculate it for s states just putting $\psi(\mathbf{r}) = \psi(0)$. This provides $\kappa = 4\pi/q^2$, and we obtain (2.86). For $\ell = 1$, the wave function of the state with projection of the orbital momentum $\ell_z = m$ ($m = \pm 1, 0$), can be written as

$$\psi_{n1m}(\mathbf{r}) = \sqrt{\frac{3}{4\pi}}r_m\chi_{n1}(r). \tag{2.90}$$

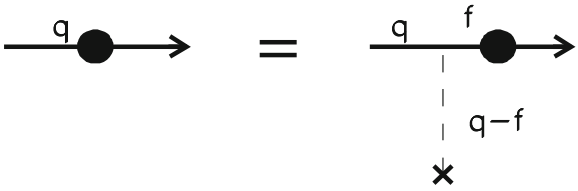

Fig. 2.2 Illustration for (2.92)–(2.95). The notation is the same as in Fig. 2.1.

Here $\chi(0) \neq 0$, and the radial part of the wave function $\psi_{n1m}(\mathbf{r})$ is $R_{n1}(r) = r\chi_{n1}(r)$. Putting $\chi_{n1}(r) = \chi_{n1}(0)$, we obtain

$$\kappa_{n1m}(\mathbf{q}) \;=\; -i\sqrt{\frac{3}{4\pi}}q_m \cdot \frac{8\pi\chi_{n1}(0)}{q^4}. \tag{2.91}$$

One can see that for $\ell \neq 0$, one needs the ℓth partial wave of the matrix element $\langle \mathbf{q}|V_{eN}|\mathbf{f_1}\rangle$ to obtain a nonzero value of κ. Thus for the bound state with orbital momentum ℓ, we can estimate $\kappa \sim q^{-2-\ell}$ and $\psi(q \gg \mu_b) \sim q^{-4-\ell}$.

One can write similar equations for the continuum wave function with asymptotic momentum $\mathbf{p}$, $p \lesssim \mu_b$:

$$\tilde{\psi}_{\mathbf{p}}(q \gg \mu_b) = \frac{8\pi\eta}{q^4}\int \frac{d^3f}{(2\pi)^3}\tilde{\psi}(\mathbf{f}) = \frac{8\pi\eta}{q^4}\psi_{\mathbf{p}}(\mathbf{r}=0). \tag{2.92}$$

These expressions for $\tilde{\psi}(q \gg \mu_b)$, illustrated by Fig. 2.2, have a clear physical meaning. The bound electron exchanges an infinite number of quanta with momenta $f \sim \mu_b$ with the nucleus and with the other electrons of the atom. There is only one exchange of the "hard" quantum carrying large momentum $q \gg \mu_b$. Exchange by a larger number of hard quanta leads to additional suppression by the powers of μ_b/q. In other words, exchange of hard quanta can be included perturbatively.

We turn now to the case in which the values of the recoil momenta can be as large as $q \sim m$. One should employ the relativistic equation (2.61):

$$\psi^{rel}(\mathbf{q}) = \int \frac{d^3f}{(2\pi)^3}\frac{d^3f_1}{(2\pi)^3}\langle \mathbf{q}|G_0^{rel}(E_b)|\mathbf{f}\rangle\langle \mathbf{f}|V|\mathbf{f_1}\rangle\gamma_0\psi^{rel}(\mathbf{f_1}), \quad E = m - \varepsilon_b. \tag{2.93}$$

In the lowest order of expansion in powers of ε_b/m (for the ground state of the Coulomb field, this parameter is $\alpha^2Z^2/2$), we can put $E_b = m$ in the propagator $G_0^{rel}(E_b)$ on the RHS, replacing also the relativistic wave function $\psi^{rel}(\mathbf{f_1})$ by a nonrelativistic one. This provides for s states

$$\psi(\mathbf{q}) \;=\; \frac{8\pi\eta}{q^4}\left(1 - \frac{\boldsymbol{\alpha}\mathbf{q}}{2m}\right)\psi(r=0)u_0. \tag{2.94}$$

Here $u_0 = u(m, 0)$ (see (2.22)), while $\psi(r = 0)$ is the value of the nonrelativistic wave function at the origin. For a bound state with orbital momentum ℓ,

$$\psi(\mathbf{q}) = \frac{2\eta}{q^2}\left(1 - \frac{\boldsymbol{\alpha}\mathbf{q}}{2m}\right)\kappa_{n\ell}u_0. \tag{2.95}$$

These equations can also be illustrated by Fig. 2.2.

Thus at $q \gg \mu_b$, the differential cross sections $d\sigma/d\omega_2 d^3q$ and $d\sigma/d\Omega_2 d^3q$ are quenched at least as $(q^2)^{-3}$. This quenching is so strong that one can assume that integration over q in (2.78) is carried out over the whole space; (2.79).

References

1. J.D. Bjorken, S.D. Drell, *Relativistic Quantum Mechanics* (McGraw-Hill Book Company, 1964)
2. V.B. Berestetskii, E.M. Lifshits, L.P. Pitaevskii, *Quantum Electrodynamics* (Pergamon, New York, 1982)
3. A.I. Akhiezer, V.B. Berestetskii, *Quantum Electrodynamics* (Pergamon, New York, 1982)
4. S. Weinberg *Quantum Field Theory* (University Press, Cambridge, 2000)
5. R. Newton, *Scattering Theory of Waves and Particles* (Springer, New York, 1982)
6. V.G. Gorshkov, A.I. Mikhailov, S.G. Sherman, Sov. Phys. JETP **37**, 572 (1973)
7. M. Inokuti, Rev. Mod. Phys. **43**, 297 (1971)
8. F.E. Low, Phys. Rev. **110**, 974 (1958)

Chapter 3
Perturbation Theory

Abstract We show that the interaction between a fast continuum electron with the nucleus can be described in perturbation theory. For processes on the Bethe ridge the plane wave can be the lowest-order approximation. For processes outside the Bethe ridge, the lowest-order approximation should include one interaction between the electron and the nucleus. We demonstrate that the interaction between the fast electron and the electrons bound in the atom (final-state interactions, abbreviated as FSI) can be presented as power series of the Sommerfeld parameter ξ_{ee}. The lowest-order FSI corrections to the cross sections are of order ξ_{ee}^2. In order to find them, one should calculate the FSI amplitude up to the second order in ξ_{ee}. The infrared divergent terms emerging in the intermediate steps cancel automatically in the expressions for the cross sections.

3.1 Interaction of the Fast Electron and the Nucleus

3.1.1 Lowest-Order Correction

We consider the motion of the electron with the asymptotic momentum $\mathbf{p}$ in the field of the nucleus V. For $V = 0$, the wave functions are just the plane waves, given by (2.10). Now we calculate the correction caused by a single act of interaction.

We start with the nonrelativistic case, when the kinetic energy of the electron is $\varepsilon = p^2/2m \ll m$. Employing the LSE equation (2.57), we find that the lowest-order correction is

$$\langle \mathbf{f}|\psi_{\mathbf{p}}^{(1)}\rangle = \int \frac{d^3q}{(2\pi)^3}\frac{\langle \mathbf{f}|\mathbf{q}\rangle\langle \mathbf{q}|V|\mathbf{p}\rangle}{p^2/2m - q^2/2m + i\delta}; \quad \delta \to 0. \tag{3.1}$$

Of course, one could have written immediately

$$\psi_{\mathbf{p}}^{(1)}(\mathbf{f}) = \frac{\langle \mathbf{f}|V|\mathbf{p}\rangle}{p^2/2m - f^2/2m + i\delta}. \tag{3.2}$$

E.G. Drukarev and A.I. Mikhailov, *High-Energy Atomic Physics*,
Springer Series on Atomic, Optical, and Plasma Physics 93,
DOI 10.1007/978-3-319-32736-5_3

However, we presented the intermediate (3.1) in order to show that it is very much like the standard expression for the lowest-order correction provided by quantum mechanics. The standard form for the latter is (see, e.g., [1])

$$|\psi_n^{(1)}\rangle = \mathscr{S}'_m |\psi_m^0\rangle \frac{\langle\psi_m^0|V|\psi_n^0\rangle}{\varepsilon_n - \varepsilon_m}. \tag{3.3}$$

Here $|\psi_m^0\rangle$ are the solutions of the wave equation $H_0\psi = \varepsilon\psi$, where the Hamiltonian H_0 is not necessarily that of the free motion. In the general case, it can have both continuum and discrete spectra; $\mathscr{S}$ denotes integration over the continuum states and the summation over the states of the discrete spectra. The prime means that the states with $\varepsilon_m = \varepsilon_n$ are excluded. If H_0 is the Hamiltonian of free motion, it has only the continuum spectrum with $\varepsilon_q = q^2/2m$.

We present the Coulomb field of the nucleus with charge Z as

$$V(r) = -\alpha Z \frac{e^{-\lambda r}}{r}; \quad \lambda \to 0, \tag{3.4}$$

and a little bit later, we shall explain the reasons. In momentum space

$$\langle \mathbf{f}|V|\mathbf{p}\rangle \;=\; \frac{-4\pi\alpha Z}{\kappa^2 + \lambda^2}, \tag{3.5}$$

where

$$\boldsymbol{\kappa} \;=\; \mathbf{f} - \mathbf{p}. \tag{3.6}$$

Employing (3.2), we can write

$$\psi_{\mathbf{p}}^{(1)}(\mathbf{f}) = \frac{4\pi\alpha Z}{\kappa^2 + \lambda^2} \cdot \frac{2m}{2\mathbf{p}\cdot\boldsymbol{\kappa} + \kappa^2 - i\delta}, \tag{3.7}$$

with $\boldsymbol{\kappa}$ defined by (3.6).

In the relativistic case

$$\psi_{\mathbf{p}}^{(1)}(\mathbf{f}) = \frac{4\pi\alpha Z}{\kappa^2 + \lambda^2} \cdot \frac{(\hat{p} + \hat{\kappa}' + m)\gamma_0 u(p)}{2\mathbf{p}\cdot\boldsymbol{\kappa} + \kappa^2 - i\delta} \tag{3.8}$$

with $\kappa' = (0, \boldsymbol{\kappa})$. Using the commutation relations expressed by (2.14) and equations of motion (2.20), we obtain

$$\psi_{\mathbf{p}}^{(1)}(\mathbf{f}) = \frac{4\pi\alpha Z}{\kappa^2 + \lambda^2} \cdot \frac{2E}{2\mathbf{p}\cdot\boldsymbol{\kappa} + \kappa^2 - i\delta} u(p) + \psi', \quad \psi' = \frac{4\pi\alpha Z}{\kappa^2 + \lambda^2} \cdot \frac{\boldsymbol{\kappa}\cdot\boldsymbol{\alpha} u(p)}{2\mathbf{p}\cdot\boldsymbol{\kappa} + \kappa^2 - i\delta}. \tag{3.9}$$

The first term in this expression for $\psi_{\mathbf{p}}^{(1)}(\mathbf{f})$ is similar to the nonrelativistic expression (3.7) with the electron mass m replaced by its energy E. The second term requires additional evaluation.

3.1.2 *Wave Function of the Continuum State Electron at the Origin*

For the nonrelativistic electron with asymptotic momentum $\mathbf{p}$, the wave function at the origin is

$$\psi_{\mathbf{p}}(\mathbf{r}=0) = N(p) = \int \frac{d^3 f}{(2\pi)^3} \tilde{\psi}_{\mathbf{p}}(\mathbf{f}). \tag{3.10}$$

One can obtain the function $N(p)$ for the nonrelativistic case by iterating the LSE (2.61). In the lowest approximation, the function $\tilde{\psi}_{\mathbf{p}}(\mathbf{f})$ is just the plane wave given by (2.10), and (3.10) provides $N^{(0)}(p) = 1$. Using (3.7), one can write the lowest-order correction caused by the field $V(r)$ determined by (3.4):

$$N^{(1)}(p) = \int \frac{d^3\kappa}{(2\pi)^3} \cdot \frac{4\pi\alpha Z}{\kappa^2+\lambda^2} \cdot \frac{2m}{2\mathbf{p}\cdot\boldsymbol{\kappa}+\kappa^2-i\delta}. \tag{3.11}$$

Carrying out the angular integration, we obtain

$$N^{(1)}(p) = \int \frac{\kappa^2 d\kappa}{(2\pi)^2} \cdot \frac{4\pi\alpha Z}{\kappa^2+\lambda^2} \cdot \frac{m}{p\kappa} \cdot \ln\frac{\kappa+2p-i\delta}{\kappa-2p-i\delta}. \tag{3.12}$$

One can see that the integral on the right-hand side of this equation has both real and imaginary parts. The former comes from all values of κ. The imaginary part is provided by $\kappa < 2p$, for which the argument of the logarithm runs negative. In the calculation of the real part, we can safely put $\lambda^2 = \delta = 0$:

$$N^{(1)}(p) = \frac{\xi}{\pi}\int_0^\infty \frac{d\kappa}{\kappa} \cdot \ln\frac{\kappa+2p}{|\kappa-2p|} = \frac{\xi}{\pi}\int_0^\infty \frac{dx}{x} \ln\frac{x+1}{|x-1|}.$$

The contribution $N^{(1)}$ is thus determined by momenta $\kappa \sim p$ transferred to the nucleus. The ratio

$$\xi = \frac{m\alpha Z}{p} \tag{3.13}$$

is the parameter of interaction between the electron with asymptotic momentum p and the nucleus. It is often referred to as the Sommerfeld parameter. One can see that

$$\xi^2 = \frac{I_Z}{\varepsilon}, \tag{3.14}$$

with I_Z the binding energy of $1s$ electron in the Coulomb field; see (2.2).

Employing

$$\int_0^\infty \frac{dx}{x} \ln \frac{x+1}{|x-1|} \;=\; \pi^2/2,$$

we obtain

$$\mathrm{Re}N^{(1)}(p) \;=\; \pi\xi/2. \tag{3.15}$$

Thus the validity of the perturbative expansion for the function $N(p)$ requires much larger energies than those determined by (2.72) and (2.73). The higher-order terms $N^{(n)}$ can be calculated by further iteration of the LSE [2].

In the relativistic case, one can calculate the lowest-order term Re $N^{(1)}(p)$ using (3.9) and (3.10). Evaluation of the first term leads to replacement of the electron mass m in the nonrelativistic expression by the energy E. Evaluation of the second term provides

$$\mathrm{Re}\int \frac{d^3\kappa}{(2\pi)^3}\cdot\frac{\boldsymbol{\kappa}}{\kappa^2+\lambda^2}\cdot\frac{1}{2\mathbf{p}\cdot\boldsymbol{\kappa}+\kappa^2} = c\mathbf{p}; \quad c=\frac{1}{p^2}\int \frac{d^3\kappa}{(2\pi)^3}\cdot\frac{1}{\kappa^2+\lambda^2}\cdot\frac{\boldsymbol{\kappa}\cdot\mathbf{p}}{2\mathbf{p}\cdot\boldsymbol{\kappa}+\kappa^2}. \tag{3.16}$$

Direct calculation provides $c = 0$. Thus in the relativistic case, (3.15) with the relativistic value

$$\xi \;=\; \frac{\alpha Z E}{p} \tag{3.17}$$

is true. Of course, (3.13) is the nonrelativistic limit of (3.17). One can write a general expression for the Sommerfeld parameter that is true for both the nonrelativistic and relativistic cases:

$$\xi \;=\; \frac{\alpha Z}{v}, \tag{3.18}$$

with $v = p/E$.

Note, however, that an attempt to calculate the second-order contribution $N^{(2)}$ for the relativistic case would fail. The corresponding integral diverges on the upper limit. This corresponds to the well-known fact that at $(\alpha Z)^2 \ll 1$, the relativistic Coulomb function behaves as $r^{-(\alpha Z)^2/2}$ for $r \to 0$ [3, 4]. Thus it is not finite in this limit.

The solution of the wave equation can be obtained up to a certain constant factor. In nonrelativistic quantum mechanics this can be the wave function at the origin. One can determine the modulus of this factor by the normalization condition. There is still uncertainty regarding the phase factor. For the nonrelativistic continuum wave function in the Coulomb field, (3.10) [1], we have

$$|N(p)|^2 \;=\; \frac{2\pi\xi}{1-e^{-2\pi\xi}}. \tag{3.19}$$

Thus

$$N(p) \;=\; \Big(\frac{2\pi\xi}{1-e^{-2\pi\xi}}\Big)^{1/2}\Phi, \tag{3.20}$$

where $|\Phi|^2 = 1$, and hence

$$\Phi \;=\; e^{i\phi}\,. \tag{3.21}$$

The value of ϕ may differ in different approaches.

We find from (3.12) that

$$\mathrm{Im}N^{(1)}(p) = \xi\int d\kappa\cdot\frac{\kappa}{\kappa^2+\lambda^2}\cdot\theta(2p-\kappa) = \xi\ln 2p/\lambda, \tag{3.22}$$

which becomes infinite if $\lambda = 0$. This is the infrared singularity, coming from small $\kappa \to 0$. It was postulated by Dalitz [5] that the infrared divergent contributions that appear in each term of the Born series can be summed into a phase factor. The hypothesis was proved by Gorshkov [6], who demonstrated that in the approach based on the LSE, the terms containing λ form the factor Φ, (3.21) with

$$\phi \;=\; \xi\ln(2p/\lambda)\,. \tag{3.23}$$

In the standard formalism of nonrelativistic quantum mechanics one can employ (3.3). The terms with $f^2 = p^2$, which provide the contributions containing $\ln\lambda$, are not included in the sum on the RHS. Thus we obtain $\phi = 0$ and $\Phi = 1$. Note that each term of the partial wave expansion of the nonrelativistic Coulomb function contains the finite phase $\delta_\ell = \arg(\Gamma(\ell+1+i\xi))$.

While the infrared divergent factors cancel for the processes in the Coulomb field, a special analysis is needed for superposition of the Coulomb field V_C and a short-range field V_H. Consider the elastic scattering in the field $V = V_C + V_H$. In the framework of partial wave analysis, one can separate the purely Coulomb term F_C in the amplitude F:

$$F \;=\; F_C + F_H\,. \tag{3.24}$$

The amplitude F_H becomes zero if $V_H = 0$. It can be viewed as the amplitude of the scattering in the field V_H, which includes the Coulomb effects as well; see, e.g., [7].

In an important special case the field V_H can be used for approximation of the strong interactions. In this case the problem becomes important for studies of the $SU(2)$ breaking effects in strong interactions.

3.1.3 *Inelastic Electron Scattering by Atoms*

We consider here the electron colliding with atom, producing the ion in the final state. The electron momentum before the collision is $\mathbf{p_1}$, while after the collision it is $\mathbf{p_1'}$. The momentum of the ejected electron is $\mathbf{p_2}$. We are considering high-energycollisions

with electron momenta greatly exceeding the binding electron momentum μ_b, i.e., $p_1, p_1', p_2 \gg \mu_b$. This enables us to calculate the amplitude in the Born approximation, including only the lowest-order interaction between the incident electron and the atom. The interaction with the nucleus does not lead to ionization, while the interaction with an atomic electron can push the latter into the continuum. We assume also that the ejected electron moves much slower than the projectile electron, i.e., $p_2 \ll p_1, p_1'$. Thus we can neglect the exchange contributions and the Coulomb corrections to the wave function of the projectile electrons. We investigate the effect on the amplitude of the Coulomb corrections to the wave functions of the ejected electrons.

To simplify the calculations we consider the nonrelativistic case with $p \ll m$. Momentum $\mathbf{q} = \mathbf{p_1} - \mathbf{p_1'}$ is transferred to the target atom. The ejected electron obtains momentum $\mathbf{p_2}$, while momentum $\mathbf{Q} = \mathbf{q} - \mathbf{p_2}$ is transferred to the nucleus. It is convenient to consider the scattering amplitude F as a function of the momenta $\mathbf{q}$ and $\mathbf{Q}$. It can be written as

$$F = \frac{4\pi\alpha}{q^2} X(\mathbf{Q}, \mathbf{q}); \quad X(\mathbf{Q}, \mathbf{q}) = \int \frac{d^3 f}{(2\pi)^3} \psi^*_{\mathbf{p_2}}(\mathbf{f}) \psi_b(\mathbf{f} - \mathbf{q}). \tag{3.25}$$

The process is illustrated by the Feynman diagram of Fig. 3.1.

We shall compare the amplitude $F^{(0)}$, in which the ejected electron is described by the plane wave and the amplitude $F^{(0)} + F^{(1)}$, where the lowest-order correction,

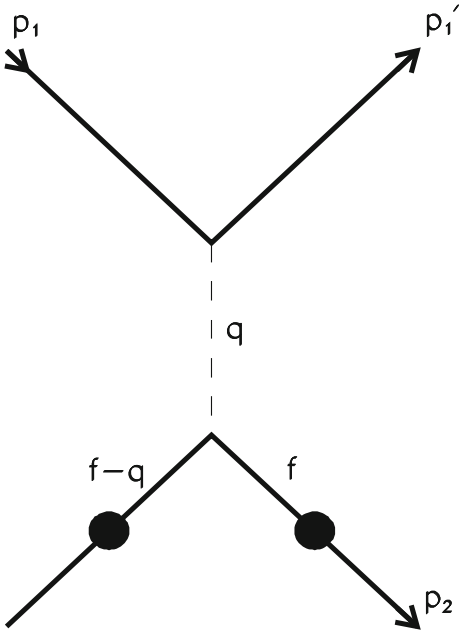

Fig. 3.1 The Feynman diagram illustrating (3.25). *Solid lines* denote the electrons. The *dark blob* stands for the atomic field. The *dashed line* is for the electron interaction (the virtual photon)

expressed by (3.2), is included. If the ejected electron is described by the plane wave, we obtain, employing (2.10),

$$F^{(0)}(\mathbf{Q}) = \frac{4\pi\alpha}{q^2}\psi_b(-\mathbf{Q}). \tag{3.26}$$

If the lowest-order correction to the wave function of the ejected electron is included, we obtain, using (3.7),

$$F^{(1)}(\mathbf{Q}) = \frac{4\pi\alpha}{q^2}\int \frac{d^3\kappa}{(2\pi)^3}\frac{-4\pi\alpha Z\psi_b(\boldsymbol{\kappa})}{(\mathbf{Q}+\boldsymbol{\kappa})^2+\lambda^2}\cdot\frac{2m}{p_2^2-(\mathbf{q}+\boldsymbol{\kappa})^2+i\delta}. \tag{3.27}$$

Recall that $\boldsymbol{\kappa} = \mathbf{f} - \mathbf{q}$.

The amplitude of the process obtains its largest values in the vicinity of region of free kinematics, which is determined by the condition

$$\mathbf{Q} = \mathbf{0}; \quad \mathbf{q} = \mathbf{p_2}. \tag{3.28}$$

In the first step we consider the amplitude exactly at $\mathbf{Q} = \mathbf{0}$. We assume also that the bound electron is in the s state. We shall compare the amplitude $F^{(0)}$, in which the ejected electron is described by the plane wave, and the amplitude $F^{(0)} + F^{(1)}$, where the lowest-order correction is included. For $\mathbf{Q} = \mathbf{0}$, (3.26) and (3.27) take the form

$$F^{(0)} = \frac{4\pi\alpha}{q^2}\tilde{\psi}_b(0); \quad F^{(1)} = \frac{4\pi\alpha}{q^2}\int\frac{d^3\boldsymbol{\kappa}}{(2\pi)^3}\frac{4\pi\alpha Z\psi_b(\boldsymbol{\kappa})}{\kappa^2+\lambda^2}\frac{2m}{2\mathbf{p}_2\cdot\boldsymbol{\kappa}+\kappa^2-i\delta}. \tag{3.29}$$

Now we evaluate the expression for $F^{(1)}$. Since the bound electron is in the s state, the function ψ_b does not depend on the direction of momentum κ. The angular integration can be carried out, providing

$$F^{(1)} = \frac{4\pi\alpha}{q^2}\xi\int\frac{d\kappa\kappa}{(2\pi)^2}\frac{4\pi\psi_b(\kappa)}{\kappa^2+\lambda^2}\ln\frac{2p_2+\kappa}{-2p_2+\kappa-i\delta}. \tag{3.30}$$

Here $\xi = \eta/p_2$ is the Sommerfeld parameter of the electron ejected from the atom.

One can see that the amplitude $F^{(1)}$ has imaginary part

$$\mathrm{Im}F^{(1)} = \pi\frac{4\pi\alpha}{q^2}\xi\int\frac{d\kappa\kappa}{(2\pi)^2}\frac{4\pi\psi_b(\kappa)}{\kappa^2+\lambda^2}\theta(2p_2-\kappa). \tag{3.31}$$

Its physical meaning becomes clear if we write (3.31) in the form

$$Im F^{(1)} = -\pi \int \frac{d^3\boldsymbol{\kappa}}{(2\pi)^3}\delta\left(\frac{p_2^2}{2m} - \frac{(\mathbf{p_2}+\boldsymbol{\kappa})^2}{2m}\right)F^{(0)}(\kappa)F_{eN}(\kappa), \tag{3.32}$$

with the lowest-order amplitude $F^{(0)}$ defined by (3.26), while $F_{eN} = -4\pi\alpha Z\theta$ $(2p_2-\kappa)/(\kappa^2+\lambda^2)$ is the amplitude of the elastic scattering of the electron on the nucleus. Thus (3.32) is a manifestation of the general statement that the imaginary part of the amplitude is due to an intermediate physical state [5, 6]. In our case, this is the electron with momentum $\mathbf{p_2}+\boldsymbol{\kappa}$ and energy $(\mathbf{p_2}+\boldsymbol{\kappa})^2/2m = p_2^2/2m$.

We turn now to the real part of the amplitude $F^{(1)}$. Consider the case $p_2 \gg \mu_b$. Since at $\kappa \sim p_2$, the wave function $\psi_b(\kappa)$ is $(\mu_b/p_2)^4$ times smaller than at $\kappa \sim \mu_b$, the integral over κ is saturated at the values $\kappa \sim \mu_b$. Putting $\ln|(2p_2+\kappa)/(2p_2-\kappa)| = \kappa/p_2$, we obtain

$$\mathrm{Re}F^{(1)} = F^{(0)}\cdot\xi\cdot\frac{1}{\pi}\int\frac{d\kappa}{p_2}\frac{\tilde{\psi}_b(\kappa)}{\tilde{\psi}_b(0)}. \tag{3.33}$$

Thus we found that

$$\frac{\mathrm{Re}F^{(1)}}{F^{(0)}} \sim \xi\frac{\mu_b}{p_2} \sim \xi^2. \tag{3.34}$$

In the special case when the bound electron is described by the Coulomb function, we have $\tilde{\psi}_b(\kappa)/\tilde{\psi}_b(0) = (\kappa^2/\eta^2+1)^{-2}$, and thus $\mathrm{Re}F^{(1)}/F^{(0)} = \xi^2/4$.

The careful reader will recall (3.15) and ask, *Where are the terms linear in* ξ?

To answer this question, let us turn again to the case in which the bound electron is in the Coulomb field. In this case, the matrix element (3.25) can be calculated explicitly. In Chap. 5, we shall introduce an easy way to calculate the amplitudes in the Coulomb field. Now we just write down the formula for the matrix element $X(\mathbf{q},\mathbf{Q})$ on the RHS of (3.25), which is true for every value of transferred momentum Q. We denote

$$X(\mathbf{Q},\mathbf{q}) = N_b N(p_2) X_1(\mathbf{Q},\mathbf{q}), \tag{3.35}$$

where $N_b = (\eta/\pi)^{3/2}$ and $N(p_2)$ defined by (3.19) are the normalization factors of the wave functions, $\eta = m\alpha Z$, $p_2 = |\mathbf{q}-\mathbf{Q}|$. In (3.35)

$$X_1(\mathbf{Q},\mathbf{q}) = 4\pi\left(-\frac{\partial}{\partial\mu}\right)Y(\mu,\mathbf{Q},\mathbf{q}), \quad \mu=\eta \tag{3.36}$$

with

$$Y(\mu,\mathbf{Q},\mathbf{q}) = \frac{1}{Q^2+\mu^2}\left(\frac{Q^2+\mu^2}{q^2-(p_2+i\mu)^2}\right)^{i\xi}; \quad \xi = \frac{\eta}{p_2}. \tag{3.37}$$

At $Q = 0$ we obtain

$$Y(\mu, 0, p_2) = \frac{1}{\mu^2}\Big(\frac{\mu}{\mu - 2ip_2}\Big)^{i\xi} = \frac{\Lambda^{i\xi} e^{\xi \arctan(\mu/2p_2)}}{\mu^2} e^{-\pi\xi/2}; \quad \Lambda = \Big(\frac{\mu^2}{\mu^2 + 4p_2^2}\Big)^{1/2}. \tag{3.38}$$

Thus in expansion in powers of ξ, the linear terms coming from the normalization factor $N(p_2)$ are canceled by the terms caused by expansion of the last factor on the RHS of (3.38).

One can see that total cancellation takes place only in the vicinity of the peak of the Bethe ridge, i.e., at $Q = |q - p_2| \ll \eta$ (recall that at the Bethe ridge, $|q - p_2| \lesssim \eta$). The general (3.37) provides

$$Y(\mu, \mathbf{Q}, \mathbf{q}) = \frac{1}{a}\Big(\frac{a}{|b|}\Big)^{i\xi} e^{\xi \arg\, b} \tag{3.39}$$

with $a = Q^2 + \mu^2$, $b = q^2 - p_2^2 + \mu^2 - 2ip_2\mu$, $\arg\, b < 0$. Thus the last factor $e^{\xi \arg b}$ is approximately equal to $e^{-\pi\xi/2}$ for $|q - p_2| \ll \eta$.

3.1.4 Use and Misuse of Plane Waves

Even in the case $\xi^2 \ll 1$, people often hesitate to check the results obtained by employing numerical functions for continuum electrons by a comparison with those obtained using plane waves. However, if they do this, the results sometimes appear to be quite different. Here we try to explain why this happens.

We have seen that the normalization factor $N(p)$ contains expansion in powers of $\pi\xi/2$, resulting in terms of the order $\pi\xi$ in the differential and total cross sections. Thus, the corrections to the plane wave calculations are linear in ξ with a rather large numerical coefficient.

Now we trace what happens to these corrections in the case of inelastic electron scattering by atoms, considered at the end of the previous subsection. It is instructive to consider the case of the hydrogenlike ion in the ground state. We begin with the case $\mathbf{Q} = 0$, considered above. As we have seen from (3.38), the terms of order $\pi\xi$ originated by $N(p)$ are totally canceled by similar terms of the expansion of the function $Y(\mu, 0, p_2)$. The plane wave approximation works with error ξ^2. Now let us increase the value of Q, remaining at the Bethe ridge $Q \sim \eta \ll p_2$. One can see from (3.39) that the compensation is not complete, becoming weaker as we increase the minimal value of $|\mathbf{Q}|_{\min} = |q - p_2|$. Thus at the Bethe ridge, the plane wave approximation works, but its accuracy becomes increasingly worse while we increase the value of Q from zero to the borders of the Bethe ridge $Q \lesssim \eta$.

The situation changes if we consider the case of large transferred momenta $Q \sim p_2$. In the amplitude $F^{(0)}$, where the ejected electron is described by the plane wave, a large momentum $Q \gg \eta$ is transferred to the nucleus by the bound electron. Thus the mechanism involves the bound-state wave function $\psi_b(Q \gg \mu_b)$, which is much smaller than that at $Q \sim \mu_b$; see (2.86). This quenching can be avoided if we include the Coulomb correction to the wave function of the ejected electron. Of course, we immediately obtain a small factor ξ. However, the continuum electron now transfers a large momentum, and the bound-state wave function ψ_b at $f \sim \mu_b$ is involved. Now we analyze the interplay of the two mechanisms.

Employing (2.86) and (3.26), we write

$$F^{(0)} = \frac{4\pi\alpha\psi_b(r=0)}{q^2} \cdot \frac{8\pi\eta}{Q^2} \cdot \frac{1}{(\mathbf{q}-\mathbf{p_2})^2}. \tag{3.40}$$

Using (3.27) and keeping κ only in the argument of the bound state wave function ψ_b, we obtain

$$F^{(1)} = \frac{4\pi\alpha\psi_b(r=0)}{q^2} \cdot \frac{8\pi\eta}{Q^2} \cdot \frac{1}{q^2-p_2^2} \tag{3.41}$$

for the lowest-order Coulomb correction. Only the last factors on the right-hand sides of these equations are different. Recall that $\mathbf{Q} = \mathbf{q} - \mathbf{p_2}$.

Thus the ratio of the amplitudes $F^{(0)}$ and $F^{(1)}$ depends on the actual values of the momenta $\mathbf{q}$ and $\mathbf{p_2}$. If $q \sim p_2 \sim |\mathbf{q} - \mathbf{p_2}|$, the two amplitudes are of the same order.

It is well known that the distributions $d\sigma/dq$ obtain the largest value at the lower limit $q_{\min}$ of the values of q, which determine also the value of the total cross section in the logarithmic approximation [1]. Since $\mathbf{q} = \mathbf{p_1} - \mathbf{p_1'}$, its lowest possible value is $q_{\min} = p_1 - p_1'$. We are considering the case in which the projectile electron transfers to the atom only a small part of its energy. Thus $p_1 - p_1' \ll p_1, p_1'$, and $q_{\min} = p_2^2/2p_1$, i.e.,

$$q_{\min} \ll p_2\,.$$

One can see that for $q \ll p_2$, the amplitudes $F^{(0)}$ and $F^{(1)}$ determined by (3.40) and (3.41) cancel up to the terms of relative order $q/p_2 \ll 1$. Thus in this case the plane wave calculation provides the qualitatively wrong result, strongly overestimating the magnitude of the amplitude. Note, however, that in the higher-order terms, a small momentum $f \sim \eta$ is transferred to the nucleus. These terms provide corrections to the higher-order terms in ξ. Thus the amplitude $F^{(0)} + F^{(1)}$ is the lowest term of the series expansion in ξ.

To summarize the analysis of Sect. 3.1.4, the plane wave calculation can be used for estimation of the amplitude at the Bethe ridge. However, one should analyze the magnitude of the higher Coulomb corrections. If larger momentum $Q \gg \mu_b$ is transferred to the nucleus, the amplitudes $F^{(0)}$ and $F^{(1)}$ may be of the same order of magnitude. In the most important kinematic region $q \sim q_{\min}$, the two amplitudes cancel each other to a large extent. The perturbative approach is possible, but the sum $F^{(0)} + F^{(1)}$ should be the zero-order approximation.

3.2 Final State Interactions Between Electrons

3.2.1 General Analysis

In previous section we saw how to include the interaction of the fast electron and the atomic nucleus. Now we will take into account its interaction with the atomic shell. Transition of the electronic shell to a particular final state is called an exclusive process. The sum of the exclusive cross sections is known as the inclusive cross section. It is important in the cases in which one wants a detailed description of the fast outgoing electron rather than the transitions of the atomic shell.

The interactions of the fast outgoing electron with the electrons of the atomic shell are determined by their Sommerfeld parameter $\xi_{ee} = \alpha/v$ with $v = |\mathbf{v_p} - \mathbf{v_i}|$, while v_p and v_i ($v_i \ll 1$) are the velocities of the fast and atomic electrons with respect to the nucleus. Since we are considering $v_p \gg v_i$, we can just put $v = v_p$ and

$$\xi_{ee} \;=\; \frac{\alpha}{v} = \frac{m\alpha}{p}. \tag{3.42}$$

We present the results in terms of the many-electron functions of the initial and final states of the atomic shell $|\Psi_i\rangle$ and $|\Phi_n\rangle$. We assume that the initial state is the ground state described by the function $|\Psi_0\rangle$. Similar equations can be obtained for the case in which the initial state is an excited one. In some cases, we find it instructive to present the equations also in terms of single-particle functions.

Transitions from the initial atomic state $|\Psi_i\rangle$ to a state of the daughter ion $|\Phi_n\rangle$ can take place even if the final-state interactions (FSI) between the fast electron and the electronic shell are neglected. Inclusion of the FSI leads to additional terms of order ξ_{ee}^2 in the cross sections. However, we shall see that in many cases, they appear to be important. We shall consider the case in which the energies transferred to the atom by the fast electron are of the order of the atomic single-particle binding energy of the daughter ion ε_b,

$$\omega_{n0} \;\equiv\; \varepsilon_n - \varepsilon_0 \;\sim\; |\varepsilon_b| \ll \varepsilon_p\,. \tag{3.43}$$

This means that we consider the final states Φ_n with $\varepsilon_n \ll \varepsilon_p$. The case of larger energies, when the amplitudes obtain additional small factors, will be analyzed in the next chapter.

There are many processes in which a fast electron can be ejected. For example, ejection of a fast electron can be caused by interaction with a charged projectile or with the photon. It can also be due to internal processes in the nucleus, which can be internal conversion during nuclear γ decay or nuclear β^- decay in which a neutron bound in the nucleus decays into a bound proton, emitting an electron and an electron antineutrino. Due to the interplay of nuclear forces, the bound proton can become heavier than the bound neutron in some nuclei. In these cases β^+ decay takes place. The bound proton can decay into a neutron, positron, and electron neutrino. In

this chapter, we study the processes in the atomic shell accompanying these "main processes."

We shall see that the amplitude of a process which includes the final state interaction between the fast electron and the electronic shell up to the terms of order ξ_{ee}^2 can be written as

$$F = F^{(0)} + F^{(1)} + F^{(2)}, \tag{3.44}$$

where the upper index $s = 0, 1, 2$ denotes the number of interactions between the fast electron and the atomic shell. In the zero order terms ($s = 0$), the FSI are neglected. In this subsection we consider the case of nonrelativistic fast electrons. We shall see that in this limit, the terms on the RHS of (3.44) contain the amplitude of the main process $\mathscr{F}$ as a factor, i.e., they can be written as (we omit the index of the initial state)

$$F_n^{(s)}(\varepsilon_p) = \mathscr{F}(\varepsilon_p) T_n^{(s)}, \tag{3.45}$$

while the amplitudes $T_n^{(s)}$ do not depend on the nature of the main process. Note that for $s = 0$, the amplitudes $F_n^{(s)}$ and $\mathscr{F}$ indeed depend on the energy of the fast outgoing electron ε_p. In the case of $s = 1, 2$, the amplitude of the main process $\mathscr{F}$ is rather a function of the energy $\varepsilon' = \varepsilon_p + \omega_{n0}$, which is shared between the fast outgoing electron and the atomic shell in the next steps. However, since $\omega_{n0}/\varepsilon_p \sim |\varepsilon_n/\varepsilon_p| \leq \xi^2 \ll 1$, while the terms with $s = 1, 2$ provide the terms of order ξ_{ee}^2, we can assume (3.45) for these terms as well.

In the relativistic case, when the spin variables are involved, the situation becomes more complicated. Some general features of the relativistic case will be discussed at the end of this chapter.

3.2.2 Zero Order Terms

We find it instructive to begin with the case of beta decay, since in this process, the charge of the nucleus changes, and the atomic shell can undergo transitions even if the FSI of the beta electron is not taken into account. If the bound electrons remain in the same state, the amplitude of the process can be written as

$$T_0^{(0)} = \langle \Phi_0 | \Psi_0 \rangle . \tag{3.46}$$

The vectors of states $|\Psi_0\rangle$ and $|\Phi_0\rangle$ describe the ground states of the Hamiltonians of the initial atom H_1 and of the daughter ion H_2 respectively,

$$H_1 = \sum_i H_{0i} + \sum_i U_{iN}(Z) + \sum_{i,j} U_{i,j}; \quad H_2 = \sum_i H_{0i} + \sum_i U_{iN}(Z+1) + \sum_{i,j} U_{i,j}, \tag{3.47}$$

with H_{0i} the free Hamiltonian (operator of the single-particle kinetic energy), $U_{iN}(Z) = -\alpha Z/r_i$ describes the interaction of the i bound electron with the nucleus with the charge Z, and $U_{i,j}$ describes the interaction between electrons i and j.

Thus for the excited states $|\Phi_n\rangle$ of the Hamiltonian H_2, the matrix elements

$$T_n^{(0)} \;=\; \langle \Phi_n | \Psi_0 \rangle \tag{3.48}$$

can obtain nonvanishing values. This requires, however, that the angular moments of the two states be the same, i.e.,

$$L_n \;=\; L_0\,. \tag{3.49}$$

This mechanism was first described in [8]. It was developed further in [9, 10]. We can write

$$F_n^{(0)}(\varepsilon_p) \;=\; \mathscr{F}(\varepsilon_p) T_n^{(0)}; \tag{3.50}$$

see Fig. 3.2a. Note that the amplitude $T_n^{(0)}$ does not contain physical intermediate states. Thus it is real.

One can see that the difference between H_1 and H_2 vanishes at large $Z \to \infty$. Thus for every exclusive inelastic process, we have

$$T_n^{(0)} \;\sim\; 1/Z \tag{3.51}$$

for large Z. We shall see in Chap. 12 that $|T_n^{(0)}| \ll 1$ for $n \neq 0$ even for the β decay of tritium with $Z = 1$. Thus we can assume that only one of the electrons undergoes inelastic transitions. Following [8], we use the term "shakeoff" for the process in which a bound electron is moved to the continuum. The process in which a bound electron moves to an upper state of the discrete spectrum is called "shakeup."

In this subsection, we shall use (3.48) for $T_n^{(0)}$. However, we shall make some comments on the possible evaluation of this expression. If only one ("active") electron changes its state, it looks reasonable to analyze the approximation in which it is described by a single-particle function. In this approach,

$$T_n^{(0)} \;=\; \langle \phi_f | \psi_i \rangle \langle \Phi_S | \Psi_S \rangle. \tag{3.52}$$

Here ψ_i and ϕ_f describe the active electron in the initial ground state $|\Psi_0\rangle$ and in the final state $|\Phi_n\rangle$. The wave vector Ψ_S describes the ground state of the rest $Z-1$ "spectator" electrons in the field of the nucleus with charge Z and the electron in state i. The wave vector Φ_S describes the $Z-1$ "spectator" electrons with a hole in state i in the field of the nucleus with charge $Z+1$. The condition expressed by (3.49) is now $\ell_f = \ell_i$. The wave equations for the functions ψ_i and ϕ_f are

$$H_1 \psi_i = \varepsilon_i \psi_i; \quad H_2 \phi_f = \varepsilon_f \phi_f, \tag{3.53}$$

with

$$H_1 = H_0 + U_{1eN}(Z) + U_{1ee}; \quad H_2 = H_0 + U_{2eN}(Z+1) + U_{2ee}. \tag{3.54}$$

Here $U_{1eN} = -\alpha Z/r$ and $U_{2eN} = -\alpha(Z+1)/r$ describe interactions of the electron with the nucleus in initial and final state correspondingly, U_{1ee} and U_{2ee} describe interaction of the active electron with the atomic shell. Treating the difference $H_2 - H_1 = V$ as a small perturbation, we can write

$$T_n^{(0)} = \frac{\langle\psi_n|V|\psi_i\rangle}{\varepsilon_n - \varepsilon_i}\langle\Phi_S|\Psi_S\rangle\,, \tag{3.55}$$

with $\varepsilon_{i(n)}$ the eigenvalues of the wave equation (3.53) with the Hamiltonian H_1, while

$$V = V_{eN} + V_{ee}; \quad V_{eN} = U_{2eN} - U_{1eN} = -\frac{\alpha}{r}; \quad V_{ee} = U_{2ee} - U_{1ee}. \tag{3.56}$$

In the case of beta decay, the term V_{eN} caused by the change of the charge of the nucleus provides the main contribution to the perturbation V. The transitions in the atomic shell take place even if we neglect all interactions between the electrons. The single-particle description (3.52) is a good approximation. However, the fast electron can be emitted from the atom by an external projectile. For example, this can be photoionization or ionization by electron impact. In these cases, we have the perturbations $V_{eN} = 0$ and $V = V_{ee}$. The problem of calculation of the amplitude $T_n^{(0)}$ becomes more complicated, and the single-particle approximation may be not good. We shall see that it can lead to quantitatively incorrect or even to qualitatively incorrect results.

Now we calculate the probabilities of the transitions in the atomic shell including the lowest-order FSI correction. We shall need the contributions to the amplitude up to order ξ_{ee}^2 [11].

3.2.3 First Order Terms

Now we include a single interaction between the outgoing beta electron and the atomic shell. We must calculate the contribution of the Feynman diagram shown in Fig. 3.2b.

Note that in looking for the terms of order ξ_{ee}^2 in the amplitude, we can describe the fast electron in the amplitude $T_n^{(1)}$ by a plane wave. The amplitude of the main process $\mathscr{F}$ depends on the interaction between the fast electron and the nucleus in terms of the parameter ξ. The dependence contains the parameter $\pi\xi$ [12], which we do not assume to be small. The fast electron with momentum p interacts with the nucleus at the distances $r \sim 1/p$, while the interactions with the atomic shell take place at the distances $r \sim 1/\mu_b$. The interactions with the nucleus after interactions with the

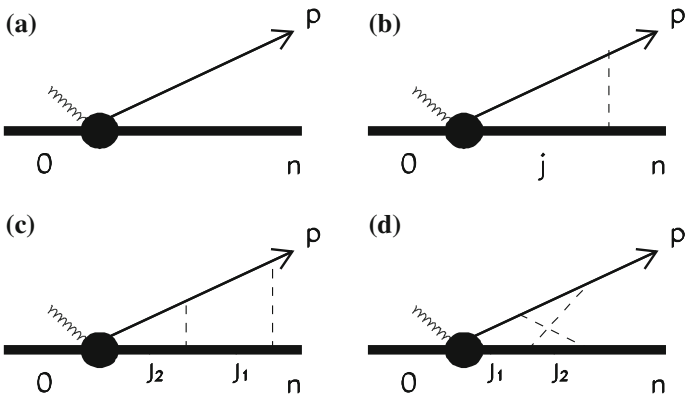

Fig. 3.2 The Feynman diagram for the amplitude that includes the final-state interactions (FSI) between the ejected electron and the electronic shell. In the case of β decay, the *wavy line* denotes an electronic antineutrino. The *solid line* with the *arrow* is for the ejected electron. The *bold line* is for the electronic shell. The *dashed lines* are for the electron interactions (the virtual photons). Here **a** corresponds to the amplitude $T_n^{(0)}$; **b** is for $T_n^{(1)}$; **c**, **d** are for $T_n^{(2)}$

atomic shell provide terms that contain an additional factor of order $\xi^2 \ll 1$, since momentum transferred to the nucleus cannot greatly exceed the binding momentum μ_b [11].

All the final-state electrons form the state $|\Phi_{n,\mathbf{p}}\rangle$, with $\mathbf{p}$ the momentum of the fast electron. If the FSI are neglected, $|\Phi_{n,\mathbf{p}}^{(0)}\rangle = |\Phi_n\rangle \cdot |\psi_{\mathbf{p}}^{(0)}\rangle$, with $|\psi_{\mathbf{p}}^{(0)}\rangle$ being the plane wave. The first-order term is determined by the LSE (see Chap. 2) with the two-particle Green function $G(\varepsilon_p + \varepsilon_n)$ (the electronic shell of the daughter ion can be treated as an entire system), which can be written as [13]

$$G(\varepsilon') = \int \frac{dq_0}{2\pi i} G_0(\varepsilon_p + q_0) g(\varepsilon_n - q_0); \quad \varepsilon' = \varepsilon_p + \varepsilon_n, \tag{3.57}$$

where G_0 is the propagator of the free electron; see (2.29). Here

$$g(\varepsilon_x) = \sum_j \frac{|\Phi_j\rangle\langle\Phi_j|}{\varepsilon_x - \varepsilon_j + i\delta} \tag{3.58}$$

is the propagator of the electronic shell. In (3.57), q_0 has the meaning of the energy transferred by the fast electron to the electronic shell of the daughter ion.

Now we can write

$$T_n^{(1)} = \langle\Phi_n| \sum_k A(\mathbf{r}^{(k)}) |\Psi_0\rangle, \tag{3.59}$$

where k labels the electrons in the atomic shell, while the integral over the loop is

$$A(\mathbf{r}^{(k)}) = \int \frac{d^3q dq_0}{(2\pi)^4 i} G_0(\varepsilon_p + q_0, \mathbf{p}+\mathbf{q}) V_{ee}(q) g(\varepsilon_n - q_0) e^{i\mathbf{q}\cdot\mathbf{r}^{(k)}}. \tag{3.60}$$

Note that (3.60) can be obtained by straightforwardly employing the rules for building Feynman diagrams [3, 4].

We write the electron interactions in a form similar to (3.4) and (3.5):

$$V(r) = \alpha \frac{e^{-\lambda r}}{r}; \quad V(q) = \frac{4\pi\alpha}{q^2+\lambda^2}; \quad \lambda \to 0. \tag{3.61}$$

Integration over the energy q_0 leads to

$$A(\mathbf{r}^{(k)}) \; = \; \sum_j B(\mathbf{r}^{(k)}) |\Phi_j\rangle\langle\Phi_j| \tag{3.62}$$

with

$$B(\mathbf{r}^{(k)}) = \int \frac{d^3q}{(2\pi)^3} \cdot \frac{2m}{p'^2 - (\mathbf{p}+\mathbf{q})^2 + i\delta} \cdot \frac{4\pi\alpha}{q^2+\lambda^2} e^{i\mathbf{q}\cdot\mathbf{r}^{(k)}}; \quad \delta \to 0, \tag{3.63}$$

where $p'^2 = p^2 + 2m\omega_{nj}$, ω_{nj} is defined by (3.43). Now

$$T_n^{(1)} \; = \; \sum_j \langle\Phi_n| \sum_k B(\mathbf{r}^{(k)}) |\Phi_j\rangle\langle\Phi_j|\Psi_0\rangle. \tag{3.64}$$

Using the formula [3, 4]

$$\frac{1}{a} \cdot \frac{1}{b} \; = \; \int_0^1 \frac{dx}{\Big(ax + b(1-x)\Big)^2} \tag{3.65}$$

and keeping only the term proportional to the large momentum p in the denominator of the electron propagator on the RHS of (3.63), i.e., putting

$$B(\mathbf{r}^{(k)}) = -\int \frac{d^3q}{(2\pi)^3} \cdot \frac{2m}{2(\mathbf{p}\cdot\mathbf{q}) - i\delta} \cdot \frac{4\pi\alpha}{q^2+\lambda^2} e^{i\mathbf{q}\cdot\mathbf{r}^{(k)}}, \tag{3.66}$$

we obtain

$$\frac{1}{2(\mathbf{p}\cdot\mathbf{q}) - i\delta} \cdot \frac{1}{q^2+\lambda^2} = \int_0^1 \frac{dx}{\Big(2(\mathbf{p}\cdot\mathbf{q})(1-x) + q^2 x + \lambda^2 x - i\delta\Big)^2}. \tag{3.67}$$

Introducing $y = (1-x)/x$, $\mathbf{q}' = \mathbf{q} + \mathbf{p}y$ and integrating over $\mathbf{q}'$ using the relation

$$\int \frac{d^3q}{(2\pi)^3} \cdot \frac{4\pi e^{i\mathbf{q}\cdot\mathbf{r}}}{(q^2 - b^2 - i\delta)^2} = \frac{1}{2b}\frac{\partial}{\partial b}\frac{e^{ibr}}{r} = i\frac{e^{ibr}}{2b}, \quad b^2 = p^2y^2 - \lambda^2 \tag{3.68}$$

we obtain

$$B(\mathbf{r}^{(k)}) = -i\alpha m \int_0^\infty \frac{dy}{b(y)} e^{ib(y)r^{(k)} - i\mathbf{p}\cdot\mathbf{r}^{(k)}y}. \tag{3.69}$$

The integral on the RHS of (3.69) can be calculated exactly:

$$B(\mathbf{r}^{(k)}) \;=\; i\xi_{ee}\Big(\ln\frac{(r^{(k)} - r_z^{(k)})\lambda}{2} + C_E\Big), \tag{3.70}$$

with z labeling the direction of the momentum p, while $C_E \approx 0.577$ is Euler's constant. The main contribution to the integral comes from $\lambda/p \ll y \ll 1$. Changing the definition of λ, we can write

$$B(\mathbf{r}^{(k)}) \;=\; i\xi_{ee}\ln(r^{(k)} - r_z^{(k)})\lambda. \tag{3.71}$$

Thus

$$T_n^{(1)} \;=\; i\xi_{ee}\sum_j \langle\Phi_n|\sum_k \ln(r^{(k)} - r_z^{(k)})\lambda|\Phi_j\rangle\langle\Phi_j|\Psi_0\rangle. \tag{3.72}$$

This equation is true for the states $|\Phi_j\rangle$ with energies of the order of the binding energy. These states saturate the closure condition $\sum_j |\Phi_j\rangle\langle\Phi_j| = 1$, since the contribution of the higher states is strongly quenched (see (2.86)). Hence, using closure, we obtain

$$T_n^{(1)} \;=\; i\xi_{ee}\langle\Phi_n|\sum_k \ln(r^{(k)} - r_z^{(k)})\lambda|\Psi_0\rangle. \tag{3.73}$$

Thus the first-order term $T_n^{(1)}$ appears to be mostly imaginary.

Recall that one should put $\lambda \to 0$ in (3.72) and (3.73). The meaning of the singularity at $\lambda = 0$ becomes clear if one writes $\ln(r^{(k)} - r_z^{(k)})\lambda = \ln(r^{(k)} - r_z^{(k)}) + \ln\lambda$ and turns to (3.72). The second term provides a nonzero value only for $j = n$. This corresponds to elastic scattering of the beta electron on the bound electrons in the state $|\Phi_n\rangle$. Hence this is just a part of the infrared divergent Coulomb phase discussed in Sect. 3.1.3. We expect the terms containing $\ln\lambda$ to cancel in the final expressions for the probability. We shall see that this indeed happens.

Thus the imaginary part $\mathrm{Im}\, T_n^{(1)}$ provides the contribution of the order ξ_{ee}^2 to the probability. Since the zero-order term $T_n^{(0)}$ is real, we must calculate also the real contributions of the order ξ_{ee}^2 to the amplitude $T_n^{(1)}$ and include their interference with $T_n^{(0)}$. The problem is simplified by the fact that $T_n^{(0)}$ obtains nonzero values only

if the angular momenta of the states $|\Psi_0\rangle$ and $\langle\Phi_n|$ are the same. Thus it is sufficient to include only the term with $\ell = 0$ in the partial wave expansion of the exponential term in the integrand on the RHS of (3.64):

$$e^{i\mathbf{q}\cdot\mathbf{r}^{(k)}} = \frac{\sin qr^{(k)}}{qr^{(k)}} + \cdots, \tag{3.74}$$

where the dots denote the terms with $\ell \neq 0$. The contribution can be obtained by calculation of the next-to-leading term of the expansion of the RHS of (3.69) in powers of $1/p$. However, we find it simpler and more instructive to return to (3.63) and to employ (3.74):

$$B(\mathbf{r}^{(k)}) = \int \frac{d^3q}{(2\pi)^3} \cdot \frac{2m}{p'^2 - (\mathbf{p}+\mathbf{q})^2 + i\delta} \cdot \frac{4\pi\alpha}{q^2+\lambda^2} \frac{\sin qr^{(k)}}{qr^{(k)}}. \tag{3.75}$$

The angular integration provides

$$\mathrm{Re}\, B(\mathbf{r}^{(k)}) = \frac{\xi_{ee}}{\pi} \int \frac{dq}{q} \cdot \frac{q^2}{q^2+\lambda^2} \cdot \frac{\sin qr^{(k)}}{qr^{(k)}} \ln \left|\frac{2pq + 2m\omega_{nj} - q^2}{2pq - 2m\omega_{nj} + q^2}\right|. \tag{3.76}$$

The leading term of the expansion of the logarithmic factor in powers of $1/p$ provides

$$\mathrm{Re}\, B(\mathbf{r}^{(k)}) = B_1 + B_2; \quad B_1 = -\frac{\xi_{ee}}{\pi} \int \frac{dq}{p} \frac{q^2}{q^2+\lambda^2} \frac{\sin qr^{(k)}}{qr^{(k)}}; \quad B_2 = \frac{2\xi_{ee}m}{\pi p} \omega_{nj} J_2, \tag{3.77}$$

with

$$J_2 = \int \frac{dq}{q^2+\lambda^2} \frac{\sin qr^{(k)}}{qr^{(k)}}. \tag{3.78}$$

The integrand of the integral that determines the contribution B_1 is finite at $\lambda = 0$. Thus, putting $\lambda = 0$, we can write

$$B_1 = -\frac{\xi_{ee}}{\pi} \int \frac{dq}{p} \frac{\sin qr^{(k)}}{qr^{(k)}}. \tag{3.79}$$

Employing

$$\int_0^\infty dx \sin x/x = \pi/2,$$

we immediately obtain $B_1 = -\xi_{ee}/2r^{(k)}p$, which can be written as

$$B_1 = -\frac{\xi_{ee}^2}{2} \cdot \frac{r_0}{r^{(k)}}, \tag{3.80}$$

where $r_0 = 1/m\alpha$ is the Bohr radius.

At first glance, the integral J_2 in expression for B_2 diverges at $\lambda = 0$, since the integrand behaves as $1/q^2$ at $q \to 0$. However, the divergence is spurious. The contribution of the region $q \ll 1/r^{(k)}$to B_2 does not depend on $r^{(k)}$, and thus does not contribute to the matrix element $\langle \Phi_n | B_2 | \Phi_j \rangle$. Separating the divergent part in J_2 (3.78),

$$J_2 = \int \frac{dq}{q^2} \left(\frac{\sin q r^{(k)}}{q r^{(k)}} - 1 \right) + \int \frac{dq}{q^2 + \lambda^2}, \tag{3.81}$$

where we put $\lambda^2 = 0$ in the first term on the RHS, we obtain

$$B_2 = \frac{-\xi_{ee} m}{2p} \omega_{nj} \left(r^{(k)} - \frac{2}{\lambda} \right), \tag{3.82}$$

where the second term in the parentheses does not contribute to the matrix element $T^{(1)}$ due to the orthogonality of the wave functions at $j \neq n$ or due to the factor ω_{nj} at $j = n$:

$$\langle \Phi_n | \omega_{nj} r^{(k)} | \Phi_j \rangle = \langle \Phi_n | [H r^{(k)}] | \Phi_j \rangle = -\langle \Phi_n | \frac{r_c}{r^{(k)}} + r_c \frac{\partial}{\partial r^{(k)}} | \Phi_j \rangle, \tag{3.83}$$

with $r_c = 1/m$ the Compton wave length of the electron. Thus

$$\mathrm{Re} T_n^{(1)} = \frac{\xi_{ee}^2}{2} \langle \Phi_n | \sum_k r_0 \frac{\partial}{\partial r^{(k)}} | \Psi_0 \rangle. \tag{3.84}$$

3.2.4 Second-Order Terms

The contribution $T_n^{(2)}$ is expressed by the sum of the diagrams shown in Fig. 3.2c, d. The fast electron exchanges momenta $\mathbf{q_1}$ and $\mathbf{q_2}$ and energies q_{10} and q_{20} with the atomic shell. We can write $T_n^{(2)} = \langle \Phi_n | \sum_{k_1,k_2} A(\mathbf{r}^{(k_1)}, \mathbf{r}^{(k_2)}) | \Psi_0 \rangle$, with $A(\mathbf{r}^{(k_1)}, \mathbf{r}^{(k_2)}) = A_c(\mathbf{r}^{(k_1)}, \mathbf{r}^{(k_2)}) + A_d(\mathbf{r}^{(k_1)}, \mathbf{r}^{(k_2)})$. The two terms correspond to the diagrams shown in Fig. 3.2c,

$$A_c(\mathbf{r}^{(k_1)}, \mathbf{r}^{(k_2)}) = \int d\Gamma_1 d\Gamma_2 f(1,2) e^{i(\mathbf{q}_1 \cdot \mathbf{r}^{(k_1)})} g(\varepsilon_n - q_{10}) e^{i\mathbf{q}_2 \cdot \mathbf{r}^{(k_2)}} g(\varepsilon_n - q_{10} - q_{20}), \tag{3.85}$$

and Fig. 3.2d,

$$A_d(\mathbf{r}^{(k_1)}, \mathbf{r}^{(k_2)}) = \int d\Gamma_1 d\Gamma_2 f(1,2) e^{i(\mathbf{q}_2 \cdot \mathbf{r}^{(k_1)})} g(\varepsilon_n - q_{20}) e^{i\mathbf{q}_1 \cdot \mathbf{r}^{(k_2)}} g(\varepsilon_n - q_{10} - q_{20}), \tag{3.86}$$

with

$$f(1,2) = G_0(\varepsilon_p + q_{10}, \mathbf{p} + \mathbf{q_1}) V_{ee}(q_1) G_0(\varepsilon_p + q_{10} + q_{20}, \mathbf{p} + \mathbf{q_1} + \mathbf{q_2}) V_{ee}(q_2),$$

and $d\Gamma_n = dq_{no} d^3 q_n / i(2\pi)^4$, while the propagators G_0 and g are given by (2.29) and (3.58).

In the nonrelativistic case, the contribution of Fig. 3.2d vanishes. In order to show this, consider q_{20} as a complex variable. Since the integrand decreases as $|q_{20}|^{-2}$ at $|q_{20}| \to \infty$, we can integrate over the closed contour consisting of the real axis and a semicircle with radius $r \to \infty$. The latter can be in the upper or lower half-plane. In both cases, the integral over the semicircle can be neglected. There is one pole in the lower half-plane, corresponding to the condition $G_0^{-1} = 0$. Its position is

$$q_{20}^p = -q_{10} + a - i\delta; \quad \delta \to +0. \tag{3.87}$$

Here a is a real value. Integrating over q_{20} in the lower half-plane, we express the result in terms of the residue at the point q_{20}^p defined by (3.87). Now in (3.86), the Green function $g(\varepsilon_n - q_{10} - q_{20}^p)$ does not depend on q_{10}, while the propagators $g(\varepsilon_n - q_{20}^p)$ and $G_0(\varepsilon_p + q_{10}, \mathbf{p} + \mathbf{q_1})$ have poles at q_{10} in the lower half-plane, and there are no poles in the upper half-plane. Now we integrate over q_{10} in the same way as we integrated over q_{20}, closing the contour in the upper half-plane. Since there are no singularities, we have $A_d = 0$.

Thus we must calculate the contribution of Fig. 3.2c. The integration over energies q_{10} and q_{20} can be carried out in the same way as in the calculation of $T^{(1)}$, providing

$$T_n^{(2)} = \sum_{k_1, k_2; j_1, j_2} \langle \Phi_n | B(\mathbf{r}^{(k_1)}) | \Phi_{j1} \rangle \langle \Phi_{j1} | C(\mathbf{r}^{(k_2)}) | \Phi_{j2} \rangle \langle \Phi_{j2} | \Psi_0 \rangle, \tag{3.88}$$

with $B(\mathbf{r}^{(k_1)})$ determined by (3.66) (with integration over $\mathbf{q}_1$), while

$$C(\mathbf{r}^{(k_2)}) = -\int \frac{d^3 q_2}{(2\pi)^3} \cdot \frac{2m}{2(\mathbf{p} \cdot (\mathbf{q}_1 + \mathbf{q}_2))} \cdot \frac{4\pi\alpha}{q_2^2 + \lambda^2} e^{i\mathbf{q}_2 \cdot \mathbf{r}^{(k_2)}}. \tag{3.89}$$

In the integral over $\mathbf{q_1}$ and $\mathbf{q_2}$, one can put

$$\frac{1}{\mathbf{pq}_1} \frac{1}{\mathbf{p}(\mathbf{q}_1 + \mathbf{q}_2)} = \frac{1}{2}\left(\frac{1}{\mathbf{pq}_1} + \frac{1}{\mathbf{pq}_2}\right) \frac{1}{\mathbf{p}(\mathbf{q}_1 + \mathbf{q}_2)} = \frac{1}{2} \frac{1}{\mathbf{pq}_1} \frac{1}{\mathbf{pq}_2}, \tag{3.90}$$

and thus we can write

$$C(\mathbf{r}^{(k_2)}) = \frac{1}{2} B(\mathbf{r}^{(k_2)}). \tag{3.91}$$

Proceeding in the same way as in the calculation of $\mathrm{Im}T_n^{(1)}$, we obtain

$$T_n^{(2)} = -\frac{\xi_{ee}^2}{2}\langle\Phi_n|\sum_{k_1}\ln\left((r^{(k_1)}-r_z^{(k_1)})\lambda\right)\sum_{k_2}\ln\left((r^{(k_2)}-r_z^{(k_2)})\lambda\right)|\Psi_0\rangle. \quad (3.92)$$

Thus the amplitude $T_n^{(2)}$ is mostly real, and its interference with the term $T_n^{(0)}$ contributes to the terms of order ξ_{ee}^2.

3.2.5 *Probabilities of the Exclusive Processes*

Now we can write an expression for any distribution $dW_n/d\Gamma$ of the main process accompanied by a transition of the atomic shell to the state $|\Phi_n\rangle$:

$$\frac{dW_n}{d\Gamma} = \frac{dW}{d\Gamma}S_n, \quad (3.93)$$

where $dW/d\Gamma$ is the distribution of the main process at the same energy ε_p, while

$$S_n = |T_n^{(0)}|^2 + 2T_n^{(0)}\mathrm{Re}T_n^{(1)} + |\mathrm{Im}T_n^{(1)}|^2 + 2T_n^{(0)}\mathrm{Re}T_n^{(2)}, \quad (3.94)$$

i.e.,

$$\begin{aligned} S_n = {} & |\langle\Phi_n|\Psi_0\rangle|^2 + \xi_{ee}^2\langle\Psi_0|\Phi_n\rangle\langle\Phi_n|\sum_k r_0\frac{\partial}{\partial r^{(k)}}|\Psi_0\rangle \\ & + \xi_{ee}^2|\sum_k\langle\Phi_n|\ln((r^{(k)}-r_z^{(k)})\lambda)|\Psi_0\rangle|^2 \\ & - \xi_{ee}^2\langle\Psi_0|\Phi_n\rangle\langle\Phi_n|\sum_{k,k_1}\ln((r^{(k)}-r_z^{(k)})\lambda)\ln((r^{(k_1)}-r_z^{(k_1)})\lambda)|\Psi_0\rangle, \end{aligned} \quad (3.95)$$

with the terms on the RHS corresponding to those on the RHS of (3.94). As expected, the terms that contain $\ln\lambda$ or $\ln^2\lambda$ cancel. Note that in some of their early papers, the authors tried to calculate the first-order term $T^{(1)}$, ignoring the second-order term $T^{(2)}$. They faced integrals that diverged at small momenta and had to introduce a regularization procedure. As we see, after inclusion of the second-order terms, the divergent terms cancel.

Sometimes, the authors of publications ask, "Which correction to the shakeoff is more important, its interference with the FSI or the FSI itself?" One can see that the question is meaningless. They are both infinite and cancel each other to a large extent.

The shakeoff term $T_n^{(0)}$ obtains a nonzero value only if the states $|\Phi_n\rangle$ satisfy the condition of (3.49). In this case, the angular integration in the matrix elements on the RHS of (3.94) can be carried out, and we obtain

$$S_n = |\langle \Phi_n|\Psi_0\rangle|^2 + \xi_{ee}^2 \langle \Psi_0|\Phi_n\rangle\langle \Phi_n| \sum_k r_0 \frac{\partial}{\partial r^{(k)}}|\Psi_0\rangle$$
$$+\xi_{ee}^2 |\sum_k \langle \Phi_n| \ln(r^{(k)}\lambda)|\Psi_0\rangle|^2$$
$$- \xi_{ee}^2 \langle \Psi_0|\Phi_n\rangle\langle \Phi_n| \sum_{k,k_1} \ln((r^{(k)}\lambda) \ln((r^{(k_1)}\lambda)|\Psi_0\rangle. \quad (3.96)$$

For the states $|\Phi_n\rangle$ with $L_n \neq L_0$, the FSI becomes the main mechanism of the process, providing

$$S_n = \xi_{ee}^2 |\langle \Phi_n| \sum_k \ln(1 - t^{(k)})|\Psi_0\rangle|^2; \quad t^{(k)} = \frac{r_z^{(k)}}{r^{(k)}}. \quad (3.97)$$

3.2.6 Probability of the Inclusive Process

Now we calculate the sum of the probabilities

$$\sum_n \frac{dW_n}{d\Gamma} = \frac{dW}{d\Gamma} \sum_n S_n. \quad (3.98)$$

One can see that for the shakeoff terms,

$$\sum_n |T_n^{(0)}|^2 = 1. \quad (3.99)$$

Turning to the contribution of the FSI, one can observe that the sums over the states $|\Phi_n\rangle$ of the two last terms on the RHS of (3.94) cancel. In other words,

$$\sum_n |\mathrm{Im}\, T_n^{(1)}|^2 + 2 \sum_n \mathrm{Re}\, T_n^{(0)} T_n^{(2)} = 0. \quad (3.100)$$

Thus we obtain

$$\sum_n S_n = 1 + 2 \sum_n \mathrm{Re}\, T_n^{(0)} T_n^{(1)} = 1 + \xi_{ee}^2 \langle \Psi_0| \sum_k r_0 \frac{\partial}{\partial r^{(k)}}|\Psi_0\rangle. \quad (3.101)$$

Employing integration by parts, we obtain

$$\sum_n S_n = 1 - \xi_{ee}^2 \langle \Psi_0| \sum_k \frac{r_0}{r^{(k)}}|\Psi_0\rangle. \quad (3.102)$$

3.2.7 The Relativistic Case

Now we assume that the kinetic energy of the outgoing electron is of the order of its mass. The amplitudes (3.45) contain the bispinor $\bar{u}$ of the outgoing electron. Thus the amplitudes take the form

$$\mathscr{F} = \bar{u}(p)w; \quad F_n^{(s)} = \bar{u}(p)T_n^{(s)}w, \quad s = 0, 1, 2, \tag{3.103}$$

where w is a certain bispinor. The amplitude $T_n^{(0)}$ is the same as in the nonrelativistic case. The amplitude $T_n^{(1)}$ is expressed by (3.64). However, the function $B(\mathbf{r}^{(\mathbf{k})})$ should be modified. The factor $2m$ on the RHS of (3.63) must be replaced by

$$\bar{u}\gamma_0(\hat{p} + \hat{q} + m) \;=\; \bar{u}(2E - \boldsymbol{\alpha}\cdot\mathbf{q}). \tag{3.104}$$

Here we employed the commutation relation (2.14) and the equation of motion (2.21). We neglected the contribution proportional to the transferred energy $q_0 \sim \mu_b^2/2m \ll \mu_b$, since $|\mathbf{q}| \sim \mu_b$, and thus $q_0 \ll |\mathbf{q}|$.

Note that in the calculations of $\operatorname{Im} T_n^{(1)}$, we employed only the lowest-order terms in the expansion in powers of q. Hence, only the first term on the RHS of (3.104) contributes. The same refers to the calculation of $\operatorname{Re} T_n^{(2)}$. Thus (3.73) for $\operatorname{Im} T_n^{(1)}$ and (3.92) for $\operatorname{Re} T_n^{(2)}$ with ξ_{ee} defined by (3.42), i.e.,

$$\xi_{ee} \;=\; \frac{\alpha E}{p} \;=\; \frac{\alpha}{v}, \tag{3.105}$$

hold in the relativistic case. Also, (3.97) for the probability of exclusive processes with $L_n \neq L_i$ is true. In the inclusive process, the cancellation expressed by (3.100) is true.

However, the situation with $\operatorname{Re} T_n^{(1)}$ is different, since here we need the next-to-leading terms of the expansion in powers of q. We can write

$$\operatorname{Re} T_n^{(1)} \;=\; X_n^a + X_n^b,$$

with the two terms corresponding to the two terms on the RHS of (3.104). One can write $X_n^a = B_1 + B_2$ with B_i defined by (3.77), while ξ_{ee} is given by (3.105). The term B_1 can be represented in the form given by (3.79), providing

$$B_1 \;=\; -\frac{\xi_{ee}^2}{2}\cdot\frac{m}{E}\cdot\frac{r_0}{r^{(k)}}.$$

The term B_2 is given by (3.82). Hence,

$$X_n^a \;=\; \frac{\xi_{ee}^2}{2}\frac{m}{E}\langle\Phi_n|\sum_k r_0\frac{\partial}{\partial r^{(k)}}|\Psi_0\rangle\,. \tag{3.106}$$

Now we must calculate

$$X_n^b \;=\; \boldsymbol{\alpha} \sum_j \langle \Phi_n | \sum_k \mathbf{B}_R(\mathbf{r}^{(k)}) | \Phi_j \rangle \langle \Phi_j | \Psi_0 \rangle, \tag{3.107}$$

with

$$\mathbf{B}_R(\mathbf{r}^{(k)}) = -\int \frac{d^3q}{(2\pi)^3} \cdot \frac{\mathbf{q}}{p'^2 - (\mathbf{p}+\mathbf{q})^2 + i\delta} \cdot \frac{4\pi\alpha}{q^2+\lambda^2} \frac{\sin qr^{(k)}}{qr^{(k)}}; \quad \delta \to 0. \tag{3.108}$$

Writing

$$\mathbf{B}_R(\mathbf{r}^{(k)}) = c\mathbf{p}, \quad c = \frac{\mathbf{B}_R(\mathbf{r}^{(k)}) \cdot \mathbf{p}}{p^2},$$

and keeping only the leading term in the denominator of the electron propagator in (3.108), i.e., putting $p'^2 - (\mathbf{p}+\mathbf{q})^2 + i\delta = -2(\mathbf{p}\cdot\mathbf{q})$, we obtain

$$c \;=\; \frac{\alpha}{p^2} \int \frac{dq}{\pi} \frac{\sin qr^{(k)}}{qr^{(k)}} \;=\; \frac{\alpha}{2r^{(k)}} \frac{1}{p^2}\,.$$

Employing also

$$\bar{u}(\boldsymbol{\alpha}\cdot\mathbf{p}) \;=\; \bar{u}(m\gamma_0 - E)\,,$$

see (2.21), we obtain

$$X_n^b = \frac{\xi_{ee}^2}{2} \frac{m}{E} \langle \Phi_n | \sum_k \frac{r_0}{r^{(k)}} | \Psi_0 \rangle (1 - \frac{m}{E}\gamma_0) \tag{3.109}$$

and

$$\mathrm{Re}\, T_n^{(1)} = \frac{\xi_{ee}^2}{2} \frac{m}{E} \langle \Phi_n | \sum_k r_0 (\frac{\partial}{\partial r^{(k)}} + \frac{1}{r^{(k)}}) | \Psi_0 \rangle - \frac{\xi_{ee}^2}{2} \frac{m^2}{E^2} \langle \Phi_n | \sum_k \frac{r_0}{r^{(k)}} | \Psi_0 \rangle \gamma_0. \tag{3.110}$$

Due to the matrix γ_0 in the last term on the RHS, the amplitude contains not only terms of the form given by (3.103), but also terms of the form $\bar{u}\gamma_0 w$. If the FSI are neglected, the probability of the process is proportional to

$$W_1 = \frac{1}{4} Sp[w\bar{w}u\bar{u}].$$

Writing $u\bar{u} = a + b_\mu \gamma^\mu$ with b_μ a four-vector, we obtain $W_1 = b_\mu p^\mu + am$. The same remains true if we include the FSI amplitudes $\mathrm{Im}\, T_n^{(1)}$ and $\mathrm{Re}\, T_n^{(2)}$. It remains true also if we include the contribution to $Re\, T_n^{(2)}$ expressed by the first term on the RHS of (3.110). However, the interference of the second term on the RHS of (3.110) with amplitude $T_n^{(0)}$ is proportional to

$$W_2 = \frac{1}{4} Sp[w\bar{w}u\bar{u}\gamma_0] = ap_0 + mb_0.$$

This contribution requires additional analysis for each particular case.

Note that in the ultrarelativistic limit $E \gg m$, we can neglect the last term on the RHS of (3.110). At these energies, we must put $\xi_{ee} = \alpha$. Thus for any exclusive process,

$$S_n = |\langle \Phi_n|\Psi_0\rangle|^2 + \alpha^2 |\langle \Phi_n| \sum_k \ln\left((r^{(k)} - r_z^{(k)})\lambda\right)|\Psi_0\rangle|^2$$
$$- \alpha^2 \langle\Psi_0|\Phi_n\rangle\langle\Phi_n| \sum_{k,k_1} \ln\left((r^{(k)} - r_z^{(k)})\lambda\right) \ln\left((r^{(k_1)} - r_z^{(k_1)})\lambda\right)|\Psi_0\rangle\,. \tag{3.111}$$

The FSI contribution for any exclusive process is of order α^2.

In the sum over n, the terms of order ξ_{ee}^2 cancel due to (3.100). In the limit $E \gg m$, the terms of order $\xi_{ee}^2 m/E$ also cancel. The terms of this order come from the interference between the zero-order amplitudes $T_n^{(0)}$ and the real parts of the first-order amplitudes $\mathrm{Re}\, T_n^{(1)}$. However,

$$\sum_n \mathrm{Re} T_n^{(1)} T_n^{(0)} = \frac{m}{E} \langle\Psi_0| \sum_k r_0 \left(\frac{\partial}{\partial r^{(k)}} + \frac{1}{r^{(k)}}\right)|\Psi_0\rangle = 0,$$

where the last equality can be obtained by integration by parts. Hence

$$\sum_n S_n \;=\; 1 + O(\alpha^2 \frac{m^2}{E^2}). \tag{3.112}$$

Thus in the ultrarelativistic limit, all the FSI contributions are very small, much smaller than the radiative corrections.

Note that in systems with a large number of electrons $N \gg 1$, all the FSI effects are increased by the factor N. An example will be presented in Chap. 10.

References

1. L.D. Landau, E.M. Lifshits, *Quantum Mechanics. Nonrelativistic Theory* (Pergamon, N.Y., 1977)
2. E. Brezin, C. Itzykson, J. Zinn-Justin, Phys. Rev. D **1**, 2349 (1970)
3. J.D. Bjorken, S.D. Drell, *Relativistic Quantum Mechanics* (McGraw-Hill Book Company, 1964)
4. V.B. Berestetskii, E.M. Lifshits, L.P. Pitaevskii, *Quantum Electrodynamics* (Pergamon, N.Y., 1982)
5. R.H. Dalitz, Proc. Roy. Soc. A. **206**, 509 (1951)
6. V.G. Gorshkov, Sov. Phys. JETP **13**, 1037 (1961)

7. J. Hamilton, I. Øverböand, B. Tromborg, Nucl. Phys. B **60**, 443 (1973)
8. E.L. Feinberg, DAN USSR **29**, 79 (1939) (in Russian)
9. E.L. Feinberg, J. Phys. USSR **4**, 423 (1941)
10. A.B. Migdal, J. Phys. USSR **4**, 449 (1941)
11. E.G. Drukarev, M.I. Strikman, Phys. Lett. B **186**, 1 (1987)
12. R.J. Blin-Stoyle, *Fundamental Interactions and the Nucleus*, (American Elsivier Publishing Company, Inc. NY, 1973)
13. J.N. Ziman, *Elements of Advanced Quantum Theory* (University Press, Cambridge, 1969)

Chapter 4
Singularities of Amplitudes and Wave Functions

Abstract We demonstrate that $2 \to 3$ processes with large recoil momenta are described by triangle diagrams with the main contributions determined by their anomalous singularities. This enables us to obtain analytical expressions for the differential distributions and for the cross sections. The transfer of large momentum between the electron and the nucleus or between electrons is related to the small values of the corresponding distances, where the shape of the wave functions is determined by the Kato cusp conditions. We explain the importance of the latter and construct the electron wave functions on the coalescence lines.

4.1 General Features of the Reactions $2 \to 3$

The singularities of amplitudes at the thresholds of physical channels are described in detail in various books; see, e.g., [1]. Also, there are many books that contain an analysis of the singularities of the pole diagrams; see [2, 3]. Here we describe the singularities of the triangle diagrams, which are less well known but appear to be important in atomic physics. We discuss also the singularities of the two-electron wave functions at the electron–nucleus and electron–electron coalescence points.

4.1.1 Amplitudes Outside the Bethe Ridge

Here we show that the processes outside the Bethe ridge can be viewed as consisting of two steps, with one of them taking place at its Bethe ridge. We begin with an example of inelastic electron scattering by atoms, which we considered in Sect. 3.1.4. Now we analyze the case of large momenta $\mathbf{Q} = \mathbf{q} - \mathbf{p_2}$ transferred to the recoil ion, i.e., $Q = |\mathbf{q} - \mathbf{p_2}| \sim q$, $p_2 \gg \mu_b$. As we have seen, the momentum $\mathbf{Q}$ is transferred to the nucleus. If the interaction between the electron with momentum $\mathbf{p_2}$ and the nucleus is neglected, the amplitude is given by (3.26). We shall discuss its role later, focusing now on the lowest-order correction provided by (3.27). It can be written as

E.G. Drukarev and A.I. Mikhailov, *High-Energy Atomic Physics*,
Springer Series on Atomic, Optical, and Plasma Physics 93,
DOI 10.1007/978-3-319-32736-5_4

$$F^{(1)}(\mathbf{Q}) = \int \frac{d^3\kappa}{(2\pi)^3} F^{(0)}(\boldsymbol{\kappa}) \frac{2m}{p_2^2 - (\mathbf{q}+\boldsymbol{\kappa})^2 + i\delta} F_{eN}(\mathbf{Q}+\boldsymbol{\kappa}), \tag{4.1}$$

where $\boldsymbol{\kappa}$ is the momentum transferred to the nucleus by the bound electron, and F_{eN} is the lowest-order amplitude of the electron–nucleus scattering in which the nucleus obtains momentum $\mathbf{Q}+\boldsymbol{\kappa}$.

The integral on the right-hand side (RHS) is dominated by small $\kappa \sim \mu_b$. Note also that the second factor of the integrand is of order m/p_2^2 unless the values of p_2 and q are close. If $|q - p_2| \sim \mu_b \ll q, p_2$, it increases, becoming of order $m/\mu_b q \gg m/q^2$. Thus the physical meaning of (4.1) is clear. In the first step, electron scattering on the Bethe ridge takes place. If the values of q and p_2 are close, the ionized electron described by the second term in the integrand passes distances of order the size of the atom approaching the nucleus at small distances of order $1/Q \ll 1/\mu_b$, where the electron–nucleus scattering takes place.

Employing (3.26) and neglecting small momentum κ in the amplitude F_{eN}, we can represent (4.1) as

$$F^{(1)}(\mathbf{q}, \mathbf{p_2}) = F_0(\mathbf{q}) \Lambda(p_2, \mathbf{q}) F_{eN}(\mathbf{Q}), \quad \mathbf{Q} = \mathbf{q} - \mathbf{p_2}, \tag{4.2}$$

with $F_0 = 4\pi\alpha/q^2$ the amplitude of free electron–electron scattering, and

$$\Lambda(p_2, \mathbf{q}) = \int \frac{d^3\kappa}{(2\pi)^3} \psi_b(\boldsymbol{\kappa}) \frac{2m}{p_2^2 - (\mathbf{q}+\boldsymbol{\kappa})^2 + i\delta}. \tag{4.3}$$

For $|q - p_2| \sim q, p_2$, the amplitudes $F^{(0)}$ (3.26) and $F^{(1)}$ (3.27) are of the same order of magnitude. However, at $|q - p_2| \sim \mu_b$, the amplitude $F^{(1)}$ appears to be enhanced by a factor q/μ_b.

The amplitude can be described by the triangle diagram shown in Fig. 4.1a.

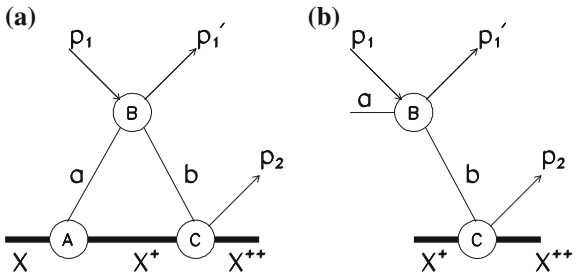

Fig. 4.1 Triangle diagram describing electron scattering on the atom X. The *bold lines* are for the atom X and the ions X^+. The *solid lines* are for electrons. Block A represents the atom X as consisting of the ion X^+ and the bound electron; block B is for the electron–electron scattering. Block C is for the electron inelastic scattering on the ion X^+. In (**b**), the bound electron a is replaced by a free electron

Here block A represents the initial atom as consisting of a bound electron described by the function $\psi(\kappa)$ (line a) and the core ion. Block B denotes the electron–electron scattering. The intermediate electron (line b) described by the second factor in the integrand of (4.1) passes through the atom. Its scattering on the nucleus of the core ion is shown by block C.

Presenting

$$\frac{1}{p_2^2-(\mathbf{q}+\boldsymbol{\kappa})^2+i\delta} = \frac{-1}{4\pi}\int d^3r e^{-i(\mathbf{q}+\boldsymbol{\kappa})\cdot\mathbf{r}}\frac{e^{ip_2r}}{r}, \tag{4.4}$$

and carrying out integration over $\boldsymbol{\kappa}$, we obtain

$$\Lambda(p_2,\mathbf{q}) = -\frac{m}{2\pi}\int d^3r\frac{\psi_b(\mathbf{r})}{r}e^{-i\mathbf{q}\cdot\mathbf{r}+ip_2r}. \tag{4.5}$$

If ψ_b describes an s state, it does not depend on the direction of $\mathbf{r}$. Thus the function Λ does not depend on the direction of the vector $\mathbf{q}$,

$$\Lambda(p_2,q)=\frac{-im}{q}M(p_2,q);\quad M(p_2,q)=\int dr\psi_b(r)\Big(e^{i(p_2-q)r}-e^{i(p_2+q)r}\Big). \tag{4.6}$$

The integral on the RHS is saturated by $r\sim 1/\mu_b$, and the second term of the integrand can be dropped:

$$M(p_2,q) = \int dr\psi_b(r)e^{i(p_2-q)r}. \tag{4.7}$$

Thus the function M depends only on $\Delta=q-p_2$, i.e., $M(p_2,q)=M(\Delta)$.

A similar expression can be obtained for the bound states with nonzero orbital momenta ℓ. If we choose the direction of momentum $\mathbf{q}$ as the axis of quantization of the angular momentum, the integral on the RHS of (4.5) obtains a nonzero value only for $\ell_z=0$. In this case, the angular integration by parts provides ($t=\mathbf{q}\cdot\mathbf{r}/qr$)

$$\int_{-1}^{1}dt\psi_b(r,\Omega)e^{-iqrt}=\frac{e^{-iqr}\psi_b(r,t=1)-e^{+iqr}\psi_b(r,t=-1)}{-iqr}-\frac{i}{qr}\int_{-1}^{1}dte^{-iqrt}\frac{\partial}{\partial t}\psi_b(r,\Omega), \tag{4.8}$$

with further integration by parts corresponding to expansion in powers of $(qr)^{-1}\sim\mu_b/q\ll 1$. Thus

$$M(\Delta) = \frac{(2\ell+1)^{1/2}}{(4\pi)^{1/2}}\int dr\psi_b^r(r)e^{-i\Delta r}, \tag{4.9}$$

with $\psi_b^r(r)$ the radial part of the wave function $\psi_b(\mathbf{r})$.

The origin of the enhancement of amplitude in the vicinity of the point

$$q^2 = p_2^2 \tag{4.10}$$

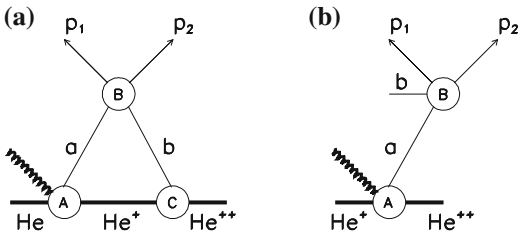

Fig. 4.2 Triangle diagram describing the double photoionization of the helium atom. The *helix line* denotes the photon. The *bold lines* are for the atom of helium and the ions He^+ and He^{++}. The *solid lines* are for electrons. The block A is for the single photoionization of the atom of helium as consisting of the ion He^+ and the bound electron; block B is for the electron–electron scattering. Block C represents the residual ion He^+ as consisting of the nucleus and the bound electron b. In (**b**), the bound electron b is replaced by a free electron

becomes clear if one considers the process on a free electron shown in Fig. 4.1b. The diagram has a pole if (4.10) is true.

These results are quite general for the reactions $2 \to 3$. In the vicinity of the point $q^2 = p_2^2$, the amplitudes represented by the diagram shown in Fig. 4.1a can be written as [4]

$$F(\mathbf{q}, \mathbf{p_2}) \;=\; F_B(\mathbf{q}) \Lambda(p_2, \mathbf{q}) F_C(\mathbf{q}, \mathbf{p_2}), \tag{4.11}$$

with the amplitudes F_B and F_C describing the two steps of the process.

The singularities of the triangle diagrams can manifest themselves in other channels [5]. Consider, for example, the process of double photoionization of the atom of helium in a simplified model, where interaction of the bound electrons is neglected. (We shall analyze double photoionization in detail in Chap. 9.) The large energy $\varepsilon \gg I$ (which we assume for simplicity to be nonrelativistic) absorbed by the atom is shared by the two outgoing electrons. The corresponding triangle diagram is shown in Fig. 4.2a.

Here block A stands for single ionization of the atom; block C shows that the residual ion consists of the bound electron (line b) and the nucleus. Block B denotes the scattering of the photoelectron a on the electron b. The position of the pole of the propagator describing the electron a in the diagram of Fig. 4.2b, corresponding to replacement of the bound electron b by a free one, is determined by condition

$$p^2 = p'^2; \quad p'^2 = 2m(\varepsilon_1 + \varepsilon_2), \tag{4.12}$$

where $p = |\mathbf{p}|$, $\mathbf{p} = \mathbf{p_1} + \mathbf{p_2}$, p_i, and ε_i $(i = 1, 2)$ are the momenta and energies of the outgoing electrons. The amplitude is

$$F(\mathbf{p_1}, \mathbf{p_2}) \;=\; F_A(\mathbf{p}) \Lambda(p', \mathbf{p}) F_B(\mathbf{p}_1, \mathbf{p}_2), \tag{4.13}$$

with the function Λ determined by (4.3).

Note that the position of singularity in the variable q^2 (4.10) in the first example as well as that of the singularity in p^2 in the second example is determined by external variables. Such singularities are known as "anomalous singularities" (see, e.g., [6]).

In the case of the Coulomb field, these features of the triangle diagrams can be illustrated by explicit calculations.

4.1.2 Triangle Diagrams in the Case of the Coulomb Field

Here we consider the inelastic scattering of electrons on a single-electron ion with the charge of the nucleus Z. More generally, we assume that the ion core in the block A in Fig. 4.1a is the source of the Coulomb field. Thus the function $\psi(\boldsymbol{\kappa})$ in (4.3) is just the nonrelativistic Coulomb function. This enables us to calculate the function $\Lambda(p_2, \mathbf{q})$ defined by (4.3) explicitly. For s electrons, $\Lambda(p_2, \mathbf{q}) = \Lambda(p_2, q)$ does not depend on direction of momentum $\mathbf{q}$. For $1s$ electrons,

$$\Lambda(p_2, \mathbf{q}) = \frac{-2mN_1}{q^2 - (p_2 + i\eta)^2}; \quad \eta = m\alpha Z; \quad N_1 = \psi_{1s}(r = 0) = \left(\frac{\eta^3}{\pi}\right)^{1/2}. \tag{4.14}$$

Thus in the Coulomb field, the pole of the amplitude is shifted from the point $q^2 = p_2^2$ to the complex plane

$$q^2 = (p_2 + i\eta)^2. \tag{4.15}$$

The function $M(p_2, q)$ defined by (4.6) is

$$M(\Delta) = \frac{-iN_1}{\Delta - i\eta}; \quad \Delta = q - p_2\,. \tag{4.16}$$

If the bound electron is in a state with a nonzero orbital momentum ℓ and its projection is given by $\ell_z = m$, the function Λ has a pole of order $\ell + 1$. For example, in the case of the $2p$ state with projection of the angular momentum $\ell_z = m$, we obtain

$$\Lambda(p_2, \mathbf{q}) = \frac{-i4mN_2\eta_2 q_m}{(q^2 - (p_2 + i\eta_2)^2)^2}; \quad \eta_2 = m\alpha Z/2; \quad N_2 = \left(\frac{\eta_2^3}{\pi}\right)^{1/2}, \tag{4.17}$$

with q_m the circular components of the vector $\mathbf{q}$.

Note that the pole singularity is an artifact of the Born approximation employed for describing the wave function of the outgoing electron. In the case of the Coulomb field, the amplitude of inelastic electron scattering given by (3.25) can be calculated explicitly; see (3.35). For the scattering on the bound electron in the $1s$ state, the last factor on the RHS of (3.35) is

$$X(\mathbf{p_2}, \mathbf{q}) \;=\; 8\pi\left(\frac{\eta(-1+i\xi)}{a} - \frac{\xi(-p+i\eta)}{b}\right)\left(\frac{a}{b}\right)^{i\xi}, \tag{4.18}$$

with $a = Q^2 + \eta^2$, $b = q^2 - (p_2 + i\eta)^2$. One can see that in the complex q-plane, the amplitude has branching points corresponding to $a = 0$ and $b = 0$. In the vicinity of the point $q = p_2 + i\eta$, at which $b = 0$, the second term in parentheses on the RHS of (4.18) dominates at large transferred momenta $q \sim p_2, q \gg \mu_b$.

4.1.3 *Triangle Diagrams in the Case of Short-Range Forces*

Now we consider the case in which block A is bound by short-range forces with the wave equation

$$\left(\frac{-\Delta}{2m} + U(\mathbf{r})\right)\psi(\mathbf{r}) \;=\; \varepsilon_b\psi_b(\mathbf{r}), \tag{4.19}$$

with $U(r) = 0$ for r exceeding a certain value a. This means that for the s states, the wave function at $r > a$ is

$$\psi_b(r) = c\frac{e^{-\mu_b r}}{r}; \quad \mu_b = (2m|\varepsilon_b|)^{1/2}, \tag{4.20}$$

with a certain constant c.

We begin with the case of the zero-range potential model (ZRPM), in which $a \to 0$. It was first used long ago by Bethe and Pierls [7] in their studies of the deuteron. The various versions of the approach differ in the prescriptions of tending to the limit $r = 0$ on the left-hand side (LHS) of the Schrödinger equation (4.19). A popular version with $U(\mathbf{r}) = A\delta(\mathbf{r})$, where A is a certain constant, is known as the Fermi pseudopotential. The ZRPM is used in many branches of physics. Nowadays, it is employed also in the physics of nanostructures [8]. The simplest example for application of ZRPM in atomic physics is the description of the outer electron in the negative ion of hydrogen. For more applications in atomic and molecular physics, see the review [9].

The ZRPM wave function of the bound s state is given by (4.20) in the whole space, and $c = (\mu_b/2\pi)^{1/2}$. The function $\Lambda(p_2, q)$ is determined by (4.7). The integral in the second equality is saturated by $1/(q + p_2) \ll r \ll 1/|q - p_2| \sim 1/\mu_b$, providing

$$M(p_2, q) \;=\; -\left(\frac{\mu_b}{2\pi}\right)^{1/2} \ln\frac{\mu_b + i(q - p_2)}{\mu_b - i(q + p_2)} \tag{4.21}$$

which depends now on $q - p_2$ and on $q + p_2$. The amplitude has branching points at $q = \pm(p_2 + i\mu_b)$. The first equality of (4.6) provides

$$\Lambda(p_2,q)=\frac{im}{q}\Big(\frac{\mu_b}{2\pi}\Big)^{1/2}\Big(-\frac{1}{2}\ln\frac{(q+p_2)^2+\mu_b^2}{(q-p_2)^2+\mu_b^2}+i(\arctan\frac{q+p_2}{\mu_b}+\arctan\frac{q-p_2}{\mu_b})\Big). \tag{4.22}$$

In the vicinity of the point given by (4.10), the amplitude is enhanced by the logarithmic factor $\ln(4q^2/(\Delta^2+\mu_b^2))$.

One can see that the function $\Lambda(p_2,q)$ has pole singularities if the integral on the RHS of (4.10) is saturated by $r\sim\mu_b^{-1}$, while the logarithmic singularities are a result of the contribution of the small distances $1/q\ll r\ll\mu_b^{-1}$.

In the case of nonzero values of a, which one can meet in the physics of nanostructures, we can write (4.6) as

$$\Lambda(p_2,q)\;=\;\Lambda_1(p_2,q)+\Lambda_2(p_2,q), \tag{4.23}$$

with the two terms on the RHS corresponding to the regions of integration $r<a$ and $r>a$ with the wave function

$$\psi_b(r)\;=\;c_1(a)\psi_{int}(r)\theta(a-r)+c_2(a)\frac{e^{-\mu_b r}}{r}\theta(r-a), \tag{4.24}$$

where $\psi_{int}(r)$ describes the bound state in the internal region where $U(r)\neq 0$. The coefficients $c_{1,2}(a)$ are determined by the normalization condition. One can see that if $a\mu_b<1$, the region $r>a$ provides the logarithmic contribution

$$\Lambda_2(q,\,p_2)\;=\;i\cdot\frac{m}{q}c_2(a)\ln\frac{\mu_b+i(q-p_2)}{\mu_b-i(q+p_2)}, \tag{4.25}$$

similar to that given by (4.21).

4.1.4 Amplitudes on the Bethe Ridge in the Presence of Singularities

In Chap. 2, we studied processes on bound electrons in the case that the amplitudes of the corresponding processes on the free electrons do not have singularities. Now we investigate the case in which there are singularities.

Consider as an example the disintegration of the negative ion of hydrogen H^- by electron impact. The momenta of the initial and scattered electron are $\mathbf{p_1}$ and $\mathbf{p_1'}$; those of the electrons ejected from the ion are $\mathbf{p_2}$ and $\mathbf{p_3}$. Momentum $\mathbf{q}=\mathbf{p_1}-\mathbf{p_1'}$ is transferred to the atom. Assuming $p_1,\,p_1'\gg p_2,\,p_3$, we can neglect the exchange terms. We consider the case in which the atom absorbs nonrelativistic energy ε.

Replacing the bound electrons by free ones and including the FSI between the ejected electrons in the lowest nonvanishing order, we obtain the diagram presented in Fig. 4.3a. For this reaction,

$$\mathbf{q}\;=\;\mathbf{p}, \tag{4.26}$$

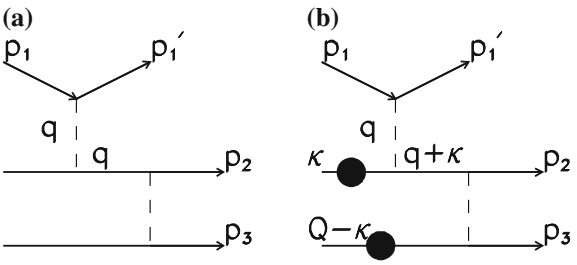

Fig. 4.3 Double ionization of the system containing two noninteracting electrons by electron impact

with $\mathbf{p} = \mathbf{p_2} + \mathbf{p_3}$ the sum of the momenta of the ejected electrons.

Including the FSI between the ejected electrons in the lowest nonvanishing order, we arrive at the diagram presented in Fig. 4.3a. Due to (4.26), the electron propagator of this diagram has a pole at

$$q^2 = p'^2; \quad p'^2 = 2m(\varepsilon_2 + \varepsilon_3), \tag{4.27}$$

with $\varepsilon_{2,3}$ the energies of the outgoing electrons. Thus we can represent the amplitude of the process on the free electrons as

$$F_0(\mathbf{p_2}, \mathbf{p_3}) \; = \; \frac{2m\,K(p_2, p_3)}{p'^2 - q^2 + i\delta}, \tag{4.28}$$

with $K(p_2, p_3) = 4\pi\alpha/p^2 \cdot 4\pi\alpha/p_3^2$.

We return now to ionization of the negative ion of hydrogen H^-. The system contains a bound electron with single-particle binding energy close to that in atomic hydrogen and an outer bound electron with the much smaller binding energy $\varepsilon_b \approx -0.7\,\text{eV}$. Thus the ratio of the corresponding binding momenta $\mu_{out}/\mu_{int} \approx 0.2$ can be treated as a small parameter. It is sufficient for our analysis to consider the lowest-order approximation.

In the region of small momenta $Q \leq \mu_{int}$ transferred to the nucleus, we obtain for the amplitude in the vicinity of the pole determined by (4.27),

$$F(\mathbf{p_2}, \mathbf{p_3}, \mathbf{Q}) \; = \; K(p_2, p_3)\Lambda_1(p', \mathbf{q}, \mathbf{Q}), \tag{4.29}$$

with

$$\Lambda_1(p', \mathbf{q}, \mathbf{Q}) = \int \frac{d^3\kappa}{(2\pi)^3}\Psi(\boldsymbol{\kappa}, \mathbf{Q} - \boldsymbol{\kappa})\frac{2m}{p'^2 - (\mathbf{q} + \boldsymbol{\kappa})^2 + i\delta}, \tag{4.30}$$

where $\Psi(\boldsymbol{\kappa}, \mathbf{Q} - \boldsymbol{\kappa})$ is the two-particle wave function of the bound electrons. We neglected terms of order $Q/p_{2,3} \sim \mu_{int}/p_{2,3} \ll 1$ in the expression for $K(\mathbf{p_2}, \mathbf{p_3})$. The two bound electrons transfer momenta $\boldsymbol{\kappa}$ and $\mathbf{Q} - \boldsymbol{\kappa}$ to the nucleus. The amplitude given by (4.29) is illustrated in Fig. 4.3b. One can see that (4.30) is very much like (4.3) for $\Lambda(p_2, \mathbf{q})$. The difference is that (4.30) contains the two-electron wave

function. Assuming that the latter can be represented in terms of the single-particle wave functions $\psi_{int,out}$ (this is not a good approximation for accurate computations), we can write

$$\Psi(\boldsymbol{\kappa}, \mathbf{Q}-\boldsymbol{\kappa}) = \frac{1}{\sqrt{2}}\Big(\psi_{out}(\boldsymbol{\kappa})\psi_{int}(\mathbf{Q}-\boldsymbol{\kappa}) + \psi_{int}(\boldsymbol{\kappa})\psi_{out}(\mathbf{Q}-\boldsymbol{\kappa})\Big). \tag{4.31}$$

It is symmetric, since the two electrons in the ion H^- form a singlet spin state. Thus (4.30) takes the form

$$\Lambda_1(p', \mathbf{q}, \mathbf{Q}) = \int \frac{d^3\kappa}{(2\pi)^3}\Big(\frac{\sqrt{2}m\psi_{out}(\boldsymbol{\kappa})\psi_{int}(\mathbf{Q}-\boldsymbol{\kappa})}{p'^2-(\mathbf{q}+\boldsymbol{\kappa})^2+i\delta} + \frac{\sqrt{2}m\psi_{out}(\mathbf{Q}-\boldsymbol{\kappa})\psi_{int}(\boldsymbol{\kappa})}{p'^2-(\mathbf{q}+\boldsymbol{\kappa})^2+i\delta}\Big). \tag{4.32}$$

Since the wave function $\psi_{out}(\boldsymbol{\kappa})$ is strongly quenched at $\kappa \gg \mu_{out}$, the first term in parentheses is saturated at $\kappa \sim \mu_{out}$. Thus we can put $\psi_{int}(\mathbf{Q}-\boldsymbol{\kappa}) = \psi_{int}(\mathbf{Q})$. For the second term in parentheses, we introduce $\boldsymbol{\kappa}' = \mathbf{Q}-\boldsymbol{\kappa}$. The integral is dominated by $\kappa' \sim \mu_{out}$. Putting $\psi_{int}(\mathbf{Q}-\boldsymbol{\kappa}') = \psi_{int}(\mathbf{Q})$, we obtain for $Q \sim \mu_{int}$,

$$F(\mathbf{p_2}, \mathbf{p_3}, \mathbf{Q}) \;=\; \frac{K(p_2, p_3)}{\sqrt{2}}\Big(\Lambda(p', q) + \Lambda(p', p)\Big)\psi_{int}(Q); \quad p = |\mathbf{p}_2 + \mathbf{p}_3|, \tag{4.33}$$

and $q = |\mathbf{p} - \mathbf{Q}|$. Here we employed that the functions ψ_{int} and ψ_{out} describe the s states. Momentum Q is transferred to the nucleus by the inner electron. The terms $\Lambda(p', q)$ and $\Lambda(p', p)$ describe the shift of the pole of the electron propagator to the complex plane due to the bound of the outer electron. The first and the second terms in parentheses correspond to absorption of momentum q by the outer bound electron and by the inner one, respectively.

Today's powerful computers enable us to obtain a very precise numerical function of the ion H^-. In the single-particle approximation, very accurate numerical functions for the outer electron ψ_{out} can be found. However, the analytical properties of the function $\Lambda(p', p)$ depend on the behavior of $\psi_{out}(r)$ at small $r \ll 1/\mu_{out}$. In earlier papers [10], the function $\psi_{out}(r)$ was approximated by combinations of the exponential terms $\sum_k c_k e^{-\mu_k r}$. In this case,

$$\Lambda(p', p) \;=\; -\sum_k c_k \frac{2m}{p^2-(p'+i\mu_k)^2} \tag{4.34}$$

and a similar expression for $\Lambda(p', q)$ are a combination of the pole terms (see (4.14)). However, the ZRPM wave function used in [11] for describing the ion H^- behaves at small r in another way (see (4.20)). This provides the logarithmic dependence

$$\Lambda(p', p) = i \cdot \frac{m}{q} \sum_k \left(\frac{\mu_k}{2\pi}\right)^{1/2} \ln \frac{\mu_k + i(p - p')}{\mu_k - i(p' + p)} \approx i \cdot \frac{m}{2q} \sum_k \left(\frac{\mu_k}{2\pi}\right)^{1/2} \ln \frac{\Delta^2 + \mu_k^2}{4p^2}, \tag{4.35}$$

with $\Delta = p - p'$, and a similar equation for $\Lambda(p', q)$.

4.1.5 Contribution of Triangle Diagrams to Differential Cross Sections

Now we calculate the contribution of the triangle diagrams to differential cross sections. Consider again the ionization of atoms by electron impact with large momentum of the outgoing electron p_2 and large momentum Q transferred to the nucleus, i.e., $Q \sim p_2 \gg \mu_b$; see Fig. 4.3. The amplitude is given by (4.2), with the differential cross section

$$d\sigma = |F|^2 d\Gamma, \tag{4.36}$$

where the phase volume (including the flux factor) can be written as

$$d\Gamma = \frac{2\pi m}{p_1} \delta(\varepsilon_1 - \varepsilon_1' - \varepsilon_2 - I) \frac{d^3 p_1'}{(2\pi)^3} \frac{d^3 p_2}{(2\pi)^3}. \tag{4.37}$$

Evaluating the phase volume at fixed value of $\mathbf{q}$,

$$\frac{d^3 p_2}{(2\pi)^3} = \frac{m Q dQ d\varepsilon_2}{q(2\pi)^2}, \tag{4.38}$$

(recall that $\mathbf{Q} = \mathbf{q} - \mathbf{p_2}$), and employing also

$$\frac{d^3 p_1'}{(2\pi)^3} = \frac{m q dq d\varepsilon_1'}{p_1(2\pi)^2}, \tag{4.39}$$

we obtain, using (4.2),

$$\frac{d\sigma}{d\varepsilon_2 dq dQ} = \frac{2\pi m}{p_1} |F_0(q)|^2 |\Lambda(p_2, q)|^2 \frac{mq}{p_1(2\pi)^2} |F_{eN}(Q)|^2 \frac{mQ}{q(2\pi)^2}. \tag{4.40}$$

Here we have assumed for simplicity that an s state is ionized, and thus the amplitudes in (4.40) do not depend on directions of momenta. Recall that F_0 is the amplitude of scattering of free electrons with exchange by momentum $\mathbf{q}$; F_{eN} is the amplitude of the eN scattering in which momentum $\mathbf{Q}$ is transferred to the nucleus. Note that in eN scattering the electron energy does not change. Thus the secondary electron carries the same energy ε_2 in both processes.

On the other hand, the cross section of free electron scattering is given by

$$d\sigma_0 \;=\; \frac{2\pi m}{p_1}|F_0|^2\delta(\varepsilon_1-\varepsilon_1'-\frac{\mathbf{q}^2}{2m})\frac{d^3p_1'}{(2\pi)^3}\,.$$

Employing (4.39) and using the delta function for integration over q, we obtain

$$\frac{d\sigma_0}{d\varepsilon_2} \;=\; \frac{m^3}{2\pi p_1^2}|F_0|^2 = \frac{\pi\alpha^2}{\varepsilon_1\varepsilon_2^2} \tag{4.41}$$

for the energy distribution of the free electron scattering ($d\sigma_0/d\varepsilon_1' = d\sigma_0/d\varepsilon_2$). For the cross section of the eN scattering, we can write

$$d\sigma_{eN} \;=\; \frac{2\pi m}{q}|F_{eN}|^2\delta(\varepsilon_2-\frac{q^2}{2m}).\frac{d^3p_2}{(2\pi)^3}\,.$$

Employing (4.38) and using the delta function for integration over ε_2, we obtain

$$\frac{d\sigma_{eN}(\varepsilon_2)}{dQ} = \frac{mQ}{4\pi\varepsilon_2}|F_{eN}|^2 = \frac{4\pi\alpha^2Z^2m}{\varepsilon_2Q^3} \tag{4.42}$$

for the distribution of the eN scattering. These expressions are well known and are presented in many books on quantum electrodynamics. However, these are the first equalities in (4.41) and (4.42) that are important for us. They enable us to write [12]

$$\frac{d\sigma(p_1)}{d\varepsilon_2 dQdq} \;=\; \frac{d\sigma_0(p_1)}{d\varepsilon_2}\frac{R(p_2,q)}{2\pi}\frac{d\sigma_{eN}(\varepsilon_2)}{dQ}, \tag{4.43}$$

where ε_2 and Q are the energy and the solid angle of the electron ejected from the target, Q is the momentum transferred to the nucleus, while $p_2 = (2m\varepsilon_2)^{1/2}$, and

$$R(p_2,q) \;=\; |M(p_2,q)|^2. \tag{4.44}$$

If the target electron is in the ground state of the Coulomb field, we obtain, employing (4.14),

$$R(p_2,q) = R(\Delta) = \frac{N_1^2}{\Delta^2+\eta^2};\quad \Delta = q-p_2. \tag{4.45}$$

If the electron is bound by the field for which $\psi_b(r=0)$ does not turn to infinity, the function R in (4.43) depends only on $\Delta = q - p_2$, and one can replace integration over q by that over Δ. This leads to

$$\frac{d\sigma(\varepsilon_1)}{d\varepsilon_2 dQ} \;=\; s\frac{d\sigma_0(\varepsilon_1)}{d\varepsilon_2}\frac{d\sigma_{eN}(\varepsilon_2)}{dQ}, \tag{4.46}$$

with

$$s \equiv \int \frac{d\Delta}{2\pi} R(\Delta)\,. \tag{4.47}$$

In the case of the Coulomb field, one obtains

$$s = \frac{N_1^2}{2\eta} = \frac{\eta^2}{2\pi} \tag{4.48}$$

for the $1s$ state.

The contribution of the small region $|\Delta| < \eta$ to the distribution $d\sigma/d\varepsilon dQ$ is thus $p_2/\eta \gg 1$ times that of the whole region $|q - p_2| \sim p_2$. This is true for every field for which $\psi_b(r = 0)$ does not turn to infinity.

Hence, if we neglect interactions of the outgoing electron with the nucleus, we shall underestimate the cross section by a factor of $p_2/\mu_b \gg 1$. This is expressed explicitly by (4.40) and (4.41).

For a process described by the diagram shown in Fig. 4.1a, one can write

$$\frac{d\sigma}{d\Gamma d\Delta} = \frac{d\sigma_0}{d\Gamma_0}\frac{R(\Delta)}{2\pi}\frac{d\sigma_C}{d\Gamma_C}, \tag{4.49}$$

where $d\Gamma_{0,C}$ and $d\Gamma = d\Gamma_0 d\Gamma_C$ are the corresponding phase volumes (compare (4.43)), and

$$\frac{d\sigma}{d\Gamma} = s\frac{d\sigma_0}{d\Gamma_0}\frac{d\sigma_C}{d\Gamma_C}. \tag{4.50}$$

Similar equations can be written for the process described by the diagram shown in Fig. 4.2.

One can obtain general expression for the parameter s [13]. Recall that for $\ell \neq 0$, the function M is nonvanishing only for states with $m = \ell_z = 0$ (the z-axis is directed along the momentum $\mathbf{q}$). Employing (4.9), we write

$$R(\Delta) = \frac{2\ell + 1}{4\pi}\delta_{m0}\int dr dr' \psi_b^{*r}(r)\psi_b^r(r')e^{i\Delta(r'-r)}. \tag{4.51}$$

Since

$$\int \frac{d\Delta}{2\pi} e^{i\Delta(r'-r)} = \delta(r' - r),$$

we obtain

$$s = (2\ell + 1)\delta_{m0}\frac{\langle\psi_{n\ell m}|r^{-2}|\psi_{n\ell m}\rangle}{4\pi}. \tag{4.52}$$

Note that these equations are written for one bound electron in each shell. One should sum over all bound electrons. For the closed subshells, we can write

$$s = \frac{\langle\Psi|\sum_k (r^{(k)})^{-2}|\Psi\rangle}{4\pi}. \tag{4.53}$$

For the subshells with $\ell \neq 0$, only the states with $\ell_z = 0$ contribute, but their contribution is enhanced by the factor $2\ell + 1$; see (4.51).

If $\psi_b(r) \sim 1/r$ as $r \to 0$, the function $d\sigma/d\varepsilon_2 dQ d\Delta$ has a peak with the height of the order $\ln^2(q^2/\Delta^2)$ at small $\Delta \sim \mu_b$; see (4.22). However, the distribution $d\sigma/d\varepsilon_2 dQ$ is determined by large $|p_2 - q| \sim q$. The region $\Delta \sim \mu_b$ provides a large correction of order $(\mu_b/q) \cdot \ln^2(q^2/\Delta^2)$.

4.2 Fast Secondary Electrons

4.2.1 Angular Correlations and Energy Distributions

Now we consider processes in which a bound electron accepts energy in interacting with an external source and shares it with another bound electron. The energies of both outgoing electrons are assumed to exceed greatly the ionization potentials.

We begin with the double ionization of the ground state of a two-electron ion (or atom) by a photon carrying energy ω. This case was mentioned briefly in Sect. 4.1.1; see Fig. 4.2 and (4.12) and (4.13). We shall discuss this process in detail in Chap. 9. Here we assume that the bound-state wave function can be represented as the product of single-particle functions. We can write, similar to (4.36) and (4.37),

$$d\sigma = 2\pi|F|^2\delta(\omega - \frac{p_2^2}{2m} - \frac{(\mathbf{p}-\mathbf{p}_2)^2}{2m} - I)\frac{d^3p}{(2\pi)^3}\cdot\frac{d^3p_2}{(2\pi)^3}, \quad \mathbf{p} = \mathbf{p}_1 + \mathbf{p}_2, \tag{4.54}$$

with the amplitude F given by (4.13). Hence

$$d\sigma = 2\pi|F_{ph}(\mathbf{p})|^2|\Lambda(p', \mathbf{p})|^2|F_{ee}(\mathbf{p}_2)|^2\cdot \tag{4.55}$$

$$\delta(\omega - \frac{p_2^2}{2m} - \frac{(\mathbf{p}-\mathbf{p}_2)^2}{2m} - I)\frac{p^2 dp d\Omega_p}{(2\pi)^3}\frac{d^3p_2}{(2\pi)^3}.$$

Here F_{ph} is the amplitude of photoionization; $\mathbf{p}$ is the momentum of the photoelectron; $F_{ee}(\mathbf{p})$ is the amplitude of the scattering of the electron with momentum $\mathbf{p}$ on the free electron at rest; $\mathbf{p}_i$ are the momenta of the outgoing electrons. Composing (4.55) with the expression

$$d\sigma_{ph} = 2\pi|F_{ph}(\mathbf{p})|^2\frac{mpd\Omega_p}{(2\pi)^3}$$

for the cross section of the photoionization and employing the delta function for integration over the angles of momentum $\mathbf{p}_2$ at fixed value of $\mathbf{p}$, we obtain

$$\frac{d\sigma}{d\varepsilon_2 dp} = \sigma_{ph}(\omega)\frac{R(p', p)}{2\pi}\frac{d\sigma_{ee}(\varepsilon)}{d\varepsilon_2}; \quad p'^2 = 2m\varepsilon, \tag{4.56}$$

with $\varepsilon = \omega - I$ the energy absorbed by the ion. The last factor on the RHS of (4.56) presents the scattering cross section of the electron with energy ε on the free electron at rest.

Thus the distribution $d\sigma/d\varepsilon_2 dp$ has a sharp maximum at $p = p'$ with the width of the order μ_b. In other words, the distribution in the angle between the momenta of the outgoing electrons (angular correlations)

$$\tau = \mathbf{p_1} \cdot \mathbf{p_2}/p_1 p_2$$

has a sharp maximum at

$$\tau = 0, \tag{4.57}$$

corresponding to the value predicted by classical mechanics. The vicinity of this point determines the distribution

$$\frac{d\sigma}{d\varepsilon_2} = s\sigma_{ph}(\omega)\frac{d\sigma_{ee}(\varepsilon)}{d\varepsilon_2}, \tag{4.58}$$

with s given by (4.52). Note that (4.58) holds at all orders of the FSI between the photoelectrons. In the lowest order of the FSI, we have

$$\frac{d\sigma_{ee}(\varepsilon)}{d\varepsilon_2} = \frac{\pi\alpha^2}{\varepsilon}\left(\frac{1}{\varepsilon_2} + \frac{1}{\varepsilon - \varepsilon_2}\right)^2. \tag{4.59}$$

We turn now to the case in which the bound electrons are described by exponential (Coulomb) functions. Since the interactions between the electrons are $1/Z$ times their interactions with the nucleus, this model becomes increasingly accurate with increase of Z. We shall see in Chap. 9 that this is a reasonable approximation for the high-energy double photoionization of heliumlike ions except the lightest ones. In the case of the Coulomb functions, one can find analytical expression for the distribution

$$\frac{d\sigma}{d\varepsilon_2 d\Delta} = \frac{1}{2\pi}\cdot\frac{N_1^2\sigma_{ph}(\omega)}{\Delta^2 + \eta^2}\cdot\frac{d\sigma_{ee}(\varepsilon)}{d\varepsilon_2}; \quad \Delta = p - p'. \tag{4.60}$$

We can also write an expression for the double distribution in the energy and angles. Since $p^2 = p_1^2 + p_2^2 + 2p_1p_2\tau$, we can write $\Delta = p - p' = 2p_1p_2\tau/(p + p') \approx p_1p_2\tau/p'$. The distribution (4.60) can be written as

$$\frac{d\sigma}{d\varepsilon_2 d\tau} = \frac{1}{2\pi a}\cdot\frac{N_1^2\sigma_{ph}(\omega)}{\tau^2 + \eta^2/a^2}\cdot\frac{d\sigma_{ee}(\varepsilon)}{d\varepsilon_2}, \tag{4.61}$$

with $a = p_1 p_2/(2m\varepsilon)^{1/2}$; $p_1 = \sqrt{2m(\varepsilon - \varepsilon_2)}$. Since $\varepsilon_{1,2} \gg I = \eta^2/2m$, we find indeed that $\tau^2 \ll 1$. The energy distribution is expressed by (4.58) with $s = \eta^2/2\pi$; see (4.48).

Note that (4.58) is quite general for processes with ejection of a fast electron carrying the energy ε. We denote the cross sections of this process and that of similar process with ejection of secondary electrons by σ_0 and σ. The high-energy part of the spectrum of the secondary electrons can be described by the formula

$$\frac{d\sigma(\varepsilon, \varepsilon_2)}{d\varepsilon_2} = s\sigma_0(\varepsilon)\frac{d\sigma_{ee}(\varepsilon)}{d\varepsilon_2}. \tag{4.62}$$

Consider now the case of very large values of $\omega \gtrsim m$, corresponding to the relativistic energies of one or both photoelectrons. Their kinetic energies are $\hat{\varepsilon_i} = E_i - m$. The point of the sharp maximum of the distribution $d\sigma/d\hat{\varepsilon}_2 dp$, corresponding to the pole of the propagator a in Fig. 4.2, is determined by the condition

$$(\omega + m)^2 - p^2 = m^2, \tag{4.63}$$

or $p = p'$ with $p'^2 = 2\omega m + \omega^2$. Since

$$\omega \approx \hat{\varepsilon} = \hat{\varepsilon_1} + \hat{\varepsilon_2}; \quad p_i^2 = 2m\hat{\varepsilon_i} + \hat{\varepsilon_i}^2, \tag{4.64}$$

(4.63) leads to a peak of the angular correlations at

$$\tau = \frac{\hat{\varepsilon_1}\hat{\varepsilon_2}}{p_1 p_2}, \tag{4.65}$$

which depends on the total energy $\hat{\varepsilon}$ and on the energy sharing $x = \hat{\varepsilon_i}/\hat{\varepsilon}$. The dependence $\tau(x)$ for several values of $\hat{\varepsilon}$ is presented in Fig. 4.4. Since the RHS of (4.65)

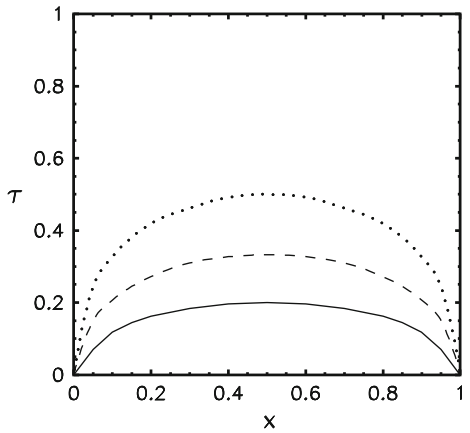

Fig. 4.4 Dependence of τ defined by (4.65) on the energy sharing $x = \hat{\varepsilon_i}/\hat{\varepsilon}$. The *solid line* is for $\hat{\varepsilon}/m = 1$ ($\hat{\varepsilon} \approx 500\,\text{keV}$). The *dashed* and *dotted lines* represent the results for $\hat{\varepsilon} = 3m/2$ and $\hat{\varepsilon} = 2m$ respectively

does not exceed unity, there is a peak in the angular correlations at any energy of the outgoing electrons. We see that $\tau \ll 1$ if one of the photoelectrons obtains a nonrelativistic energy. If both electrons are ultrarelativistic, with $\hat{\varepsilon}_i \gg m$ we find that $\tau \to 1$. The high-energy part of the spectrum of the secondary electrons can be written similar to (4.62):

$$\frac{d\sigma(\hat{\varepsilon}, \hat{\varepsilon_2})}{d\hat{\varepsilon_2}} = s\sigma_0(\hat{\varepsilon})\frac{d\sigma_{ee}(\hat{\varepsilon})}{d\hat{\varepsilon_2}}. \tag{4.66}$$

Now we can formulate the main features of the distribution of fast secondary electrons.

- The distribution $d\sigma/d\varepsilon_2 d\tau$ has a sharp and narrow peak with the point τ_0 determined by the energies of the outgoing electrons. In the nonrelativistic limit $\tau_0 = 0$, the width of the peak is of order $\mu_b/(2m\varepsilon)^{1/2}$.
- The distribution $d\sigma/d\varepsilon_2$ is determined by the values of τ close to the vicinity of the peak.
- The shape of the spectrum of the photoelectrons is the same as that in free electron–electron scattering.
- The spectrum is proportional to the expectation value of the sum $\sum_k (r^{(k)})^{-2}$ of the ionized atom.

For the case $\psi_b(r) \to 1/r$ as $r \to 0$, the first feature is also true. However, the peak is much lower, and all values of τ contribute to the energy distribution, while the vicinity of the peak provides a large correction of the order $(\mu_b/p_2) \cdot \ln^2(\mu_b/p_2)$.

4.2.2 Internal Energy Loss

If an atom remains in the ground state after ejection of a fast electron, its wave function changes from $|\Psi_0\rangle$ to $|\Phi_0\rangle$, while the energy changes from $\varepsilon_0^{(i)}$ to $\varepsilon_0^{(f)}$ ($\varepsilon_0^{(i,f)} < 0$). The ground-state energies $\varepsilon_0^{(i,f)}$ can be usually measured and calculated with good accuracy.

If the atom moves to an excited state, the fast electron obtains a smaller energy. We shall calculate the energy loss of the fast electron connected with possible excitation of the atomic states. For the sake of simplicity, we consider the nonrelativistic case. The extension of the result to the relativistic case is straightforward.

The energy distribution of the fast electrons in the process accompanied by excitation of the electronic shell to the state $|\Phi_n\rangle$ with energy $\varepsilon_n \ll \varepsilon$ can be written, following (4.67), as

$$\frac{d\sigma_n}{d\varepsilon} = \frac{d\sigma}{d\varepsilon} S_n\,, \tag{4.67}$$

with $d\sigma/d\varepsilon$ the distribution of the fast electrons, with the final state of the electronic shell being $|\Phi_0\rangle$. Here S_n is determined by (3.94) and (3.95). The internal energy loss of the fast electron is defined as

$$\langle\varepsilon\rangle \;=\; \frac{\sum_n(\varepsilon_n^{(f)}-\varepsilon_0^{(f)})d\sigma_n/d\varepsilon}{d\sigma/d\varepsilon}, \tag{4.68}$$

with $\sum_n$ denoting the sum over the discrete spectrum and the integral over the continuum. Thus

$$\langle\varepsilon\rangle \;=\sum_n(\varepsilon_n^{(f)}-\varepsilon_0^{(f)})S_n \tag{4.69}$$

for every process in which the fast electron is ejected. In applications, one often needs the sum on the RHS, which includes only the states for which ε_n does not exceed a certain value

$$\varepsilon_n^{(f)} \;\le\; \varepsilon_{\max}^{(f)}. \tag{4.70}$$

If $\varepsilon_{\max}^{(f)}$ is larger than all the single-particle ionization potentials, we can obtain several general relations.

If the transitions in the electronic shell are treated in the SO approximation, we can obtain an expression for the energy loss $\langle\varepsilon\rangle_1$ in closed form. We write

$$\langle\varepsilon\rangle_1 \;=\sum_n(\varepsilon_n^{(f)}-\varepsilon_0^{(i)})S_n-\delta\varepsilon_0\,, \tag{4.71}$$

with $\delta\varepsilon_0=\varepsilon_0^{(f)}-\varepsilon_0^{(i)}$ the change of energy of the ground state. Since $S_n=T_n^{(0)2}$ decreases with ε_n as ε^{-4}, the first term on the RHS can be obtained by employing the closure condition. We may write $\sum_n(\varepsilon_n^{(f)}-\varepsilon_0^{(i)})S_n=\sum_n\langle\Psi_0|\Phi_n\rangle(\varepsilon_n^{(f)}-\varepsilon_0^{(i)})\langle\Phi_n|\Psi_0\rangle=\sum_n\langle\Psi_0|V|\Phi_n\rangle\langle\Phi_n|\Psi_0\rangle$, with $V=H_2-H_1$ the difference of the electronic shell Hamiltonians in their final and initial states. Thus

$$\langle\varepsilon\rangle_1 \;=\; \langle\Psi_0|V|\Psi_0\rangle-\delta\varepsilon_0\,. \tag{4.72}$$

Here the first term on the RHS represents the total energy transferred to the electronic shell. It includes the change in its ground state energy after ejection of the fast electron, which is subtracted by the second term. In the case of beta decay, we have $V=-\sum_k\alpha/r^{(k)}$.

Going beyond the SO approximation, we find that due to the FSI, the probability for excitation of the high-energy continuum states with $\varepsilon_n\gg I_b$ decreases as $1/\varepsilon_n^2$; see (4.59) and (4.60). The contribution of these states to the energy loss behaves as $\ln\varepsilon_{\max}$ and cannot be calculated by employing the closure condition. The FSI provide the contribution $\langle\varepsilon\rangle_2$ to the energy loss. The high-energy excited states with $I_b\ll\varepsilon_n\lesssim\varepsilon_{\max}$ determine

$$\langle\varepsilon\rangle_2^h \;=\; \xi_{ee}^2\,\frac{\langle r^{-2}\rangle}{2m}\,\ln\frac{\varepsilon_{\max}}{I_b}. \tag{4.73}$$

Here the upper index h indicates that this is the contribution of the high-energy excited states, $\xi_{ee}^2 = \alpha^2/v^2$, and $\langle r^{-2}\rangle = \langle\Psi_0|\sum_k r^{(k)-2}|\Psi_0\rangle$. The sum over the initial state bound electrons is carried out. The low-energy excited states with $\varepsilon \sim I_b$ provide the contribution $\langle\varepsilon\rangle_2^\ell \sim \xi_{ee}^2 I_b$. The upper index ℓ indicates that this is the contribution of the low-energy part of the spectrum. For each single-particle bound state $I_b \sim \langle r^{-2}\rangle/2m$, we can write

$$\langle\varepsilon\rangle_2 \;=\; \langle\varepsilon\rangle_2^h + \langle\varepsilon\rangle_2^\ell = \xi_{ee}^2\,\frac{\langle r^{-2}\rangle}{2m}\,\ln\frac{\varepsilon_{\max}}{B} \tag{4.74}$$

for the total FSI generated contribution to the energy loss, with $B \approx I_b$.

The total energy loss is thus

$$\langle\varepsilon\rangle \;=\; \langle\varepsilon\rangle_1 + \langle\varepsilon\rangle_2\,,$$

with the SO contribution $\langle\varepsilon\rangle_1$ given by (4.72). The parameter B should be calculated separately in each particular case. In Chap. 12, we shall calculate it for the tritium atom. For very large energies $\varepsilon_{\max}$ with $\ln(\varepsilon_{\max}/I_b) \gg 1$, one can put $B = I_b$. For smaller energies, the expression for $\langle\varepsilon\rangle_2$ with $B = I_b$,

$$\langle\varepsilon\rangle \;=\; \xi_{ee}^2\,\frac{\langle r^{-2}\rangle}{2m}\,\ln\frac{\varepsilon_{\max}}{I_b}, \tag{4.75}$$

can be used as an estimate that enables one to get a feel for the size of the effect. One can see that (4.74) and (4.75) can be expanded to the relativistic case. The largest value $\varepsilon_{\max}$ of the nonrelativistic kinetic energy $\varepsilon = p^2/2m$ should be replaced by the largest value of the kinetic energy $\hat{\varepsilon} = E - m$.

4.3 Kato Cusp Conditions

Here we analyze the electron wave functions in configurations in which the electron and nucleus of the atom or two electrons approach each other. The triple coalescence in the helium atom, whereby all three charged particles are at the same point, will be discussed in the next section.

4.3.1 Electron–Nucleus Coalescence Point

Consider an atomic electron moving in a certain central field described by the local potential $U(r) = U_{eN}(r) + U_{ee}(r)$, where the two terms stand for the interaction of the electron with the nucleus and with the other electrons. The wave equation for the radial part $R(r)$ of the wave function $\psi(\mathbf{r})$ describing an s electron is

$$R''(r) + \frac{2}{r}R'(r) - 2mU(r)R(r) \;=\; -2m\varepsilon R(r)\,. \tag{4.76}$$

Let us consider small $r \to 0$. In this limit, we can put $U(r) = U_{eN}(r) = -\alpha Z/r$, with Z the charge of the nucleus. Since $R(r)$ does not turn to zero at $r = 0$ [1], the last term on the LHS of (4.76) becomes singular. On the other hand, the RHS does not have singularities. The only way to make the two statements consistent is to assume that this singularity is compensated by that of the second term, i.e.,

$$\frac{dR(r)}{dr}|_{r=0} \;=\; -\eta R(r)_{r=0}\,, \tag{4.77}$$

as found by Kato [14]. Surprisingly, this observation was made thirty years after the Schrödinger equation was first written down. Note that for the ground state of a hydrogenlike ion, we have $R(r) = N_1 e^{-\eta r}$, and (4.77) holds for all values of r.

A nonzero value of the derivative $R'(r = 0)$ is the consequence of the singularity of the potential $U(r)$ at $r = 0$. Without singularities of $U(r)$, the wave function $R(r)$ would have been an analytic function of r^2, for which $dR(r)/dr = 2r\,dR(r)/dr^2$, and thus $dR(r)/dr = 0$ at $r = 0$. In our case, dR/dr^2 goes to infinity at $r = 0$, since $dR(r)/dr$ has a nonzero value expressed by (4.77), which is usually called the first Kato cusp condition. The Kato condition remains true if nonlocal exchange interactions are taken into account, since the exchange terms do not have singularities at $r = 0$.

A similar condition can be written for the single-particle states with orbital momentum $\ell \neq 0$. In this case, the wave equation for the radial function $R_\ell(r)$ is

$$R''_\ell(r) + \frac{2}{r}R'_\ell(r) - 2mU(r)R_\ell(r) - \frac{\ell(\ell+1)}{r^2}R_\ell(r) \;=\; -2m\varepsilon R_\ell(r). \tag{4.78}$$

One can write $R_\ell(r) = r^\ell \chi_\ell(r)$ with $\chi_\ell(0) \neq 0$. The RHS behaves as r^ℓ as $r \to 0$. The contributions proportional to $r^{\ell-2}$ at $\ell > 1$ on the LHS cancel identically, and cancellation of the terms of order $r^{\ell-1}$ takes place if

$$\frac{d\chi(r)}{dr}|_{r=0} \;=\; -\frac{\eta}{\ell+1}\chi(r=0)\,. \tag{4.79}$$

The Kato conditions are true also if the wave function ψ describes a single-particle state in a multielectron system. For the multielectron function $\Psi(\mathbf{r_1}, \mathbf{r_2}, \ldots)$, the first Kato condition takes the form

$$\frac{\partial \hat{\Psi}(\mathbf{r_1}, \mathbf{r_2}, \ldots)}{\partial r_1}|_{r_1=0} \;=\; -\eta \Psi(0, \mathbf{r_2}, \ldots), \tag{4.80}$$

where $\hat{\Psi}$ means that the function is averaged over the sphere with a small radius $r_1 \to 0$. This can be proved by expansion of the function $\Psi(\mathbf{r_1})$ (other variables are fixed) in partial waves near the origin. We write $\Psi(\mathbf{r_1}) = \sum_{\ell,m} \Psi_{\ell,m}$, where $\Psi_{\ell,m} = \sum_n c_{n\ell} R_{n\ell}(r_1) Y_{\ell m}(\Omega)$. Thus $\partial \Psi_{\ell,m}(\mathbf{r_1})/\partial r_1 = \sum_n c_{n\ell} R'_{n\ell}(r_1) Y_{\ell m}(\Omega)$. Now we check (4.80) for the partial waves $\Psi_{\ell,m}$, recalling that $R_{n\ell}(r_1) \sim r_1^\ell$. For $\ell = 0$, (4.79) can be obtained in the same way as for the single-particle case. For $\ell \geq 2$, both the RHS and LHS go to zero, since $R_{n\ell}(0) = R'_{n\ell}(0) = 0$. For $\ell = 1$, we have $\Psi_{1,m}(\mathbf{r}_1) = 0$, while $\partial \Psi_{1,m}(r_1)/\partial r_1|_{r_1=0} \sim Y_{\ell m}(\Omega)$, which goes to zero after integration over the sphere.

4.3.2 Electron–Electron Coalescence Point

We begin by considering an S state of a two-electron atom. The two-electron wave function Ψ can be considered as a function of three scalars $r_1 = |\mathbf{r_1}|$, $r_2 = |\mathbf{r_2}|$, and $r_{12} = |\mathbf{r_1} - \mathbf{r_2}|$, with $\mathbf{r_i}$ the positions of the electrons with respect to the nucleus. In the wave equation $H\Psi = \varepsilon\Psi$, the Hamiltonian

$$H \;=\; -\frac{\Delta_1}{2m} - \frac{\Delta_2}{2m} - \frac{\alpha Z}{r_1} - \frac{\alpha Z}{r_2} + \frac{\alpha}{|\mathbf{r_1} - \mathbf{r_2}|} \tag{4.81}$$

takes the form $H = H_1 + H_2 + H_{12}$ with

$$H_i = H_i^{(0)} + V_i; \quad H_i^{(0)} = \frac{-1}{2m}\Big(\frac{\partial^2}{\partial r_i^2} + \frac{2}{r_i}\frac{\partial}{\partial r_i}\Big); \quad V_i = \frac{-\alpha Z}{r_i}, \tag{4.82}$$

while

$$H_{12} = H_{12}^{(0)} + V_{12}; \quad H_{12}^{(0)} = \frac{-1}{m}\Big(\frac{\partial^2}{\partial r_{12}^2} + \frac{2}{r_{12}}\frac{\partial}{\partial r_{12}} + h_1\frac{\partial^2}{\partial r_1 \partial r_{12}} + h_2\frac{\partial^2}{\partial r_2 \partial r_{12}}\Big), \tag{4.83}$$

with

$$h_1 = \frac{r_1^2 - r_2^2 + r_{12}^2}{2r_1 r_{12}}; \quad h_2 = h_1(1 \leftrightarrow 2); \quad V_{12} = \frac{\alpha}{r_{12}}. \tag{4.84}$$

Cancellation of the singularities at $r_{12} = 0$ in the term H_{12} leads to the second Kato cusp condition for the spin–singlet states

$$\frac{\partial \Psi(r_1, r_2, r_{12})}{\partial r_{12}}|_{r_{12}=0} \;=\; \frac{\nu}{2}\Psi(r_1, r_2, r_{12} = 0); \quad \nu = m\alpha. \tag{4.85}$$

For the spin–triplet states, the wave function is space-antisymmetric. Hence $\Psi(r_{12} = 0) = 0$, and (4.85) means that expansion of the wave function $\Psi(r_{12})$ in powers of r_{12} begins with the terms r_{12}^2. This cusp condition holds for every multielectron system near the point of a two-electron coalescence.

For the two-electron states with total angular momentum $L \neq 0$, the requirement that the terms that have singularities at $r_{12} = 0$ cancel also leads to certain relations between the wave function and its derivative at this point. We shall not consider this case here, referring the reader to the original papers [15, 16].

4.3.3 A Wave Function Based on the Kato Cusp Condition

Here we consider the Schrödinger equation for the electron moving in the Yukawa potential

$$U(r) = -g\frac{e^{-\lambda r}}{r}; \quad \lambda, g > 0\,. \tag{4.86}$$

Initially, this potential was supposed to describe the nucleon interactions. However, the situation with strong interactions appeared to be more complicated. In recent decades, the Yukawa potential has been used in atomic physics, and numerical solutions have been obtained. This potential is weaker than the Coulomb potential with the same coupling constant g. At λ exceeding a certain critical value λ_c, the bound state in this field ceases to exist. We demonstrate that a simple wave function based only on the requirement to have proper asymptotics at small and large r reproduces the value of λ_c fairly well [17].

The wave equation describing the s state in the Yukawa potential is

$$R''(r) + \frac{2}{r}R'(r) + 2mg\frac{e^{-\lambda r}}{r}R(r) = -2m\varepsilon(g,\lambda)R(r)\,. \tag{4.87}$$

At $\lambda = 0$, the energy of the ground state is $\varepsilon = -mg^2/2$, since U is just the Coulomb potential of the nucleus with charge $Z = g/\alpha$ (recall that $\alpha = e^2 = 1/137$). Increasing λ, we make the field weaker, thus making $|\varepsilon|$ smaller. The value λ_c corresponds to the ground-state energy

$$\varepsilon(g,\lambda_c) = 0\,. \tag{4.88}$$

This equation determines the value of the ratio λ_c/g. This happens because the scale transformation $r' = \zeta r$ of (4.87) leads to the relation $\varepsilon(g,\lambda) = \zeta^2\varepsilon(g/\zeta, \lambda/\zeta)$. Putting $\zeta = g$ (for $g = \alpha$, this means that we express all parameters in atomic units), we obtain $\varepsilon(g,\lambda) = g^2\varepsilon(1,\lambda/g)$, and (4.88) can be written as

$$\varepsilon(1,\lambda_c^*) = 0 \quad \lambda_c^* = \lambda_c/g\,. \tag{4.89}$$

It was understood long ago that $\lambda_c/mg \approx 1$ [18]. Later, (4.88) was solved more accurately by numerical methods; see, e.g., [19].

We can write

$$\frac{\int dr\phi^*(r)H(r)\phi(r)}{\int dr\phi^*(r)\phi(r)} = \varepsilon \tag{4.90}$$

for the wave functions that provide the solution of (4.87), where H the Hamiltonian in the Yukawa field,

$$H = -\frac{1}{2m}\frac{d^2}{dr^2} + U(r)\,, \tag{4.91}$$

and the wave equation (4.87) is

$$H\phi = \varepsilon\phi; \quad \phi(r) \equiv rR(r)\,. \tag{4.92}$$

Now we try to build an approximate solution of (4.87) or (4.92). The large-distance behavior can be found by setting $U = 0$ on the LHS of (4.92). Thus at $r \to \infty$, we have

$$R(r) = \frac{e^{-\mu r}}{r}; \quad \mu = (-2m\varepsilon)^{1/2}. \tag{4.93}$$

However, this function does not satisfy the Kato condition (4.77), which requires $R' = -mgR$ at $r = 0$. Therefore, we add an exponential term to the numerator of (4.93):

$$R(r) = \frac{e^{-\mu r} - e^{-\kappa r}}{r}\,, \tag{4.94}$$

with $\kappa > \mu$, which does not change the asymptotics at large r and ensures the Kato condition if

$$\kappa = 2\eta - \mu; \quad \eta = mg. \tag{4.95}$$

Note that the binding energy is $\varepsilon(\lambda) = -\mu^2/2m$, while $\varepsilon(0) = -\eta^2/2m$.

Since the exponential factor on the RHS of (4.86) makes the field weaker, we see that $\mu < \eta$. Thus indeed, we have $\kappa > \mu$.

Now substituting the wave function (4.94) into (4.90) and putting $\varepsilon = 0$, we find that

$$\frac{\lambda_c}{\eta} = 2(\sqrt{\frac{e_h}{e_h - 1}} - 1); \quad e_h \equiv e^{1/2} \approx 1.6487. \tag{4.96}$$

This provides the value $\lambda_c/\eta \approx 1.1884$, which is very close to the value $\lambda_c/\eta = 1.1906$ found in [19].

The binding energy for $\lambda < \lambda_c$ can be expressed in terms of μ, λ, and η using (4.90). An explicit formula is given in [17]. Here we present results for $g = \alpha$. For $\lambda/m\alpha = 1.1$, i.e., in the vicinity of the critical value, this approach provides $\varepsilon = -2.189 \times 10^{-3}$ atomic units (a.u.), while numerical computations [19] lead to $\varepsilon = -2.287 \times 10^{-3}$ a.u. At smaller values of λ, the deviation diminishes. At $\lambda/m\alpha = 0.8$, for example, the function (4.94) gives $\varepsilon = -0.0444$ a.u., while $\varepsilon = -0.0447$ a.u. was obtained in [17].

4.4 Wave Functions of Helium and Heliumlike Ions

4.4.1 Three-Particle Coalescence Point

In the early days of quantum mechanics, there were attempts to calculate the binding energy of the ground state of the helium atom by employing approximate functions written as

$$\Psi_a(r_1, r_2, r_{12}) \;=\; e^{-a(r_1+r_2)}\, P(r_1, r_2, r_{12})\,, \tag{4.97}$$

with the parameter a and the coefficients of the polynomial $P(r_1, r_2, r_{12}) = \sum c_{ijk} r_1^i r_2^j r_{12}^k$ determined by the variational principle. The exponential drop at $r_{1,2} \to \infty$ is due to the behavior of the Hamiltonian H given by (4.82) as $r_1, r_2, r_{12} \to \infty$. In this limit, the interactions $-\alpha Z/r_i$ and α/r_{12} can be neglected, and the Hamiltonian can be written as a sum of two Hamiltonians for free noninteracting electrons $H = H_1^{(0)} + H_2^{(0)}$. The corresponding solution of the wave equation is $\Psi \sim e^{-a(r_1+r_2)}$, with $a = (-m\varepsilon)^{1/2}$.

However, by 1935, it was understood that the solution of the wave equation cannot take the form of (4.97), since it is unable to describe the configuration in which both electrons and the nucleus are at the same point [20]. Soon, Barlett [21] suggested that inclusion of the logarithmic terms might solve the problem. In 1954, Fock found an expansion of the helium wave function near the three-particle coalescence point involving the logarithmic terms and proved it to be capable of solving the Schrödinger equation [22].

The Fock expansion is written in hyperspherical coordinates, in which the limit $r_1, r_2, r_{12} \to 0$ corresponds to only one hyperradial variable $r = (r_1^2 + r_2^2)^{1/2} \to 0$. The two hyperangular variables can be chosen, e.g., as $\alpha_h = 2\tan^{-1}(r_2/r_1)$ and $\theta_h = \cos^{-1}((r_1^2 + r_2^2 - r_{12}^2)/2r_1r_2)$. In these variables, the expansion near $r = 0$ can be written as

$$\Psi(r, \alpha_h, \theta_h) \;=\; \sum_{k=0}^{\infty} \sum_{m}^{[k/2]} r^k (\ln r)^m \psi_{k,m}(\alpha_h, \theta_h), \tag{4.98}$$

where $[k/2]$ is the greatest integer that does not exceed $k/2$. It was proved in [22] that it is possible in principle to find all the functions $\psi_{k,m}(\alpha_h, \theta_h)$. It was shown in [23] that the radius of convergence of the Fock series is about half the radius of the helium atom. The terms of the expansion up to $k = 6$ are presented in [24].

While the expression on the RHS of (4.98) satisfies the Kato cusp conditions, each term of the expansion may not. For example, the contribution that includes the terms linear in r written in the variables r_i, r_{12} takes the form (in this subsection we are using the normalization $\Psi(0, 0, 0) = 1$)

$$\Psi_F^{(1)}(r_1, r_2, r_{12}) = 1 - \eta(r_1 + r_2) + \nu r_{12}/2; \quad \eta = m\alpha Z; \quad \nu = m\alpha, \tag{4.99}$$

for which (4.77) and (4.85) are not true. Thus the approximate wave functions can be improved either by ensuring the Kato cusp conditions or by including several terms of the Fock expansion.

4.4.2 Account of Analytical Properties in Approximate Wave Functions

The binding energy of the ground state of the helium atom that is measured with relative error 2×10^{-7} [25] is the standard test for the accuracy of the approximate wave functions. Today's computers make it possible to calculate the value with high accuracy without worrying about the analytical properties; see, e.g., [26]. However, Kato predicted in his 1957 paper [14] that proper treatment of singularities improves the rate of convergence of the computations with approximate functions.

Pioneering calculations employing the Fock expansion [27] confirmed the statement. The calculation of the binding energy of the helium atom with accuracy 10^{-9} required 52 parameters, while the same accuracy of the computations employing the functions represented by (4.97) needed 1078 parameters. It was noticed that the variational calculations of the coefficients of the functions involving the logarithmic terms mimic those of the Fock expansion [16].

If the approximate wave function is chosen in a reasonable form, the variational procedure finds the parameters that ensure the validity of the Kato cusp condition. For example, the wave function of the form

$$\Psi_a(r_1, r_2, r_{12}) \;=\; e^{-a(r_1+r_2)+br_{12}}\, P(r_1, r_2, r_{12}) \tag{4.100}$$

with four parameters satisfies the first Kato cusp condition with an accuracy of 6% [28, 29]. The error diminishes if a larger number of parameters is employed. The function given by (4.100), with 14 parameters, reproduces the binding energy with an accuracy of 3×10^{-5}. One needs 210 parameters to obtain this accuracy, employing functions of the form represented by (4.97).

Since the function [30]

$$\phi(r_1, r_2, r_{12}) \;=\; \exp\left(\Psi_F^{(1)}(r_1, r_2, r_{12})\right), \tag{4.101}$$

with $\Psi_F^{(1)}$ defined by (4.99), satisfies both Kato cusp conditions and reproduces the lowest term of the Fock expansion, it is reasonable to look for the solution of the wave equation in the form [31]

$$\Psi \;=\; \phi\Phi\,. \tag{4.102}$$

The function $\Phi(r_1, r_2, r_{12})$ satisfies the equation

$$H'\Phi \;=\; \varepsilon'\Phi\,. \tag{4.103}$$

Here $H' = H_1^{(0)} + H_2^{(0)} + H_{12}^{(0)} + V'$, where the free Hamiltonians $H_i^{(0)}$, $i = 1, 2$, are represented by (4.82), while the Hamiltonian $H_{12}^{(0)}$ is given by (4.83). The interactions are described by the operator

$$V' = \Big(\nu - \eta(h_1 + h_2)\Big)\frac{\partial}{\partial r_{12}} - \frac{\nu}{2}\left(h_1\frac{\partial}{\partial r_1} + h_2\frac{\partial}{\partial r_2}\right)$$

with $\eta = m\alpha Z$, $\nu = m\alpha$, and h_i determined by (4.84). The operator V' does not contain the Coulomb singularities. In (4.103), we have $\varepsilon' = \varepsilon + \eta^2/m + \nu^2/4m$.

The wave functions for the S states of the helium atom and of heliumlike ions in the form (4.101) were suggested in [31, 32]. The locally correct function Φ was obtained by the correlation function hyperspherical harmonic (CFHH) method. The function Φ includes the logarithmic terms. It behaves as $r_{1,2}^2$ as $r_{1,2} \to 0$ and as r_{12}^2 as $r_{12} \to 0$. The CFHH functions with a more complicated form of the function $\Psi_F^{(1)}$ also succeeded in describing the negative hydrogen ion H^-. Thus they satisfy both Kato cusp conditions. We shall employ the CFHH functions in Chap. 9.

4.4.3 *Approximate Wave Functions on Coalescence Lines*

On the electron–nucleus coalescence lines $r_1 = 0$ (or $r_2 = 0$) and on the electron–electron coalescence line $r_{12} = 0$, rather simple wave functions that respect the analytical properties appear to be capable of ensuring good accuracy. Assuming that on the electron–nucleus coalescence line where $r_1 = 0$, $r_2 = r_{12} = R$, the approximate wave function is given by $\Psi_a(0, R, R) = N\phi(0, R, R)$ with ϕ defined by (4.101), i.e., $\phi(0, R, R) = Ne^{-(\eta-\nu/2)R}$, we obtain

$$\Psi_a(R) \;=\; Ne^{-(\eta-\nu/2)R}\,. \tag{4.104}$$

Recall that we set $\nu = m\alpha$. Similarly, on the electron–electron coalescence line $r_{12} = 0, r_1 = r_2 = R$, we obtain the approximate function

$$\Psi_a(R) \;=\; Ne^{-2\eta R}\,. \tag{4.105}$$

In (4.104) and (4.105), we have $N = \Psi(0, 0, 0)$. The CFHH calculations provide $N = 0.07\nu^3$ for the ion H^- and $N = 1.55\nu^3$ for helium. At large Z, we can expect that N becomes close to its Coulomb value $N_C = \nu^3 Z^3/\pi$. In helium, the CFHH calculations give $r = 0.61$ for the ratio $r = N/N_C$, while they give $r = 0.83$ for $Z = 6$. These simple wave functions approximate accurate numerical functions with an error that does not exceed several percent. They work not only for heliumlike ions, but also for the negative hydrogen ion H^-.

To characterize the accuracy of these approximate functions, we introduce

$$y_{1,2}(R) \;=\; \log\left|\frac{\Psi_a(R)-\Psi_{CFHH}(R)}{\Psi_{CFHH}(R)}\right|,$$

where y_1 corresponds to the wave function (4.104) on the electron–nucleus coalescence line, while y_2 corresponds to the wave function (4.105) on the electron–electron coalescence line. The functions $y_{1,2}(R)$ for several bound systems containing two electrons are shown in Fig. 4.5.

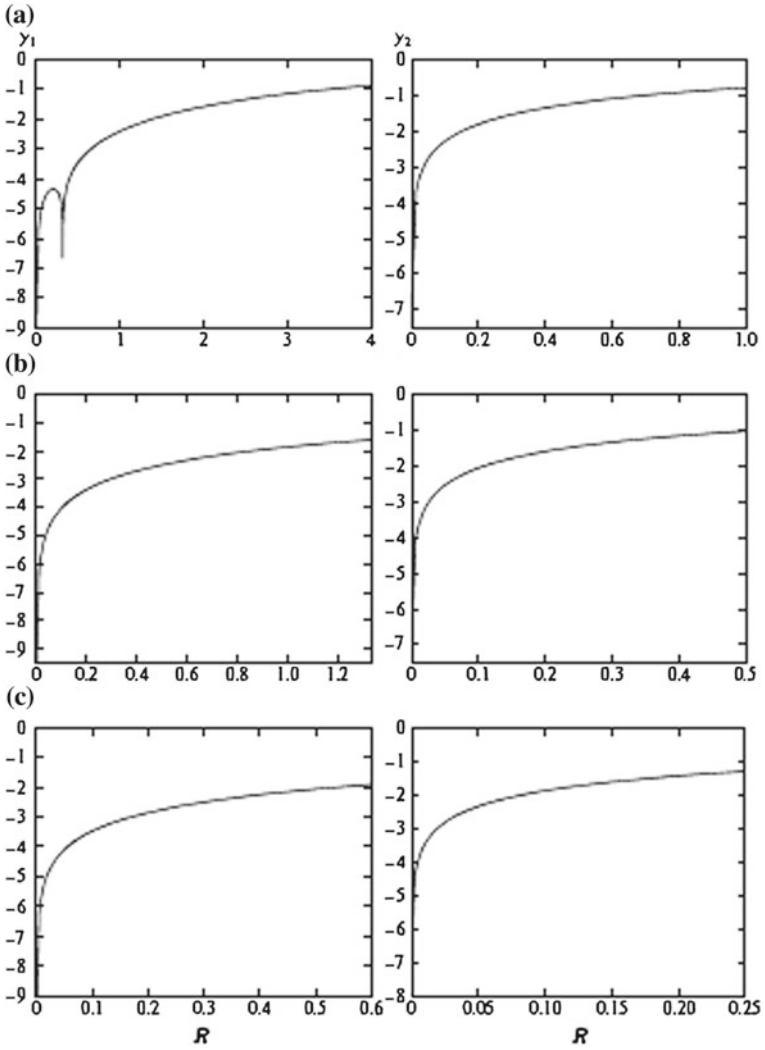

Fig. 4.5 The functions $y_{1,2}(R)$ for the negative ion H^- (**a**), for the helium atom (**b**), and for the ion Be^+ (**c**). The horizontal axis is for the distance R in atomic units [33]

The accuracy of the wave functions (4.104) and (4.105) becomes worse for large R, since they do not have proper asymptotics as $R \to \infty$. The accuracy is improved by applying the two-exponential representation [34] of the function $\Psi_a(R)$. For the approximate function on the electron–nucleus coalescence line, we have

$$\Psi_a(R) \equiv f(R) = C(e^{-\lambda R} + \gamma e^{-\beta R}), \tag{4.106}$$

where the second term is required to have proper asymptotics as $R \to \infty$. Two other parameters γ and λ are determined by the condition that at $R \to 0$, they should reproduce the terms of order R and R^2 of the Fock expansion. This means that the first and second derivatives in R of the function $f(R)$ should be the same as those of the Fock expansion on the electron–nucleus coalescence line:

$$\Psi_F^{(2)}(0, R, R) = 1 - \nu R\left(Z - \frac{1}{2}\right) + \frac{\nu^2 R^2}{12}\left(4Z^2 - 2Z(3 - \ln 2) + 1 - \frac{2\varepsilon}{\nu^2}\right) + 0(R^2). \tag{4.107}$$

The normalization coefficient C can be found, e.g., by computation of the value of the CFHH function at $R = 0$.

This provides two equations that connect the parameters λ, β, and γ. For example, equating the terms of order R in (4.106) and (4.107) provides

$$\lambda = (\eta - \beta - \nu/2)(1 + \gamma) + \beta. \tag{4.108}$$

Analysis involving the second derivatives in R shows that $\lambda > \beta$. Thus the first term on the RHS of (4.106) decreases more rapidly than the second one. Hence the asymptotic of $f(R)$ at large R is indeed determined by the second term on the RHS of (4.106) for every Z.

To find $f(R)$ at large R, note that in the limit $r_2 \gg r_1$, we can put $r_{12} = r_2$, and the variables r_1 and r_2 are separated in the wave equation

$$\left(\frac{-\Delta_1}{2m} + \frac{-\Delta_2}{2m} - \frac{\alpha Z}{r_1} - \frac{\alpha(Z-1)}{r_2}\right)\Psi = \varepsilon\Psi, \tag{4.109}$$

where ε is the energy of the ground state. For the helium atom, we have $\varepsilon \approx -78.9$ eV. Thus, the solution of (4.109) can be represented as $\Psi(\mathbf{r_1}, \mathbf{r_2}) = \psi_1(r_1)\psi_2(r_2)$. It is reasonable to look for the solution on the assumption that

$$\left(\frac{-\Delta_1}{2m} - \frac{\alpha Z}{r_1}\right)\psi(r_1) = -I_Z\psi(r_1),$$

with $I_Z = \eta^2/2m$. This means that the bound electron located at the point r_1 does not feel the electron that is far away at $r_2 \gg r_1$. Thus in the asymptotic $r_2 \to \infty$, we have $(-\Delta_2/2m)\psi_2(r_2) = (\varepsilon + I_Z)\psi(r_2)$ with $I_Z = \eta^2/2m$), providing $\psi_2(r_2) \sim e^{-kr_2}$ with $k = (-2\varepsilon m - \eta^2)^{1/2}$. Hence, $f(R) \sim e^{-kR}$ at large R, and we can put $\beta = k = (-2\varepsilon m - \eta^2)^{1/2}$. For the helium atom, we have $\lambda = 1.59\nu$, $\beta = 1.34\nu$, $\gamma = 0.55$, while $\eta = 2\nu$. Thus we can write

$$\Psi_a(R) \;=\; N_1 e^{-\lambda_1 R} + N_2 e^{-\lambda_2 R}\,. \tag{4.110}$$

For helium, the CFHH calculations provide $\lambda_1 = 1.59\nu$, $\lambda_2 = 1.34\nu$ and $N_1 = 0.65\nu^3$, $N_2 = 0.35\nu^3$.

A similar procedure was carried out for the wave function on the electron–electron coalescence line. The Fock expansion on this line is

$$\Psi_F^{(2)}(R,\,R,\,0) \;=\; 1 - 2\nu RZ + \nu^2 R^2\left(\frac{2Z}{3}\left(\frac{2}{\pi} - 1\right)\ln \nu R - \frac{2\varepsilon}{3} + \frac{5}{3}Z^2 - \frac{3Z}{10} + \frac{3}{2}\right), \tag{4.111}$$

and the parameters of this function are $\lambda = 5.54\nu$, $\beta = 3.41\nu$, $\gamma = 2.60$. The wave function on the electron–electron coalescence line takes the form (4.110). For the helium atom, we have $\lambda_1 = 5.54\nu$, $\lambda_2 = 3.41\nu$, while $N_1 = 0.38\nu^3$, $N_2 = 0.99\nu^3$.

References

1. L.D. Landau, E.M. Lifshits, *Quantum Mechanics. Nonrelativistic Theory* (Pergamon, N.Y., 1977)
2. J.D. Bjorken, S.D. Drell, *Relativistic Quantum Mechanics* (McGraw-Hill Book Company, 1964)
3. V.B. Berestetskii, E.M. Lifshits, L.P. Pitaevskii, *Quantum Electrodynamics* (Pergamon, N.Y., 1982)
4. V.G. Gorshkov, S.G. Sherman, JETP Lett. **17**, 374 (1973)
5. E.G. Drukarev, V.G. Gorshkov, A.I. Mikhailov, S.G. Sherman, Phys. Lett. A **46**, 467 (1974)
6. J.D. Bjorken, S.D. Drell, *Relativistic Quantum Fields* (McGraw-Hill Book Company, 1965)
7. H. Bethe, R. Pierls, Proc. R. Soc. Ser. A **148**, 146 (1935)
8. V. Adamyan, S. Tishchenko, J. Ph, Condens. Matter **18**, 186206 (2007)
9. G. Drukarev, Adv. Quantum Chem. **11**, 251 (1979)
10. H.A. Bethe, E.E. Salpeter, *Quantum Mechanics of One- and Two-Electron Atoms* (Dover Publications, NY, 2008)
11. B.H. Armstrong, Phys. Rev. **131**, 1132 (1963)
12. V.G. Gorshkov, F.F. Karpeshin, A.I. Mikhailov, JETP **41**, 444 (1975)
13. E.G. Drukarev, Nucl. Phys. A **541**, 131 (1992)
14. T. Kato, Commun. Pure Appl. Math. **10**, 151 (1957)
15. R.T. Pack, W.B. Brown, J. Chem. Phys. **45**, 556 (1966)
16. C.R. Myers, C.J. Umrigar, J.P. Sethna, J.D. Morgan III, Phys. Rev. A **44**, 5537 (1991)
17. E.Z. Liverts, E.G. Drukarev, V.B. Mandelzweig, Ann. Phys. (NY) **322**, 2958 (2007)
18. R.G. Sachs, M. Göppert-Mayer, Phys. Rev. **53**, 991 (1938)
19. O.A. Gomes, H. Ghacham, J.R. Mohallem, Phys. Rev. A **50**, 228 (1994)
20. J.H. Barlett Jr., J.J. Gibbons Jr., C.G. Dunn, Phys. Rev. **47**, 679 (1935)
21. J.H. Barlett, Phys. Rev. **51**, 661 (1937)
22. V. Fock, Izv. Akad. Nauk. SSSR, Ser. Fiz. **18**, 161 (1954); K. Nor. Vidensk. Selsk. Forth. **31**, 138 (1958), **31**, 145 (1958)
23. J.H. Macek, Phys. Rev. **160**, 170 (1967)
24. P.C. Abbot, E.N. Maslen, J. Phys. A **20**, 2043 (1987)
25. K.S.E. Eikema, Phys. Rev. Lett. **71**, 1690 (1993)
26. V.A. Korobov, Phys. Rev. A **66**, 024501 (2004)
27. A.M. Ermolaev, Vestn. Leningr. Univ. **14**, 48 (1958)
28. A.M. Ermolaev, G.B. Sochilin, Soviet Phys.-Doklady **9**, 292 (1964)

29. Z. Teng, R. Shakeshaft, Phys. Rev A. **47**, R3487 (1993)
30. P.C. Abbot, E.N. Maslen, J. Phys. B **19**, 1595 (1986)
31. M.I. Haftel, V.B. Mandelzweig, Ann. Phys. (NY) **189**, 29 (1989)
32. E.Z. Liverts, N. Barnea, Comput. Phys. Commun. **10**, 151 (2011)
33. E.G. Drukarev, E.Z. Liverts, M.Ya. Amusia, R. Krivec, V.B. Mandelzweig, JETP **103**, 690 (2006)
34. E.Z. Liverts, M.Ya, Amusia, R. Krivec, V.B. Mandelzweig. Phys. Rev. A. **73**, 012514 (2006)

Chapter 5
The Coulomb Field. Nonrelativistic Case

Abstract We introduce a technique that simplifies calculations in the Coulomb field. We apply it for calculating first- and second-order processes. In other words, we calculate the differential distributions and the total cross sections for the photoeffect and also for the Rayleigh scattering, for the Raman scattering, and for the Compton effect.

5.1 Wave Functions and Propagator

5.1.1 General Remarks

In this section, we carry out calculations for the nonrelativistic electron moving in the Coulomb field of a nucleus with charge Z. The potential energy of the electron in the Coulomb field is known to be

$$U(r) = \frac{-\alpha Z}{r}. \tag{5.1}$$

Such calculations are important, since it is instructive to understand how the processes go on or the mechanisms of the processes in the simplest case of the hydrogen atom or hydrogenlike ion before studying more complicated atoms. The nonrelativistic electron wave functions in the Coulomb field are available in closed form [1, 2]. The same refers to the nonrelativistic Coulomb Green function [3–5]. This enables us to investigate processes of higher order. The technique developed in [6–8] simplifies the calculations. Thus we can trace how the quantitative estimates are supported by the results of the calculations.

Moreover, the development of physics of multicharged ions requires their theoretical investigation. In such systems, the interaction between electrons can be included perturbatively, with the Coulomb field calculations as the zero-order approximation. This expansion in powers of $1/Z$ appears to be useful for a large number of systems, even in the case of helium.

E.G. Drukarev and A.I. Mikhailov, *High-Energy Atomic Physics*,
Springer Series on Atomic, Optical, and Plasma Physics 93,
DOI 10.1007/978-3-319-32736-5_5

In this chapter, we do not include relativistic corrections to the bound state wave functions, which are usually of order $(\alpha Z)^2$. Even for uranium, with $Z = 92$, we obtain $(\alpha Z)^2 = 0.45$, and the nonrelativistic results can be employed as estimates.

Recall that in every central field, the dependence of the nonrelativistic single-electron wave functions on the angular variables is separated in the spherical harmonics $Y_{\ell m}(\Omega)$, where ℓ and m are the angular momentum and its projection on a certain axis. The bound-state wave functions can be written as $\psi_{n\ell m}(\mathbf{r}) = R_{n\ell}(r)Y_{\ell m}(\Omega)$, with the radial parts $R_{n\ell}(r)$ satisfying the equation

$$-R''_{n\ell} - \frac{2}{r}R'_{n\ell} + \frac{\ell(\ell+1)}{r^2}R_{n\ell}(r) + 2mU(r)R_{n\ell} = 2m\varepsilon_{n\ell}R_{n\ell}\,. \tag{5.2}$$

It is due to the specifics of the Coulomb field that the energies of the bound states do not depend on ℓ:

$$\varepsilon_{n\ell} = \varepsilon_n = -\frac{\eta^2}{2m}\frac{1}{n^2}; \quad \eta = m\alpha Z\,. \tag{5.3}$$

This was found by Niels Bohr a century ago, before quantum mechanics was formulated.

For a continuum electron with energy $\varepsilon > 0$, the radial function $R_{\varepsilon\ell m}$ satisfies the equation similar to (5.2):

$$-R''_{\varepsilon\ell} - \frac{2}{r}R'_{\varepsilon\ell} + \frac{\ell(\ell+1)}{r^2}R_{\varepsilon\ell}(r) + 2mU(r)R_{\varepsilon\ell} = 2m\varepsilon R_{\varepsilon\ell}\,. \tag{5.4}$$

The continuum radial wave function is given by $R_{\varepsilon\ell} = Cr^{\ell-1}F(i\eta/p + \ell + 1, 2\ell + 2, -2ipr)$, where the last factor is the confluent hypergeometric function, $p = (2m\varepsilon)^{1/2}$, while C is the normalization constant. The radial wave function of the bound states $R_{n\ell}$ is described by the same equation with $\varepsilon = \varepsilon_n$, while the latter is given by (5.3).

In an alternative description of the continuum wave functions, we can choose the three components of the asymptotic momentum $\mathbf{p}$ as three independent quantum numbers. In this case, the continuum wave function $\psi_{\mathbf{p}}(\mathbf{r})$ is determined by the value of the asymptotic momentum $\mathbf{p}$. We shall employ both forms, focusing, however, on the latter one.

5.1.2 *Technique of Calculations*

The key point of the approach is to present the nonrelativistic electron wave functions in momentum space as the matrix elements of the Yukawa potential

$$V_{i\lambda}(r) = \frac{e^{-\lambda r}}{r}; \quad \langle \mathbf{r}_1|V_{i\lambda}|\mathbf{r}_2\rangle = V_{i\lambda}(r_1)\delta(\mathbf{r}_1 - \mathbf{r}_2), \tag{5.5}$$

in the plane wave basis

$$\langle \mathbf{f}_1|V_{i\lambda}|\mathbf{f}_2\rangle = \langle \mathbf{f}_2|V_{i\lambda}|\mathbf{f}_1\rangle = \int d^3r \frac{e^{-\lambda r}}{r} e^{-i\mathbf{f}_1\cdot\mathbf{r}+i\mathbf{f}_2\cdot\mathbf{r}} = \frac{4\pi}{(\mathbf{f}_2-\mathbf{f}_1)^2+\lambda^2}. \tag{5.6}$$

The definition of λ with the factor i appears to be convenient for calculations with the continuum wave functions. Integration over the momenta is carried out by employing the closure relation

$$\int \frac{d^3f}{(2\pi)^3}|\mathbf{f}\rangle\langle\mathbf{f}| \;=\; 1, \tag{5.7}$$

leading to the products of two Yukawa potentials. The latter can be evaluated as

$$-\frac{\partial}{\partial\lambda}V_{i\lambda}V_{i\tau} \;=\; V_{i(\lambda+\tau)}\,. \tag{5.8}$$

5.1.3 Wave Functions of the Bound States

We begin with the ground state $1s$. In the spatial representation, the wave function is

$$\psi_{1s}(\mathbf{r}) = N_1 e^{-\eta r}; \quad \eta = m\alpha Z, \quad N_1 = (\frac{\eta^3}{\pi})^{1/2}. \tag{5.9}$$

Presenting

$$e^{-\eta r} = -\frac{\partial V_{i\eta}(r)}{\partial\eta}, \tag{5.10}$$

we obtain for the wave function in momentum representation

$$\psi_{1s}(\mathbf{f}) \;=\; \frac{8\pi\eta N_1}{(f^2+\eta^2)^2}\,, \tag{5.11}$$

or

$$\psi_{1s}(\mathbf{f}) \;=\; N_1\Big(-\frac{\partial}{\partial\eta}\Big)\langle\mathbf{f}|V_{i\eta}|0\rangle\,. \tag{5.12}$$

The wave functions of the higher ns bound states in spatial representation are

$$\psi_{ns}(\mathbf{r}) = N_n\mathscr{L}_n^1(2\eta_n r)e^{-\eta_n r}; \quad \eta_n = m\alpha Z/n, \quad \eta_1 = \eta, \quad N_n = \Big(\frac{\eta_n^3}{\pi}\Big)^{1/2}, \tag{5.13}$$

with $\mathscr{L}_n^1$ the associated Laguerre polynomials. Thus there is a finite number $k < n$ of terms $(2\eta_n r)^k$. Since one can write

$$r^k e^{-\lambda r} \;=\; (-1)^k \frac{\partial^k e^{-\lambda r}}{(\partial\lambda)^k}\,, \tag{5.14}$$

the wave functions in momentum space can be written as

$$\psi_{ns}(\mathbf{f}) = N_n \mathscr{L}_n^1\Big(-2\lambda\frac{\partial}{\partial\eta_n}\Big)\Big(-\frac{\partial}{\partial\eta_n}\Big)\langle\mathbf{f}|V_{i\eta_n}|0\rangle; \quad \lambda=\eta_n\,, \tag{5.15}$$

while the derivatives do not act on λ. In particular, for the $2s$ state,

$$\psi_{2s}(\mathbf{f}) = N_2\Big(1+\eta_2\frac{\partial}{\partial\eta_2}\Big)\Big(-\frac{\partial}{\partial\eta_2}\Big)\langle\mathbf{f}|V_{i\eta_2}|0\rangle\,. \tag{5.16}$$

In order to illustrate how this technique works, let us prove the orthogonality of the functions ψ_{1s} and ψ_{2s}. We calculate

$$J = \int \frac{d^3 f}{(2\pi)^3}\psi_{1s}(\mathbf{f})\psi_{2s}(\mathbf{f}) = \tag{5.17}$$
$$= N_1 N_2\Big(-\frac{\partial}{\partial\eta_1}\Big)\Big(1+\eta_2\frac{\partial}{\partial\eta_2}\Big)\Big(-\frac{\partial}{\partial\eta_2}\Big)\int\frac{d^3 f}{(2\pi)^3}\langle 0|V_{i\eta_1}|\mathbf{f}\rangle\langle\mathbf{f}|V_{i\eta_2}|0\rangle.$$

The derivatives should be calculated at $\eta_1=\eta$; $\eta_2=\eta/2$.
This equality can be evaluated as

$$J = N_1 N_2\Big(-\frac{\partial}{\partial\eta_1}\Big)\Big(1+\eta_2\frac{\partial}{\partial\eta_2}\Big)\Big(-\frac{\partial}{\partial\eta_2}\Big)\langle 0|V_{i\eta_1}V_{i\eta_2}|0\rangle = \tag{5.18}$$

$$= N_1 N_2\Big(1+\eta_2\frac{\partial}{\partial\eta_2}\Big)\Big(-\frac{\partial}{\partial\eta_1}\Big)\langle 0|V_{i\eta_1+i\eta_2}|0\rangle; \quad \langle 0|V_{i\eta_1+i\eta_2}|0\rangle \;=\; \frac{4\pi}{(\eta_1+\eta_2)^2}.$$

The first equality is due to (5.7); the second follows from (5.8). Direct calculation of the derivatives indeed provides $J=0$.

We begin the representation of the functions with the orbital momentum $\ell\neq 0$, considering the $2p$ state. In the spatial representation, the function of the $2p$ state with the projection m of the orbital momentum $\ell=1$ is

$$\psi_{21m}(\mathbf{r}) \;=\; N_2\eta_2 r_m e^{-\eta_2 r}\,. \tag{5.19}$$

Writing

$$\mathbf{r} \;=\; -i\nabla_q e^{i(\mathbf{q}\cdot\mathbf{r})}|_{q=0}\,. \tag{5.20}$$

and carrying out the Fourier transformation, we obtain

$$\psi_{21m}(\mathbf{f}) \;=\; iN_2\eta_2\frac{\partial}{\partial\eta_2}(\nabla_q)_m\langle\mathbf{f}|V_{i\eta_2}|\mathbf{q}\rangle|_{\mathbf{q}=0}\,. \tag{5.21}$$

For every value of the orbital momentum ℓ, the angular part of the wave function is described by the spherical harmonics $Y_{\ell m}(\Omega) = P_\ell^m(\cos\theta)e^{im\phi}$. Here

$$P_\ell^m(t) \;=\; (1-t^2)^{m/2}\frac{d^m P_\ell}{(dt)^m}$$

are the associated Legendre functions, while P_ℓ are the Legendre polynomials. (the functions P_ℓ^m are often referred to as the "associated Legendre polynomials," although the functions $P_\ell^m(t)$ are not polynomials in general. However, $P_\ell^m(\cos\theta)$ are polynomials for even m). The radial part contains the factor r^ℓ. These are common features of the nonrelativistic bound state wave functions in a central field. Thus except for the Laguerre polynomials, the Coulomb wave function contains a factor of the form

$$A_{\ell m} \;=\; r^\ell\Big[\sin\theta e^{i\phi}\Big]^m\sum_{k=0}^{\ell-m}c_k^{\ell m}(\cos\theta)^k, \tag{5.22}$$

where $c_k^{\ell m}$ can be expressed in terms of the coefficients of the Legendre polynomials. Labeling the axis of quantization of the angular momentum by z, we can write in the terms of the cyclic components $q_0 = q_z$, $q_+ = -(q_x + iq_y)/\sqrt{2}$, $q_- = (q_x - iq_y)/\sqrt{2}$:

$$r^m[\sin\theta e^{i\phi}]^m = [i\nabla_+]^m e^{i\mathbf{q}\cdot\mathbf{r}}|_{q=0}; \quad r^k[\cos\theta]^k = [-i\nabla_0]^m e^{i\mathbf{q}\cdot\mathbf{r}}|_{q=0}.$$

Here the operator ∇ acts on the vector $\mathbf{q}$. Thus

$$A_{\ell m} \;=\; \Big(i\sqrt{2}\nabla_+\Big)^m\sum_{k=0}^{\ell-m}c_k^{\ell m}(-i\nabla_0)^k r^{\ell-k-m}e^{i\mathbf{q}\cdot\mathbf{r}}|_{q=0}\,. \tag{5.23}$$

Employing (5.14), we have

$$\psi_{n\ell m}(\mathbf{f}) = N_n(-1)^\ell\mathscr{L}_{n+\ell}^{2\ell+1}\Big(-2\eta_n\frac{\partial}{\partial\eta_n}\Big)\Big(i\sqrt{2}\nabla_+\Big)^m\cdot \tag{5.24}$$

$$\sum_{k=0}^{\ell-m}c_k^{\ell m}(-i\nabla_0)^k\frac{\partial^{\ell-k-m}}{\partial(\eta_n)^{\ell-k-m}}\langle\mathbf{f}|V_{i\eta_n}|\mathbf{q}\rangle|_{\mathbf{q}=0}.$$

5.1.4 *Wave Functions of the Continuum States*

The nonrelativistic Coulomb wave function with the asymptotic momentum $\mathbf{p}$ can be expressed in the spatial representation as

$$\psi_{\mathbf{p}}(\mathbf{r}) = N_p e^{i(\mathbf{p}\cdot\mathbf{r})} F(i\xi, 1, ipr - i\mathbf{p}\cdot\mathbf{r}); \quad \xi = \frac{\eta}{p}. \tag{5.25}$$

Here $F(i\xi, 1, ipr - i\mathbf{p}\cdot\mathbf{r})$ is the confluent hypergeometric function. The normalization factor $N_p = N(p)$ is given by (3.20). In the asymptotic $r \to \infty$, this wave function is the superposition of the plane wave and the outgoing wave.

In order to represent the wave function (5.25) in terms of the matrix element of the Yukawa potential, we employ the representation (see, e.g., [2])

$$F(a, b, z) = \frac{1}{2\pi i} \frac{\Gamma(1-a)\Gamma(b)}{\Gamma(b-a)} \oint \frac{dx}{x} \left(\frac{-x}{1-x}\right)^a (1-x)^{b-1} e^{zx}. \tag{5.26}$$

Here the contour of integration is a closed loop encircling the cut between the branch points $x = 0$ and $x = 1$ in the counterclockwise direction. This is true for every $\mathrm{Re}(b-a) > 0$. Now we can write the last factor on the RHS of (5.25) as

$$F(i\xi, 1, ipr - i\mathbf{p}\cdot\mathbf{r}) = \hat{J}_x e^{ix(pr - \mathbf{p}\cdot\mathbf{r})}, \tag{5.27}$$

where

$$\hat{J}_x = \frac{1}{2\pi i} \oint \frac{dx}{x} \left(\frac{-x}{1-x}\right)^{i\xi}, \tag{5.28}$$

with the same contour of integration as in (5.26).

Multiplying the integrand in (5.27) by $1 = -(e^{-\lambda r}/r)'$, where the prime denotes the derivative in λ at $\lambda = 0$, and carrying out the Fourier transformation, we obtain

$$\psi_{\mathbf{p}}(\mathbf{f}) = -N_p \frac{\partial}{\partial\lambda} \hat{J}_x \langle \mathbf{f} | V_{px+i\lambda} | \mathbf{p}(1-x) \rangle |_{\lambda=0}. \tag{5.29}$$

The integrand on the RHS decreases as $|x|^2$ as $|x| \to \infty$. Thus we can modify the contour of integration, which begins at the real axis at a certain $x_0 > 1$, makes a closed loop encircling the cut between the branch points $x = 0$ and $x = 1$ in the counterclockwise direction, runs along the positive real axis, makes a circle with $R \to \infty$, and returns to x_0 along the real axis. The only singularity of the integrand inside this contour is the pole at the point determined by the equality $(\mathbf{f} - \mathbf{p}(1-x))^2 = (px + i\lambda)^2$. The residue at this point provides

$$\psi_{\mathbf{p}}(\mathbf{f}) = \frac{8\pi\eta N_p}{A_0 B_0} \left(\frac{A_0}{B_0}\right)^{i\xi}; \quad A_0 = (\mathbf{p} - \mathbf{f})^2; \quad B_0 = f^2 - p^2. \tag{5.30}$$

The lower index 0 recalls that the values correspond to $\lambda = 0$. This is an explicit expression for the continuum wave function. However, (5.29) is more useful for applications.

5.1.5 Examples of Applications

This technique enables us to obtain easily the two expressions that were given above without derivation. In Sect. 3.1.4, we presented the result of calculation of the integral

$$X(\mathbf{q},\mathbf{Q}) = \int \frac{d^3 f}{(2\pi)^3}\psi^*_{\mathbf{p_2}}(\mathbf{f})\psi_{1s}(\mathbf{f}-\mathbf{q}); \quad \mathbf{Q}=\mathbf{q}-\mathbf{p_2}, \tag{5.31}$$

with the Coulomb wave functions. In Sect. 4.1.1, we gave expression for the integral

$$\Lambda(p_2,\mathbf{q}) = \int \frac{d^3\kappa}{(2\pi)^3}\psi_{1s}(\boldsymbol{\kappa})\frac{2m}{p_2^2-(\mathbf{q}+\boldsymbol{\kappa})^2+i\delta}; \quad \delta\to 0, \tag{5.32}$$

for the Coulomb function ψ_{1s}.

We begin with the latter case. Presenting

$$\frac{2m}{p_2^2-(\mathbf{q}+\boldsymbol{\kappa})^2+i\delta} = -\frac{m}{2\pi}\langle\boldsymbol{\kappa}|V_{p_2+i\delta}|-\mathbf{q}\rangle \tag{5.33}$$

and using (5.12), we can write

$$\Lambda(p_2,\mathbf{q}) = -\frac{m}{2\pi}N_1\Big(-\frac{\partial}{\partial\eta}\Big)\int\frac{d^3\kappa}{(2\pi)^3}\langle 0|V_{i\eta}|\boldsymbol{\kappa}\rangle\langle\boldsymbol{\kappa}|V_{p_2+i\delta}|-\mathbf{q}\rangle. \tag{5.34}$$

Employing the closure condition expressed by (5.7), we find

$$\Lambda(p_2,\mathbf{q}) = -\frac{m}{2\pi}N_1\Big(-\frac{\partial}{\partial\eta}\Big)\langle 0|V_{i\eta}V_{p_2+i\delta}|-\mathbf{q}\rangle. \tag{5.35}$$

Using (5.8), we obtain

$$\Lambda(p_2,\mathbf{q}) = -\frac{m}{2\pi}N_1\langle 0|V_{p_2+i\eta}|\mathbf{q}\rangle\,, \tag{5.36}$$

providing (4.14).

Turning to (5.31) and employing (5.29) for the continuum wave function, we obtain, similar to (5.34) and (5.35),

$$X(\mathbf{q},\mathbf{Q}) = -N_p N_1\frac{\partial}{\partial\eta}\hat{J}_x\langle\mathbf{q}|V_{p_2x+i\eta}|\mathbf{p}_2(1-x)\rangle\,. \tag{5.37}$$

The integrand on the RHS can be calculated in the same way as that in (5.29), leading to

$$\hat{J}_x \langle \mathbf{q}|V_{p_2 x+i\eta}|\mathbf{p}_2(1-x)\rangle = \frac{4\pi}{A}\left(\frac{A}{B}\right)^{i\xi}; \quad A = Q^2+\eta^2; \quad B = q^2-(p_2+i\eta)^2. \tag{5.38}$$

This provides the value given by (3.36) for $X(\mathbf{q},\mathbf{Q})$.

5.1.6 Green Function

While the Coulomb electron wave functions were obtained in the early days of quantum mechanics, a closed expression for the nonrelativistic Coulomb propagator was found only in the 1960s [3–5]. We mark only the milestones of the derivation, referring the reader to the paper [5] for the details.

The Green function can be written in the form

$$\langle \mathbf{r_2}|G(\varepsilon)|\mathbf{r}_1\rangle = \mathscr{S}_{n\ell m}\frac{\langle \mathbf{r}_2|\psi_{n\ell m}\rangle\langle\psi_{n\ell m}|\mathbf{r}_1\rangle}{\varepsilon-\varepsilon_n}, \tag{5.39}$$

where $\mathscr{S}$ denotes the sum over the states of the discrete spectrum and integration over the continuum states. Introducing

$$p^2 = 2m\varepsilon, \quad \zeta = \eta/p, \tag{5.40}$$

one can find that for $|\zeta|<1$,

$$\langle \mathbf{r_2}|G(\varepsilon)|\mathbf{r}_1\rangle = \hat{J}_y\langle \mathbf{r}_2|g(\varepsilon)|\mathbf{r}_1\rangle; \quad \hat{J}_y = 2m\int_1^\infty dy\left(\frac{y+1}{y-1}\right)^{i\zeta}, \tag{5.41}$$

with

$$\langle \mathbf{r}_2|g(\varepsilon)|\mathbf{r}_1\rangle = \frac{ip}{4\pi}e^{ipy(r_1+r_2)}J_0(\gamma u); \quad \gamma^2 = p^2(y^2-1); \quad u^2 = 2(r_1r_2+\mathbf{r}_1\cdot\mathbf{r}_2), \tag{5.42}$$

where J_0 is the Bessel function of order 0. For $|\zeta|<1$, the integral over y converges. The condition $|\zeta|<1$ is true for $|\varepsilon|>I_Z$, i.e., for $\varepsilon>I_Z$ and negative values of ε for which $-\varepsilon>I_Z$. In the former case, ζ is real, while in the latter it is purely imaginary.

We introduce a more complicated operator, which will be useful in applications:

$$\Upsilon(\varepsilon;\lambda_1,\lambda_2) = V'_{i\lambda_2}g(\varepsilon)V'_{i\lambda_1}, \tag{5.43}$$

where $V'_{i\lambda} = \partial V_{i\lambda}/\partial\lambda$. Since

$$V'_{i\lambda}|_{\lambda=0} = -1, \tag{5.44}$$

we can write

$$g(\varepsilon) = \Upsilon(\varepsilon;0,0). \tag{5.45}$$

The Green function can be viewed as a special case of the operator

$$\mathscr{G}(\varepsilon;\lambda_1,\lambda_2) \;=\; V'_{i\lambda_2} G(\varepsilon) V'_{i\lambda_1}, \tag{5.46}$$

i.e.,

$$G(\varepsilon) \;=\; \mathscr{G}(\varepsilon;0,0)\,, \tag{5.47}$$

and the matrix element in spatial representation can be written, similar to (5.41),

$$\langle \mathbf{r_2}|\mathscr{G}(\varepsilon;\lambda_1,\lambda_2)|\mathbf{r}_1\rangle = \hat{J}_y \langle \mathbf{r}_2|\Upsilon(\varepsilon;\lambda_1,\lambda_2))|\mathbf{r}_1\rangle\,. \tag{5.48}$$

Since

$$-\langle \mathbf{r}|V'_{i\lambda}|\mathbf{r}'\rangle \;=\; e^{-\lambda r}\delta(\mathbf{r}-\mathbf{r}')\,, \tag{5.49}$$

we have

$$\langle \mathbf{r}_2|\Upsilon(\varepsilon;\lambda_1,\lambda_2)|\mathbf{r}_1\rangle = \frac{ip}{4\pi} e^{i(z_1 r_1 + z_2 r_2)} J_0(\gamma u); \quad z_i = py + i\lambda_i\,, \tag{5.50}$$

with γ and u defined by (5.42).

In order to obtain the momentum space matrix element $\langle \mathbf{f}_2|\Upsilon|\mathbf{f}_1\rangle$, one can employ an integral representation of the Bessel function (see, e.g., [9]):

$$J_0(v) \;=\; \frac{1}{2\pi i}\oint \frac{dt}{t} e^{t-\frac{v^2}{4t}}\,, \tag{5.51}$$

with the contour running around the point $t = 0$. Thus

$$\langle \mathbf{r}_2|\Upsilon(\varepsilon;\lambda_1,\lambda_2)|\mathbf{f}_1\rangle = \int d^3 r_1 e^{i(\mathbf{f}_1\cdot\mathbf{r}_1)} \langle \mathbf{r}_2|\Upsilon(\varepsilon;\lambda_1,\lambda_2))|\mathbf{r}_1\rangle = \tag{5.52}$$

$$= -ipe^{iz_2 r_2}\left(\frac{-\partial}{\partial\lambda_1}\right)\frac{1}{z_1^2 - f_1^2}\frac{1}{2\pi i}\oint \frac{dte^t}{t - iA(\mathbf{f_1}\mathbf{r_2} - z_1 r_2)},$$

with $z_i = py + i\lambda_i$ $(i = 1, 2)$, $A = \gamma^2/(z_1^2 - f_1^2)$, $\gamma^2 = p^2(y^2 - 1)$. The integral is determined by the pole of the integrand, providing

$$\langle \mathbf{r}_2|\Upsilon(\varepsilon;\lambda_1,\lambda_2)|\mathbf{f}_1\rangle = \hat{\Gamma}\frac{e^{i(z_2 - z_1 A)r_2} e^{i(\mathbf{f}_1\cdot\mathbf{r}_2)A}}{z_1^2 - f_1^2}; \quad \hat{\Gamma} = \frac{\partial}{\partial\lambda_1}\frac{\partial}{\partial\lambda_2}\,. \tag{5.53}$$

This enables us to calculate

$$\langle \mathbf{f}_2|\Upsilon(\varepsilon;\lambda_1,\lambda_2)|\mathbf{f}_1\rangle \;=\; -ip\hat{\Gamma}\frac{\langle \mathbf{f}_2|V_{z_2 - z_1 A}|\mathbf{f}_1 A\rangle}{z_1^2 - f_1^2} \tag{5.54}$$

and

$$\langle \mathbf{f_2}|\mathscr{G}(\varepsilon;\lambda_1,\lambda_2)|\mathbf{f}_1\rangle \;=\; -ip\hat{J}_y\hat{\Gamma}\frac{\langle \mathbf{f}_2|V_{z_2-z_1A}|\mathbf{f}_1A\rangle}{z_1^2-f_1^2}\,. \tag{5.55}$$

In (5.54) and (5.55), one can make permutations $\mathbf{f}_1, z_1 \longleftrightarrow \mathbf{f}_2, z_2$.

We can represent the matrix element $\langle \mathbf{f}_2|\mathscr{G}(\varepsilon)|\mathbf{f}_1\rangle$ in symmetric form. Direct evaluation of the RHS of (5.54) provides

$$\langle \mathbf{f}_2|\Upsilon(\varepsilon;\lambda_1,\lambda_2)|\mathbf{f}_1\rangle = -i\hat{\Gamma}\frac{4\pi p}{\gamma^4+2(\mathbf{f}_2\cdot\mathbf{f}_1-z_1z_2)\gamma^2+(f_1^2-z_1^2)(f_2^2-z_2^2)}. \tag{5.56}$$

Replacing integration over y in the operator $\hat{J}_y$ by integration over $t=(y+1)/(y-1)$, we obtain another form of the matrix element, namely

$$\langle \mathbf{f}_2|\Upsilon(\varepsilon;\lambda_1,\lambda_2)|\mathbf{f}_1\rangle \;=\; i16\pi mp\hat{\Gamma}\int_1^\infty dt\frac{t^{i\zeta}}{at^2-2bt+\bar{a}}\,. \tag{5.57}$$

Here

$$\begin{gathered} a=\alpha_1\alpha_2;\quad \alpha_j=f_j^2-(p+i\lambda_j)^2;\quad \bar{a}=\bar{\alpha}_1\bar{\alpha}_2;\quad \bar{\alpha}_j=f_j^2-(p-i\lambda_j)^2; \\ b \;=\; \beta_1\beta_2-4p^2(\mathbf{f}_1\cdot\mathbf{f}_2);\quad \beta_j \;=\; p^2+f_j^2+\lambda_j^2. \end{gathered} \tag{5.58}$$

For $\varepsilon>0$, p is real, and $\bar{a}=a^*$. Due to (5.47), the matrix element of the Green function in momentum representation is

$$\langle \mathbf{f}_2|G(\varepsilon)|\mathbf{f}_1\rangle \;=\; \langle \mathbf{f}_2|\mathscr{G}(\varepsilon;0,0)|\mathbf{f}_1\rangle. \tag{5.59}$$

This can be demonstrated directly, since (5.44) leads to

$$-\langle \mathbf{f}|V'_{i\lambda}|\mathbf{f}'\rangle|_{\lambda=0} \;=\; \delta(\mathbf{f}-\mathbf{f}'), \tag{5.60}$$

and thus

$$\begin{gathered} \langle \mathbf{f}_2|\mathscr{G}(\varepsilon;0,0)|\mathbf{f}_1\rangle=\int\frac{d^3f_1'}{(2\pi)^3}\frac{d^3f_2'}{(2\pi)^3}\langle \mathbf{f}_2|V'_{i\lambda_2}|\mathbf{f}_2'\rangle\langle \mathbf{f}_2'|G(\varepsilon)|\mathbf{f}_1'\rangle\langle \mathbf{f}_1'|V'_{i\lambda_1}|\mathbf{f}_1\rangle|_{\lambda_{1,2}=0}= \\ \langle \mathbf{f}_2|G(\varepsilon)|\mathbf{f}_1\rangle. \end{gathered} \tag{5.61}$$

Thus for the matrix elements

$$\mathscr{T}(\varepsilon;\lambda_1,\lambda_2) \;=\; V_{i\lambda_2}G(\varepsilon)V_{i\lambda_1}\,, \tag{5.62}$$

we can write

$$\langle \mathbf{f_2}|\mathscr{T}(\varepsilon;\lambda_1,\lambda_2)|\mathbf{f}_1\rangle = -ip\hat{J}_y \frac{\langle \mathbf{f}_2|V_{z_2-z_1A_1}|\mathbf{f}_1A_1\rangle}{z_1^2-f_1^2} = -ip\hat{J}_y \frac{\langle \mathbf{f}_2A_2|V_{z_1-z_2A_2}|\mathbf{f}_1\rangle}{z_2^2-f_2^2};$$
$$A_i = \frac{p^2(y^2-1)}{z_i^2-f_i^2}. \tag{5.63}$$

It is important that in the first equality, the dependence on $\mathbf{f}_2$ is contained only in the state $\langle \mathbf{f}_2|$, while in the second one, dependence on $\mathbf{f}_1$ is contained only in the state $|\mathbf{f}_1\rangle$. Also, similar to (5.57), we have

$$\langle \mathbf{f}_2|\mathscr{T}(\varepsilon;\lambda_1,\lambda_2)|\mathbf{f}_1\rangle = i16\pi mp\int_1^\infty dt \frac{t^{i\zeta}}{at^2-2bt+\bar{a}}. \tag{5.64}$$

We shall see that these expressions will be useful in applications.

Note that for $|\zeta|<1$, the matrix element on the LHS of (5.57) can be written in terms of the hypergeometric functions. One can write

$$I(\zeta) = \int_1^\infty dt \frac{t^{i\zeta}}{at^2-2bt+\bar{a}} = \frac{1}{a}\cdot\frac{X(i\zeta,z_+)-X(i\zeta,z_-)}{z_+-z_-}, \tag{5.65}$$

where $z_\pm = (b\pm\sqrt{b^2-a\bar{a}})/a$ are the roots of the denominator of the integrand, while

$$X(i\zeta,z) = \int_1^\infty dt \frac{t^{i\zeta}}{t-z} = -\frac{{}_2F_1(1,-i\zeta,1-i\zeta,z)}{i\zeta}. \tag{5.66}$$

Thus (5.57) can be represented as

$$\langle \mathbf{f}_2|\Upsilon(\varepsilon;\lambda_1,\lambda_2)|\mathbf{f}_1\rangle = \frac{-16\pi mp^2}{\eta}\cdot\frac{{}_2F_1(1,-i\zeta,1-i\zeta,z_+)-{}_2F_1(1,-i\zeta,1-i\zeta,z_-)}{a(z_+-z_-)}. \tag{5.67}$$

A more rigorous analysis [4, 5] shows that this form for the matrix element is true also for $-I_Z<\varepsilon<0$. In this case, ζ is purely imaginary, and the real parameter $\chi = i\zeta$ changes in the interval $0<\chi<\infty$. The RHS of (5.67) has poles at $\chi = n$ $(n=1,2,3,\ldots)$ since the hypergeometric functions ${}_2F_1(a,b,c,z)$ has poles in parameter c at $c=0,1,2,\ldots$ corresponding to the bound states. More explicitly, one can write for $Im\zeta>0$,

$$X(i\zeta,z) = -\frac{1}{i\zeta}+zX(i\zeta-1,z) = -\sum_{k=0}^{N-1}\frac{1}{i\zeta-k}+z^NX(i\zeta-N,z). \tag{5.68}$$

At $Im\zeta \leq 0$, (5.68) is true for the function $X(i\zeta, z) = -{}_2F_1(1, -i\zeta, 1 - i\zeta, z)/(i\zeta)$ (see (5.67)) and $N > \chi$. As expected, the matrix element has poles at $\chi = k$ ($k = 1, 2, 3, \dots$) corresponding to the bound states.

5.2 Photoeffect

This effect is the lowest-order process of interaction between the photon and a bound electron. The photon interacts with the bound electron, moving it to continuum. The process is caused by the first-order term of the Hamiltonian $H = -e(\mathbf{A} \cdot \mathbf{f})/m$ with $\mathbf{A}$ the vector potential of the electromagnetic field; $\mathbf{f}$ is the electron momentum. The amplitude of the process is

$$F_{ph} \;=\; N(\omega)\langle\psi_{\mathbf{p}}|\gamma|\psi_i\rangle\;; \quad N(\omega) = \sqrt{\frac{4\pi\alpha}{2\omega}},. \tag{5.69}$$

Here ψ_i and $\psi_{\mathbf{p}}$ are the nonrelativistic Coulomb functions of the initial bound state and final continuum state, $\gamma = \mathbf{e} \cdot \mathbf{f}/m$ is the vertex of the electron–photon interaction in the nonrelativistic approximation, and $\mathbf{e}$ is the polarization vector of the absorbed photon, $\mathbf{e} \cdot \mathbf{k} = 0$. We can write

$$F_{ph} \;=\; N(\omega)\int \frac{d^3 f}{(2\pi)^3}\langle\psi_{\mathbf{p}}|\mathbf{f}\rangle\frac{\mathbf{e}\cdot\mathbf{f}}{m}\langle\mathbf{f}-\mathbf{k}|\psi_i\rangle\,. \tag{5.70}$$

Recall that in our system of units, the photon energy is $\omega = k$. We consider the photoionization of the ground state electron in the Coulomb field; the final state is the continuum electron with asymptotic momentum $\mathbf{p}$. Its energy is $\varepsilon = \omega_1 - I_Z = p^2/2m$. Our calculations are carried out for a single-electron ion. In the case of a complete K shell, one should multiply the result by the factor 2, corresponding to the number of electrons. The electron wave functions are described by (5.12) and (5.29). Integration over momenta $\mathbf{f}$ can be carried out using the relation

$$\mathbf{f}\Big(-\frac{\partial}{\partial\mu}\Big)\langle\mathbf{k}|V_{i\mu}|\mathbf{f}\rangle = \hat{\mathbf{h}}(\mu)\langle\mathbf{k}|V_{i\mu}|\mathbf{f}\rangle; \quad \hat{\mathbf{h}}(\mu) = \mu\nabla_k - \mathbf{k}\frac{\partial}{\partial\mu}\,, \tag{5.71}$$

which is true for every μ. Thus

$$\mathbf{f}\psi_{1s}(\mathbf{f}-\mathbf{k}) = N_1\mathbf{f}(-\frac{\partial}{\partial\eta})\langle\mathbf{k}|V_{i\eta}|\mathbf{f}\rangle = N_1\hat{\mathbf{h}}(\eta)\langle\mathbf{k}|V_{i\eta}|\mathbf{f}\rangle. \tag{5.72}$$

Since $\mathbf{e} \cdot \mathbf{k} = 0$, we can put

$$\hat{\mathbf{h}}(\eta) \;=\; \eta\nabla_k. \tag{5.73}$$

We obtain, employing (5.38),

$$F_{ph} = N(\omega)N_p N_1 \frac{\mathbf{e}\nabla_k}{m}\frac{4\pi\eta}{A}\left(\frac{A}{B}\right)^{i\xi}, \tag{5.74}$$

with $A = (\mathbf{k}-\mathbf{p})^2+\eta^2$, $B = k^2-(p+i\eta)^2$. In other words,

$$F_{ph} = \mathbf{e}\mathbf{n}_\mathbf{p} M; \quad \mathbf{n}_p = \frac{\mathbf{p}}{p}; \quad M = N(\omega)N_1 N_p \frac{p(1-i\xi)}{m}T(\eta); \tag{5.75}$$

$$T(\eta) = \frac{8\pi\eta}{A^2}\left(\frac{A}{B}\right)^{i\xi}.$$

The differential cross section

$$d\sigma_{ph}^{nr} = \frac{mp}{\pi}|F_{ph}|^2\frac{d\Omega}{4\pi} \tag{5.76}$$

after the averaging over the photon polarizations can be written as

$$d\sigma_{ph}^{nr} = \frac{mp}{2\pi}|M|^2(1-t^2)\frac{d\Omega}{4\pi}; \quad t = \mathbf{k}\cdot\mathbf{p}/\omega_1 p. \tag{5.77}$$

Thus the angular distribution vanishes if the direction of the electron momentum $\mathbf{p}$ is the same as that of the photon momentum $\mathbf{k}$. Since $k \ll max(p,\eta)$, one can put $k=0$ on the RHS of (5.75) after calculation of the gradient. In this limit, the amplitude M does not depend on the angular variables. Its expansion in powers of ω^2/η^2 (at $\omega \sim I_Z$) or in powers of ω^2/p^2 (at larger values of ω) provides terms of order $(\alpha Z)^2$ and ε/m respectively. Thus they are of the same order of magnitude as the relativistic corrections and cannot be included in nonrelativistic calculation of the cross section. However, inclusion of the terms linear in $\mathbf{k}$ can be useful for analysis of the contributions of the higher multipoles.

The total cross section of photoionization of the $1s$ state is thus

$$\sigma_{ph}^{nr} = \frac{2^9\pi^2}{3}\alpha r_0^2\frac{1}{Z^2}\left(\frac{I_Z}{\omega}\right)^4 \cdot \frac{\exp\left(-4\xi\arctan(1/\xi)\right)}{1-\exp\left(-2\pi\xi\right)}. \tag{5.78}$$

Recall that $r_0 = 1/m\alpha$ is the Bohr radius. In the high-energy limit $\omega \gg I_Z$, one can put $1-\exp(-2\pi\xi) = 2\pi\xi$, which yields the well-known behavior $\sigma_{ph} \sim \omega^{-7/2}$. We shall discuss the possibility and limits of the asymptotic analysis in Chap. 7. Note that this can be obtained without calculations and for any binding field. Indeed, in this limit, a large momentum $\mathbf{q} = \mathbf{k}-\mathbf{p}$ is transferred to the nucleus, and $q \approx p \gg \eta$. It is transferred by the initial electron, and the amplitude contains the factor $\psi_i(p)(\mathbf{e}\cdot\mathbf{p})$. Following the analysis of Chap. 2, we find that $\psi(p) \sim 1/p^4$. This estimate leads to the asymptotic law.

Note that the approach developed in Sect. 5.2 enables us to obtain the cross section of photoionization of any bound state with quantum numbers n, ℓ, m. The amplitude M in (5.75) should be replaced by

$$M = N(\omega)N_n N_p \frac{p(1-i\xi)}{m} T_{n\ell m}; \quad T_{n\ell m} = \Gamma_{n\ell m} T(\eta_n), \tag{5.79}$$

with $\Gamma_{n\ell m}$ certain differential operators. In particular, for $2s$ and $2p$ electrons, we can write, following Sect. 5.2,

$$\Gamma_{200} = (1 + \eta_2 \frac{\partial}{\partial \eta_2}); \quad \Gamma_{21m} = i\eta_2 (\nabla_k)_m \,. \tag{5.80}$$

5.3 Second Order Processes I

5.3.1 General Analysis

The nonrelativistic Hamiltonian of interaction between photons and electrons is

$$H = -e\frac{\mathbf{A}\cdot\mathbf{f}}{m} + e^2\frac{\mathbf{A}^2}{2m}\,. \tag{5.81}$$

To obtain the amplitude of a second-order scattering process, one should include the first term of the Hamiltonian in the second order of perturbation theory. This provides the pole terms shown in Fig. 5.1a, b. The second term should be included in the first order, providing the "seagull" contribution known also as the A^2 term. It is shown in Fig. 5.1c. One can write general expressions for every binding field.

There are two pole terms. In the first, shown in Fig. 5.1a, the initial electron absorbs the photon with momentum $\mathbf{k}_1$ and polarization $\mathbf{e}_1$. This is followed by ejection of the photon with momentum $\mathbf{k}_2$ and polarization $\mathbf{e}_2$. In the second, illustrated in Fig. 5.1b,

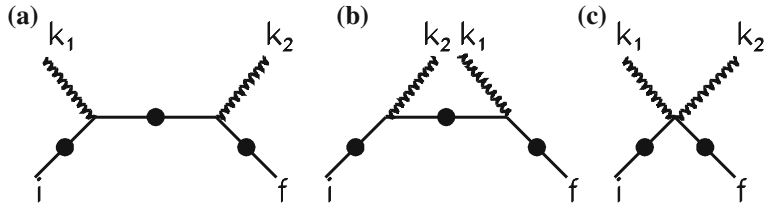

Fig. 5.1 The Feynman diagrams for a second-order process. *Helix lines* denote the absorbed photon with momentum $\mathbf{k}_1$ and the scattered photon with momentum $\mathbf{k}_2$. The *solid lines* stand for electrons; the *dark blobs* denote the binding field. The diagrams *a* and *b* illustrate the pole terms, and diagram *c* is for the seagull term

ejection of the photon with momentum $\mathbf{k}_2$ occurs before absorption of the photon with momentum $\mathbf{k}_1$. The pole terms for the process in which the initial state of the electron is $|\psi_i\rangle$, while the final state electron is $\langle\psi_f|$, can be represented as

$$F_a = N(\omega_1)N(\omega_2)\int \frac{d^3f_1}{(2\pi)^3}\frac{d^3f_2}{(2\pi)^3}\langle\psi_f|\mathbf{f}_2-\mathbf{k}_2\rangle\frac{\mathbf{e}_2^*\cdot\mathbf{f}_2}{m}\langle\mathbf{f}_2|G(p_a)|\mathbf{f}_1\rangle\frac{\mathbf{e}_1\cdot\mathbf{f}_1}{m}\langle\mathbf{f}_1-\mathbf{k}_1|\psi_i\rangle. \tag{5.82}$$

Here $p_a = \sqrt{2m(\omega_1 - I_i)}$, I_i is the potential of ionization of the initial state, $I_i = I_Z$ for the $1s$ electron in the Coulomb field, and

$$F_b = N(\omega_1)N(\omega_2)\int \frac{d^3f_1}{(2\pi)^3}\frac{d^3f_2}{(2\pi)^3}\langle\psi_f|\mathbf{f}_2+\mathbf{k}_1\rangle\frac{\mathbf{e}_1\cdot\mathbf{f}_2}{m}\langle\mathbf{f}_2|G(p_b)|\mathbf{f}_1\rangle\frac{\mathbf{e}_2^*\cdot\mathbf{f}_1}{m}\langle\mathbf{f}_1+\mathbf{k}_2|\psi_i\rangle, \tag{5.83}$$

with $p_b = i\sqrt{2m(\omega_2 + I_i)}$.

The seagull term can be written immediately as

$$F_c = \frac{\mathbf{e}_1\cdot\mathbf{e}_2^*}{m}N(\omega_1)N(\omega_2)\int\frac{d^3f}{(2\pi)^3}\langle\psi_f|\mathbf{f}\rangle\langle\mathbf{f}-\mathbf{q}|\psi_i\rangle;\quad \mathbf{q}=\mathbf{k}_1-\mathbf{k}_2. \tag{5.84}$$

The total amplitude is

$$F = F_a + F_b + F_c\,. \tag{5.85}$$

We shall carry out the calculations for the $1s$ state of the Coulomb field as the initial state, discussing also the general features of the processes that are common to all binding fields.

There are three characteristic values of the photon energy $\omega_1 = k_1$. These are the electron binding energy $I_Z = \eta^2/2m$; the energy $\omega = \eta$ at which the wavelength of the photon is equal to the size of the bound state; and the relativistic scale $\omega = m$. Recall that in the case of the hydrogen atom, $I_1 = 13.6\,\text{eV}$, $\eta = 3.7\,\text{keV}$. At $\omega \lesssim \eta$, the transferred momentum $q \le 2\omega \le \eta$. The cases $\omega \sim I_Z$, $I_Z \ll \omega \ll \eta$, and $\omega \sim \eta$ need separate analysis. We shall consider also the high-energy nonrelativistic asymptotics $\eta \ll \omega_1 \ll m$. To have a picture for every binding field, one should just replace η by the average binding momentum μ.

In the following sections, we consider elastic scattering, i.e., $|\psi_i\rangle = |\psi_f\rangle = |\psi\rangle$. The equations will be written for one electron in each state. If there are two electrons, the amplitudes are summed coherently, and the equations for the differential distributions and for the cross sections should be multiplied by the factor 4.

5.3.2 Amplitude of Rayleigh Scattering

We begin our investigation of the processes of the second order in photon–electron interactions by considering the scattering of photons on atoms in which the bound

electrons do not undergo transitions. The photon can scatter on the bound electrons. It can also scatter on the nucleus. There can also be scattering in the Coulomb field (Delbrück scattering). We shall discuss contributions of the two latter channels in Sect. 5.3.3. For the energies considered in this subsection, scattering on the bound electrons, known also as Rayleigh scattering, is the dominant mechanism. The amplitude of the process is connected with an important parameter of the atom known as polarizability.

Since the photon energy does not change, $\omega_1 = \omega_2 = \omega$ and $k_1 = |\mathbf{k}_1| = k_2 = |\mathbf{k}_2|$ (recall that in our system of units, $\omega_i = k_i$). The cross section σ and the amplitude F of the process are related by the equation

$$d\sigma \;=\; 2\pi |F|^2 \delta(\omega_2 - \omega_1) \frac{d^3k_2}{(2\pi)^3} \;=\; \frac{\omega^2 |F|^2 d\Omega}{(2\pi)^2}\,, \tag{5.86}$$

where averaging over polarizations of the initial-state photons and summation over polarizations of the final-state photons is carried out.

Before beginning the calculations, we estimate the relative role of the pole and seagull terms. These estimates as well as (5.82)–(5.85) are true for every binding field. We begin with the photon energies ω of the order of the binding energy I_Z. Recall that $I_Z = 13.6\,\mathrm{eV}$ for hydrogen, while $I_Z = 1.36\,\mathrm{keV}$ for neon. The integrals on the RHS of (5.82)–(5.84) are saturated by $f \sim \eta$. The photon momenta are $k_i \sim I_Z \ll \eta$, and they can be neglected while we perform estimates. Since the matrix element $\langle \mathbf{f_2}|G|\mathbf{f}_1\rangle$ at these energies is of order $1/I_Z$, the RHS of (5.82) and (5.83) are of order $4\pi\alpha(\eta/m)^2/I_Z \sim 4\pi\alpha/m$, i.e., of the same order as the seagull term F_c. Thus at $\omega \sim I_Z$, all three terms on the RHS of (5.85) are important. At $\omega \gg I_Z$, the seagull term dominates.

We return now to the case of Rayleigh scattering in the Coulomb field. Recall that here $\psi_i = \psi_f = \psi_{1s}$, the wave function of $1s$ electron; its energy is $\varepsilon = -I_Z$ with $I_Z = \eta^2/2m$, $\eta = m\alpha Z$. We begin with the pole terms $F_{a,b}$. Integration over momenta $\mathbf{f}_{1,2}$ carried out using (5.71)–(5.73) provides

$$F_a = N^2(\omega) N_1^2 \eta^2 (\mathbf{e}_2^* \cdot \boldsymbol{\nabla}_{\mathbf{k}_2})(\mathbf{e}_1 \cdot \boldsymbol{\nabla}_{\mathbf{k}_1}) \langle \mathbf{k}_2 | \mathscr{T}(\varepsilon_a; \eta, \eta) | \mathbf{k}_1 \rangle; \quad \varepsilon_a = \omega - I_Z, \tag{5.87}$$

with the matrix element on the RHS defined by (5.64) with $\mathbf{f}_j = \mathbf{k}_j$.

While we consider the energies $\omega \sim I_Z$, we have $p_{a,b} \sim \eta$, while $k_j = \omega_j \sim \eta(\alpha Z) \ll \eta$, $p_{a,b}$. Thus, although (5.87) provides exact dependence of the amplitude F_a on the photon momenta $\mathbf{k}_{1,2}$, we must include only the leading nonvanishing terms of the expansion in powers of ω_j^2/η^2. The higher terms are of order $(\alpha Z)^2$, and their inclusion is beyond the nonrelativistic approximation. This approach is usually called the dipole approximation, since it is equivalent to inclusion of the partial wave with $\ell = 1$ only. Thus we must put $\mathbf{k}_1 = \mathbf{k_2} = 0$ after we calculate the derivatives. In this approximation, we find that

$$F_a \;=\; \mathbf{e}_1 \cdot \mathbf{e}_2^* \Phi_a\,, \tag{5.88}$$

with

$$\Phi_a = -iN^2(\omega)\frac{2^7 m p_a \eta^5}{(p_a + i\eta)^8} X(\zeta_a); \quad \zeta_a = \frac{\eta}{p_a}, \tag{5.89}$$

where $p_a = \sqrt{2m(\omega - I_Z)}$, and

$$X(\zeta_a) = \int_0^\infty \frac{dt t^{i\zeta_a+1}}{(t-\kappa(\zeta_a))^4} = \frac{{}_2F_1(4, 2-i\zeta_a, 3-i\zeta_a, \kappa)}{2-i\zeta_a}; \quad \kappa = \frac{(1-i\zeta_a)^2}{(1+i\zeta_a)^2}. \tag{5.90}$$

The contribution of the pole term $F_b = \mathbf{e}_1 \cdot \mathbf{e}_2 \Phi_b$ can be represented in a similar way, with momentum p_a replaced by $p_b = i\sqrt{2m(\omega + I_Z)}$.

The seagull amplitude is

$$F_c = \mathbf{e}_1 \cdot \mathbf{e}_2^* \Phi_c; \quad \Phi_c = -\frac{N^2(\omega) N_1^2}{m} \langle \mathbf{k}_2 | V'_{i\eta+i\lambda} | \mathbf{k}_1 \rangle, \tag{5.91}$$

with V' denoting the derivative with respect to η, and $\lambda = \eta$. While $\omega \ll \eta$, we can put $\mathbf{k}_1 = \mathbf{k}_2 = 0$, thus obtaining $\Phi_c = N^2(\omega)/m$. Note that this is true for every binding field, since for $\mathbf{q} = 0$,

$$\Phi_c = \frac{N^2(\omega)}{m} \int \frac{d^3 f}{(2\pi)^3} \langle \psi | \mathbf{f} \rangle \langle \mathbf{f} | \psi \rangle = \frac{N^2(\omega)}{m}. \tag{5.92}$$

The last equality is due to the normalization condition $\int d^3 f/(2\pi)^3 \langle \psi | \mathbf{f} \rangle \langle \mathbf{f} | \psi \rangle = 1$.

Finally, the amplitude of the Rayleigh scattering is

$$F = \mathbf{e}_1 \cdot \mathbf{e}_2 \Phi(\omega); \quad \Phi(\omega) = \Phi_a(\omega) + \Phi_b(\omega) + \Phi_c(\omega). \tag{5.93}$$

Note that in the limiting case $\omega \ll I_Z$, the amplitude is proportional to ω^2 in every binding field. This happens because at $\omega = 0$, the seagull term, which does not depend on ω, is canceled by the pole terms. We shall demonstrate this in Chap. 7. In expansion of the pole terms in powers of ω/ε_n, the linear terms cancel.

At $\omega \ll \eta$, i.e., while the dipole approximation is valid, the amplitude of the Rayleigh scattering is connected with an important characteristic of the atom known as dipole polarizability. We shall give a more detailed analysis of these points in Chap. 7.

Consider now another limiting case, $\omega \gg I_Z$. If, however, $\omega \ll \eta = m\alpha Z$, the photon momenta $k_i \ll \eta$ can be neglected while we make estimates, as in the previous case. For hydrogen, the condition $I_Z \ll \omega \lesssim \eta$ means that $10\,\mathrm{eV} \ll \omega \lesssim 4\,\mathrm{keV}$, for neon $1\,\mathrm{keV} \ll \omega \lesssim 40\,\mathrm{keV}$. The matrix elements of the Green function are now of order $1/\omega$; see (5.39). Thus each of the pole terms is of order $4\pi\alpha/m \cdot I_Z/\omega$, i.e., $F_{a,b} \sim F_c \cdot I_Z/\omega \ll F_c$. Also, the energies of the Green functions are $\varepsilon_a = \omega - I_z$, $\varepsilon_b = -\omega - I_Z$, and the contributions $F_{a,b}$ cancel up to terms of order I_Z/ω.

Therefore, at these energies, the amplitude is determined by the seagull term F_c with the sum of the pole terms $F_a + F_b$ providing a correction of order I_Z^2/ω^2.

Hence in the whole region $\omega \gg I_Z$, the amplitude is determined by the seagull term. If also $\omega \ll \eta$, it is given by (5.92). Momentum transferred to the nucleus $q \ll \eta$ can be neglected, and the amplitude is equal to that on a free electron,

$$F = F_0 = \frac{\mathbf{e}_1 \cdot \mathbf{e}_2^* N^2(\omega)}{m}. \tag{5.94}$$

At larger energies $\omega \gtrsim \eta$, one can no longer neglect the transferred momentum q in (5.84). In the general case (the binding field is not necessarily a Coulomb field), we can write for the amplitude

$$F_c = \frac{\mathbf{e}_1 \cdot \mathbf{e}_2^* N^2(\omega) f(q^2)}{m}; \quad f(q^2) = \int \frac{d^3 f}{(2\pi)^3} \langle \psi | \mathbf{f} \rangle \langle \mathbf{f} - \mathbf{q} | \psi \rangle = \tag{5.95}$$

$$\int d^3 r |\psi(\mathbf{r})|^2 e^{i(\mathbf{q}\cdot\mathbf{r})}.$$

The function $f(q^2)$ is usually called a form factor. In the Coulomb case, we obtain, employing (5.91),

$$f(q^2) = \frac{16\eta^4}{(q^2 + 4\eta^2)^2}. \tag{5.96}$$

The amplitude of the Rayleigh scattering on the other bound states can be obtained by applying certain differential operators acting on η and λ to the RHS of (5.82)–(5.84); see Sect. 5.1.

5.3.3 *Cross Section of the Rayleigh Scattering*

In the whole region $\omega \ll \eta$, the dependence of the differential distribution on the angles comes only from the common factor $\mathbf{e}_1 \cdot \mathbf{e}_2^*$. Thus one can write

$$\frac{d\sigma}{dt} = \frac{\omega^2 |\Phi(\omega)|^2}{4\pi}(1 + t^2); \quad t = \mathbf{k_1} \cdot \mathbf{k}_2/\omega_1\omega_2, \tag{5.97}$$

with $\Phi(\omega) = \Phi_a(\omega) + \Phi_b(\omega) + \Phi_c$, $\Phi_{a,b}$ defined by (5.87), (5.62); Φ_c is given by (5.92).

Following the analysis of the previous subsubsection, we find that for $\omega \ll I_Z$, the cross section is proportional to ω^4. This was found by Lord Rayleigh in 1871. For $\omega \sim I_Z$, the cross section is

$$\sigma(\omega) = \frac{2}{3\pi}\omega^2|\Phi(\omega)|^2. \tag{5.98}$$

For $I_Z \ll \omega \ll \eta$, we can put $\Phi = \Phi_c$, and the cross section is equal to the cross section of scattering by the free electron σ_{Th}, known as the Thomson cross section, i.e.,

$$\sigma = \sigma_{Th} = \frac{8\pi}{3}r_e^2, \quad r_e = \frac{\alpha}{m}, \tag{5.99}$$

and the field which binds the electron is not necessarily a Coulomb field. Note that this equation can be obtained in the framework of classical electrodynamics (see, e.g., [10]). The cross section σ_{Th} represents the ratio of the flux of radiated energy to that of the incoming energy.

At $\omega \sim \eta$, the equations become more complicated. We have still $\Phi = \Phi_c$, but one cannot neglect the transferred momentum $q^2 = 2\omega(1-t)$ unless the angle of scattering is small, i.e., unless $1 - t \ll 1$. In the latter case, the angular distribution is given by (5.97), with $\Phi = \Phi_c$ determined by (5.92). For every value of t at these values of the photon energies,

$$\frac{d\sigma}{dt} = \pi r_e^2(1+t^2)|f(q^2)|^2; \quad q^2 = 2\omega^2(1-t), \tag{5.100}$$

This equation with $f(q^2)$ defined by (5.95) is true for every $I_Z \ll \omega \leq \eta$. For $\omega \ll \eta$, one can put $q^2 = 0$. As we have seen, $f(0) = 1$.

In the whole region $I_Z \ll \omega \ll m$, the total cross section of the Rayleigh scattering can be expressed as

$$\sigma = \sigma_{Th}\frac{1 + x + x^2/2}{(1+x)^3}; \quad x = \frac{\omega^2}{\eta^2}. \tag{5.101}$$

One can see that $\sigma < \sigma_{Th}$, with the limiting value $\sigma = \sigma_{Th}$ in the limit $\omega \ll \eta$. In the asymptotics $\omega \gg \eta$, we expect $\sigma \sim 1/\omega^2$, since one can put $dt = qdq/\omega^2$ in the phase volume, while the integral over q is saturated by $q \sim \eta$ and does not depend on ω. For $\omega \gg \eta$, (5.101) provides

$$\sigma(\omega) = \sigma_{Th}\frac{\eta^2}{2\omega^2}, \tag{5.102}$$

thus confirming the estimate.

As we mentioned above, the photon can undergo elastic scattering on the nucleus. Treating the latter as a heavy spinless particle with the mass $M \gg m$ and considering the process in its rest frame, we find that the amplitude is determined by the seagull term. Hence, it becomes smaller than the value on the bound electrons by a factor of $m/M \ll 1$. The situation becomes more complicated if we take into account that the nucleus is a system of nucleons. Here the case in which the photon energy is close to the excitation energy of the nucleus requires additional analysis. Otherwise,

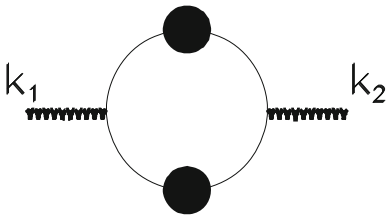

Fig. 5.2 Photon scattering in the Coulomb field of the nucleus. Notation is the same as in Fig. 5.1

the amplitude is at least m/m_N times the value on the bound electrons, with $m_N \approx 940\,\text{MeV}$ standing for the mass of the nucleon.

Photon scattering in the Coulomb field known as Delbrück scattering is a quantum-electrodynamic effect that can be viewed as a renormalization of its wave function. The process can be considered as the conversion of a photon to an off-mass shell electron–positron pair converting later back to a photon; see Fig. 5.2. The details of the process are described, e.g., in [11]. The amplitude of the Delbrück scattering F^D contains at least two interactions of the e^+e^- pair with the nucleus. Also, the gauge invariance requires that F^D contains the energy of each photon as a factor. Thus F^D contains an additional small factor of order $(\alpha Z)^2\omega^2/m^2$, and can be neglected at the energies considered here.

5.4 Second Order Processes II: Raman and Compton Scattering

Now we study the processes in which absorption of a photon with energy ω_1 by a bound electron is followed by radiation of the photon with energy ω_2 and transition of the bound electron to an excited state of the discrete or continuum spectrum. The equations will be written for one electron in each state. For the case of two electrons, the equations for the differential distributions and for the cross sections should be multiplied by the factor 2.

5.4.1 Raman Scattering

In Raman scattering, the bound electron is transferred to another bound state. The differential distribution is now

$$\frac{d\sigma}{d\Omega} = \frac{\omega_2^2|F|^2}{4\pi^2}, \tag{5.103}$$

while $\omega_2 = \omega_1 - (I_i - I_f)$, with $I_{i,f}$ the ionization potentials of initial and final bound states.

For every binding field, the amplitude of the process is given by (5.82)–(5.85). The same refers to the estimates given in this section, which we present for the Coulomb case. At $\omega \sim I_Z \ll \eta$, the pole terms of the amplitude obtains the parametrically largest values if the orbital momenta of the initial and final states satisfy the inequality

$$\Delta\ell \;=\; |\ell_f - \ell_i| \;=\; 0, 2\,. \tag{5.104}$$

This happens because in each vertex of the pole terms, the electron undergoes mainly a dipole transition, which can be described by putting $\mathbf{k}_1 = \mathbf{k}_2 = 0$. Transitions with other values of $\Delta\ell$ require inclusion of the higher powers of the expansion in $k_i/f_i \sim k_i/\eta \ll 1$. As to the seagull term, it vanishes for $\mathbf{q} = 0$ due to orthogonality of the wave functions. Thus, if condition (5.104) is satisfied, the amplitude is determined by the pole diagrams and is of the order of the Rayleigh amplitude.

At larger energies, the contribution of the pole terms obtains an additional small factor $(I_Z/\omega)^2$. On the other hand, the transitions with $\Delta\ell = 1$ described by the seagull term require only the lowest term of the expansion in powers of q/f_i. They become dominative at $\omega_1/\eta \gg (I_Z/\omega_1)^2$, i.e., at $\omega_1 \gg \eta(\alpha Z)^{2/3}$. For hydrogen, this means $\omega_1 \gg 120\,\mathrm{eV}$. The amplitude of these transitions is much smaller than the Rayleigh amplitude. At $\omega_1 \sim \eta$, the amplitudes are dominated by the seagull terms. The processes with all values of $\Delta\ell$ are important, and the amplitudes are of the same order as in Rayleigh scattering. Note, however, that parametric estimates do not exclude additional numerical quenching.

In the case of the Coulomb field, the amplitude of the Raman scattering with any initial and final electronic states can be expressed in terms of the matrix elements given by (5.82)–(5.84). Here we present the results for scattering on the $1s$ electron with its excitation to the L shell. Thus the photon carrying the energy ω_1 is absorbed by the $1s$ electron, which is moved to the $2s$ or $2p$ state, and a photon with the energy $\omega_2 = \omega_1 - 3I_Z/4$ is radiated.

Proceeding similar to Sect. 5.2, one can represent the amplitudes of excitations to the $2s$ and to $2p$ states in terms of the matrix elements

$$\begin{aligned} F_a &= N(\omega_1)N(\omega_2)N_1N_2\eta(\mathbf{e}_2^*\cdot\boldsymbol{\nabla}_{\mathbf{k}_2})(\mathbf{e}_1\cdot\boldsymbol{\nabla}_{\mathbf{k}_1})\Gamma_{2\ell m}\eta_2\langle\mathbf{k}_2|\mathscr{T}(\varepsilon_a;\eta_2,\eta)|\mathbf{k}_1\rangle,\\ F_b &= N(\omega_1)N(\omega_2)N_1N_2\eta(\mathbf{e}_2^*\cdot\boldsymbol{\nabla}_{\mathbf{k}_2})(\mathbf{e}_1\cdot\boldsymbol{\nabla}_{\mathbf{k}_1})\Gamma_{2\ell m}\eta_2\langle\mathbf{k}_1|\mathscr{T}(\varepsilon_b;\eta_2,\eta)|\mathbf{k}_2\rangle, \end{aligned} \tag{5.105}$$

with $\varepsilon_a = \omega_1 - I_Z$, $\varepsilon_b = -\omega_2 - I_Z/4$, while operators $\Gamma_{2\ell m}$ are defined by (5.80). Also, for the seagull term,

$$\Phi_c \;=\; \frac{-N(\omega_1)N(\omega_2)N_1N_2}{m}\,\Gamma_{2\ell m}\langle\mathbf{k}_2|V'_{i\eta+i\eta_2}|\mathbf{k}_1\rangle. \tag{5.106}$$

Thus for excitation of $2s$ state,

$$F_c = \mathbf{e}_1\cdot\mathbf{e}_2^*\Phi_c;\quad \Phi_c = \frac{N(\omega_1)N(\omega_2)}{m}\,\frac{4\sqrt{2}\eta^4q^2}{(q^2+\lambda^2)^3};\quad \lambda \;=\; \frac{3\eta}{2}, \tag{5.107}$$

while for excitation of $2p$ state with projection of the angular momentum $\ell_z = m$,

$$\Phi_c = i\frac{N(\omega_1)N(\omega_2)}{m}\frac{6\sqrt{2}\eta^5 q^m}{(q^2+\lambda^2)^3}, \tag{5.108}$$

with q^m the cyclic component of the vector $\mathbf{q}$.

As we have seen, the seagull term dominates if the energy ω_1 is large enough. In the case of the $2s$ state, this is $\omega_1 \gg \eta(\alpha Z)^{2/3}$ (for hydrogen, $\omega_1 \gg 120\,\mathrm{eV}$), while in the case of the $2p$ state, this is $\omega_1 \gg I_Z$ (for hydrogen, $\omega_1 \gg 14\,\mathrm{eV}$). For heavier atoms, we can just write $\omega_1 \gg I_Z$. At these energies, one can put $\omega_1 = \omega_2$, and the angular distributions for transitions to ns states are given by (5.100) with

$$f_{2s}^2 = \frac{32\eta^8 q^4}{(q^2+\lambda^2)^6}; \quad f_{2p}^2 = \frac{72\eta^{10}q^2}{(q^2+\lambda^2)^6}. \tag{5.109}$$

Thus at $\omega_1 \sim I_Z$ the transitions $1s \to 2s$ and $1s \to 2p$ are dominated by the pole diagrams. The $1s \to 2s$ transition is allowed in the dipole approximation, while $1s \to 2p$ is not. Thus the cross section for $1s \to 2p$ is about $\alpha^2 Z^2$ times that for $1s \to 2s$.

The situation changes for $\omega_1 \gg I_Z$. If also $\omega_1 \ll \eta$, we can neglect q in the denominators of the expressions in (5.109), finding the limiting equations for the cross sections

$$\sigma_{2s} = \sigma_{Th}\cdot\left(\frac{4}{9}\right)^5\cdot 64\cdot\frac{56}{45}\frac{\omega_1^4}{\eta^4} \approx \sigma_{Th}\cdot 1.38\frac{\omega_1^4}{\eta^4}; \tag{5.110}$$

$$\sigma_{2p} = \sigma_{Th}\left(\frac{4}{9}\right)^5\cdot 64\cdot\frac{\omega_1^2}{\eta^2} \approx \sigma_{Th}\cdot 1.11\frac{\omega_1^2}{\eta^2},$$

with domination of the $1s \to 2p$ transition. For $\omega_1 \gg I_Z$ (however, $\omega_1 \ll m$), the cross sections of excitation of the $2s$ and $2p$ states are

$$\sigma_{2s} = \sigma_{Th}\frac{8}{5}\left(\frac{2}{3}\right)^8\beta^2\frac{7+2\beta+\beta^2}{(1+\beta)^5}; \tag{5.111}$$

$$\sigma_{2p} = \sigma_{Th}\frac{4}{5}\left(\frac{2}{3}\right)^8\beta\frac{20+16\beta+11\beta^2+3\beta^3}{(1+\beta)^5}; \quad \beta = \frac{16}{9}\frac{\omega_1^2}{\eta^2}.$$

These equations are illustrated in Fig. 5.3.

In the high-energy nonrelativistic asymptotics $\omega_1 \gg \eta$ and [12]

$$\sigma_{2s} \approx \sigma_{Th}\cdot\frac{2^6}{3^6}\cdot\frac{2}{5}\frac{\eta^2}{\omega_1^2} \approx \sigma_{Th}\cdot 3.5\cdot 10^{-2}\frac{\eta^2}{\omega_1^2}; \tag{5.112}$$

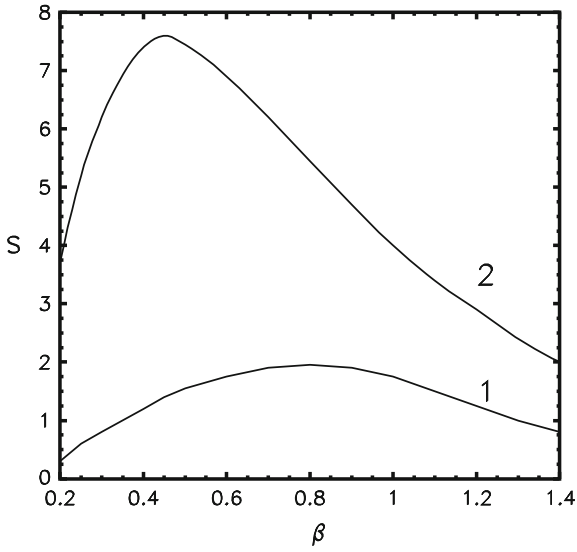

Fig. 5.3 Energy dependence for the cross sections of photon scattering accompanied by transition of the bound electron from the $1s$ state to the $2s$ state (curve *1*) and to the $2p$ state (curve *2*) for $\omega_1 \sim \eta$. The horizontal axis is for $\beta = 16\omega_1^2/9\eta^2$. The vertical axis shows $S = \sigma_{2s,2p}/\sigma_{Th} \times 10^{-2}$

$$\sigma_{2p} \approx \sigma_{Th} \cdot \frac{2^6}{3^6} \cdot \frac{3}{5}\frac{\eta^2}{\omega_1^2} \approx \sigma_{Th} \cdot 5.3 \cdot 10^{-2} \cdot \frac{\eta^2}{\omega_1^2}.$$

Here the two cross sections are of the same order of magnitude. For calculations of the Raman scattering cross sections in several particular cases, see, e.g., [13, 14].

5.4.2 *Compton Scattering*

Now interaction of the photon with a bound electron moves the latter to continuum state with momentum $\mathbf{p}$. We shall find the energy distribution $d\sigma(\omega_1)/d\omega_2$ and the cross section $\sigma(\omega_1)$. Before carrying out the calculations, we can write expression for the energy distribution at $\omega_2 \to 0$. The pole term with the photon carrying momentum $\mathbf{k}_2 \to 0$ behaves as $1/\omega_2$ as $\omega_2 \to 0$, while the other contributions obtain finite values in this limit. This term can be written as

$$F(\mathbf{p}, \mathbf{k}_2) \;=\; \langle \mathbf{p}, \mathbf{k}_2 | \gamma G^0(\varepsilon') | \mathbf{p}' \rangle F_{ph}(\mathbf{p}'). \tag{5.113}$$

Here $\mathbf{p}' = \mathbf{p} + \mathbf{k}_2$; F_{ph} is the amplitude of photoionization; γ is the vertex of interaction between the electron and the photon with momentum $\mathbf{k}_2$. One can represent this equation as

$$F(\mathbf{p}, \mathbf{k}_2) = \phi(\mathbf{p}, \mathbf{k}_2) F_{ph}(\mathbf{p}); \quad \phi(\mathbf{p}, \mathbf{k}_2) = \frac{N(\omega_2)}{2m\omega_2} \frac{\mathbf{e}_2^* \cdot \mathbf{p}}{m}. \tag{5.114}$$

Here we kept only the terms that increase as $1/\omega_2$ and neglected the terms of the relative order p/m in the denominator of the Green function. Writing

$$d\sigma \;=\; |F_{ph}(p)|^2 |\phi(\mathbf{p}, \mathbf{k}_2)|^2 d\Gamma \frac{d^3k_2}{(2\pi)^3}\,, \tag{5.115}$$

with $d\Gamma$ the phase volume for photoionization, we obtain

$$\frac{d\sigma(\omega_1)}{d\omega_2} = \sigma_{ph}(\omega_1) w(\omega_1, \omega_2); \quad w(\omega_1, \omega_2) = \frac{2\alpha}{3\pi}\frac{p^2}{m^2}\frac{1}{\omega_2}. \tag{5.116}$$

Here σ_{ph} is the photoionization cross section of the same electronic state. This expression is true for every initial electronic state and for every binding field. Note that (5.116) is a very general relation connecting the cross sections of the processes with and without radiation of a soft photon [11, 15].

Below we focus on Compton scattering on the $1s$ electron in the Coulomb field [16]. The energy conservation law is

$$\omega_1 - I_Z \;=\; \varepsilon + \omega_2\,. \tag{5.117}$$

Here $\varepsilon = p^2/2m$ is the energy of the outgoing electron. The differential cross section of the process can be written as

$$\frac{d\sigma}{d\omega_2} \;=\; \frac{\omega_2^2 m p |F|^2 d\Omega_e d\Omega_\gamma}{(2\pi)^5}\,. \tag{5.118}$$

Here $d\Omega_{e,\gamma}$ are the solid angles of the final-state particles; the amplitude F is given by (5.82)–(5.85).

Compare the contributions of the pole and seagull terms to the amplitude. For $\omega_1 \ll \eta$, one can neglect $\mathbf{k}_{1,2}$ in the pole terms, but not in the seagull term, since the latter vanishes at $\mathbf{k}_1 - \mathbf{k}_2 = 0$ due to the orthogonality of the wave functions. Hence the seagull term contains an additional small factor of order ω_1/η. Thus at $\omega_1 \sim I_Z$, the pole terms dominate. The seagull term contributes at $\omega_1 \geq \eta(\alpha Z)^{2/3}$. Recall that for hydrogen, this means that $\omega_1 \geq 200\,\mathrm{eV}$. The pole terms of the amplitudes can be written in terms of the matrix elements defined by (5.57):

$$F_a = N(\omega_1)N(\omega_2)N_1 N_p (\mathbf{e}_1 \cdot \boldsymbol{\nabla}_1)\hat{J}_x \hat{\Gamma} \langle \mathbf{k}_2 + \mathbf{p}(1-x)|\mathscr{T}(\varepsilon_a; \lambda - ipx, \eta)|\mathbf{k}_1\rangle, \tag{5.119}$$
$$\varepsilon_a = \omega_1 - I_Z, \quad \lambda = 0,$$

with the operator $\hat{J}_x$ defined by (5.28), $\hat{\Gamma} = \mathbf{e}_2^* \cdot (\boldsymbol{\nabla}_2 - \mathbf{p}(1/x - 1)\partial/\partial\lambda)$, and N_1 and N_p are the normalization factors of the $1s$ and continuum electrons. The operators $\boldsymbol{\nabla}_{1,2}$ act on momenta $\mathbf{k}_{1,2}$. For $\omega_1 \ll \eta$, we can put $\mathbf{k}_1 = \mathbf{k}_2 = 0$ in the matrix element after calculation of the derivatives.

Thus

$$F_a = 8\pi \frac{N(\omega_1)N(\omega_2)N_1N_p}{m\eta^3}\Big(\mathbf{e}_1\cdot\mathbf{e}_2^* S_a + (\mathbf{e}_1\cdot\mathbf{n})(\mathbf{e}_2^*\cdot\mathbf{n})T_a\Big);\quad r_e = \frac{\alpha}{m}. \tag{5.120}$$

Here $\mathbf{n} = \mathbf{p}/p$. We introduce the dimensionless parameters

$$x_i \;=\; \omega_i/I_Z\,. \tag{5.121}$$

Recall that earlier we introduced $\varepsilon/I_Z = \xi^{-2}$. Employing the technique developed in Sect. 5.1, we obtain

$$\begin{aligned} S_a &= -i\int_0^1 \frac{dyyf(y)}{\lambda(y)} A^{-1+i\xi}B^{-1-i\xi};\\ T_a &= \frac{2(1-i\xi)(2-i\xi)}{\xi^2}\int_0^1 dyyf(y)A^{-3+i\xi}B^{-i\xi}. \end{aligned} \tag{5.122}$$

Here $\lambda(y) = [x_1(1-y)-1]^{1/2}$,

$$f(y) \;=\; \Big(\frac{i\zeta-1}{i\zeta+1}\frac{\zeta\lambda+1}{\zeta\lambda-1}\Big)^{i\zeta},$$

while $\zeta = \eta/p_a = (x_1-1)^{-1/2}$, $A = \lambda^2 - \xi^{-2}$, $B = (\lambda+\xi^{-1})^2$. The amplitude F^b can be obtained by changing $(\mathbf{k}_1, \omega_1, \mathbf{e}_1)$ to $(-\mathbf{k}_2, -\omega_2, \mathbf{e}_2)$.

To calculate the seagull term, we introduce

$$\boldsymbol{\kappa} \;=\; \mathbf{k}_1 - \mathbf{k}_2. \tag{5.123}$$

The seagull contribution can be expressed explicitly:

$$F_c = 8\pi\alpha Z N(\omega_1)N(\omega_2)N_1N_p(\mathbf{e}_1\cdot\mathbf{e}_2^*)\Big(\frac{1-i\xi}{A_0}+\frac{1+i\xi}{B_0}\Big)A_0^{-1+i\xi}B_0^{-i\xi}. \tag{5.124}$$

Here $A_0 = q^2+\eta^2$ with $q^2 = |\mathbf{p}-\boldsymbol{\kappa}|^2$, while $B_0 = \kappa^2 - (p+i\eta)^2$. For $\omega_1 \ll \eta$, this expression can be simplified:

$$F_c = 8\pi\frac{N(\omega_1)N(\omega_2)N_1N_p}{m\eta^3}\frac{\mathbf{p}\cdot\boldsymbol{\kappa}}{\eta^2}(\mathbf{e}_1\cdot\mathbf{e}_2^*)\frac{\xi^6(1-i\xi)}{(\xi^2+1)^3}\cdot\exp\left(-2\xi\arctan(1/\xi)\right). \tag{5.125}$$

One can see that at least for $\omega_1 \ll \eta$, the interference between the pole and the seagull terms vanishes after integration of the angular distribution. Thus the energy distributions can be written as

$$\frac{d\sigma(\omega_1)}{d\omega_2} \;=\; \frac{d\sigma_P(\omega_1)}{d\omega_2} + \frac{d\sigma_{SG}(\omega_1)}{d\omega_2}\,, \tag{5.126}$$

with the lower indices P and SG denoting the respective contributions of the pole and seagull terms.

We begin our calculation of the energy distributions, considering the case $\omega_1 \sim I_Z$. One can see that the seagull contribution to the amplitude is quenched by a factor of order αZ. This provides a correction of order $(\alpha Z)^2$ to the cross section, which cannot be included in the framework of the nonrelativistic approach. Thus we include only the pole terms. In terms of the dimensionless variables $x_{1,2}$ and ξ_Z, we can write $d\sigma(\omega_1)/d\omega_2 = d\sigma_P(\omega_1)/d\omega_2$. The general expression for the latter is

$$\frac{1}{\sigma_{Th}}\frac{d\sigma_P}{dx_2} = 32\frac{x_2}{x_1}\frac{X(x_1,x_2)}{1-\exp(-2\pi\xi)}, \tag{5.127}$$

with

$$X = |S|^2 + \frac{2}{3}Re(S^*T) + \frac{1}{3}|T|^2; \quad S = S_a + S_b; \quad T = T_a + T_b. \tag{5.128}$$

Thus the energy spectrum is expressed in terms of the "universal" (scaled) function $X(x_1, x_2)$.

In the case $\eta \gg \omega_1 \gg I_Z$ ($x_1 \gg 1$), we can distinguish two regions of the spectrum. At electron energy $\varepsilon \sim I_Z$, the transferred momentum $q \sim \eta$ is small, and the amplitude obtains the largest values. The distribution becomes much smaller at larger values of the energy of the outgoing electron. In any case, we must add the contribution of the seagull term, which is

$$\frac{1}{\sigma_{Th}}\frac{d\sigma_{SG}}{dx_2} = \frac{2^8}{3}\frac{\omega_1^2}{\eta^2}V(\xi); \quad V(\xi) = \frac{\xi^{10}}{(1+\xi^2)^5}\frac{\exp(-4\xi\,\mathrm{arctan}(1/\xi))}{1-\exp(-2\pi\xi)}. \tag{5.129}$$

This expression presents the distribution in terms of the universal parameters $x_{1,2}$ and the ratio ω_1/η. In other words, the distribution depends on parameters x_i and on the nuclear charge Z separately. As we estimated above, the energy distribution on the Bethe ridge $x_1 - x_2 \sim 1 \ll x_{1,2}$ is dominated by the seagull term for $\omega_1 \gg \eta(\alpha Z)^{2/3}$. From (5.129), one can find that the local maximum at small values of the electron energy $x_1 - x_2 \ll x_1$ is reached at $\varepsilon = 0.16 I_Z$ (for hydrogen, it is $\varepsilon = 2.1\,\mathrm{eV}$).

At $\varepsilon \gg I_Z$, a large momentum $q \sim p \gg \eta$ is transferred to the nucleus. Thus we are outside the Bethe ridge. If the outgoing electrons (as well as the intermediate electrons in the pole terms) are described by plane waves, a large momentum q is transferred to the nucleus by the initial-state electron. Hence both pole and seagull terms contain the factor $\psi_{1s}(q)$. However, the contribution to the seagull term calculated in this approximation is canceled by that containing the lowest-order Coulomb correction to the wave function of the outgoing electron, which contains an additional factor of order $\omega_1/p \ll 1$, which is due to a partial cancelation of the two leading terms in the wave function of the outgoing electron corresponding to the plane wave $F_c^{(0)}$ and to the lowest-order Coulomb correction $F_c^{(1)}$. We demonstrated this for the initial s states.

The plane-wave term is

$$F_c^{(0)} = \frac{\mathbf{e}_1 \cdot \mathbf{e}_2^*}{m} N(\omega_1) N(\omega_2) \psi_i(\mathbf{q}) \tag{5.130}$$

with $\mathbf{q} = \mathbf{p} - \boldsymbol{\kappa}$. The term containing the lowest Coulomb correction is (see Sect. 3.1.3)

$$F_c^{(1)} = \frac{\mathbf{e}_1 \cdot \mathbf{e}_2^*}{m} \int \frac{d^3 f}{(2\pi)^3} \frac{-4\pi\alpha Z}{(\mathbf{q}+\mathbf{f})^2} \cdot \frac{2m}{p^2 - (\boldsymbol{\kappa} - \mathbf{f})^2} \psi_i(\mathbf{f}), \tag{5.131}$$

with the integral saturated at $f \sim \eta$. Thus we can neglect f everywhere except the wave function ψ_i. Since $\omega_1 \ll \eta$, we can also put $\boldsymbol{\kappa} = 0$ and $\mathbf{q} = \mathbf{p}$. Hence

$$F_c^{(1)} = \frac{\mathbf{e}_1 \cdot \mathbf{e}_2^*}{m} N(\omega_1) N(\omega_2) \int \frac{d^3 f}{(2\pi)^3} \psi_i(\mathbf{f}) \cdot \frac{-8\pi\eta}{q^4}. \tag{5.132}$$

Employing (2.86) for the wave function $\psi_i(\mathbf{q})$, we find that indeed, $F_c^{(0)} = -F_c^{(1)}$. The errors in this equality are of order η/p and ω_1/η. Thus at $\varepsilon \gg I_Z$, the energy distribution is determined by the pole terms. This is true for every binding field.

Examples of photon spectra are presented in Fig. 5.4.

As expected, the distribution obtains the largest values at small x_2, in agreement with (5.116).

Now we calculate the total cross section. Due to the infrared divergence at $\omega_2 \to 0$ (5.116), we must ensure the proper treatment of the soft photon region. We assume that the detector of the ejected electrons can distinguish the electrons with the largest available energy $\varepsilon_m = \omega_1 - I_Z$ from those with energy $\varepsilon_\lambda < \varepsilon_m$, but cannot distinguish the electrons with energies $\varepsilon_\lambda < \varepsilon < \varepsilon_m$. This is equivalent to the introduction of a cutoff $\omega_2 > \omega_\lambda = \omega_1 - I_Z - \varepsilon_\lambda$ in the spectrum of the ejected photons. In Chap. 8, we shall carry out a more rigorous procedure for treatment of soft photons. Here we only investigate dependence of our results on the actual value of ω_λ.

We have seen that a large part of the cross section can be estimated as coming from the region of the ejected soft photons, where the spectrum is described by (5.116). The upper limit of the values of x_2 where this equation is valid is a certain $x_2 = c(x_1 - 1)$, with c an unknown coefficient. Employing (5.78) for σ_{ph}, we find that this part of the cross section can be represented as

$$\frac{\sigma'_P}{\sigma_{Th}} = U(x_1) \ln\left(\frac{c(x_1-1)}{\omega_\lambda/I_Z}\right); \quad U(x_1) = \frac{2^7}{3} \frac{x_1 - 1}{x_1^4} \frac{\exp\left(-4\xi \arctan(1/\xi)\right)}{1 - \exp\left(-2\pi\xi\right)}. \tag{5.133}$$

The lower index P reminds the reader that this contribution comes from the pole terms. Now we can look for the values of ω_1 where the ratio σ'_P/σ_{Th} reaches it largest values by calculation of the derivative with respect to x_1. Assuming that the resolution threshold is proportional to the energy of the photoelectron, i.e., $\omega_\lambda = \lambda(\omega_1 - I_Z)$ with $\lambda \ll 1$, we obtain that the contribution (5.133) reaches its largest value at

$$x_1 = \frac{\omega_1}{I_Z} = 1.56, \tag{5.134}$$

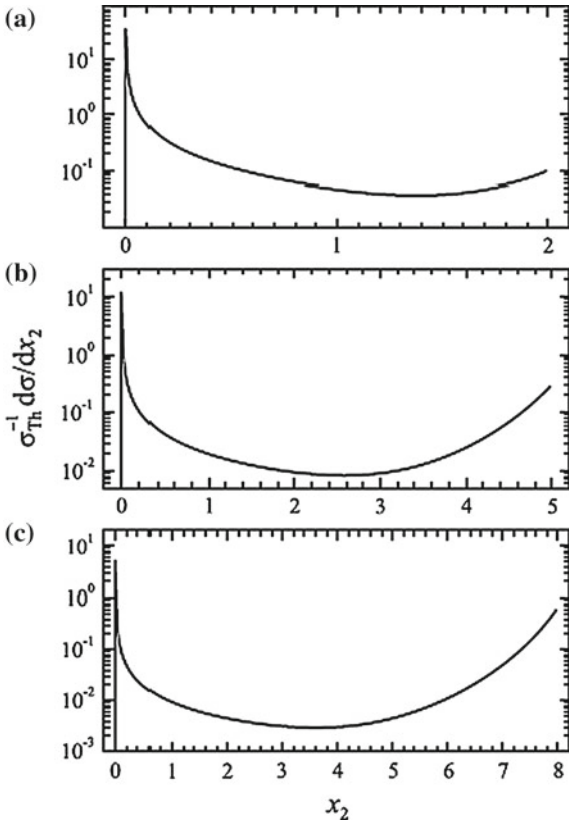

Fig. 5.4 Photon energy distributions for $Z = 20$ in three cases: **a** the total cross section is dominated by the pole terms ($x_1 = 2$); **b** the pole and seagull terms provide equal contributions to the cross section ($x_1 = 5$); **c** the cross section is dominated by the seagull term ($x_1 = 8$) [16]

which is $\omega_1 = 21.2\,\mathrm{eV}$ for hydrogen. If ω_λ does not depend on ω_1 (or depends on it in a more complicated way), the maximum of (5.133) is shifted from the value (5.134). In changing the value of λ from 10^{-3} to $2 \cdot 10^{-3}$, we change the value of σ'_P by about 10% if $c \sim 10^{-1}$.

The contribution of the seagull term (5.129) is

$$\frac{\sigma_{SG}}{\sigma_{Th}} = \frac{64}{3}(\alpha Z)^2 x_1^2 \int_0^{x_1-1} dx_p V(x_p); \quad x_p = \varepsilon/I_Z = \xi^{-2}. \tag{5.135}$$

The cross section of the Compton scattering depends on x_1 and Z separately. The energy dependence of the cross section for several values of Z, calculated by employing (5.82–5.85) for the amplitude, is shown in Fig. 5.5. The maxima, which are close to those predicted by (5.134), originate from the soft photon region.

One can see that the contribution of the low-energy photons (5.133) decreases with energy, while the contribution of the low-energy electrons (5.135) increases with energy. At $x_1 \gg 1$, i.e., at $\omega_1 \gg I_Z$ (but still $\omega_1 \ll \eta$), the integral on the RHS of (5.135) does not depend on the actual value of the upper limit, being saturated

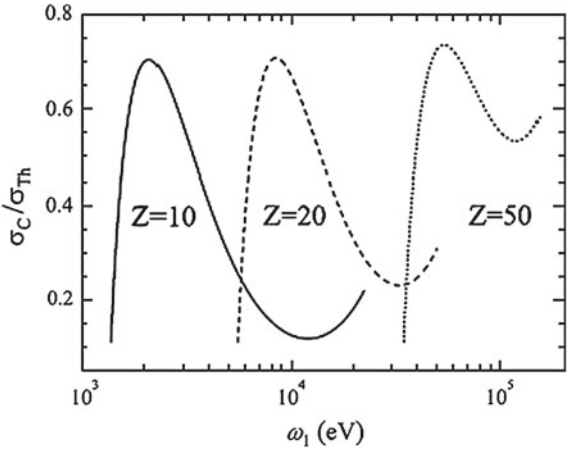

Fig. 5.5 Energy dependence of the Compton scattering cross section for several values of the nuclear charge Z [16]

by $x_p \sim 1$. Direct calculation provides $\int_0^\infty dx_p V(x_p) = 6.6 \cdot 10^{-3}$, leading to the limiting relation

$$\frac{\sigma}{\sigma_{Th}} = 0.14(\alpha Z)^2 x_1^2 = 0.56\frac{\omega_1^2}{\eta^2} \tag{5.136}$$

for $I_Z \ll \omega_1 \ll \eta$. Analysis of the case $\omega_1 \sim \eta$ can be carried out in a similar way. Here the cross section is determined by the seagull terms, but its dependence on the energies is more complicated.

As well as in the cases of Rayleigh and Raman scattering, the calculations for the other states in the Coulomb field can be carried out by applying certain differential operators to the RHS of (5.82)–(5.84); see Sect. 5.2.

In the high-energy nonrelativistic limit $\eta \ll \omega_1 \ll m$, the momenta of the outgoing electrons satisfy the condition $p \gg \eta$ in most of the Bethe ridge. The cross section is determined by $q \sim \eta$, where the amplitude is

$$F = F_0 \psi_i(\mathbf{q}) , \tag{5.137}$$

where F_0 determined by (5.94) is the amplitude for the process on the free electron at rest. Following the general analysis carried out in Sect. 2.2.2, we obtain in this limit

$$\sigma = \sigma_{Th} . \tag{5.138}$$

This is true for every bound state in every binding field.

5.4.3 Total Cross Section of Photon Scattering

Now we can draw some conclusions regarding the total cross section σ_{tot} of the photon scattering on an atom, which is summed over the final states of the electrons (inclusive cross section). One can write

$$\sigma_{tot} = \sigma_{el} + \sigma_R + \sigma_C \,, \tag{5.139}$$

with the first term on the RHS standing for the cross sections of the elastic (Rayleigh) scattering, the second term is the sum of the cross sections of the Raman scattering, while the last one is the cross section of the Compton scattering. The amplitude of the process, in which the final state of the electron is labeled by the lower index x, can be written as

$$F_x = F_0 T_x(\mathbf{q}); \quad T_x(\mathbf{q}) = \langle \psi_x | e^{i\mathbf{q}\cdot\mathbf{r}} | \psi_{in} \rangle. \tag{5.140}$$

Proceeding similarly to what we did in Sect. 2.2.2, we obtain

$$\frac{d\sigma_{tot}}{d\Omega_2 d^3q} = \mathscr{S}_x |T_x(\mathbf{q})|^2 \frac{d\sigma_{Th}}{d\Omega_2}. \tag{5.141}$$

Due to the completeness (closure) condition

$$\mathscr{S}_x |\psi_x\rangle\langle\psi_x| = 1, \tag{5.142}$$

we obtain

$$\int \frac{d^3q}{(2\pi)^3} \mathscr{S}_x |T_x(\mathbf{q})|^2 = 1, \tag{5.143}$$

and thus

$$\frac{d\sigma_{tot}}{d\Omega_2} = \frac{d\sigma_{Th}}{d\Omega_2}, \tag{5.144}$$

and also

$$\sigma_{tot} = \sigma_{Th}. \tag{5.145}$$

We have seen earlier that at $I_Z \ll \omega_1 \ll \eta$, the sum (5.139) is dominated by Rayleigh scattering, while at $\eta \ll \omega_1 \ll m$, it is dominated by Compton scattering. This is also true for every binding field. The new content is that (5.145) is true also for $\omega_1 \sim \eta$ for every bound state and for every binding field. In this energy region, all three possible processes are important. The distribution between the channels depends on the initial state and on the nature of the binding field.

5.5 Expansion in Powers of $1/Z$

Now we shall include interactions between the electrons moving in the Coulomb field of the nucleus. Since the strength of this interaction is $1/Z$ times that between the electrons and the nucleus, it is expected to be determined by the parameter $1/Z$. Unexpectedly, the lowest-order terms appear to provide a rather accurate description even for the case of helium, where $Z = 2$.

5.5.1 Ground-State Energies of Heliumlike Ions

If the interactions between the bound electrons is neglected, the energy of the ground state of the helium atom is $\varepsilon_0 = -2I_Z \approx -109\,\mathrm{eV}$. This differs strongly from the experimental value $\varepsilon \approx -78.9\,\mathrm{eV}$. Now let us include the lowest-order correction caused by interaction between the bound electrons. It is

$$\varepsilon_{ee} \;=\; \langle \Psi | U_{ee} | \Psi \rangle \,. \tag{5.146}$$

Here $\Psi(\mathbf{r_1}, \mathbf{r_2}) = \psi(r_1)\psi(r_2)$, while the single-particle wave functions $\psi(r)$ are determined by (5.9), and $U_{ee} = \alpha/|\mathbf{r}_1 - \mathbf{r}_2|$ is the interaction between the electrons. Hence

$$\varepsilon_{ee} \;=\; \int d^3r_1 d^3r_2 \rho(r_1) \frac{\alpha}{|\mathbf{r}_1 - \mathbf{r}_2|} \rho(r_2)\,, \tag{5.147}$$

with $\rho(r_i) = \psi^*(r_i)\psi(r_i)$. Since only the monopole term of the partial wave expansion for the function $1/|\mathbf{r}_1 - \mathbf{r}_2|$ contributes, we can put

$$\frac{1}{|\mathbf{r}_1 - \mathbf{r}_2|} = \frac{1}{r_1} \quad (r_1 > r_2); \quad \frac{1}{|\mathbf{r}_1 - \mathbf{r}_2|} = \frac{1}{r_2} \quad (r_2 > r_1), \tag{5.148}$$

$$\varepsilon_{ee} \;=\; 2(4\pi)^2 \int_0^\infty dr_1 r_1 \rho(r_1) \int_0^{r_1} dr_2 r_2^2 \rho(r_2). \tag{5.149}$$

Direct calculation provides

$$\varepsilon_{ee} \;=\; \frac{5}{4} Z I_1; \quad I_1 = \frac{m\alpha^2}{2} \;\approx\; 13.6\,\mathrm{eV}. \tag{5.150}$$

One can obtain this expression as well by employing the technique developed in Sect. 5.1. We suggest that the reader carry out this exercise.

For helium, (5.150) provides $\varepsilon_{ee} = 34.0\,\mathrm{eV}$. This leads to the energy $\varepsilon = \varepsilon_0 + \varepsilon_{ee} = -74.8\,\mathrm{eV}$, which differs by about 5% from the experimental value. One could expect the accuracy to be about $1/Z^2 = 1/4$. However, it appears to be much better.

It is instructive to compare this result with the ground-state energy value obtained by assuming that the approximate wave function of two $1s$ electrons takes the form $\Psi_a(\mathbf{r_1}, \mathbf{r_2}) = \psi(Z_{eff}; r_1)\psi(Z_{eff}; r_2)$, with $\psi(Z_{eff}; r_i)$ the functions in the Coulomb field of the nucleus with certain effective charge Z_{eff} [1]. Of course, such a function is not a solution of the wave equation for helium. However, we can try to minimize the discrepancy between its LHS and RHS by requiring that $F(Z_{eff}) = \langle\Psi_a(Z_{eff})|H - \varepsilon|\Psi_a(Z_{eff})\rangle$, with the Hamiltonian H determined by (4.81) reaching its smallest value. This is known as the variational principle. The condition $\partial F(Z_{eff})/\partial Z_{eff} = 0$ provides the equation

$$Z_{eff}^2 + Z_{eff}(\frac{5}{8} - 2Z) \;=\; 0; \quad Z_{eff} \;=\; Z - \frac{5}{16}, \tag{5.151}$$

and the binding energy is

$$\varepsilon \;=\; -2I_1 Z^2(1 - \frac{5}{16Z})^2. \tag{5.152}$$

Note that the lowest correction of the order $1/Z$ coincides with that obtained in the perturbative approach; (5.150).

For helium, we have $Z_{eff} = 27/16$, and the energy is $\varepsilon = -77.5\,\text{eV}$. This deviates from the experimental value by less than 2%.

5.5.2 *Photoionization of Helium Near the Threshold*

At relatively small photon energies ω, corresponding to the energies of the photoelectrons $\varepsilon \leq I_Z$, the hydrogenlike formula (5.78) does not reproduce the experimental values for the cross sections. For example, for helium, it provides the value $\sigma_{ph} = 3.15\,\text{Mb}$ at the threshold of the process ($\varepsilon \to 0$), while the experimental value is $\sigma_{ph} = 7.40\,\text{Mb}$. Now we shall see how the situation changes if we include the electron interactions in the lowest order of perturbation theory.

We must add the amplitude (5.75), in which the electrons do not interact, and the amplitudes in which the initial-state or final-state electrons interact in the lowest order of perturbation theory. In the latter case, the amplitude can be written as

$$F^{(1)} \;=\; N(\omega)\int \frac{d^3q}{(2\pi)^3} J_1(\mathbf{q})\frac{4\pi\alpha}{q^2} J_2(\mathbf{q}) + \cdots, \tag{5.153}$$

with

$$J_1(\mathbf{q}) \;=\; \int \frac{d^3f}{(2\pi)^3}\frac{d^3f_1}{(2\pi)^3}\langle\psi_{\mathbf{p}}|\mathbf{f}-\mathbf{q}\rangle\langle\mathbf{f}|G(p)|\mathbf{f_1}\rangle\frac{\mathbf{e}\cdot\mathbf{f_1}}{m}\langle\mathbf{f_1}-\mathbf{k}|\psi\rangle; \tag{5.154}$$

$$J_2(\mathbf{q}) = \int \frac{d^3 f_2}{(2\pi)^3} \langle \psi | \mathbf{f}_2 \rangle \langle \mathbf{f}_2 - \mathbf{q} | \psi \rangle .$$

Here ψ and $\psi_{\mathbf{p}}$ are the Coulomb wave functions describing the bound $1s$ electron and the photoelectron. The dots on the RHS of (5.153) denote the contribution in which the final-state single-particle electron functions are permuted. A similar expression can be written for the amplitude that includes electron interactions in the initial state.

One can evaluate the integrals on the RHS of (5.153) and (5.154) by employing the technique developed in Sect. 5.2. Integration over $\mathbf{f}_1$ provides

$$\int \frac{d^3 f_1}{(2\pi)^3} \langle \mathbf{f} | G(p) | \mathbf{f_1} \rangle \frac{\mathbf{e} \cdot \mathbf{f_1}}{m} \langle \mathbf{f_1} - \mathbf{k} | \psi \rangle = \frac{N_1 \eta}{m} \mathbf{e} \cdot \boldsymbol{\nabla}_k \langle \mathbf{f} | G(p) V_{i\eta} | \mathbf{k} \rangle |_{k=0}. \quad (5.155)$$

Integration over $\mathbf{f}$ can be carried out by employing (5.29), providing

$$J_1(\mathbf{q}) = \eta N_1 N_p \frac{\mathbf{e} \cdot \boldsymbol{\nabla}_k}{m} \Big(- \frac{\partial}{\partial \lambda} \Big) \hat{J}_x \langle \mathbf{p}(1-x) + \mathbf{q} | \mathscr{T}(\varepsilon, -ipx + \lambda, \eta) | \mathbf{k} \rangle |_{k=0, \lambda=0}. \quad (5.156)$$

Integration over $\mathbf{f}_2$ provides

$$J_2 = N_1^2 \Big(- \frac{\partial}{\partial \eta} \Big) \langle \mathbf{q} | V_{i\eta + i\kappa} | 0 \rangle , \quad (5.157)$$

where me must put $\kappa = \eta$ after calculation of the derivative. Now we write

$$\frac{1}{q^2} \langle \mathbf{q} | V_{i\mu} | 0 \rangle = \frac{1}{\mu^2} \Big(\langle \mathbf{q} | V_0 | 0 \rangle - \langle \mathbf{q} | V_{i\mu} | 0 \rangle \Big). \quad (5.158)$$

The matrix element on the RHS of (5.156) can be represented in the form (5.63), with dependence on $\mathbf{q}$ contained only in $|\mathbf{q}\rangle$. This enables us to calculate the integral over $\mathbf{q}$. Thus the amplitude $F^{(1)}$ can be written in terms of one-dimensional integrals, which are presented in [17].

As we have seen in Chap. 3, the electron interactions are determined by the parameter $\xi_{ee} = \alpha / v$, where v is their relative velocity. The bound state does not have a definite momentum, but we can characterize it by the average momentum $\eta = m\alpha Z$. Thus the effective value of ξ is $1/Z$ for initial-state interactions. In the final state, it is of the same order for all $\varepsilon \lesssim I_Z$. As we have seen in Chap. 4, at large energies $\varepsilon \gg I_Z$, the real part of the amplitude $F^{(1)}$ is proportional to ξ_{ee}, but it obtains also additional quenching due to large values of the photoelectron momenta $p \gg \eta$. There is no such quenching at $\varepsilon \sim I_Z$, and Re $F^{(1)} \sim \xi = 1/Z$. Thus the corrections of order $1/Z$ to the cross section come from the interference terms $F^{(0)} \cdot$ Re $F^{(1)}$.

Inclusion of these corrections makes the deviations from the experimental data much smaller. The threshold value of the cross section for helium becomes $\sigma_{ph} = 7.19\,\text{Mb}$, with 3% deviation from the experimental data.

References

1. H.A. Bethe, E.E. Salpeter, *Quantum Mechanics of One- and Two-Electron Atoms* (Dover Publications, NY, 2008)
2. L.D. Landau, E.M. Lifshits, *Quantum Mechanics. Nonrelativistic Theory* (Pergamon, N.Y., 1977)
3. L. Hostler, R.H. Pratt, Phys. Rev. Lett. **10**, 469 (1963)
4. L. Hostler, J. Math. Phys. **5**, 591 (1964)
5. V.G. Gorshkov, ZhETF **47**, 352 (1964); Sov. Phys. JETP **20**, 234 (1965)
6. V.G. Gorshkov, A.I. Mikhailov, ZhETF **44**, 2142 (1963)
7. V.G. Gorshkov, V.S. Polikanov, ZhETF Lett. **9**, 464 (1969)
8. V.S. Polikanov, Theoret. Math. Phys. **26**, 26 (1976)
9. E.T. Whittaker, G.N. Watson, *A Course of Modern Analysis* (Cambridge University Press, Cambridge, 1996)
10. J.D. Jackson, *Classical Electrodynamics* (Willey, NY-London, 1998)
11. A.I. Akhiezer, V.B. Berestetskii, *Quantum Electrodynamics* (Pergamon, N.Y., 1982)
12. L.F. Vitushkin, A.I. Mikhailov, Sov. Phys. JETP **43**, 917 (1976)
13. B.A. Zon, A.N. Manakov, L.P. Rapoport, Sov. Phys. JETP **28**, 480 (1969)
14. A.I. Mikhailov, A.N. Moskalev, G.V. Frolov, Opt. Spectrosc. **54**, 599 (1983)
15. F.E. Low, Phys. Rev. **110**, 974 (1958)
16. E.G. Drukarev, A.I. Mikhailov, I.A. Mikhailov, Phys. Rev. A **82**, 023404 (2010)
17. A.I. Mikhailov, A.V. Nefiodov, G. Plunien, Phys. Lett. A **368**, 391 (2007)

Chapter 6
The Coulomb Field. Relativistic Case

Abstract We obtain the relativistic electron Coulomb functions as power series in $\alpha^2 Z^2$ with the Furry–Sommerfeld–Maue functions as the lowest order approximation. The results are employed for calculation of photoionization angular distribution and the cross section with inclusion of the terms of order $\alpha^3 Z^3$. We consider also second-order processes. We study the role of various mechanisms for photon elastic scattering on atoms. We present the characteristics of Compton scattering on the Bethe ridge with inclusion of the $\alpha^2 Z^2$ terms. Employing the results of Chap. 4, we calculate the differential distributions for the Compton scattering outside the Bethe ridge.

6.1 Wave Functions

6.1.1 Wave Functions with Fixed Angular Momentum

The relativistic electron in the Coulomb field is described by the Dirac equation

$$\left(\boldsymbol{\alpha}\cdot\mathbf{p}+\beta m-\frac{\alpha Z}{r}\right)\psi = E\psi;\quad \mathbf{p}=-i\nabla. \tag{6.1}$$

Solutions of (6.1) are analyzed in books on quantum electrodynamics; see, e.g., [1]. Here we recall the main points.

We do not now assume the velocities of the bound and continuum electrons (in units of the speed of light) to be small. Thus we do not consider $\alpha^2 Z^2$ to be a small parameter. We also employ relativistic kinematics.

As in any central field, the state of the electron can be determined by the energy E, the total momentum j, which is the sum of the orbital momentum and spin, and its projection $j_z = m$. Each state is the combination of the states with the orbital angular momenta $\ell = j \pm 1/2$, thus having different spatial parities. The wave functions $\psi_{Ej\ell m}$ with $\ell = j \pm 1/2$ of both discrete and continuum spectra can be obtained in closed form:

E.G. Drukarev and A.I. Mikhailov, *High-Energy Atomic Physics*,
Springer Series on Atomic, Optical, and Plasma Physics 93,
DOI 10.1007/978-3-319-32736-5_6

$$\psi_{Ej\ell m}(\mathbf{r}) = \begin{pmatrix} g_{Ej\ell}(r)\Omega_{j\ell m}(\mathbf{n}) \\ i f_{Ej\ell'}(r)\Omega_{j\ell' m}(\mathbf{n}) \end{pmatrix}; \quad \Omega_{j\ell' m}(\mathbf{n}) = -(\boldsymbol{\sigma}\cdot\mathbf{n})\Omega_{j\ell m}(\mathbf{n}); \quad \mathbf{n} = \frac{\mathbf{r}}{r}; \tag{6.2}$$
$$\ell, \ell' = j \pm 1/2\,,$$

with $\Omega_{j\ell m}(\mathbf{n})$ the spherical spinors. Below, we shall omit the lower indices of the functions $g(r)$ and $f(r)$.

The radial functions $g(r)$ and $f(r)$ are singular at the origin:

$$g(r),\, f(r) \sim r^{\gamma-1} \quad r \to 0, \tag{6.3}$$

where

$$\gamma = \sqrt{(j+1/2)^2 - (\alpha Z)^2}. \tag{6.4}$$

For the discrete spectrum the energy is

$$E = m\Big(1 + \frac{(\alpha Z)^2}{(n - j - 1/2 + \gamma)^2}\Big)^{-1/2}, \tag{6.5}$$

with $n = 1, 2, \ldots$.

Considering the nonrelativistic limit $(\alpha Z)^2 \to 0$, one can see that n is the analogue of the principal quantum number of the nonrelativistic case. For the bound states we have $j \le n - 1/2$ and $\ell \le n - 1$. Thus for $n = 1$ there is only one state; its angular momentum is $j = 1/2$. This state has also a definite value of the angular momentum $\ell = 0$. To keep a connection with the nonrelativistic notation, it is usually denoted by $1s_{1/2}$. There are states with $j = 1/2$ and $j = 3/2$ for $n = 2$. The former can be treated as the superposition of the states with $\ell = 0$ and $\ell = 1$, i.e., of the $2s_{1/2}$ and $2p_{1/2}$ states. The latter is usually notated as $2p_{3/2}$.

In the spectrum of the Dirac equation, the energy levels corresponding to the same n and j but different $\ell = j \pm 1/2$ remain doubly degenerate. The observable difference between these values, called the Lamb shift, can be calculated by means of quantum electrodynamics. The point is described in detail in the book [2] for small Z and in the review [3] for large Z.

We present as an example the wave function of the ground state ($n = 1$, $j = 1/2$):

$$\psi_{1s}(\mathbf{r}) = \begin{pmatrix} g(r)\chi \\ -i(\boldsymbol{\sigma}\cdot\mathbf{n}) f(r)\chi \end{pmatrix}; \quad \mathbf{n} = \frac{\mathbf{r}}{r}, \tag{6.6}$$

with χ the two-component Pauli spinor,

$$g(r) = N_1 e^{-\eta r}(\eta r)^{\gamma-1} h_1(\gamma); \quad f(r) = -N_1 e^{-\eta r}(\eta r)^{\gamma-1} h_2(\gamma); \quad \eta = m\alpha Z, \tag{6.7}$$

where $\gamma = \sqrt{1 - \alpha^2 Z^2}$ while $N_1 = (\eta^3/\pi)^{1/2}$ is the value of the nonrelativistic wave function at the origin, and

$$h_1(\gamma) = \left(\frac{1+\gamma}{2\Gamma(1+2\gamma)}\right)^{1/2}; \quad h_2(\gamma) = h_1(\gamma)\frac{1-\gamma}{\alpha Z}. \tag{6.8}$$

Note that the product of the first two factors in the expressions for $g(r)$ and $f(r)$ forms the nonrelativistic wave function ψ_{1s}^{nr} of the $1s$ state. The energy of the electron in the ground state is

$$E_{1s} \;=\; m\sqrt{1-\alpha^2 Z^2} = m\gamma\,. \tag{6.9}$$

Thus the relativistic electron appears to be bound more strongly than the nonrelativistic one.

The wave function ψ_{Ejm} of the continuum state also can be written as the sum of the functions (6.2) with $\ell = j \pm 1/2$. The radial functions $g(r)$ and $f(r)$ can be represented in terms of the confluent hypergeometric functions $F(\gamma+1+i\xi, 2\gamma+1; 2ipr)$, with γ defined by (6.4). Explicit expressions for the functions $\psi_{Ejm}(\mathbf{r})$ are given in [1].

However, in contrast to the nonrelativistic case, a closed representation for the continuum wave function $\psi_{\mathbf{p}}$ with the asymptotic momentum $\mathbf{p}$ is unknown. The continuum wave functions at $E \gg m$ make an exception [4].

6.1.2 *The Continuum Wave Function in the Ultrarelativistic Limit*

To find the expression for the continuum function, we begin with the Dirac equation (6.1) written in the form

$$\Big(E - \boldsymbol{\alpha}\cdot\mathbf{p} - \beta m - V\Big)\psi_{\mathbf{p}} = 0,$$

with $V = -\alpha Z/r$ and $\mathbf{p} = -i\nabla$. We use the notation

$$\tilde{\mathbf{k}} \;=\; \boldsymbol{\alpha}\cdot\mathbf{k} \tag{6.10}$$

for any three-dimensional vector $\mathbf{k}$, and multiply the wave equation on the left by the operator $E + \tilde{\mathbf{p}} + \beta m - V$. This leads to the equation

$$\Big(\nabla^2 + p^2 - 2EV + i(\tilde{\boldsymbol{\nabla}}V) + V^2\Big)\psi_{\mathbf{p}} \;=\; 0; \quad p^2 = E^2 - m^2. \tag{6.11}$$

Substituting $\psi_{\mathbf{p}}(\mathbf{r}) = e^{i\mathbf{p}\cdot\mathbf{r}}F(\mathbf{r})u_{\mathbf{p}}$, with the spinor $u_{\mathbf{p}}$ corresponding to the free motion, we find that the function $F(\mathbf{r})$ satisfies the equation

$$\Big(\nabla^2 + 2i\mathbf{p}\nabla - 2EV + V^2 + i(\tilde{\boldsymbol{\nabla}}V)\Big)F(\mathbf{r})u_{\mathbf{p}} \;=\; 0. \tag{6.12}$$

We try to find the wave function at $r \gtrsim 1/m$ corresponding to momentum $q \lesssim m$ transferred to the nucleus. Thus $pr \gg 1$. In this limit, we can omit two last terms in the parentheses on the right-hand side (RHS) of (6.12). Thus

$$\left(\nabla^2 + 2i\mathbf{p}\nabla - 2EV\right)F(\mathbf{r}) \;=\; 0. \tag{6.13}$$

Now we solve a simpler equation, in which the first term in parentheses is neglected:

$$\left(i\mathbf{p}\nabla - EV\right)F(\mathbf{r}) = 0, \tag{6.14}$$

We shall analyze the value of the neglected term in the next step. Putting $F(\mathbf{r}) = e^{iw(\mathbf{r})}$, we write (6.14) as

$$\mathbf{p}\nabla w + EV \;=\; 0. \tag{6.15}$$

The solution of this equation is

$$w(r_z, r_t) \;=\; \alpha Z \ln(pr + pr_z) f(r_t), \tag{6.16}$$

the z-direction of the momentum $\mathbf{p}$, r_t is orthogonal to $\mathbf{p}$, $r_t^2 = r^2 - r_z^2$, and f is an arbitrary function of r_t. The choice $f = 1$ leads to the wave function (we omit the phase factor)

$$\psi_{\mathbf{p}} \;=\; e^{i\mathbf{p}\cdot\mathbf{r}} e^{i\alpha Z \ln(pr+pr_z)} u_{\mathbf{p}}. \tag{6.17}$$

Putting $f(r_t) = -\alpha Z \ln(p^2 r_t^2)$ on the RHS of (6.16), we obtain another solution,

$$\psi_{\mathbf{p}} \;=\; e^{i\mathbf{p}\cdot\mathbf{r}} e^{-i\alpha Z \ln(pr-pr_z)} u_{\mathbf{p}}. \tag{6.18}$$

The solutions (6.17) and (6.18) are known as distorted plane waves. Calculating the first term on the left-hand side (LHS) of (6.13) with the functions determined by (6.17) and (6.18), we obtain an additional condition for the validity of these wave functions,

$$pr \pm \mathbf{p}\cdot\mathbf{r} \;\gg\; 1\,. \tag{6.19}$$

Thus at $E \gg m$, the wave functions represented by (6.17) and (6.18) obtained by Pratt [4] are the solutions of the wave equation (6.11) under the restriction expressed by (6.19). The corrections to these functions are of order m/E.

Analysis of the wave equation enables us to obtain an approximate wave function that is free from the limitation (6.19). The condition $r \gg 1/E$ enables us to neglect the last two terms on the LHS of (6.11). We come to the equation

$$(\nabla^2 + p^2 - 2EV)\psi_{\mathbf{p}} \;=\; 0\,, \tag{6.20}$$

which is just the nonrelativistic equation for the electron in the Coulomb field with the mass m replaced by the total energy E. Its solution is the modified nonrelativistic

wave function $\psi_{\mathbf{p}}^{nr}(\mathbf{r}) = e^{i\mathbf{p}\cdot\mathbf{r}} F^{nr}(\mathbf{r})$ with the same replacement $m \to E$. In the next step, we include all the terms except the last one on the LHS of (6.11),

$$\left(\nabla^2 + p^2 - 2EV + i(\tilde{\nabla} V)\right)\psi_{\mathbf{p}} \;=\; 0. \tag{6.21}$$

In neglecting the term V^2, we have neglected the terms of higher order in αZ. Representing the solution of (6.21) in the form $\psi_{\mathbf{p}}(\mathbf{r}) = e^{i\mathbf{p}\cdot\mathbf{r}}(F^{nr}(\mathbf{r})u_{\mathbf{p}} + \phi(\mathbf{r}))$, we obtain, employing (6.20) [5],

$$\phi(\mathbf{r}) \;=\; -i\frac{\tilde{\nabla}}{2E} F^{nr}(\mathbf{r})u_{\mathbf{p}}\,. \tag{6.22}$$

This is the lowest correction to the nonrelativistic wave function; the higher correction yields the additional factor αZ.

The latter equation is a special case of the Furry–Sommerfeld–Maue (FSM) functions [5, 6], which are the combination of the nonrelativistic terms and the first-order correction proportional to αZ. We shall try to find an expansion of the relativistic functions in powers of the relativistic parameter αZ. The coefficients of this expansion will be the functions of the Coulomb parameter $\xi = \alpha ZE/p$. The zero-order terms are the FSM functions.

6.1.3 *Furry–Sommerfeld–Maue Approximation*

Let us find the ground-state function for $(\alpha Z)^2 \to 0$, i.e., $\gamma \to 1$. In this limit, the functions $h_{1,2}$ defined by (6.8) are $h_1 = 1/\sqrt{2}, h_2 = \alpha Z/2\sqrt{2}$. Thus the ground-state wave function can be written as

$$\psi_{1s}^{FSM}(\mathbf{r}) \;=\; (1 - \frac{i\tilde{\nabla}}{2m})\psi_{1s}^{nr}(\mathbf{r})u_0, \tag{6.23}$$

with u_0 the bispinor of the free electron at rest. Thus for the ground state, the FSM function is expressed in terms of the nonrelativistic one. In momentum representation,

$$\psi_{1s}^{FSM}(\mathbf{f}) \;=\; \left(1 + \frac{\tilde{\mathbf{f}}}{2m}\right)\psi_{1s}^{nr}(\mathbf{f})u_0\,. \tag{6.24}$$

Using the technique developed in Sect. 5.2, one can find a similar relation between the FSM and the nonrelativistic functions for every bound state. Note that for small $f = |\mathbf{f}| \sim \eta$, the second term in parentheses on the RHS of (6.23) provides a small correction of order αZ to the first term. At large $f \sim m$, both terms are of the same order.

For the continuum states, the dependence of the functions $\psi_{Ejm}(\mathbf{r})$ on $(\alpha Z)^2$ is contained in the parameter γ defined by (6.4). In the FSM approximation, we must put

$$\gamma \;=\; j + 1/2\,. \tag{6.25}$$

Under this assumption, the series for the continuum wave function

$$\psi_{\mathbf{p}}(\mathbf{r}) = \sum_{jm} a_{jm}\psi_{Ejm}(\mathbf{r}); \quad p = |\mathbf{p}| = \sqrt{E^2 - m^2} \tag{6.26}$$

was found to be

$$\psi_{\mathbf{p}}^{FSM}(\mathbf{r}) = N_p e^{i(\mathbf{p}\cdot\mathbf{r})}\Big(1 - \frac{i\tilde{\boldsymbol{\nabla}}}{2E}\Big)\,{}_1F_1(i\xi, 1, ipr - i\mathbf{p}\cdot\mathbf{r})u_{\mathbf{p}}. \tag{6.27}$$

Here

$$N_p = N(p) = \sqrt{\frac{2\pi\xi}{1 - e^{-2\pi\xi}}}$$

is the normalization factor of the nonrelativistic continuum function with three-momentum p and total energy E; see (3.19). Note that we keep the relativistic value of the energy E on the RHS of (6.27), and $\xi = \alpha ZE/p$; see (3.17) and (3.18). Neglecting the second term in the parentheses on the RHS of (6.27), we would obtain the corresponding nonrelativistic function with the electron rest energy m replaced by E; see (5.25).

Carrying out the Fourier transform, we find that in the momentum space,

$$\psi_{\mathbf{p}}^{FSM}(\mathbf{f}) \;= \Big(1 + \frac{\tilde{\mathbf{f}} - \tilde{\mathbf{p}}}{2E}\Big)\psi_{\mathbf{p}}^{nr}(\mathbf{f})u_{\mathbf{p}}. \tag{6.28}$$

Similarly to the case of the discrete spectrum, the second term in parentheses on the RHS provides a small correction of order αZ to the first term for small $q = |\mathbf{f} - \mathbf{p}| \ll E$. At large $q \sim E$, both terms are of the same order.

Employing the explicit expression (5.30) for the nonrelativistic function, we can also represent the FSM function as

$$\psi_{\mathbf{p}}^{FSM}(\mathbf{f}) = N_p\Big(-\frac{\partial}{\partial\lambda} + \frac{ip\tilde{\nabla}_{\mathbf{p}}}{2E}\Big)\Phi_{\mathbf{p}}(\mathbf{f},\lambda)u_{\mathbf{p}}|_{\lambda=0} = \tag{6.29}$$

$$N_p\Big(-\frac{\partial}{\partial\lambda} + \alpha Z\frac{i\tilde{\nabla}_{\mathbf{p}}}{2\xi}\Big)\Phi_{\mathbf{p}}(\mathbf{f},\lambda)u_{\mathbf{p}}|_{\lambda=0}.$$

In the second equality, the factor αZ manifests itself explicitly. In (6.29),

$$\Phi_{\mathbf{p}}(\mathbf{f},\lambda)=\frac{4\pi}{a}\left(\frac{a}{b}\right)^{i\xi};\quad a=q^2+\lambda^2;\quad b=(\mathbf{q}+\mathbf{p})^2-(p+i\lambda)^2;\quad \mathbf{q}=\mathbf{f}-\mathbf{p}. \tag{6.30}$$

The operator $\nabla_{\mathbf{p}}$ in (6.29) does not act on ξ and q.

These expressions for the FSM continuum wave function can be obtained by comparing the Lippmann–Schwinger equations for the nonrelativistic wave function (with the relativistic value of the energy E) and for the relativistic one. We define, separating the bispinor of free motion $u_{\mathbf{p}}$,

$$\psi_{\mathbf{p}}\ =\ \varphi_{\mathbf{p}}u_{\mathbf{p}}\,. \tag{6.31}$$

In the nonrelativistic case, we have just $\psi^{nr}_{\mathbf{p}}=\varphi^{nr}_{\mathbf{p}}$. Note that $\varphi_{\mathbf{p}}$ is a 4×4 matrix acting on the Lorentz indices of the bispinor $u_{\mathbf{p}}$. The nonrelativistic $\varphi^{nr}_{\mathbf{p}}$ is a unit matrix. The LSE can be written as

$$\varphi^{nr}_{\mathbf{p}}=\varphi^{(0)}_{\mathbf{p}}-G_0(p)V_0\varphi^{nr}_{\mathbf{p}};\quad \varphi_{\mathbf{p}}=\varphi^{(0)}_{\mathbf{p}}-G_0(p)\gamma_0V_0\varphi_{\mathbf{p}}. \tag{6.32}$$

Here $\varphi^{(0)}_{\mathbf{p}}$ describes free motion, $p=|\mathbf{p}|$, while the propagator

$$\langle\mathbf{f}|G_0(p)|\mathbf{f}_1\rangle=G_0(p,\mathbf{f})\delta(\mathbf{f}-\mathbf{f}_1);\quad G_0(p,\mathbf{f})=\frac{2E}{p^2-f^2+i\delta};\quad \delta\to 0, \tag{6.33}$$

with $p^2=E^2-m^2$, differs from the nonrelativistic Green function of free motion given by (2.29) by the factor E/m. The Coulomb interaction between the nucleus and the electron is represented as

$$V=-\alpha ZV_0;\quad \langle\mathbf{r}|V_0|\mathbf{r}_1\rangle=\frac{\delta(\mathbf{r}-\mathbf{r}_1)}{r};\quad \langle\mathbf{f}|V_0|\mathbf{f}_1\rangle=\frac{4\pi}{(\mathbf{f}-\mathbf{f}_1)^2}. \tag{6.34}$$

It is instructive to write these equations in terms of the Möller operator

$$|\varphi^{nr}_{\mathbf{p}}\rangle=\mathscr{M}^{nr}|\varphi^{(0)}_{\mathbf{p}}\rangle=\mathscr{M}^{nr}|\mathbf{p}\rangle\,. \tag{6.35}$$

The nonrelativistic operator $\mathscr{M}^{nr}$ satisfies the equation

$$\mathscr{M}^{nr}\ =\ 1-\alpha ZG_0(p)V_0\mathscr{M}^{nr}, \tag{6.36}$$

while in the relativistic case,

$$|\varphi_{\mathbf{p}}\rangle=\mathscr{M}|\mathbf{p}\rangle\quad \mathscr{M}\ =\ 1-\alpha ZG(p)\gamma_0V_0\mathscr{M}\,, \tag{6.37}$$

with the Green function of the free Dirac equation G given by (2.35). The equations for the Möller operator presented above are the direct consequence of the LSE (see Sect. (2.1.3)). For further calculations, we introduce $G_+ = G\gamma_0$ and $G_- = G_+ - G_0$, i.e.,

$$\langle \mathbf{f}_1|G_\pm(p)|\mathbf{f}_2\rangle = G_\pm(p,\mathbf{f_1})\delta(\mathbf{f}_1-\mathbf{f}_2); \quad G_\pm(p;\mathbf{f}) = \frac{\tilde{\mathbf{f}}+\beta m \pm E}{p^2-f^2+i\delta}. \tag{6.38}$$

We write (6.37) as

$$\mathscr{M} \;=\; 1-\alpha Z G_+ V_0 \mathscr{M}\,. \tag{6.39}$$

Here and below, we omit the argument p of the electron propagators.

Now we solve (6.39) in the FSM approximation, i.e., we keep only corrections of order αZ to the nonrelativistic operator $\mathscr{M}^{nr}$. Thus

$$\mathscr{M}^{FSM} \;=\; 1-\alpha Z G_+ V_0 \mathscr{M}^{nr}. \tag{6.40}$$

Comparing this expression with (6.36), we obtain

$$\mathscr{M}^{FSM} \;=\; (1-\alpha Z G_- V_0)\mathscr{M}^{nr}. \tag{6.41}$$

Using (6.35), we obtain

$$\psi_{\mathbf{p}}^{FSM}(\mathbf{f}) \;=\; \Big(\varphi_{\mathbf{p}}^{nr}(\mathbf{f}) - \alpha Z\langle \mathbf{f}|G_- V_0|\varphi_{\mathbf{p}}^{nr}\rangle\Big)u_{\mathbf{p}}\,. \tag{6.42}$$

Due to the equation of motion $(m\gamma_0 - E)u_{\mathbf{p}} = -\tilde{\mathbf{p}}u_{\mathbf{p}}$, we can write

$$\varphi_{\mathbf{p}}^{FSM}(\mathbf{f}) - \varphi_{\mathbf{p}}^{nr}(\mathbf{f}) \;=\; -\alpha Z\frac{\tilde{\mathbf{f}}-\tilde{\mathbf{p}}}{2E}\langle \mathbf{f}|G_0 V_0|\varphi_{\mathbf{p}}^{nr}\rangle. \tag{6.43}$$

Employing (6.36), we obtain $-\alpha Z G_0 V_0|\varphi_{\mathbf{p}}^{nr}\rangle = -|\mathbf{p}\rangle + |\varphi_{\mathbf{p}}^{nr}\rangle$, coming to (6.28).

For the Coulomb Green function in the FSM approximation, we obtain

$$G_c^{FSM} = \mathscr{M}^{FSM} G_+; \quad \langle \mathbf{f}|G_c^{FSM}|\mathbf{f}_1\rangle = \langle \mathbf{f}|\mathscr{M}^{FSM}|\mathbf{f}_1\rangle G_+(\mathbf{f}_1). \tag{6.44}$$

Note that since the difference between the right-hand sides of (6.4) and (6.25) is of the order $(\alpha Z)^2/\ell$, the FSM functions become increasingly accurate for processes in which high values of the orbital momenta are involved. For example, if an electron scatters on a small angle $\theta \ll 1$, the momentum $q \approx p\theta$ is transferred to the target. The transverse distances $r_t \sim 1/q$ are important, and effective values of angular momentum are $\ell = p/q \gg 1$. Thus the corrections to the FSM functions are of order $(\alpha Z)^2 q/p$.

6.2 The αZ Dependence of Electron Functions

6.2.1 Power Series for Wave Functions

Now we obtain the relativistic Möller operator as a power series of the parameter αZ:

$$\mathscr{M} = \sum_{n=0} (\alpha Z)^n \mathscr{M}^{(n)}, \tag{6.45}$$

where the term with $n = 0$ corresponds to the nonrelativistic approximation, and $\mathscr{M}^{(0)} = \mathscr{M}^{nr}$. We also find from (6.41) that $\mathscr{M}^{(1)} = -G_- V_0 \mathscr{M}^{nr}$. Note that the terms $\mathscr{M}^{(n)}$ on the RHS of (6.45) depend on the Coulomb parameter $\xi = \alpha Z E/p$.

It follows from (6.39) that for $n \geq 1$,

$$\mathscr{M}^{(n)} = (-G_+ V_0)^{n-1} \mathscr{M}^{(1)}, \tag{6.46}$$

i.e., all the terms are expressed through the operator $\mathscr{M}^{(1)}$. Thus the continuum wave function can written as

$$\varphi_{\mathbf{p}} = \varphi^{nr}_{\mathbf{p}} + \alpha Z \sum_{n=0} (-\alpha Z)^n (G_+ V_0)^n \varphi^1_{\mathbf{p}}, \tag{6.47}$$

with $\varphi^1_{\mathbf{p}} = \varphi^{FSM}_{\mathbf{p}} - \varphi^{nr}_{\mathbf{p}} = \mathscr{M}^{(1)} \varphi^{(0)}_{\mathbf{p}}$. For example, up to the terms $(\alpha Z)^3$,

$$\varphi_{\mathbf{p}} = \varphi^{nr}_{\mathbf{p}} + \alpha Z \varphi^1_{\mathbf{p}} - (\alpha Z)^2 G_+ V_0 \varphi^1_{\mathbf{p}} + (\alpha Z)^3 G_+ V_0 G_+ V_0 \varphi^1_{\mathbf{p}}. \tag{6.48}$$

Since the continuum wave functions can be obtained only as the αZ series, it is reasonable to have the bound state wave functions in a similar form. The wave function of the ground state can be written as

$$\psi_{1s}(\mathbf{r}) = N_1 \phi_{1s} u_0; \quad \phi_{1s} = (r + i\tau \tilde{\mathbf{r}}) e^{-\eta r} \Gamma(1+\sigma) r^{-\sigma-1}, \tag{6.49}$$

with $\Gamma(x)$ the Euler gamma function, while

$$\eta = m\alpha Z; \quad \gamma = \sqrt{1-(\alpha Z)^2}; \quad \tau = \left(\frac{1-\gamma}{1+\gamma}\right)^{1/2}; \quad \sigma = 1-\gamma. \tag{6.50}$$

We shall see that the additional factor $\Gamma(1+\sigma)$ is introduced to make further calculations more convenient. The normalization factor is now

$$N_1^2 = \frac{(2\eta)^{2\gamma+1}(1+\gamma)}{8\pi \Gamma(2\gamma+1)\Gamma^2(1+\sigma)}.$$

In the limit $(\alpha Z)^2 \to 0$, we obtain $\gamma = 1$, $\tau = \alpha Z/2$, and $\psi_{1s} = \psi_{1s}^{FSM}$. In the limit $\alpha Z \to 0$, we obtain $\tau = 0$ and $\psi_{1s} = \psi_{1s}^{nr}$.

Now we find the ground-state wave function in momentum space. For the FSM function, we can put $\sigma = 0$, $r^{-\sigma-1} = r^{-1}$, and the wave function can be represented in terms of the matrix elements of the Yukawa potential, as was done in Sect. 5.2 for the nonrelativistic case:

$$\phi_{1s}(\mathbf{f}) = \Gamma_\eta \langle \mathbf{f}|V_{i\eta}|\mathbf{k}\rangle; \quad \Gamma_\eta = \Big(-\frac{\partial}{\partial\eta} + \frac{\alpha Z}{2}\tilde{\nabla}_{\mathbf{k}}\Big)|_{\mathbf{k}=0}. \tag{6.51}$$

In order to include the higher terms of the αZ series, we employ the relation

$$r^{-1-\sigma}\Gamma(1+\sigma) = \int_0^\infty d\lambda e^{-r\lambda}\lambda^\sigma, \tag{6.52}$$

and write

$$\phi_{1s}(\mathbf{f}) = \Gamma_\lambda \langle \mathbf{f}|V_{i\eta+i\lambda}|\mathbf{k}\rangle\,, \tag{6.53}$$

with

$$\Gamma_\lambda = \Gamma_\eta\Big(-\frac{\partial}{\partial\eta}\Big)\int_0^\infty d\lambda\lambda^\sigma. \tag{6.54}$$

Setting here $\lambda^\sigma = e^{\sigma\ln\lambda} = 1 + \sigma\ln\lambda + \cdots$, we obtain an expansion in powers of σ. Expanding also the parameter τ in powers of αZ, we obtain an expansion of the function ϕ_{1s} in powers of αZ. For the first two terms of the expansion, we obtain

$$\Big(-\frac{\partial}{\partial\eta}\Big)\int_0^\infty d\lambda\langle \mathbf{f}|V_{i\eta+i\lambda}|\mathbf{k}\rangle = \Big(-\frac{\partial}{\partial\eta}\Big)\int_\eta^\infty d\rho\langle \mathbf{f}|V_{i\rho}|\mathbf{k}\rangle = \langle \mathbf{f}|V_{i\eta}|\mathbf{k}\rangle,$$

and we arrive at (6.51). For the terms up to $(\alpha Z)^3$, we obtain

$$\Gamma_\lambda = \Gamma_\eta + \frac{(\alpha Z)^2}{2}\Gamma_\eta\Big(-\frac{\partial}{\partial\eta}\Big)\int_0^\infty d\lambda\ln\lambda. \tag{6.55}$$

Returning to the continuum wave functions, note that they depend on αZ directly and also through the Sommerfeld parameter $\xi = \alpha Z/v$. Equations (6.45) and (6.47) include both. In the next section, we obtain an equation that treats the dependence on these two parameters separately.

6.2.2 *Relativistic Functions in Terms of FSM Functions*

We have seen that relativistic functions can be expressed in terms of the lowest-order Möller operators $\mathscr{M}^{nr}$ and $\mathscr{M}^1$. Now we shall represent them as power series in

$\alpha^2 Z^2$ with the coefficients expressed in terms of the FSM operators [7]. We begin by representing the functions in terms of $\mathscr{M}^{nr}$ and $\mathscr{M}^{FSM}$. Putting

$$\mathscr{M} \;=\; \mathscr{M}^{FSM}\Lambda\,, \tag{6.56}$$

we write (6.39), employing (6.41), as

$$(1-\alpha ZG_-V_0)\mathscr{M}^{nr}\Lambda = 1-\alpha ZG_+V_0\mathscr{M}^{nr}\Lambda+\alpha^2Z^2A\Lambda;\quad A=G_+V_0G_-V_0\mathscr{M}^{nr}. \tag{6.57}$$

We evaluate

$$-1+(1-\alpha ZG_-V_0)\mathscr{M}^{nr}\Lambda+\alpha ZG_+\mathscr{M}^{nr}\Lambda=(1+\alpha ZG_0V_0)\mathscr{M}^{nr}\Lambda-1=\Lambda-1. \tag{6.58}$$

Employing (6.36), we find that $\alpha ZG_0V_0\mathscr{M}^{nr}\Lambda = 1-\mathscr{M}^{nr}\Lambda$. Thus we arrive at an equation for Λ:

$$\Lambda \;=\; 1+(\alpha Z)^2A\Lambda\,, \tag{6.59}$$

which represents the Möller operator in terms of $\mathscr{M}^{nr}$ and $\mathscr{M}^{FSM}$. The iteration procedure demonstrates that Λ can be written as a sum of the terms A^n. Thus $\Lambda A = A\Lambda$, and we can write (6.59) as

$$\Lambda \;=\; 1+(\alpha Z)^2\Lambda A\,. \tag{6.60}$$

Now we demonstrate that the operator A depends only on the parameter ξ. Writing (6.60) for the matrix elements

$$\langle \mathbf{f}|\Lambda|\mathbf{p}\rangle = \langle \mathbf{f}|\mathbf{p}\rangle + (\alpha Z)^2\int\frac{d^3f_1}{(2\pi)^3}\langle \mathbf{f}|\Lambda|\mathbf{f}_1\rangle\langle \mathbf{f}_1|A|\mathbf{p}\rangle \tag{6.61}$$

and representing

$$\langle \mathbf{f}_1|A|\mathbf{p}\rangle = \int\frac{d^3k}{(2\pi)^3}\langle \mathbf{f}_1|A_1|\mathbf{k}\rangle\langle \mathbf{k}|A_2|\mathbf{p}\rangle;\quad A_1=G_+V_0G_-;\quad A_2=V_0\mathscr{M}^{nr}, \tag{6.62}$$

we can write $(\tilde{\mathbf{f}}_1+E+m\beta)(\tilde{\mathbf{k}}-E+m\beta)=\tilde{\mathbf{f}}_1\tilde{\mathbf{k}}-p^2+(\tilde{\mathbf{k}}-\tilde{\mathbf{f}}_1)(E-m\beta)$ for the spinor structure of the numerator. Since this matrix acts on the bispinor $u_{\mathbf{p}}$, the factor $(E-m\beta)$ in the last term can be replaced by $\tilde{\mathbf{p}}$, and we have

$$\langle \mathbf{f}_1|A|\mathbf{p}\rangle = \int\frac{d^3k}{(2\pi)^3}\frac{\tilde{\mathbf{f}}_1\tilde{\mathbf{k}}+(\tilde{\mathbf{k}}-\tilde{\mathbf{f}}_1)\tilde{\mathbf{p}}-p^2}{(p^2-f_1^2+i\delta)(\mathbf{f}_1-\mathbf{k})^2(p^2-k^2+i\delta)}\langle \mathbf{k}|A_2|\mathbf{p}\rangle. \tag{6.63}$$

Employing the technique developed in Sect. 5.2, we obtain for the last factor on the RHS of (6.63),

$$\langle \mathbf{k}|A_2|\mathbf{p}\rangle = \int \frac{d^3q}{(2\pi)^3}\langle \mathbf{k}|V_0|\mathbf{q}\rangle\langle \mathbf{q}|\varphi^{nr}_{\mathbf{p}}\rangle = \frac{4\pi N(\xi)}{a}\left(\frac{a}{b}\right)^{i\xi}; \tag{6.64}$$

$$a = (\mathbf{k}-\mathbf{p})^2; \quad b = k^2 - p^2,$$

with $N(\xi)$ the normalization factor of the nonrelativistic continuum function. Introducing

$$\mathbf{v} = \frac{\mathbf{f}}{p}; \quad \mathbf{v}_1 = \frac{\mathbf{f}_1}{p}; \quad \mathbf{u} = \frac{\mathbf{k}}{p}; \quad \mathbf{n} = \frac{\mathbf{p}}{p}, \tag{6.65}$$

we can write (6.63) in the form

$$\langle \mathbf{f}_1|A|\mathbf{p}\rangle = \frac{1}{p^3}\langle \mathbf{v}_1|A|\mathbf{n}\rangle, \tag{6.66}$$

$$\langle \mathbf{v}_1|A|\mathbf{n}\rangle = \int \frac{d^3u}{(2\pi)^3}\frac{\tilde{\mathbf{v}}_1\tilde{\mathbf{u}} + (\tilde{\mathbf{u}}-\tilde{\mathbf{v}}_1)\tilde{\mathbf{n}} - 1}{(1-v_1^2+i\delta)(\mathbf{v}_1-\mathbf{u})^2(1-u^2+i\delta)}\langle \mathbf{u}|A_2|\mathbf{n}\rangle,$$

where

$$\langle \mathbf{u}|A_2|\mathbf{n}\rangle \;=\; p^2\langle \mathbf{k}|A_2|\mathbf{p}\rangle.$$

Since also $\langle \mathbf{f}|\mathbf{p}\rangle = \langle \mathbf{v}|\mathbf{n}\rangle/p^3 = \delta(\mathbf{v}-\mathbf{n})/p^3$, we find that

$$\langle \mathbf{f}|\Lambda|\mathbf{p}\rangle = \frac{1}{p^3}\langle \mathbf{v}|\Lambda|\mathbf{n}\rangle, \tag{6.67}$$

and (6.61) can be written as

$$\langle \mathbf{v}|\Lambda|\mathbf{n}\rangle = \langle \mathbf{v}|\mathbf{n}\rangle + (\alpha Z)^2\int \frac{d^3v_1}{(2\pi)^3}\langle \mathbf{v}|\Lambda|\mathbf{v}_1\rangle\langle \mathbf{v}_1|A|\mathbf{n}\rangle. \tag{6.68}$$

Here the matrix element of the operator A does not contain any dependence on the parameter $(\alpha Z)^2$. Its dependence on the parameter ξ is determined by (6.64) and (6.66).

Thus iteration of (6.59) and (6.60) provides the expansion of the relativistic wave function in powers of $(\alpha Z)^2$ with the coefficients of the power series being functions of ξ:

$$\Lambda((\alpha Z)^2, \xi) \;=\; 1 + (\alpha Z)^2 A(\xi)\Lambda\Big((\alpha Z)^2, \xi\Big). \tag{6.69}$$

Its solution in operator form is

$$\Lambda((\alpha Z)^2, \xi) \;=\; \frac{1}{1-(\alpha Z)^2 A(\xi)}\,. \tag{6.70}$$

An actual solution can be obtained by iteration of (6.69).

Thus the relativistic Coulomb wave function of a continuum electron with asymptotic momentum $\mathbf{p}$ can be represented in terms of the nonrelativistic Coulomb wave function

$$\psi_{\mathbf{p}}(\mathbf{f}) \;=\; \mathscr{M}\varphi^0_{\mathbf{p}} u_{\mathbf{p}}\,, \tag{6.71}$$

with operator $\mathscr{M}$ given by (6.56), while Λ is determined by (6.70). Similarly, one can represent the relativistic Coulomb propagator as

$$G_C(E) \;=\; \mathscr{M} G_+(E)\,, \tag{6.72}$$

while G_+ is given by (6.38).

Note that there is no sense in calculating too many terms of the expansion in powers of $(\alpha Z)^2$. The solution of the Dirac equation does not include the radiative corrections, which are of order $\alpha \sim 0.01$. For example, at $Z \le 50$, we obtain $(\alpha Z)^4 \le 2 \times 10^{-2}$, and for these values of Z, inclusion of the terms of the order $(\alpha Z)^4$ is beyond the accuracy of the approach.

Applications will be presented in next three sections.

6.3 Photoeffect

6.3.1 General Remarks

Calculation of the angular distribution and of the total cross section is a more difficult task than it was in the nonrelativistic case. The spin variables are involved, making the calculations more complicated. The continuum wave function cannot be represented in closed form, and can be obtained only as a power series of the parameter αZ. Also, the ratio of the photon-to-electron momenta is $k/p \sim 1$. Thus all angular momenta of the outgoing electron may provide a noticeable contribution, and (5.70) is no longer valid. The angular distribution becomes much more complicated.

The general expression for the angular distribution of the photoelectrons is very much like the expression in the nonrelativistic case. For a single bound electron in the initial state, we have

$$d\sigma_{ph} = pE|\bar{F}_{ph}|^2 \frac{d\Omega}{4\pi^2}; \quad t = \mathbf{k}\cdot\mathbf{p}/\omega p\,. \tag{6.73}$$

The overbar indicates that averaging over polarizations in the initial state and summation over those in the final state are carried out. For the photoelectron energy we have $E^2 = p^2 + m^2$, and in the limit $E - m \ll m$, we arrive at (5.76). However, now

$$F_{ph} = \langle \psi_{\mathbf{p}} | \hat{A} | \psi_i \rangle; \quad \hat{A} = -\mathbf{A}\boldsymbol{\gamma} \tag{6.74}$$

while ψ_i and $\psi_{\mathbf{p}}$ are the relativistic wave functions of the initial and final electrons, and $\boldsymbol{\gamma}$ are the Dirac matrices. We carry out calculations for the bound electron in $1s$ state. A similar analysis can be carried out for any bound state in the Coulomb field.

We shall present all equations for the case of one electron in the $1s$ state. The results for the closed K shell can be obtained by multiplying by the factor 2. In the nonrelativistic case, this was trivial, since the two K electrons are independent. In the relativistic case, the spin variables are involved, and one should carry out a simple calculation. The amplitude is proportional to the matrix element $M = \langle \Psi_f | \gamma_1 + \gamma_2 | \Psi_0 \rangle$. Here 1 and 2 stand for the space and spin coordinates of the two electrons, $\gamma_i = (a\mathbf{e} \cdot \mathbf{p} + ib\boldsymbol{\sigma}_i \cdot \mathbf{h}) e^{i\mathbf{k}\cdot\mathbf{r}_i}$ $(i = 1, 2)$, and the vector $\mathbf{h}$ is a composition of vectors $\mathbf{k}$, $\mathbf{e}$ and $\mathbf{p}$. Also, $\Psi_0 = \varphi_{1s}(1)\varphi_{1s}(2)\mathscr{S}_0$ is the initial-state wave function, with $\mathscr{S}_0$ describing the two-electron state with spin $S = 0$. The final-state wave function is $\Psi_f = \Phi_s \mathscr{S}_0 + \Phi_a \mathscr{S}_{1\mu}$, with $\mathscr{S}_{1\mu}$ describing the two-electron state with spin $S = 1$ and its projection μ. Here $\Phi_s = (\varphi_{\mathbf{p}}(1)\varphi_{1s}(2) + \varphi_{\mathbf{p}}(2)\varphi_{1s}(1))/\sqrt{2}$ and $\Phi_a = (\varphi_{\mathbf{p}}(1)\varphi_{1s}(2) - \varphi_{\mathbf{p}}(2)\varphi_{1s}(1))/\sqrt{2}$ are respectively the symmetric and antisymmetric space wave functions. Employing the relation $(\boldsymbol{\sigma}_1 + \boldsymbol{\sigma}_2)\mathscr{S}_0 = 0$, we obtain $M = [a\mathbf{e} \cdot \mathbf{p}\mathscr{S}_0^* \mathscr{S}_0 + ib\mathscr{S}_{1\mu}^* \boldsymbol{\sigma} \cdot \mathbf{h}\mathscr{S}_0]\sqrt{2}\langle \varphi_{\mathbf{p}} | e^{i\mathbf{k}\cdot\mathbf{r}} | \varphi_{1s} \rangle$. After summation over the spin variables of the final-state electrons, we obtain $|M|^2 = 2[(a^2(\mathbf{e} \cdot \mathbf{p})^2 + b^2h^2)\langle \varphi_{\mathbf{p}} | e^{i\mathbf{k}\cdot\mathbf{r}} | \varphi_{1s} \rangle^2]$. Since the expression in square brackets corresponds to the case of one electron in the K shell, this proves our statement.

There are two relativistic parameters in our process. In the nonrelativistic case, we considered photoionization in the lowest order in powers of αZ. Now we go beyond this approximation. Also, in the nonrelativistic case, the energies of the photons were limited by the condition $E - m \ll m$. Now we analyze mostly the case of fast electrons with $E - m \gtrsim m$. We begin, however, with the case in which the photon energy ω is close to the ionization potential of the $1s$ state, which is now $I_Z = m(1 - \gamma)$, and the photoelectrons absorb the energy $\omega - I_Z \ll m$.

6.3.2 *Threshold Ionization of Heavy Ions*

The amplitude of the photoeffect can be obtained by direct employing (6.74) with the electron wave functions described by (6.2). Considering the ionization of the $1s$ state, we represent its wave function as

$$\psi_{1s}(\mathbf{r}) = \begin{pmatrix} g(r)\Omega_{\frac{1}{2}0M}(\mathbf{n}) \\ if(r)\Omega_{\frac{1}{2}1M}(\mathbf{n}) \end{pmatrix}; \quad \mathbf{n} = \frac{\mathbf{r}}{r}, \tag{6.75}$$

where $M = \pm 1/2$ is the projection of the total angular momentum $j = 1/2$ of the $1s$ electron.

Integration over the angular variables in (6.74) by expansion of the exponential factor in spherical harmonics leads to the set of radial integrals $R_\kappa^\pm$. Here we use the conventional notation $\kappa = \ell$ for $j = \ell - 1/2$, while $\kappa = -\ell - 1$ is used for $j = \ell + 1/2$. The upper indices of $R_\kappa^\pm$ correspond to the values $M = \pm 1/2$. The integrands contain the products $g(r) f_\kappa(r)$ and $f(r) g_\kappa(r)$. For example,

$$R_\kappa^+ = -\frac{\sqrt{\ell(\ell^2-1)}}{2\ell+1} \int_0^\infty dr r^2 F(r) g_\ell(r) (j_{\ell-1}(kr) + j_{\ell+1}(kr)), \tag{6.76}$$

where $j_{\ell\pm1}$ are the spherical Bessel functions. The cross section of the photoeffect is

$$\sigma_{ph} = \frac{16\pi\alpha p E}{\omega} \cdot \sum_{\kappa=\pm n} (|R_\kappa^+|^2 + |R_\kappa^-|^2), \tag{6.77}$$

with integer values of $n \neq 0$.

If $p \gtrsim m$, the integrals $R_\kappa^\pm$ are saturated at $r \sim 1/p$ and can be estimated as $R_\kappa^\pm \sim (k/p)^{\ell-1} \sim 1$. Thus, strictly speaking, one needs an infinite number of terms on the RHS of (6.77). It was shown in [8] that $n = 8$ terms are necessary to achieve an accuracy of 10% at $E \approx 1$ MeV. Of course, this is easy for today's computational facilities. However, it is useful to have a simple analytical formula. In the threshold region such a formula can be obtained.

If the photon energy is close to the binding energy of the ionized state, and thus the momentum of the photoelectron $p \to 0$, the photoionization proceeds at distances of order the size of the K shell $r_K = 1/\eta$, with $\eta = m\alpha Z$. Since $\omega \to I_Z \approx m\alpha^2 Z^2/2$, we can estimate

$$R_\kappa^\pm \sim (k/\eta)^{\ell-1} \sim (\alpha Z)^{\ell-1}, \tag{6.78}$$

except $R_{-1}^- \sim (\alpha Z)^2$. Thus the series on the RHS of (6.77) can be rearranged to a power series in $\alpha^2 Z^2$. The number of terms is determined by the required accuracy of computations. For example, if we want to achieve the accuracy $\alpha^6 Z^6$, we need $-4 \leq \kappa \leq 3$ [9].

In the nonrelativistic limit, we can write

$$\sigma_{ph} = \sigma_{ph}^{nr} = \sigma_0 f(\tau), \tag{6.79}$$

with σ_{ph}^{nr} determined by (5.78), $\tau = p^2/\eta^2$, while

$$\sigma_0 = \frac{2^8 \pi^2 \alpha e^{-4}}{3m\omega} = \frac{168}{1-\gamma} \text{ [barn]} \tag{6.80}$$

is the nonrelativistic value of σ_{ph} at the threshold where $\omega = m(1-\gamma)$.

Employing the explicit equations for the Coulomb functions g_κ and f_κ, one can simplify calculations in the vicinity of the threshold, where $p \ll \eta$ [9]. For

$$\omega - I_Z \lesssim \alpha^2 Z^2 I_Z \approx \frac{m\alpha^4 Z^4}{2}, \tag{6.81}$$

where $p \lesssim \alpha Z\eta$ (this makes about 50 keV above the threshold in the case of uranium), expansion in powers of k/η and p/η provides

$$\sigma_{ph}(p) = \sigma_0\Big(f(\tau) - 0.393a - 0.144a^2 + 1.023\tau a + O(a^3)\Big). \tag{6.82}$$

Here $a = \alpha^2 Z^2$, $\tau = p^2/\eta^2$, while

$$f(\tau) = 1 - 5\tau/3 + 94\tau^2/45 + O(\tau^3). \tag{6.83}$$

The threshold value ($p = 0$) for uranium $\sigma = 0.793\sigma_0$ provided by (6.82) appears to be very close to the result of direct numerical computations $\sigma = 0.789\sigma_0$ presented in [10].

6.3.3 The αZ Dependence of Amplitude

Now we consider the case in which the photoelectron carries a large energy $E - m \gtrsim m$. We calculate the angular distribution and the total cross section of photoionization of the hydrogenlike atoms, taking into account the terms of relative order $(\alpha Z)^2$. Since the process cannot proceed for a free electron, the lowest-order amplitude is proportional to αZ. Thus we must include the terms up to $(\alpha Z)^3$.

The wave function of the $1s$ state is expressed by (6.53). The wave function of the continuum state is given by (6.48). Combining these expressions, we can write

$$F_{ph} = N(\omega) N_p N_1 \bar{u}_{\mathbf{p}} T u_0, \tag{6.84}$$

where $u_{\mathbf{p}}$ and u_0 are the Dirac bispinors corresponding to the free motion, while

$$T = T_0 + \alpha Z T_1 + (\alpha Z)^2 T_2 + (\alpha Z)^3 T_3, \tag{6.85}$$

with the terms on the RHS corresponding to the expansion of the wave function of the photoelectron (6.48):

$$T_0 = \langle\varphi^{nr}_{\mathbf{p}}|V_{i\mu}|\mathbf{k}\rangle\hat{e}\Gamma_\lambda; \quad T_1 = \langle\varphi^1_{\mathbf{p}}|V_{i\mu}|\mathbf{k}\rangle\hat{e}\Gamma_\lambda; \quad T_2 = -\langle\varphi^1_{\mathbf{p}}|\hat{V}_0 G V_{i\eta}|\mathbf{k}\rangle\hat{e}\Gamma_\eta,$$
$$T_3 = \Big(-\frac{\partial}{\partial\eta}\Big)\langle\varphi^1_{\mathbf{p}}|\hat{V}_0 G \hat{V}_0 G V_{i\eta}|\mathbf{k}\rangle\hat{e}\,. \tag{6.86}$$

The operators Γ_λ and Γ_η act on the left. Since the process can not take place on the free electron, the term T_0 is actually proportional to αZ. In the lowest-order term $T_0 + \alpha Z T_1$, only the contributions of order αZ are included in the wave function of the photoelectron. The corrections up to order $(\alpha Z)^2$ are included in the wave function of the $1s$ electron. In the term $(\alpha Z)^2 T_2$, the wave function of the $1s$ electron is included in the FSM approximation. The contribution $(\alpha Z)^3 T_3$ contains the nonrelativistic wave function of the $1s$ electron.

Note that the functions T_n $(n = 0, 1, 2, 3)$ contain two more parameters that depend on αZ. These are the Coulomb parameter $\xi = \alpha Z E/p$ and momentum $\eta = m\alpha Z$.

6.3.4 Calculations in the Lowest Order in αZ

Here we calculate the amplitude T in the lowest nonvanishing order in αZ. It can be represented as

$$T^{LO} \;=\; T_0^{LO} + \alpha Z T_1^{LO}\,. \tag{6.87}$$

The upper index LO is for "leading order." The terms on the RHS of (6.87) are

$$T_0^{LO} = \langle\varphi_{\mathbf{p}}^{nr}|V_{i\eta}|\mathbf{k}\rangle\hat{e}\Gamma_\eta; \quad T_1^{LO} = (-\frac{\partial}{\partial\eta})\langle\varphi_{\mathbf{p}}^{1}|V_{i\eta}|\mathbf{k}\rangle\hat{e}. \tag{6.88}$$

Employing the technique developed in Sect. 5.2 we obtain

$$T_0^{LO} = -\hat{e}\frac{\partial}{\partial\eta}\Phi_{\mathbf{p}}(\mathbf{k},\eta); \quad T_1^{LO} = -\frac{\tilde{\mathbf{c}}}{b}\Phi_{\mathbf{p}}(\mathbf{k},\eta), \tag{6.89}$$

with $\Phi_{\mathbf{p}}(\mathbf{k},\eta)$ and b defined by (6.30), while $\mathbf{c} = \mathbf{q} - i\eta\mathbf{p}/p$, and momentum $\mathbf{q} = \mathbf{k} - \mathbf{p}$ is transferred to the nucleus. Recall that $\eta = m\alpha Z$.

While we are calculating the lowest nonvanishing terms of the αZ expansion, we put $\eta = 0$ in all ingredients of (6.89) except the function

$$\Theta \;=\; \Big(\frac{a}{b}\Big)^{i\xi} = \Big(\frac{q^2+\eta^2}{k^2-(p+1\eta)^2}\Big)^{i\xi}, \tag{6.90}$$

which enters the amplitude (6.87) as a factor.

In the lowest order of expansion in powers of $(\alpha Z)^2$, the energy conservation law can be written as

$$E \;=\; \omega + m; \quad p^2 - k^2 \;=\; 2m\omega\,. \tag{6.91}$$

Thus, employing (6.87), we can write

$$\bar{u}_{\mathbf{p}} T^{LO} u_0 = \frac{4\pi\alpha Z\Theta}{q^2}\bar{u}_p\Big(\frac{2m\hat{\mathbf{e}}(1-\tilde{\mathbf{q}}/2m)}{q^2} - \frac{2E(1-\tilde{\mathbf{q}}/2E)\hat{\mathbf{e}}}{2m\omega}\Big)u_0. \tag{6.92}$$

Here we evaluated the second term by employing equation of motion $\bar{u}_p m\gamma_0 = \bar{u}_p(E+\tilde{\mathbf{p}})$. The first and second terms in the parentheses describe the transfer of large momentum $q \gg \eta$ to the nucleus by the bound electron and by the photoelectron respectively. One can immediately recognize the FSM structure of both terms. Writing the numerator of the second term as $\bar{u}_p(E-m-\tilde{\mathbf{k}})\hat{\mathbf{e}}u_0$, we see that for $\omega \ll m$, the first term dominates, as it should be in the nonrelativistic limit.

Thus the amplitude of the photoeffect is

$$F_{ph} \;=\; N(\omega)N_p\Theta X\,, \tag{6.93}$$

where

$$X = N_1 X_1; \quad X_1 = \frac{4\pi\alpha Z}{q^2}\bar{u}_{\mathbf{p}}\Big(\frac{\hat{\mathbf{e}}(2m-\tilde{\mathbf{q}})}{q^2} - \frac{(2E-\tilde{\mathbf{q}})\hat{\mathbf{e}}}{2m\omega}\Big)u_0. \tag{6.94}$$

Recall that $N_1 = (\eta^3/\pi)^{1/2}$ is the value of the nonrelativistic Coulomb wave function of the $1s$ electron at the origin. These equations have a clear physical meaning. The amplitude X describes the process in which the electrons interact with the nucleus only once, transferring large momentum $q \gg \eta$. The first term in parentheses describes this interaction in the initial state, while the second corresponds to interaction in the final state. All exchanges by small momenta $f \sim \eta$ are described by the factors N_1, N_p, and Θ on the RHS of (6.93).

As well as in the nonrelativistic case, the amplitude turns to zero for the photon and photoelectron moving along the same line, i.e., for $t = \pm 1$. In the nonrelativistic case, this happened because the spin of the electron was neglected, and the amplitude was proportional to the product $\mathbf{e}\cdot\mathbf{p}$. However, in the relativistic case, there are also structures proportional to $\mathbf{e}[\mathbf{k}\boldsymbol{\sigma}]$ and $\mathbf{e}[\mathbf{p}\boldsymbol{\sigma}]$. They do not vanish for $\mathbf{p}$ parallel to $\mathbf{k}$. One should do some algebra of γ matrices to prove the statement for the relativistic case.

One can evaluate the factor Θ, writing it as

$$\Theta = e^{-\pi\xi}\chi(\xi)\Phi(\xi); \quad \chi(\xi) = \exp(\xi \arctan\frac{2p\eta}{p^2-k^2-\eta^2}); \quad \Phi(\xi) = e^{i\xi\phi}, \tag{6.95}$$

with $\phi = \ln|a/b|$. Since $\chi(\xi) \approx \exp(\alpha^2 Z^2 E/\omega) \approx 1$, we can put

$$\Theta \;=\; e^{-\pi\xi}\Phi\,. \tag{6.96}$$

Thus the amplitude depends on ξ in terms of the parameter $\pi\xi$, i.e., the coefficients of the expansion in powers of ξ are numerically large. We do not carry out this expansion, keeping the dependence on ξ given by (6.96).

Employing (6.94), we obtain for the angular distribution

$$\frac{d\sigma_{ph}}{dt} = \frac{pM}{\omega}\frac{F(\theta)}{q^4}; \quad dt = \sin\theta d\theta, \tag{6.97}$$

with θ the angle between the directions of momenta $\mathbf{k}$ and $\mathbf{p}$,

$$M(\xi) = 2\pi \cdot 4\pi\alpha(\alpha Z)^2 N_p^2 N_1^2 e^{-2\pi\xi}, \tag{6.98}$$

and

$$F(\theta) = \frac{4mp^2\sin^2\theta}{q^4}\Big(1 + \frac{q^2}{4m^2}(\frac{\omega}{m} - 1)\Big). \tag{6.99}$$

Here $q^2 = p^2 + \omega^2 - 2p\omega\cos\theta$. One can see that the distribution (6.99) turns to zero at $\theta = 0$ and at $\theta = \pi$.

Integration of (6.97) provides an expression for the cross section

$$\sigma_{ph}(\omega) = \frac{M(\xi)}{4m^5}\frac{\zeta^2(1-\zeta^2)^{3/2}}{(1-\zeta)^5}\Big(\frac{4}{3} + \frac{1-2\zeta}{\zeta(\zeta+1)}\cdot(1 - \frac{\zeta^2}{2\sqrt{1-\zeta^2}}\ln\frac{1+\sqrt{1-\zeta^2}}{1-\sqrt{1-\zeta^2}})\Big), \tag{6.100}$$

with

$$\zeta = \frac{m}{E}. \tag{6.101}$$

In the limit $\pi\xi \ll 1$, i.e., for $N_p = 1$, $e^{-2\pi\xi} = 1$, this formula was obtained by Sauter in the early days of quantum mechanics [11]. In the ultrarelativistic limit $E \gg m$, the asymptotic of the cross section is

$$\sigma_{ph}(\omega) = \frac{M(\alpha Z)}{4m^5}\cdot\frac{m}{\omega}. \tag{6.102}$$

6.3.5 *Inclusion of Higher-Order Terms*

In order to increase the region of the values of Z where our calculations are valid, we must include the higher-order terms of the expansion in powers of αZ. Also, the angular distribution (6.97) turns to zero for the forward and backward photoemission ($\sin\theta = 0$). Thus to obtain a nonvanishing contribution for these angles, we must include the higher-order terms.

The lowest-order amplitudes (LOA) (6.89) are proportional to αZ; the corresponding angular distribution (6.97) is proportional to $(\alpha Z)^2$. The $(\alpha Z)^3$ term of the angular distribution also vanishes for $\sin\theta = 0$, since it comes from the interference between LOA and the term of order $(\alpha Z)^2$. Thus the lowest-order nonvanishing contribution comes from the terms of order $(\alpha Z)^2$ of the amplitude. Hence the amplitude (6.85) gives the leading nonvanishing contribution and a correction of order αZ to the angular distributions at small angles and at those close to π. It describes the angular distribution with relative error $(\alpha Z)^3$ at other angles.

The higher-order terms of the amplitude (6.85) can be calculated by employing the technique developed in Sect. 5.1 [12]. The last term T_3 can be evaluated in the limit $\eta = 0$. Here we employ a useful relation:

$$F(\mathbf{k}_1, \mathbf{k}) \equiv \Big(- \frac{\partial}{\partial \eta} \Big) \langle \mathbf{k}_1 | V_{i\eta} | \mathbf{k} \rangle |_{\eta=0} = (2\pi)^3 \delta(\mathbf{k}_1 - \mathbf{k}). \tag{6.103}$$

One can see that indeed, $F(\mathbf{k}, \mathbf{k}_1) = 0$, unless $\mathbf{k} = \mathbf{k}_1$ while $\int d^3k F(\mathbf{k}_1, \mathbf{k})/(2\pi)^3 = 1$. Thus one can write

$$T_3 = \langle \varphi^1_{\mathbf{p}} | \hat{V}_0 G \hat{V}_0 | \mathbf{k} \rangle G(\mathbf{k}) \hat{e} \,. \tag{6.104}$$

One can find that all the terms that compose the amplitude (6.85) contain the factors $(a/b)^{i\xi}$ and $1/q^2$. The amplitude can be written as

$$T = \Big(\frac{a}{b} \Big)^{i\xi} \frac{\alpha Z}{q^2} \Big(\tau_0 + \alpha Z \tau_1 + (\alpha Z)^2 \tau_2 + (\alpha Z)^3 \tau_3 \Big), \tag{6.105}$$

where τ_n do not depend on αZ. The angular distribution is thus

$$\frac{d\sigma_{ph}}{dt} = M(\xi) \frac{p}{\omega} \frac{A(\theta)}{q^4} \,, \tag{6.106}$$

with $M(\xi)$ defined by (6.98), and

$$A(\theta) = F(\theta) + \alpha Z G(\theta) + (\alpha Z)^2 F_1(\theta) + (\alpha Z)^3 G_1(\theta) \,, \tag{6.107}$$

with $F(\theta)$ determined by (6.99). Here $F(\theta)$ comes from the square of the LOA; G originates from interference between the LOA and the leading correction of order αZ, etc. Employing notation introduced in (6.105), we can write

$$F = \langle \tau_0 \tau_0 \rangle; \quad G = 2\mathrm{Re} \langle \tau_1 \tau_0^+ \rangle; \quad F_1 = \langle \tau_1 \tau_1^+ \rangle + 2\mathrm{Re} \langle \tau_2 \tau_0^+ \rangle; \tag{6.108}$$

$$G_1 = 2\mathrm{Re} \langle \tau_2 \tau_1^+ \rangle + 2\mathrm{Re} \langle \tau_3 \tau_0^+ \rangle,$$

where the angle brackets denote averaging over the electron spins.

Now we calculate the angular distribution, including the terms up to those of the order αZ, i.e., neglecting the contributions of the order $\alpha^2 Z^2$. For large $\theta \sim 1$ (excluding those close to π), we can neglect the last two terms on the RHS of (6.107). Employing the technique worked out in Sect. 5.2, we obtain

$$G(\theta) \;=\; \frac{\pi}{2}\,\frac{p^2\sin^2\theta}{q^3}\Big(2-\frac{\omega}{m}\Big)\Big(1+\frac{\omega-m}{2m-\omega}\cdot\frac{q^2(pm+Eq)}{mp(pq-\mathbf{p}\cdot\mathbf{q})}\Big). \qquad (6.109)$$

Note that the denominator of the last factor never turns to zero. This is because $p = \sqrt{\omega^2+2m\omega} > k$, and thus $\mathbf{p}\cdot\mathbf{q} = (k^2-p^2-q^2)/2 < 0$. The contribution comes from the interference between the LOA and the leading correction. Although the latter does not vanish for $\theta = 0, \pi$ [13], the function $G(\theta)$ does.

Consider now the case of small angles. Recall that the functions F and G become zero for $\theta = 0$. Hence for small values of θ, the higher-order terms containing the functions F_1 and G_1 should be included. The distribution (6.106) depends on the angle θ in terms of the structures $(\mathbf{ep})^2$ and $(\mathbf{kp})^2$. At small θ, the former is proportional to θ^2, while the latter has a constant value. Thus as $\theta \to 0$, $\langle\tau_0\tau_i^+\rangle$ $(i = 1, 2, 3)$ are proportional to θ^2. Hence at small $\theta \ll 1$, we can write $F(\theta) = \theta^2 f$, $G(\theta) = \theta^2 g$, presenting

$$A(\theta) \;=\; \theta^2 f + \alpha Z\theta^2 g + (\alpha Z)^2 F_1(0) + (\alpha Z)^3 G_1(0), \qquad (6.110)$$

with $F_1 = \langle\tau_1\tau_1^+\rangle$, $G_1 = 2Re\langle\tau_2\tau_1^+\rangle$.

For $\theta^2 \sim \alpha Z$, the first term on the RHS of (6.110) gives the leading contribution, with the second and third terms providing corrections of the order αZ. Here we need

$$F_1(0) = \frac{\omega}{16q^2}(1-\frac{q}{2\omega})^2[(\pi\frac{\omega}{p})^2 + 4(1-\frac{q^2}{2\omega p}\ln\frac{h}{q})^2]; \quad h = p+\omega, \qquad (6.111)$$

with $q = p - \omega$. For smaller angles $\theta \sim \alpha Z$, the first and third terms dominate on the RHS, while the second and the fourth give a correction of order αZ. We do not show here a complicated expression for the function $G_1(0)$. However, we shall need its ultrarelativistic limit

$$G_1(0) \;\approx\; -\frac{0.23\pi}{2}\,\frac{\omega}{m^2}\Big(1+O(\frac{m}{E})\Big). \qquad (6.112)$$

Analysis of the region of small angles becomes increasingly important in the ultrarelativistic case.

6.3.6 Ultrarelativistic Case

Now we consider the case of ultrarelativistic photoelectrons with energies $E \gg m$. This requires very large photon energies $\omega \gg m$. In the lowest nonvanishing order of expansion in powers of m/E, we obtain $p = k$, $p - k = m$. The momentum transferred to the nucleus is

$$q^2 = m^2\gamma^2 + 4E^2 \sin^2(\theta/2); \quad E = \omega + m\gamma; \quad \gamma = \sqrt{1 - \alpha^2 Z^2}. \tag{6.113}$$

As we have seen, the angular distribution is proportional to q^{-4}, reaching its largest values near the lowest limit of possible variations of q. Thus we are mostly interested in studying the region of small $\theta \sim m/E$, where q^2 is of order m^2 and can be represented as

$$q^2 = q_1^2 E^2; \quad q_1^2 = \zeta^2\gamma^2 + \theta^2, \tag{6.114}$$

where $\zeta = m/E$.

We shall carry out our calculations in the lowest order of expansion in powers of m/E [4, 14]. In this limit, the amplitude is determined by (6.74) with the photoelectron described by the modified nonrelativistic Coulomb wave function, in which the electron mass is replaced by its energy E. The FSM and higher corrections are quenched by the powers of the parameter $\alpha Z\zeta$.

We begin with calculation of the angular distribution in the FSM approximation. It is determined by (6.97), and the second term dominates in the expression (6.99) for the function $F(\theta)$. Putting $\gamma = 1$ in the expression (6.114) for q_1^2, we obtain

$$\frac{d\sigma_{ph}}{dt} = \frac{M(\xi)}{m^5} \cdot \frac{\zeta^3\theta^2}{q_1^6}. \tag{6.115}$$

We must put $\xi = \alpha Z$ in the factor $M(\xi)$ defined by (6.98). The distribution obtains the largest value at $\theta^2 = \theta_0^2 = \zeta^2/2 = m^2/2E^2$. The cross section is determined by the values of $\theta^2 \sim \zeta^2$, being given by (6.102).

Inclusion of the correction of order αZ given by (6.109) modifies the shape of the angular distribution, providing

$$\frac{d\sigma_{ph}}{dt} = \frac{M(\xi)}{m^5} \frac{\zeta^3\theta^2}{q_1^6} \left(1 - \frac{\pi\alpha Z}{2} \cdot \frac{m}{q}\right). \tag{6.116}$$

For moderate values of Z this shifts the position θ_0 of the peak. For $\theta = 0$ expression in parentheses on the RHS of (6.116) runs negative if $Z \geq 74$. This signals the importance of the higher-order corrections.

The wave function (6.17) enables us to calculate the amplitude as a function of the parameter αZ. Also, the amplitude can be calculated in all orders of expansion in powers of αZ. Employing the exact relativistic wave function of the $1s$ electron given by (6.53), we obtain

$$T = \hat{e}\Gamma_\lambda \Phi_{\mathbf{p}}(\mathbf{k}, \mu); \quad \mu = \nu + \lambda, \tag{6.117}$$

with $\Phi_{\mathbf{p}}(\mathbf{k}, \mu)$ determined by (6.30).

This amplitude can be written as

$$T = \hat{e}(-2p)^{i\xi}\sigma\Gamma_\eta I; \quad I = \int_0^\infty d\lambda\lambda^{\sigma-1}(q^2+\mu^2)^{i\xi-1}(z+i\mu)^{-i\xi}; \tag{6.118}$$

$$z = m\gamma; \quad \gamma = \sqrt{1-\alpha^2 Z^2}; \quad \sigma = 1-\gamma\,.$$

However, the expressions are too complicated for actual calculations. That is why we employ expansion in powers of αZ.

For very small angles $\theta \ll \zeta$, we can put $q^2 = m^2\gamma^2$, and obtain

$$\frac{d\sigma_{ph}}{dt} = \frac{M(\xi)E^3}{m^5}(\theta^2 f_1(\alpha Z) + (\alpha Z\zeta)^2 f_2(\alpha Z)). \tag{6.119}$$

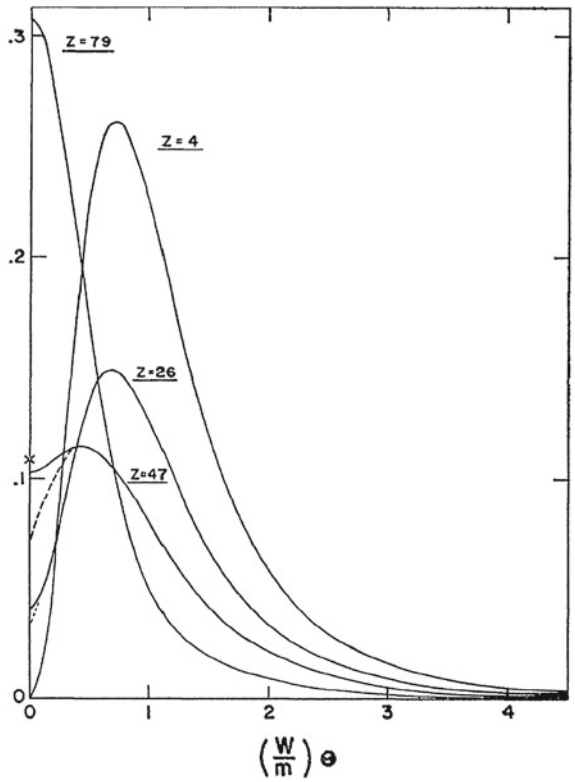

Fig. 6.1 The angular distribution of photoelectrons. The *horizontal axis* is for $E\theta/m(W = E)$. The *vertical axis* is the function $F = (d\sigma/dt)/\sigma_0$ with $\sigma_0 = 8\pi\alpha(\alpha Z)^3 E/m^3$. Reproduced from [15] with permission of AIP

Hence, the second term becomes important for $\theta \leq \alpha Z\zeta$. Employing (6.99), (6.109), (6.111), (6.112), and (6.118), we find that up to the terms of order $\alpha^3 Z^3$,

$$f_1(x) \;=\; 1 - 1.57x - 2.58x^2 + 1.49x^3; \quad f_2(x) \;=\; 0.87 - 0.37x - 0.86x^2\,. \tag{6.120}$$

The distribution (6.120) reaches its local minimum at $\theta = 0$ if $Z \leq 56$, since $f_1 > 0$ for those values of Z. It changes to a peak at $Z > 56$, when f_1 runs negative.

Employing (6.119) and (6.120), one can trace the shape of the angular distribution with variation of the nuclear charge Z [15] (Fig. 6.1).

6.4 Elastic Scattering of the High Energy Photons on Atoms

6.4.1 Channels of the Process

Now we consider scattering of photons with energies $\omega \gtrsim m$ on an atom in which the state of the atom does not change. If we assume the nucleus to be an infinitely heavy particle without excited states, there are two channels of the process. Besides the scattering of the photon on the bound electrons (Rayleigh scattering), the photon can be scattered by the Coulomb field of the nucleus (Delbrück scattering). Roughly speaking, the latter process can be viewed as conversion of the photon to an electron–positron pair moving in the Coulomb field, annihilating into a photon in a further step. Thus the amplitude of the process can be written as $F = F_R + F_D$.

If we treat the nucleus as a heavy particle without internal structure, we must include the nuclear Thomson scattering. Taking into account possible excitations of the nucleus, we must include the nucleus resonance scattering, which can provide a noticeable contribution if the photon energy is close to the excitation energy. Now the amplitude of the process can be written as

$$F \;=\; F_R + F_D + F_{NTh} + F_{NR}\,, \tag{6.121}$$

with the four terms on the RHS corresponding to the amplitudes of the four channels listed above.

6.4.2 Rayleigh Scattering

We begin by considering the process at the Bethe ridge, i.e., at $q \sim \eta = m\alpha Z$. In the lowest order of expansion in powers of αZ, the amplitude is represented by the diagram shown in Fig. 6.2a and the diagram with permutation of the photons.

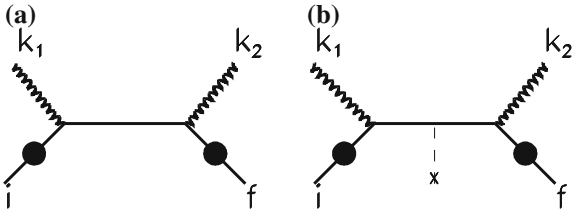

Fig. 6.2 Feynman diagrams for the Rayleigh scattering on the bound electron. The *helix lines* are for the photons. The *solid lines* denote the electrons. The *dark blobs* in (**a**) and (**b**) are for the Coulomb field of the nucleus. The *dashed line* in (**b**) shows the interaction between the nucleus and the intermediate-state electron, i.e., the lowest-order correction to the free electron propagator

The propagators are those of the free motion, and we can write for any two-photon process [16]

$$F_R = F_R^a + (1 \leftrightarrow 2); \quad F_R^a = -N(\omega_1)N(\omega_2)\int \frac{d^3f}{(2\pi)^3}\bar{\psi}_f(\mathbf{f})\hat{\mathbf{e}}_2^* G(p_1, \mathbf{f}+\mathbf{k}_2)\hat{\mathbf{e}}_1\psi_i(\mathbf{f}-\mathbf{q}); \tag{6.122}$$

$$\mathbf{q} = \mathbf{k}_1 - \mathbf{k}_2,$$

where G is the Green function of the free Dirac equation, and $p_1^2 = (\omega_1 + E_{1s})^2 - m^2$. The amplitude $F_R^a(1 \leftrightarrow 2)$ corresponds to permutation of the two photons. It can be obtained by the replacement $\mathbf{k}_1 \longleftrightarrow -\mathbf{k}_2$, $\omega_1 \longleftrightarrow -\omega_2$, $\mathbf{e}_1 \longleftrightarrow \mathbf{e}_2^*$ in the amplitude F^a. In the case of Rayleigh scattering, $\psi_f = \psi_i$ and $\omega_1 = \omega_2 = \omega$. We focus on the case of a $1s$ electron with $\psi_f = \psi_i = \psi_{1s}$.

In the lowest order of expansion in powers of αZ the small momentum $f \sim \eta$ should be neglected in the propagators. After a simple calculation, we find that at $q \sim \eta$, which determines the cross section, the nonrelativistic equation (5.95) is true for the relativistic case as well for any binding field. In the special case of the $1s$ electron in the Coulomb field, we obtain (5.96).

For the calculation that includes terms of order αZ, it is sufficient to calculate the amplitude F^a with the wave functions taken in the FSM approximation. The lowest Coulomb correction to the Green function, see Fig. 6.2b, provides a contribution of the order $\alpha^2 Z^2$. To prove the statement, we include this contribution in the amplitude. Now

$$F_R \;=\; F_R^a + F_R^b + (1 \leftrightarrow 2)\,, \tag{6.123}$$

with the term F_R^b containing the Coulomb correction to the propagator. We can write

$$F_R^b = \alpha Z N(\omega_1)N(\omega_2)\int \frac{d^3f}{(2\pi)^3}\frac{d^3s}{(2\pi)^3}\bar{\psi}_f(\mathbf{f})\hat{\mathbf{e}}_2^* G(p_1, \mathbf{f}+\mathbf{k}_2)\gamma_0 V_0(\mathbf{s})\times \tag{6.124}$$

$$G(p_1, \mathbf{f}+\mathbf{k}_2-\mathbf{s})\hat{\mathbf{e}}_1\psi_i(\mathbf{f}-\mathbf{q}-\mathbf{s}).$$

The amplitude F_R^b contains an additional integral over $\mathbf{s}$, which is saturated at $s \sim \eta$. Thus we can put $G(p_1, \mathbf{f} + \mathbf{k}_2 - \mathbf{s}) = G(p_1, \mathbf{k}_2)$, yielding

$$F_R^b = N(\omega_1)N(\omega_2) \cdot \alpha Z \int \frac{d^3 f}{(2\pi)^3} \bar{\psi}_f(\mathbf{f}) \hat{\mathbf{e}}_2^* G(p_1, \mathbf{f} + \mathbf{k}_2) \gamma_0 G(p_1, \mathbf{k}_2) \hat{\mathbf{e}}_1 \times \quad (6.125)$$

$$\int \frac{d^3 s}{(2\pi)^3} V_0(\mathbf{s}) \psi_i(\mathbf{f} - \mathbf{q} - \mathbf{s}).$$

Considering the scattering on the $1s$ state (one can easily generalize for any bound state), we see that the amplitude F^b differs from the amplitude F^a by replacement of the function $\psi_{1s}(\mathbf{f} - \mathbf{q})$ in the integrand by

$$\tau(\mathbf{f} - \mathbf{q}) = -\alpha Z \gamma_0 G(p_1, \mathbf{k}_2) \int \frac{d^3 s}{(2\pi)^3} V_0(\mathbf{s}) \psi_i(\mathbf{f} - \mathbf{q} - \mathbf{s}) = \quad (6.126)$$

$$= -\alpha Z \gamma_0 G(p_1, \mathbf{k}_2) N_1 \langle \mathbf{q} | V_{i\eta} | \mathbf{f} \rangle.$$

Since $f \sim \eta$, we can estimate for $\omega \sim m$,

$$\frac{F_R^b}{F_R^a} \sim \frac{q^2}{m^2}. \quad (6.127)$$

Note that we did not make any assumptions on the value of q. At the Bethe ridge, where $q \sim \eta$, we have indeed $F^b/F^a \sim \alpha^2 Z^2$.

Now we calculate the amplitude on the Bethe ridge, taking into account the terms of the order $\alpha^2 Z^2$. The wave function of the $1s$ electron that includes the $\alpha^2 Z^2$ terms is given by (6.53), with operator Γ_λ defined by (6.55), where we can put $\Gamma_\eta = -\partial/\partial\eta$ in the second term on the RHS. Including also the terms of order q^2/m^2 in the amplitude F_R^a, we obtain for one electron in the $1s$ state,

$$F_R = \frac{\mathbf{e}_1 \cdot \mathbf{e}_2^*}{m} N^2(\omega) f(q) \chi_2^* \Big(1 - \frac{q^2}{4m^2} - i \frac{\boldsymbol{\sigma}[\mathbf{k}_1 \mathbf{k}_2]}{2m\omega} + \frac{\alpha^2 Z^2}{2} \kappa(q)\Big) \chi_1; \quad (6.128)$$

$$f(q) = \Big(\frac{\lambda^2}{q^2 + \lambda^2}\Big)^2; \quad \lambda = 2\eta; \quad \omega = \omega_1 = \omega_2.$$

Here $\chi_{1,2}$ are the Pauli spinors,

$$\kappa(q) = \ln \frac{q^2 + \lambda^2}{\lambda^2} + \frac{q^2 - \lambda^2}{q\lambda} \arctan \frac{q}{\lambda}. \quad (6.129)$$

Note that $f(q)$ in (6.128) is the nonrelativistic form factor defined by (5.95). If there are two electrons in the K shell, we must sum the amplitude (6.128) for both

electrons. The term containing the Pauli matrix vanishes, since the electrons compose the state with spin $S = 0$.

Now we can calculate the angular distribution for small values of the angle θ between directions of the photon momenta $\mathbf{k}_1$ and $\mathbf{k}_2$. For a single electron in the $1s$ state we obtain

$$\frac{d\sigma}{d\Omega} = r_e^2 f^2(q)\Big(1 - \frac{q^2}{4m^2} - \frac{q^2}{2\omega^2} + \alpha^2 Z^2 \kappa(q)\Big), \tag{6.130}$$

where $q^2 = \omega^2\theta^2$. For two electrons in the K shell,

$$\frac{d\sigma}{d\Omega} = 4r_e^2 f^2(q)\Big(1 - \frac{q^2}{2m^2} - \frac{q^2}{2\omega^2} + \alpha^2 Z^2 \kappa(q)\Big). \tag{6.131}$$

Here we replaced the characteristic factor $1 + \cos^2\theta$ by $2 - q^2/\omega^2$. Both equations describe the distribution for $\theta \lesssim \eta/\omega \ll 1$.

We turn now to the kinematic region outside the Bethe ridge, i.e., $q \sim \omega \gg \eta$. In the amplitude F_R^a, a large momentum q is transferred to the nucleus by the initial-state or final-state electron. In the former case, the integral over f is saturated at $f \sim \eta$, while in the latter case, it is dominated by large $\mathbf{f} \approx \mathbf{q}$, with $|\mathbf{f} - \mathbf{q}| \sim \eta$. In the amplitude F_R^b, a large momentum is transferred to the nucleus in the propagator, and the integral over s is dominated by large $\mathbf{s} \approx \mathbf{q}$, with $|\mathbf{s} + \mathbf{q}| \sim \eta$. Since the angular distribution at these values of q is much smaller than in the region of small q, we carry out calculations in the lowest order of expansion in powers of $\alpha^2 Z^2$. For one electron in the K shell, we obtain

$$F_R = N^2(\omega)\frac{16\eta^4}{mq^4}\chi_2^*\Big\{(\mathbf{e}_1\cdot\mathbf{e}_2^*)\Big[1 - \frac{q^2}{8m^2}(1 + \mathbf{n}_1\mathbf{n}_2)\Big] + \frac{q^2}{8m^2}(\mathbf{e}_1\cdot\mathbf{n}_2)(\mathbf{e}_2^*\cdot\mathbf{n}_1) + \\ + \frac{i}{4m}\Big[(\boldsymbol{\sigma}\mathbf{q})(\mathbf{u}[\mathbf{e}_1\mathbf{e}_2^*]) + (\boldsymbol{\sigma}\cdot[\mathbf{wq}])\Big]\Big\}\chi_1\,. \tag{6.132}$$

Here $\mathbf{n}_i = \mathbf{k}_i/\omega$, $\mathbf{u} = \mathbf{n}_1 - \mathbf{n}_2$, $\mathbf{w} = \mathbf{n}_1(\mathbf{e}_1\cdot\mathbf{e}_2^*) + \mathbf{n}_2(\mathbf{e}_1\cdot\mathbf{e}_2^*) - \mathbf{e}_2^*(\mathbf{e}_1\cdot\mathbf{n}_2) - \mathbf{e}_1(\mathbf{e}_2^*\cdot\mathbf{n}_1)$.

For two electrons in the K shell,

$$F_R = 2N^2(\omega)\frac{16\eta^4}{mq^4}\Big\{(\mathbf{e}_1\cdot\mathbf{e}_2^*)\Big[1 - \frac{q^2}{8m^2}(1 + \mathbf{n}_1\mathbf{n}_2)\Big] + \frac{q^2}{8m^2}(\mathbf{e}_1\cdot\mathbf{n}_2)(\mathbf{e}_2^*\cdot\mathbf{n}_1)\Big\}. \tag{6.133}$$

The angular distribution for the closed K shell at $\theta \gg \eta/\omega$ is

$$\frac{d\sigma}{d\Omega} = \frac{2^9 r_e^2 \eta^8}{q^8}\Big(1 + t^2 - \frac{q^2}{4m^2}(1 - \frac{q^2}{8m^2})(1 + t)^2\Big). \tag{6.134}$$

Here $q^2(t) = 2\omega^2(1 - t)$, $t = \cos\theta$. Combining this equation with (6.131), we can write an expression for the angular distribution that is valid for all values of θ for the closed K shell:

$$\frac{d\sigma}{d\Omega} = 2r_e^2 f^2(q)(1+t^2)\Big(1+\alpha^2 Z^2\kappa(q) - \frac{q^2}{4m^2}(1-\frac{q^2}{8m^2})\frac{(1+t)^2}{1+t^2}\Big). \quad (6.135)$$

The cross section is dominated by small $\theta \lesssim \eta/\omega$ ($q \lesssim \eta$). The region of $\theta \sim 1$ ($q \sim \omega$) contributes to the correction of order $(\alpha Z)^6$. Up to the terms of order $\alpha^2 Z^2$, we obtain for one electron in the $1s$ state,

$$\sigma_1 = \sigma_{Th}(\alpha Z)^2 \frac{m^2}{2\omega^2}\Big(1+\alpha^2 Z^2(\frac{7}{6} - \frac{3\pi^2}{16} - \frac{m^2}{\omega^2})\Big), \quad (6.136)$$

while for the closed K shell,

$$\sigma_2 = 2\sigma_{Th}(\alpha Z)^2 \frac{m^2}{\omega^2}\left(1+\alpha^2 Z^2\Big(\frac{2}{3} - \frac{3\pi^2}{16} - \frac{m^2}{\omega^2}\Big)\right). \quad (6.137)$$

Here $\sigma_{Th} = 8\pi r_e^2/3$ is the Thomson cross section; see (5.99). Note that the relativistic effects strongly diminish the value of $\sigma_{1,2}$. At $\omega = m \approx 500\,\text{keV}$, the expression in parentheses on the RHS of (6.137) becomes of order $\alpha^4 Z^4$ for $Z \gtrsim 85$. As we have seen, in the lowest approximation, the ratio of cross sections of elastic scattering on the atom with one and two electrons σ_1 and σ_2 is just $r = \sigma_2/\sigma_1 = 4$. The spin-dependent terms that manifest themselves in the contributions of the order $\alpha^2 Z^2$ lead to deviations from this law.

Note that (6.132) and (6.133) can be employed for investigation of the polarization effects in the elastic scattering of the photons on atoms. Experiments in which polarization of both incident and scattered photons is fixed have recently been planned [17, 18].

6.4.3 Delbrück Scattering

The photon can undergo elastic scattering in the Coulomb field of the nucleus; see Fig. 5.2. The process requires at least two interactions with the nucleus, since the sum of the diagrams with an odd number of interactions vanishes. The latter statement is known as Furry theorem [1]. Thus the amplitude can be written as

$$F_D = N^2(\omega)(\alpha Z)^2 \cdot \frac{\mathbf{e}_1 \cdot \mathbf{e}_2^*}{m}(a_1(\omega,q) + i a_2(\omega,q)), \quad (6.138)$$

where $a_{1,2}$ are real. The amplitude $a_2(\omega,0)$ ($q=0$ at $\theta=0$) is related to the cross section of creation of e^+e^- pairs in the Coulomb field.

If we include both the Rayleigh and Delbrück mechanisms, the amplitude is given by $F = F_R + F_D$. The angular distribution is

$$\frac{d\sigma}{d\Omega} = \frac{d\sigma_R}{d\Omega} + \frac{d\sigma_{int}}{d\Omega} + \frac{d\sigma_D}{d\Omega}, \quad (6.139)$$

with the first and last terms standing for purely Rayleigh and Delbrück contributions, while the second term describes their interference. At small $q \sim \eta$, the first term on the RHS is described by (6.131), while

$$\frac{d\sigma_{int}}{d\Omega} = 4r_e^2(\alpha Z)^2 f(q) a_1(\omega, 0)\,, \tag{6.140}$$

thus contributing to the corrections of order $\alpha^2 Z^2$ in the angular distribution. The role of the interference term increases at $\omega \gg m$, since $a_1 \sim \omega/m$ at these energies.

Inclusion of the interference terms (6.140) modifies the distributions (6.136) and (6.137) [19]:

$$\sigma_1 = \sigma_{Th}(\alpha Z)^2 \frac{m^2}{2\omega^2}\left[1 + \alpha^2 Z^2\left(\frac{7}{6} - \frac{3\pi^2}{16} - \frac{m^2}{\omega^2} + 6a_1(\omega, 0)\right)\right], \tag{6.141}$$

while for the closed K shell,

$$\sigma_2 = 2\sigma_{Th}(\alpha Z)^2 \frac{m^2}{\omega^2}\left[1 + \alpha^2 Z^2\left(\frac{2}{3} - \frac{3\pi^2}{16} - \frac{m^2}{\omega^2} + 3a_1(\omega, 0)\right)\right]. \tag{6.142}$$

The function $a_1(\omega, 0)$ was calculated in [20].

In the ultrarelativistic limit $\omega \gg m$,

$$a_1(\omega, 0) = \frac{7}{18}\frac{\omega}{m}\left(1 + O\left(\frac{m}{\omega}\right)\right), \tag{6.143}$$

and the interference terms determine the corrections of order $\alpha^2 Z^2$.

At large $q \sim \omega$, the three terms on the RHS of (6.139) are of respective orders $r_e^2(\alpha Z)^8 \cdot m^4/\omega^4$, $r_e^2(\alpha Z)^6 \cdot m^2/\omega^2$, and $r_e^2(\alpha Z)^4$, with domination of the Delbrück scattering.

6.4.4 *Scattering on the Nucleus*

In the first step, we treat the nucleus as a single free particle with the charge $e' = eZ$ and mass $M = Am_N$, where A is the atomic number. Recall that the nucleon mass is $m_N \approx 940\,\text{MeV}$. Such a target, which may also have the anomalous magnetic moment μ_A, can be described by the Dirac equation

$$\left(\hat{p} + e'\hat{A} - M - \frac{i}{2}\mu_A \sigma_{\mu\nu} F_{\mu\nu}\right)\psi = 0; \quad F_{\mu\nu} = \frac{\partial A_\nu}{\partial x_\mu} - \frac{\partial A_\mu}{\partial x_\nu}. \tag{6.144}$$

The anomalous magnetic moment is caused by the strong interactions. We can employ this equation to describe the photon scattering on the nuclei. In any case, for

the photon energies $\omega \ll M$ (even for hydrogen, this means $\omega \ll 1\,\mathrm{GeV}$), the spin terms are not important [21], and we arrive at the Thomson amplitude

$$F_{NTh} = -\mathbf{e}_1 \cdot \mathbf{e}_2^* \frac{N^2(\omega) Z^2}{A m_N}, \tag{6.145}$$

which provides the cross section

$$\sigma_{NTh} = \sigma_{Th} \cdot \frac{m^2}{m_N^2} \cdot \frac{Z^4}{A^2}. \tag{6.146}$$

For the photon energies ω close to the excitation energy of the nucleon E_r, the amplitude contains the characteristic factor $(E_r - \omega - i\Gamma/2)^{-1}$, with Γ the width of the excited state. Thus the amplitude is enhanced at $|\omega - E_r| \lesssim \Gamma$. The process is called nuclear resonant scattering. Its cross section has the Breit–Wigner shape. For the dipole excitations we obtain, neglecting the Thomson scattering and including only one channel of decay,

$$\sigma_{NR} = \frac{\pi}{\omega^2} \cdot \frac{\Gamma^2}{(E_r - \omega)^2 + \Gamma^2/4}. \tag{6.147}$$

6.4.5 *Isolation of Partial Contributions*

The angular distribution of the Rayleigh scattering has a sharp peak at small angles. Its contribution is easily isolated in a number of experiments [22].

It follows from the analysis presented above that at large angles $\theta \gg \eta/\omega$, the process is the interplay of the Delbrück scattering and nuclear Thomson scattering. The amplitudes describing these two mechanisms behave with Z in the same way. The amplitude of the Thomson scattering is also proportional to $1/A$. Thus the role of the Thomson scattering increases at small values of the atomic number A. This is supported by the results of the experiment [23] on elastic scattering of photons with energy $\omega = 1.6\,\mathrm{MeV}$ by the light nuclei H, Li, C, and Al. The results are in very good agreement with those predicted by (6.146); see Fig. 6.3.

At large angles, the Delbrück scattering dominates for heavier atoms. The results for scattering of photons carrying energy $\omega = 1.33\,\mathrm{MeV}$ on the nucleus ^{208}Pb ($Z = 82$) [22] are presented in Fig. 6.4. They demonstrate that inclusion of the contribution of the Delbrück scattering is necessary to obtain agreement between experimental and theoretical results at $\theta \geq 90\,\mathrm{deg}$.

It is instructive to look at the results on small-angle scattering of photons with energy $\omega = 7278\,\mathrm{keV}$ on ^{208}Pb presented in Table 6.1 [24]. Calculating the distribution $X_S = d\sigma/d\Omega$, corresponding to superposition of the Rayleigh and Delbrück scattering (the nuclear Thomson amplitude is small), we find the discrepancy between the experimental data and theoretical results. Inclusion of the contribution

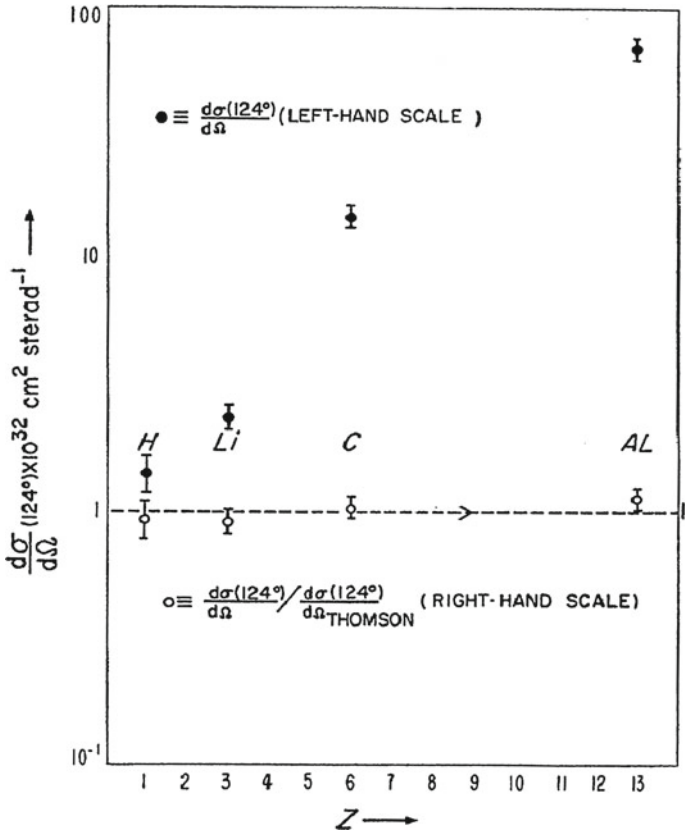

Fig. 6.3 Dependence of the elastic scattering differential cross section at angle 124° for 1.6-MeV gamma rays on the value of nuclear charge Z. The *open circles* are ratios of the measured cross sections to the classical Thomson cross section. Reproduced from [23] with permission of AIP

of the nuclear resonant scattering ($E_r = 7.28\,\text{MeV}$) X_{NR} and its interference with the Rayleigh and Delbrück amplitudes X_{INT} provides $X_T = X_S + X_{NR} + X_{INT}$, which is close to the experimental value X_{EXP}.

6.5 Compton Scattering

6.5.1 General Relations

Now a photon with energy ω_1 is absorbed by a bound electron in $1s$ state. There is a scattered photon with energy ω_2 as well as the continuum electron with energy E in the final state. The energies of the particles participating in the process are bound by the condition

$$\omega_1 + E_{1s} = \omega_2 + E\,. \tag{6.148}$$

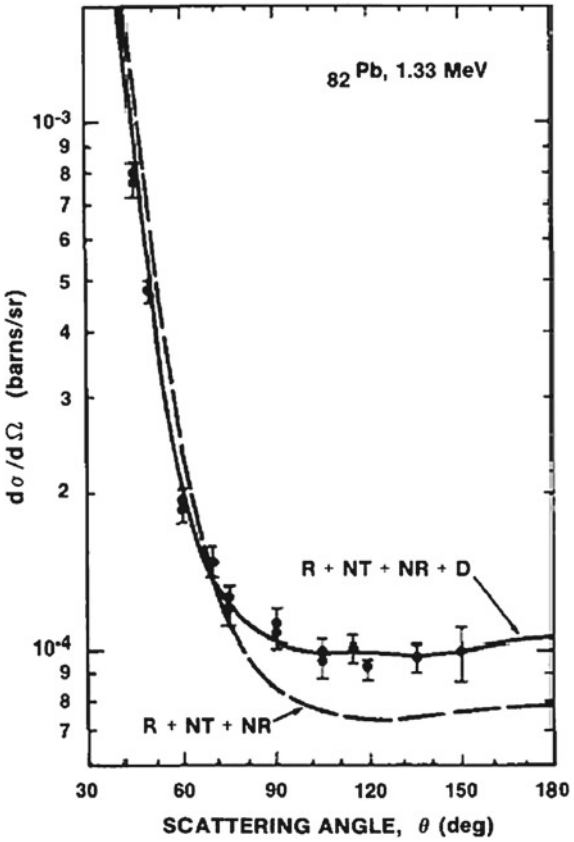

Fig. 6.4 Theoretical values for the angular distribution of elastic photon scattering on Pb at 1.33 MeV with and without inclusion of Delbrück scattering (D) compared with experimental data. Here NT and NR are for the nuclear Thomson scattering and nuclear resonant scattering respectively. The experiment clearly indicates that the Delbrück amplitudes must be included to obtain satisfactory agreement. Reproduced from [22] with permission of Elsevier Publishing

Table 6.1 Role of nuclear resonant scattering in the elastic scattering of a photon with energy $\omega = 7278$ keV on the nucleus of lead

X in mb/sr	$\theta = 1.0dg$	$\theta = 1.7dg$
X_S	920	244
X_{NR}	347	347
X_{INT}	182	105
X_T	1449	696
X_{EXP}	1490 ± 80	663 ± 30

Reproduced from [24] with permission of AIP

The nucleus transfers momentum $\mathbf{q}$ to the electrons, and

$$\mathbf{k}_1 + \mathbf{q} = \mathbf{p} + \mathbf{k}_2\,, \tag{6.149}$$

with photon momenta $\mathbf{k}_i$ and electron momentum $\mathbf{p}$. The differential cross section of the process can be written as

$$d\sigma = |\bar{F}|^2 d\Gamma; \quad d\Gamma = 2\pi\delta(\omega_1 + E_{1s} - \omega_2 - E)\cdot\frac{d^3p}{(2\pi)^3}\cdot\frac{d^3k_2}{(2\pi)^3}. \tag{6.150}$$

As usually, the overbar indicates that averaging over polarizations in the initial state and summation over those in the final state are carried out. Multiplying by $\delta(\mathbf{k_1} - \mathbf{k_2} - \mathbf{p} + \mathbf{q})d^3q$, we can write the phase volume in (6.150) as

$$d\Gamma \;=\; d\Gamma_0\cdot\frac{d^3q}{(2\pi)^3}\,, \tag{6.151}$$

where

$$d\Gamma_0 = (2\pi)^4\delta(\omega_1 + E_{1s} - \omega_2 - E)\cdot\delta(\mathbf{k_1} - \mathbf{k_2} - \mathbf{p} + \mathbf{q})\frac{d^3p}{(2\pi)^3}\cdot\frac{d^3k_2}{(2\pi)^3} \tag{6.152}$$

is the phase volume for Compton scattering on the free electron.

We shall focus on Compton scattering on the $1s$ electron. Similar calculations can be carried out for other states in the Coulomb field by employing the technique described in Sect. 5.2. We discuss also features of the process that are common for the process on the bound state in any field.

6.5.2 *Lowest Order Calculations on the Bethe Ridge*

We begin with analysis of the process on the Bethe ridge, i.e., in the kinematic region where the recoil momentum can be made small, $q \lesssim \eta$ [25]. The energies of the outgoing particles are limited by the conditions

$$\varepsilon \;\equiv\; E - m \le \frac{\omega_1}{1 + m/2\omega_1}; \quad \omega_2 \;\ge\; \frac{\omega_1}{1 + 2\omega_1/m}\,. \tag{6.153}$$

Thus the electron energy cannot be too large, while the photon energy cannot be too small. Note that in the process on the free electrons the energy ω_2 is determined by the scattering angle θ between momenta $\mathbf{k}_1$ and $\mathbf{k}_2$:

$$\omega_2 = \omega_{20} \;=\; \frac{\omega_1}{1 + \omega_1(1-t)/m}; \quad t \;=\; \cos\theta\,. \tag{6.154}$$

Consider first ejection of relatively slow electrons with momentum $p \lesssim \eta = m\alpha Z$, and thus $\varepsilon \lesssim I_Z$. We find that on the Bethe ridge, $\omega_1^2(1-t) \lesssim \eta^2$ in this case. Thus for $\varepsilon \sim I_Z$, the Bethe ridge corresponds to the small scattering angles of outgoing photons:

$$\theta \lesssim \frac{m}{\omega_1} \cdot \alpha Z\,. \tag{6.155}$$

Also, the energies ω_2 may differ from ω_{20} by values of the order $m\alpha^2 Z^2$.

Since at $p \lesssim \eta$, the condition $q \lesssim \eta$ corresponds to $\kappa \lesssim \eta$ with $\boldsymbol{\kappa} = \mathbf{k}_1 - \mathbf{k}_2$, we can use the results obtained for Rayleigh scattering. The amplitude of the process, which is valid for all values of kinematic variables, is presented by (6.122)–(6.125), where ψ_f is the Coulomb continuum function $\psi_{\mathbf{p}}$. On the Bethe ridge, the amplitude F^b provides a correction of order $\alpha^2 Z^2$. Thus in the lowest order of αZ expansion,

$$F = F^a + (1 \leftrightarrow 2) = \frac{\mathbf{e}_1 \cdot \mathbf{e}_2^*}{m} N(\omega_1) N(\omega_2) \bar{u}_{\mathbf{p}} W(\mathbf{p}, \boldsymbol{\kappa}) u_0; \quad W(\mathbf{p}, \boldsymbol{\kappa}) = -N_p N_1 \frac{\partial}{\partial \eta} \Phi_{\mathbf{p}}(\boldsymbol{\kappa}, \eta). \tag{6.156}$$

Direct calculation provides

$$-\frac{\partial}{\partial \eta} \Phi_{\mathbf{p}}(\boldsymbol{\kappa}, \eta) = 8\pi \left(\frac{\eta(1 - i\xi)}{a^2} + \frac{i\xi(p + i\eta)}{ab} \right) \cdot \Theta, \tag{6.157}$$

with $a = (\boldsymbol{\kappa} - \mathbf{p})^2 + \eta^2$, $b = \kappa^2 - (p + i\eta)^2$, while Θ is defined by (6.90). It can be written as

$$\Theta = \Phi(\xi) e^{\xi \arg b}; \quad \Phi(\xi) = e^{i\xi \ln \left| \frac{a}{b} \right|}. \tag{6.158}$$

For the distributions of slow electrons at the Bethe ridge, we obtain

$$\frac{d\sigma}{d\omega_2 d\Omega d\Omega_e} = r_e^2 (1 + t^2) \frac{pE\omega_2}{\omega_1} \frac{|W|^2}{(2\pi)^3}\,, \tag{6.159}$$

with Ω_e the solid angle of the ejected electron. Note that $|W|^2$ contains the factor $|\Theta|^2 = \exp(2\xi \arg b)$, where $b = b_1 - 2i\eta p$, with $b_1 = \kappa^2 - p^2 + \eta^2$. Thus $\arg b = -\arctan(2\eta p / b_1)$ for $b_1 > 0$, while $\arg b = -\pi + \arctan(2\eta p / |b_1|)$ for $b_1 < 0$. After some algebra, we obtain

$$\arg b = -\frac{\pi}{2} + \arctan\left(\frac{\kappa^2 - p^2 + \eta^2}{2\eta p} \right) \tag{6.160}$$

and

$$|\Theta|^2 \;=\; \exp(-\pi\xi)\exp(2\xi\chi); \quad \chi \;=\; \arctan\Big(\frac{\kappa^2 - p^2 + \eta^2}{2\eta p}\Big). \tag{6.161}$$

The dependence on the angular variables of the ejected electron is contained only in the parameter a; (6.157). Carrying out this integration and taking into account that (6.159) is true for small θ and $p \lesssim \eta$, we obtain

$$\frac{d\sigma}{dtd\omega_2} = \pi r_e^2 \cdot \frac{2^8(1+t^2)m\eta^6\omega_2\kappa^2(p^2+3\kappa^2+\eta^2)}{3\omega_1[(p-\kappa)^2+\eta^2]^3[(p+\kappa)^2+\eta^2]^3} \cdot \frac{\exp(-\pi\xi)\exp(2\xi\chi)}{1-\exp(-2\pi\xi)}, \tag{6.162}$$

which is true for all $\omega_1 \gg I_Z$. Further evaluation of this expression requires numerical computations.

Now we turn to the case in which the outgoing electron carries large momentum $p \gtrsim m \gg \eta$, and thus the energy $\varepsilon \gtrsim m$. Analysis similar to that carried out above for the slow electrons shows that $F^b/F^a \sim q^2/m^2$, and thus in the lowest orders of αZ series, it is sufficient to put $F = F^a + (1 \leftrightarrow 2)$, with

$$F^a = -N(\omega_1)N(\omega_2)\int \frac{d^3f}{(2\pi)^3}\bar{\psi}_{\mathbf{p}}(\mathbf{f})\hat{\mathbf{e}}_2^* G(p_1, \mathbf{f}+\mathbf{k}_2)\hat{\mathbf{e}}_1\varphi_{1s}(\mathbf{f}-\boldsymbol{\kappa})u_0, \tag{6.163}$$

where $\boldsymbol{\kappa} = \mathbf{k}_1 - \mathbf{k}_2$, G is the Green function of the free Dirac equation, and $p_1^2 = (\omega_1 + E_{1s})^2 - m^2$. Of course, if $\varphi_{\mathbf{p}}(\mathbf{f})$ is the plane wave, we obtain immediately

$$F^a \;=\; F_0\psi_i(\mathbf{q})\,, \tag{6.164}$$

with F_0 the amplitude of the Compton scattering on the free electron at rest. This is true for every bound state in any field.

Hence, the energy distribution at the Bethe ridge is equal to that of the Compton scattering on the free electron at rest,

$$\frac{d\sigma}{d\omega_2} \;=\; \frac{d\sigma_0}{d\omega_2}\,, \tag{6.165}$$

and also for the total cross section,

$$\sigma(\omega_1) \;=\; \sigma_0(\omega_1)\,. \tag{6.166}$$

Thus the cross section of the Compton scattering on a bound electron is equal to that on the free electron.

The characteristics of the free process are usually presented in books on quantum electrodynamics; see, e.g., [1]. The energy distribution is known to be

$$\frac{d\sigma_0}{d\omega_2} = 2\pi r_e^2 \frac{m}{\omega_1^2} \cdot f_0(\omega_1, \omega_2)\,, \tag{6.167}$$

with

$$f_0(\omega_1, \omega_2) = \frac{1}{2}\Big[\frac{\omega_1}{\omega_2} + \frac{\omega_2}{\omega_1} + 2(\frac{m}{\omega_1} - \frac{m}{\omega_2}) + (\frac{m}{\omega_1} - \frac{m}{\omega_2})^2\Big]. \tag{6.168}$$

The total cross section is

$$\sigma_0(\omega_1) = 2\pi r_e^2\Big[\frac{1+\beta}{\beta^3}\Big(\frac{2\beta(1+\beta)}{1+2\beta} - \ln(1+2\beta)\Big) + \frac{\ln(1+2\beta)}{2\beta} - \frac{1+3\beta}{(1+2\beta)^2}\Big], \tag{6.169}$$

$\beta = \omega_1/m$. At $\omega_1 \gg m$

$$\sigma(\omega_1) = \pi r_e^2 \frac{m}{\omega_1}\left(\ln\frac{2\omega_1}{m} + \frac{1}{2}\right). \tag{6.170}$$

In order to estimate the accuracy of (6.165) and (6.166) and to find the leading-order corrections, we calculate the amplitude with the Coulomb functions of both initial and final states. This enables us to include the αZ and $\alpha^2 Z^2$ terms in the next steps. Also, we shall be able to trace dependence on the parameter $\pi\xi$, which we do not necessarily assume to be small.

Since the integral on the RHS of (6.163) is saturated by $|\mathbf{f} - \boldsymbol{\kappa}| \lesssim \eta \ll p$, we can put $G(p_1, \mathbf{f} + \mathbf{k}_2) = G(p_1, \mathbf{k}_1)$ in the integrand for the lowest-order term of expansion in powers of αZ. This provides

$$F = F_0 W(\mathbf{p}, \boldsymbol{\kappa})\,, \tag{6.171}$$

with $W(\mathbf{p}, \boldsymbol{\kappa})$ defined by (6.156). However, now we must include only the lowest-order term of the expansion in powers of ξ. Thus

$$W(\mathbf{p}, \mathbf{k}_2) = 8\pi \frac{\eta N_1 N_p \Theta}{a^2}; \quad a = (\boldsymbol{\kappa} - \mathbf{p})^2 + \eta^2\,, \tag{6.172}$$

and

$$\frac{d\sigma}{d\omega_2 dt} = \frac{d\sigma_0}{dt} \cdot \frac{8}{3\pi} \cdot \frac{\omega_1}{\omega_{20}\kappa} \frac{m\eta^5}{(\Delta^2+\eta^2)^3} \cdot N_p^2 \cdot |\Theta|^2; \quad \Delta = \kappa - p. \tag{6.173}$$

Note that

$$\frac{d\sigma_0}{dt} = 2\pi \frac{\omega_{20}^2}{\omega_1^2} \cdot f_0(\omega_1, \omega_{20})\,, \tag{6.174}$$

with $\omega_{20}(t)$ determined by (6.154), is the angular distribution of the Compton scattering on the free electron. The distribution (6.173) reaches its largest values at $\Delta \sim \eta \ll p, \kappa$. It peaks at $\Delta = 0$.

As expected, (6.171) turns into (6.164) for the $1s$ state of the Coulomb field if we put $N_p = 1$, $\Theta = 1$. We have kept these factors, since they include dependence on the parameter $\pi\xi$, which is not assumed to be small. Employing (6.161) and also writing

$$N_p^2 = \frac{2\pi\xi}{1 - exp(-2\pi\xi)} = e^{\pi\xi}(1 - \frac{\pi^2}{6}\xi^2 + O(\xi^4)), \tag{6.175}$$

we find that

$$N_p^2\Theta^2 = \exp(2\xi\chi)\Big(1 - \frac{\pi^2}{6}\xi^2\Big). \tag{6.176}$$

In the vicinity of the center of the peak where $|\Delta| \ll I_Z \sim m\alpha^2 Z^2$, we can put $\chi = \eta/2p$, and

$$N_p^2\Theta^2 = 1 + \left(\frac{m}{E} - \frac{\pi^2}{6}\right)\xi^2 + O(\xi^4)\,. \tag{6.177}$$

While we neglect terms of order αZ, we can put $N_p^2\Theta^2 = 1$ on the RHS of (6.173).

As we shall see, the region of large recoil momenta $q \gg \eta$ provides contributions of order $\alpha^4 Z^4$ to the differential and total cross sections. Thus the leading corrections to (6.164), (6.165), and (6.166) come from more accurate calculations at the Bethe ridge.

6.5.3 *Inclusion of Higher Order Terms on the Bethe Ridge*

Now we carry out more accurate calculations on the Bethe ridge. We begin with calculation of the terms of order αZ. Since the amplitude F^b provides a correction of the order $\alpha^2 Z^2$, we have still $F = F^a$. The wave functions φ_{1s} and $\varphi_{\mathbf{p}}$ on the RHS of (6.163) should be taken in the FSM approximation, and only the corrections of order ξ should be included in the expansion of F^a.

Omitting the intermediate steps of the calculation (they are presented in [25]), we write the angular distribution

$$\frac{d\sigma}{d\omega_2 d\Delta} = \frac{d\sigma_0}{d\omega_2} \cdot \frac{8}{3\pi} \frac{\eta^5}{(\Delta^2 + \eta^2)^3}(1 + \gamma\Delta/m). \tag{6.178}$$

The parameter γ can be expressed in terms of the function f_0 defined by (6.168). We define also

$$f_1(\omega_1,\omega_2)=\omega_1\frac{\partial f_0(\omega_1,\omega_2)}{\partial\omega_1}=\frac{1}{2}\left[\frac{\omega_1}{\omega_2}-\frac{\omega_2}{\omega_1}-\frac{2m}{\omega_1}\left(1+\frac{m}{\omega_1}-\frac{m}{\omega_2}\right)\right] \quad (6.179)$$

and

$$f_2(\omega_1,\omega_2) = \omega_2\frac{\partial f_0(\omega_1,\omega_2)}{\partial\omega_2}=f_1(\omega_1\leftrightarrow-\omega_2). \quad (6.180)$$

With this notation,

$$\gamma = \frac{3E}{2p}+\frac{\mathbf{k}_1\cdot\boldsymbol{\kappa}\, f_1}{\omega_1\kappa f_0}+\frac{\mathbf{k}_2\cdot\boldsymbol{\kappa}\, f_2}{\omega_2\kappa f_0}. \quad (6.181)$$

The peak of the distribution $d\sigma/d\omega_2 dt$ is reached at $\omega_2=\omega_{20}+\delta\omega_2$, where

$$\delta\omega_2=\frac{\eta^2}{12m}\cdot\frac{E\omega_{20}}{m\omega_1}\left[1+2\frac{E-m}{E}\left(1+\frac{m}{\omega_1})(1+\frac{f_1}{f_0}\right)+(t+\frac{E}{\omega_1})\cdot\frac{f_2}{f_0}\right)\right], \quad (6.182)$$

with an error of order α^2Z^2. In (6.182), we have $f_i=f_i(\omega_1,\omega_{20})$.

This equation can be simplified in special cases. For example, if $\omega_1\ll m$, we obtain

$$\delta\omega_2 = \frac{\eta^2}{12m}\left(1+\frac{\omega_1}{m}(1-t)+O\left(\frac{\omega_1^2}{m^2}\right)\right). \quad (6.183)$$

In the ultrarelativistic case, $\omega_1\gg m$, and if also $\omega_{20}\gg E$, we obtain

$$\delta\omega_2 = \frac{\eta^2}{12m}\cdot\frac{3E-2m}{m}\cdot\left(1-\frac{E-m}{\omega_1}\cdot\frac{3E-4m}{3E-2m}+O(\frac{E^2}{\omega_1^2})\right). \quad (6.184)$$

The term proportional to $\gamma\Delta/m$ on the RHS of (6.178) vanishes after one integration of the distribution. Thus there are no αZ corrections to (6.165) and (6.166)

Consider now corrections of the order α^2Z^2. Now $F=F^a+F^b$. In the amplitude F^a, we must take the relativistic functions φ_{1s} and $\varphi_{\mathbf{p}}$ up to terms of the order α^2Z^2, following the approach developed in Sect. 5.2.1. As we have seen, the amplitude F^b is α^2Z^2 times smaller than F^a. It can be calculated in the lowest order of expansion in powers of ξ. Thus F_b can be described by (6.125):

$$F^b = \alpha ZN(\omega_1)N(\omega_2)\bar{u}_{\mathbf{p}}\hat{\mathbf{e}}_2^*G(p_1,\mathbf{p}+\mathbf{k}_2)\gamma_0G(p_1,\mathbf{k}_2)\hat{\mathbf{e}}_1u_0\tau(\kappa); \quad (6.185)$$

$$\tau(\kappa) = \int\frac{d^3s}{(2\pi)^3}V_0(\mathbf{s})\varphi_{1s}(\boldsymbol{\kappa}-\mathbf{s}) = \frac{4\pi N_1}{\kappa^2+\eta^2}.$$

The rather complicated final expressions for the distributions and for the shift $\delta\omega_2$ are given in [25]. We present only the angular and energy distributions in the limit $\omega_1\gg m$ and the high-energy asymptotics of the cross section. For $\theta\gg\sqrt{\eta/\omega_1}$, we have

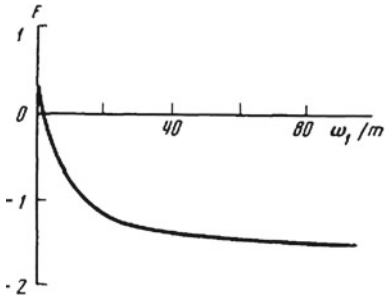

Fig. 6.5 Function $F(\omega_1)$ defined by (6.188) [26]

$$\frac{d\sigma}{dt} = \frac{d\sigma_0}{dt} \cdot (1 + \alpha^2 Z^2 f(\omega_1, t)); \quad f(\omega_1, t) = \ln 2 - \frac{5}{3} - \frac{5t}{6} + O(\frac{m}{\omega_1}), \tag{6.186}$$

while the energy distribution is

$$\frac{d\sigma}{d\omega_2} = \frac{d\sigma_0}{d\omega_2} \cdot (1 + \alpha^2 Z^2 f(\omega_1, \omega_2)); \quad f(\omega_1, \omega_2) = \ln 2 - \frac{5}{2} + \frac{5}{6} \cdot \frac{m(\omega_1 - \omega_2)}{\omega_1 \omega_2} + O(\frac{m}{\omega_1}). \tag{6.187}$$

For the total cross section, we obtain

$$\sigma(\omega_1) \; = \; \sigma_0(\omega_1) \cdot (1 + \alpha^2 Z^2 F(\omega_1)) \, , \tag{6.188}$$

with the function $F(\omega_1)$ shown in Fig. 6.5. Its high-energy asymptotic is

$$F(\omega_1) \; = \; \ln 2 - \frac{5}{2} \approx -1.81 \, , \tag{6.189}$$

with errors of order $(\ln \omega_1/m)^{-1}$. Note that for $Z \gtrsim 92$, the high-energy limit of the expression $1 + \alpha^2 Z^2 F(\omega_1)$ becomes of order $\alpha^4 Z^4$, and the higher-order terms should be calculated.

6.5.4 Outside the Bethe Ridge

As we shall see, here it is convenient to analyze the distribution of the ejected electrons rather than that of the scattered photons. On the Bethe ridge, the energies of the ejected electrons are limited by condition (6.153). In the free process, the angle θ_e between the direction of the electron momentum and that of the incoming photon is determined by the relation

$$t_e \; \equiv \; \cos\theta_e = t_0 = \frac{\varepsilon(\omega_1 + m)}{p\omega_1}; \quad \varepsilon = E - m \, . \tag{6.190}$$

Thus on the Bethe ridge, $|t_e - t_0| \lesssim \eta/\omega_1 \ll 1$.

Consider now the case in which the energy of the ejected electron is limited by the condition (6.153), but the scattering angle differs from that determined by (6.190) by values larger than a small value η/ω_1. This requires a large recoil momentum $q \gg \eta$. Following the theory developed in Sect. 4.1, the process can be viewed as consisting of two steps. In the first step, Compton scattering with small recoil momentum of order η takes place. It is followed by scattering of the ejected electron on the nucleus in which a large momentum $q \gg \eta$ is transferred. In other words, the Compton effect with the scattering angle of the electron determined by (6.190) is followed by scattering on the nuclei, which leads to additional rotation of the electron linear momentum. The triple differential cross section takes the form (see (4.49))

$$\frac{d\sigma}{d\varepsilon dq d\kappa} = \frac{d\sigma_0}{d\varepsilon} \cdot \frac{R(\Delta)}{2\pi} \cdot \frac{d\sigma_{eN}(\varepsilon)}{dq}. \tag{6.191}$$

Recall that

$$R(\Delta) = \frac{N_1^2}{\Delta^2 + \eta^2}; \quad \Delta = \kappa - p; \quad N_1^2 = \frac{\eta^3}{\pi}, \tag{6.192}$$

while σ_{eN} is the cross section of the electron scattering on the nucleus. The vicinity of the surplus of the distribution determines the double differential cross sections

$$\frac{d\sigma}{d\varepsilon dq} = \frac{\eta^2}{2\pi} \cdot \frac{d\sigma_0}{d\varepsilon} \cdot \frac{d\sigma_{eN}(\varepsilon)}{dq}; \quad \frac{d\sigma}{d\varepsilon d\Omega_e} = \frac{\eta^2}{2\pi} \cdot \frac{d\sigma_0}{d\varepsilon} \cdot \frac{d\sigma_{eN}(\varepsilon)}{d\Omega_e}. \tag{6.193}$$

Since $d\sigma_{eN}(\varepsilon)/d\Omega_e$ is proportional to $\alpha^2 Z^2$, this mechanism provides corrections of order $\alpha^4 Z^4$ to the energy distribution in the interval determined by (6.153) and to the total cross section.

At larger electron energies outside the interval (6.153), a large momentum q can be transferred to the nucleus by the electron in the initial, intermediate, or final state. All these contributions are of the same order of magnitude. Since $\xi \ll 1$, interaction of the outgoing electron with the nucleus can be treated perturbatively. However, in agreement with the analysis carried out in Sect. 3.1, the plane wave and the lowest-order Coulomb correction provide contributions of the same order. These contributions make up the two terms in the expression for the amplitude F^a in the lowest order of expansion in powers of ξ and αZ:

$$F^a = -\frac{\alpha Z N(\omega_1) N(\omega_2) N_1}{q^4} \bar{u}_{\mathbf{p}} \hat{\mathbf{e}}_2^* G(p_1, \mathbf{k}_2) \hat{\mathbf{e}}_1 u_0 + \tag{6.194}$$

$$\frac{\alpha Z N(\omega_1) N(\omega_2) N_1}{q^2} \bar{u}_{\mathbf{p}} \gamma_0 G(p_2, \boldsymbol{\kappa}) \hat{\mathbf{e}}_2 G(p_1, \mathbf{k}_1) \hat{\mathbf{e}}_1 u_0.$$

The amplitude is $F = F^a + F^b + (1 \leftrightarrow 2)$, with F^b describing exchange by hard momentum $q \gg \eta$ with the nucleus in the intermediate state

$$F^b = \frac{\alpha Z N(\omega_1) N(\omega_2) N_1}{q^2} \bar{u}_{\mathbf{p}} \hat{\mathbf{e}}_2 G(p_1, \mathbf{k}_1 + \mathbf{q}) \gamma_0 G(p_1, \mathbf{k}_1) \hat{\mathbf{e}}_1 u_0 \,. \tag{6.195}$$

Due to the common factor $N_1 \eta \sim (\alpha Z)^{5/2}$ in the amplitudes F^a and F^b, the part of the spectrum outside the interval (6.153) provides a contribution to the cross section of order $\alpha^5 Z^5$.

References

1. A.I. Akhiezer, V.B. Berestetskii, *Quantum Electrodynamics* (Pergamon, New York, 1982)
2. M.I. Eides, H. Grotch, V.A. Shelyuto, *Theory of Light Hydrogenic Bound States* (Springer, Heidelberg, 2007)
3. P.J. Mohr, G. Plunien, G. Soff, Phys. Rep. **293**, 227 (1998)
4. R.H. Pratt, Phys. Rev. **117**, 1017 (1960)
5. W.H. Furry, Phys. Rev. **46**, 391 (1934)
6. A. Sommerfeld, A.W. Maue, Ann. Phys. **22**, 629 (1935)
7. V.G. Gorshkov, Sov. Phys. JETP **20**, 1331 (1965)
8. R.H. Pratt, R.D. Levee, R.L. Pexton, W. Aron, Phys. Rev. **134**, A898 (1964)
9. A.I. Mikhailov, Sov. Phys. JETP **28**, 3266 (1969)
10. B. Nagel, P. Olsson, Arkiv. Fysik **18**, 29 (1960)
11. F. Sauter, Ann. der Phys. **11**, 454 (1931)
12. V.G. Gorshkov, A.I. Mikhailov, V.S. Polikanov, Nucl. Phys. **55**, 273 (1964)
13. M. Gavrila, Phys. Rev. **113**, 514 (1959)
14. V.G. Gorshkov, A.I. Mikhailov, ZhETF **42**, 2142 (1963)
15. T.A. Weber, C.J. Mullin, Phys. Rev. **126**, 615 (1962)
16. V.B. Berestetskii, E.M. Lifshits, L.P. Pitaevskii, *Quantum Electrodynamics* (Pergamon, New York, 1982)
17. U. Spillmann et al., Rev. Sci. Instrum. **79**, 083101 (2008)
18. G. Weber et al., J. Instrum **5**, 07010 (2010)
19. A.I. Mikhailov, S.G. Sherman, Sov. Phys. JETP. **42**, 958 (1975)
20. H. Bethe, F. Rohrlich, Phys. Rev. **86**, 10 (1952)
21. M. Gell-Mann, M.L. Goldberger, Phys. Rev. **96**, 1433 (1954)
22. P.P. Kane, L. Kissel, R.H. Pratt, S.C. Roy, Phys. Rep. **140**, 76 (1986)
23. L.W. Alvarez, F.S. Crawford Jr., M.L. Stevenson, Phys. Rev. **112**, 1267 (1958)
24. S. Kahane, R. Moreh, O. Shahal, Phys. Rev. C **28**, 1519 (1983)
25. V.G. Gorshkov, A.I. Mikhailov, S.G. Sherman, Sov. Phys. JETP **37**, 572 (1973)
26. V.G. Gorshkov, A.I. Mikhailov, S.G. Sherman, Sov. Phys. JETP **50**, 15 (1979)

Chapter 7
Photoionization of Atoms

Abstract We show that in the high-energy nonrelativistic limit the leading deviations of the energy dependence of the bound-states photoionization cross sections from the asymptotic laws are described by the same factor (called the Stobbe factor). The Stobbe factor cancels in the cross section ratios, making possible an asymptotic analysis. We demonstrate that the variety of forms of electron–photon interactions is connected with the gauge invariance of quantum electrodynamics. We show that the asymptotics for photoionization of s states can be calculated by employing the plane waves in the velocity form for the electron–photon interaction. In the length form one should include also the lowest nonvanishing term of interaction between the photoelectron and the nucleus. The latter should be included in calculations of the asymptotics for ionization of states with $\ell \neq 0$ in both forms. We analyze the Thomas–Reiche–Kuhn sum rules for the case of a nonlocal field. We carry out asymptotic analysis also for the relativistic case. We present the method of inclusion of screening corrections for the relativistic case near the threshold and far away from it. We demonstrate that inclusion of correlations beyond the independent particle approximation (IPA) in the framework of the perturbative approach developed in Chap. 3 enables us to remove the discrepancy between the experimental data and the results of IPA calculations. We show also how inclusion of IPA breaking effects changes the asymptotic behavior of the photoionization cross sections.

7.1 High-Energy Nonrelativistic Asymptotics

Here we assume that the atomic electrons move in a certain central field V. The electron single-particle wave functions describing the states of the discrete and continuum spectra are respectively $\psi_{n\ell m}$ and $\psi_{\mathbf{p}}$.

E.G. Drukarev and A.I. Mikhailov, *High-Energy Atomic Physics*,
Springer Series on Atomic, Optical, and Plasma Physics 93,
DOI 10.1007/978-3-319-32736-5_7

7.1.1 Ionization of s States

The amplitude is given by (5.69) and (5.70) with ψ_i describing an s state. We consider the limit $p \gg \mu_b$ with $\mu_b = (2mI_b)^{1/2}$ the averaged momentum of the bound state. Thus in our limit, $\varepsilon \gg I_b$.

A large momentum $\mathbf{q} = \mathbf{k} - \mathbf{p} \approx -\mathbf{p}$, $q \gg I_b$, should be transferred to the nucleus. As we demonstrated in Sect. 2.1.4, the transfer of a large momentum can be treated perturbatively. The ion accepts the large recoil momentum from either the initial or ejected electron. To investigate the relative role of the two mechanisms, we include the two lowest-order terms of the perturbative series of the photoelectron wave function:

$$\langle\psi_{\mathbf{p}}| = \langle\psi_{\mathbf{p}}^{(0)}| + \langle\psi_{\mathbf{p}}^{(1)}|; \quad \langle\psi_{\mathbf{p}}^{(0)}| = \langle\mathbf{p}|; \quad \langle\psi_{\mathbf{p}}^{(1)}| = \langle\psi_{\mathbf{p}}^{(0)}|VG = \langle\mathbf{p}|VG. \tag{7.1}$$

The amplitude of the photoionization can be written as

$$F = F_0 + F_1; \quad F_k = N(\omega)\langle\psi_{\mathbf{p}}^{(k)}|\gamma|\psi_i\rangle; \quad k = 0, 1. \tag{7.2}$$

Here ψ_i is the wave function of the bound electron, $\gamma = \mathbf{e}\cdot\mathbf{f}/m$ is the vertex of the electron–photon interaction in the nonrelativistic approximation, $\mathbf{e}$ is the polarization vector of the absorbed photon, $\mathbf{e}\cdot\mathbf{k} = 0$. Recall that $N(\omega) = (4\pi\alpha/2\omega)^{1/2}$.

We find immediately that

$$F_0 \;=\; \frac{\mathbf{e}\cdot\mathbf{p}}{m} N(\omega)\,.\psi_i(\mathbf{p}). \tag{7.3}$$

The general analysis carried out in (2.4) provides $\psi_i(\mathbf{p}) \sim p^{-4}$.

We can write also

$$F_1 = N(\omega)J; \quad J = \int \frac{d^3f}{(2\pi)^3}\langle\mathbf{p}|VG|\mathbf{f}\rangle\frac{\mathbf{e}\cdot\mathbf{f}}{m}\langle\mathbf{f}|\psi_i\rangle. \tag{7.4}$$

Here a large momentum is transferred to the nucleus by the outgoing electron, and J is saturated at $f \sim \mu_b$. Now we write

$$\langle\mathbf{p}|VG|\mathbf{f}\rangle \;=\; V(\mathbf{p}-\mathbf{f})\frac{2m}{p^2 - f^2}\,. \tag{7.5}$$

Since the interaction with a large transferred momentum $|\mathbf{p}-\mathbf{f}| \gg \mu_b$ is dominated by that with the nucleus (see (2.4)), we can estimate $V \approx -4\pi\alpha Z/(\mathbf{p}-\mathbf{f})^2$. At large $f \gg \mu_b$, the wave function $\langle\mathbf{f}|\psi_i\rangle$ is quenched by a factor μ_b^4/f^4. Thus the integral J is saturated by $f \sim \mu_b$. Expanding

$$V(\mathbf{p}-\mathbf{f}) \;\approx\; V(p)(1 + 2\mathbf{pf}/p^2), \tag{7.6}$$

we see that the second term is needed to obtain a nonvanishing value. This is because the ejected electron carries angular momentum $\ell = 1$, and the corresponding partial wave is needed. Note that we cannot calculate the amplitude F_1 in such a way, since the integral J diverges after evaluation (7.6). A rigorous calculation requires knowledge of the shape of the wave function $\psi_i(\mathbf{f})$. However, we can make an order-of-magnitude estimate. Integration over the region $f \sim \mu_b$ provides $F_1 \sim F_0 \mu_b^2/p^2$, and the amplitude is dominated by the contribution F_0. Hence we can put $F = F_0$.

This has a simple explanation. In the amplitude F_0, the initial electron transfers a large momentum q to the nucleus, while in the amplitude F_1, the photoelectron does it. In both cases, the wave functions are quenched at large q. This corresponds to a small probability of approaching the nucleus. The photoelectron carries orbital momentum $\ell = 1$, with the wave function obtaining an additional factor r^ℓ. That is why the quenching of the amplitude F_1 appears to be stronger.

Now we write

$$F = \frac{\mathbf{e}\cdot\mathbf{p}}{m} N(\omega) \int d^3 r e^{-i\mathbf{p}\cdot\mathbf{r}} \psi(r)\,. \tag{7.7}$$

Here and below we omit the index i of the function ψ_i. Since the integral is dominated by small $r \sim 1/\mu_b$, we can expand the initial-state wave function near the origin $\psi(r) = \psi(0) + r\psi'(0)$. Multiplying the integrand by $e^{-\lambda r}|_{\lambda=0}$, we calculate

$$F = \frac{\mathbf{e}\cdot\mathbf{p}}{m} N(\omega) \left(\psi(0) - \psi'(0)\frac{\partial}{\partial\lambda}\right) \int d^3 r e^{-i\mathbf{p}\cdot\mathbf{r}-\lambda r}|_{\lambda=0}. \tag{7.8}$$

Since

$$\int d^3 r e^{-i\mathbf{p}\cdot\mathbf{r}-\lambda r} = \frac{8\pi\lambda}{(p^2+\lambda^2)^2}\,, \tag{7.9}$$

we obtain

$$F = -\frac{\mathbf{e}\cdot\mathbf{p}}{m} \cdot N(\omega) \frac{8\pi\psi'(0)}{p^4}\,, \tag{7.10}$$

or, employing the first Kato condition $\psi'(0) = -\eta\psi(0)$, see (4.77),

$$F = \frac{\mathbf{e}\cdot\mathbf{p}}{m} \cdot N(\omega) \frac{8\pi\eta\psi(0)}{p^4}; \quad \eta = m\alpha Z. \tag{7.11}$$

Thus the angular distribution of a photoelectron knocked out from $1s$ state averaged over the polarizations of the photon is

$$\frac{d\sigma}{dt} = \frac{3(1-t^2)}{4} \frac{A_{1s}}{\omega^{7/2}}; \quad A_{1s} = \frac{(4\pi)^2\sqrt{2}}{3} \cdot \alpha \cdot (\alpha Z)^2 \frac{|\psi(0)|^2}{m^{3/2}}, \tag{7.12}$$

with $t = \mathbf{k}\cdot\mathbf{p}/kp$. The cross section is

$$\sigma(\omega) = \frac{A_{1s}}{\omega^{7/2}}\,. \tag{7.13}$$

Note also the expression for A_{1s} in terms of the radial wave function $R_{1s}(r) \equiv \chi(r) = \sqrt{4\pi}\psi_{1s}(r)$:

$$A_{1s} \;=\; \frac{4\pi\sqrt{2}}{3}\cdot\alpha\cdot(\alpha Z)^2\frac{|\chi(0)|^2}{m^{3/2}}\,. \tag{7.14}$$

For an s state, the value $|\psi(0)|^2$ can be expressed in terms of the potential $V(r)$:

$$|\psi(0)|^2 \;=\; \frac{m}{2\pi}\langle\psi|V'|\psi\rangle\,. \tag{7.15}$$

To prove the statement, we set $\psi(r) = R(r)/\sqrt{4\pi}$, i.e., $R(r)$ is the radial part of the wave function, and we introduce $u(r) = rR(r)$. We now multiply both sides of the wave equation

$$-u''(r) \;=\; 2m(\varepsilon_b - V(r))u(r) \tag{7.16}$$

by the function $u'(r)$ and integrate over r. Evaluation of the LHS provides

$$-\int_0^\infty dr\,u''(r)u'(r) = -\frac{1}{2}\int_0^\infty dr[u'^2(r)]' = -\frac{1}{2}u'^2(r)|_0^\infty = \frac{1}{2}|R(0)|^2 = 2\pi\psi^2(0). \tag{7.17}$$

On the other hand, evaluation of the RHS leads to

$$\begin{aligned} 2m\int_0^\infty dr(\varepsilon_b - V(r))u(r)u'(r) \;&=\; m\int_0^\infty dr(\varepsilon_b - V(r))(u^2(r))' \\ &=\; m\int_0^\infty dr\,V'(r)u^2(r) \;=\; m\int d^3r\,V'(r)\psi^2(r), \end{aligned} \tag{7.18}$$

proving the relation (7.15).

7.1.2 *Ionization of States with $\ell \neq 0$*

One can expect that the amplitude obtains an additional factor $p^{-\ell}$. This is because the wave functions behave as r^ℓ at $r \to 0$, while the distances $r \sim 1/p$ are important. We demonstrate how this happens, beginning with the case $\ell = 1$.

The wave function of the bound state with orbital momentum $\ell = 1$ and its projection m can be written as

$$\psi_{n1m}(\mathbf{r}) = \sqrt{\frac{3}{4\pi}}r_m\chi(r); \quad R_{n1}(r) = r\chi(r); \quad \chi(0) \neq 0. \tag{7.19}$$

We denote the amplitude describing photoionization of the state $n, 1, m$ by F_m. In the first step, we neglect the interaction of the photoelectron with the residual ion. We obtain, similar to (7.3),

$$F_{m0} = \sqrt{\frac{3}{4\pi}} \frac{\mathbf{e}\cdot\mathbf{p}}{m} N(\omega) \int d^3 r r_m e^{-i\mathbf{p}\cdot\mathbf{r}} \chi(r) . \tag{7.20}$$

Since $r_m e^{-i\mathbf{p}\cdot\mathbf{r}} = i(\nabla_p)_m e^{-i\mathbf{p}\cdot\mathbf{r}}$, we obtain, after integration by parts,

$$F_{m0} = -i\sqrt{\frac{3}{4\pi}} \frac{\mathbf{e}\cdot\mathbf{p}}{m} N(\omega)(\nabla_p)_m \cdot \frac{8\pi\chi'(0)}{p^4} , \tag{7.21}$$

and finally

$$F_{m0} = -i\sqrt{\frac{3}{4\pi}} \cdot \frac{\mathbf{e}\cdot\mathbf{p}}{m} \cdot N(\omega) \frac{16\pi\eta p_m \chi(0)}{p^6} . \tag{7.22}$$

Here we employed the Kato condition $\chi'(0) = -\eta\chi(0)/2$; see (4.79). Thus indeed, the amplitude F_0 for the ionization of p states is of order $1/p^5$. Compared with the amplitude for s states, it contains an additional factor of order $1/p$.

Now we include the first-order correction to the wave function of the photoelectron caused by interaction with the residual ion. Recall that interactions of a photoelectron with bound electrons followed by the transfer of a large momentum $q \gg \mu_b$ with the bound electrons are quenched by additional powers of $1/q \approx 1/p$. Thus we must include only interactions with the nucleus. To calculate the corresponding contribution to the amplitude F_{m1}, we employ the Fourier transform of the function (7.19),

$$\psi_{n1m}(\mathbf{f}) = i\sqrt{\frac{3}{4\pi}} (\nabla_f)_m \chi(\mathbf{f}) , \tag{7.23}$$

and write, similar to (7.4),

$$F_{m1} = i\sqrt{\frac{3}{4\pi}} N(\omega) J_1; \quad J_1 = \int \frac{d^3 f}{(2\pi)^3} \langle \mathbf{p}|VG|\mathbf{f}\rangle \frac{\mathbf{e}\cdot\mathbf{f}}{m} (\nabla_f)_m \chi(f). \tag{7.24}$$

In integration by parts, the action of operator ∇_f on the matrix element $\langle \mathbf{p}|VG|\mathbf{f}\rangle$ provides additional powers of p in the denominator. The corresponding terms should be neglected in the asymptotics. Thus we obtain

$$J_1 = -e_m \int \frac{d^3 f}{(2\pi)^3} \langle \mathbf{p}|VG|\mathbf{f}\rangle \frac{\chi(f)}{m} . \tag{7.25}$$

Here we can put $\langle \mathbf{p}|VG|\mathbf{f}\rangle = \langle \mathbf{p}|VG|0\rangle = 2mV(p)/p^2$. This happens because the ejected electron can carry angular momentum $\ell = 0$. At large p, we can put $V(p) = -4\pi\alpha Z/p^2$, obtaining

$$F_{m1} \;=\; i\sqrt{\frac{3}{4\pi}}\cdot\frac{e_m}{m}N(\omega)\cdot\frac{8\pi\eta\chi(0)}{p^4};\quad \chi(0)\;=\;\chi(r=0). \tag{7.26}$$

Thus $F_{m1} \sim 1/p^4$ is of the same order as F_0 and should be included in the asymptotics

$$F_m \;=\; F_{m0} + F_{m1}\,. \tag{7.27}$$

At first glance, this looks a little bit unexpected, since in a process with small transferred momentum $q \sim \mu_b$, one would expect the Coulomb correction to be ξ times smaller than the contribution of the plane wave. However, in the high-energy photoionization, a large momentum $q \gg \mu_b$ is transferred to the nucleus. In the amplitude F_0, the photoelectron does not interact with the nucleus, and the momentum q is transferred by the bound electron. Thus the amplitude contains the factor $\psi(\mathbf{q})$, corresponding to small distances from the nucleus. In the amplitude F_1, momentum q is transferred by the photoelectron. This also provides a small factor. However, the bound-state wave function enters the amplitude F_1 with small momentum $f \sim \mu_b$. Thus the bound electron remains on the distances $r \sim 1/\mu_b$, where its density obtains the largest values, and $|\psi(\mathbf{f})| \gg |\psi(\mathbf{q})|$. Due to the interplay of these factors, the amplitudes F_0 and F_1 become of the same order of magnitude.

Note that the angular distribution related to one electron in the $2p$ state,

$$\frac{d\sigma}{d\Omega} \;=\; \frac{mp}{(2\pi)^2}\cdot\frac{\sum_m |F_{m0}+F_{m1}|^2}{3}, \tag{7.28}$$

is isotropic, since the sum $\sum_m |F_{m0}+F_{m1}|^2$ does not contain angular dependence. A simple way to see this is to choose the direction of the photon polarization as the axis of quantization of the angular momentum, i.e., $e_m = e\delta_{m0}$. Direct calculation (we ignore the common factor i in the amplitudes F_{m0} and F_{m1}) demonstrates that $\sum_m (F_{m0}^2 + 2F_{m0}F_{m1}) = 0$, and thus $\sum_m |F_m|^2 = \sum_m |F_{m1}|^2$, which does not contain angular dependence. Thus (7.28) can be written as

$$\frac{d\sigma}{dt} = \frac{A_{21}}{2}\cdot\frac{1}{\omega^{9/2}};\quad A_{21} = 2\sqrt{2}\pi\alpha(\alpha Z)^2\cdot\frac{|\chi(0)|^2}{m^{5/2}}. \tag{7.29}$$

This provides an instructive example of a possible misuse of plane waves. Assuming that since the photoelectron moves fast, it can be described by the plane waves, thus putting $F_m = F_{m0}$, one would obtain the qualitatively incorrect angular distribution $d\sigma/dt \sim 1 - t^2$. In particular, it would vanish for electrons moving along the direction of the photon momentum. This is not the case for the real angular distribution. Also, such an "approach" would overestimate the cross section for ionization of a $2p$ electron by the factor $4/3$.

The cross section for the ionization of one $2p$ electron is

$$\sigma_{2p}(\omega) \;=\; \frac{A_{21}}{\omega^{9/2}}\,. \tag{7.30}$$

Similarly, one can show that for ionization of any state with $\ell \neq 0$, one should include the interaction of the ejected electron with the residual ion. The cross section has the form

$$\sigma_{n\ell}(\omega) = \frac{A_{n\ell}}{\omega^{7/2+\ell}}, \tag{7.31}$$

where $A_{n\ell}$ does not depend on the photon energy and contains the factor $|\chi_\ell(0)|^2$, where $\chi_\ell(r) = R_{n\ell}(r)/r^\ell$.

The energy behavior of the cross sections $\sigma_{n\ell}$ is well known; see, e.g., [1].

7.1.3 Possibility of Asymptotic Analysis

Recent experiments on high-energy photoionization demonstrate that (7.31) is satisfied with poor accuracy. To understand what happens, let us return to the Coulomb case. Employing (5.79), we obtain an expression for the cross section of the photoionization of a hydrogenlike ion with nuclear charge Z, which includes the lowest-order term of the expansion in powers of $1/\omega$, but does not contain the expansion in powers of $\pi\xi$:

$$\sigma_{1s}(\omega) = \frac{16\sqrt{2}\pi}{3Z^2}\alpha r_0^2\left(\frac{m\alpha^2Z^2}{\omega}\right)^{7/2} e^{-\pi\xi}; \quad r_0 = \frac{1}{m\alpha}. \tag{7.32}$$

Recall that $\xi = m\alpha Z/p$, and $p = \sqrt{2m(\omega - I)}$ is the momentum of the photoelectron. Thus the high-energy equation that includes the leading correction to the asymptotics is

$$\sigma_{1s}(\omega) = \frac{16\sqrt{2}\pi}{3Z^2}\alpha r_0^2\left(\frac{m\alpha^2Z^2}{\omega}\right)^{7/2}(1 - \pi\xi). \tag{7.33}$$

Hence, in the case $Z = 1$, (7.29) holds with an accuracy of 10% for $\omega \geq 14\,\mathrm{keV}$. For the hydrogenlike ion with $Z = 2$, the condition is $\omega \geq 56\,\mathrm{keV}$. However, at these energies, $\omega/m \geq 0.1$, and the relativistic corrections are of this order. Thus for $Z > 2$, there is no region where the high-energy nonrelativistic asymptotics of the cross section work.

Now we show that the deviations of the cross sections of photoionization of the states $n\ell$ from their asymptotic values are described by a common factor. To illustrate the statement, consider the wave equation for the single-particle wave function in the state n, which can belong to either the discrete or continuum spectrum:

$$H\psi(\mathbf{r}) = \varepsilon\psi(\mathbf{r}); \quad H = \frac{p^2}{2m} + V(\mathbf{r}); \quad \mathbf{p} = -i\frac{\nabla}{m}. \tag{7.34}$$

We can write

$$V(r) = -\alpha Z/r + V_{ee}, \tag{7.35}$$

where the first term on the RHS is the interaction of the electron in the state n with the nucleus, while V_{ee} stands for its interaction with the other electrons. Since in the asymptotics we deal with wave functions at distances r that are much smaller than the characteristic distances in the atom, we can put $V_{ee}(r) = V_{ee}(0)$ on the RHS of (7.35). Thus the wave equation (7.34) can be written as

$$-\frac{\Delta}{2m}\psi(\mathbf{r}) - \frac{\alpha Z}{r}\psi(\mathbf{r}) = \tilde{\varepsilon}\psi(\mathbf{r}); \quad \tilde{\varepsilon} = \varepsilon - V_{ee}(0). \tag{7.36}$$

This is just the equation for the electron in the Coulomb field with the shifted value of energy. For large $Z \gg 1$, we can employ the Thomas–Fermi model estimate $V_{ee}(0) = 1.45m\alpha^2 Z^{4/3}$. For small $Z \sim 1$, we have $V_{ee}(0) \sim m\alpha^2$. Thus the energy dependence of the cross section is the same as in the case of the Coulomb field with nuclear charge Z.

We turn now to (5.74) for the photoionization amplitude of the ground state in the Coulomb field. Treating $\pi\xi$ as a separate parameter, we find that the dependence is reproduced by the factor

$$h(\pi\xi) \;=\; N(\pi\xi)e^{-\pi\xi}\,. \tag{7.37}$$

Recall that $N(\pi\xi) = N_p$ is the normalization factor of the continuum wave function. The factor $e^{-\pi\xi}$ comes from the ratio $(A/B)^{i\xi}$ in (5.74). It emerges just because in the photoionization $p \gg k$. This stresses the "model-independent" nature of this term. Using the technique developed in Sect. 5.2, one can demonstrate (see, e.g., [2]) that the factor

$$\left(\frac{A}{B}\right)^{i\xi} = \left[\frac{(\mathbf{p}-\mathbf{k})^2 + \mu_n^2}{k^2 - (p + i\mu_n)^2}\right]^{i\xi} \tag{7.38}$$

has the same form for amplitudes of photoionization of any bound state. Thus the amplitudes of ionization of $n\ell$ states contain the common factor

$$Q_n(\xi) \;=\; h(\pi\xi)\exp\left(2\xi \arctan \xi/n\right), \tag{7.39}$$

and the energy dependence of the photoionization cross section has the form

$$\sigma_{n\ell}(\omega) \;=\; C\frac{D(\pi\xi)\exp\left(4\xi \arctan \xi/n\right)P_{n\ell}(\xi^2/n^2)}{\omega^{7/2+\ell}}. \tag{7.40}$$

Here C is a constant factor,

$$D(\pi\xi) = h^2(\pi\xi) = N^2(\pi\xi)\exp(-2\pi\xi); \quad N^2(\pi\xi) = \frac{2\pi\xi}{1-\exp(-2\pi\xi)}\,, \tag{7.41}$$

while $P_{n\ell}$ are the polynomial ratios. For the lowest states,

$$P_{10} = 1; \quad P_{20} = 1 + \frac{3(\xi/2)^2}{1 + (\xi/2)^2}; \quad P_{21} = 1 + \frac{8(\xi/2)^2}{3[1 + (\xi/2)^2]}.$$

Hence we have obtained the factor

$$S_n \;=\; D(\pi\xi)\exp\left(4\xi \arctan \xi/n\right), \tag{7.42}$$

which is common for photoionization cross sections of every state in the nth shell.

The factor $D(\pi\xi)$ is the same for every bound state. Note that the values of the parameter $\xi = m\alpha Z/(2m\varepsilon)^{1/2}$, with the energy of the photoelectron $\varepsilon = \omega - I_n$, differ for different n. However, with accuracy $I_{n\ell}/\omega$, we can replace ξ by

$$\hat{\xi} \;\equiv\; \frac{m\alpha Z}{(2m\omega)^{1/2}}. \tag{7.43}$$

Thus the high-energy behavior of the cross section of photoionization of the single-particle $n\ell$ state is determined by the factor $\omega^{7/2+\ell}$ and by the factor D defined by (7.41), which varies with the energy much more slowly. It can be written as

$$\sigma_{n\ell}(\omega) \;=\; \frac{A_{n\ell} D(\hat{\xi})}{\omega^{7/2+\ell}}. \tag{7.44}$$

The corrections to (7.44) are of order ξ^2/n. Note that corrections to (7.30) are much larger. They are of order $\pi\xi$.

We can write

$$D(\pi\xi) \;=\; \frac{2\pi\xi}{e^{\pi\xi} - e^{-\pi\xi}} S(\pi\xi), \tag{7.45}$$

where

$$S(\pi\xi) \;=\; \exp\left(-\pi\xi\right), \tag{7.46}$$

often referred to as the Stobbe factor, contains the sharpest dependence on the parameter $\pi\xi$.

Thus the ratio of the cross sections of photoionization of the same state at the high energies ω_1 and ω_2 is [3]

$$\frac{\sigma(\omega_1)}{\sigma(\omega_2)} \;\approx\; \frac{D_1}{D_2}\left(\frac{\omega_2}{\omega_1}\right)^{7/2+\ell}, \tag{7.47}$$

with $D_{1,2}$ denoting the factor $D(\pi\xi)$ given by (7.45) corresponding to the energies $\omega_{1,2}$. Also, the ratios of cross sections from different states, e.g.,

$$R_{n\ell}(\omega) \;=\; \frac{\sigma_{n0}(\omega)}{\sigma_{n\ell}(\omega)}, \tag{7.48}$$

converge to their nonrelativistic high-energy limit much faster than the cross sections themselves.

7.1.4 Preasymptotic Behavior of the Cross Sections

Preasymptotic behavior of the cross sections manifests itself in corrections of order $1/\omega$. Besides the direct numerical calculations, it is desirable to find approximate analytical formulas. The analytic perturbation theory developed in [4] provides a possibility to find analytical expressions for the wave functions of both discrete and continuum states. The approach is based on the assumption that the atomic potential can be represented as that of the Coulomb field of the point nucleus multiplied by a factor, which can be written as a series in powers of λr with $\lambda \approx m\alpha Z^{1/3}$ of the order of the inverse Thomas–Fermi radius of the atom:

$$V(r) \;=\; -\frac{\alpha Z}{r}\Big(1 + c_1\lambda r + c_2(\lambda r)^2 + c_3(\lambda r)^3 + \cdots\Big). \tag{7.49}$$

Such a representation enables us to find analytical expressions for the electron wave functions of both discrete and continuum spectra in the region $\lambda r \lesssim 1$. This means that for the lowest bound states such as the K shell in most atoms and the L shell for high Z, the approach describes the wave functions in the region $r \lesssim 1/\mu_b$, where these functions obtain the largest values. Introducing

$$\nu \;=\; \frac{\lambda}{\eta}; \quad \eta \;=\; m\alpha Z \tag{7.50}$$

($\nu \sim Z^{-2/3}$), one obtains for the wave function of the $1s$ state up to the terms $\lambda^3 r^3$,

$$\psi_{1s}(r) = N\psi^C_{1s}(r)\cdot s(r); \quad s(r) = 1 + \frac{c_2}{2}\lambda^2 r^2 + c_3\lambda^2 r^2\nu + \frac{c_3}{3}\lambda^3 r^3. \tag{7.51}$$

Here ψ^C_{1s} is the Coulomb function,

$$N \;=\; 1 - \frac{3}{2}c_2\nu^2 - \frac{11}{2}c_3\nu^3; \tag{7.52}$$

is the normalization factor. Note that deviations of the shape of the wave functions from the Coulomb functions begin with terms of order λ^2. The second-order

perturbative corrections are of order λ^4. Similar expressions are obtained for the continuum wave functions. The terms linear in λ lead only to a shift of the binding energies from the Coulomb values. For the ground state, the Coulomb value $I_Z = \eta^2/2m$ is shifted to $\varepsilon = I_Z(1 - 2c_1\nu - 3c_2\nu^2 - 6\nu^3)$.

This enables us to find analytical formulas for the photoionization cross sections as functions of the parameter ξ [5]. For the $1s$ electron, it is

$$\sigma(\omega) \;=\; N^2\sigma^C(\omega)\, f(c_n, \xi^2), \tag{7.53}$$

with σ^C the Coulomb cross section given by (5.78). The analytical expression for the function $f(c_n, \xi^2)$ is presented in [5]. The preasymptotic behavior of the cross section is determined by the lowest-order terms of the expansion in powers of ξ^2 of the cross section σ^C and of the function

$$f(c_n, \xi^2) \;=\; 1 + \xi^2\Big(-\frac{1}{2}c_2\nu^2 + 7c_3\nu^3\Big) + O(\xi^4)\,. \tag{7.54}$$

The value of λ is chosen as the inverse Thomas–Fermi radius of the atom, i.e., $\lambda = 1.13m\alpha Z^{1/3}$. Thus $\nu = 1.13/Z^{2/3}$ is the ratio of the size of the K shell to that of the Thomas-Fermi atom. The values of the coefficients c_n are obtained by fitting the Hermann–Skillman atomic potential (a modification of the Hartree–Fock field in which the nonlocal exchange term is approximated by an effective local one) in the internal region of the atom, i.e., at $\lambda r \le 1$ for each value of the nuclear charge Z.

To illustrate the accuracy of the approach, we compare the result for the cross section of ionization of the K shell of the Ca atom ($Z = 20$) at $\omega = 20\,\mathrm{keV}$ to the result obtained by application of direct numerical methods. In the described approach, one obtains $\sigma = 7.511\,\mathrm{barn}$, while in numerical calculations, it is $7.544\,\mathrm{barn}$.

7.2 Forms of Electromagnetic Interactions

7.2.1 Forms of Interaction and Gauge Invariance

Here we analyze the various forms of interaction between the nonrelativistic atomic electron and the photon. We are looking for expressions in the dipole approximation, i.e., in the lowest order of expansion in the photon momentum $\mathbf{k}$.

A variety of forms occurs, since the vector potential of electromagnetic field is not uniquely defined. Interaction of the electron with an electromagnetic field described by a four-dimensional vector A with time-component A_0 and space components $A_i = (\mathbf{A})_i$, written usually as $A = (A_0, \mathbf{A})$, is determined by the contribution

$$L_I(x) \;=\; -eA_\mu(x)\, j^\mu(x) \tag{7.55}$$

(for the electron, $e = -|e|$) to the Lagrangian density. Here $x = (t, \mathbf{r})$ is a point in four-dimensional space, $j = (\psi_e^* \psi_e, \psi_e^* \boldsymbol{\alpha} \psi_e)$ is the electron current, while ψ_e is the operator of the electron field. In the nonrelativistic limit, $j^i = \psi_e^* \mathbf{v}^i \psi_e$. Only three of the four components A_μ are independent, corresponding to the three possible projections of the photon spin $S = 1$. The only possible relativistic invariant condition that can tie up the components A_μ is the Lorentz condition $\partial A_\mu / \partial x_\mu = 0$. Equations of motion are invariant under the gauge transform

$$A'_\mu = A_\mu + \nabla_\mu \lambda(x); \quad \nabla_\mu = \left(\frac{\partial}{\partial t}, -\nabla_j \right); \quad j = 1, 2, 3\,, \tag{7.56}$$

with the function $\lambda(x)$ satisfying the condition

$$\frac{\partial}{\partial x_\mu} \frac{\partial \lambda(x)}{\partial x^\mu} = 0. \tag{7.57}$$

The standard choice for interaction of an electron with an external photon is $A_0 = 0$. In this case,

$$\mathbf{A}(x) = \mathbf{A}(\mathbf{r}) e^{-i\omega t}; \quad \mathbf{A}(\mathbf{r}) = \sqrt{\frac{2\pi}{\omega}} \mathbf{e} e^{i\mathbf{k}\cdot\mathbf{r}}; \quad \omega = |\mathbf{k}|; \quad \mathbf{e} \cdot \mathbf{k} = 0, \tag{7.58}$$

with $\mathbf{e}$ the polarization vector (direction of the electric field in the electromagnetic wave). Thus

$$L_I(x) = e \bar{\psi}_e(x) \mathbf{v} \cdot \mathbf{A}(\mathbf{r}) \psi_e(x) e^{-i\omega t}; \quad \mathbf{v} = \frac{-i\nabla}{m} = \frac{\mathbf{p}}{m}. \tag{7.59}$$

On the other hand, we can choose

$$\lambda(x) = \lambda(t, \mathbf{r}) = \mathbf{r} \cdot \mathbf{A}(t, \mathbf{r}), \tag{7.60}$$

with $\mathbf{A}$ determined by (7.58). Direct calculation confirms that (7.57) is satisfied. Carrying out the transformation (7.56), we obtain

$$A'_0(x) = A'_0(\mathbf{r}) e^{-i\omega t}; \quad A'_0(\mathbf{r}) = -i\omega \mathbf{r} \cdot \mathbf{A}(\mathbf{r}), \quad A'_i(x) = A'_i(\mathbf{r}) e^{-i\omega t}; \tag{7.61}$$

$$A'_i(\mathbf{r}) = -i k_i \mathbf{r} \cdot \mathbf{A}(\mathbf{r}).$$

In the nonrelativistic approximation, $v \ll 1$, and we put $A'_\mu j^\mu = A'_0 j^0$. Employing (7.61), we obtain

$$L_I(x) = -e \bar{\psi}_e(x) A'_0(x) \psi_e(x) e^{-i\omega t} = i\omega e \bar{\psi}_e(x) \cdot \mathbf{A}(\mathbf{r}) \psi_e(x) e^{-i\omega t}\,, \tag{7.62}$$

with $\mathbf{A}$ determined by (7.58).

The matrix element $S_{n'n}$ describing the transition between the states $|n\rangle$ and $\langle n'|$ of atomic electrons with energies E_n and $E_{n'}$ can be written as

$$S_{n'n} = \langle n'| \int d^4x H_I(x)|n\rangle = -\langle n'| \int d^4x L_I(x)|n\rangle,$$

with H_I the Hamiltonian of the interaction. Since the time dependence of the electron wave functions can be singled out as $\psi_n(x) = \psi_n(\mathbf{r})e^{-iE_n t}$ and $\bar{\psi}_{n'}(x) = \bar{\psi}_{n'}(\mathbf{r})e^{+iE'_n t}$, the integral over t can be calculated as

$$\int dt e^{i(E_{n'}-E_n-\omega)t} = 2\pi\delta(E_{n'} - E_n - \omega).$$

The delta function ensures energy conservation. We obtain the amplitude

$$M_{n'n} = -e \int d^3r A_\mu(\mathbf{r}) j^\mu_{n'n}(\mathbf{r}), \tag{7.63}$$

with $j^\mu_{n'n}(\mathbf{r}) = \bar{\psi}_{n'}(\mathbf{r})\gamma^\mu\psi(\mathbf{r})$, and in the nonrelativistic limit, $j^i_{n'n}(\mathbf{r}) = \psi^*_{n'}(\mathbf{r})\mathbf{v}^i\psi(\mathbf{r})$. Details of the derivation of (7.63) are given, e.g., in the book [6]. To obtain the amplitudes in the dipole approximation, we must put $\mathbf{k} = 0$ in expressions (7.58) for $\mathbf{A}(\mathbf{r})$. Thus, if the vector potential is determined by (7.58), we obtain

$$M^v_{n'n} = N(\omega)h^v_{n'n}; \quad h^v_{n'n} = \langle\Psi_{n'}| \sum_k \mathbf{e}\cdot\mathbf{v}^{(k)}|\Psi_n\rangle\,. \tag{7.64}$$

Here k labels the atomic electrons. The upper index v corresponds to the operator $\mathbf{v}^k$ in the integrand on the RHS. This is known as the "velocity" or "gradient" form of the electron–photon interaction. However, if the vector potential is given by (7.61), we obtain

$$M^r_{n'n} = N(\omega)h^r_{n'n}; \quad h^r_{n'n} = i\varepsilon_{n'n}\langle\Psi_{n'}| \sum_k \mathbf{e}\cdot\mathbf{r}^{(\mathbf{k})}|\Psi_n\rangle; \quad \varepsilon_{n'n} = \varepsilon_{n'} - \varepsilon_n. \tag{7.65}$$

The upper index r corresponds to the operators $\mathbf{r}^{(k)}$ on the RHS of the integrand. This is the "length" form for the electron–photon interaction.

If the states n and n' are described by wave functions that satisfy the Schrödinger equation with Hamiltonian

$$H = -\sum_k \frac{\Delta_k}{2m} + \sum_k \frac{-\alpha Z}{r_k} + \sum_{k'>k} \frac{\alpha}{|\mathbf{r}_{k'} - \mathbf{r}_k|}\,, \tag{7.66}$$

where k and k' label the atomic electrons and Δ_k is the Laplace operator acting on the electron, labeled by k, we have

$$M^v_{n'n} = M^r_{n'n}; \quad h^v_{n'n} = h^r_{n'n}\,. \tag{7.67}$$

However, one actually uses certain approximations for the interaction V, and relation between the two forms requires additional analysis.

Now we assume that the many-electron functions $\Psi_{n',n}$ are described by combinations of the one-electron functions that satisfy (7.34), with V a *local* potential. The two forms of interaction with the photon that cause a transition between the single-particle states $|i\rangle$ and $\langle f|$ are

$$h^v_{fi} = \langle\psi_f|\mathbf{e}\cdot\mathbf{v}|\psi_i\rangle; \quad h^r_{fi} = i\varepsilon_{fi}\langle\psi_f|\mathbf{e}\cdot\mathbf{r}|\psi_i\rangle, \tag{7.68}$$

and $h^v_{fi} = h^r_{fi}$. This can be demonstrated in the following way. Since $|i\rangle$ and $\langle f|$ are the eigenstates of the same Hamiltonian H given by (7.34), the amplitude h^r_{fi} can be evaluated as $\varepsilon_{fi}\langle\psi_f|\mathbf{r}|\psi_i\rangle = \langle\psi_f|H\mathbf{r} - \mathbf{r}H|\psi_i\rangle$. Direct calculation provides

$$[H,\mathbf{r}] = -i\frac{\mathbf{p}}{m} + [V,\mathbf{r}]\,, \tag{7.69}$$

and hence [7]

$$h^r_{fi} = \langle\psi_f|\frac{\mathbf{e}\cdot\mathbf{p}}{m}|\psi_i\rangle + i\langle\psi_f|\mathbf{e}\cdot[V,\mathbf{r}]|\psi_i\rangle\,. \tag{7.70}$$

For the local field V, the last term on the RHS vanishes, proving the statement. Similarly, one can show that in the local field, the "accelerator form" for the matrix element

$$h^a_{fi} = i\langle\psi_f|\frac{\mathbf{e}\cdot\boldsymbol{\nabla}V}{m\varepsilon_{fi}}|\psi_i\rangle \tag{7.71}$$

(in the classical equation of motion, the electron acceleration is proportional to ∇V) is equivalent to two other elements. One could see that the variety of forms for the electron–photon interactions is connected with the gauge invariance of quantum electrodynamics.

Note that

$$h^v_{fi} = h^r_{fi} = h^a_{fi} \tag{7.72}$$

for the exact solutions of the wave equation (7.34). In fact, approximate wave functions are usually used. For them, the results may differ, and a small value of the deviations between computations in various forms would signal good accuracy of the employed wave functions.

We turn now to the case of a self-consistent field, where the single-particle function of each electron depends on the distributions of the other electrons. In the Hartree approximation, the potential V in (7.34) is

$$V(r) = -\frac{\alpha Z}{r} + W(r)\,, \tag{7.73}$$

where

$$W(r) = \alpha \int d^3r' \frac{\rho(\mathbf{r}')}{|\mathbf{r}' - \mathbf{r}|}; \quad \rho(\mathbf{r}') = \sum_k \psi_k^*(\mathbf{r}')\psi_k(\mathbf{r}'),$$

with k labeling the atomic electrons. The potential $W(r)$ is a local one. However, the states $|i\rangle$ and $\langle f|$ belong to different Hamiltonians, since the density of the atomic electrons $\rho(\mathbf{r}')$ changes if one of the electrons undergoess a transition. The forms remain equivalent under the assumption that this change is numerically small and thus is unimportant. This assumption is known as the "frozen core approximation."

The Hartree–Fock approximation includes also the nonlocal exchange potential. In this case,

$$V(r) \;=\; V_{HF}(r) \;=\; -\frac{\alpha Z}{r} + W(r) + K(r)\,, \tag{7.74}$$

with the exchange potential

$$K(r) = -\alpha \int d^3r' \frac{u(\mathbf{r}', \mathbf{r})}{|\mathbf{r}' - \mathbf{r}|}; \quad u(\mathbf{r}', \mathbf{r}) = \sum_k \psi_k^*(\mathbf{r}')\psi_k(\mathbf{r}). \tag{7.75}$$

It provides a nonzero contribution to the second term on the RHS of (7.70). Now we try to calculate it.

Recall that the general expression for the result of the action of the operator V on the state $|\psi\rangle$ is

$$\langle \mathbf{r}|V|\psi\rangle \;=\; \int d^3r' \langle \mathbf{r}|V|\mathbf{r}'\rangle\langle \mathbf{r}'|\psi\rangle \;=\; \int d^3r' \langle \mathbf{r}|V|\mathbf{r}'\rangle\psi(\mathbf{r}'). \tag{7.76}$$

For the exchange potential, we have

$$\langle \mathbf{r}|K|\mathbf{r}'\rangle \;=\; -\alpha \frac{\sum_k \psi_k(\mathbf{r})\psi_k^*(\mathbf{r}')}{|\mathbf{r}' - \mathbf{r}|}, \tag{7.77}$$

with the sum over the occupied states k. For a local potential,

$$\langle \mathbf{r}|W|\mathbf{r}'\rangle \;=\; W(\mathbf{r})\delta(\mathbf{r} - \mathbf{r}') \tag{7.78}$$

and $\langle \mathbf{r}|W|\psi\rangle \;=\; W(\mathbf{r}) \cdot \psi(\mathbf{r})$. Now we express the function $\psi(\mathbf{r}')$ on the RHS of (7.76) in terms of the function $\psi(\mathbf{r})$. This can be done using the relation (see, e.g., [8])

$$\psi(\mathbf{r}') \;=\; e^{i\mathbf{a}\cdot\mathbf{p}}\psi(\mathbf{r}); \quad \mathbf{a} \;=\; \mathbf{r}' - \mathbf{r}, \tag{7.79}$$

where the operator $\mathbf{p} = -i\nabla$ acts on $\mathbf{r}$. Note that (7.79) is just the Taylor series expansion of the function $\psi(\mathbf{r}')$ about the point $\mathbf{r}$. Thus we can write

$$V(\mathbf{r};\mathbf{p}) = \int d^3r' \langle \mathbf{r}|V|\mathbf{r}'\rangle e^{i\mathbf{a}\cdot\mathbf{p}}. \tag{7.80}$$

For the case of the local potential, the LHS does not depend on $\mathbf{p}$, due to (7.78).

The matrix element of the interaction with the electromagnetic field is $M_{fi} = \langle \psi_f|H_I|\psi_i\rangle$. The Hamiltonian of interaction $H_I = H_A - H$ is the difference between the atomic Hamiltonian in the external field A and that without the field. The operator H_I can be obtained by replacing $\mathbf{p}$ by $\mathbf{p} - e\mathbf{A}$ in the atomic Hamiltonian (7.34). Note that now the matrix element of the potential V depends on $\mathbf{p}$. Employing (7.80), we obtain

$$\langle \psi_f|V(\mathbf{p})|\psi_i\rangle = \int d^3r \int d^3r' \psi_f^*(\mathbf{r})\langle \mathbf{r}|V|\mathbf{r}'\rangle e^{i\mathbf{a}\cdot\mathbf{p}}\psi_i(\mathbf{r}). \tag{7.81}$$

For a description of photoionization, we must include only the lowest order of the electron charge e. In the dipole approximation, i.e., putting $\mathbf{k} = 0$ in the second equality of (7.58), we obtain $\mathbf{A} = \sqrt{2\pi/\omega}\mathbf{e}$. Setting $M_{fi} = N(\omega)h_{fi}$, we obtain

$$h_{fi} = \int d^3r \psi_f^*(\mathbf{r})\frac{\mathbf{e}\cdot\mathbf{p}}{m}\psi_i(\mathbf{r}) + i\int d^3r\psi_f^*(\mathbf{r})\mathbf{e}\Bigg[\int d^3r'\langle \mathbf{r}|V|\mathbf{r}'\rangle(\mathbf{r}'\psi_i(\mathbf{r}')) - \\ - \int d^3r'\langle \mathbf{r}|V|\mathbf{r}'\rangle(\mathbf{r}\psi_i(\mathbf{r}'))\Bigg]. \tag{7.82}$$

Since

$$\int d^3r\psi_f^*(\mathbf{r})\Bigg[\int d^3r'\langle \mathbf{r}|V|\mathbf{r}'\rangle(\mathbf{r}'\psi_i(\mathbf{r}')) - \int d^3r'\langle \mathbf{r}|V|\mathbf{r}'\rangle(\mathbf{r}\psi_i(\mathbf{r}'))\Bigg] = \langle \psi_f|[V,\mathbf{r}]|\psi_i\rangle\,, \tag{7.83}$$

we obtain, employing (7.70),

$$h_{fi} = h_{fi}^r\,. \tag{7.84}$$

Hence one must use the length form of interaction with the electromagnetic field in the case of a nonlocal potential [9, 10].

In practical computations, one sometimes replaces the exchange potential by an effective local potential. This can be done, e.g. by calculation of the function $u(\mathbf{r}', \mathbf{r})$, assuming that the atomic electrons are described by plane waves with momenta $p \le p_F$, while the Fermi momentum p_F is determined by the density $\rho(\mathbf{r})$. In this Hartree–Fock–Slater approximation, the exchange potential is replaced by the local potential $K_{eff}(\rho(\mathbf{r}))$. In this approach, one is free to use any form of interaction.

7.2.2 Thomas–Reiche–Kuhn Sum Rule

In the case of local potentials, when the length and velocity forms are equivalent, their combination provides the simplest way to obtain an important relation between the probabilities of the photoexcitation and photoionization processes. Returning to the many-electron states, we can write expressions for probabilities of transitions between the states $|n\rangle$ and $\langle n'|$.

We introduce the dimensionless characteristics of such transitions $f_{nn'}$, called the "dipole oscillator strength." They are defined as

$$f_{n'n} = 2m\varepsilon_{n'n}|\hat{x}_{n'n}|^2 \quad \varepsilon_{n'n} = \varepsilon_{n'} - \varepsilon_n; \quad f_{nn'} = -f_{n'n}. \tag{7.85}$$

Here x is the projection of the vector $\mathbf{r}$ on an arbitrary chosen direction, $\hat{x} = \sum_k x^{(k)}$ with k labeling atomic electrons. Employing (7.64) and (7.65), we can express the squared amplitude of the transition between the states n and n' caused by absorption of a photon in terms of the oscillator strength

$$|M_{n'n}|^2 \;=\; \pi r_e f_{n'n}\,. \tag{7.86}$$

As we have seen, this expression is true even if the interaction V contains nonlocal terms.

We turn now to the case of a local field $V(r)$. Employing the equivalence of the length and velocity forms, we can write

$$f_{n'n} = 2i(\hat{p}_x)_{nn'}(\hat{x})_{n'n} = -2i(\hat{x})_{nn'}(\hat{p}_x)_{n'n}; \quad \hat{\mathbf{p}} = \sum_k \mathbf{p}^{(k)}\,. \tag{7.87}$$

The sum over a complete set of the states n' provides

$$\mathscr{S}_{n'} f_{n'n} \;=\; i[\hat{p}_x, \hat{x}]_{nn}\,. \tag{7.88}$$

Here $\mathscr{S}_{n'}$ denotes the sum over the states of the discrete spectrum and integration over the continuum states with weight $d^3p'/(2\pi)^3$. For each electron,

$$i[p_i, r_j] \;=\; \delta_{ij}\,, \tag{7.89}$$

and thus $i[\hat{p}_x, \hat{x}]_{nn} = N_e$, with N_e the number of atomic electrons in the state n. Hence we come to the Thomas–Reiche–Kuhn sum rule

$$\mathscr{S}_{n'} f_{n'n} \;=\; N_e\,. \tag{7.90}$$

This equation enables us to investigate the relative probability of various channels of excitation.

The contributions of the discrete and continuum states to the left-hand side of (7.90) can be written separately. We illustrate this by considering the case of single-particle excitations, i.e., only one of the electrons in the state n undergoes excitation. Generalization to many-particle excitations is straightforward.

Employing (7.64) and (7.65), one can write the photoionization cross section of the state n in terms of the oscillator strength

$$\sigma_{ph}(\omega) = 2\pi^2 r_e \int \frac{d^3p'}{(2\pi)^3}\delta(\omega - \frac{p'^2}{2m} - I_n) f_{\mathbf{p}'n}; \quad r_e = \frac{\alpha}{m}, \tag{7.91}$$

with I_n the ionization potential of the initial state n, $\mathbf{p}'$ the photoelectron momentum. Integrating both sides over ω, we obtain

$$\frac{1}{2\pi^2 r_e}\int_{I_n}^{\infty} d\omega\sigma(\omega) \; = \int \frac{d^3p'}{(2\pi)^3} f_{\mathbf{p}'n}\,, \tag{7.92}$$

with the term on the RHS being just the contribution of the continuum states to the LHS of (7.90). Thus the Thomas–Reiche–Kuhn sum rule can be written as

$$\sum_{n''} f_{n''n} + \frac{1}{2\pi^2 r_e}\int_{I_n}^{\infty} d\omega\sigma_{ph}(\omega) \; = \; N_e\,. \tag{7.93}$$

Here n'' labels the states of the discrete spectrum.

The relation (7.93) is known also as the "golden sum rule." Note that both terms on the LHS can be measured experimentally. The "golden sum rule" is widely used in the analysis of experimental data on photoionization and photoexcitation. For the case of many-particle excitations, σ_{ph} is the cross section of the photoabsorption process in which at least one electron is moved to the continuum.

Recall that (7.90) and (7.93) are obtained under the assumption that the velocity and the length forms of the interaction are equivalent. This is true for the exact solutions of the wave equation with the Hamiltonian (7.66). However, it can be violated if approximate functions are employed. If the approximate Hamiltonian contains a nonlocal term, it is reasonable to write (7.85) as

$$f_{n'n} = 2m\varepsilon_{n'n}|\hat{x}_{n'n}|^2 = 2m\hat{x}_{n'n}[H,\hat{x}]_{n'n}\,. \tag{7.94}$$

Using (7.69) projected onto the x-axis, we obtain

$$\sum_{n''} f_{n''n} + \frac{1}{2\pi^2 r_e}\int_{I_n}^{\infty} d\omega\sigma_{ph}(\omega) + f_n^{nloc} \; = \; N_e\,, \tag{7.95}$$

with

$$f_n^{nloc} \; = \; m[\hat{x},[H,\hat{x}]]_{nn}\,. \tag{7.96}$$

7.2.3 Amplitude of Photoionization in Length Form

Here we calculate the asymptotics of the amplitude for the photoionization of a bound s state in length form. As we have seen, the final-state wave function can be treated perturbatively. The calculation presented below illustrates the fact that the number of perturbative terms depends on the form of electromagnetic interaction employed in the calculations.

As we have seen in Sect. 7.1.1, in velocity form, the amplitude is given by (7.7) and (7.10). It corresponds to description of the photoelectron by the plane wave. In length form, one should write the vertex of the electron–photon interaction in (7.2) as $\gamma = -\omega \mathbf{e} \nabla_f$. The contributions to the amplitude corresponding to the description of the photoelectron by the plane wave are given by (7.7) and (7.10) with momentum $\mathbf{p}$ replaced by the operator $-m\omega\nabla_p$. This provides

$$F_0^r = -\frac{\mathbf{e}\cdot\mathbf{p}}{m}\cdot N(\omega)\frac{16\pi\psi'(r=0)}{p^4}; \quad \eta = m\alpha Z \tag{7.97}$$

which is twice the contribution of the plane-wave term in the velocity form given by (7.10).

To understand what happened, we turn now to the contribution of the lowest correction to the wave function of the outgoing electron. As we know, it comes from the interaction with the nucleus V. We obtain, instead of (7.4),

$$F_1^r = N(\omega)J; \quad J = -\omega\int\frac{d^3f}{(2\pi)^3}\cdot\langle\mathbf{p}|VG|\mathbf{f}\rangle\cdot\mathbf{e}\cdot\nabla_f\langle\mathbf{f}|\psi_i\rangle, \tag{7.98}$$

with ∇_f acting on $\mathbf{f}$. Employing (7.5), we put

$$\langle\mathbf{p}|VG|\mathbf{f}\rangle = -\frac{8\pi\eta}{p^2(\mathbf{p}-\mathbf{f})^2} \approx -\frac{8\pi\eta}{p^4} - \frac{16\eta}{p^6}\mathbf{p}\cdot\mathbf{f} \tag{7.99}$$

in the integral. Integration by parts over $\mathbf{f}$ provides

$$F_1^r = -\frac{\mathbf{e}\cdot\mathbf{p}}{m}\cdot N(\omega)\frac{8\pi\eta\psi(0)}{p^4}. \tag{7.100}$$

Thus the contribution of the plane wave F_0 and that of the lowest correction F_1 provide contributions of the same order. Their sum is

$$F^r = F_0^r + F_1^r = -\frac{\mathbf{e}\cdot\mathbf{p}}{m}\cdot N(\omega)\frac{8\pi}{p^4}\cdot(2\psi'(0)+\eta\psi(0)). \tag{7.101}$$

Due to the first Kato condition, $2\psi'(0) + \eta\psi(0) = -\eta\psi(0)$. As expected, the amplitude F^r is equal to that calculated in the velocity form; (7.10).

Note that if the approximate functions employed in the computations do not satisfy the Kato condition, the equivalence of the two forms is lost. Note also that a calculation that includes only the plane wave overestimates the cross section by a factor of 4. This would be one more example of the possible misuse of plane waves.

7.2.4 Amplitude of Rayleigh Scattering in Length Form

As we have seen in Chap. 5, the nonrelativistic amplitude of Rayleigh scattering can be presented as the sum of the seagull and pole terms. In the velocity form for the interaction between the photon and electron, it can be written as

$$F = \frac{N^2(\omega)}{m^2} X;$$

$$X = \mathbf{e}_2^* \cdot \mathbf{e}_1 N_e m + \mathscr{S}_n \Big(\frac{\langle \Psi_1 | \mathbf{e}_2^* \hat{\mathbf{p}} | \Psi_n \rangle \langle \Psi_n | \mathbf{e}_1 \hat{\mathbf{p}} | \Psi_1 \rangle}{\omega + \varepsilon_{1n}} + \frac{\langle \Psi_1 | \mathbf{e}_1 \hat{\mathbf{p}} | \Psi_n \rangle \langle | \Psi_n | \mathbf{e}_2^* \hat{\mathbf{p}} | \Psi_1 \rangle}{-\omega + \varepsilon_{1n}} \Big). \tag{7.102}$$

Here we put $\Psi_i = \Psi_f = \Psi_1$ and $\varepsilon_f = \varepsilon_i = \varepsilon_1$.

Now we try to obtain an expression for the amplitude in length form. Due to (7.89), we can write $\mathbf{e}_2^* \cdot \mathbf{e}_1 = e_{2i}^* e_{1j} \delta_{ij} = i e_{2i}^* e_{1j} [p_i, r_j] = i \mathbf{e}_2^* \cdot \mathbf{p}\, \mathbf{e}_1 \cdot \mathbf{r} - i \mathbf{e}_1 \cdot \mathbf{r}\, \mathbf{e}_2^* \cdot \mathbf{p}$. This enables us to write

$$\mathbf{e}_2^* \cdot \mathbf{e}_1 N_e = \mathscr{S}_n \Big(i \langle \Psi_1 | \mathbf{e}_2^* \hat{\mathbf{p}} | \Psi_n \rangle \langle \Psi_n | \mathbf{e}_1 \hat{\mathbf{r}} | \Psi_1 \rangle - i \langle \Psi_1 | \mathbf{e}_1 \hat{\mathbf{r}} | \Psi_n \rangle \langle \Psi_n | \mathbf{e}_2^* \hat{\mathbf{p}} | \Psi_1 \rangle \Big). \tag{7.103}$$

The sum of the first terms in the parentheses on the RHS of (7.102) and (7.103) is

$$\langle \Psi_1 | \mathbf{e}_2^* \hat{\mathbf{p}} | \Psi_n \rangle \Big(\frac{\langle \Psi_n | \mathbf{e}_1 \hat{\mathbf{p}} | \Psi_1 \rangle}{\omega + \varepsilon_{1n}} + im \langle \Psi_n | \mathbf{e}_1 \hat{\mathbf{r}} | \Psi_1 \rangle \Big) = im \frac{\omega \langle \Psi_1 | \mathbf{e}_2^* \hat{\mathbf{p}} | \Psi_n \rangle \langle \Psi_n | \mathbf{e}_1 \hat{\mathbf{r}} | \Psi_1 \rangle}{\omega + \varepsilon_{1n}} \tag{7.104}$$

for each value of n. After a similar evaluation of the second terms in the same parentheses, we obtain the amplitude in length form:

$$F = 2\pi \alpha \omega \mathscr{S}_n \Big(\frac{\langle \Psi_1 | \mathbf{e}_2^* \hat{\mathbf{r}} | \Psi_n \rangle \langle \Psi_n | \mathbf{e}_1 \hat{\mathbf{r}} | \Psi_1 \rangle}{\omega + \varepsilon_1 - \varepsilon_n} + \frac{\langle \Psi_1 | \mathbf{e}_1 \hat{\mathbf{r}} | \Psi_n \rangle \langle | \Psi_n | \mathbf{e}_2^* \hat{\mathbf{r}} | \Psi_1 \rangle}{-\omega + \varepsilon_1 - \varepsilon_n} \Big). \tag{7.105}$$

One can see that the velocity and length forms have their strong points. In the velocity gauge, there is a separate seagull term, which provides the main contribution to the cross section in a large interval of values of the photon energy. There is no such thing as the seagull term in the length gauge. However, (7.105) enables us to present the elastic scattering of a photon by an atom in terms of the operator of dipole momentum

$$\mathbf{d} \;=\; e\sum_k \mathbf{r}^{(k)}\,. \tag{7.106}$$

This can be done by representing (7.105) as [8]

$$F \;=\; -2\pi\omega e^*_{2i}e_{1j}\alpha_{ij}(\omega)\,, \tag{7.107}$$

with

$$\alpha_{ij}(\omega) = -\mathscr{S}_n\Big(\frac{\langle\Psi_1|d_i|\Psi_n\rangle\langle\Psi_n|d_j|\Psi_1\rangle}{\omega-\varepsilon_{n1}+i\delta} + \frac{\langle\Psi_1|d_j|\Psi_n\rangle\langle|\Psi_n|d_i|\Psi_1\rangle}{-\omega-\varepsilon_{n1}+i\delta}\Big);\quad \delta\to 0, \tag{7.108}$$

the tensor of dipole polarizability, which can be defined in such a way for any system. Recall that $\mathscr{S}$ means the sum over the states of the discrete spectrum and integration over continuum states. If the system has a spherical symmetry, we can put $\alpha_{ij}(\omega) = \delta_{ij}\alpha_d(\omega)$ with

$$\alpha_d(\omega) \;=\; \frac{2}{3}\mathscr{S}_n\frac{\varepsilon_{n1}|\langle\Psi_1|\mathbf{d}|\Psi_n\rangle|^2}{\varepsilon_{n1}^2-\omega^2+i\delta\theta(\varepsilon_{n1})}. \tag{7.109}$$

Here the lower index d stands for dipole. Note that $\varepsilon_{n1} > 0$. The static characteristic

$$\alpha_d(0) \;=\; \frac{2}{3}\mathscr{S}_n\frac{|\langle\Psi_1|\mathbf{d}|\Psi_n\rangle|^2}{\varepsilon_{n1}} \tag{7.110}$$

is called a polarizability. It describes the leading (second perturbative order) shift of the energy caused by the electrostatic field. For the ground state of hydrogen, $\alpha(0) = 4.5r_0^3$ [8]. Another role of polarizability is that it characterizes modification of the amplitude describing the interaction between the photon and the electronic shell. We shall meet with this aspect of polarizability in Chap. 10.

7.3 Relativistic Case

7.3.1 The Lowest Order αZ Terms

Here we calculate the cross section of photoionization of a single-particle electron state by photons carrying energies $\omega \gtrsim m$. The analysis is similar to that carried out in Sect. 6.1, but the wave function ψ is no longer a Coulomb function. As we have seen in Sects. 6.1 and 6.3, the lowest order of the αZ series for the amplitude can be written in terms of the nonrelativistic wave function $\psi(\mathbf{r})$. The large momentum $q = |\mathbf{q}| \gtrsim m$ ($\mathbf{q} = \mathbf{k} - \mathbf{p}$) can be transferred to the recoil ion in either the initial or final state.

Employing (2.94) and (2.95), we find that for every s state, the amplitude and the cross section are described by (6.97)–(6.99) with N_1 replaced by the nonrelativistic wave function of the s state at the origin $\psi^{nr}_{ns}(r=0)$. The factor $M(\xi)$ defined by (6.98) can be represented as

$$M(\xi) \;=\; 2\pi\cdot 4\pi\alpha(\alpha Z)^2 D(\pi\xi)|\psi^{nr}_{ns}(r=0)|^2\,, \tag{7.111}$$

with the factor $D(\xi)$ defined by (7.45).

To understand what happens for the bound states with $\ell\neq 0$, it is sufficient to analyze the contribution in which the large momentum q is transferred to the recoil ion by the initial-state electron. In this contribution, the photoelectron is described by a plane wave, and the amplitude can be evaluated as

$$F_{ph} \;=\; \langle\psi_{\mathbf{p}}|\hat{A}|\psi\rangle \;=\; N(\omega)\bar{u}_{\mathbf{p}}\hat{\mathbf{e}}\varphi(\mathbf{q})u_0\,. \tag{7.112}$$

Recall that $\psi=\varphi u_0$. Following the analysis carried out in Sect. 2.2.3, we can write

$$\psi(\mathbf{q}) \;=\; \frac{2\eta}{q^2}\Big(1-\frac{\boldsymbol{\alpha}\mathbf{q}}{2m}\Big)\int\frac{d^3f}{(2\pi)^3}\frac{\varphi(\mathbf{f})}{(\mathbf{q}-\mathbf{f})^2}u_0\,. \tag{7.113}$$

The integral is saturated by f of order the characteristic momentum of the bound state μ_b. Thus we can assume that $f\ll q$, and the integral on the RHS obtains a nonzero value only if we expand the denominator up to the terms $(f/q)^\ell$, while for s states, we could put $(\mathbf{q}-\mathbf{f})^2=q^2$ there. Thus the amplitude has different q dependence for different values of ℓ. This changes the shape of the angular distribution, which obtains also an additional small factor $\mu_b^{2\ell}/q^{2\ell}\sim\mu_b^{2\ell}/m^{2\ell}$. In the hydrogenlike approximation, this factor is $(\alpha Z)^{2\ell}$. Also, the shape of the ω dependence of the cross section varies with the value of ℓ.

In the ultrarelativistic case, momenta $q\sim m$ determine the cross section. Thus the cross section decreases as ω^{-1} for every value of the orbital momentum ℓ. It can be written as

$$\sigma_{n\ell}(\omega) \;=\; \frac{C_{n\ell}D(\pi\alpha)}{m\omega}\,, \tag{7.114}$$

with

$$C_{n\ell}=\alpha\cdot(\alpha Z)^2\Big(\frac{\mu_{n\ell}}{m}\Big)^{2\ell}\frac{|\chi_{n\ell}(r=0)|^2}{m^3}c_{n\ell}\,, \tag{7.115}$$

where $\chi_{n\ell}(r)$ is related to the radial part of the function $\varphi(\mathbf{r})$ as $R_{n\ell}(r)=r^\ell\chi_{n\ell}(r)$, and $c_{n\ell}$ is a dimensionless numerical coefficient.

Note that in the ultrarelativistic case, the quenching of the angular distribution for large ℓ is more pronounced at $q\sim\omega\gg m$. In this region, it contains the factor $\mu_b^{2\ell}/\omega^{2\ell}$ instead of $\mu_b^{2\ell}/m^{2\ell}$ at $q\sim m$.

Further computations require separate calculations of the parameter $\chi(0)$. For the internal shells, perturbative calculations of deviations from the Coulomb field are possible, except for a very small nuclear charge Z. They will be considered in the next two sections.

7.3.2 *Far Away from the Threshold*

Here we consider the case in which the photoelectron carries the energy $\varepsilon \gg I_Z$. We carry out calculations for ionization of the electron in $1s$ state.

The Coulomb cross section of the process is modified by interaction of the electronic shell with both the bound electron and the photoelectron. It is often referred to as the "screened cross section," while its difference from the Coulomb cross section is usually called the "screening correction." Using the results obtained in Sect. 3.4.7, we find that the screening corrections for the photoelectron change the cross section of the photoeffect by magnitudes of relative order $\xi_{ee}^2 Z < \alpha$. This is smaller than the influence of the radiative corrections. Thus we have to study only the interaction between the electronic shell and the electron of the ionized state.

The ionized electron is bound by the field $V(r)$, which is the sum of the field of the nucleus $V_{eN} = -\alpha Z/r$ and the field created by $Z-1$ electrons of the atomic shell V_{ee}, $V = V_{eN} + V_{ee}$. We calculate the screening corrections, treating V_{ee} as a perturbation:

$$V(r) = V_0(r) + V_1(r); \quad V_0 = V_{eN}; \quad V_1 = V_{ee}\,. \tag{7.116}$$

In the standard formalism, the expressions for perturbative corrections involve all functions of the Coulomb spectrum. Here we employ another method, in which the correction to the wave function of the $1s$ electron is expressed solely in terms of the Coulomb $1s$ wave function. Such an approach was suggested by Zeldovich [11]. It was realized by Polikanov [12] for the Schrödinger equation and was employed for the Dirac equation in [13, 14].

In this approach, the expressions for the higher-order perturbative corrections are less complicated than in the standard one. We shall use this feature in the next section.

We demonstrate that the screened and Coulomb cross sections σ and σ^C are linked by a simple relation,

$$\sigma(\omega) = (1+\tau(Z))\sigma^C(\omega)\,, \tag{7.117}$$

which does not depend on the accuracy of calculation of the Coulomb cross section. In other words, it does not depend on the number of terms of the αZ series.

The wave function of the electron in the $1s$ state of the screened Coulomb field can be written as

$$\psi_{1s}(\mathbf{r}) = \frac{1}{r}\begin{pmatrix} G(r)\Omega_{\frac{1}{2}0M}(\mathbf{n}) \\ iF(r)\Omega_{\frac{1}{2}1M}(\mathbf{n}) \end{pmatrix}; \quad \mathbf{n} = \frac{\mathbf{r}}{r}. \tag{7.118}$$

For the Coulomb field without screening, this is just (6.6), where we put $G(r) = rg(r)$ and $F(r) = rf(r)$. The radial wave functions $G(r)$ and $F(r)$ satisfy the set of equations

$$G' - \frac{1}{r}G - (E - V + m)F = 0; \quad F' + \frac{1}{r}F + (E - V - m)G = 0. \tag{7.119}$$

Putting $F(r) = G(r)\Phi(r)$, we obtain another set of equations. Now we have a Riccati equation for the function $\Phi(r)$:

$$\Phi' + \frac{2}{r}\Phi + B\Phi^2 + B - 2m = 0; \quad B(r) \equiv E - V(r) + m, \tag{7.120}$$

while the equation for $G(r)$ is

$$G' - (\frac{1}{r} + B\Phi)G = 0. \tag{7.121}$$

The latter equation enables us to represent the function $G(r)$ in terms of $\Phi(r)$. Since for the ground state, the radial function has no nodes, we can assume that $G(r) \geq 0$, writing (7.121) as $d \ln G(r)/dr = 1/r + B(r)\Phi(r)$. Thus

$$G(r) = C(Z)r \exp\left(\int_0^r dx B(x)\Phi(x)\right), \tag{7.122}$$

with C a numerical coefficient depending only on the nuclear charge Z.

Now we calculate the lowest-order screening correction to the Coulomb wave function. We put $G = G_0 + G_1$, $\Phi = \Phi_0 + \Phi_1$, $B = B_0 + B_1$, $E = E_0 + E_1$, and $C = C_0(1 + C_1)$. The wave functions and energies with the lower index 0 are the Coulomb ones; see Sect. 6.1. Those with lower index 1 are caused by perturbation V_1. Note that

$$\Phi_0(r) = -\frac{\alpha Z}{1 + \gamma}; \quad \gamma = (1 - \alpha^2 Z^2)^{1/2}, \tag{7.123}$$

does not depend on r. The perturbative correction $\Phi_1(r)$ satisfies the equation

$$\Phi_1' + 2\Big(\frac{1}{r} + B_0\Phi_0\Big)\Phi_1 + (E_1 - V_1)(1 + \Phi_0^2) = 0. \tag{7.124}$$

Since (7.121) enables us to write $1/r + B_0\Phi_0 = G_0'/G_0$, we find that

$$\Phi_1(r) = -(1+\Phi_0^2)G_0^{-2}(r)\int_0^r dx(E_1 - V_1(x))G_0^2(x)$$
$$= -\frac{2}{1+\gamma}G_0^{-2}(r)\int_0^\infty dx(E_1 - V_1(x))G_0^2(x). \qquad (7.125)$$

Employing the boundary conditions $G, F \to 0$ at $r \to \infty$ and the normalization condition

$$\int_0^\infty dr(G_0^2(r) + F_0^2(r)) = \int_0^\infty dr(1+\Phi_0^2(r))G_0^2(r) = 1,$$

we find that

$$E_1 \;=\; \int_0^\infty dx\, V_1(x)G_0^2(x)\,. \qquad (7.126)$$

We assume that the field created by the atomic shell V_{ee} is described by the Thomas–Fermi potential and can be approximated by a sum of several Yukawa terms [15]:

$$V_{ee} \;=\; -\frac{\alpha(Z-1)}{r}\sum_i^n a_i \exp(-b_i\lambda r). \qquad (7.127)$$

Here $\lambda = 1.13m\alpha Z^{1/3}$ is the Thomas–Fermi radius; a_i and b_i are the dimensionless coefficients. We put $a_n = -1$, $b_n = 0$, and impose the additional condition

$$\sum_i^n a_i \;=\; 0\,. \qquad (7.128)$$

The potential $V(r) = V_{eN} + V_{ee}$ with V_{ee} defined by (7.127) has proper asymptotics at large distances $V(r \to \infty) = -\alpha/r$, as well as at small distances $V(r \to 0) = -\alpha Z/r$.

For $\lambda r \ll 1$, we obtain $V_{ee} \approx \alpha(Z-1)/r \cdot \sum_i^n a_i b_i \lambda r$. For $r \sim 1/m$, we have $V_{ee}/V_{eN} \sim \lambda r \approx \alpha Z^{1/3} \ll 1$. Thus at these distances, the electron interaction $V_{ee} = V_1$ can be treated as a perturbation. We assume that $n = 4$ and accept the numerical values of a_i and b_i presented in [15]. These are $a_1 = 0.1$, $a_2 = 0.55$, $a_3 = 0.35$, $a_4 = -1$, while $b_1 = 6.0$, $b_2 = 1.2$, $b_3 = 0.3$, $b_4 = 0$.

Introducing for a function $f(\lambda)$,

$$\hat{S}f(\lambda) \;=\; \sum_i^n a_i f(b_i\lambda)\,, \qquad (7.129)$$

we obtain after straightforward evaluation of (7.125),

$$\Phi_1(r) = \Phi_0 \hat{S}(1+\nu/2)^{-2\gamma}\left(\gamma^{-1} + 2\int_0^{\nu/2} dv \exp(-2\eta r v)(1+v)^{2\gamma-1}\right);\ \nu = \frac{\lambda}{\eta}. \tag{7.130}$$

The power of the exponent is $2\eta r v < b_1 \lambda r \ll 1$. One can see immediately that $\Phi_1 \sim \eta r \cdot \nu^2$ at small r. Thus we can put $\Phi_1(r) = 0$ for $r \sim 1/m$.

Employing (7.122), we can write the function $G(r) = G_0(r) + G_1(r)$ for any value of r as

$$G(r) = G_0(r)(1+C_1)\left(1 + \int_0^r dx[B_0(x)\Phi_1(x) + B_1(x)\Phi_0]\right). \tag{7.131}$$

Following our previous analysis, we can put $\Phi_1 = 0$ for $r \sim 1/m$. For these values of r, the integral on the RHS is of order $\eta r \nu^2 \ll 1$ and can be neglected. Hence the main effect of screening is the modification of the normalization constant C. Thus we find that indeed, for $r \sim 1/m$, one can put

$$G_1(r) = C_1 G_0(r); \quad F_1 = C_1 F_0(r). \tag{7.132}$$

The values of $C_1(Z)$ can be found from the normalization condition

$$\int_0^\infty dr\left(1 + \Phi^2(r)\right)G^2(r) = 1, \tag{7.133}$$

for the functions $G = G_0 + G_1$ and $\Phi = \Phi_0 + \Phi_1$. Note that here we need the functions $\Phi_1(r)$ and $G_1(r)$ for all values of r; (7.125) and (7.122).

Using the well-known explicit expressions for the Coulomb functions G_0 and Φ_0, we obtain

$$C_1 = M(Z) = -(1+\gamma)(1+2\gamma)(1-\gamma/2)\frac{\nu^2}{4}\sum_i a_i b_i^2; \quad \nu = \frac{\lambda}{\eta}, \tag{7.134}$$

and

$$F_{ph} = (1+M(Z))F_{ph}^C; \quad d\sigma = (1+2M(Z))d\sigma_{ph}^C; \quad \sigma = (1+2M(Z))\sigma_{ph}^C. \tag{7.135}$$

Recall that $\gamma = (1-\alpha^2 Z^2)^{1/2}$. One can demonstrate that the second-order perturbative correction is of order λ^4/η^4. Thus the screening correction does not modify the shape of the energy dependence of the ionization cross section. Since $M(Z) < 0$, the screening diminishes the value of the cross section. Relative corrections to the parameter $M(Z)$ are of order λ^2/η^2. They are smaller than 0.1 already for $Z \geq 7$.

Employing the numerical values of the coefficients a_i and b_i presented above, we obtain

$$M(Z) = -1.414(1+\gamma)(1+2\gamma)(1-\gamma/2)Z^{-4/3}. \tag{7.136}$$

In the limit $\alpha^2 Z^2 \ll 1$, we can put $\gamma = 1$, which gives

$$M(Z) \;=\; -4.24 Z^{-4/3}. \tag{7.137}$$

The screening corrections for the electrons from the higher shells can be calculated in a similar way. Note that in this case, the wave functions have nodes, and evaluation of (7.120) is not as straightforward as it was in the case of the K shell.

7.3.3 *In the Vicinity of the Threshold*

Now we consider the case of very slow photoelectrons, with momenta p much smaller than the binding momenta μ_b. This means that $\omega \approx \varepsilon_b$. For the $1s$ electrons, this means that $\omega - \varepsilon_b \lesssim \alpha^2 Z^2 I_Z$, with I_Z the Coulomb value of the binding energy. In Sect. 6.3.2, we carried out calculations for the unscreened Coulomb field. Now we include screening, employing the technique developed in [16].

The Coulomb cross section is dominated by the first term in parentheses on the RHS of (6.82), which provides about 80% of the total cross section. This is the nonrelativistic limit of the cross section, and we include screening only for this term.

First we must find the screening corrections for the wave functions of the bound $1s$ and continuum electrons. We need these functions at the distances of order the size of the K shell, $r \sim 1/\eta$. Employing (7.122), we obtain in the first order of perturbative theory

$$\psi_{1s} \;=\; \psi^C_{1s}\Big[1 + \frac{\hat{S}}{4}\nu^2\Big[-3 + \eta^2 r^2 + \frac{\nu}{3}\Big(11 - 2\eta^2 r^2 - \frac{2}{3}\eta^3 r^3\Big)\Big]\Big]. \tag{7.138}$$

The second perturbative correction is of order $(\hat{S}\nu^2)^2$.

Carrying out a similar calculation for the partial wave with $\ell = 1$ of the continuum wave function, we obtain an expression for the screened Coulomb cross section, which differs from the unscreened one (6.82) by a factor

$$\phi(\nu) \;=\; 1 + \hat{S}\nu^2\Big(-\frac{103}{30} + \frac{541}{126}\nu^2\Big). \tag{7.139}$$

The screened cross section is expressed in terms of the parameter $\tau = p_c^2/\eta^2$, where $p_c = \sqrt{2m(\omega - I_Z)}$ is the momentum of the photoelectron in the unscreened case:

$$\sigma_{ph}(p) \;=\; \sigma_0\Big(f(\tau)\phi(\nu) - 0.393a - 0.144a^2 + 1.023\tau a + O(a^3)\Big). \tag{7.140}$$

Here $a = \alpha^2 Z^2$, while $f(\tau)$ is determined by (6.83), σ_0 is the value of the Coulomb cross section at the threshold; see (6.80).

For the uranium atom, the physical threshold is $\omega = 116\,\text{keV}$. Here (7.140) provides $\sigma = 1.41 \times 10^3$ barn (for two electrons in the K shell). This is very close to $\sigma = 1.37 \times 10^3$ barn obtained earlier [17] by numerical calculations.

7.4 Photoionization Beyond the Independent Particle Approximation

7.4.1 Correlations in the L Shell

About fifty years ago, all the existing data on photoionization could be described in the framework of the independent particle approximation (IPA), where the wave function of the atomic electronic shell was presented as a composition of single-particle functions. It was found in the 1960s that IPA does not always reproduce the experimental data at photon energies not far from the threshold. However, for a long time there was a general belief that at photon energies far above the thresholds, photoionization could be described in the framework of IPA.

Experiments on photoionization of the L shell of the neon atom [18] ($Z = 10$) forced researchers to doubt the latter statement. The $2s$ to $2p$ cross section ratio $R_{21}(\omega) = \sigma_{20}(\omega)/\sigma_{21}(\omega)$ defined by (7.48) was measured at photon energies of about 1 keV. The binding energies of $2s$ and $2p$ electrons are about 40 and 20 eV; a small energy shift of 0.1 eV between $2p_{1/2}$ and $2p_{3/2}$ states can be neglected. Following analysis carried out in Sect. 7.1, the ratio R_{21} was expected to be proportional to ω, i.e., $R^I_{21}(\omega) = a^I\omega$. (In this subsection, the upper index I indicates that the values are related to the IPA case.) Experiments demonstrated that the ratio is indeed a linear function of ω. However, the line was shifted, $R_{21}(\omega) = a\omega + b$, and the value of the slope a differed from that obtained by the Hartree–Fock (HF) calculations.

To understand what happens, we employ the results obtained in (6.1). In the IPA picture, the photon interacts with the $2p$ electron directly. The latter transfers large momentum p to the nucleus, approaching it at small distances $r \sim 1/p$. This leads to a small factor $(\mu_L/p)^4$ in the amplitude, with μ_L the average momentum of the electron in the L shell. Beyond the IPA, another channel of the process is possible. Instead of interacting with the $2p$ state, the photon interacts with the $2s$ electron, creating a hole. The photoelectron pushes the $2p$ electron into the $2s$ hole by electron impact. In the first step, the $2s$ electron transfers large momentum to the nucleus. This provides a small factor of order $(\mu_L/p)^3$. Thus it is not as small as in the case of a $2p$ electron. The second step takes place at distances of order the size of the L shell (rather than at the small distances at which photoionization takes place), and thus we avoid suppression by powers of momentum. However, interaction of the outgoing electron with the bound electron provides the Sommerfeld factor $\xi_{ee} = \alpha m/p$; see (3.42). Hence, the IPA breaking correction to the amplitude is of order $\alpha m/\mu_L$ and does not depend on the photon energy. In the hydrogenlike approximation, this is $2/Z$, making 20% for the case of neon. Thus it should be included.

Now we calculate the IPA breaking effects for photoionization of $2p$ and $2s$ electrons, tracing the lowest-order terms of expansion of the amplitude in powers of ξ_{ee} [19]. We assume that the atomic electrons move in a certain effective field, and we carry out calculations in nonrelativistic approximation. The calculations are very much like those carried out in Sect. 3.2. Note that our analysis does not require the asymptotic behavior of the cross sections σ_{2p} and σ_{2s}.

We begin with the ionization of the $2p$ state. We write the two-electron states consisting of one $2p$ and one $2s$ electron as $|i,\, j\rangle$, where i denotes the set of quantum numbers $2,\, 1,\, m$ ($m = 0, \pm 1$), while j stands for the set $2,\, 0,\, 0$. The IPA amplitude of photoionization of the $2p$ state is

$$F_i^I \;=\; f_i \;=\; \langle \mathbf{p},\, j|\gamma|i,\, j\rangle\,, \tag{7.141}$$

with $\mathbf{p}$ denoting the state of the photoelectron; γ is the vertex of the electron–photon interaction. Here the $2s$ electron is just a spectator (we neglect a small change of the effective field caused by creation of the hole in the $2p$ state). Now we assume that the final-state interactions (FSI) of the photoelectron with the bound electrons are neglected in the amplitude f_i, and we include the admixture of other two-electron states by the lowest-order FSI between the electrons V_{ee}. The amplitude becomes

$$F_i = f_i + \sum_k \frac{\langle \mathbf{p},\, j|V_{ee}|k,\, j\rangle\langle k,\, j|\gamma|i,\, j\rangle}{\omega + \varepsilon_i - \varepsilon_k} - \sum_k \frac{\langle \mathbf{p},\, j|V_{ee}|k,\, i\rangle\langle k,\, i|\gamma|j,\, i\rangle}{\omega + \varepsilon_j - \varepsilon_k}, \tag{7.142}$$

with k standing for vacancies in both continuum and discrete spectra,

$$\langle \mathbf{p},\, j|V_{ee}|k,\, i\rangle = \int d^3r\, d^3r'\, \psi^*_{\mathbf{p}}(\mathbf{r})\psi_k(\mathbf{r})\frac{\alpha}{|\mathbf{r}-\mathbf{r}'|}\psi^*_j(\mathbf{r}')\psi_i(\mathbf{r}'). \tag{7.143}$$

The second term on the RHS of (7.142) describes the scattering of the photoelectron ejected from the $2p$ state on the bound $2s$ electron. This is just a correction to the IPA amplitude f_i. The third term represents the IPA breaking mechanism described above. It is illustrated by the Feynman diagram shown in Fig. 7.1.

The interaction V_{ee} does not depend on the spin variables. Thus the spin projections of the states $2s$ and $2p$ in the IPA breaking term should be the same. Hence the space part of the function describing the two-electron state should be antisymmetric.

The main contribution to the sum over k in the IPA breaking term comes from the continuum states with momentum $\mathbf{p}'$ close to $\mathbf{p}$. To prove the statement, we introduce $\mathbf{p}' = \mathbf{p} + \mathbf{q}$, and write

$$\langle \mathbf{p},\, j|V_{ee}|\mathbf{p}',\, i\rangle \;=\; \frac{4\pi\alpha}{q^2+\lambda^2}\langle j|e^{i\mathbf{q}\cdot\mathbf{r}}|i\rangle\,. \tag{7.144}$$

Recall that $\lambda \to 0$ is introduced to avoid divergence in integrations over q at the lower limit. It vanishes in the final expressions for the cross sections. The last factor decreases rapidly for $q \gg \mu_L$. Thus we can put

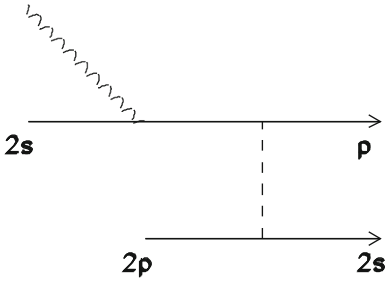

Fig. 7.1 The main IPA breaking contribution to the amplitude of the high-energy photoionization of the $2p$ state. *Solid lines* stand for electrons, p labels the photoelectron carrying momentum $\mathbf{p}$. The *helix line* is for the photon. The *dashed line* denotes the electron interaction (exchange by virtual photon) in the final state

$$\langle k, i|\gamma|j, i\rangle \;=\; \langle \mathbf{p}, i|\gamma|j, i\rangle = f_j \tag{7.145}$$

in the IPA breaking term. This enables us to write

$$F_i \;=\; f_i + F_i^{(1)}; \quad F_i^{(1)} \;=\; -\sum_j f_j B_{ji}\,, \tag{7.146}$$

where $F_i^{(1)}$ represents the IPA breaking effects caused by the FSI, while

$$B_{ji} = \int \frac{d^3q}{(2\pi)^3}\,\frac{1}{\omega + \varepsilon_j - \varepsilon_{\mathbf{p}+\mathbf{q}}}\cdot\frac{4\pi\alpha}{q^2+\lambda^2}\langle j|e^{i\mathbf{q}\cdot\mathbf{r}}|i\rangle \equiv \langle j|B(\mathbf{r})|i\rangle. \tag{7.147}$$

We omitted the second term on the RHS of (7.142), since it provides just a correction to f_i due to scattering of the photoelectron on the $2s$ electron. One can see that the operator $B(\mathbf{r})$ is just the one defined by (3.66) with $p'^2 = 2m(\omega + \varepsilon_j)$.

The initial-state interaction beyond the effective (self-consistent) field also provides the IPA breaking effect, mixing the $2s, 2p$ two-electron state with a $2s, k$ state, where k labels an unoccupied p state of the discrete or continuum spectrum. The corresponding amplitude written in the lowest order of perturbation theory is

$$F_{2p}^{in} = \mathscr{S}_k f_k G_{k,2p}^{(2s)}; \quad G_{k,2p}^{(2s)} = \frac{\langle k, 2s|V_{ee}|2p, 2s\rangle}{\varepsilon_{2p} - \varepsilon_k}\,. \tag{7.148}$$

If the state k belongs to the discrete spectrum, then f_k is the IPA amplitude of photoionization. If it belongs to the continuum, then f_k is the amplitude of the absorption of the photon by the electron moving in the field of the atom. Unlike the FSI case, the IPA breaking amplitude F_{2p}^{in} can be calculated only numerically. We expect the contribution to be small, since the amplitudes of ionization from excited states are small. For the heavy atoms with large Z, it is quenched by a factor $m\alpha/\mu_L \sim 1/Z$. In any case, a large value of IPA breaking effects in the initial state

would mean that single-particle representation is not a good approximation for this state. We shall neglect these contributions in our equations. We shall estimate the contribution of the IPA breaking terms in the initial state for the special case of ionization of the L shell of neon several paragraphs below.

Employing the results of Sect. 3.2, we obtain

$$B_{ji} \;=\; i\xi_{ee} S_{ji}\,, \tag{7.149}$$

with $S_{ji} = \langle j|\ln(r - r_z)\lambda|i\rangle = \langle j|\ln(r\lambda(1-t))|i\rangle$; see (3.71). Here the direction of the photoelectron momentum is chosen as the axis of quantization of the angular momentum. Writing $\ln(r\lambda(1-t)) = \ln(r\lambda) + \ln(1-t)$, we note that the term $\ln(r\lambda)$ vanishes due to the orthogonality of the angular parts of the wave functions. Thus

$$S_{ji} \;=\; \langle j|\ln(1-t)|i\rangle\,, \tag{7.150}$$

and

$$F_i \;=\; f_i - i\xi_{ee} f_j S_{ji}\,. \tag{7.151}$$

Direct calculation provides

$$S_{200,21m} \;=\; b_1 d_{2s,2p}\delta_{m0}\,, \tag{7.152}$$

with

$$b_1 \;=\; \frac{\sqrt{3}}{2}\int_{-1}^{1} dt\, t\ln(1-t) \;=\; -\frac{\sqrt{3}}{2}\,, \tag{7.153}$$

while

$$d_{2s,2p} \;=\; \int_0^\infty dr r^2 \psi^r_{2s}(r)\psi^r_{2p}(r) \tag{7.154}$$

is the overlap integral of the radial functions with angular momenta 1 and 0. Note that the matrix element $S_{200,21m}$ obtains a nonzero value only for the state with $m = 0$.

We use a conventional definition in which the bound-state wave functions with $m = 0$ are real. Since the amplitude of photoionization of a p state with $m = 0$ contains the factor i, both terms on the RHS of (7.151) are purely imaginary. The squared amplitude for ionization of the state $i = 2, 1, 0$ can be written as

$$|F_i|^2 \;=\; |f_i|^2 - 2\mathrm{Re}(i\xi_{ee} f_j S_{ji} f_i^*) + \xi_{ee}^2 |f_j S_{ji}|^2. \tag{7.155}$$

The asymptotics of the photoionization amplitude from a p state with $m = 0$ can be represented as $f_i = -i\hat{f}_i$ with $\mathrm{Im}\,\hat{f}_i = 0$. Thus (7.155) can be written in terms of real variables as

$$|F_i|^2 \;=\; |f_i|^2 + 2\xi_{ee} f_j S_{ji} \hat{f}_i + \xi_{ee}^2 |f_j S_{ji}|^2. \tag{7.156}$$

Now we can carry out integration over the angular variables and consider the IPA breaking effects in terms of the cross sections. This is possible, since the angular dependence of the amplitude f_{2s} is determined by the product of $\mathbf{e}\cdot\mathbf{n}$ and $\mathbf{n}=\mathbf{p}/p$. For the amplitude f_{2p} of photoionization from the state with azimuthal quantum number m there are two terms, proportional to e_m and to $(\mathbf{e}\cdot\mathbf{n})n_m$. For the axis of quantization of the angular momentum along the vector $\mathbf{n}$ and $m=0$, all three structures coincide, being just e_z. The influence of $2s$ electrons on the photoionization of $2p$ electrons can be written as [19]

$$\frac{\sigma_{2p}(\omega)}{\sigma^I_{2p}(\omega)} = 1 + 2\xi_{ee} b_1 d_{2s,2p}\sqrt{\frac{R^I_{21}(\omega)}{3}} + \xi^2_{ee} b_1^2 d^2_{2s,2p} R^I_{21}(\omega). \tag{7.157}$$

Only two of six $2p$ electrons (those with $m=0$) contribute to the IPA breaking amplitude. Note that (7.157) is true also for the multicharged ions that have $n<6$ electrons in the $2p$ state, with R^I_{21} the IPA cross section ratio for this ion.

An analysis analogous to that carried out in Chap. 3 shows that the amplitude $F^{(1)}_{2p}$ has also a small real part with $\mathrm{Re}F^{(1)}_{2p}\sim(\mu_L/p)\cdot\mathrm{Im}F^{(1)}_{2p}\ll\mathrm{Im}F^{(1)}_{2p}$. Also, the second-order perturbative amplitude $F^{(2)}_{2p}$ is mostly real with $\mathrm{Re}\,F^{(2)}_{2p}\sim\xi_{ee}\mathrm{Im}\,F^{(1)}_{2p}\ll\mathrm{Im}\,F^{(1)}_{2p}$. These terms do not interfere with those on the RHS of (7.146), providing small corrections of order μ_b^2/p^2 and ξ^2 to the IPA breaking terms on the RHS of (7.157).

Recall that $\xi_{ee}=(I_1/\omega)^{1/2}$ with $I_1=13.6\,\mathrm{eV}$. Therefore, if the IPA cross section ratio exhibits the asymptotic behavior

$$R^I_{21}(\omega) \;=\; a^I\omega\,, \tag{7.158}$$

where a^I does not depend on ω, the RHS of (7.157) does not depend on the photon energy ω. Introducing the dimensionless parameter $\kappa=(a^I I_1)^{1/2}$, we obtain

$$\frac{\sigma_{2p}(\omega)}{\sigma^I_{2p}(\omega)} \;=\; 1+\frac{2b_1 d_{2s,2p}}{\sqrt{3}}\kappa + b_1^2 d^2_{2s,2p}\kappa^2, \tag{7.159}$$

and the RHS does not depend on ω.

Now we study the influence of $2p$ electrons on the photoionization of $2s$ electrons. We can write, similar to (7.155),

$$|F_j|^2 \;=\; |f_j|^2 - 2\mathrm{Re}(i\xi_{ee} f_i S_{ij} f_j^*) + \xi^2_{ee}|f_i S_{ij}|^2, \tag{7.160}$$

with $S_{ij}=S_{ji}$. Comparing (7.155) and (7.160), one can see that the second terms on the RHS contain the amplitudes f^*_{2p} and f_{2p} respectively. Thus they have different signs, and

$$\frac{\sigma_{2s}(\omega)}{\sigma_{2s}^{I}(\omega)} = 1 - 2\xi_{ee}\frac{b_1 d_{2s,2p}}{\sqrt{3R_{21}^{I}(\omega)}} + \xi_{ee}^{2}\frac{b_1^2 d_{2s,2p}^2}{3R_{21}^{I}(\omega)}\,. \tag{7.161}$$

If (7.158) is satisfied, we obtain

$$\frac{\sigma_{2s}(\omega)}{\sigma_{2s}^{I}(\omega)} = 1 - 2\sqrt{\frac{I_1}{3a^I}}\frac{b_1 d_{2s,2p}}{\omega} + \frac{I_1}{3a^I}\frac{b_1^2 d_{2s,2p}^2}{\omega^2}\,. \tag{7.162}$$

Thus the IPA breaking effects vanish in the asymptotics.

How do the IPA breaking effects change the asymptotic law given by (7.158)? Employing (7.159) and (7.162), we obtain

$$R_{21}(\omega) = a\omega + b + c/\omega\,. \tag{7.163}$$

Here

$$a = \frac{a^I}{K};\quad b = -2\frac{\kappa}{\sqrt{3}}\frac{b_1 d_{2s,2p}}{K};\quad c = I_1\frac{b_1^2 d_{2s,2p}^2}{3K}, \tag{7.164}$$

where,

$$K = 1 + 2b_1 d_{2s,2p}\frac{\kappa}{\sqrt{3}} + b_1^2 d_{2s,2p}^2\kappa^2, \tag{7.165}$$

is the RHS of (7.159). The last term on the RHS of (7.163) can be neglected, since $\omega \ll I_1$. Thus the dependence $R_{21}(\omega)$ remains linear. The value of b_1 is given by (7.153). As to the overlap matrix element $d_{2s,2p}$ defined by (7.154), its calculation with the Coulomb functions give $d_{2s,2p} = -\sqrt{3}/2 \approx -0.87$ for every value of the nuclear charge Z, and we can expect that its Hartree–Fock value is always negative as well. Since b_1 is also negative, we find that $K > 1$. Hence, the correlations diminish the slope of the line (7.158) and shift it downward.

We return to ionization of neon, which we mentioned at the beginning of this section. The HF calculations provide the behavior (7.158) for the photon energies between 0.7 and 1.0 keV with $a^I = 2.19\ \text{keV}^{-1}$. Hence we can put $\kappa = 0.17$. The HF computation provides $d_{2s,2p} = -0.95$. We obtain $K - 1 = 0.19$ from correlations in the final state determined by (7.157) and (7.162). An additional contribution -0.02 to $K - 1$ comes from correlations in the initial state; see (7.157). Thus we arrive at the value $K = 1.17$. Hence, in (7.163),

$$a = 1.87\ \text{keV}^{-1};\quad b = -0.14\,, \tag{7.166}$$

which is much closer to the observed values; see Fig. 7.2.

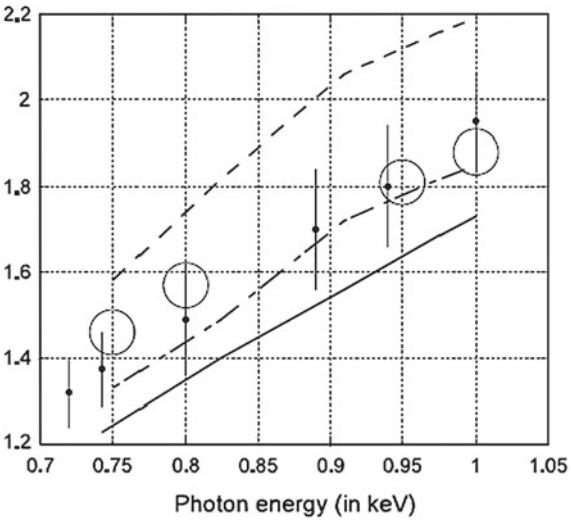

Fig. 7.2 Ratio of the $2s$ to $2p$ photoionization cross sections for neon. The *dots* and *large circles* are the experimental data obtained in [18] and [20] respectively. The *solid line* shows the results based on the perturbative calculations described in the text. The *dashed* and *chain curves* are results obtained in [19] in the Hartree–Fock and RPAE approximations respectively [19]

7.4.2 Random Phase Approximation with Exchange

In the calculations carried in the previous subsubsection, we actually calculated the sum

$$\sum_k \frac{|k,\, j\rangle\langle k,\, j|}{\omega + \varepsilon_j - \varepsilon_k}$$

in the plane-wave basis for the states k. A more accurate approach requires calculations in which all electrons are moving in the field of the atom.

The IPA amplitude of the process in which an atomic electron is moved from the single-particle bound state $|i\rangle$ to a vacant single-particle state $\langle f|$, which can belong to the discrete or continuum spectrum, is $F_0 = \langle f|\gamma|i\rangle$. We omit the indices of the other bound electrons, since they do not change their states, contributing only to the effective field, acting in the states $|i\rangle$ and $\langle f|$. Now we assume that one of the bound electrons, i.e., that in state j, can also undergo transitions. The photon can interact directly with state j, and the interaction between the electrons can push the electron from state $|i\rangle$ to the hole in state $|j\rangle$. This leads to the amplitude

$$F_{1a} = \sum_k \frac{\langle f,\, j|V_{ee}|i,\, k\rangle\langle k|\gamma|j\rangle}{\omega + \varepsilon_j - \varepsilon_k + i\delta}\,, \tag{7.167}$$

with the two-particle matrix element of the ee interaction given by (7.143). Here the photon interacts directly with the electron in state j, transferring it to an unoccupied state k. The electron interaction moves it to the hole in state j and pushes the electron from state i to the continuum. The amplitude

$$F_{1b} = -\sum_k \frac{\langle j, f|V_{ee}|i, k\rangle\langle k|\gamma|j\rangle}{\omega + \varepsilon_j - \varepsilon_k + i\delta}, \tag{7.168}$$

with permutation $\langle f, j| \to \langle j, f|$, describes the process in which the photoelectron knocked out from state j moves to the continuum, also pushing the bound electron from state i to the hole in state j. One can see that the process considered in Sect. 7.4.1 is described by the amplitude F_{1b} with $i = 2, 1, 0$, $j = 2, 0, 0$, and $\langle f| = \langle \mathbf{p}|$.

Another possibility is that the interaction V_{ee} transfers the electrons from the bound states $|i\rangle$ and $|j\rangle$ to unoccupied states $\langle f|$ and $\langle k|$. The latter can belong to the discrete or continuum spectrum. The photon interacts with the electron in state $\langle k|$, pushing it back to the hole in state j. The amplitude is

$$F_{2a} = \sum_k \frac{\langle j|\gamma|k\rangle\langle k, f|V_{ee}|j, i\rangle}{-\omega + \varepsilon_j - \varepsilon_k + i\delta}. \tag{7.169}$$

The replacement $|i, j\rangle \to -|j, i\rangle$ provides the amplitude F_{2b}. These contributions to the amplitude are shown in Fig. 7.3.

We denote the amplitude by

$$F = F_0 + F_{1a} + F_{1b} + F_{2a} + F_{2b}, \tag{7.170}$$

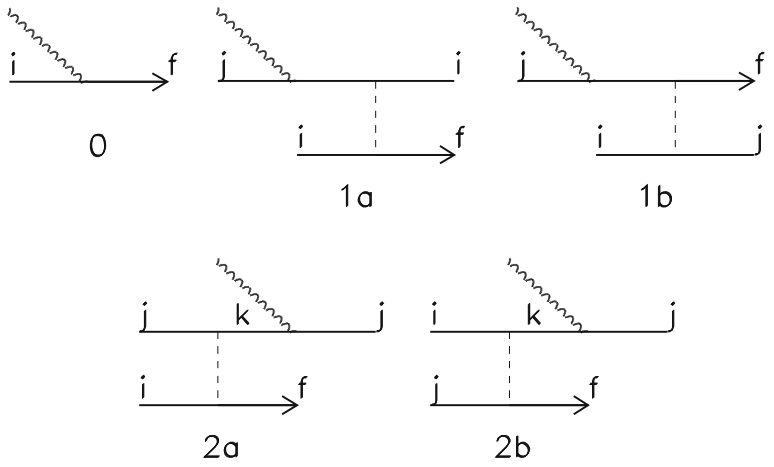

Fig. 7.3 The Feynman diagram for photoionization of the bound state i in the random phase approximation with exchange (RPAE). The photoelectron is labeled by f. The diagram 0 is for direct interaction of the photon with the electron in state i. In diagram $1a$, the photon interacts with a bound electron in state j, moving it to an unoccupied intermediate state. In next step, the electron moves back to state j, transferring the energy to the bound electron in state i. The latter is moved to the continuum. In the exchange diagram $1b$, the photon also creates a hole in state j. The bound electron moves from state i to the vacancy in state j, transferring the energy to the photoelectron. In the diagrams $2a$ and $2b$, the electron interaction mixes the two-electron state of the bound electrons i and j to the vacant states k and f, and the photon moves the electron from state k to the vacancy in state j. Diagram $2b$ differs from $2a$ by a permutation of the initial single-particle states i and j

summed over all bound states j as $F = \langle f|M|i\rangle$, where M can be treated as the operator of the γe interaction beyond the IPA. Thus we obtain

$$\langle f|M|i\rangle = \langle f|\gamma|i\rangle + \sum_{k,j} \frac{\langle \tilde{f}, \tilde{j}|V_{ee}|i,k\rangle\langle k|\gamma|j\rangle}{\omega + \varepsilon_j - \varepsilon_k + i\delta} + \sum_{k,j} \frac{\langle j|\gamma|k\rangle\langle k, f|V_{ee}|\tilde{j}, \tilde{i}\rangle}{-\omega + \varepsilon_j - \varepsilon_k + i\delta}, \tag{7.171}$$

with $\langle \tilde{a}, \tilde{b}| = \langle a, b| - \langle b, a|$. In (7.171), the sum is carried out over all occupied states j and over all vacant states k.

This equation presents the amplitude of the transition between a bound state and a vacant state with the IPA effects included in the lowest order of the perturbative theory. It can be treated as the first iteration of the general equation that ties the amplitudes of the bound-to-vacant transitions of the electron,

$$\langle f|M|i\rangle = \langle f|\gamma|i\rangle + \sum_{k,j} \frac{\langle \tilde{f}, \tilde{j}|V_{ee}|i,k\rangle\langle k|M|j\rangle}{\omega + \varepsilon_j - \varepsilon_k + i\delta} + \sum_{k,j} \frac{\langle j|M|k\rangle\langle k, f|V_{ee}|\tilde{j}, \tilde{i}\rangle}{-\omega + \varepsilon_j - \varepsilon_k + i\delta}. \tag{7.172}$$

This equation with the Hartree–Fock functions as the single-particle basis forms the "random phase approximation with exchange" (RPAE). The approach in which the exchange terms are neglected, i.e., $\langle \tilde{f}, \tilde{j}| = \langle f, j|$; $\langle \tilde{j}, \tilde{i}| = \langle j, i|$, is known as the "random phase approximation" (RPA). Derivation of (7.172) is given in a number of books; see, e.g., [21, 22]. Therefore, we do not repeat it here.

The calculations pioneered by Amusia and his collaborators [22] demonstrated that the RPAE succeeds in describing the correlation effects in the low-energy photoionization. Note a strong point of the approach: the length and velocity forms of the electron–photon interactions are equivalent. After photoionization has taken place, the effective field felt by the electron–spectators changes. The RPAE does not account for this effect. It is included in the generalized version of the RPAE known as the GRPAE [23].

One can see that it works well for investigations of the correlations at high energies also. The results of the RPAE calculations for ionization of the L shell of neon are presented in Fig. 7.2. The amplitude F_{1b} dominates, since at amplitude F_{1a}, the electron interaction transfers large energy. Therefore, inclusion of the exchange terms is of crucial importance. Below, we shall meet also the relativistic version of the random phase approximation (RRPA) [24], based on the Dirac wave equation. The relativistic approach becomes increasingly important for the internal shells of heavy atoms.

Note, however, that the RPAE does not pick the terms in which the photon connects two vacant states. Thus, for example, the IPA breaking effects in the initial state described by (7.147) are not included in RPAE calculations and should be analyzed separately.

7.4.3 Correlations in the Higher Subshells

Now we consider the higher subshells, which contain the states with the angular momenta $\ell > 1$. We focus on their correlations with the s electrons of the same subshell.

The lowest-order IPA breaking amplitude is described by (7.151) with $i = n, \ell, m$, $j = n, 0, 0$, where

$$S_{ji} = b_\ell d_{n0,n\ell}\delta_{m0}\,, \tag{7.173}$$

with

$$d_{n0,n\ell} = \int_0^\infty dr r^2 \psi^r_{ns}(r)\psi^r_{n\ell}(r)\,, \tag{7.174}$$

while

$$b_\ell = \frac{\sqrt{2\ell+1}}{2}X_\ell; \quad X_\ell = \int_{-1}^{1} dt\, P_\ell(t)\ln(1-t)\,, \tag{7.175}$$

where $P_\ell(t)$ is the Legendre polynomial. Employing the Rodrigues formula [25]

$$P_\ell(t) = \frac{1}{2^\ell \cdot \ell!}\frac{d^\ell}{dt^\ell}(t^2-1)^\ell, \tag{7.176}$$

and integrating ℓ times by parts, one can find that $X_\ell = -2/\ell(\ell+1)$ for $\ell > 0$, and

$$b_\ell = -\frac{\sqrt{2\ell+1}}{\ell(\ell+1)}\,. \tag{7.177}$$

The squared amplitude is described by (7.155) for every value of ℓ. However, the second term on the RHS, which describes the interference between the IPA and IPA breaking amplitudes, has a nonzero value only for odd values of ℓ. This is because the IPA amplitude contains the factor i^ℓ, while the leading IPA breaking amplitude is mostly imaginary. There is no interference in the case of even values of ℓ, and this term vanishes.

Thus for odd values of ℓ, the influence of the ns electron on the cross section of ionization of $n\ell$ states is

$$\frac{\sigma_{n\ell}(\omega)}{\sigma^I_{n\ell}(\omega)} = 1 + 2\xi_{ee}b_\ell d_{n0,n\ell}\sqrt{\frac{R^I_{n\ell}(\omega)}{2\ell+1}} + \xi^2_{ee}b^2_\ell d^2_{n0,n\ell}R^I_{n\ell}(\omega), \tag{7.178}$$

while the influence of $n\ell$ electrons on ionization of ns states can be written as

$$\frac{\sigma_{ns}(\omega)}{\sigma^I_{ns}(\omega)} = 1 - 2\xi_{ee}\frac{b_\ell d_{n0,n\ell}}{\sqrt{(2\ell+1)R^I_{n\ell}(\omega)}} + \xi^2_{ee}\frac{b^2_\ell d^2_{n0,n\ell}}{\sqrt{(2\ell+1)R^I_{n\ell}(\omega)}}. \tag{7.179}$$

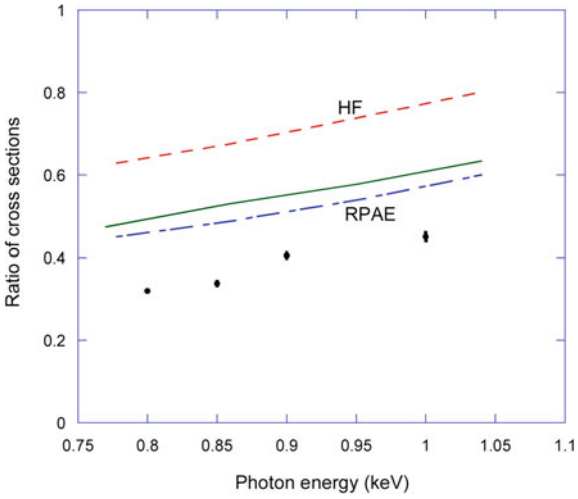

Fig. 7.4 Ratio of the $3s$ to $3p$ photoionization cross section for argon. The *dots* show the experimental data obtained in [26]. The *solid line* shows the results based on perturbative calculations described in the text. The *dashed* and *chain curves* are results obtained in [19] in the Hartree–Fock and RPAE approximations respectively [19]

An instructive example is provided by photoionization of the $3p$ state in argon by photons carrying energies of about 1 keV [26]; see Fig. 7.4. One can see that there is a large discrepancy between the experimental data and the results of the IPA HF calculations. The HF value of the $3s$ to $3p$ photoionization ratio at $\omega = 1$ keV is $R_{31} = 0.78$. Employing (7.178) and (7.179), we find that since $R_{31} < 1$, the influence of the $3p$ electron on the ionization of the $3s$ state is larger than that of the $3s$ electron on the ionization of the $3p$ state. The IPA breaking effects diminish the slope of the IPA curve and shift it downward. The IPA breaking effects in ionization of the $3s$ and $3p$ states add -0.090 and -0.077 respectively to R_{31}. This provides $R_{31} = 0.61$. Note that the RPAE value is $R_{31} = 0.58$.

For even values of ℓ,

$$\frac{\sigma_{n\ell}(\omega)}{\sigma^I_{n\ell}(\omega)} = 1 + \xi^2_{ee} b^2_\ell d^2_{n0,n\ell} R^I_{n0}(\omega), \tag{7.180}$$

with $d_{n0,n\ell}$ and b_ℓ determined by (7.174) and (7.177). Although at large energies for $\ell \geq 2$, the last terms on the RHS of (7.178) and (7.180) dominate, one cannot discriminate other contributions at finite energies, since the factors b^2_ℓ and $d^2_{\ell 0}$ can be small. For example, $b^2_2 \approx 0.14$. Note that in such a way, one can find correlations between the electrons with any orbital momenta ℓ and ℓ'.

In Fig. 7.5, we demonstrate an example illustrating the correlations in the M shell in the ionization of krypton ($Z = 36$) by photons with energies in the region of 1 keV. The RRPA calculations of the cross section ratios demonstrate that the correlations provide a noticeable contribution and improve agreement with the experimental data [27].

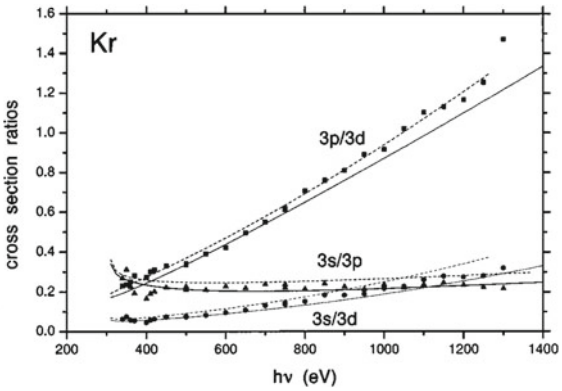

Fig. 7.5 Ratio among $3s$, $3p$, and $3d$ cross sections of Kr. The *points* are the experimental data obtained in [27]. The *solid* and *dashed curves* show the theoretical results for the fully coupled RRPA) and RRPA with couplings between different subshells omitted. The horizontal axis is for the photon energies in eV. Reproduced from [27] with permission of AIP

7.4.4 Intershell Correlations

If the photon energy is much larger than the binding energies of the states $i = n, \ell, m$ and $j = n', \ell', m'$, the amplitude that includes correlations between these sates is given by (7.151) with

$$S_{ji} = s_{n'\ell',n\ell}\delta_{m'm}; \quad s_{n'\ell',n\ell} = b_{\ell'\ell}d_{n'\ell',n\ell}, \tag{7.181}$$

where

$$d_{n'\ell',n\ell} = \int_0^\infty dr r^2 \psi^r_{n'\ell'}(r)\psi^r_{n\ell}(r)\,, \tag{7.182}$$

while

$$b_{\ell'\ell} = \frac{\sqrt{(2\ell'+1)(2\ell+1)}}{2}\int_{-1}^{1} dt\, P_{\ell'}(t)\,P_\ell(t)\ln(1-t). \tag{7.183}$$

The squared amplitude of photoionization of the state $|i\rangle$, which includes correlations with states j, is

$$|F_i|^2 = |f_i|^2 + 2\mathrm{Re}\sum_j (i\xi_{ee} f_j S_{ji} f_i^*) + \xi_{ee}^2 |\sum_j f_j S_{ji}|^2. \tag{7.184}$$

To express (7.184) in terms of the cross sections, we must take into account that some of the contributions to the RHS vanish, since the amplitudes of photoionization of states with orbital momenta ℓ contain the factors i^ℓ. Also, the azimuthal quantum numbers of the electrons participating in correlations should be the same, i.e., $m = m' = m''$. Denote the state n', ℓ', m' by j', and define $\theta_{\ell\ell'} = (1-(-1)^{\ell-\ell'})/2$. Thus $\theta_{\ell\ell'} = 1$ for odd values of $\ell - \ell'$, turning to zero for even values of this difference. The

cross section of photoionization of a state i with orbital momentum ℓ that includes correlation with the states having momenta ℓ', $\ell'' < \ell$ can be written as

$$\sigma_i = \sigma_i^I + 2\xi_{ee} \sum_{j'} s_{j'i} \left(\sigma_i^I \sigma_{j'}^I N_{j'i}\right)^{1/2} \theta_{\ell\ell'} + \xi_{ee}^2 \sum_{j',j''} s_{j'i} s_{j''i} (1 - \theta_{\ell'\ell''}) \left(\sigma_{j'}^I \sigma_{j''}^I\right)^{1/2}. \tag{7.185}$$

Here $s_{j'i} = b_{\ell'\ell} d_{n'\ell',n\ell}$, and the factor $N_{j'i} = (2\ell' + 1)/(2\ell + 1)$ reflects the fact that only the terms with $m' = m$ contribute to the second term on the RHS.

Now we consider the case of very high photon energies, which exceed strongly the binding energy in the K shell. The RPAE calculations of $2p$ photoionization of nitrogen and neon for energies up to 10 keV [28] demonstrated a strong cancellation between correlations with the $2s$ and $1s$ states in the angular distributions of the photoelectrons. Now we demonstrate that in our perturbative approach, such cancellation takes place at the amplitude level. We show also that this is a general tendency [29].

Note first that when we include the inner shells, the whole picture becomes more complicated. For example, the photon can interact directly with the $2s$ electron, while the $1s$ electron undergoes shakeup into the hole in the $2s$ state of the ion. The latter step is described by the overlap matrix element $\langle \psi_{2s}^{\prime r} | \psi_{1s}^r \rangle$, with $\psi_{2s}^{\prime r}$ the radial wave function of the $2s$ electron in the field of the ion. In the final step, the photoelectron pushes the $2p$ electron to the $1s$ hole of the final-state ion. We can neglect the contribution of such channels, assuming that $|\langle \psi_{n's}^{\prime r} | \psi_{ns}^r \rangle| \ll 1$. Under this assumption, the inclusive cross section with the sum over all possible states of the final ion coincides with the exclusive cross section in which the spectator electrons do not undergo transitions.

We begin with ionization of the $2p$ state. The term with $i = 2, 1, 0$ on the RHS of (7.151) contains the factor $d_{2s,2p}$. Its value for $Z = 1$ is -0.87. The HF calculation provides $d_{2s,2p} = -0.91$ for $Z = 5$, becoming closer to -1 for larger Z. The corresponding factor $d_{1s,2p}$ for correlation with the $1s$ state is positive, since the function ψ_{1s}^r is always positive, while the function ψ_{2p}^r is positive except at the point $r = 0$, where it becomes zero. These two contributions have different signs, exhibiting the tendency to cancellation. Correlations with other $n's$ ($n' \geq 2$) electrons, if there are any, are much smaller. This happens for two reasons. The high-energy IPA amplitudes $f_{n's}$ decrease with n'. Also, closure requires that $\mathscr{S}_x |\langle \psi_{xs}^r | \psi_{2p}^r \rangle|^2 = 1$, with summation over states of both the discrete and continuum spectra. Thus the values of $d_{2s,2p}$ and $d_{1s,2p}$ (the Coulomb value is 0.48 in the latter case) almost saturate the closure condition, and the values of the overlap integrals $d_{n's,2p}$ with $n' > 1$ are much smaller. Hence only correlations with $2s$ and $1s$ electrons are important. For the same reason, in ionization of the np state, the correlations with ns and $1s$ electrons are the largest.

Now we analyze the influence of the s electrons from various n' shells on the cross section of ionization of the np states. We can write (7.185) as

$$\sigma_{np} = \sigma^I_{np} + 2\xi_{ee} \sum_{j'} s_{j'i} \left(\frac{\sigma^I_i \sigma^I_{j'}}{3}\right)^{1/2} + \xi^2_{ee} \sum_{j',j''} s_{j'i} s_{j''i} (\sigma^I_{j'} \sigma^I_{j''})^{1/2}, \tag{7.186}$$

with j' and j'' denoting the $n's$ and $n''s$ states respectively. We can rearrange the RHS as

$$\sigma_{np} = \sigma^I_{np} + 2\xi_{ee} \Big[\sum_{j'} s_{j'i} \Big(\frac{\sigma^I_i \sigma^I_{j'}}{3}\Big)^{1/2} + \frac{\xi_{ee}}{2} s^2_{j'i} \sigma^I_{j'} \Big] + \xi^2_{ee} \sum_{j' \neq j''} s_{j'i} s_{j''i} (\sigma^I_{j'} \sigma^I_{j''})^{1/2}. \tag{7.187}$$

Here the term in square brackets on the RHS describes the "individual" contribution to the IPA breaking effect of $n's$ electrons, while the last term provides the interference of correlations with $n's$ and $n''s$ electrons. In the asymptotics, the RHS does not depend on ω, and the correlation effects change the slope r^I_n of the line $R_{n1} \equiv \sigma_{ns}/\sigma_{np} = a^I_n \omega$ to $a_{n1} = a^I_{n1}/K$. Putting $K = 1 + \lambda$, we can write

$$\lambda = \sum_{n'} \lambda_{n'} + \sum_{n'' \neq n'} \tau_{n',n''}\,. \tag{7.188}$$

Here each $\lambda_{n'}$ is the contribution of an $n's$ electron; the sum $\sum_{n'} \lambda_{n'}$ corresponds to the term in square brackets on the RHS of (7.187). The cross terms $\tau_{n',n''}$ contain the products of contributions of $n's$ and $n''s$ electrons. The sum $\sum_{n'' \neq n'} \tau_{n',n''}$ corresponds to the third term on the RHS of (7.187).

We use (7.188) to analyze the interplay of the partial contributions. For nitrogen, we have $\lambda_1 = -0.29$, $\lambda_2 = 0.44$, while $\tau_{1,2} = -0.23$. Thus $\lambda = -0.08$. For neon, $\lambda_1 = -0.17$, $\lambda_2 = 0.18$, while $\tau_{1,2} = -0.03$, providing $\lambda = -0.02$. The correlations of the $2p$ electrons with those in the $2s$ and $1s$ states compensate each other to a large extent. For ionization of the $3p$ state in argon, $\lambda_1 = 0.086$, $\lambda_3 = -0.077$, while the other parameters are much smaller. Thus we face the tendency of compensation of the correlations once again.

Ionization of $3d$ electrons in titanium ($Z = 22$) provides another illustration of the tendency. Nonrelativistic calculations carried out for $\omega = 50\,\text{keV}$ gave $\lambda \approx 0.04$, while the individual contributions are about ten times larger.

7.4.5 *Nonrelativistic High-Energy Asymptotics*

Now we calculate the leading terms of the expansion in powers of $1/\omega$ of the cross sections for ionization of $n\ell$ states beyond the IPA. As we have seen in Sect. 7.1.3, the IPA amplitudes have a common factor $h(\xi)$ representing the dependence on the parameter $\pi\xi$-(7.37). Thus the IPA cross sections contain the factor $D(\xi) = h^2(\xi)$; see (7.41). Since we presented the IPA breaking amplitudes as linear combinations of the IPA amplitudes, the cross section beyond the IPA will also contain the factor $D(\xi)$.

We begin with IPA breaking effects in the final state. As we have seen, in the case of s states, the IPA breaking effects manifest themselves beyond the leading terms of the asymptotics. The cross section can be expressed by (7.44) with $\ell = 0$,

$$\sigma_{n0}(\omega) = \frac{\mathscr{A}_{n0} D(\hat{\xi})}{\omega^{7/2}}, \tag{7.189}$$

with $\mathscr{A}_{n0}$ equal to its IPA value A_{n0}, i.e., $\mathscr{A}_{n0} = A_{n0}$.

For the states with $\ell = 1$, the IPA and IPA breaking terms depend on the photon energy in the same way. Thus all the terms on the RHS of (7.155) contribute to the asymptotics. Also, only correlations with s states contribute to the asymptotics. We obtain

$$\sigma_{n1}(\omega) = \frac{\mathscr{A}_{n1} D(\hat{\xi})}{\omega^{9/2}}. \tag{7.190}$$

Now $\mathscr{A}_{n1}$ differs from its IPA value A_{n1}:

$$\mathscr{A}_{n1} = A_{n1} + 2b_1 \sum_{n'} d_{n'0,n1} \left(\frac{A_{n1} A_{n'0} I_1}{3} \right)^{1/2} + I_1 b_1^2 \left(\sum_{n'} d_{n'0,n1} A_{n'0}^{1/2} \right)^2, \tag{7.191}$$

with the sum over all occupied $n's$ states, and $I_1 = m\alpha^2/2 \approx 13.6\,\mathrm{eV}$.

For $\ell \geq 1$, the asymptotics are determined by the IPA breaking contribution, expressed by the last term on the RHS of (7.190). As in the case $\ell = 1$, only correlations with s states contribute to the asymptotics. We obtain

$$\sigma_{n\ell}(\omega) = \frac{\mathscr{A}_{n\ell} D(\hat{\xi})}{\omega^{9/2}}, \tag{7.192}$$

with

$$\mathscr{A}_{n\ell} = I_1 b_\ell^2 \left(\sum_{n'} (d_{n'0,n\ell} A_{n'0}^{1/2} \right)^2. \tag{7.193}$$

The amplitude describing the IPA breaking in the initial state for photoionization of $2p$ states is given by (7.147). A similar equation can be written for the photoionization of any $n\ell$ state. The $n\ell$ electron can be transferred to a vacant $n'\ell$ state by the ee interaction. In the next step, it undergoes direct interaction with the photon. The amplitude has the same energy dependence as the IPA amplitude. This mechanism contributes to the terms beyond the asymptotics if $\ell > 1$. For $\ell = 0, 1$, it should be included. However, usually it is numerically small, due to the small amplitude of photoionization from the excited states. For strongly bound states with binding energies $\varepsilon_b \gg I_1$, it is quenched by the factor $m\alpha/\mu_{n\ell}$. In any case, in the high-energy limit, the amplitude of photoionization can be expressed in terms of a single parameter that is the derivative of the wave function of this state at the origin. Hence, the IPA breaking effect in the initial state can be treated as a certain renormalization of the single-particle wave function.

Thus the IPA breaking effects do not alter the asymptotic law for s states. For p states they do not change the energy dependence of the cross section, but modify the coefficient of the asymptotics. For $\ell \geq 2$, the IPA breaking effects determine the asymptotics and change their energy dependence from $D(\xi)/\omega^{7/2+\ell}$ to $D(\xi)/\omega^{9/2}$ [30].

7.4.6 Peculiarities of the Relativistic Case

Now we consider the correlations for relativistic photoelectrons. The ratio ω/m is no longer a small parameter. As in the nonrelativistic case, the q dependence of the IPA amplitudes contains the factor $(\mu_{n\ell}/q)^{\ell}$. However, now one cannot neglect the photon momentum $\mathbf{k}$ in the expression for the recoil momentum $q = |\mathbf{k} - \mathbf{p}|$. Employing the results of Sect. 7.4.3, one can see that (7.156), or more generally (7.184), which presents the squared IPA breaking amplitude in terms of the IPA amplitudes, is true in the relativistic case. However, the relation between the amplitudes and the cross sections is not as simple as in the nonrelativistic case. It requires a complicated angular integration.

Recall that in the nonrelativistic case, the second term on the RHS of (7.155) vanishes for even values of ℓ, since the bound-state wave functions are real. The relativistic amplitudes contain both real and imaginary parts of the same order of magnitude for all values of ℓ. Neither part can be neglected without a more detailed analysis.

Employing the results of Sect. 7.4.1, we can estimate the IPA breaking corrections to the cross sections as

$$\frac{\sigma_{n\ell}(\omega) - \sigma_{n\ell}^{(I)}(\omega)}{\sigma_{n\ell}^{(I)}(\omega)} \sim \frac{\alpha}{\zeta_{n\ell}^{\ell}}; \quad \frac{\alpha^2}{\zeta_{n\ell}^{2\ell}}, \tag{7.194}$$

with $\zeta_{n\ell} = \mu_{n\ell}/m$. The first and second terms on the RHS correspond to the second and third terms on the RHS of (7.155). In the hydrogenlike approximation, $\zeta_{n\ell} = \alpha Z/n$, and

$$\frac{\sigma_{n\ell}(\omega) - \sigma_{n\ell}^{(I)}(\omega)}{\sigma_{n\ell}^{(I)}(\omega)} \sim \frac{\alpha}{(\alpha Z)^{\ell}}; \quad \frac{\alpha^2}{(\alpha Z)^{2\ell}}. \tag{7.195}$$

Here we do not trace the n dependence.

Thus in the ionization of s states, the IPA breaking effects provide small corrections of order α, i.e., of the same order as the relativistic corrections. In the ionization of p states, the IPA breaking effects are of order $1/Z$, being determined by the second term on the RHS of (7.155). The third term provides a correction of order $1/Z^2$. For higher values of ℓ, one cannot make a definite conclusion about the relative role of the two terms. The relative role of the third term with respect to the second one can be described by the parameter $\gamma_{\ell} = (\alpha Z)^{1-\ell}/Z$. We obtain $\gamma_2 = 0.31$ and $\gamma_3 = 0.10$

for the lightest atoms containing d and f electrons with the charges of the nuclei $Z = 21$ and $Z = 57$ respectively. Thus one cannot neglect the third term on the RHS of (7.184) without additional analysis.

In the ultrarelativistic limit $\omega \gg m$, the energy dependence of the photoionization amplitudes is the same for all bound states. Thus the left-hand sides of (7.194) and (7.195) do not depend on ω.

The strong cancellation between the partial contributions to the correlations in the nonrelativistic case makes the relativistic calculations increasingly important. For example, in the ionization of neon and argon at energies of about 70 keV, the relativistic corrections to contributions of correlations of the electrons from different shells are of order 0.14. However, these corrections become of order the total correlation effect, calculated in the nonrelativistic approximation. It is still not clear whether the cancellations obtained in the nonrelativistic approximation still take place after taking relativistic effects into account.

References

1. H.A. Bethe, E.E. Salpeter, *Quantum Mechanics of One- and Two -Electron Atoms* (Dover Publications, NY, 2008)
2. V.G. Gorshkov, A.I. Mikhailov, V.S. Polikanov, Nucl. Phys. **55**, 273 (1964)
3. N.B. Avdonina, E.G. Drukarev, R.H. Pratt, Phys. Rev. A **65**, 052705 (2002)
4. J. McEnnan, L. Kissel, R.H. Pratt, Phys. Rev. A **13**, 532 (1976)
5. S.D. Oh, J. McEnnan, R.H. Pratt, Phys. Rev. A **14**, 1428 (1976)
6. A.I. Akhiezer, V.B. Berestetskii, *Quantum Electrodynamics* (Pergamon, N.Y., 1982)
7. R.G. Sachs, N. Aysten, Phys. Rev. **84**, 705 (1951)
8. L.D. Landau, E.M. Lifshits, *Quantum Mechanics Nonrelativistic Theory*. Pergamon, New York, 1977)
9. M.Y. Amusia, L.V. Chernysheva, N.A. Cherepkov, S.I. Sheftel. Sov. Phys. JETP **29**, 1018 (1969)
10. A.F. Starace, Phys. Rev. A **3**, 1242 (1971)
11. Y.B. Zeldovich, ZhETF, **31**, 1101 (1956)
12. V.S. Polikanov, Sov. Phys. JETP **25**, 882 (1967)
13. A.I. Mikhailov, V.S. Polikanov, Sov. Phys. JETP **27**, 95 (1968)
14. C.K. Au, G.W. Rodgers, Phys. Rev. A **22**, 1820 (1980)
15. G. Moliere, Z. Naturforsch **2A**, 133 (1947)
16. A.I. Mikhailov, Sov. Phys. JETP **71**, 465 (1990)
17. G. Racavy, A. Ron, Phys. Rev. **159**, 50 (1967)
18. E.W.B. Dias et al., Phys. Rev. Lett. **78**, 4553 (1997)
19. E.G. Drukarev, N.B. Avdonina, J. Phys. B **36**, 2033 (2003)
20. O. Hemmers et al., J. Electron. Spectrosc. **123**, 157 (2002)
21. D.T. Touless, *Quantum Mechanics of Many-Body Systems* (Academic Press, NY, London, 1961)
22. M.Y. Amusia, in *Atomic Photoeffect* (Plenum Press, NY, 1990)
23. M.Y. Amusia, V.G. Yarzhemsky, L.V. Chernysheva, *Handbook of Theoretical Atomic Physics, Data for Photon Absorption, Electron Scattering, Vacancies Decay* (Springer, Berlin, 2012)
24. S.T. Manson, Can. J. Phys. **87**, 5 (2009)
25. E.T. Whittaker, G.N. Watson, *A Course of Modern Analysis* (University Press, Cambridge, 1996)

26. D.L. Hansen et al., Phys. Rev. A **60**, R2641 (1999)
27. H.S. Chakraborty, D.L. Hansen, O. Hemmers, P.C. Deshmukh, P. Focke, I.A. Sellin, C. Heske, D.W. Lindle, S.T. Manson, Phys. Rev. A **63**, 042708 (2001)
28. V.K. Dolmatov, A.S. Baltenkov, S.T. Manson, Phys. Rev. A **64**, 042718 (2001)
29. E.G. Drukarev, R.H. Pratt, Phys. Rev. A **72**, 062701 (2005)
30. E.G. Drukarev, N. Avdonina, R.H. Pratt, Bull. Amer. Phys. Soc. **44**, 132 (1999)

Chapter 8
Ionization and Excitation by Photon Impact at Higher Energies

Abstract Since the nonrelativistic photoionization cross section decreases rapidly with an increase of the photon energy, the higher-order processes dominate in the formation of ions at larger values of photon energy. We carry out relativistic analysis of the second- and third-order processes. If the photon energy is large enough, the Compton scattering becomes the dominant mechanism for creation of ions. We show that the seagull term of the nonrelativistic Compton scattering amplitude can be viewed as the contribution of the negative-energy intermediate states in the relativistic amplitude. We obtain the general equations for the characteristics of the Compton scattering on the Bethe ridge and show their connection with equations of the impulse approximation. Employing the results obtained in Chap. 4, we obtain the differential distributions outside the Bethe ridge. We demonstrate the infrared stability of the sum of the contribution to the Compton scattering cross section coming from the soft scattered photons and the photoionization cross section that includes the radiative corrections. At still larger photon energies exceeding certain value ω_0, the ions are produced mainly accompanied by the creation of electron–positron pairs. We determine the energy distribution of the electrons ejected due to this mechanism. We calculate the dependence of ω_0 on the value of the nuclear charge Z for the single-electron ions and for the atoms containing Z electrons. We find also the photon energy region where this mechanism dominates in the creation of excited atoms.

8.1 Compton Scattering

8.1.1 Interpretation of the Seagull Term

In both photoeffect and Compton scattering, the final state contains an ion. At low energies, the photoelectric effect dominates, while the relative contribution of the Compton scattering is of order the fine-structure constant α. As we have seen, at very large energies the ratio of the cross sections of these processes, $R(\omega) = \sigma_C(\omega)/\sigma_{ph}(\omega)$ (in this section, the lower index C stands for "Compton"), is of order $\alpha/(\alpha Z)^5$, which

E.G. Drukarev and A.I. Mikhailov, *High-Energy Atomic Physics*,
Springer Series on Atomic, Optical, and Plasma Physics 93,
DOI 10.1007/978-3-319-32736-5_8

is larger than unity for $Z \leq 52$. The cross section of the Compton scattering is larger than that of the photoeffect for $\omega > \omega_1(Z)$. The value of ω_1 amounts to several kilo-electron volts for the lightest atoms, becoming about 1 MeV for the heaviest ones [1].

Before calculating the cross section σ_C, we discuss the matching of the general relativistic approach with the nonrelativistic one. The relativistic amplitude of the Compton scattering in the single-particle approximation can be written as [2]

$$F_C = -N(\omega_1)N(\omega_2)X;$$

$$X = \int \frac{d^3f_1}{(2\pi)^3}\frac{d^3f_2}{(2\pi)^3}\Big[\langle\psi_f|\mathbf{f}_2 - \mathbf{k}_2\rangle\hat{e}_2^*\langle\mathbf{f}_2|G(\omega_1 + E_i)|\mathbf{f}_1\rangle\hat{e}_1\langle\mathbf{f}_1 - \mathbf{k}_1|\psi_i\rangle + \tag{8.1}$$

$$+\langle\psi_f|\mathbf{f}_2 + \mathbf{k}_1\rangle\hat{e}_1\langle\mathbf{f}_2|G(-\omega_2 + E_i)|\mathbf{f}_1\rangle\hat{e}_2^*\langle\mathbf{f}_1 + \mathbf{k}_2|\psi_i\rangle\Big],$$

with G the relativistic electron propagator in the atomic field. The polarization vectors e_k have only the space components, and thus $\hat{e}_k = -(e_k)_i\gamma_i$, $(i = 1, 2, 3)$. The first term describes the process in which the absorption of a photon with energy ω_1 by an atomic electron is followed by radiation of a photon with energy ω_2. In the second term, the radiation precedes the absorption. In the nonrelativistic limit (see Sect. 5.4), we have also the $\mathbf{A}^2$ or seagull term with absorption and radiation at the same point.

To find the nonrelativistic limit of the amplitude (8.1), we present each propagator as the sum of the contributions of the positive-energy and negative-energy states:

$$G(E) = G^+(E) + G^-(E); \quad G^+ = \sum_s \frac{|\psi_s\rangle\langle\psi_s|}{E - E_s + i\delta}; \quad G^- = \sum_q \frac{|\psi_q\rangle\langle\psi_q|}{E - E_q - i\delta}. \tag{8.2}$$

Here s denote the states with $E_s > 0$, while q stand for the states with $E_q < 0$ (actually, $E_q < -m$). The amplitude can be written as $F_C^+ + F_C^-$, with the two terms corresponding to the two terms on the RHS of the first equality in (8.2).

In the nonrelativistic limit $\omega_{1,2} \ll m$, the energies of the final-state and initial-state electrons $E_{f,i}$ should be close to m, i.e., $|E_{f,i} - m| \ll m$. In this limit, the amplitude F_C^+ describes the nonrelativistic pole contributions. Now we focus on the contribution $F_C^- = -N(\omega_1)N(\omega_2)X^-$; of the intermediate states with negative energies E_q:

$$X_C^- = \int \frac{d^3f_1}{(2\pi)^3}\frac{d^3f_2}{(2\pi)^3}\Big[\sum_q \frac{\langle\psi_f|\mathbf{f}_2 - \mathbf{k}_2\rangle\hat{e}_2^*\langle\mathbf{f}_2|\psi_q\rangle\langle\psi_q|\mathbf{f}_1\rangle\hat{e}_1\langle\mathbf{f}_1 - \mathbf{k}_1|\psi_i\rangle}{\omega_1 + E_i - E_q - i\delta} +$$

$$+ \sum_q \frac{\langle\psi_f|\mathbf{f}_2 + \mathbf{k}_1\rangle\hat{e}_1\langle\mathbf{f}_2|\psi_q\rangle\langle\psi_q|\mathbf{f}_1\rangle\hat{e}_2^*\langle\mathbf{f}_1 + \mathbf{k}_2|\psi_i\rangle}{-\omega_2 + E_i - E_q - i\delta}\Big]. \tag{8.3}$$

Note that the sum over the states $|\psi_q\rangle$ is saturated by those with three-dimensional momenta $q = |\mathbf{q}| \ll m$. This is because the bound states determine important values

of momenta $f_1 \sim \mu_b \ll m$, and the wave functions $\langle \mathbf{f}_1|\psi_q\rangle$ are strongly quenched at $q \gtrsim m$. Thus we can put $E_q = -m$ in the denominators of both terms on the RHS of (8.3), which become $E_i - E_q \approx 2m$. Also, we can neglect the terms corresponding to the kinetic and potential energies in the wave equation for ψ_q, which is just $(\gamma_0 + 1)|\psi_q\rangle = 0$. Hence we can put

$$|\psi_q\rangle \;=\; \frac{1-\gamma_0}{2}|\psi_q\rangle\,, \tag{8.4}$$

and write

$$X_C^- = \frac{1}{4m}\int \frac{d^3f_1}{(2\pi)^3}\frac{d^3f_2}{(2\pi)^3}\Big[\sum_q \langle\psi_f|\mathbf{f}_2 - \mathbf{k}_2\rangle\hat{e}_2^*(1-\gamma_0)\langle\mathbf{f}_2|\psi_q\rangle\langle\psi_q|\mathbf{f}_1\rangle\hat{e}_1\langle\mathbf{f}_1 - \mathbf{k}_1|\psi_i\rangle + \\ + \sum_q \langle\psi_f|\mathbf{f}_2 + \mathbf{k}_1\rangle\hat{e}_1(1-\gamma_0)\langle\mathbf{f}_2|\psi_q\rangle\langle\psi_q|\mathbf{f}_1\rangle\hat{e}_2^*\langle\mathbf{f}_1 + \mathbf{k}_2|\psi_i\rangle\Big]. \tag{8.5}$$

To evaluate the sum over the negative energy states, we employ the closure condition

$$\sum_s |\psi_s\rangle\langle\psi_s| + \sum_q |\psi_q\rangle\langle\psi_q| \;=\; 1, \tag{8.6}$$

and replace $\sum_q |\psi_q\rangle\langle\psi_q|$ by $1 - \sum_s |\psi_s\rangle\langle\psi_s|$ on the RHS of (8.5). In the sum over the positive energy states, those with large momentum $s = |\mathbf{s}| \gtrsim m$ are quenched, since the integrals are determined by $f_{1,2} \sim \mu_b \ll m$. For the states with $s \ll m$, we obtain $(1-\gamma_0)|\psi_s\rangle = 0$ in the nonrelativistic limit. Thus we can put $\sum_q |\psi_q\rangle\langle\psi_q| = 1$ on the RHS of (8.5), and $\sum_q \langle\mathbf{f}_2|\psi_q\rangle\langle\psi_q|\mathbf{f}_1\rangle = (2\pi)^3\delta(\mathbf{f}_1 - \mathbf{f}_2)$. Integrating over $\mathbf{f}_2$ and changing the variable $\mathbf{f}_1$ of integration in the second term on the RHS of (8.5) to $\mathbf{f}_1 - \mathbf{k}_1 - \mathbf{k}_2$, we obtain

$$F_C^- = -\frac{N(\omega_1)N(\omega_2)}{4m}\int \frac{d^3f_1}{(2\pi)^3}\langle\psi_f|\mathbf{f}_1 - \mathbf{k}_2\rangle\Big(\hat{e}_2^*(1-\gamma_0)\hat{e}_1 + \hat{e}_1(1-\gamma_0)\hat{e}_2^*\Big)\langle\mathbf{f}_1 - \mathbf{k}_1|\psi_i\rangle. \tag{8.7}$$

Now we employ the commutation relations $\gamma_0\hat{e}_{1,2} = -\hat{e}_{1,2}\gamma_0$ and $\hat{e}_2^*\hat{e}_1 + \hat{e}_1\hat{e}_2^* = 2e_2^*e_1 = -2\mathbf{e}_2^*\mathbf{e}_1$. Since also in the nonrelativistic limit $\gamma_0|\psi_i\rangle = |\psi_i\rangle$, we find that

$$F_C^- = \frac{\mathbf{e}_2^*\cdot\mathbf{e}_1}{m}N(\omega_1)N(\omega_2)\int \frac{d^3f_1}{(2\pi)^3}\langle\psi_f|\mathbf{f}_1 - \mathbf{k}_2\rangle\langle\mathbf{f}_1 - \mathbf{k}_1|\psi_i\rangle. \tag{8.8}$$

Replacing $\mathbf{f}_1 - \mathbf{k}_1$ by $\mathbf{f}_1$ in the integrand, we arrive at (5.84) for the seagull term.

Thus the seagull term approximates the sum over the negative energy states in (8.1). It is amusing that the nonrelativistic Thomson cross section, which corresponds to the amplitude described by the seagull diagram, is expressed in terms of essentially relativistic characteristics.

8.1.2 Distribution of the Scattered Photons

Recall that we denote momenta and energies of the incoming and scattered photons by $\mathbf{k}_{1,2}$ and $\omega_{1,2} = k_{1,2} \equiv |\mathbf{k}_{1,2}|$. The total energies of the initial and outgoing electrons are E_i and E. Treating the recoil ion as just a source of an external field, we can write for the differential cross section

$$d\sigma_C = (2\pi)^4 |F_C(\mathbf{k_1}, \mathbf{k_2})|^2 \delta(\omega_1 + E_i - E - \omega_2) d\Gamma; \quad d\Gamma = \frac{d^3p}{(2\pi)^3} \frac{d^3k_2}{(2\pi)^3}, \tag{8.9}$$

with $\mathbf{p}$ the three-dimensional momentum of the outgoing electron, and $p = |\mathbf{p}|$. Considering the recoil ion to be one of the final-state particles, which obtains momentum $-\mathbf{q}$, we can write (8.9) in the form

$$d\sigma_C = (2\pi)^4 |F_C(\mathbf{k_1}, \mathbf{k_2}, \mathbf{q})|^2 \delta(\omega_1 + E_i - E - \omega_2) \delta(\mathbf{k}_1 + \mathbf{q} - \mathbf{k}_2 - \mathbf{p}) d\Gamma', \tag{8.10}$$

$$d\Gamma' = \frac{d^3p}{(2\pi)^3} \frac{d^3k_2}{(2\pi)^3} \frac{d^3q}{(2\pi)^3}.$$

The case of soft scattered photons with $\omega_2 \ll \omega_1$ will be analyzed in Sect. 8.1.4. Here we focus on the energies of the scattered photons $\omega_2 \sim \omega_1$.

As we have seen in Chap. 2, for large energies

$$\omega_1 \gg \mu_b \tag{8.11}$$

(in other words, for the case in which the wavelength of the incoming photon is much smaller than the size of the bound state), the amplitude is enhanced on the Bethe ridge, where the momentum q transferred to the recoil ion can be as small as the average binding momentum μ_b. This requires that the energy of the scattered photon be not too small:

$$\omega_2 \geq \frac{\omega_1}{1 + 2\omega_1/m}. \tag{8.12}$$

If also the kinetic energy of the outgoing electron is large enough, $\varepsilon \gg I_b$, i.e., its momentum satisfies the condition $p \gg \mu_b$, one can neglect q everywhere except the bound state wave function ψ_i in the general equation for the amplitude (8.1). The latter can be written as [3]

$$F_C(\mathbf{k_1}, \mathbf{k_2}, \mathbf{q}) = \psi_i(\mathbf{q}) F_0(\omega_1, \omega_2), \tag{8.13}$$

with F_0 the amplitude of the Compton scattering on an electron at rest; momentum $\mathbf{q} = -\mathbf{k}_1 + \mathbf{k}_2 + \mathbf{p}$ is transferred from the nucleus. Further, we omit the lower index i labeling the wave function of the initial state electron. Note that the accuracy of this factorized form is μ_b^2/ω^2.

For small $q \sim \mu_b \ll k_1, k_2, p$, the amplitude F_C takes the form determined by (8.13). Thus (8.10) can be written as

$$d\sigma_C = (2\pi)^4 |F_0(\omega_1, \omega_2)|^2 |\psi(\mathbf{q})|^2 \delta(\omega_1 + E_i - E - \omega_2) \delta(\mathbf{k}_1 - \mathbf{k}_2 - \mathbf{p}) \frac{d^3p}{(2\pi)^3} \frac{d^3k_2}{(2\pi)^3} \frac{d^3q}{(2\pi)^3}. \tag{8.14}$$

Here we have neglected momentum $\mathbf{q}$ in the argument of the delta function of the three-dimensional momenta. We also employed that $|\psi(-\mathbf{q})|^2 = |\psi(\mathbf{q})|^2$. This equation can be represented as

$$d\sigma_C = d\sigma_0 \frac{|\psi(\mathbf{q})|^2 d^3q}{(2\pi)^3}, \tag{8.15}$$

with $d\sigma_0$ the cross section of the process on the free electron at rest.

Recall that this relation is true for $q \lesssim \mu_b$. To obtain the distribution of the scattered photons, we must integrate over q in this region. However, these are the very values of q that saturate the normalization integral $\int d^3q |\psi(\mathbf{q})|^2/(2\pi)^3 = 1$. This enables us to find the energy distribution in the region of ω_2 limited by condition (8.12):

$$\frac{d\sigma_C}{d\omega_2} = \frac{d\sigma_0}{d\omega_2}, \tag{8.16}$$

where the term on the RHS is the energy distribution for the Compton scattering on the free electron at rest. Note that for $\omega_1 \ll m$, we find from (8.12) that $\omega_1 - \omega_2 \leq 2\omega_1^2/m \ll \omega_1$. Thus for $\omega_1 \sim \mu_b$, the kinetic energy of the outgoing electron is of the order of the electron binding energy, and its interaction with the atomic field should be included.

Also, for the total cross section, we obtain for every bound state

$$\sigma_C(\omega_1) = \sigma_0(\omega_1), \tag{8.17}$$

up to the terms μ_b^2/ω_1^2. Thus for the Compton scattering on the atom,

$$\sigma_C(\omega_1) = N_e \sigma_0(\omega_1), \tag{8.18}$$

with N_e the number of bound electrons.

Now we analyze the double differential cross section $d\sigma/d\omega_2 dt$ with $t = \mathbf{k}_1 \cdot \mathbf{k}_2/\omega_1\omega_2$. For Compton scattering on the free electron, the magnitude of the momentum of a radiated photon and the angle between the momenta of the ejected particles are linked by (6.154). The distribution is given by the Klein–Nishina formula

$$\frac{d\sigma_0}{d\omega_2 dt} = U(\omega_2, t)\delta(\omega_2 - \omega_{20}), \tag{8.19}$$

with

$$U(\omega_2, t) \;=\; \pi r_0^2 \frac{\omega_2^2}{\omega_1^2}\left[\frac{\omega_1}{\omega_2} + \frac{\omega_2}{\omega_1} + t^2 - 1\right], \tag{8.20}$$

while ω_{20} is defined by (6.154). For a similar distribution in the free Compton scattering, there is a single line with frequency ω_{20} for each scattering angle. For the bound electrons, one can expect that at a fixed value of the scattering angle, the distribution has a peak in the vicinity of the point ω_{20}. Introducing $\boldsymbol{\kappa} = \mathbf{k}_1 - \mathbf{k}_2$, we obtain

$$\frac{d\sigma_C}{d\omega_2 dt} \;=\; U(\omega_{20}, t) pE \int \frac{d\Omega_p}{(2\pi)^3} |\psi(\mathbf{p} - \boldsymbol{\kappa})|^2; \quad E = \omega_1 + E_i - \omega_2\,, \tag{8.21}$$

for $|\mathbf{p} - \boldsymbol{\kappa}| \lesssim \mu_b \ll \omega_1$. The integral on the RHS is saturated by small values of the angle θ_p between the directions of $\boldsymbol{\kappa}$ and $\mathbf{p}$. For every fixed value of t, the distribution reaches its peak at $\omega_2 = \omega_{20}$, determined by (6.154) shifted by the binding energy. (An additional shift of relative order $\alpha^2 Z^2$ was discussed in Sect. 5.3.5 for the special case of the Coulomb field.)

Many studies of high-energy Compton scattering are based on the impulse approximation, which was formulated in its nonrelativistic form in the early days of quantum mechanics; see, e.g., [4]. Compton scattering on bound electrons is viewed like that on free electrons with momenta $\mathbf{q}'$ distributed with density $\rho(\mathbf{q}') = |\psi(\mathbf{q}')|^2$. Indeed, this means that the amplitude is described by (8.13). The momentum $\mathbf{q}'$ in the impulse approximation is not equivalent to the recoil momentum $\mathbf{q}$. We demonstrate, however, that the difference is relatively small.

In the impulse approximation, the energy delta function on the RHS of (8.14) is used for integration over one of the components of the vector $\mathbf{q}'$. In the nonrelativistic case, this can be written

$$\delta\left(\omega_2 + \frac{(\boldsymbol{\kappa} + \mathbf{q}')^2}{2m} - \omega_1 - \frac{q'^2}{2m}\right) = \delta\left(\omega_2 + \frac{\kappa q'_z}{m} - \omega_1 + \frac{\kappa^2}{2m}\right), \tag{8.22}$$

where the z-axis runs in the direction of the vector $\boldsymbol{\kappa}$. Employing cylindrical coordinates for the vector $\mathbf{q}'$, one can write

$$\frac{d\sigma}{d\omega_2 dt} \;=\; \frac{d\sigma_0}{dt}\frac{m}{\kappa} j(q'_z), \tag{8.23}$$

with

$$j(q'_z) \;=\; 2\pi \int_{q'_z}^{\infty} |\psi(q')|^2 q' dq' \tag{8.24}$$

(here we have employed the spherical symmetry of the density $|\psi(q')|^2$), while

$$q'_z \;=\; -\frac{\kappa}{2} + \frac{m(\omega_1 - \omega_2)}{\kappa}\,. \tag{8.25}$$

The impulse approximation is justified only on the Bethe ridge, where $q \lesssim \mu_b$, since outside this region, a momentum q can be transferred to the nucleus not only by the bound electron, but by the outgoing electron, as well as by the electron in an intermediate state. In other words, it is expected to describe the distribution in the vicinity of the peak. On the other hand, at the Bethe ridge the results provided by the impulse approximation are expected to be close to those obtained by a straightforward use of (8.13) and (8.14). Proceeding in the same way as in (8.22)–(8.25), we see that the two approaches differ only in the values of q_z, and this difference is small. The delta function on the RHS of (8.14) can be written as

$$\delta(\omega_2 + \frac{(\boldsymbol{\kappa} + \mathbf{q})^2}{2m} - \omega_1 + I_b) \;=\; \delta\left(\omega_2 + \frac{\kappa q_z}{m} - \omega_1 + I_b + \frac{\kappa^2 + q^2}{2m}\right) \tag{8.26}$$

($I_b > 0$). Thus

$$q_z \;=\; q_z' - \frac{m}{\kappa}\left(I_b + \frac{q^2}{2m}\right), \tag{8.27}$$

where $q_z' \sim \mu_b$ is the impulse approximation value determined by (8.25). Since at the Bethe ridge $\kappa \approx p \gg \mu_b$, we find that $(q_z - q_z')/q_z \sim \mu_b/p \ll 1$.

The factorized form of the amplitude (8.13) requires that $\mu_b \ll m$. Thus one cannot expect it to work well for the K shells of heavy atoms. However, in the example presented in Fig. 8.1 [5], the results of the impulse approximation calculations (in relativistic form) appeared to be close to those of direct computations based on (8.1).

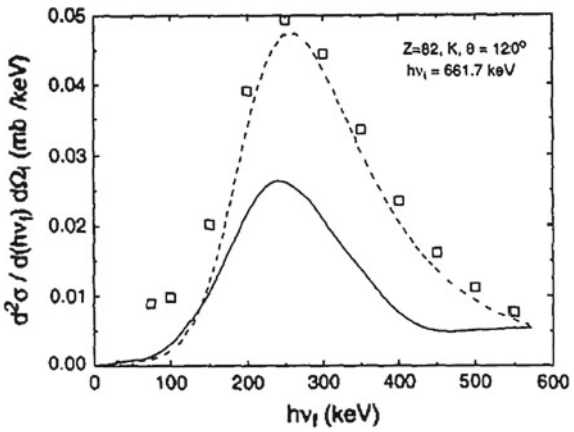

Fig. 8.1 Photon energy distribution at fixed angle $\theta = 120°$ for the scattering of the unpolarized photon beam with energy $\omega_1 = 662\,\text{keV}$ on the target with $Z = 82$. The *boxes* show the result of direct numerical calculations. The *dashed line* is for the results obtained by employing the relativistic impulse approximation. The *solid line* is for the nonrelativistic impulse approximation. Reproduced from [5] with permission of Elsevier Publishing

8.1.3 Distribution of Ejected Electrons

We turn now to the distribution of the outgoing electrons. Here we set $\varepsilon = E - m$ with E the total energy of the ejected electron and $t_e = \cos\theta_e$ with the angle θ_e between the direction of momentum of the incoming photon and that of the ejected electron. For every value of the electron energy limited by condition (6.153), the distribution $d\sigma_C/d\varepsilon dt_e$ peaks at $t_e = t_0 = \cos\theta_0$, where θ_0 is the value of θ_e corresponding to the free process. The latter is given by (6.190). For the Compton scattering on the free electron, we obtain, employing (8.19),

$$\frac{d\sigma_0}{d\varepsilon dt_e} = U(\varepsilon, t_e)\delta(\varepsilon - \varepsilon_0)\,, \tag{8.28}$$

with $\varepsilon_0 = \omega_1 - \omega_2$, while U written in terms of the parameters of the outgoing electron,

$$U(\varepsilon, t_e) = \pi r_0^2 \frac{\omega_2^2}{\omega_1^2}\left[\frac{\omega_1}{\omega_2} + \frac{\omega_2}{\omega_1} - \frac{p^2}{\omega_2^2}(1 - t_e^2)\right]; \quad \omega_2 = \omega_1 - \varepsilon. \tag{8.29}$$

Here the last term in the square brackets is obtained by using the sine theorem $p/\sin\theta = k_2/\sin\theta_e$ and $k_2 = \omega_2$.

The value of the angular distribution in the vicinity of the peak $t_e = t_0$ can be obtained in the same way as for the photon distribution; see (8.21):

$$\frac{d\sigma_C}{d\varepsilon dt_e} = U(\varepsilon, t_0)\omega_2^2 \int \frac{d\Omega}{(2\pi)^3}|\psi(\mathbf{k}_2 - \mathbf{q}_1)|^2; \quad \omega_2 = \omega_1 + E_i - E, \tag{8.30}$$

with $\mathbf{q}_1 = \mathbf{k}_1 - \mathbf{p}$, while Ω is the solid angle of the scattered photon. The vicinity of the peak is determined by the inequality $|\mathbf{k}_2 - \mathbf{q}_1| \lesssim \mu_b \ll \omega_1$.

We can calculate the value of this distribution for any value of the angle t_e if the energy of the outgoing electron satisfies (6.153). If the values of t_e are not close to t_0, a large recoil momentum $q \gg \mu_b$ is transferred to the nucleus. Following the analysis carried out in Chaps. 4 and 6, we can consider the process as consisting of two steps. The first is the Compton scattering with small transferred momentum $q \sim \mu_b$ and energy ε of the outgoing electron. In the second step, the ejected electron transfers momentum $q \gg \mu_b$ to the recoil ion. The energy of the outgoing electron does not change, while the direction of its momentum does.

Employing (4.50) and (4.53), we find that the distribution of the outgoing electrons in energies and in recoil momenta is

$$\frac{d\sigma_C}{d\varepsilon dq^2} = \frac{\langle\psi_i|r^{-2}|\psi_i\rangle}{4\pi} \cdot \frac{d\sigma_0}{d\varepsilon} \cdot \frac{d\sigma_{el}(\varepsilon)}{dq^2}. \tag{8.31}$$

Here $d\sigma_{eI}$ is the cross section for the scattering of the outgoing electron on the recoil ion, and (8.31) holds in all orders of their interaction. In the Born approximation,

$$\frac{d\sigma_{eI}(\varepsilon)}{dq^2} = \frac{|V_{eI}(q^2)|^2}{2\pi}\frac{E^2}{p^2}\left(1-\frac{q^2}{4E^2}\right), \tag{8.32}$$

where V_{eI} is the interaction between the outgoing electron and the recoil ion. If the recoil momentum q greatly exceeds the binding momenta of the internal electrons, it is transferred primarily to the nucleus, and one can put $V_{eI} = V_{eN} = -4\pi\alpha Z/q^2$.

The distribution (8.31) can be written in terms of the angular variables of the ejected electron. We can write the squared recoil momentum as $q^2 = 2p^2(1-t')$. Here $t' = \cos\theta'$, with θ' the angle between the momentum of the ejected electron and that of the outgoing electron with the same energy ε in the Compton scattering on the free electron. Hence $d\sigma_{eI}/dt' = 2p^2/q^2 \cdot d\sigma_{eI}/dq^2$, and

$$\frac{d\sigma_C}{d\varepsilon dt'} = \frac{\langle\psi_i|r^{-2}|\psi_i\rangle}{4\pi}\cdot\frac{d\sigma_0}{d\varepsilon}\cdot\frac{d\sigma_{eI}}{dt'}. \tag{8.33}$$

This enables us to write the double differential distribution in the system with the polar axis directed along the momentum of the incoming photon $\mathbf{k}_1$. Since $t' = t_e t_0 + \sqrt{1-t_0^2}\sqrt{1-t_e^2}\cos\varphi$, we have

$$\frac{d\sigma_C}{d\varepsilon d\Omega_e} = \frac{\langle\psi_i|r^{-2}|\psi_i\rangle}{(4\pi)^2}\cdot\frac{d\sigma_0}{d\varepsilon}\cdot\frac{2p^2 d\sigma_{eI}}{dq^2}\cdot\left(t_0 - \frac{t_e\sqrt{1-t_0^2}\cos\varphi}{\sqrt{1-t_e^2}}\right), \tag{8.34}$$

with Ω_e the solid angle of the ejected electron.

In the ultrarelativistic case $\omega_1 \gg m$, the momenta of the incoming photons and ejected electrons are almost parallel in the free process. Thus we can put $d\sigma_C/d\varepsilon d\Omega' = d\sigma_C/d\varepsilon d\Omega_e$. In this case, we have $t_0 = 1$ in the last factor on the RHS of (8.34). This turns this factor to unity.

8.1.4 Radiation of Soft Photons

As we have seen in Sect. 5.5.2, at $\omega_2 \to 0$, the amplitude of the Compton scattering obtains a pole, corresponding to radiation of the photon by the outgoing electron after its interaction with the recoil ion. There is no infrared singularity in the term describing the radiation of such a photon by the bound electron. This is because for $\omega_2 \to 0$, only the radiation of the electric dipole photon survives, and the states n of the Green functions on the RHS of (8.1) contributing to the process cannot coincide with the initial state. Thus the denominator of the electron propagator does not become zero at $\omega_2 \to 0$. This argument does not work for the continuum wave functions, since the states with fixed energy are degenerate with respect to the directions of the electron momentum.

This remains true in the relativistic case, where we find the factorized form for the double differential cross section to be [6, 7]

$$\frac{d\sigma_C}{d\omega_2 d\Omega} = \frac{\alpha}{\pi}\cdot\frac{v^2}{\omega_2}\cdot\int\frac{d\Omega_e}{4\pi}\cdot\frac{1-\tau^2}{(1-v\tau)^2}\frac{d\sigma_{ph}}{d\Omega};\quad \tau=\frac{\mathbf{p}\cdot\mathbf{k}_2}{p\omega_2}\,, \tag{8.35}$$

with $\mathbf{v} = \mathbf{p}/E$ the velocity of the photoelectron. The distribution increases if the energy of the scattered photon decreases. This leads to the logarithmically divergent contribution of the soft photons to the total cross section of the Compton scattering.

In practice, the resolution of the detector of the outgoing photons is limited by a certain value $\bar{\varepsilon}$. For $\omega_2 < \bar{\varepsilon}$, the Compton scattering is indistinguishable from the photoionization. As we shall see, the sum of the differential cross section for the Compton scattering integrated in the interval $0 \le \omega_2 \le \bar{\varepsilon}$ and the cross section for photoionization including the lowest-order radiative corrections

$$\sigma \;=\; \sigma_{ph}^{rad} + \int_0^{\bar{\varepsilon}} d\omega_2 \frac{d\sigma_C}{d\omega_2} \tag{8.36}$$

does not contain infrared divergent terms. This is a special case of a more general statement. The combination of the cross section σ_1 for a radiative process and the cross section σ_0 for the radiationless process with the radiative corrections included,

$$\sigma \;=\; \sigma_0^{rad} + \int_0^{\bar{\varepsilon}} d\omega_2 \frac{d\sigma_1}{d\omega_2}, \tag{8.37}$$

is infrared stable.

We illustrate this by considering the Compton scattering of photons with energies $I_b \ll \omega_1 \ll m$. The amplitude of the process for $\omega_2 \ll \omega_1$ can be written as

$$F_C \;=\; \frac{\mathbf{e}_2\mathbf{p}}{m\omega_2} N(\omega_2) F_{ph}\,, \tag{8.38}$$

with F_{ph} the amplitude of the photoeffect for the same energy of the incoming photon ω_1. Thus after summation over the polarizations of the photon, we obtain

$$d\sigma_C = \sigma_{ph}\Phi(\mathbf{k}_2)\frac{d^3k_2}{(2\pi)^3};\quad \Phi(\mathbf{k}_2) = 4\pi\alpha\frac{p^2(1-t^2)}{m^2\omega_2^3}\,, \tag{8.39}$$

leading to

$$\frac{d\sigma_C}{d\omega_2} = \sigma_{ph}\cdot\frac{4\alpha}{3\pi}\frac{v^2}{\omega_2};\quad v^2 = \frac{p^2}{m^2}. \tag{8.40}$$

Consider now the radiative corrections to the photoionization in the lowest order of α. These are the self-energy corrections to the wave functions of the final and initial states and the vertex function. We calculate the radiative corrections, focusing on the infrared divergent terms. The corrections contain the four-dimensional integrals

over momentum of the virtual photon f. One can see that the infrared divergent terms originate from the pole $f_0 = f$ in the contour of integration over f_0. Following the analysis done above, we find that there are no infrared divergent terms if the virtual photon is coupled to the bound electron. Hence, such terms are contained only in the self-energy of the outgoing electron.

As we know from quantum electrodynamics [2], the radiative correction for the electron with four-momentum p can be included by multiplying its wave function by the factor $(1 - \Sigma')^{-1/2}$, with the self-energy

$$\Sigma(p) = \alpha \int \frac{d^4 f}{(2\pi)^4 i} \gamma^\mu G(p - f) \gamma^\nu D_{\mu\nu}(f). \tag{8.41}$$

Here $D_{\mu\nu}$ and $G = (\hat{p} - \hat{f} - m)^{-1}$ are the photon and electron propagators, and the derivative is taken with respect to $\hat{p}$. The photoionization cross section, which includes the lowest-order radiative corrections, is thus $\sigma_{ph}^{rad} = \sigma_{ph}(1 + \Sigma')$. Note that we are tracing only the infrared divergent terms.

Since we are tracing the infrared divergent terms, we can assume that integration over f is carried out in a limited volume $f \leq L \ll m$. Hence we can employ the nonrelativistic electron propagator determined by (2.29). It is reasonable to use the photon propagator in the Coulomb gauge; see (2.50). Only the space components D_{ij} of the photon propagator contribute to the infrared divergent terms. In the nonrelativistic approximation, the electron–photon vertices $\gamma_{i,j}$ can be replaced by $p_{i,j}/m$. Therefore,

$$\Sigma(\varepsilon, \mathbf{p}) = -\int \frac{df_0 d^3 f}{(2\pi)^4 i} \cdot \frac{4\pi\alpha}{m^2 \kappa(f)} \cdot \frac{|\mathbf{p}|^2 (1 - \tau_f^2)}{f_0^2 - f^2 + i\delta}; \quad \tau_f = \frac{\mathbf{f} \cdot \mathbf{p}}{f|\mathbf{p}|}, \tag{8.42}$$

with $\kappa(f) = \varepsilon - f_0 - m - (\mathbf{p} - \mathbf{f})^2/2m + i\delta$. Now $\Sigma' = \partial\Sigma/\partial\varepsilon$, and we must put $\varepsilon = |\mathbf{p}|^2/2m$ after calculation of the derivative. Integrating over f_0 in the complex plane, one finds that the infrared divergent term comes from the contribution of the pole $f_0 = -f + i\delta$. At this point, we have $\kappa = f(1 - v\tau_f)$, with $v = |\mathbf{p}|/m$ the velocity of the ejected electron. We can put $v = 0$ for the nonrelativistic electron. This provides

$$\Sigma' = -\int \Phi(\mathbf{f}) \frac{d^3 f}{(2\pi)^3}, \tag{8.43}$$

with Φ determined by (8.39). Hence,

$$\sigma_{ph}^{rad} = \sigma_{ph}\left(1 - \frac{4\alpha}{3\pi} v^2 \int_\lambda^L \frac{df}{f}\right). \tag{8.44}$$

Here we assumed that the lower limit of integration over the three-dimensional momentum f is $\lambda \to 0$. Under the latter assumption, the contribution of soft photons with energies $\omega_2 \leq \bar{\varepsilon}$ to the cross section of the Compton scattering is

$$\int_{\lambda}^{\bar{\varepsilon}} d\omega_2 \frac{d\sigma_C}{d\omega_2} = \sigma_{ph} \cdot \frac{4\alpha}{3\pi} v^2 \int_{\lambda}^{\bar{\varepsilon}} \frac{d\omega_2}{\omega_2}, \tag{8.45}$$

and thus the sum

$$\sigma_{ph}^{rad} + \int_{\lambda}^{\bar{\varepsilon}} d\omega_2 \frac{d\sigma_C}{d\omega_2} = \sigma_{ph}\Big(1 - \frac{4\alpha}{3\pi} v^2 \int_{\bar{\varepsilon}}^{L} \frac{d\omega_2}{\omega_2}\Big). \tag{8.46}$$

does not contain infrared-divergent terms.

The logarithmic dependence on the upper-limit cutoff L remains in a more rigorous calculation, where one assumes $L \gg m$ in the integral on the RHS of (8.41) and employs the relativistic Green electron function and the total photon propagator. The terms containing $\ln L$ are contained in the vertex functions. These terms cancel in the standard renormalization procedure of quantum electrodynamics; see, e.g., [8]. A more detailed analysis of the radiative corrections to the photoionization cross section is given in [9].

8.2 Ionization Accompanied by Creation of Pairs

8.2.1 Vacuum Assistance Mechanism

Now we turn to the mechanism in which formation of ions (or excitation of atoms and ions) is accompanied by creation of electron–positron pairs. This is possible for $\omega > 2m \approx 1\,\text{MeV}$. We shall see that in the high-energy asymptotics $\omega \gg m$, the cross section reaches a constant value. Thus for the photon energies exceeding a certain value $\omega_0(Z)$, the cross section exceeds that of the Compton scattering. We shall see that the energy $\omega_0(Z)$ is of order several dozens of MeV. Thus we analyze the case $\omega \gg m$, carrying out the calculations in the leading order of the parameter m/ω.

We carry out calculations for the spectrum of the electrons and for the cross section, focusing on the case of not very large values of nuclear charge $\alpha^2 Z^2 \ll 1$, adding, however, several comments about the case in which $\alpha^2 Z^2$ is not considered a small parameter.

Before writing expressions for the amplitude, we present the relevant Feynman diagrams in Fig. 8.2 [10]. Figure 8.2a shows the creation of pairs by an incoming photon with further scattering on the bound electron. In Fig. 8.2b, the photon energy absorbed by the bound electron is shared between the ejected electron and the electron–positron pair. We begin with the case in which the three-dimensional momentum $\mathbf{p}_1$ of the ejected electron is much larger than the average momentum of the bound electron μ_b. Following our general strategy, we must find the amplitude in the kinematic region where the process on the free electron can take place. In this

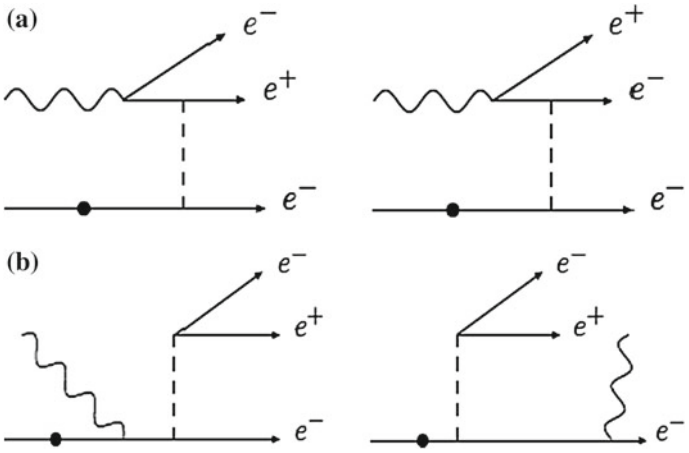

Fig. 8.2 Feynman diagrams describing ionization of e^+e^- pairs. **a** The pair created by the photon interacts with the bound electron. **b** The photon interacts with the bound electron and the absorbed energy is shared between the electron knocked out from the atom and the e^+e^- pair

region, a momentum **q** is transferred to the nucleus by the bound electron. The other electrons can be described by functions of free motion [11].

In this approximation, the diagrams of Fig. 8.2a do not interfere with those of Fig. 8.2b. The interference terms in the cross section contain the electron–positron loop with an odd number (three) of electron–photon vertices, and the contribution vanishes due to Furry theorem [8]. Hence

$$d\sigma \;=\; d\sigma^a + d\sigma^b\,, \tag{8.47}$$

with the two terms corresponding to Fig. 8.2a, b.

We shall not consider the configurations in which all the outgoing electrons carry the energy $E \gg m$. As we shall see, here the amplitude of the process is strongly quenched. For the same reason, we shall not consider the case in which only one of the outgoing particles is ultrarelativistic. Thus we focus on the case of two ultrarelativistic particles in the final state.

In order to trace the leading contribution to the amplitude, recall that each propagator carrying a large momentum provides a small factor in the amplitude. For $p_1 \sim k = \omega$, all diagrams of Fig. 8.2a, b contain two propagators with large momenta. For $p_1 \ll k$, there is one propagator with large momentum in each of the diagrams of Fig. 8.2a. There are two of them in each of Fig. 8.2b. Thus the main mechanism is described by the diagrams shown in Fig. 8.2a. The incoming photon creates the e^-e^+ pair that knocks out the atomic electron to the continuum. This is called the "vacuum assistance mechanism" (VAM) [10].

Now we can easily extend our analysis to the case of slow ejected electrons with $p_1 \sim \mu_b$. The wave function of the ejected electron should include interactions with

the residual ion. Momentum $\mathbf{q}$ can be transferred to the nucleus by either the bound electron or the ejected electron.

Denote the four-dimensional momentum of the electron ejected from the atom by p_1, while the respective momenta of the electron and positron of the e^-e^+ pair are p_e and p_p, and $P = p_e + p_p$. The three-dimensional momentum $\boldsymbol{\kappa} = \mathbf{k} - \mathbf{P}$ and the energy $\varepsilon_1 + I_b$ are transferred to the atom, with $\varepsilon_1 = E_1 - m$ the kinetic energy of the ejected electron. This momentum is shared between the ejected electron and the nucleus, i.e., $\boldsymbol{\kappa} = \mathbf{p}_1 + \mathbf{q}$. The amplitude can be written as

$$F = \alpha N(\omega)\Phi_\nu \bar{u}(p_e)[\hat{e}G(p_e - k)\gamma^\mu + \gamma^\mu G(k - p_p)\hat{e}]u(-p_p)D_{\mu\nu}(\kappa)\Phi^\nu, \quad (8.48)$$

with G and $D_{\mu\nu}$ the relativistic propagator of free electron and the photon propagator respectively, $\kappa = (\kappa_0, \boldsymbol{\kappa})$, while

$$\Phi^\nu(\mathbf{p}_1, \boldsymbol{\kappa}) = \int d^3r \bar{\psi}_{\mathbf{p}_1}(\mathbf{r})\gamma^\nu \psi_i(\mathbf{r})e^{-i\boldsymbol{\kappa}\mathbf{r}} = \int \frac{d^3f}{(2\pi)^3}\bar{\psi}_{\mathbf{p}_1}(\mathbf{f} - \boldsymbol{\kappa})\gamma^\nu \psi_i(\mathbf{f}), \quad (8.49)$$

with relativistic electron wave functions ψ. For $\varepsilon_1 \gg \mu_b$, the wave function of the outgoing electron on the RHS of (8.49) can be replaced by the plane wave.

For nonrelativistic $p_1 \ll m$, it is reasonable to employ the propagator $D_{\mu\nu}$ in the Coulomb gauge. The dominating contribution to the amplitude comes from the time component D_{00}. In this case,

$$\Phi^\nu(\mathbf{p}_1, \boldsymbol{\kappa}) = \Phi(\mathbf{p}_1, \kappa)\delta_{\nu 0}; \quad \Phi(\mathbf{p}_1, \boldsymbol{\kappa}) = \int d^3r \psi^*_{\mathbf{p}_1}(\mathbf{r})\psi_i(\mathbf{r})e^{-i\boldsymbol{\kappa}\mathbf{r}} = \quad (8.50)$$

$$\int \frac{d^3f}{(2\pi)^3}\psi^*_{\mathbf{p}_1}(\mathbf{f} - \boldsymbol{\kappa})\psi_i(\mathbf{f}).$$

The electrons can be described by the nonrelativistic functions ψ_i and $\psi_{\mathbf{p}_1}$. If $\psi^*_{\mathbf{p}_1}(\mathbf{r})$ is replaced by $\psi^*_i(\mathbf{r})$, then (8.48) represents the amplitude of creation of e^-e^+ pairs in the field of the bound electron. Putting $\Phi = -Z$, we would obtain the amplitude F_{BH} for pair creation in the field of the nucleus, which was first calculated by Bethe and Heitler; see, e.g., [8].

Now we look for the energy distribution of the ejected electrons.

8.2.2 *Energy Distribution of the Ejected Electrons*

For relatively fast electrons ejected from the atom with $\omega \gg \varepsilon_1 \gg I_b$, we can write now

$$d\sigma = d\sigma_0 \frac{|\psi(\mathbf{q})|^2 d^3q}{(2\pi)^3}, \quad (8.51)$$

with

$$d\sigma_0 \;=\; N^2(\omega)|F_0|^2\,\frac{d^3p_1}{(2\pi)^3}\,\frac{d^3p_e}{(2\pi)^3}\,, \tag{8.52}$$

where F_0 is the amplitude of the process in which the bound electron is replaced by the free electron at rest.

Recall that for the scattering on the free electron, the four-dimensional momenta of the particles involved in the process are related by the conservation law

$$k+\tilde{p} \;=\; P+p_1\,, \tag{8.53}$$

where $\tilde{p}=(m,0)$ is the momentum of the initial-state electron, and $P=p_e+p_p$ is the momentum of the e^-e^+ pair.

We employ an expression for the distribution $d\sigma_0/d^3p_1$ of the ejected electrons obtained in [12] in terms of their energies and the invariant variable $\Delta^2=P^2$. Using (8.53), one can express the latter in terms of variables of the ejected electron:

$$\Delta^2 \;=\; -2\varepsilon_1(\omega+m)+2\omega p_1 t_1; \qquad t_1 \;=\; \mathbf{kp_1}/\omega p_1. \tag{8.54}$$

Thus

$$\frac{d\sigma}{d^3p_1} \;=\; \frac{d\sigma_0}{d^3p_1} \;=\; \frac{\omega_1}{\pi E_1}\,\frac{d\sigma_0}{d\varepsilon_1 d\Delta^2}\,. \tag{8.55}$$

The interval of the values of Δ^2 can be obtained by employing (8.53) and the inequality

$$k_1k_2 \;\geq\; m_1m_2\,, \tag{8.56}$$

which is true for any two particles with masses $m_{1,2}$ and the four-momenta $k_{1,2}$. This can be checked directly. The definition of Δ^2 provides $\Delta^2\geq 4m^2$. Since $(k+\tilde{p})^2=(P+p_1)^2\geq(\sqrt{\Delta^2}+m)^2$, we obtain $\Delta^2\leq 2m\omega$. Hence

$$4m^2\leq\Delta^2\leq 2m\omega.$$

It follows from (8.54) that at $\Delta^2\sim 4m^2$, the momentum of the ejected electron is $|\mathbf{p}_1|\ll m$. In particular, $p_{1z}\approx 2m^2/\omega$ (the z-axis runs along the direction of the photon momentum $\mathbf{k}$). At $\Delta^2\sim 2m\omega$, we find that $\omega\gg p_{1z}\gg m$ and $p_{1t}\leq m$, with p_{1t} denoting the component of the vector $\mathbf{p}_1$ orthogonal to the z-axis.

Calculation of the distribution (8.55) can be done by the standard methods of quantum electrodynamics. Referring the interested reader, to [12] for the details (several limiting cases have been studied earlier), we just present a result. For the energy of the ejected electron $I_b\ll\varepsilon_1\ll\omega$, the distribution is

$$\frac{d\sigma_0}{d\varepsilon_1 d\Delta^2} \;=\; \alpha^3 W(\varepsilon_1,\Delta^2)\,, \tag{8.57}$$

with

$$W(\varepsilon_1, \Delta^2) = \frac{A(\varepsilon_1, \Delta^2)}{\varepsilon_1 B(\varepsilon_1, \Delta^2)}. \tag{8.58}$$

Here $B(\varepsilon_1, \Delta^2) = (\Delta^2 + 2m\varepsilon_1)^2$, while

$$A(\varepsilon_1, \Delta^2) = 4\beta\left(1 - L + 4m\frac{[\Delta^2(m - 4\varepsilon_1)] + L[2m^2(2\varepsilon_1 + m) + \Delta^2(\varepsilon_1 - m)]}{B(\varepsilon_1, \Delta^2)}\right), \tag{8.59}$$

with $\beta = [(\Delta^2 - 4m^2)/\Delta^2]^{1/2}$ and $L = (1/\beta)\ln[(1+\beta)/(1-\beta)]$. The energy distribution for $I_b \ll \varepsilon_1 \ll \omega$ can be obtained by integration over Δ^2 in the interval between $4m^2$ and $2m\omega$:

$$\frac{d\sigma}{d\varepsilon_1} = \frac{\alpha r_e^2}{m} T_f\left(\frac{\varepsilon_1}{m}\right) \tag{8.60}$$

with $r_e = \alpha/m$, and the lower index f comes from "fast" ($\varepsilon_1 \gg I_b$)

$$T_f(x) = \frac{2}{x}\left[-\frac{x^3 + x^2 + 2x - 1}{x^2(2+x)^2} + \frac{2(2x^4 + 7x^3 + 16x^2 + 5x - 3)}{3x^{5/2}(2+x)^{5/2}}\ln\left(\sqrt{x/2} + \sqrt{x/2+1}\right) - \frac{2(1-4x)}{15}\,{}_2F_1\left(2, 4, \frac{7}{2}, -\frac{x}{2}\right)\right]. \tag{8.61}$$

Here $x = \varepsilon_1/m$. At $x \ll 1$, we obtain

$$T_f(x) = \frac{14}{9}\cdot\frac{1}{x}. \tag{8.62}$$

Since at $\varepsilon_1 \ll m$, the distribution behaves as ε_1^{-1}, the region $\varepsilon_1 \sim I_b$ provides a contribution of the same order of magnitude to the total cross section as the region $\varepsilon_1 \gg I_b$.

Consider now the case of slow ejected electrons with kinetic energies $\varepsilon_1 \sim I_b$. Here the momentum p_1 and the recoil momentum q are of the same order of magnitude. Following the analysis made at the end of Sect. 8.2.1, we can write for each bound electron

$$F = -\frac{1}{Z}F_{BH}\Phi(\mathbf{p}_1, \boldsymbol{\kappa}). \tag{8.63}$$

Since the outgoing electron is slow, at moderate values of Z we can use the non-relativistic functions for the bound and ejected electrons for the function Φ defined by (8.50). Now we can write

$$d\sigma = \frac{1}{Z^2}d\sigma_{BH}|\Phi(\mathbf{p}_1, \boldsymbol{\kappa})|^2\frac{d^3p_1}{(2\pi)^3}. \tag{8.64}$$

The Bethe–Heitler distribution is

$$d\sigma_{BH} = R d\Gamma'; \quad d\Gamma' = dp_{et} dp_{e\ell} dp_{pt} dp_{p\ell} dE_p d\varphi, \tag{8.65}$$

with the indices e and p corresponding to the electron and positron of the $e^- e^+$ pair, the lower indices ℓ and t labeling the directions along the momentum of the photon and orthogonal to it, while

$$R = \frac{8\alpha r_e^2 Z^2 E_e E_p}{\pi \kappa^4 \omega^3} H, \tag{8.66}$$

and

$$H = -\frac{\delta_-^2}{(1+\delta_-^2)^2} - \frac{\delta_+^2}{(1+\delta_+^2)^2} + \frac{\omega^2}{2E_e E_p} \cdot \frac{\delta_-^2 + \delta_+^2}{(1+\delta_-^2)(1+\delta_+^2)} + \tag{8.67}$$

$$\left(\frac{E_e}{E_p} + \frac{E_p}{E_e}\right) \frac{\delta_- \delta_+ \cos\varphi}{(1+\delta_-^2)(1+\delta_+^2)}.$$

Here $\delta_{-,+} = p_{et,pt}/m$. The distribution should be evaluated at $p_{et,pt} \sim m$, as in the Bethe–Heitler case. However, now we need $\kappa_t = |\mathbf{p}_{et} + \mathbf{p}_{pt}| \lesssim \mu_b \ll p_{et,pt}$. In this kinematic region, we can represent (8.67) in the form

$$H = \frac{\kappa^2}{m^2 (1+\delta_+^2)^2} \left(\Lambda + \frac{4\delta_+^2 t^2}{(1+\delta_+^2)^2} \right), \tag{8.68}$$

with $t = (p_{et} - p_{pt})/\kappa$ $(-1 \le t \le 1)$ and

$$\Lambda = \frac{E_e^2 + E_p^2}{2E_e E_p}. \tag{8.69}$$

The phase volume in (8.65) becomes

$$d\Gamma' = dE_p p_{pt}^2 dp_{pt} d\kappa^2 \frac{dt}{2(1-t^2)^{1/2}}. \tag{8.70}$$

After integration over the positron variables and over t, we obtain

$$d\sigma = \frac{14}{9} \alpha r_e^2 |\Phi(\mathbf{p}_1, \kappa)|^2 \frac{d\kappa^2}{\kappa^2} \frac{d^3 p_1}{(2\pi)^3}. \tag{8.71}$$

At $\kappa = 0$, the factor $\Phi(\mathbf{p}_1, \kappa)$ becomes zero due to the orthogonality of the wave functions involved. Thus the function $|\Phi(\mathbf{p}_1, \kappa)|^2$ contains κ as a factor at $\kappa \to 0$, and integration of the RHS over κ provides a finite value.

The factors $\Phi(\mathbf{p}_1, \kappa)$ have been computed for many cases in connection with electron–atomic scattering. Here we present evaluation of (8.71) for the hydrogenlike

ion with one electron in the $1s$ state. The function $\Phi(\mathbf{p}_1, \kappa)$ is calculated by employing the nonrelativistic Coulomb functions for describing electrons. In this case, the average binding momentum is given by $\mu_b = \eta = m\alpha Z$. Employing (8.50) and writing $d^3p_1 = mp_1 d\varepsilon_1 d\Omega$, we obtain

$$\int \frac{d\Omega}{(2\pi)^3} |\Phi(\mathbf{p}_1, \kappa)|^2 = \kappa^2 X(p_1, \kappa); \quad X(p_1, \kappa) = \frac{2^7 N_p^2}{3\pi} \exp(2\xi\gamma) \cdot \frac{u(p_1, \kappa)}{v(p_1, \kappa)}. \tag{8.72}$$

Here $u(p_1, \kappa) = \eta^5(p_1^2+3\kappa^2+\eta^2)$ and $v(p_1, \kappa) = [(\kappa^2-p_1^2)^2+2\eta^2(\kappa^2+p_1^2)+\eta^4]^3$, while $\gamma = \arg(\kappa^2+\eta^2-p_1^2-2i\eta p_1)$. Recall that $\xi = \eta/p_1$ and N_p is the normalization factor of the outgoing electron wave function determined by (3.20). Combining (8.71) and (8.72), we can write

$$\frac{d\sigma}{d\varepsilon_1} = \frac{14}{9}\alpha r_e^2 m p_1 \int d\kappa^2 X(p_1, \kappa). \tag{8.73}$$

We express the kinetic energy of the outgoing electron in "units" of the binding energy $I_Z = m\alpha^2 Z^2/2$, introducing $\tilde{\varepsilon} = p_1^2/\eta^2 = \varepsilon_1/I_Z$. Writing also $\kappa^2 = y\eta^2$, we find that

$$\frac{d\sigma}{d\tilde{\varepsilon}} = \frac{14}{9}\alpha r_e^2 K(\tilde{\varepsilon}), \tag{8.74}$$

with

$$K(\tilde{\varepsilon}) = \frac{2^7}{3(1-e^{-2\pi\xi})} \int_0^\infty dy\, e^{-2\xi\gamma_1} \frac{\mu+3y}{(y^2+2\nu y+\mu^2)^3}, \tag{8.75}$$

with $\xi = 1/\sqrt{\tilde{\varepsilon}}$, while $\mu = 1+\tilde{\varepsilon}$, $\nu = 1-\tilde{\varepsilon}$, and $\gamma_1 = \arg(y+\nu+2i\sqrt{\tilde{\varepsilon}})$.

Thus we can write the energy distribution of the "slow" electrons with kinetic energy $\varepsilon_1 \sim I_Z$ in the form similar to (8.60):

$$\frac{d\sigma}{d\varepsilon_1} = \frac{\alpha r_e^2}{I_Z} T_s\left(\frac{\varepsilon_1}{I_Z}\right), \tag{8.76}$$

with

$$T_s(\tilde{\varepsilon}) = \frac{14}{9} K(\tilde{\varepsilon}). \tag{8.77}$$

One can calculate $K(0) = 1 - 7e^{-4}/3 \approx 0.957$, and thus $T_s(0) \approx 1.5$.

At $\varepsilon_1 \gg I_Z$, i.e., at $\tilde{\varepsilon} \gg 1$, the lowest order of expansion of $K(\tilde{\varepsilon})$ in powers of $1/\tilde{\varepsilon}$, corresponding to a plane-wave description of the outgoing electron, leads to

$$K(\tilde{\varepsilon}) = \frac{1}{\tilde{\varepsilon}}. \tag{8.78}$$

Thus for $I_Z \ll \varepsilon_1 \ll m$,

$$T_s(\tilde{\varepsilon}) \;=\; \frac{14}{9}\cdot\frac{1}{\tilde{\varepsilon}}\,, \tag{8.79}$$

in agreement with the nonrelativistic limit of (8.60); see (8.62).

One can find a more accurate approximate expression for the function $T_s(\tilde{\varepsilon})$ at $\tilde{\varepsilon} \gg 1$. At $p_1 \gg \eta$, the integral on the RHS of (8.73) is dominated by κ close to p_1, with $|\kappa - p_1| \sim \eta$. This is because momentum transferred to the nucleus is of order η. Thus the integral on the RHS of (8.75) is dominated by $y \gg 1$, $|y - \tilde{\varepsilon}| \sim \sqrt{\tilde{\varepsilon}}$. After some algebra [11], we obtain

$$K(\tilde{\varepsilon}) \;=\; \frac{1}{\tilde{\varepsilon}+1}\Big[1 + 0(\tilde{\varepsilon}^{-5/2})\Big]. \tag{8.80}$$

Thus several next-to-leading-order corrections to the high-energy limit of the function $T_s(\tilde{\varepsilon})$ can be included by a simple factor:

$$g(\tilde{\varepsilon}) \;=\; \frac{\tilde{\varepsilon}}{\tilde{\varepsilon}+1}\,. \tag{8.81}$$

The function

$$\tilde{T}_s(\tilde{\varepsilon}) \;=\; \frac{14}{9}\frac{1}{\tilde{\varepsilon}+1} \tag{8.82}$$

approximates the function (8.77) well enough even at small values of $\tilde{\varepsilon}$. The largest relative deviations between the RHS of (8.77) and (8.82) take place at $\tilde{\varepsilon} = 0$. Employing the value of $K(0)$ obtained earlier, one can see the deviation to be about 4 %.

8.2.3 Total Cross Section

Now we calculate the total cross section of the process. We can write $\sigma = \sigma_s + \sigma_f$, with the two terms corresponding to slow and fast ionized electrons. For a value ε_0 satisfying the inequality $I_Z \ll \varepsilon_0 \ll m$, we can write

$$\sigma_s = \frac{\alpha r_e^2}{I_Z}\int_0^{\varepsilon_0} d\varepsilon_1 T_s(\frac{\varepsilon_1}{I_Z}); \quad \sigma_f = \frac{\alpha r_e^2}{m}\int_{\varepsilon_0}^{\omega} d\varepsilon_1 T_f(\frac{\varepsilon_1}{m}). \tag{8.83}$$

Since $T_f(x)$ decreases as $\ln x/x^2$ at $x \to \infty$, see (8.61), the contribution σ_f has a finite value at $\omega \to \infty$. Using (8.62) and (8.79), we obtain

$$\sigma_s = \frac{14}{9}\alpha r_e^2\Big(\ln\frac{\varepsilon_0}{I_Z} + c_s\Big); \quad \sigma_f = \frac{14}{9}\alpha r_e^2\Big(\ln\frac{m}{\varepsilon_0} + c_f\Big). \tag{8.84}$$

The contributions c_s and c_f come from the regions $\varepsilon_1 \sim I$ and $\varepsilon_1 \sim m$ respectively. In this form, the equations for σ_s and σ_f hold for every bound state.

We obtain first the total cross section for the $1s$ electron in a hydrogenlike ion. Since the low-energy limit of the function T_f coincides with the high-energy limit of the function T_s, one can expect that the function

$$\tilde{T}(\varepsilon_1) = T_f\Big(\frac{\varepsilon_1}{m}\Big) g\Big(\frac{\varepsilon_1}{I_Z}\Big) = T_f\Big(\frac{\varepsilon_1}{m}\Big) \frac{\varepsilon_1}{\varepsilon_1 + I_Z} \tag{8.85}$$

approximates the energy distribution in the whole interval $0 \le \varepsilon_1 \ll \omega$. The actual numerical calculations employing the function $\tilde{T}$ provide

$$\sigma \;=\; \frac{14}{9}\alpha r_e^2 \Big(\ln \frac{2}{\alpha^2 Z^2} + C \Big), \tag{8.86}$$

with the values of C changing from 1.23 for $Z = 1$ to 1.31 for $Z = 50$. On the other hand, one can calculate

$$c_s \;=\; \int_0^\infty d\tilde{\varepsilon} [T_s(\tilde{\varepsilon}) - \tilde{T}_s(\tilde{\varepsilon})] \;\approx\; -0.027, \tag{8.87}$$

with the integral saturated by $\tilde{\varepsilon} \sim 1$. Thus c_s does not depend on the charge of the nucleus. The same refers to the contribution c_f. Hence $C = c_s + c_f$ also should not depend on Z, and its small variation with the value of Z is an uncertainty caused by employing the approximate function $\tilde{T}$. Thus for the $1s$ state of the hydrogenlike ion, the cross section is given by (8.86) with $C \approx 1.3$.

For the many-electron atoms, (8.84) remains true. The value of c_f is the same for all electrons and is the same as for the hydrogenlike case. To understand what happens to c_s, note that it is caused by interaction of the outgoing electron with the recoil atom. This interaction reaches the largest value for the hydrogenlike case. Thus the value of $|c_s|$ becomes even smaller and can be neglected. Hence, for every electron state j, we can write

$$\sigma_j \;=\; n_j \frac{14}{9}\alpha r_e^2 \Big(\ln \frac{m}{I_{jb}} + C \Big); \quad C \;\approx\; 1.3, \tag{8.88}$$

with n_j the number of electrons in the state j. For the ionization of the atom, we have

$$\sigma \;=\; \sum_j n_j \frac{14}{9}\alpha r_e^2 \Big(\ln \frac{m}{I_{jb}} + C \Big); \quad C \;\approx\; 1.3. \tag{8.89}$$

Note that our cross sections reach constant values at $\omega \to \infty$. On the other hand, cross sections of pair creation in the field of the nucleus and in the field of free electrons increase as $\ln \omega$ in this limit. This happens because the logarithmic terms are caused by the lower limits m^2/ω of integration over the momentum transferred to

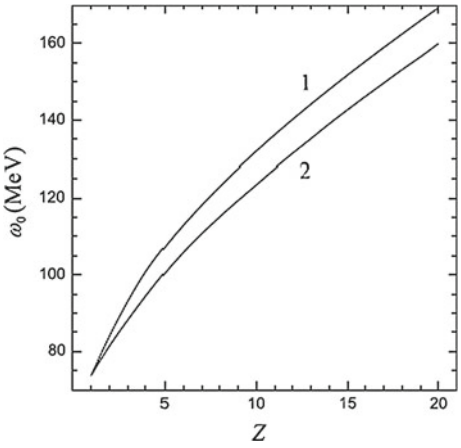

Fig. 8.3 Dependence of the energy ω_0 on the value of the nuclear charge Z. For $\omega > \omega_0$, the VAM photoionization cross section for ionization of the $1s$ state is larger than that for the Compton scattering. *Line 1* corresponds to the single-electron ions; *line 2* is for atoms with Z electrons [11]

the nucleus or to the electron. In our case, the lower limit of such integration actually is of the order of the binding momentum. In the Coulomb case, we have $\ln 1/(\alpha Z)^2$ instead of $\ln \omega/m$.

Comparing the cross section with that of the Compton scattering, we find that for the $1s$ state of the hydrogen atom, the VAM of ionization becomes more important at $\omega > \omega_0 = 73.6\,\text{MeV}$. The value of ω_0 may become smaller for external electrons of many-electron atoms if their binding energy is smaller than that in hydrogen. For example, the binding energies in Na and K are 4.9 and 4.1 eV respectively, providing the values $\omega_0 = 66.7\,\text{MeV}$ and 65.6 MeV. The dependence of ω_0 on the nuclear charge Z is shown in Fig. 8.3.

Ionization of internal shells in coincidence with pair creation was measured in [13] for silver and gold. The results for the K shell are 18 ± 6 mb for Ag and 8.3 ± 6.2 mb for Au. The equations presented above provide 7.8 mb and 5.9 mb, respectively. Note that in the latter case, $Z = 79$, and the errors of calculation are about 30 %. Improvement in the accuracy of both experimental and theoretical results is still ahead.

8.3 Excitation Accompanied by the Pair Creation

8.3.1 Mechanisms of the Excitation Processes

Now we consider excitation of atoms during interactions with high-energy photons with energies $\omega > 2m$ [14]. If the atom (ion) contains at least two bound electrons, the lowest-order process is the shakeup following the photoionization; see Chap. 3. As we have seen in Sect. 7.3, the photoionization cross section reaches the largest values for ionization of the K shell. Assume for simplicity that the bound electrons

are described by single-particle functions. We find that bound electron can undergo transition from the initial state i in the field of the atom described by the function ψ_i to an excited state f in the field of the ion described by the function ψ_f. We shall analyze this type of process in Chap. 9. The cross section can be represented as

$$\sigma_S \;=\; \sigma_{ph} S_{fi}; \quad S_{fi} \;=\; |\langle \varphi_f | \psi_i \rangle|^2. \tag{8.90}$$

The lower index S reminds about the shakeoff origin of the contribution. Employing (7.114) and (7.115), we find that

$$\sigma_S \;\sim\; \alpha(\alpha Z)^5 S_{fi}/m\omega\,. \tag{8.91}$$

Note that due to the closure condition, $S_{fi} < 1$.

The second-order process is the Raman scattering of the photon. The photon interacts with a bound electron, causing its transition to an unoccupied state of the discrete spectrum and radiation of the photon with momentum $\mathbf{k}'$. The amplitude F_R of the Raman scattering can be described by (8.1), with the free relativistic propagators G and the wave function ψ_f describing an excited state of the discrete spectrum:

$$F_R \;=\; F_0 \Phi(q)\,, \tag{8.92}$$

with F_0 standing for the amplitude of the Compton scattering on the free electron at rest with momentum of the outgoing electron going to zero. Momentum $\mathbf{q} = \mathbf{k} - \mathbf{k}'$ is transferred to the atom, while $\Phi(q)$ is determined by (8.50), with $\psi^*_{\mathbf{p}_1}$ replaced by ψ^*_f. Note that Φ is proportional to q if the states $|i\rangle$ and $\langle f|$ have opposite parities, being proportional to q^2 if they have the same parity. Since the energy of the scattered photon is given by $\omega' = \omega - I_i + I_f$, and $\omega - \omega' \ll \omega$, we put $\omega' = \omega$. Thus

$$\sigma_R \;=\; \frac{\pi r_e^2}{\omega^2} \int_0^{4\omega^2} dq^2 |\Phi(q)|^2. \tag{8.93}$$

The integral is dominated by $q^2 \sim \mu^2$ with $\mu = \mu_i + \mu_f$, while $\mu_{i,f}$ are the averaged momenta of the bound electrons in the initial and final states. Thus

$$\sigma_R \;=\; \pi r_e^2 \frac{\mu^2}{\omega^2} b_{fi}\,, \tag{8.94}$$

with $b_{fi} \;=\; \int_0^{4\omega^2} dq^2 |\Phi(q)|^2/\mu^2$. Since the integral is saturated by small $q^2 \sim \mu^2$, we can replace the upper limit of integration by infinity. Therefore,

$$b_{fi} \;=\; \int_0^{\infty} \frac{dq^2}{\mu^2} |\Phi(q)|^2. \tag{8.95}$$

These are dimensionless coefficients of order unity.

In the third order, the excitation of atoms (ions) can be caused by the VAM, discussed in Sect. 8.2. The amplitude is expressed by (8.63), with the function Φ expressed by (8.50), in which the continuum wave function $\psi_{\mathbf{p_1}}$ is replaced by the wave function of the discrete spectrum ψ_f. Now momentum $\mathbf{q} = \mathbf{k} - \mathbf{P}$, with $\mathbf{P} = \mathbf{p}_e + \mathbf{p}_p$ the sum of momenta of the electron and positron composing the $e^- e^+$ pair, is transferred to the atom. The cross section can be obtained by integration of the distribution

$$\frac{d\sigma_V}{dq^2} = \frac{14}{9}\alpha r_e^2 \frac{|\Phi(q)|^2}{q^2}, \tag{8.96}$$

in the interval $q^2_{\min} \le q^2 \le q^2_{\max}$. The lower index V corresponds to VAM. For $\omega \gg m$, we obtain $q_{\max} = 2\omega$, corresponding to directions of momenta $\mathbf{p}_e$ and $\mathbf{p}_p$ opposite to that of the photon momentum $\mathbf{k}$. For a fixed value of $P = |\mathbf{P}|$, the lower limit is given by $q_{\min} = \omega - P$. For any value of the energy of the outgoing electron, it is reached at $P = p_e + p_p$. Thus $q_{\min} = \omega - p_e - p_p$. Writing $p_j = E_j - m^2/2E_j$ $(j = e, p)$, we find that for every value of the energy of the outgoing electron, we have $q_{\min} = I_i - I_f + m^2\omega/2E_eE_p$. The lowest value corresponds to $E_e = E_p = \omega/2$. Thus

$$q_{\min} \approx I_i - I_f + \frac{2m^2}{\omega}. \tag{8.97}$$

Since the function $\Phi(q)$ is quenched at $q > \mu$, it is important to find the region where $q_{\min} \lesssim \mu$. Noting that $I_i - I_f \sim \mu^2/2m \ll \mu$, we obtain that $q_{\min} < \mu$ if the photon energy is greater than a certain characteristic value

$$\omega_c = \frac{2m^2}{\mu}. \tag{8.98}$$

For $\omega \gg \omega_c$, we obtain $q_{\min} \ll \mu$. In this case, we can put

$$\sigma_V = \frac{14}{9}\alpha r_e^2 c_{fi}; \quad c_{fi} = \int_0^\infty dq^2 \frac{|\Phi(q)|^2}{q^2}, \tag{8.99}$$

where the coefficients c_{fi} do not depend on ω. We replaced the lower and upper limits of integration $q^2_{\min}$ and $q^2_{\max}$ by 0 and infinity respectively, since the integral is saturated by the values $q^2 \sim \mu^2$.

In order to expand our results to the region $\omega \lesssim \omega_c$, we should employ (8.97) for $q^2_{\min}$:

$$\sigma_V = \frac{14}{9}\alpha r_e^2 d_{fi}(\omega); \quad d_{fi}(\omega) = \int\limits_{q^2_{\min}}^\infty dq^2 \frac{|\Phi(q)|^2}{q^2}. \tag{8.100}$$

The bound-state wave functions can be approximated as $\psi_b(\mathbf{r}) = \mathscr{F}(\mathbf{r})e^{-\eta_b r}$, with $\mathscr{F}$ containing polynomials in r and spherical functions. The function Φ can be expressed in terms of the function

$$J(\mu) \;=\; \int d^3r \exp\left(-i\mathbf{q}\cdot\mathbf{r}\right) \exp\left(-\mu r\right) \;=\; \frac{8\pi\mu}{(q^2+\mu^2)^2}\,. \tag{8.101}$$

As we have seen in Chap. 5, (5.13) and (5.23), the polynomials in r and the spherical functions can be represented in terms of the function $J(\mu)$. Noting also that at $q \ll \mu$, the function $\Phi(q)$ vanishes for $q = 0$ due to the orthogonality of the wave function, one obtains

$$d_{fi}(\omega) \;=\; \frac{c_{fi}}{(1+q^2_{\min}(\omega)/\mu^2)^n} \;=\; \frac{c_{fi}}{(1+\omega_c^2/\omega^2)^n} \tag{8.102}$$

for the terms that contain the main dependence on $q^2_{\min}$, where the coefficients c_{fi} do not depend on ω. In (8.102), $n = 5$ for the states $|i\rangle$ and $\langle f|$ with opposite parities, while $n = 4$ if they have the same parity. The cross section (8.100) drops sharply when the photon energy becomes smaller than the characteristic value ω_c.

8.3.2 *Competition of the Contributions*

We begin with the case of single-electron ions, when we must compare the cross sections of the Raman scattering σ_R and the excitation by VAM. We introduce

$$R \;=\; \frac{\sigma_V}{\sigma_R} \;=\; \frac{14}{9\pi}\frac{d_{fi}(\omega)}{b_{fi}}\frac{\alpha\omega^2}{\mu^2}\,, \tag{8.103}$$

with b_{fi} and $d_{fi}(\omega)$ defined by (8.95) and (8.102). The VAM dominates at

$$\omega \;>\; \omega_c; \quad \omega \;>\; \omega_e\,, \tag{8.104}$$

with ω_e defined by the condition $R(\omega_e) = 1$.

The electron states can be described by wave functions of the Coulomb field. One can obtain analytical expressions for the parameters involved. If the electron is excited to a state with principal quantum number n, we obtain $\mu = \eta(1 + 1/n)$ with $\eta = m\alpha Z$, and thus

$$\omega_c \;=\; \frac{2m}{\alpha Z}\cdot\frac{n}{n+1}\,. \tag{8.105}$$

The region of VAM domination is $\omega > \omega_c(Z,n)$ if $\omega_c(Z,n) > \omega_e(Z,n)$, and $\omega > \omega_e(Z,n)$ if $\omega_e(Z,n) > \omega_c(Z,n)$. Since ω_e increases with Z, the lowest energy of VAM domination is reached for the value of Z determined by the equation

$$\omega_c(Z,n) \;=\; \omega_e(Z,n)\,, \tag{8.106}$$

Table 8.1 Values of Z_0 corresponding to the solution of (8.106) for $1s \to 2p$ transition (case 1) and $1s \to 2p$ transition (case 2) in hydrogenlike ions and to excitation of $1s$ electrons in multielectron atoms (case 3)

	1	2	3
Z	18.82	14.72	19.99
$\omega_{c,e}$	9.71	12.41	13.71
Z_0	19	15	20
$\omega_c(Z_0)$	9.62	12.18	13.70
$\omega_e(Z_0)$	9.67	12.31	13.70

The two last lines show the values of ω_c and ω_e in MeV corresponding to physical (integer) nuclear charge values Z_0 closest to Z

if its solution corresponds to physically reasonable values of Z. Examples for physical (integer) values Z_0 closest to Z are presented in Table 8.1.

For excitation of the K electrons to the L shell, we have $\mu = 3\eta/2$. We obtain

$$\omega_c = \frac{4m}{3\alpha Z}. \tag{8.107}$$

Direct calculation provides

$$|\Phi_{2s}(q)|^2 = \frac{32\eta^8 q^4}{(q^2+\mu^2)^6}; \quad |\Phi_{2p}(q)|^2 = \frac{72\eta^{10} q^2}{(q^2+\mu^2)^6}. \tag{8.108}$$

The lower index of the function Φ labels the state in the L shell. The summation over the quantum numbers is carried out for $2p$ states. Now we obtain, for the coefficients defined by (8.95) and (8.99),

$$b_{1s2s} = \frac{2^{14}}{5\cdot 3^{11}} \approx 1.86\cdot 10^{-2}; \quad b_{1s2p} = \frac{2^{11}}{5\cdot 3^{11}} \approx 1.86\cdot 10^{-2}, \tag{8.109}$$

and

$$c_{1s2s} = \frac{2^{11}}{5\cdot 3^{8}} \approx 6.24\cdot 10^{-2}; \quad c_{1s2p} = \frac{2^{11}}{5\cdot 3^{8}} \approx 6.24\cdot 10^{-2}. \tag{8.110}$$

The region of VAM domination for the $1s \to 2p$ transition for ionization of a single-electron ion is shown in Fig. 8.4. The smallest energy value for the VAM domination $\omega = 10\,\text{MeV}$ is reached at $Z = 19$. One can see that the lower limit of the VAM region exhibits a very weak dependence on Z. A similar calculation for the $1s \to 2s$ transition provides $\omega = 12\,\text{MeV}$ as the smallest energy value for the VAM domination. It is reached at $Z = 15$.

For excitation of the K shell in an atom with a larger number of electrons, we must include the shakeup excitations that follow photoionization. For large Z, we can put $S_{fi} = s_{fi}/Z^2$ with $s_{fi} < 1$. We shall see in the next chapter that this estimate

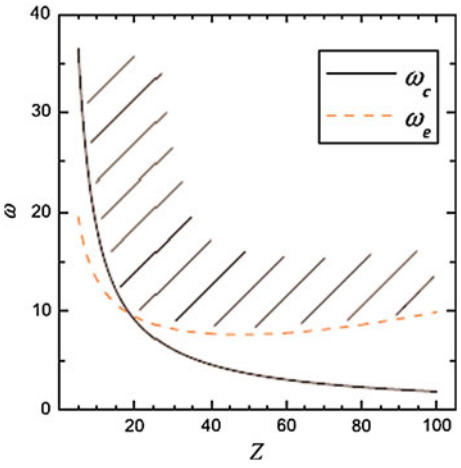

Fig. 8.4 Transition from the $1s$ to the $2p$ state in a hydrogenlike ion with nuclear charge Z. The *solid* and *dashed curves* show the energies ω_c defined by equation (8.107) and ω_e defined by the condition $R(\omega_e) = 1$. The region of VAM domination is *shaded* [14]

works well even for $Z = 2$. We can neglect μ_f with respect to μ_i and assume the Coulomb value $\mu_i = \eta = m\alpha Z$ for the latter. Thus $\omega_c = 2m/\alpha Z$. Comparing the cross sections of excitations caused by the shakeup and VAM, we obtain

$$\frac{\sigma_V}{\sigma_S} \sim \frac{\omega}{m\alpha^3 Z^3}, \tag{8.111}$$

and thus for $\omega > \omega_c$, the VAM dominates. Assuming also $c_{fi}/b_{fi} \approx 1$, we find a minimum value of the VAM domination energy to be $\omega = 20\,\text{MeV}$, corresponding to $Z = 20$.

Except in the case of very low Z, the results shown in Fig. 8.4 can be used for estimates for ions with two electrons in the K shell. For excitation to the L shell, of an ion with two electrons in the K shell, we have

$$\sigma = \frac{28}{9}\alpha r_e^2 \cdot \frac{2^{11}}{3^8} = 0.56\,\text{mb}, \tag{8.112}$$

with 0.11 mb and 0.45 mb coming from excitation of the $2s$ and $2p$ states respectively. This cross section is about one-tenth that for ionization of the ground states of heavy atoms by the VAM mechanism.

We can make estimates for excitation of external electrons. They "feel" the strongly screened charge $Z \approx 1$. Thus we can put $\mu_i = \mu_f = m\alpha$. Employing (8.98), we find that the VAM is "switched on" at energies of about 100 MeV. Employing (8.94), one can see that the contribution of the Raman scattering is negligible at these energies. It follows from (8.91) that for moderate values of Z, VAM definitely dominates over the shakeup, while the case of large Z requires additional analysis.

References

1. D.E. Cullen, J.H. Hubbel, L. Kissel, *UCRLR-50400*, vol. 6 (Livermore, 1997)
2. V.B. Berestetskii, E.M. Lifshits, L.P. Pitaevskii, *Quantum Electrodynamics* (Pergamon, N.Y., 1982)
3. V.G. Gorshkov, A.I. Mikhailov, S.G. Sherman, Sov. Phys. JETP **37**, 572 (1973)
4. R.H. Pratt, L.A. LaJohn, V. Florescu, T. Surić, B.K. Chaterjee, S.C. Roy, Radiat. Phys. Chem. **79**, 124 (2010)
5. P.M. Bergstrom Jr., R.H. Pratt, Radiat. Phys. Chem. **50**, 3 (1997)
6. T. Surić, K. Pisk, P.M. Bergstrom Jr., R.H. Pratt, Phys. Rev. Lett. **67**, 189 (1991)
7. L. Rosenberg, F. Zhou, Phys. Rev. A **44**, 4283 (1991)
8. A.I. Akhiezer, V.B. Berestetskii, *Quantum Electrodynamics* (Pergamon, N.Y., 1982)
9. J. McEnnan, M. Gavrila, Phys. Rev. A **15**, 1537 (1977)
10. D.C. Ionescu, A.H. Sorensen, A. Belkacem, Phys. Rev. A **59**, 3527 (1999)
11. E.G. Drukarev, A.I. Mikhailov, I.A. Mikhailov, KhYu. Rakhimov, W. Scheid, Phys. Rev. A **75**, 032717 (2007)
12. V.I. Baier, V.S. Fadin, V.A. Khose, Sov. Phys. JETP **23**, 104 (1966)
13. D. Dauvergne et al., Phys. Rev. Lett. **90**, 153002 (2003)
14. E.G. Drukarev, A.I. Mikhailov, I.A. Mikhailov, W. Scheid, J. Phys. B **40**, 1501 (2007)

Chapter 9
Double Photoionization and Related Processes

Abstract We analyze three mechanisms of double photoionization. They are shakeoff (SO), final-state interactions (FSI) and the quasifree mechanism (QFM). We study their role in the distribution of photoelectrons and their contribution to the double-to-single cross section ratio $R_0(\omega) = \sigma^{++}(\omega)/\sigma^{+}(\omega)$ in the photoionization of the K shell of the helium atom and heliumlike ions. In the latter case, we analyze the nuclear charge dependence of characteristics of the process. The QFM is at work only beyond the dipole approximation. The QFM manifested itself in experiments on the distribution in the recoil momentum at photon energies $\omega \approx 800\,\text{eV}$. It modifies the shape of the spectrum curve at the energies of several keV. We demonstrate that the approximate wave functions employed in computations of the spectrum at these energies should satisfy the second Kato cusp condition. Otherwise, they can provide a qualitatively incorrect result. At energies of several hundred keV the QFM dominates in the large part of the photoelectron's energy distribution. It is also the main mechanism of breaking the nonrelativistic high-energy asymptotics of the ratio $R_0(\omega)$.

9.1 The General Picture

9.1.1 Objects of Investigation

Now we consider the process in which a single photon moves two bound electrons to the continuum. We focus on ionization of the ground state of the helium atom and of two-electron ions with both electrons in the K shell. The case of helium is best studied both in experimental and theoretical works.

There are three channels for interaction of the photon with the two bound electrons, which can be separated experimentally. In single ionization, one electron is moved to the continuum, while the second electron remains in the ground state. We denote the cross section by $\sigma^{+}(\omega)$. In ionization with excitation, the second electron moves to a state of the discrete spectrum with quantum numbers n, ℓ. The corresponding cross section is $\sigma^{+*}_{n\ell}(\omega)$. We denote the total cross section of ionization with excitation

E.G. Drukarev and A.I. Mikhailov, *High-Energy Atomic Physics*,
Springer Series on Atomic, Optical, and Plasma Physics 93,
DOI 10.1007/978-3-319-32736-5_9

by $\sum_{n\ell}\sigma^{+*}_{n\ell}(\omega) = \sigma^{+*}(\omega)$. In double ionization, both electrons are moved to the continuum. The cross section of this process is $\sigma^{++}(\omega)$. It is convenient to study the ratios

$$R(\omega) = \frac{\sigma^{++}(\omega)}{\sigma^{+}(\omega)+\sigma^{+*}(\omega)}, \tag{9.1}$$

which is the ratio of the cross sections of formation of the ions with $Z-2$ and $Z-1$ electrons and

$$R_0(\omega) = \frac{\sigma^{++}(\omega)}{\sigma^{+}(\omega)}, \tag{9.2}$$

representing the double-to-single cross section ratio with all the other electrons remaining in their states. The relative probability of excitations are described by the ratios

$$R^*_{n\ell}(\omega) = \frac{\sigma^{+*}_{n\ell}(\omega)}{\sigma^{+}(\omega)}; \quad R^*(\omega) = \sum_{n,\ell} R^*_{n\ell}(\omega)\,. \tag{9.3}$$

In double photoionization of the ground state of a two-electron ion,

$$\omega + E_b = \varepsilon_1 + \varepsilon_2, \tag{9.4}$$

with E_b the total energy of the system of two bound electrons, $\varepsilon_i = E_i - m$, $E_i^2 = p_i^2 + m^2$, E_i and $\mathbf{p}_i$ are the energies and momenta of the photoelectrons, and $p_i = |\mathbf{p}_i|$. Momentum

$$\mathbf{q} = \mathbf{p}_1 + \mathbf{p}_2 - \mathbf{k} \tag{9.5}$$

is transferred to the electrons by the nucleus. Here $\mathbf{k}$ is the photon momentum, $k \equiv |\mathbf{k}| = \omega$. If $\omega \ll m$, both photoelectrons carry the energies $\varepsilon_i \ll m$, and (9.4) can be written as

$$\omega - I^{2+} = \varepsilon_1 + \varepsilon_2 = \varepsilon; \quad \varepsilon_i = p_i^2/2m\,, \tag{9.6}$$

with $I^{2+} = 2m - E_b$; ε is the total energy carried by the photoelectrons.

Besides the total cross sections, studies of the double photoionization have focused on distributions of photoelectrons. There are also experimental and theoretical investigations of distributions of recoil momenta.

9.1.2 Mechanisms of the Process

At the photon energies $\omega - I^{++} \sim I_Z$, with $I_Z = m\alpha^2 Z^2/2$, the energies of both photoelectrons are of order $\varepsilon_{1,2} \lesssim I_Z$. There are no small parameters, and one should

just try to employ the most accurate functions Ψ_i and Ψ_f for describing the initial and final states in the double photoionization amplitude

$$F^{++} = N(\omega)\langle\Psi_f|\gamma|\Psi_i\rangle\,. \tag{9.7}$$

In the position representation, $\Psi_i(\mathbf{r}_1, \mathbf{r}_2)$ describes the ground state of a two-electron system bound by the field of the nucleus (further, we omit its lower index), $\Psi_f(\mathbf{r}_1, \mathbf{r}_2)$ describes the system of two interacting photoelectrons in the field of the nucleus. In (9.7),

$$\gamma(\mathbf{r}_1, \mathbf{r}_2) = \gamma_1 + \gamma_2 \tag{9.8}$$

describes the interaction of the photon with the bound system, with the two terms on the RHS corresponding to two electrons. In the nonrelativistic case,

$$\gamma_i = -ie^{i\mathbf{k}\cdot\mathbf{r}_i}\frac{\mathbf{e}\cdot\nabla_i}{m}\,. \tag{9.9}$$

Considering the energies $\omega \gg I_Z$ (for helium, this means that $\omega \gg 55\,\mathrm{eV}$), we have a small parameter

$$\frac{I_Z}{\omega} \ll 1\,, \tag{9.10}$$

and we can separate several mechanisms of the process, tracing their contributions to the amplitude. Also, in the region (9.10), the calculations become simpler, since at least one of the photoelectrons obtains the energy $\varepsilon \gg I_Z$, and its interactions with the nucleus can be treated perturbatively due to the small value of its Sommerfeld parameter $\xi = E\alpha Z/p \ll 1$. This photoelectron moves rapidly relative to the second one, with Sommerfeld parameter of their interaction $\xi_{ee} \approx E\alpha/p \ll 1$. This interaction also can be treated perturbatively.

Double photoionization can take place even if the FSI interactions between the photoelectrons are neglected. A bound electron interacts with the photon directly (we call it the "primary electron" and label it $i = 1$) and is knocked out to the continuum. Another bound electron (we call it the "secondary electron" and label it $i = 2$) is moved to the continuum due to a sudden change of the Hamiltonian of the system. This is the "shakeoff" (SO) mechanism, described in Sect. 3.2. It is reasonable to trace the acts of exchange by large momenta (much larger than the binding momentum), since each of them provides a small factor in the amplitude. In the shakeoff mechanism, a large momentum $q \approx p \gg \mu_b$ is transferred by one of the bound electrons to the nucleus. Thus this electron approaches the nucleus at the distance $r \sim 1/p \ll 1/\mu_b$. The configuration in which both electrons obtain large energies $\varepsilon_i \gg I_Z$ requires that both of them approach the nucleus at small distances.

In an alternative FSI mechanism, a bound electron is moved to the continuum by interaction with the photon. The photoelectron pushes the secondary one to the continuum in the next step. If the secondary electron is slow ($\varepsilon_2 \sim I_Z$), there is only one act of transfer of large momentum, when the first electron approaches the nucleus. Both final-state electrons can obtain $\varepsilon_{1,2} \gg I_Z$ if the electrons exchange large momentum in the final state.

The electron that directly interacts with the photon can transfer large momentum to the second one without participation of the nucleus. The interelectron distance r_{12} becomes small, i.e., $r_{12} \ll \mu_b^{-1}$, while both r_1 and r_2 are of order μ_b^{-1}. The photoelectrons leave the atom, transferring only small momentum $q \sim \mu_b$ to the nucleus. Following the general analysis presented in Chap. 2, the amplitude describing this quasifree mechanism (QFM) is proportional to that of the process on the system of free electrons. Such a process is possible if

$$\mathbf{p}_1 + \mathbf{p}_2 \;=\; \mathbf{k}\,. \tag{9.11}$$

This limits the difference between the energies of photoelectrons

$$\beta \;\equiv\; \frac{\varepsilon_1 - \varepsilon_2}{\varepsilon_1 + \varepsilon_2}\,. \tag{9.12}$$

Since $|\mathbf{k}| \geq |p_1 - p_2|$, we obtain

$$|\beta| \;\leq\; \sqrt{\frac{\varepsilon}{\varepsilon + m}}\,; \quad \varepsilon \;=\; \varepsilon_1 + \varepsilon_2\,. \tag{9.13}$$

Recall that $\varepsilon = \varepsilon_1 + \varepsilon_2 = \omega - I^{++}$ is the energy carried by the photoelectrons.

In the nonrelativistic case, we have $|\beta| \ll 1$, and the QFM manifests itself only in the vicinity of the center of the spectrum. Here $p_i \approx (m\omega)^{1/2}$.

Since in all mechanisms, exchange by large momenta takes place at distances $1/p_i$, in the nonrelativistic case, the partial wave expansion manifests itself as a power series in $k/p \sim \sqrt{\omega/m}$. The SO and FSI can be calculated in the dipole approximation, corresponding to $\mathbf{k} = 0$ in the power of the exponential factor on the RHS of (9.9). However, the QFM does not work in the dipole approximation. Indeed, since $\varepsilon_{1,2} = \varepsilon(1 \pm \beta)/2$, we can write the amplitude, describing absorption of the photon by the system of two free electrons as

$$F_0 = (\mathbf{e}\cdot\mathbf{p}_1) f(\omega, \varepsilon_1) + (\mathbf{e}\cdot\mathbf{p}_2) f(\omega, \varepsilon_2) = (\mathbf{e}\cdot\mathbf{p}_1) f(\omega, \beta) + (\mathbf{e}\cdot\mathbf{p}_2) f(\omega, -\beta). \tag{9.14}$$

The explicit form of the function $f(\omega, \beta)$ is not important. Since $|\beta| \ll 1$, we find that in the lowest order of expansion in powers of β,

$$F_0 \;=\; (\mathbf{e}\cdot(\mathbf{p}_1 + \mathbf{p}_2)) f(\omega, \beta = 0) = (\mathbf{e}\cdot\mathbf{k}) f(\omega, \beta = 0) = 0\,, \tag{9.15}$$

and the lowest nonvanishing term is

$$F_0 \;=\; 2(\mathbf{e}\cdot\mathbf{p}_1)\beta f'(\omega, \beta = 0)\,, \tag{9.16}$$

with f' the derivative with respect to β. Since for the free process $\beta = \mathbf{k}\cdot(\mathbf{p}_1 - \mathbf{p}_2)/2m\omega$, the QFM requires going beyond the dipole approximation, which would correspond to the lowest order of expansion in powers of k/p_i.

As we shall see, the QFM manifests itself in differential characteristics of the double photoionization of helium in the vicinity of the center of the spectrum at photon energies of order 1 keV and larger. It becomes increasingly important at higher energies. These points will be analyzed in Sects. 9.3 and 9.4. In Sect. 9.2, we consider the process in the dipole approximation, where it is a superposition of the SO and FSI contributions. The electrons are described by nonrelativistic functions, and the electron–photon vertex is described by the lowest order of expansion in powers of k/p.

9.2 Double Ionization in the Dipole Approximation

9.2.1 Nonrelativistic High-Energy Asymptotics for Helium

Here we demonstrate that the main contribution to the nonrelativistic high-energy asymptotics of the double photoionization cross section $\sigma^{2+}(\omega)$ is determined by the SO mechanism. The value of the cross section is determined by the "edge" part of the spectrum, where the primary electron carries most of the energy $\varepsilon_1 \approx \omega$, while the secondary electron carries the small energy $\varepsilon_2 \sim I_Z$. The angular distribution of the fast electrons is the same as in single photoionization. The secondary electrons carry angular momenta $\ell = 0$, and they have uniform angular distribution [1].

We begin with analysis of this case. In the asymptotics, the fast electron should be described by a plane wave, and the slow one by a nonrelativistic Coulomb function. In (9.7),

$$\Psi_f(\mathbf{r}_1, \mathbf{r}_2) = \frac{1}{\sqrt{2}}\Big(e^{i\mathbf{p}_1\cdot\mathbf{r}_1}\psi^C_{\mathbf{p}_2}(\mathbf{r_2}) + e^{i\mathbf{p}_1\cdot\mathbf{r}_2}\psi^C_{\mathbf{p}_2}(\mathbf{r_1})\Big), \tag{9.17}$$

with the upper index C standing for Coulomb. In the dipole approximation, we put $e^{i\mathbf{k}_1\cdot\mathbf{r}_1} = 1$ on the RHS of (9.8). The leading contribution to the amplitude comes from the first term on the RHS of (9.17) (the contribution of the second term is smaller by a factor of p_2/p_1). The amplitude is

$$F^{++} = \frac{\mathbf{e}\cdot\mathbf{p}_1}{m} N(\omega)\sqrt{2}\int d^3r_2 \psi^{C*}_{\mathbf{p}_2}(\mathbf{r_2}) J(\mathbf{p}_1; \mathbf{r}_2), \tag{9.18}$$

with

$$J(\mathbf{p}_1; \mathbf{r}_2) = \lim_{\lambda\to 0}\int d^3r_1 \Psi(\mathbf{r}_1, \mathbf{r}_2) e^{-i\mathbf{p}_1\cdot\mathbf{r}_1} e^{-\lambda r_1}. \tag{9.19}$$

Introducing $\zeta = \mathbf{r}_1\cdot\mathbf{r}_2$, we can write, in the same way as in Sect. 7.1, i.e., keeping the terms up to first order in the Taylor expansion,

$$\Psi(\mathbf{r}_1, \mathbf{r}_2) = \Psi(r_1, \zeta, r_2) = \Psi(0, 0, r_2) + \zeta\Psi'(0, \zeta, r_2)|_{\zeta=0} + r_1\Psi'(r_1, 0, r_2)|_{r_1=0}. \tag{9.20}$$

Similar to Sect. 7.1, we see that only the last term of the expansion provides a nonzero contribution to the integral on the RHS of (9.19). We find that

$$J(\mathbf{p}_1;\mathbf{r}_2) \;=\; -\frac{8\pi\Psi'(0,\mathbf{r}_2)}{p_1^4}(1+O(p_1^{-1})) \;=\; \frac{8\pi\eta\Psi(0,\mathbf{r}_2)}{p_1^4}(1+O(p_1^{-1})). \quad (9.21)$$

Here Ψ' denotes the derivative with respect to r_1 at $r_1 = 0$. The last equality is due to the first Kato cusp condition. Note that the RHS of (9.21) cannot be represented as a Taylor series at $r_2 \to 0$ due to the singularity of the wave function at $\mathbf{r}_1 = \mathbf{r}_2 = 0$. We obtain

$$F^{++} = \frac{\mathbf{e}\cdot\mathbf{p}_1}{m}N(\omega)\frac{8\pi\eta}{p_1^4}\sqrt{2}\Phi(\mathbf{p}_2); \quad \Phi(\mathbf{p}_2) = \int d^3r_2\psi^{C*}_{\mathbf{p}_2}(\mathbf{r}_2)\Psi(0,\mathbf{r}_2), \quad (9.22)$$

with $\eta = m\alpha Z$. The factor $\sqrt{2}$ is due to two electrons in the K shell.

Note that by approximating Ψ by a product of two single-particle functions $\psi^{s\cdot p\cdot}$, i.e., putting

$$\Psi_{appr}(\mathbf{r}_1,\mathbf{r}_2) \;=\; \psi^{s\cdot p\cdot}(\mathbf{r}_1)\psi^{s\cdot p\cdot}(\mathbf{r}_2), \quad (9.23)$$

we would obtain

$$F^{++} \;=\; F_{ph}\sqrt{2}\int d^3r\,\psi^{C*}_{\mathbf{p}_2}(\mathbf{r})\psi^{\mathbf{s}\cdot\mathbf{p}\cdot}(\mathbf{r}), \quad (9.24)$$

with F_{ph} the amplitude of single photoionization in the independent particle approximation expressed by (5.69). We shall see that (9.23) is not a good approximation for describing the asymptotics of double photoionization.

The SO amplitude of every photoionization process in a two-electron ion can be written in a similar way. Introducing

$$\psi(r_2) \;=\; \Psi(0,\mathbf{r}_2)\,, \quad (9.25)$$

we can write, for photoionization accompanied by transition of the secondary electron to the final state f,

$$F^{++} = F_{SO} = M\Phi_f; \quad M = M(\omega,\mathbf{p}_1) = N(\omega)\frac{\mathbf{e}\cdot\mathbf{p}_1}{m}\frac{8\pi\eta}{p_1^4}\sqrt{2}; \quad \Phi_f = \langle\psi_f^C|\psi\rangle. \quad (9.26)$$

We omit the index of the final state in the amplitudes F^{++} unless it is necessary to avoid misunderstanding. For the continuum states, we write $\Phi_{\mathbf{p}_2} = \Phi(\mathbf{p}_2)$. In the special case in which the secondary electron remains in the $1s$ state, this is just the amplitude of single photoionization, which we denote by F^+ in this section:

$$F^+ = M(\omega,\mathbf{p}_1)\Phi_{1s}; \quad \Phi_{1s} = \int d^3r_2\psi^C_{1s}(r_2)\psi(r_2) = \langle\psi^C_{1s}|\psi\rangle. \quad (9.27)$$

The integrals over r_2 on the RHS of (9.22) and (9.27) are saturated by $r_2 \sim 1/\mu_b$.

Now we consider another situation, in which the first electron absorbs only a small part of the photon energy $\varepsilon_1 \sim I_Z$, while the secondary electron carries a large energy $\varepsilon_2 \sim \omega$. If the secondary electron is described by a plane wave, a large momentum $q \approx p_2$ is transferred by the bound electron to the nucleus. Thus the amplitude contains a small factor μ_b^4/p_2^4, similar to that in (9.22). However, the photon–electron vertex now provides a factor of order μ_b/m instead of a factor of order $\sqrt{m\omega}/m$ in (9.22). Thus the amplitude corresponding to this mechanism is smaller than that described by (9.22) by a factor of at least $\mu_b/\sqrt{m\omega} \ll 1$.

In fact, the quenching is stronger due to cancellation of the contributions coming from the two lowest terms of the perturbative expansion for the wave function of the fast photoelectron. If we include the lowest-order Coulomb correction, a large momentum q can be transferred to the nucleus by the secondary electron. We put $\Psi_f(\mathbf{r}_1, \mathbf{r}_2) = \psi^C_{\mathbf{p}_1}(\mathbf{r_1})\psi_{\mathbf{p}_2}(\mathbf{r_2})$, where $\psi_{\mathbf{p}_2} = \psi^{(0)}_{\mathbf{p}_2} + \psi^{(1)}_{\mathbf{p}_2}$ is the sum of the plane wave and the lowest Coulomb correction; see (3.29). The corresponding contribution to the amplitude can be written as

$$F^{++} = F_0 + F_1; \quad F_k = \int d^3r_2 \Lambda(\mathbf{r}_2)\psi^{(k)*}_{\mathbf{p}_2}(\mathbf{r}_2), \tag{9.28}$$

with

$$\Lambda(\mathbf{r}_2) = N(\omega)\sqrt{2}\int d^3r_1 \psi^{C*}_{\mathbf{p}_1}(\mathbf{r}_1)\gamma(\mathbf{r}_1)\Psi(\mathbf{r}_1, \mathbf{r}_2); \quad \gamma(\mathbf{r}_1) = \frac{-i\mathbf{e}\cdot\nabla_1}{m}.$$

We find immediately that

$$F_0 = \tilde{\Lambda}(\mathbf{p_2}) = N(\omega)\sqrt{2}\int d^3r_1 \psi^{C*}_{\mathbf{p}_1}(\mathbf{r}_1)\gamma(\mathbf{r}_1)\int d^3r_2 \Psi(\mathbf{r}_1, \mathbf{r}_2)e^{-i\mathbf{p}_2\cdot\mathbf{r}_2}. \tag{9.29}$$

Recall that now $p_2 \gg \mu_b$. Integrating over r_2 using (9.19)–(9.21), we obtain

$$F_0 = -\frac{8\pi\Lambda'}{p_2^4}, \tag{9.30}$$

where Λ' denotes the derivative with respect to r_2 at $r_2 = 0$. Since the integral over r_1 is saturated at $r_1 \sim \mu_b$, the amplitude F_0 is suppressed by a small factor of order $\mu_b/\sqrt{m\omega}$ relative to that determined by (9.22). This is in agreement with the estimate given above.

One can see that the sum $F_0 + F_1$ is suppressed more strongly. We write (see (7.5))

$$F_1 = \int \frac{d^3f}{(2\pi)^3}\tilde{\Lambda}(\mathbf{f})\frac{-4\pi\alpha Z}{(\mathbf{p_2}-\mathbf{f})^2}\frac{2m}{p_2^2 - f^2}. \tag{9.31}$$

The integral converges at $f \sim \mu_b \ll p_2$. Neglecting f in two last factors, we obtain

$$F_1 = \frac{-8\pi\eta A(r_2=0)}{p_2^4}; \quad \eta = m\alpha Z, \tag{9.32}$$

and $F_0 + F_1 = 0$ due to the Kato condition. The higher Coulomb corrections provide the contributions of order $(\mu_b^2/p_2^2)F_0$ (recall that $p_2 \approx (2m\omega)^{1/2}$). Thus the contribution to the amplitude of the configuration with a fast secondary electron is smaller than that with a fast primary electron by a factor of μ_b^3/p_2^3 (we do not make difference between η and μ_b here).

If both primary and secondary electrons are fast, i.e., $p_{1,2} \gg \mu_b$, the amplitude obtains a small factor of order μ_b^4/p_2^4 relative to the amplitude (9.22) if the secondary electron is described by the plane wave. A calculation similar to (9.28)–(9.32) provides an additional small factor μ_b^2/p_2^2 if we include the lowest-order Coulomb correction $\psi^{(1)}_{\mathbf{p}_2}$. Thus, in spite of the large phase volume, the region $p_{1,2} \gg \mu_b$ provides a small contribution to the total cross section. The latter is described by the region $p_2 \sim \mu_b$ of the differential cross section

$$d\sigma^{++} = 2\pi\delta(\varepsilon_1 + \varepsilon_2 - \varepsilon)|F^{++}|^2 \frac{d^3p_1}{(2\pi)^3}\frac{d^3p_2}{(2\pi)^3}. \tag{9.33}$$

For $p_2 \sim \mu_b$, it can be written as

$$d\sigma^{++} = \frac{32\pi^2\sqrt{2}}{3} \cdot \frac{\alpha\cdot(\alpha Z)^2}{m^{3/2}\omega^{7/2}}|\Phi(\mathbf{p}_2)|^2\frac{d^3p_2}{(2\pi)^3}. \tag{9.34}$$

The cross section for single photoionization from the K shell, i.e., for the process in which one of the electrons is moved to the continuum while the second one remains in the $1s$ state, is

$$\sigma^{+} = \frac{32\pi^2\sqrt{2}}{3} \cdot \frac{\alpha\cdot(\alpha Z)^2}{m^{3/2}\omega^{7/2}}\Phi_{1s}^2; \tag{9.35}$$

see (7.13)–(7.14).

Note that since the function $\Psi(0, \mathbf{r}_2)$ depends only on the scalar r_2, the function Φ depends only on the energy of the secondary electron ε_2. This means that the secondary electrons are ejected with orbital momenta $\ell = 0$. Hence the function $\Phi(\mathbf{p}_2)$ does not depend on the direction of momentum $\mathbf{p_2}$ and can be represented as $\Phi(\varepsilon_2)$. The cross section can be represented as

$$\sigma^{++}(\omega) = \frac{16\sqrt{2}}{3} \cdot \frac{\alpha\cdot(\alpha Z)^2}{m^{1/2}\omega^{7/2}}\int_0^\omega d\varepsilon_2 p_2|\Phi(\varepsilon_2)|^2. \tag{9.36}$$

Here the integral over the energies of the secondary electrons is saturated at $\varepsilon_2 \sim I_b \ll \omega$.

Thus the SO contribution to the cross section comes from the edge region of the spectrum $\varepsilon_2 \lesssim I_Z$. Its contribution to the ratios $R(\omega)$ and $R_0(\omega)$ defined by (9.2) reaches constant values at $\omega \to \infty$. As to the FSI, they provide corrections of order ξ_{ee}^2 at $\varepsilon_2 \lesssim I_Z$. The contribution of the FSI of two fast electrons to these ratios can be obtained by integrating the energy distribution provided by (4.62) and (4.53) over the interval $\varepsilon_2 \sim \varepsilon$. Since $\langle r^{-2} \rangle \sim \mu_b^2$, we obtain the contribution to the cross section $\sigma^{++} \sim (\alpha^2 \mu_b^2/\omega^2)\sigma^+$, and thus for $\omega \gg I_Z$, the relative contribution of the FSI is much smaller than unity.

Employing (9.26) and (9.27), we obtain

$$\lim_{\omega\to\infty} R_0(\omega) \;=\; C_0; \quad C_0 \;=\; \frac{m}{2\pi^2 \Phi_{1s}^2} \int_0^\infty d\varepsilon_2 p_2 |\Phi(\varepsilon_2)|^2. \tag{9.37}$$

Since the integral converges at $\varepsilon_2 \lesssim I_Z \ll \omega$, we replaced the upper limit of integration ω by infinity. The Stobbe factors of both processes, which include the most important corrections caused by the interaction of the primary electrons with the nucleus, cancel in the ratio.

Note that in the early days of studies of double photoionization processes, investigators faced a paradox. Computations carried out employing the length form of electromagnetic interactions provided the behavior $F^{++} \sim F^+ p/\mu_b$ for the amplitude and thus $R_0 \sim \omega$ for the cross section ratio. The contribution came from the configuration in which the secondary electron carried most of the absorbed energy. In the length form, $\gamma = i\omega \mathbf{e} \mathbf{r}_1$. Proceeding in the same way as in (9.28)–(9.32), we write

$$F^{++} = \omega(F_{0L} + F_{1L}); \quad F_{kL} = \int d^3 r_2 \Lambda_L(\mathbf{r}_2) \psi_{\mathbf{p}_2}^{(k)*}(\mathbf{r}_2); \quad k = 0, 1 \tag{9.38}$$

with

$$\Lambda_L(\mathbf{r}_2) = N(\omega)\sqrt{2} \int d^3 r_1 \psi_{\mathbf{p}_1}^{C*}(\mathbf{r}_1) \gamma_L(\mathbf{r}_1) \Psi(\mathbf{r}_1, \mathbf{r}_2); \quad \gamma_L(\mathbf{r}_1) = i\omega \mathbf{e} \cdot \mathbf{r}_1,$$

and obtain

$$F_{0L} \;=\; -\frac{8\pi \Lambda_L'(r_2 = 0)}{p_2^4}; \quad F_{1L} \;=\; -\frac{8\pi \eta \Lambda_L(r_2 = 0)}{p_2^4}, \tag{9.39}$$

and the amplitude

$$F^{++} \;=\; -\frac{8\pi\omega}{p^4} c; \quad c \;=\; \Lambda_L'(r_2 = 0) + \eta \Lambda_L(r_2 = 0)\,, \tag{9.40}$$

which is indeed p/μ_b times larger than the amplitude of single photoionization F^+ if $c \neq 0$. The computations were carried out by employing approximate wave functions that do not satisfy the Kato condition. The latter provides $c = 0$ and

eliminates the spurious contribution. This was found by Åberg [2], who introduced the Kato conditions into atomic physics. This is an instructive example showing why theoretical analysis should precede computations.

The first calculations of the asymptotic value $R_0 = C_0$ for atomic helium were carried out with the approximate initial-state wave functions written as the products of single-particle wave functions; see (9.23). Taking ψ as the screened Coulomb functions with the effective charge $Z_{eff} = 27/16$ provided $C_0 = 7.2 \times 10^{-3}$. The Hartree–Fock functions gave $C_0 = 5.1 \times 10^{-3}$. Employing more complicated functions that include dependence on the interelectron distance $r_{12} = |\mathbf{r}_1 - \mathbf{r}_2|$ [3] provided the much larger value $C_0 \approx 1.7 \times 10^{-2}$, and a more contemporary CFHH approach described in Sect. 4.4.2 provided $C_0 = 1.74 \times 10^{-2}$ [4]. The latter results have been confirmed by the experimental data [5] presented in Fig. 9.1. The accuracy of the calculations is greater than that of the measurements. The uncorrelated wave functions failed to reproduce the asymptotic value of the double-to-single cross section ratio, since they do not describe the dynamics of the relative motion of the two bound electrons.

In similar way, one can calculate the cross section of photoionization with excitation of the secondary electron to the $n\ell$ state. This can be done by replacing $\Phi(\varepsilon_2)$ in (9.34) by

$$\Phi_{n\ell} = \int d^3 r_2 \psi^{C^*}_{n\ell}(\mathbf{r}_2)\Psi(0, \mathbf{r}_2). \tag{9.41}$$

The integral on the RHS becomes zero for $\ell \neq 0$. Thus we can put $\Phi_{n\ell} = \Phi_{ns}\delta_{\ell 0}$. The cross section can be written, similar to (9.34),

$$\sigma^{+*}_{ns}(\omega) = \frac{32\pi^2\sqrt{2}}{3} \cdot \frac{\alpha \cdot (\alpha Z)^2}{m^{3/2}\omega^{7/2}} \Phi^2_{ns}, \tag{9.42}$$

and thus the asymptotics of the ratios

$$R^*_n = \frac{\sigma^{+*}_{ns}(\omega)}{\sigma_{1s}(\omega)} = \frac{\Phi^2_{ns}}{\Phi^2_{1s}} = C_n \tag{9.43}$$

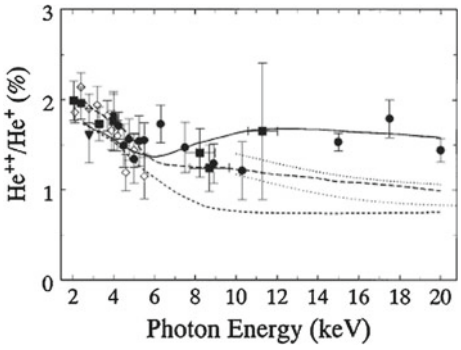

Fig. 9.1 Double-to-single ionization ratio for helium. The *horizontal* axis is for the photon energy in keV. The *dots* show the experimental points. The *lines* show the results of calculations in various approaches (see [5] for references) [5]

do not depend on the photon energy. Excitations to the states with $\ell \geq 1$ contribute beyond the asymptotics. The CFHH calculations provided $C_2 = 4.80 \times 10^{-2}$, $C_3 = 0.59 \times 10^{-2}$, $C_4 = 0.20 \times 10^{-2}$, while $R^* = 5.8 \times 10^{-2}$, and $R = 1.645 \times 10^{-2}$.

A smooth transition between excitations of discrete and continuum states requires that

$$\lim_{\varepsilon_2 \to 0} \frac{d\sigma^{++}}{d\varepsilon_2} = \lim_{n \to \infty} \frac{n^3 \sigma_n^{+*}}{2I_Z}\,. \tag{9.44}$$

Thus C_n^* decreases as n^{-3} at large n. One can see that (9.44) provides

$$\lim_{\varepsilon_2 \to 0} \frac{mp_2 \Phi(\varepsilon_2)}{4\pi^2} = \lim_{n \to \infty} n^3 C_n\,. \tag{9.45}$$

Due to the normalization factor of the continuum wave function, $\Phi(\varepsilon_2) \sim \varepsilon_2^{-1/2}$ at $\varepsilon_2 \to 0$, and the LHS of (9.45) obtains a finite value.

Employing the closure condition for the Coulomb functions, one obtains

$$\sum_{n=1}^{\infty} \Phi_{ns}^2 + \int \frac{d\varepsilon_2 mp_2}{2\pi^2} |\Phi(\varepsilon_2)|^2 = \int d^3r |\Psi(0, \mathbf{r})|^2, \tag{9.46}$$

leading to a remarkable sum rule [6]:

$$\sigma^+ + \sigma^{+*} + \sigma^{++} = \frac{32\pi^2\sqrt{2}}{3} \cdot \frac{\alpha \cdot (\alpha Z)^2}{m^{3/2}\omega^{7/2}} \int d^3r |\Psi(0, \mathbf{r})|^2. \tag{9.47}$$

9.2.2 *Nuclear Charge Dependence of Asymptotics for Heliumlike Ions*

Consider now the double photoionization of two-electron ions with $Z > 2$. It is reasonable to try a perturbative model in which interaction between electrons and the nucleus is included exactly, while interaction of the bound electrons is included in the lowest nonvanishing order of perturbation theory [7]; see Fig. 9.2. This corresponds to the lowest order of expansion in powers of $1/Z$. In the asymptotics, one can neglect the FSI of the photoelectrons. Since in atoms the K electrons are well separated from the others, we can expect that the approach can be applied at least for estimating the effects in atoms as well.

The wave function of the K shell electrons can be written as

$$\Psi = \Psi_0 + G V_{ee} \Psi_0\,. \tag{9.48}$$

Here G is the nonrelativistic two-electron Green function in the Coulomb field, while $\Psi_0(\mathbf{r}_1, \mathbf{r}_2) = \psi_{1s}(\mathbf{r}_1)\psi_{1s}(\mathbf{r}_2)$, with ψ_{1s} the single-particle function in the Coulomb

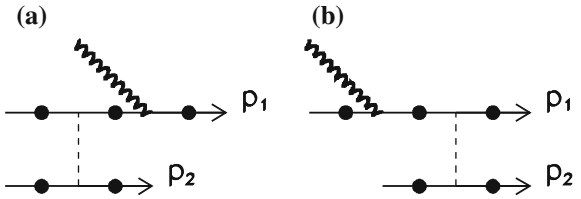

Fig. 9.2 Feynman diagrams illustrating the perturbative model for double photoionization. The *solid lines* stand for the electrons in the Coulomb field of the nucleus (labeled by *dark blobs*). The *helical line* is for the photon. The *dashed line* stands for the electron interaction in the initial state (**a**) or in the final state (**b**). In the asymptotics, only the diagram shown in (**a**) contributes

field. The final-state wave function is given by (9.17). Due to orthogonality of the wave functions, the first term on the RHS of (9.48) does not contribute to the amplitude.

In terms of the single-particle functions, the amplitude of the process can be written as

$$F^{++} = \sqrt{2}\frac{\mathbf{e}\cdot\mathbf{p}_1}{m}N(\omega)\int\frac{d^3f}{(2\pi)^3}X_2(\mathbf{f})\frac{4\pi\alpha}{f^2}X_1(\mathbf{f})\,, \tag{9.49}$$

where

$$X_1(\mathbf{f}) = \int\frac{d^3f_1}{(2\pi)^3}\langle\mathbf{p}_1|G(\varepsilon)|\mathbf{f}_1\rangle\langle\mathbf{f}_1+\mathbf{f}|\psi_{1s}\rangle;\quad X_2(\mathbf{f}) = \int\frac{d^3f_2}{(2\pi)^3}\langle\psi_{\mathbf{p}_2}|\mathbf{f}_2\rangle\langle\mathbf{f}_2-\mathbf{f}|\psi_{1s}\rangle. \tag{9.50}$$

The energy of the Coulomb propagator is $\varepsilon = -I^{2+} - \varepsilon_2 < 0$. Since we include the electron interactions in the lowest order of perturbative theory, we must put $I^{2+} = 2I_Z$, and $\varepsilon = -2I_Z - \varepsilon_2 < 0$. Note that the integrals are saturated by $f_1 \sim f \sim \mu_b = \eta$, while $p_1 \gg \eta$.

Under the latter condition, one can write for $p_1 \gg f_1$, similar to (2.86),

$$\langle\mathbf{p}_1|G|\mathbf{f}_1\rangle = \frac{8\pi\eta}{p_1^4}\int\frac{d^3q}{(2\pi)^3}\langle\mathbf{q}|G|\mathbf{f}_1\rangle\,, \tag{9.51}$$

writing

$$X_1(\mathbf{f}) = \frac{8\pi\eta}{p_1^4}X(\mathbf{f});\quad X(\mathbf{f}) = \int\frac{d^3f_1}{(2\pi)^3}\frac{d^3q}{(2\pi)^3}\langle\mathbf{q}|G(\varepsilon)|\mathbf{f}_1\rangle\langle\mathbf{f}_1+\mathbf{f}|\psi_{1s}\rangle. \tag{9.52}$$

Thus we can write, similar to (9.22),

$$F^{++} = M(\omega,\mathbf{p_1})\Phi(\varepsilon_2);\quad \Phi(\varepsilon_2) = \int\frac{d^3f}{(2\pi^3)}X(\mathbf{f})\frac{4\pi\alpha}{f^2}X_2(\mathbf{f}). \tag{9.53}$$

Integration over the electron momentum on the RHS of (9.53) can be carried out analytically, and the function $\Phi(\varepsilon)$ may be expressed through a one-dimensional integral. This can be done by employing the technique worked out in Sect. 5.1. Representing the 1s wave function in the form (5.12) and applying (5.55), we can integrate over $\mathbf{f}_1$ on the RHS of (9.52):

$$X(\mathbf{f}) = N_1 \hat{\Gamma} \int \frac{d^3q}{(2\pi)^3} \langle \mathbf{q}|V_{i\nu}G(\varepsilon)V_{i\lambda}|-\mathbf{f}\rangle|_{\nu=0,\lambda=\eta}; \quad N_1 = \left(\frac{\eta^3}{\pi}\right)^{1/2}, \tag{9.54}$$

$$\hat{\Gamma} = \frac{\partial}{\partial\nu}\frac{\partial}{\partial\lambda}.$$

Introducing $p = \sqrt{2m\varepsilon_2 + 2\eta^2}$, we obtain

$$\langle \mathbf{q}|V_{i\nu}G(\varepsilon)V_{i\lambda}|-\mathbf{f}\rangle \;=\; -p\hat{\Gamma}\hat{J}_y \frac{\langle \mathbf{q}|V_{i\mu}|\mathbf{f}A\rangle}{f^2+z_\lambda^2}, \tag{9.55}$$

with

$$z_\nu = py + \nu; \quad z_\lambda = py + \lambda; \quad \mu = z_\nu - z_\lambda A; \quad A = -\frac{p^2(y-1)}{f^2+z_\lambda^2}, \tag{9.56}$$

while

$$\hat{J}_y \;=\; 2m\int_1^\infty dy\left(\frac{y+1}{y-1}\right)^\zeta; \quad \zeta \;=\; \frac{m\alpha Z}{p}. \tag{9.57}$$

After calculation of the derivatives, we must put $\nu = 0$, $\lambda = \eta$.

In spite of the complicated dependence of the RHS of (9.55) on $\mathbf{f}$, integration over $\mathbf{q}$ leads to a very simple expression. One can see that

$$\frac{\partial}{\partial\nu}\langle \mathbf{q}|V_{i\mu}|\mathbf{a}\rangle \;=\; \frac{-\mu}{2\pi}\langle \mathbf{a}|V_{i\mu}|\mathbf{q}\rangle\langle \mathbf{q}|V_{i\mu}|\mathbf{a}\rangle \tag{9.58}$$

for every vector $\mathbf{a}$. Note that all dependence of the RHS of (9.55) on ν is contained in the parameter z_ν. Employing (5.46) and (5.8), we integrate over $\mathbf{q}$ and find that

$$\frac{\partial}{\partial\nu}\int\frac{d^3q}{(2\pi)^3}\langle \mathbf{q}|V_{i\mu}|\mathbf{f}A\rangle = -\frac{\mu}{2\pi}\int\frac{d^3q}{(2\pi)^3}\langle \mathbf{f}A|V_{i\mu}|\mathbf{q}\rangle\langle \mathbf{q}|V_{i\mu}|\mathbf{f}A\rangle = -1. \tag{9.59}$$

Thus we obtain

$$X(\mathbf{f}) = pN_1\hat{J}_y\frac{\partial}{\partial\lambda}\frac{1}{f^2+z_\lambda^2}; \quad X_1(\mathbf{f}) = \frac{2p\eta N_1}{p_1^4}\hat{J}_y\frac{\partial}{\partial\lambda}\langle \mathbf{f}|V_{iz_\lambda}|0\rangle. \tag{9.60}$$

Evaluating

$$X_2(\mathbf{f}) \;=\; N_1\Big(-\frac{\partial}{\partial\kappa}\Big)\langle\psi_{\mathbf{p}_2}|V_{i\kappa}|\mathbf{f}\rangle|_{\kappa=\eta} \tag{9.61}$$

and writing

$$\langle\mathbf{f}|V_{iz_\lambda}|0\rangle\cdot\frac{1}{f^2}=\frac{1}{z_\lambda^2}\Big(\langle\mathbf{f}|V_0|0\rangle-\langle\mathbf{f}|V_{iz_\lambda}|0\rangle\Big), \tag{9.62}$$

we carry out integration over $\mathbf{f}$ in the second equality on the RHS of (9.53):

$$\Phi(\varepsilon_2)=\alpha p N_1^2\hat{J}_y\frac{\partial}{\partial\lambda}\frac{1}{z_\lambda^2}\langle\psi_{\mathbf{p}_2}|V_{i\eta}-V_{i(\eta+z_\lambda)}|0\rangle|_{\lambda=\eta}. \tag{9.63}$$

Employing (5.28), we calculate, for every $\mathbf{p}$ and μ,

$$\langle\psi_{\mathbf{p}}|V_{i\mu}|0\rangle=4\pi N_p\frac{(\mu+ip)^{i\xi-1}}{(\mu-ip)^{i\xi+1}}=\frac{4\pi N_p}{p^2+\mu^2}exp(-2\xi\,\arctan 1/\xi);\quad \xi=\eta/p. \tag{9.64}$$

Finally, we obtain

$$\Phi(\varepsilon_2) \;=\; -8\pi\alpha p N_1^2 N_{p_2}\hat{J}_y\frac{T(y)}{(py+\eta)^3}\,. \tag{9.65}$$

Here

$$T(y) \;=\; \varphi_1(\eta)-\varphi_1(\rho)-(py+\eta)^2\varphi_2(\rho);\quad \rho \;=\; 2\eta+py, \tag{9.66}$$

$$\varphi_k(x)=\frac{(x+ip_2)^{i\xi_2-k}}{(x-ip_2)^{i\xi_2+k}}=\frac{exp(-2\xi_2\,\arctan\,p_2/x)}{(p^2+x^2)^k}\,.$$

Carrying out numerical integration on the RHS of (9.36), we find that in the asymptotics,

$$R(\omega) \;=\; C;\quad C \;=\; \frac{c}{Z^2};\quad c \;=\; 0.090. \tag{9.67}$$

Note that for the ratios defined by (9.1) and (9.2), we must put $R = R_0$ in the lowest order of the Z^{-1} expansion. For the case of helium, the perturbative model overestimates the value by about 30%.

It is amusing that the same result can be obtained from a very simple estimation for the magnitude of the effect. It is known that $1s$ electron in an atom with $Z \geq 3$ can be described roughly by the Coulomb function with the effective value of the nuclear charge $Z_{eff} = Z - s$, with $s \approx 0.3$ describing the "internal screening" [8]. The main contribution to the value of s comes from another $1s$ electron. After one of the electrons is moved to the continuum, the wave function of the remaining one changes by a value of order s/Z, and the probability of the SO is of order s^2/Z^2, where $s^2 \approx 0.09$.

The nuclear charge dependence of the asymptotic ratio R was traced for $Z \leq 10$ using variational functions of the ground state of the ion [9]. For the largest values of Z from this interval, the ratio exhibited the behavior

$$R \approx \frac{0.09}{Z^2} - \frac{0.03}{Z^3}. \tag{9.68}$$

The authors of [10] fitted their results by employing the CFHH functions (see Sect. 4.4.2), and the results of [9] by a three-terms formula,

$$R = \frac{a}{Z^2} + \frac{a'}{Z^3} + \frac{a''}{Z^4}, \tag{9.69}$$

for $2 \leq Z \leq 10$. The values of a, a', a'' were found by least squares fitting. The best fit for the data of [9] was obtained for $a = 0.090$, $a' = -0.022$, $a'' = -0.052$, while for the results of [10], it was $a = 0.090$, $a' = -0.021$, $a'' = -0.053$. Thus the perturbative approach indeed provides a proper value of the ratio R in the lowest nonvanishing order of the Z^{-1} expansion.

Photoionization accompanied by excitation can be calculated in framework of the perturbative model [11]. As we have seen, only excitations of s states can take place in the asymptotics. For ionization accompanied by excitation of the ns state,

$$R_n^*(\omega) = C_n = \frac{\Phi_{ns}^2}{\Phi_{1s}^2}, \tag{9.70}$$

where Φ_{ns} is given by the second equality of (9.53) with

$$X_2(\mathbf{f}) = \int \frac{d^3 f_1}{(2\pi)^3} \psi_{ns}^*(\mathbf{f_1}) \psi_{1s}(\mathbf{f_1} - \mathbf{f}), \tag{9.71}$$

while $X_1(\mathbf{f})$ is still given by the first equality of (9.50). There is no need to carry out new calculations. The function Φ_{ns} is determined by (9.65) with several changes. Now $p = \eta\sqrt{2 - n^{-2}}$, the normalization factor of the continuum wave function $N(\xi_2)$ should be replaced by that of the discrete spectrum $N_{ns} = \left(\eta^3/n^3\pi\right)^{1/2}$, and one should change p_2 to $i\eta/n$ and $i\xi_2$ to n in the functions $\varphi_{1,2}$ on the RHS of (9.66).

For the case of helium, the model provides the value of the cross section ratio for excitation of the $2s$ state $C_{2s}^* = 0.023$. This underestimates the results obtained with precise wave functions carried out by several groups by a factor of about 2. The discrepancy diminishes for larger values of n. The approach provides $C_{5s}^* = 7.6 \times 10^{-4}$, which differs from accurate results by about 15%.

Setting

$$C_n = \frac{c_n}{Z^2}, \tag{9.72}$$

Table 9.1 Values of a_n and a'_n in (9.73) calculated with the CFHH functions and the values of c_n obtained in the perturbative approach in units of 10^{-2}

n	a_n	a'_n	c_n
2	8.9	15.0	9.2
3	1.7	1.4	1.7
4	0.61	0.46	0.64
5	0.30	1.16	0.30
6	0.17	0.08	0.17

we obtain the values of c_n given in Table 9.1. The deviations from the behavior $c_n \cdot n^3 = \text{const}$ become less than 3% for $n \geq 5$.

Now we compare the results with those carried out with the CFHH functions for $Z \leq 10$ approximated by two terms of the Z^{-1} series

$$C_n = \frac{a_n}{Z^2} + \frac{a'_n}{Z^3}. \tag{9.73}$$

One can see that $c_n = a_n$ with good accuracy. Thus again, the perturbative approach provides the values of the ratios R_n^* in the lowest nonvanishing order of the Z^{-1} expansion. In contrast to the case of double photoionization, the perturbative model underestimates the values of the excitation cross sections.

In photoionization of the ground state, the secondary electron remains mostly in the $1s$ state and does not undergo transitions. The situation is different in photoionization of an excited state. We introduce the total cross section for absorption of the photon by the ion $\sigma_{tot} = \sigma^+ + \sigma^{+*} + \sigma^{++}$ and the relative probabilities for the channels with the secondary electrons in ns states of the discrete spectrum $r_{ns} = \sigma_{ns}^{+*}/\sigma_{tot}$ and in the continuum $r = \sigma^{++}/\sigma_{tot}$. The photon interacts mostly with the $1s$ electron, and usually two channels dominate [9]. For example, in the case of the metastable 2^1S state of helium, $r_{1s} = 0.049$, $r_{2s} = 0.535$, $r_{3s} = 0.399$. For the double photoionization, $r = 9 \times 10^{-3}$.

The negative ion of hydrogen is a very special case. The results obtained in [10] demonstrate that the probabilities of finding the secondary electron in the $1s$ state or in an excited ns state of the discrete spectrum are of the same order of magnitude: $r_{1s} = 0.590$; $\sum_{n=2} r_{ns} = 0.394$, and $r = 0.016$.

9.2.3 *Double Photoionization at Intermediate Energies*

Here we focus on the case of helium, discussing the cases of heavier atoms at the end of the subsection.

One can see from Fig. 9.1 that in helium, the asymptotic value of the double-to-single cross section ratio is reached at photon energies of order several keV. This can

be understood, since the contribution of the FSI to the cross section of the double photoionization is proportional to ξ_{ee}^2. The SO becomes the dominant mechanism if the asymptotic value $R_0 = C_0 \approx 1.7 \times 10^{-2}$ satisfies the condition

$$C_0 \gg \xi_{ee}^2 . \tag{9.74}$$

For helium, this is equivalent to $\omega \gg 800\,\text{eV}$. By "intermediate energies," we mean the values of the photon energies $\omega \gg I_Z$, where a perturbative description of at least one of the photoelectrons is possible, but on the other hand, deviations of the cross section ratios from their high-energy limit is noticeable (with the relative deviations exceeding 10%). For atomic helium, this is the region from 300–400 eV to 2 keV. This is in agreement with terminology of the review [12].

We move from the high-energy region by including next-to-leading terms of the expansion in powers of ω. There are several attractive points in this approach. It provides the possibility of clarifying the role of various mechanisms representing their contributions in terms of certain characteristics of the initial-state wave function. Within the framework of this approach, one can estimate the magnitude of the neglected terms, thus controlling the accuracy [13].

Corrections which behave as $1/p_1$ and $1/p_1^2$, with p_1 the momentum of the fast photoelectron, can be originated by correlations in both initial and final states. The amplitude can be written as

$$F^{++} = F^{SO} + F^{ISI} + F^{FSI} , \tag{9.75}$$

where ISI and FSI stand for the initial-state and final-state electron interactions. The leading amplitude F^{SO} is given by (9.22). Now we can write

$$R_0(\omega) = C_0 + \Delta^{corr}(\omega) , \tag{9.76}$$

with

$$\Delta^{corr}(\omega) = \frac{1}{|F^+|^2} \int \frac{d^3 p_2}{(2\pi)^3} \Big(|F^{SO} + F^{ISI} + F^{FSI}|^2 - |F^{SO}|^2 \Big). \tag{9.77}$$

We calculate $\Delta^{corr}(\omega)$ in the leading order of the $1/\omega$ series. Indeed, we have two small parameters, which are the Sommerfeld parameter of the FSI between the outgoing electrons $\xi_{ee} \approx m\alpha/p_1$ and the Sommerfeld parameter of the fast photoelectron $\xi_1 = \eta/p_1$. We shall write the final expressions in terms of ξ_{ee}, employing that $\xi_1 = 2\xi_{ee}$. Recall that the amplitude F^{SO} is real. As we have seen in Chap. 3, the amplitude F^{FSI} describing the final-state interactions has imaginary part proportional to $1/p_1$ and real part proportional to $1/p_1^2$. As we show below, the same refers to the amplitude F^{ISI}. Hence we can write

$$\Delta^{corr}(\omega) = \frac{1}{|F^+|^2} \int \frac{d^3 p_2}{(2\pi)^3} \Big[2F^{SO}(F_2^{ISI} + F_2^{FSI}) + |F_1^{ISI} + F_1^{FSI}|^2 \Big], \tag{9.78}$$

with

$$F^{ISI} = iF_1^{ISI} + F_2^{ISI}; \quad F^{FSI} = iF_1^{FSI} + F_2^{FSI}, \tag{9.79}$$

where F_i^{ISI} and F_i^{FSI} $(i = 1, 2)$ are real.

One can write similar corrections to the amplitude of a single photoionization F^+ when the second electron remains in the $1s$ state. However, the corresponding contributions to Δ^{corr} will be of order $\xi_{ee}^2 C_0$, and we have neglected them, since $C_0 \ll 1$. Nevertheless, we shall include the main correction of order $\xi_{ee}^2 C_0$, since it contributes with a numerically large coefficient. This is a kinematic correction that is due to the difference between the momentum of the fast photoelectron of double photoionization p_1 and that of single photoionization p. The corresponding contribution to the ratio is

$$\Delta^{kin}(\omega) = \frac{1}{|F^+(p)|^2 p} \int \frac{d^3 p_2}{(2\pi)^3} \Big[|F^{SO}(\mathbf{p}_2, p_1)|^2 - |F^{SO}(\mathbf{p}_2, p)|^2 \Big] p_1 \,. \tag{9.80}$$

In the single photoionization momentum of the photoelectron is

$$p = \sqrt{2m(\omega - I^+)}\,, \tag{9.81}$$

while the double photoionization momentum of the fast photoelectron is

$$p_1 = \sqrt{2m(\omega - I^{2+} - \varepsilon_2)} = p\left(1 - \frac{I_Z + \varepsilon_2}{2\omega}\right). \tag{9.82}$$

Here we neglected the higher-order terms of the expansion in powers of $1/\omega$, and employed that $I^{2+} - I^+ = I_Z$, with $I_Z = m\alpha^2 Z^2/2$, for helium $I_Z = 54.4\,\text{eV}$. We trace the corrections that are due to the difference between the value of the momentum of the fast electron p_1 and the value p determined by (9.81), which corresponds to single photoionization.

The amplitude F^{SO} behaves as p_1^{-3}, while the phase volume of the fast electron contains the factor p_1. Thus the double photoionization cross section is proportional to p_1^{-5}. The dependence on photoelectron momentum manifests itself also in corrections for the wave functions of the fast outgoing electrons. As we have seen in Chap. 7, in the case of single photoionization, we can separate the corrections depending on the parameter $\pi\xi$ $(\xi = \eta/p)$. This dependence manifests itself in the Stobbe factor $S(\pi\xi_1) = e^{-\pi\xi_1}$; see (7.46). There is a similar factor $S(\pi\xi_1)$ with $\xi_1 = \eta/p_1$ in the cross section of the double photoionization. Note that $\pi\xi = 1$ at $\omega \approx 560\,\text{eV}$, and we do not treat $\pi\xi$ as a small parameter. Thus (9.80) can be evaluated as

$$\Delta^{kin}(\omega) = \frac{m}{2\pi^2 |\Phi_{1s}|^2} \int_0^{\omega/2} d\varepsilon_2 p_2 \left[\frac{p^5}{p_1^5} e^{-\pi(\xi_1 - \xi)} - 1 \right] |\Phi(\varepsilon_2)|^2. \tag{9.83}$$

This provides

$$\Delta^{kin}(\omega) = \frac{\xi^2}{2}(5-\pi\xi)\Big(1+\frac{\langle\varepsilon_2\rangle}{I_Z}\Big)C_0, \tag{9.84}$$

where

$$\langle\varepsilon_2\rangle = \frac{\int_0^{\omega/2} d\varepsilon_2 p_2 |\Phi(\varepsilon_2)|^2 \varepsilon_2}{\int_0^{\omega/2} d\varepsilon_2 p_2 |\Phi(\varepsilon_2)|^2}. \tag{9.85}$$

Note that $\Delta^{kin} > 0$.

Now we calculate the contributions caused by correlations in the initial state. To calculate the amplitude F^{ISI}, we must include the higher corrections of the expansion in powers of $1/p_1 \approx 1/p$ on the RHS of (9.21). Since the process takes place at the distances $r_1 \sim p_1$, expansion of the amplitude in powers of $1/p_1$ corresponds to expansion in powers of $\mathbf{r}_1$ of the integrand on the RHS of (9.19). To obtain these terms, we carry out the Taylor expansion for the wave function $\Psi(\mathbf{r}_1, \mathbf{r}_2)$ near the point $\mathbf{r_1} = 0$:

$$\Psi(r_1, r_2, r_{12}) = \Psi(0, r_2, r_2) + r_1 \frac{\partial\Psi}{\partial r_1}|_{r_1=0} + (r_{12}-r_2)\frac{\partial\Psi}{\partial r_{12}}|_{r_{12}=r_2} + \cdots. \tag{9.86}$$

As we have seen in Chap. 7, the leading contribution is provided by the term containing the first derivative. Thus to obtain corrections to the cross section of the relative order p_1^{-2}, we must include the Taylor expansion up to the third order. The terms of the expansion contain the powers of r_1 and $\mathbf{r}_1 \cdot \mathbf{r}_2$. The integrals containing the powers of r_1 are

$$X_n = \lim_{\lambda\to 0}\int d^3 r_1 r_1^n e^{-i\mathbf{p}_1\cdot\mathbf{r}_1} e^{-\lambda r_1}; \quad X_0 = \lim_{\lambda\to 0}\frac{8\pi\lambda}{(p_1^2+\lambda^2)^2} = 0; \tag{9.87}$$

$$X_1 = \frac{-8\pi}{p_1^4}; \quad X_2 = 0; \quad X_3 = \frac{96\pi}{p_1^6}.$$

The integrals containing the powers of $\mathbf{r}_1 \cdot \mathbf{r}_2$ are calculated using the relation $\mathbf{r}_1 e^{-i\mathbf{p}_1\cdot\mathbf{r}_1} = i\nabla e^{-i\mathbf{p}_1\cdot\mathbf{r}_1}$, with the gradient taken with respect to $\mathbf{p}_1$. Thus the contribution of the odd powers of the product $\mathbf{r}_1 \cdot \mathbf{r}_2$ are imaginary. Note also that $\lim_{\lambda\to 0}\int d^3 r_1 r_1^n (\mathbf{r}_1\cdot\mathbf{r}_2)^k e^{-i\mathbf{p}_1\cdot\mathbf{r}_1} e^{-\lambda r_1} = 0$ for even n and every integer k. Thus some of the terms on the RHS of (9.86) vanish after integration over r_1.

Keeping only the terms that will survive, we write

$$\Psi(r_1, r_2, r_{12}) = r_1\psi^{10} + r_1\delta\psi^{11} + \frac{r_1\delta^2}{2}\psi^{12} + \frac{r_1^3}{6}\psi^{30}. \tag{9.88}$$

Here we defined

$$\delta \;=\; r_{12} - r_2 \;=\; -\frac{\mathbf{r}_1 \cdot \mathbf{r}_2}{r_2} - \frac{(\mathbf{r}_1 \cdot \mathbf{r}_2)^2}{2r_2^3} + \frac{r_1^2}{2r_2} \tag{9.89}$$

and

$$\psi^{nk}(r_2) \;=\; \frac{\partial^{n+k}\Psi(r_1, r_2, r_{12})}{\partial^n r_1 \partial^k r_{12}}|_{r_1=0, r_{12}=r_2}\,. \tag{9.90}$$

Employing (9.87) for integration over $\mathbf{r}_1$ on the RHS of (9.22), we can write for the ISI amplitude

$$F_1^{ISI} = \xi_{ee} M(\omega, \mathbf{p}_1)\Phi_1^{ISI}(\mathbf{p}_2); \quad F_2^{ISI} = \xi_{ee}^2 M(\omega, \mathbf{p}_1)\Phi_2^{ISI}(\mathbf{p}_2),$$

with M determined by (9.26), and

$$\Phi_1^{ISI}(\mathbf{p}_2) = -\frac{4}{\eta\nu}\langle\psi_{\mathbf{p}_2}^C|\mathbf{n}\cdot\mathbf{r}/r|\psi^{11}\rangle; \quad \Phi_2^{ISI}(\mathbf{p}_2) = \frac{8}{\eta\nu^2}\langle\psi_{\mathbf{p}_2}^C|\frac{1-3(\mathbf{n}\cdot\mathbf{r})^2/2r^2}{r}|\psi^{11}\rangle - \tag{9.91}$$
$$\frac{4}{\eta\nu^2}\langle\psi_{\mathbf{p}_2}^C|1-6(\mathbf{n}\cdot\mathbf{r})^2/r^2|\psi^{12}\rangle + \frac{2}{\eta\nu^2}\langle\psi_{\mathbf{p}_2}^C|\psi^{30}\rangle; \quad \eta = m\alpha Z; \quad \nu = m\alpha,$$

and $\mathbf{n} = \mathbf{p}_1/p_1$. Note that $F_1^{ISI}(\mathbf{p}_2)$ describes ejection of the secondary electrons with orbital momenta $\ell = 1$. The amplitude $F_2^{ISI}(\mathbf{p}_2)$ corresponds to ejection of the electrons with orbital momenta $\ell = 0$ and $\ell = 2$. Only the terms describing the secondary electrons with $\ell = 0$ interfere with the SO terms.

For the FSI amplitude we obtain, employing the results of Chap. 3,

$$F_1^{FSI} = \xi_{ee} M(\omega, \mathbf{p}_1)\Phi_1^{FSI}(\mathbf{p}_2); \quad F_2^{FSI} = \xi_{ee}^2 M(\omega, \mathbf{p}_1)\Phi_2^{FSI}(\mathbf{p}_2); \tag{9.92}$$

$$\Phi_1^{FSI}(\mathbf{p}_2) = \langle\psi_{\mathbf{p}_2}^C|\ln(r - r_z)\lambda)|\psi\rangle;$$

$$\Phi_2^{FSI}(\mathbf{p}_2) = \frac{1}{2}\langle\psi_{\mathbf{p}_2}^C|r_0\frac{\partial}{\partial r}|\psi\rangle - \frac{1}{2}\langle\psi_{\mathbf{p}_2}^C|\ln^2(r - r_z)\lambda|\psi\rangle,$$

with $\lambda \to 0$, while z denotes the direction of the fast photoelectron momentum. Recall that here $\psi = \Psi(0, \mathbf{r})$. Thus we can write

$$\Delta^{corr}(\omega) = \frac{1}{\Phi_{1s}^2}\int\frac{d^3p_2}{(2\pi)^3}(2\Phi(\mathbf{p}_2)\Phi_2^{ISI}(\mathbf{p}_2) + 2\Phi(\mathbf{p}_2)\Phi_2^{FSI}(\mathbf{p}_2) + \tag{9.93}$$

$$+ |\Phi_1^{ISI}(\mathbf{p}_2) + \Phi_1^{FSI}(\mathbf{p}_2)|^2),$$

with the terms containing $\ln\lambda$ canceling on the RHS.

For illustration, we carry out computations employing a ground-state wave function depending on its variables explicitly. We use a simple version of the Bonham–Kohl(BK) functions [14]

$$\Psi(r_1, r_2, r_{12}) \;=\; N_0\Big(e^{-\mu_1 r_1-\mu_2 r_2}+e^{-\mu_2 r_1-\mu_1 r_2}\Big)\Big(1-ce^{-\lambda r_{12}}\Big), \tag{9.94}$$

with $\mu_1 = 2.21\nu$, $\mu_2 = 1.41\nu$, $\lambda = 0.24\nu$, $c = 0.61$, and $N_0 = 1.64\nu^2$, while $\nu = m\alpha$. This wave function provides the proper value of the binding energy and reproduces the true value of the asymptotics C_0. The BK functions provide $\langle\varepsilon_2\rangle/I_Z = 0.58$, and thus $\Delta^{kin} = (0.068 - 0.014\pi\xi)\xi^2$. Recall that $\xi = m\alpha Z/p$. The contributions to Δ^{corr} depend on the parameter $\xi_{ee} \approx m\alpha/p$. For the BK functions, $\Delta^{corr} = 0.87\xi_{ee}^2$. Note that $\pi\xi = 0.96$ for $\omega = 600\,\text{eV}$, while $\pi\xi = 0.42$ for $\omega = 3\,\text{keV}$. Thus we can put $\pi\xi \approx 0.7$, leading to

$$\Delta^{kin}(\omega) \;=\; 0.23\xi_{ee}^2, \tag{9.95}$$

with the final result

$$\Delta(\omega) \;=\; \Delta^{kin}(\omega)+\Delta^{corr}(\omega) \;=\; 1.10\xi_{ee}^2. \tag{9.96}$$

Thus we have obtained

$$R_0(\omega) \;=\; C_0 + 1.10\xi_{ee}^2; \quad \xi_{ee}^2 \;=\; \frac{13.6\,\text{eV}}{\omega} \tag{9.97}$$

for the preasymptotic behavior of the cross section ratio; see Fig. 9.3. The FSI determines about 70% of the value. Since $\Delta(\omega) > 0$, the cross section ratio approaches the asymptotic value from above. Since at the threshold, the cross section of the double photoionization vanishes (just due to the vanishing phase volume), while that for single photoionization does not, the ratio also becomes zero. Hence, it peaks at a certain finite value of the photon energy above the threshold. This peak was observed in a number of experiments.

The contribution of the final-state interactions is dominated by the imaginary part of the amplitude F_1^{FSI} represented by second term on the RHS of (9.92). This is because the real part of the amplitude F_2^{FSI} is multiplied by the SO matrix element $\langle\psi_{\mathbf{p}_2}^C|\psi\rangle$, which is numerically small. Neglecting the correlations in the initial state, we have $\Delta^{corr} = \Delta^{FSI}$. The value of Δ^{FSI} does not depend strongly on the correlations in the ground state. The Hartree–Fock functions, which we have seen to underestimate the SO value for the cross section, provide $\Delta^{FSI} = 0.75\xi_{ee}^2$. Even neglecting the electron interactions in the ground state, i.e., describing the ground state by the product of two single-particle Coulomb functions with $Z = 2$ (9.23), we obtain $\Delta^{FSI} = 0.91\xi_{ee}^2$.

While the SO mechanism provides the monopole secondary electrons, the correction $\Delta(\omega)$ is a superposition of contributions Δ_ℓ. The distribution over the angular

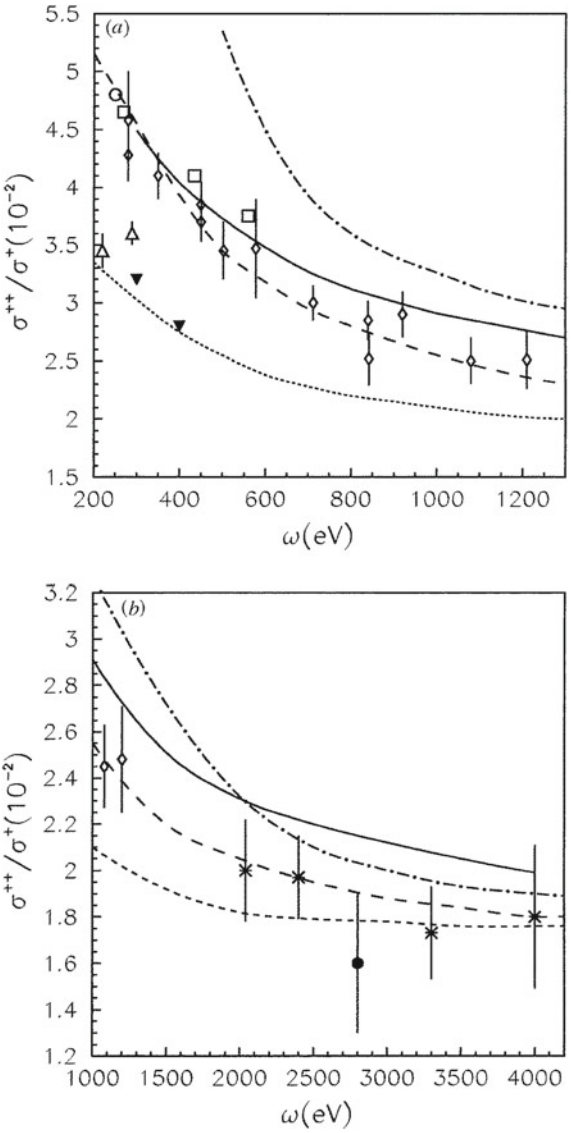

Fig. 9.3 Double-to-single photoionization ratio for the helium atom. The *horizontal* axis is for the photon energy in eV. The *black dots*, *triangles*, and *square* show the experimental data (the references are listed in [13]). The *solid line* represents the results of calculation employing (9.97). The other *lines* are for the calculations carried out in other approaches (see [13] for references) [13]

momenta is characterized by the parameter

$$a_\ell = \frac{\Delta_\ell}{\Delta}; \quad \Delta = \sum \Delta_\ell \,. \tag{9.98}$$

Employing the functions defined by (9.94) we find

$$a_0 = 0.29; \quad a_1 = 0.48; \quad a_2 = 0.12; \quad a_3 = 0.05, \tag{9.99}$$

with domination of dipole and monopole terms.

For the double photoionization of the K shell of heliumlike ions, it is reasonable to try the perturbative model formulated in Sect. 9.2.2, extending it to the lower energies $\omega \sim I_Z$. This was done in [15]. The initial-state wave function was given by (9.48), while the final-state wave function was represented as

$$\Psi_f = \Psi_f^0 + G V_{ee} \Psi_f^0 , \tag{9.100}$$

where Ψ_f^0 is the symmetrized product of two Coulomb functions describing the photoelectrons with momenta $\mathbf{p}_{1,2}$. As in (9.48), G is the nonrelativistic two-electron Green function in the Coulomb field. The second terms on the RHS of (9.48) and (9.100) contain the Sommerfeld factors of electron interaction $\xi_{ee} = \alpha/v$, with v the velocity of relative motion of the electrons. In the initial state $v \approx \alpha Z$, and the Sommerfeld parameter for the electron interaction is $\xi_{ee}^i \approx 1/Z$. At $\omega \sim I_Z$, the same refers to the final state. Thus the amplitude

$$F^{++} = N(\omega)\Big(\langle \Psi_f^0 | \gamma G(\varepsilon_a) V_{ee} | \Psi \rangle + \langle \Psi_f^0 | V_{ee} G(\varepsilon_b) \gamma | \Psi \rangle \Big), \tag{9.101}$$

with $\varepsilon_a = \varepsilon_1 - \omega$; $\varepsilon_b = \omega - I_Z$, and γ the operator of the $e-\gamma$ interaction determined by (9.8), provides the amplitude in the lowest order of expansion in powers of $1/Z$.

At $\omega \gg I_Z$, the first term on the RHS of (9.101) is still of order $\xi_{ee}^i \approx 1/Z$, while the second term is of order $\xi_{ee} \approx \alpha\sqrt{m/2\omega}$. Inclusion of higher terms in the interaction V_{ee} would provide the higher terms of expansions in powers of $1/Z$ and ξ_{ee}. Thus for $\omega \gg I_Z$, the amplitude (9.101) reproduces the leading terms of expansion in powers of $1/Z$ and ξ_{ee}. Note that the amplitude does not contain infrared logarithmic divergent terms (see Sect. 3.2). Recall the origin of such terms. After one of the electrons leaves the atom (ion), the field that is felt by the secondary electron changes and is shaken to an excited state. In the next step, the photoelectron undergoes elastic scattering on the shaken one. This provides the logarithmic divergent phase. In the present model all electrons move in the same field, and such terms do not emerge.

Since the K electrons are well separated from the other bound electrons, the results can be, with some modifications, used for the process in the neutral atoms. We employ the only modification of assuming that the K electrons move in the Coulomb field with the effective charge of the nucleus Z_{eff} determined by the condition that the experimental single-electron binding energy is equal to its nonrelativistic Coulomb field value with charge Z_{eff}, i.e., $I_{\rm exp} = m\alpha^2 Z_{eff}^2/2$. Some of results are given in Table 9.2.

Table 9.2 The double-to-single photoionization ratio for a number of neutral atoms; $w = \omega/I_{exp}$ is the energy carried by the photoelectrons

Z	I_{exp}, keV	w	Z_{eff}	R_{exp}	R_{theor}
10	0.87	5.75	8.0	3.2(−3) [16]	2.8(−3)
22	4.97	3.50	19.1	5.3(−4) [17]	5.1(−4)
26	7.12	2.44	22.9	2.4(−4) [17]	2.3(−4)
29	8.99	2.22	25.7	1.3(−4) [18]	1.1(−4)

The numbers in parentheses are the powers of 10. The theoretical data are taken from paper [15]

9.2.4 *Photoionization Followed by Excitation: Intermediate Energies*

Recall that in the nonrelativistic high-energy limit, the excitation of an electron to the shell with a principal quantum number n following photoionization is due to the specific correlation in the initial state known as the shakeup (SU). Only s states can be excited by this mechanism. Excitation of the states with nonzero angular momenta are quenched by factors that decrease as ω^{-1}. Similar to the double photoionization, we can write for the ratios defined by (9.3)

$$R^*_{ns}(\omega) \;=\; C^*_{ns} + \Delta_{ns}(\omega) \tag{9.102}$$

for $\ell = 0$, and

$$R^*_{n\ell}(\omega) \;=\; \Delta_{n\ell}(\omega), \tag{9.103}$$

for $\ell \geq 1$. For excitation of s states, we calculate the lowest-order correction of the asymptotics. For excitation of the states with $\ell > 0$, we obtain the leading contribution of the expansion in powers of $1/\omega$.

We begin with the excitation of s states. As in the case of double photoionization, there are contributions of kinematic corrections and corrections caused by correlations in the initial and final states. The contributions of the kinematic corrections can be obtained by replacing $\langle \varepsilon_2 \rangle$ by $-I_Z/n^2$ on the RHS of (9.84). Recalling that $\xi = 2\xi_{ee}$, we obtain

$$\Delta^{kin}_{ns}(\omega) \;=\; 2\xi^2_{ee}(5 - \pi\xi)(1 - \frac{1}{n^2})C^*_{ns}, \tag{9.104}$$

with $\xi = \eta/p$, where p is the momentum of photoelectron, and we put $p = (2m\omega)^{1/2}$.

One can obtain the amplitudes that describe the contributions of correlations in the initial and final states from expressions for the amplitudes F^{ISI} and F^{FSI} for the double photoionization given by (9.93) and (9.92), replacing $\psi^C_{\mathbf{p}_2}$ by ψ^C_{ns}. Now we need only the real part of the amplitude F^{ISI}. Setting $F^{ISI}_{ns} = \xi^2_{ee} M U_n$ and employing (9.91), we obtain for the contribution corresponding to the orbital momentum $\ell = 0$ of the secondary electron

$$U_n = \frac{4}{\eta\nu^2}\int_0^\infty drrR_{ns}(r)\psi^{11}(r) + \frac{4}{\eta\nu^2}\int_0^\infty drr^2R_{ns}(r)\psi^{12}(r) + \tag{9.105}$$

$$+\frac{2}{\eta\nu^2}\int_0^\infty drr^2R_{ns}(r)\psi^{30}(r),$$

with $R_{ns}(r)$ the radial part of $\psi^C_{ns}(\mathbf{r})$, $\nu = m\alpha$. Hence

$$\Delta^{ISI}_{ns}(\omega) = 2\xi^2_{ee}\frac{\Phi_{ns}U_n}{\Phi^2_{1s}}. \tag{9.106}$$

In the description of the FSI correlations, we omit the contributions of order $\xi^2_{ee}C^*_{ns}$, since they contain two small factors. We write $F^{FSI}_{ns} = i\xi_{ee}MS_n + \xi^2_{ee}MT_n$, with

$$S_n = \int_0^\infty drr^2R_{ns}(r)\ln(r\lambda)\psi(r); \quad T_n = \frac{r_0}{2}\int_0^\infty drr^2R_{ns}(r)\psi'(r) -$$

$$-\frac{1}{2}\int_0^\infty drr^2R_{ns}(r)\ln^2(r\lambda)\psi(r). \tag{9.107}$$

This leads to

$$\Delta^{FSI}_{ns}(\omega) = \xi^2_{ee}\frac{2\Phi_{ns}T_n + S^2_n}{\Phi^2_{1s}}. \tag{9.108}$$

Finally,

$$\Delta_{ns}(\omega) = \Delta^{kin}_{ns}(\omega) + \Delta^{ISI}_{ns}(\omega) + \Delta^{FSI}_{ns}(\omega). \tag{9.109}$$

Excitation of the p states can take place only beyond the SU approximation. The ISI and FSI contributions can be obtained by changing $\psi^C_{\mathbf{p}_2}$ to ψ^C_{n1m} in the expressions for F^{ISI}_1 and F^{FSI}_2 in (9.92). Choosing the direction of momentum of the photoelectron as the axis of quantization of the angular momentum, we find that the secondary electrons can be excited only to the states with $m = 0$. We obtain

$$F^{ISI}_{np} = i\xi_{ee}M(\omega,\mathbf{p}_1)V_n; \quad V_n = -\frac{4\sqrt{3}}{3}r^2_0\int_0^\infty drr^2R_{np}(r)\psi^{11}(r); \tag{9.110}$$

$$F^{FSI}_{np} = i\xi_{ee}M(\omega,\mathbf{p}_1)W_n; \quad W_n = -\frac{\sqrt{3}}{2}\int_0^\infty drr^2R_{np}(r)\psi(r),$$

leading to

$$\Delta_{np}(\omega) \;=\; \xi_{ee}^2 \frac{(V_n + W_n)^2}{\Phi_{1s}^2}\,. \tag{9.111}$$

For $\ell \geq 1$, only the FSI contribute to the asymptotics. Replacing $\psi_{\mathbf{p}_2}^C$ by $\psi_{n\ell 0}^C$ in the expression (9.92) for F_1^{FSI}, we obtain

$$\Delta_{n\ell}(\omega) \;=\; \xi_{ee}^2 \frac{2\ell+1}{\ell^2(\ell+1)^2} \frac{D_{n\ell}^2}{\Phi_{1s}^2}; \quad D_{n\ell} = \int\limits_0^\infty dr r^2 R_{n\ell}(r)\psi(r). \tag{9.112}$$

Here we employed (7.176) for calculation of the angular integral.

Calculations for the helium atom carried out by employing the CFHH functions [19] demonstrate that in the excitation of s states, all the components of the energy-dependent contributions to the ratios $R_{n\ell}^*$ presented by (9.109) are important, and there are some cancellations between them. In the excitation of p states, the contribution of FSI provides about 4/5 of the ratios R_{np}^*. Excitations of s and p states provide contributions of the same order of magnitude to the total cross section of excitation of the shell with the given principal quantum number. Excitation of d states gives about 10% of the latter. Contributions of the states with $\ell \geq 3$ are much smaller. For example, the cross section for excitation of the $4f$ state is about 1/20 that of the $4d$ state. For all n and ℓ, we write $\Delta_{n\ell} = \xi_{ee}^2 B_{n\ell}$, where B_{ns} depends on the photon energy in terms of the parameter $\zeta = \pi\xi_1$. For $\ell \geq 1$, the parameter $B_{n\ell}$ does not depend on ω. We present some numerical results for $B_{n\ell}$ and $B_n = \sum_\ell B_{n\ell}$ in Table 9.3.

The calculated ratios R_n^* for helium can be compared with the unique set of experimental data obtained by Wehlitz et al. [20]; see Fig. 9.4. As expected, a noticeable discrepancy takes place only for $\omega \leq 300$ eV. The largest deviations of theoretical results from experimental data are reached for $n = 2$. For $n = 6$, experimental data

Table 9.3 Values of $B_{n\ell}$ for ionization accompanied by excitation of a secondary electron to the $n\ell$ state and $B_n = \sum_\ell B_{n\ell}$; $\zeta = \pi\xi$

State	$B_{n\ell}$	B_n
$2s$	$0.19 - 0.07\zeta$	
$2p$	0.13	$0.32 - 0.07\zeta$
$3s$	$(3.0 - 1.1\zeta) \times 10^{-2}$	
$3p$	1.9×10^{-2}	
$3d$	3.1×10^{-3}	$(5.2 - 1.1\zeta) \times 10^{-2}$
$4s$	$(1.0 - 0.4\zeta) \times 10^{-2}$	
$4p$	6.2×10^{-3}	
$4d$	1.4×10^{-3}	
$4f$	7.9×10^{-5}	$(1.8 - 0.4\zeta) \times 10^{-2}$

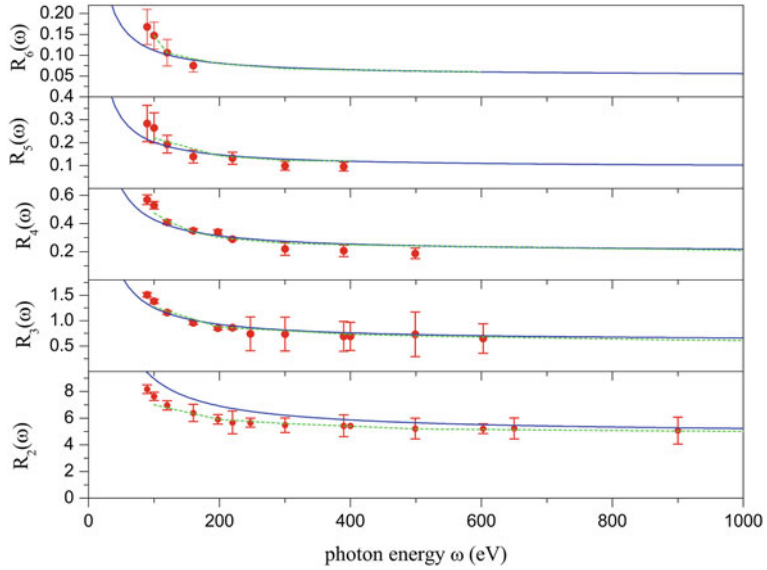

Fig. 9.4 The ratio $R_n(\omega)$ for the photoionization cross section of the helium atom accompanied by excitation of the second electron to the shell with the main quantum number n related to the single photoionization cross section. The *horizontal* axis is for the photon energy in eV. The *dots* show the experimental data obtained in [20]. The *solid line* shows the results of calculation based on (9.112) by employing the CFHH functions [19]

are available only for $\omega \leq 160$ eV. However, even here, the discrepancy between the experimental and theoretical results is not large.

In Sect. 9.2.3, we described a model of double photoionization developed in [15] in which all the electron interactions with the nucleus are included exactly, while the interactions between the electrons are treated in the lowest order of perturbation theory. The approach was extended to studies of photoionization accompanied by excitation [21]. The universal functions $H_{n\ell}(\xi)$ that determine the ratios

$$R^*_{n\ell}(\omega) = \frac{H_{n\ell}(\xi)}{Z^2 n^3} \tag{9.113}$$

have been obtained. It was found that all $H_{n\ell}(\xi)$ increase strongly in the region $\xi \gtrsim 1$. Here the cross sections for excitation of the ns and np states are of the same order of magnitude, while those with $\ell \geq 2$ are much smaller. At $n \geq 3$, the functions $H_{n\ell}(\xi)$ exhibit only weak dependence on n.

9.2.5 Two Fast Photoelectrons

Now we consider the case in which both photoelectrons carry energies $\varepsilon_{1,2}$ that strongly exceed the binding energies I_Z. Now the FSI determine the process, while the SO provides only a small correction. Indeed, in the SO amplitude $\Phi(\mathbf{p}_2) = \int d^3r_2 \psi^{C*}_{\mathbf{p}_2}(\mathbf{r}_2)\Psi(0,\mathbf{r}_2)$, one can treat the interaction between the secondary electron and the nucleus perturbatively if its momentum satisfies $p_2 \gg \mu_b$. At zero order, the wave function $\psi^{C*}_{\mathbf{p}_2}(\mathbf{r}_2)$ is just the plane wave; a large momentum p_2 is transferred to the nucleus by the initial-state electron, and the amplitude is quenched by a factor of order p_2^{-4}; see Sect. 7.1.1. Momentum p_2 is transferred to the nucleus by the secondary photoelectron if the lowest Coulomb correction is included. This contribution also decreases as p_2^{-4}. Similar to the case of ejection of electrons in electron scattering on atoms considered in Sect. 3.1, the leading terms of these contributions cancel, and the SO amplitude decreases as p_2^{-5}.

If the FSI between the photoelectrons are included, a large momentum p_2 is transferred to the secondary electron by the primary one. If the FSI is treated in the lowest order of perturbative theory, the final-state wave function can be represented by (9.100). Since the energies of all electrons are large, one can describe the state Ψ_f^0 by the composition of two plane waves.

We discussed the main features of the FSI mechanism in Sect. 4.2. The double photoionization proceeds in two steps. In the first one, a single photoionization takes place. The real photoelectron passes from the vicinity of the nucleus to the region where the density of the electron cloud reaches its largest values. Here it knocks out the secondary electron by electron impact.

In Sect. 4.2, we described electrons by single-particle functions. The corresponding equations can be easily generalized to two-particle functions. Proceeding in the same way as in Sect. 4.2, we can represent the lowest-order FSI amplitude as

$$F^{++} = \sqrt{2}N(\omega)\int \frac{d^3f}{(2\pi)^3}\frac{\langle \mathbf{p}_1,\mathbf{p}_2|V_{ee}|\mathbf{p}-\mathbf{f},\mathbf{f}\rangle\langle \mathbf{p}-\mathbf{f},\mathbf{f}|\gamma|\Psi\rangle}{\varepsilon-(\mathbf{p}-\mathbf{f})^2/2m-f^2/2m} + (\mathbf{p}_2 \leftrightarrow \mathbf{p}_1),$$
$$\mathbf{p} = \mathbf{p}_1 + \mathbf{p}_2; \quad \varepsilon = \varepsilon_1 + \varepsilon_2, \tag{9.114}$$

where Ψ is the wave function of the K shell electrons, while γ is the operator of interaction between the photon and one of the electrons. Since V_{ee} is proportional to p_2^{-2}, the FSI amplitude can be expected to decrease as p_2^{-4}. As we demonstrated in Chap. 4, in the kinematic region that determines the energy distribution, the FSI amplitude is enhanced and behaves as p_2^{-3}. Thus, the FSI dominates the process at $\varepsilon_{1,2} \gg I_Z$. This equation can be evaluated as

$$F^{++} = \sqrt{2}\int \frac{d^3f}{(2\pi)^3}\frac{4\pi\alpha}{(\mathbf{p}_2-\mathbf{f})^2}\frac{2m}{p'^2-(\mathbf{p}-\mathbf{f})^2-f^2}M(\omega,\mathbf{p}-\mathbf{f})\psi(\mathbf{f}) + (\mathbf{p}_2 \leftrightarrow \mathbf{p}_1), \tag{9.115}$$

with $p' = (2m\varepsilon)^{1/2}$, while $\psi(\mathbf{f})$ is the Fourier transform of the function $\psi(\mathbf{r}_2)$ defined by (9.25). The function M is given by (9.26). One can see that the first factor is the amplitude of free ee scattering F_{ee}. Since the integral is saturated by $f \sim \mu_b \ll p_2$, we can put $F_{ee}(\mathbf{p}_2 - \mathbf{f}) = F_{ee}(\mathbf{p}_2)$. This provides a direct analogue of (4.11):

$$F^{++} = 4\pi\alpha \left(\frac{1}{p_1^2} + \frac{1}{p_2^2} \right) M(\omega, \mathbf{p}) \Lambda(p, p'); \tag{9.116}$$

$$\Lambda(p, p') = \int \frac{d^3 f}{(2\pi)^3} \frac{2m}{p'^2 - (\mathbf{p} - \mathbf{f})^2 - f^2} \psi(\mathbf{f}).$$

The wave function of the ground state of a two-electron system on the electron–nucleus coalescence line $\Psi(0, \mathbf{r})$ can be well approximated by the superposition of two exponential terms; see Sect. 4.4.3. One can write $\Psi(0, \mathbf{r}) = \psi(r) = N_1 e^{-\lambda_1 r} + N_2 e^{-\lambda_2 r}$, where $\lambda_{1,2}$ are of order the binding momentum μ_b. For the helium atom, $\lambda_1 = 1.34\nu$, $\lambda_2 = 1.59\nu$, and $N_1 = 0.35\nu^3$, $N_2 = 0.65\nu^3$, $\nu = m\alpha$; see (4.110).

Thus

$$\psi(\mathbf{f}) = \frac{8\pi N_1 \lambda_1}{(f^2 + \lambda_1^2)^2} + \frac{8\pi N_2 \lambda_2}{(f^2 + \lambda_2^2)^2}. \tag{9.117}$$

This provides

$$\Lambda(p, p') = -\sum_i \frac{2m N_i}{p^2 - (p' + i\lambda_i)^2}; \quad i = 1, 2, \tag{9.118}$$

and we can put

$$|\Lambda(p, p')|^2 = \frac{m^2}{p'^2} \left(\frac{N_1^2}{\kappa_1} + \frac{N_2^2}{\kappa_2} + \frac{2N_1 N_2}{\lambda_1 + \lambda_2} \left(\frac{\lambda_1}{\kappa_1} + \frac{\lambda_2}{\kappa_2} \right) \right); \quad \kappa_i = (p - p')^2 + \lambda_i^2. \tag{9.119}$$

Representing the differential cross section as

$$d\sigma = |F^{++}|^2 d\Gamma; \quad d\Gamma = 2\pi\delta(\varepsilon_1 + \varepsilon_2 - \omega + I^{++}) \frac{d^3 p}{(2\pi)^3} \frac{d^3 p_2}{(2\pi)^3}, \tag{9.120}$$

putting $\varepsilon_1 = (\mathbf{p} - \mathbf{p}_2)^2/2m$ and employing the delta function for integrating over the angles of $\mathbf{p}_1$, we obtain

$$d\sigma^{++} = |F^{++}|^2 \frac{m^2}{p} \frac{d^3 p}{(2\pi)^3} \frac{d\varepsilon_2}{2\pi}. \tag{9.121}$$

The integral over p is saturated by the values close to p', i.e., $|p - p'| \sim \lambda_{1,2}$. Thus, quite similar to the single-particle approach presented in Sect. 4.2, the distribution $d\sigma^{++}/d\varepsilon_2 dp$ peaks at $p = p'$ with the width of the peak of order μ_b. In other words, the distribution in the angle between the momenta of the outgoing electrons (angular

correlations) $\tau = \mathbf{p_1} \cdot \mathbf{p_2}/p_1 p_2$ has a sharp maximum at $\tau = 0$ corresponding to the value predicted by classical mechanics for elastic scattering of electrons. The vicinity of this point determines the distribution

$$\frac{d\sigma^{++}}{d\varepsilon_2} = C \frac{\sigma^+(\omega)}{\Phi_{1s}^2} \frac{\pi r_e^2}{\varepsilon_1 \varepsilon_2^2}, \tag{9.122}$$

with $\sigma^+(\omega)$ the cross section of single photoionization, while Φ_{1s} is defined by (9.27),

$$C = \frac{N_1^2}{\lambda_1} + \frac{N_2^2}{\lambda_2} + \frac{4N_1 N_2}{\lambda_1 + \lambda_2}. \tag{9.123}$$

The last factor is just the energy distribution of the free $e - e$ scattering in the Born approximation, in agreement with the results of Sect. 4.1.5.

Proceeding in the same way as in Sect. 4.1.5, we can demonstrate the domination of small values of $|p - p'| \ll p, p'$ without specifying the shape of the wave function on the electron–nucleus coalescence line. We obtain, analogous to (4.62),

$$\frac{d\sigma^{++}}{d\varepsilon_2} = s \frac{\sigma^+(\omega)}{\Phi_{1s}^2} \frac{d\sigma_{ee}(\varepsilon)}{d\varepsilon_2}, \tag{9.124}$$

with

$$s = \int d^3 r \frac{|\Psi(0, \mathbf{r})|^2}{r^2}. \tag{9.125}$$

Recall that domination of the values of p close to p', i.e., of τ close to zero, corresponds to domination of the real intermediate state in the process. One of the electrons absorbs the photon and moves to the continuum. In the next step, it shares its momentum with the second bound electron.

Now we consider another type of differential cross sections that are differential in energy and in angle of the same photoelectron. Such studies are traditionally carried out for the linear polarization of the photons. Here we define $\cos\theta_i = t_i = \mathbf{e} \cdot \mathbf{p}_i / p_i$ for each photoelectron and employ the standard parameterization for the double differential distribution in the dipole approximation

$$\frac{d\sigma^{++}}{d\varepsilon_1 dt_1} = \frac{1}{2}\Big(1 + \beta_{asym}(\varepsilon, \varepsilon_1) P_2(t_1)\Big), \tag{9.126}$$

with $P_2(t_1) = (3t_1^2 - 1)/2$ the Legendre polynomial of second order; β_{asym} is called the "asymmetry function", $\varepsilon = \omega - I^{++}$. Here we calculate the asymmetry function for the case in which both photoelectrons are fast, i.e., $\varepsilon_1 \gg I_Z$ and $\varepsilon - \varepsilon_1 \gg I_Z$.

We write the differential cross section

$$d\sigma = |F^{++}|^2 d\Gamma; \quad d\Gamma = 2\pi \delta(\varepsilon_1 + \varepsilon_2 - \varepsilon) \frac{d^3 p_1}{(2\pi)^3} \frac{d^3 p_2}{(2\pi)^3} \tag{9.127}$$

in terms of the variables $\varepsilon_{1,2}, t_{1,2}$ and $p^2 = p_1^2 + p_2^2 + 2p_1p_2\tau$, where $\tau = \cos\theta_{12}$, while θ_{12} is the angle between the directions of the momenta $\mathbf{p}_1$ and $\mathbf{p}_2$. Employing the well-known relation $\tau = t_1t_2 + \sqrt{1-t_1^2}\sqrt{1-t_2^2}\cos(\varphi_1 - \varphi_2)$, we obtain

$$d\sigma = 2\pi F_{ee}^2 |\Lambda(p, p')|^2 M^2(\omega, \mathbf{p})\delta(\varepsilon_1 + \varepsilon_2 - \varepsilon)\frac{m^2 p d\varepsilon_1 d\varepsilon_2 dt_1 dt_2 dp}{A(\tau, t_1, t_2)(2\pi)^5}, \quad (9.128)$$

$$F_{ee} = \frac{2\pi\alpha}{m}\left(\frac{1}{\varepsilon_1} + \frac{1}{\varepsilon_2}\right).$$

Here $\tau = (p^2 - p_1^2 - p_2^2)/2p_1p_2$, while

$$A(\tau, t_1, t_2) = \left[(1-t_1^2)(1-t_2^2) - (\tau - t_1t_2)^2\right]^{1/2}. \quad (9.129)$$

Note that this distribution is symmetric relative to the photoelectrons.

During integration over p, we can put $p = p'$ everywhere except in the denominators κ_i. We put $\tau = 0$ in (9.129) for $A(\tau, t_1, t_2)$. Thus the triple differential distribution is

$$\frac{d\sigma}{d\varepsilon_1 dt_1 dt_2} = \frac{m^4 F_{ee}^2}{16\pi^3 p'}\frac{CM^2(\omega, \mathbf{p})}{\sqrt{1-t_1^2-t_2^2}}, \quad (9.130)$$

for $t_1^2 + t_2^2 \le 1$, with C defined by (9.123). Note that here the lower indices just label the photoelectrons. Each of them can be a primary one or a secondary one. The value $\tau = 0$ can be reached only if $t_1^2 + t_2^2 \le 1$. As one can see, the distribution $d\sigma/d\varepsilon_1 dt_1 dt_2$ is quenched by a factor of order $\mu_b/p' \ll 1$ outside this region. For the photon energy $\omega = 1\,\text{keV}$, one finds that $\mu_b/p' \approx 0.2$.

Since the angular dependence of the function $M(\omega, \mathbf{p})$ defined by (9.26) is determined by the sum $p_1t_1 + p_2t_2$, we can write (9.130) as

$$\frac{d\sigma}{d\varepsilon_1 dt_1 dt_2} = \frac{(p_1t_1 + p_2t_2)^2}{\sqrt{1-t_1^2-t_2^2}}X(\varepsilon_1, \varepsilon_2), \quad (9.131)$$

where X is a symmetric function of the energies of the photoelectrons. Carrying out integration over t_1 and t_2, one can see that

$$X = \frac{3}{4\pi m\varepsilon}\frac{d\sigma}{d\varepsilon_1}, \quad (9.132)$$

while the double differential distribution indeed takes the form (9.126) [23] with the asymmetry function

$$\beta(\varepsilon, \varepsilon_i) = f\left(\frac{\varepsilon_i}{\varepsilon}\right) = 3\frac{\varepsilon_i}{\varepsilon} - 1. \quad (9.133)$$

Recall that this expression is obtained for the case of two fast photoelectrons with $\varepsilon_i \gg I_b$. Only the FSI mechanism of the process is included. If $\varepsilon_2 \sim I_b$, i.e., $\varepsilon_1 \approx \varepsilon$, the process can be viewed as a single ionization with ejection of the fast electron, with the second electron moved to the continuum due to the shakeoff (SO). The double differential distribution is proportional to t_1^2, and thus can be written as

$$\frac{d\sigma}{d\varepsilon_1 dt_1} = \frac{3t_1^2}{2}\frac{d\sigma}{d\varepsilon_1}, \tag{9.134}$$

and $\beta_{asym} \to 2$. Thus (9.133) reproduces the limit $\varepsilon_1 \to \varepsilon$, although the mechanism of the process is quite different. For small $\varepsilon_1 \sim I_b \ll \varepsilon$, the electron labeled by the lower index 1 is moved to the continuum by the SO mechanism, carrying the angular momentum $\ell = 0$. Hence, the right-hand side of (9.133) does not depend on t_1, and $\beta_{asym} = 0$. Thus (9.133), which provides $\beta_{asym} = -1$ for $\varepsilon_1 = 0$, does not work for small $\varepsilon_1 \sim I_b$.

The validity of (9.133) is illustrated by comparing it with the numerical results obtained in a number of papers. Computations of the function β_{asym} for the energy $\varepsilon = 1\,\text{keV}$ and $\varepsilon_1 = 920\,\text{eV}$ carried out in [22] in two different approaches provided $\beta_{asym} = 1.70$ and $\beta_{asym} = 1.86$, while (9.133) gives $\beta_{asym} = 1.76$. In the earlier paper [24], the asymmetry coefficient was calculated for several values of the photon energy ω. The results of [24] and our asymmetry function (9.133) are presented in Fig. 9.5. As expected, the region of the values $\varepsilon_1/\varepsilon$ where our results agree with those of [24] increases as we increase the value of the photon energy.

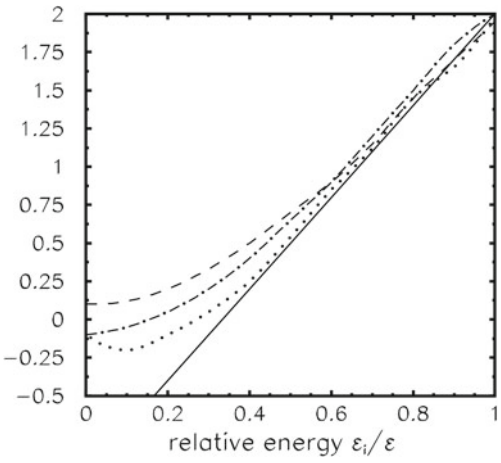

Fig. 9.5 Dependence of the asymmetry coefficient β_{asym} on the fraction of energy carried by a photoelectron in double photoionization of helium. The *solid line* corresponds to (9.113) of the text. The other *curves* represent the results of reference [23]. *Dashed curve*: $\omega = 280$ eV. *Dashed-dotted curve*: $\omega = 1$ keV. The *dotted curve* is for $\omega = 2.8$ keV

9.3 Quasifree Mechanism

9.3.1 The Amplitude

Now we turn to analysis of the quasifree mechanism (QFM) [7, 25] in which the nucleus accepts small momentum $q \sim \mu_b \ll p_i$. While we consider the photon energies corresponding to nonrelativistic photoelectrons, i.e., $\omega \ll m$, the QFM is possible only in the vicinity of the center of the energy distribution, where the relative difference of the electron energies $\beta = (\varepsilon_1 - \varepsilon_2)/(\varepsilon_1 + \varepsilon_2)$ is small, $\beta \ll 1$ (in this section, we assume that $\varepsilon_1 \geq \varepsilon_2$ and hence $\beta \geq 0$). If $\omega \ll \mu_b$, i.e., the photon wavelength is much larger than the size of the bound state, one can neglect $\mathbf{k}$ in the expression (9.5) for the recoil momentum $\mathbf{q}$. The QFM is possible if

$$\beta \lesssim \sqrt{\frac{\mu_b^2}{m\omega}}\,. \tag{9.135}$$

For atomic helium, these are the energies $\omega \ll 6\,\mathrm{keV}$. For $\omega \approx \mu_b$, we obtain $\beta \lesssim 0.11$. If $\mu_b \ll \omega \ll m$, one can replace the condition $q \lesssim \mu_b$ by that of free kinematics $q = 0$. This provides

$$\beta \lesssim \sqrt{\frac{\omega}{m}}\,. \tag{9.136}$$

The QFM leads to a strong correlation of the photoelectrons. They move approximately "back to back" with nearly opposite directions of the momenta.

In the standard formalism of quantum mechanics, we present the QFM amplitude describing photoelectrons by plane waves. We introduce

$$\mathbf{R} = (\mathbf{r}_1 + \mathbf{r}_2)/2; \quad \boldsymbol{\rho} = \mathbf{r}_1 - \mathbf{r}_2\,, \tag{9.137}$$

and represent the ground state wave function in terms of these variables:

$$\Psi(\mathbf{r}_1, \mathbf{r}_2) = \hat{\Psi}(\mathbf{R}, \boldsymbol{\rho})\,. \tag{9.138}$$

Introducing also $\boldsymbol{\kappa} = (\mathbf{p}_1 - \mathbf{p}_2)/2 \approx \mathbf{p}_1$, we write for the QFM amplitude

$$F_{QFM} = \sqrt{2}N(\omega)\int d^3R d^3\rho e^{-i\mathbf{q}\mathbf{R}+i(\boldsymbol{\kappa}-\mathbf{k}/2)\cdot\boldsymbol{\rho}}\left(\frac{i\mathbf{e}\cdot\boldsymbol{\nabla}_\rho}{m} - \frac{i\mathbf{e}\cdot\boldsymbol{\nabla}_R}{2m}\right)\hat{\Psi}(\mathbf{R}, \boldsymbol{\rho}) + (\mathbf{p}_1 \leftrightarrow \mathbf{p}_2), \tag{9.139}$$

with $\mathbf{q} = \mathbf{p}_1 + \mathbf{p}_2 - \mathbf{k}$. Integrating by parts, we find that since $|\boldsymbol{\kappa}| \gg q$, the first integral on the RHS dominates, providing

$$F_{QFM} = \sqrt{2}N(\omega)\frac{\mathbf{e}\boldsymbol{\kappa}}{m}\int d^3R d^3\rho e^{-i\mathbf{q}\mathbf{R}+i(\boldsymbol{\kappa}-\mathbf{k}/2)\cdot\boldsymbol{\rho}}\hat{\Psi}(\mathbf{R}, \boldsymbol{\rho}) + (\mathbf{p}_1 \leftrightarrow \mathbf{p}_2). \tag{9.140}$$

The integral is determined by $R \sim 1/q \sim 1/\mu_b$, i.e., the characteristic values of R is of the order the size of the bound state. The important values of ρ are much smaller, being of order $1/\kappa \ll 1/\mu_b$. To pick the quadrupole terms, we represent the wave function analogously to (9.20), i.e.,

$$\hat{\Psi}(\mathbf{R}, \boldsymbol{\rho}) = \hat{\Psi}(R, 0, 0) + \zeta \hat{\Psi}'(R, \zeta, 0)|_{\zeta=0} + \rho \hat{\Psi}'(R, 0, \rho)|_{\rho=0} + 0(\rho^2), \quad (9.141)$$

with $\zeta = \mathbf{R} \cdot \boldsymbol{\rho}$. Substituting this expansion into the integral over ρ in (9.140),

$$J(\mathbf{a}, R) = \int d^3\rho e^{i\mathbf{a}\cdot\boldsymbol{\rho}} \hat{\Psi}(\mathbf{R}, \boldsymbol{\rho}); \quad \mathbf{a} = \frac{\mathbf{p}_1 - \mathbf{p}_2 - \mathbf{k}}{2}, \quad (9.142)$$

we see that only the third term on the RHS of (9.141) contributes, providing

$$J(\mathbf{a}, R) = -\frac{8\pi \hat{\Psi}'(R, 0, \rho)|_{\rho=0}}{a^4} = -\frac{4\pi m\alpha}{a^4} \hat{\Psi}(\mathbf{R}, 0). \quad (9.143)$$

The second equality is due to the second Kato cusp condition given by (4.85). Thus the amplitude

$$F_{QFM} = \sqrt{2} N(\omega) \frac{\mathbf{e}\boldsymbol{\kappa}}{m} \int d^3R e^{-i\mathbf{q}\mathbf{R}} J(\mathbf{a}, R) + \left(\mathbf{p}_1 \leftrightarrow \mathbf{p}_2\right) \quad (9.144)$$

can be written as

$$F_{QFM} = F_0 S(q). \quad (9.145)$$

Here

$$S(q) = \int d^3r e^{-i\mathbf{q}\mathbf{r}} \Psi(\mathbf{r}, \mathbf{r}) = \int \frac{d^3f}{(2\pi)^3} \tilde{\Psi}(\mathbf{q} - \mathbf{f}, \mathbf{f}) \quad (9.146)$$

describes the transfer of momentum $-\mathbf{q}$ to the nucleus by the bound electrons. The factor

$$F_0 = -4\pi\sqrt{2}\alpha N(\omega) \frac{\mathbf{e}\boldsymbol{\kappa}}{a^4} + \left(\mathbf{p}_1 \leftrightarrow \mathbf{p}_2\right); \quad a^2 = m\omega \quad (9.147)$$

is the amplitude of the process in which the photon moves a system consisting of two free electrons in the spin-singlet state to the continuum. Hence, (9.145) can be viewed as a generalization of the single-particle relation expressed by (2.75) for the two-particle case.

Note that in the dipole approximation $e^{-i\mathbf{k}\cdot\boldsymbol{\rho}} = 1$, direct evaluation of the RHS of (9.139) provides the amplitude

$$F^{(0)}_{dip} = -8\pi\sqrt{2}\alpha N(\omega) \frac{\mathbf{e}\mathbf{q}}{m^2\omega^2} \int d^3\mathrm{R} e^{-i\mathbf{q}\mathbf{R}} r_0 \hat{\Psi}'(R, 0, \rho)|_{\rho=0}. \quad (9.148)$$

The upper index (0) means that we neglected the FSI of the photoelectrons. For $\omega \ll \mu_b$, this contribution is much larger than the quadrupole one (9.144). As noticed by Surić et al. [26], inclusion of the interaction between the photoelectrons in the lowest nonvanishing order leads to the amplitude

$$F_{dip}^{(1)} = 4\pi\sqrt{2}\alpha N(\omega)\frac{\mathbf{eq}}{m^2\omega^2}\int d^3\mathrm{Re}^{-i\mathbf{qR}}\hat{\Psi}(\mathbf{R},0). \tag{9.149}$$

We find that each of the amplitudes $F_{dip}^{(0,1)}$ treated separately would provide a surplus in the center of the energy distribution. However, due to the second Kato condition, we have $F_{dip}^{(0)} + F_{dip}^{(1)} = 0$, and there is no such thing as a dipole contribution to the QFM.

The literature on the subject includes several direct numerical computations carried out in the dipole approximation and employing approximate functions that do not satisfy the second Kato cusp condition. They report a peak in the center of the spectrum. We see that it is a spurious one. This provides an instructive example that a theoretical analysis should precede computations. We address the reader to the review [27] for more details.

Even if the quadrupole terms are separated, in calculations of the contribution of the QFM one should employ a ground-state function that satisfies the second Kato condition. Of course, every approximate function Ψ_{approx} with a nonzero value of the derivative $\Psi'_{approx}(R,\rho)|_{\rho=0}$ would provide a surplus in the center of the energy distribution. However, for the quantitative results one needs an approximate function that satisfies the Kato condition. Note that the combinations of the products of the single-particle functions $\psi^{s.p.}$ do not reproduce any trace of the QFM. Such functions

$$\Psi_{approx}(\mathbf{R},\boldsymbol{\rho}) \;=\; \psi^{s.p.}\left(\mathbf{R}+\frac{\boldsymbol{\rho}}{2}\right)\psi^{s.p.}\left(\mathbf{R}-\frac{\boldsymbol{\rho}}{2}\right) \tag{9.150}$$

are the even functions of ρ, and for them, $\Psi'_{approx}(R,\rho)|_{\rho=0} = 0$.

9.3.2 *Evaluation of the Shape of the Spectrum Curve*

Now we trace the change of the shape of the spectrum curve with the growth of the value of the photon energy ω [28]. We have seen that the photoelectron spectrum has sharp peaks at the edges of the energy interval $\varepsilon_{1,2} \to 0$, where the process is dominated by the SO mechanism. At $\varepsilon_{1,2} \gg I_b$, the energy distribution is the result of interplay between the FSI and QFM. Since the amplitude of the FSI is mostly imaginary while that of the QFM is real, we neglect the interference terms and write

$$\frac{d\sigma^{++}}{d\varepsilon_1} \;=\; V_1(\omega,\beta) + V_2(\omega,\beta)\,, \tag{9.151}$$

with V_1 and V_2 standing for contributions of the FSI and QFM respectively. The FSI contribution was found in Sect. 9.2.5. Setting $\varepsilon_i = \omega(1 \pm \beta)/2$, we can write

$$V_1(\omega, \beta) = \frac{2\alpha^2 s v_1(\omega)}{\omega^3(1-\beta^2)^2}; \quad v_1(\omega) = \frac{2^{11/2}\pi^2\alpha(\alpha Z)^2}{3m^5}(\frac{m}{\omega})^{7/2}, \tag{9.152}$$

with s defined by (9.125). The function $v_1(\omega)$ is defined in such a way that the asymptotics of the cross section for photoionization of the K shell in the single-particle approximation is $\sigma^+(\omega) = \psi_{1s}^2(0)v_1(\omega)$. To obtain the QFM contribution V_2, we represent the differential cross section corresponding to the QFM as

$$d\sigma^{++}(\omega) = \delta\Big(\varepsilon - 2\varepsilon_1 - \frac{p_1 q_z}{m} - \frac{q^2}{2m}\Big)|F_{QFM}|^2 \frac{d^3 p_1}{(2\pi)^3}\frac{dq^2 dq_z}{4\pi}, \tag{9.153}$$

with z the direction of momentum $\mathbf{p}_1 - \mathbf{k}$, and we put $\mathbf{p}_1 - \mathbf{k} = \mathbf{p_1}$ in the argument of the delta function. Using the delta function for integration over q_z, we obtain for the energy distribution

$$\frac{d\sigma_{QFM}^{++}}{d\varepsilon_1} = \frac{m^2}{2}\int |F_{QFM}|^2 \frac{dq^2 dt}{(2\pi)^3}; \quad t = \mathbf{p}_1\mathbf{k}/p_1 k, \tag{9.154}$$

which can be written as

$$V_2(\omega, \beta) = v_2(\omega)\int_{-1}^{1} dt t^2(1-t^2)\Phi(\omega, \beta, t); \quad v_2(\omega) = 32\alpha^3\Big(\frac{m}{\omega}\Big)^3, \tag{9.155}$$

while

$$\Phi(\omega, \beta, t) = \int_{q_{min}^2}^{4p_1^2} dq^2 D(q); \quad D(q) = S^2(q). \tag{9.156}$$

The function $S(q)$ is defined by (9.146). The smallest possible value of the recoil momentum q is $q_{min} = ||\mathbf{p}_1 - \mathbf{k}| - p_2|$. Introducing $p = (m\omega)^{1/2}$ and estimating $|\mathbf{p}_1 - \mathbf{k}| \approx p_1 - \mathbf{p}_1 \cdot \mathbf{k}/p_1$ and $p_1 - p_2 \approx p\beta$, we obtain

$$q_{min}^2 = (p\beta - \omega t)^2; \quad p = (m\omega)^{1/2}. \tag{9.157}$$

In the QFM, the nucleus obtains the momentum $q \sim \mu_b$, which is much smaller than the momenta of the photoelectrons. The values $q \sim \mu_b$ are inside the interval of integration on the RHS of (9.156) if the value of β is small enough. In any case, the QFM kinematics are available at the central point $\beta = 0$.

If the QFM is neglected, the spectrum curve is **U**-shaped, with a minimum at the central point. The values of ω where the spectrum curve with a minimum at the central point converts into a curve with a maximum, and vice versa, are determined by the equation

$$V_1''(\omega, \beta)|_{\beta=0} + V_2''(\omega, \beta)|_{\beta=0} = 0, \tag{9.158}$$

with $V''_{1,2}$ the second derivatives of the functions $V_{1,2}$ with respect to β. Calculation of V''_1 is trivial. The first derivative is given by $V'_2 = -pv_2(\omega)\int_{-1}^{1} dtt^2(1-t^2)(p\beta - \omega t)D(q_{min})$. Noting that

$$\frac{\partial D(q_{min})}{\partial \beta} = -\frac{p}{\omega}\frac{\partial D(q_{\min})}{\partial t}$$

and employing integration by parts, we obtain

$$V''_2(\omega,\beta)|_{\beta=0} = -v_2(\omega)\frac{p}{\omega}\int_{-1}^{1} dtt^2(1-t^2)\frac{\partial D(\omega t)}{\partial t}.$$

Integration by parts enables us to represent (9.158) in the form

$$\frac{16\alpha^2 s}{\omega^3} + \frac{6\sqrt{2}}{\pi^2 Z^2}\omega m\left(\frac{\omega}{m}\right)^{1/2} A(\omega) = 0. \tag{9.159}$$

Here

$$A(\omega) = \int_{-1}^{1} dtt^2(1-2t^2)D(\omega t). \tag{9.160}$$

We can estimate the value $\omega = \omega_1$ where (9.159) is satisfied. Estimating $s \sim \mu_b^5$, we obtain $\omega_1 \sim \mu_b(\alpha Z)^{4/9}$. The exact value of ω_1 is obtained by finding a numerical solution of (9.159). One can find also an approximate analytical solution that is true with relative accuracy αZ. Since the integral on the RHS of (9.146) is saturated by $r \sim \mu_b^{-1}$ while $\omega_1 \sim \mu_b(\alpha Z)^{4/9}$, we can assume that $\omega^2 r^2 \sim \alpha Z \ll 1$. Thus we can calculate $S_0 \equiv S(q_{min})$ by putting $\exp(-i\mathbf{q}\cdot\mathbf{r}) = 1$ on the RHS of (9.146). We obtain

$$A = -\frac{2}{15}B, \tag{9.161}$$

with

$$B = |\int d^3 r\Psi(\mathbf{r},\mathbf{r})|^2.$$

Assuming that the function $A(\omega)$ is given by (9.161), we obtain the solution of (9.159):

$$\omega_1^* = 5^{2/9}(\pi\alpha Z)^{4/9}\left(\frac{8s^2}{B^2 m}\right)^{1/9}. \tag{9.162}$$

As one can see from Table 9.4, the values of ω_1 and ω_1^* are very close indeed. For helium, $\omega_1^* = 1.9\,\text{keV}$. Employing (9.162), one can trace the Z-dependence of ω_1^*:

$$\omega_1^* = 0.65Z^{14/9}. \tag{9.163}$$

One can see that at $\omega = \omega_1$, the QFM contribution to the energy distribution V_2 is still much smaller than the FSI contribution V_1. Thus the evaluation of the spectrum curve begins with a small QFM surplus on the smooth FSI curve.

Thus at certain $\omega_1 \ll \mu_b$, the **U** shape of the spectrum curve changes to a **W** shape. On the other hand, for much larger energies $\omega \gg \mu_b$, we can write

$$d\sigma^{++}_{QFM}(\omega) = 2\pi\delta\Big(\varepsilon_1 + (\mathbf{k}-\mathbf{p_1})^2/2m - \omega + I^{2+}\Big)|F_{QFM}|^2 \frac{d^3p_1}{(2\pi)^3}\frac{d^3q}{(2\pi)^3}. \quad (9.164)$$

Employing (9.49), we obtain

$$\frac{d\sigma^{++}}{d\varepsilon_1} = 2^8\pi^2\alpha^3\frac{\beta^2}{m\omega^5}\Big(1 - \frac{m\beta^2}{\omega}\Big)\tilde{I}; \quad \beta^2 \le \frac{\omega}{m}, \quad (9.165)$$

with

$$\tilde{I} = \int \frac{d^3q}{(2\pi)^3}|S(q)|^2 = \int d^3r|\Psi(\mathbf{r},\mathbf{r})|^2. \quad (9.166)$$

Thus at $\omega \gg \mu_b$ (for helium, this means $\omega \gg 6\,\mathrm{keV}$), the spectrum curve has two peaks at

$$\varepsilon' = \frac{\varepsilon}{2}\Big(1 \pm \frac{1}{2}\sqrt{\frac{2\omega}{m}}\Big). \quad (9.167)$$

There are also three local minima. One of them is at the center of the energy distribution $\varepsilon_i = \varepsilon/2$, while the two others are at

$$\varepsilon' = \frac{\varepsilon}{2}\Big(1 \pm \sqrt{\frac{\omega}{m}}\Big). \quad (9.168)$$

This structure is due to the quadrupole nature of the QFM.

Due to the free kinematics $\mathbf{p}_1 + \mathbf{p}_2 = \mathbf{k}$, the angular variables of the photoelectrons are linked to the parameter β:

$$t_1 = \beta\sqrt{\frac{m}{\omega}}; \quad t_2 = -\beta\sqrt{\frac{m}{\omega}}; \quad t_i = \frac{\mathbf{p}_i\cdot\mathbf{k}}{p_i\omega}; \quad i = 1,2. \quad (9.169)$$

Thus employing (9.165), we obtain the angular distribution

$$\frac{d\sigma^{++}}{dt_1} = 2^7\pi^2\alpha^3\frac{1}{m^2\omega^3}\sqrt{\frac{\omega}{m}}\,t_1^2(1-t_1^2)\tilde{I}, \quad (9.170)$$

with $\tilde{I}$ defined by (9.166).

We demonstrated that at $\omega = \omega_1 \ll \mu_b$, the **U** shape of the spectrum curve changes to a **W** shape. At certain $\omega = \omega_2$, the central peak splits into two peaks at the points close to the center $|\varepsilon_i - \varepsilon_2| \ll \varepsilon/2$. One can see that ω_2 cannot be

Table 9.4 The values of ω_1, ω_1^*, ω_2, ω_2^* for the ground states of two-electron ions with nuclear charge Z

Z	1	2	3	4	5
ω_1	0.55	1.93	3.70	5.89	8.49
ω_1^*	0.54	1.89	3.57	5.61	7.96
ω_2	4.0	8.94	13.7	18.5	23.3
ω_2^*	4.0	9.72	14.5	19.4	24.3

The results are obtained by employing CFHH functions. The column with $Z = 1$ shows the data for the negative hydrogen ion

much smaller than μ_b, since there is only one solution of (9.158), and it is ω_1. Also, ω_2 cannot be much larger than μ_b, since we found the energy distribution for these values of the photon energies just now. Hence, ω_2 is of order μ_b. One can see that in the region $\omega_2 \sim \mu_b$, the FSI contribution is smaller than that of QFM by more than a factor of α. Thus the value ω_2 is determined by condition $V_2'' = 0$ or

$$\int_{-1}^{1} dt t^2(1-2t^2)D(\omega t) \;=\; 0. \tag{9.171}$$

The values of ω_2 obtained by numerical solution of this equation for $Z \leq 5$ are presented in Table 9.4. The approximate solution ω_2^* can be found by employing (9.156) for the function D based on (4.105) for the wave function. In this case, (9.171) takes the form

$$\int_{-1}^{1} dt \frac{t^2(1-2t^2)}{(t^2+a^2)^4} = 0; \quad a = \frac{2\eta}{\omega}. \tag{9.172}$$

This equation has a solution $a = 1.534$, and thus

$$\omega_2^* \;=\; 1.30\eta \;=\; 4.86Z\,\mathrm{keV}; \quad \eta \;=\; m\alpha Z. \tag{9.173}$$

Evaluation of the shape of the spectrum curve is shown in Fig. 9.6.

9.3.3 *High Energy Behavior of Ionization Cross Section Ratios*

Now we calculate the contribution of the QFM to the double-to-single photoionization cross section ratio. Employing (9.170), we see that the contribution of the QFM to the cross section of the double photoionization is

$$\sigma_{QFM}^{++}(\omega) \;=\; \frac{2^8\pi^2\alpha^3}{15m^2\omega^3}\sqrt{\frac{\omega}{m}}\tilde{I}. \tag{9.174}$$

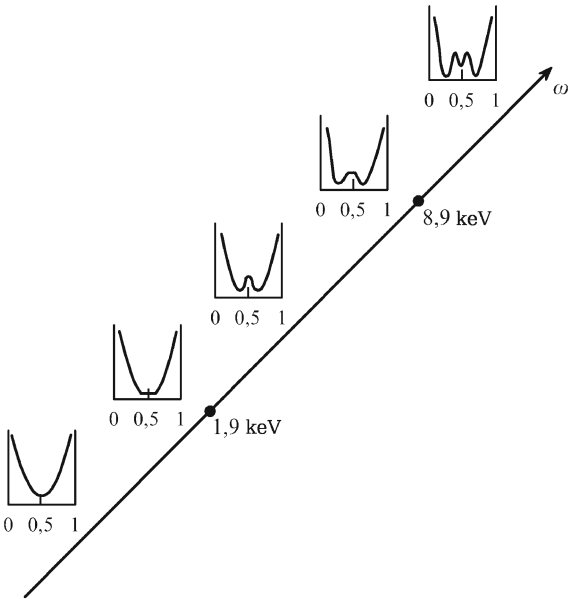

Fig. 9.6 Evaluation of the shape of the spectrum *curve* for the double photoionization of helium with increase of the photon energy ω. The lowest image corresponds to the energies $\omega < \omega_1$ with the FSI causing the knockout of two fast electrons. In the next figure, corresponding to $\omega = \omega_1 = 1.9\,\text{keV}$, the QFM becomes noticeable in the vicinity of the center. At $\omega_1 < \omega < \omega^*$ (the third figure), the spectrum *curve* peaks at its center due to the QFM. At $\omega \geq \omega^* = 8.9$ keV (next two figures), the central peak obtains an internal structure due to the quadrupole nature of the QFM [27]

The double-to-single cross section ratio in the high-energy nonrelativistic limit becomes [29–31]

$$R(\omega) \;=\; C + \frac{4\sqrt{2}}{5Z^2}\,\frac{\tilde{I}}{\Phi_{1s}^2}\,\frac{\omega}{m}\,. \tag{9.175}$$

Here the first term corresponding to the SO does not depend on ω (see Sect. 9.2.1). The second term, which is the QFM contribution, thus provides the lowest-order energy-dependent correction. As to the FSI contributions, one can see, employing (9.122), that they provide a small correction of order $\alpha^2\mu_b^2/\omega^2$ to the ratio of the cross sections.

Recall that employing the standard formalism of quantum mechanics would provide the second term on the RHS of (9.175), where

$$\tilde{I}' = \int d^3R|2r_0\Psi'(R,\,\rho=0)|^2,$$

and Ψ' denotes the derivative of the function Ψ with respect to ρ. For the exact solution of the wave equation, we have $\tilde{I} = \tilde{I}'$, due to the second Kato cusp condition. However, these two values can differ for approximate functions employed in computations.

The dimensionless quantity

$$\mathscr{I} \;=\; \frac{\tilde{I}}{\Phi_{1s}^2} \tag{9.176}$$

appears to be quite sensitive to the choice of the wave function in the case of helium. One obtains $\mathscr{I} = 1/8$ if Ψ is approximated by the product of single-particle Coulomb functions. This value does not depend on the charge of the nucleus. One can put $Z = 2$ or can employ a certain effective value Z_{eff}. For the old variational functions of Hylleraas [8] containing three and six parameters, one obtains $\mathscr{I} = 0.070$ and 0.068 respectively. For the Kinoshita wave function [8], one has $\mathscr{I} = 0.055$. The Hartree–Fock approximation provides $\mathscr{I} = 0.11$. The CFHH value is $\mathscr{I} = 0.060$. Thus the QFM provides a correction of order 5% at $\omega = 100\,\text{keV}$.

The nuclear charge dependence of $\mathscr{I}$ for two-electron ions traced in [32] is shown in Fig. 9.7. In the limit $Z \gg 1$, one obtains $\mathscr{I} \to 1/8$. The same result can be obtained by employing the product of the Coulomb functions for describing the initial state. The result is not a trivial one, since one could not expect such a description to work on the electron–electron coalescence line. The contribution of QFM reaches the largest value in the negative ion of hydrogen H^-, where $\mathscr{I} = 0.017$.

Anyway, as we have seen in Chap. 8, photoionization is not the main mechanism of ionization if the photon energy is large enough. In the case of helium, the cross section of the Compton scattering exceeds that of the photoionization if the energy of the incoming photon satisfies $\omega_1 \gtrsim 6\,\text{keV}$. Thus it reasonable to study the double-to-single cross section ratio for ionization by Compton scattering.

We have seen that in contrast to photoionization, Compton scattering can take place on the free electrons. The Compton scattering on a bound electron is determined by the kinematic region where the process on the free electron is possible. This requires that most of the energy be carried by the scattered photon and that the electron energy be limited by the condition $\varepsilon \lesssim \omega_1^2/m$. The asymptotics of the cross section are reached when the outgoing electron can be described by a plane wave, i.e., $\omega_1 \gg \eta$. For helium, this means $\omega_1 \gg 6\,\text{keV}$. The asymptotics of the amplitude at the Bethe ridge can be written as

$$F_{Compt} = \sqrt{2} N(\omega_1) N(\omega_2) \frac{\mathbf{e}_2^* \cdot \mathbf{e}_1}{m} \int d^3 r_1 d^3 r_2 \psi_{1s}^C(\mathbf{r}_2) e^{-i\mathbf{q}\cdot\mathbf{r}_1} \Psi(\mathbf{r}_1, \mathbf{r}_2), \quad (9.177)$$

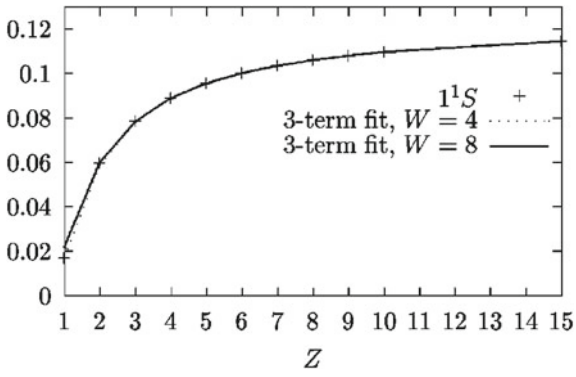

Fig. 9.7 The nuclear charge dependence of the parameter $\mathscr{I}$ determined by (9.176) for the ground state of the two-electron ion. The *horizontal* axis is for the charge of the nucleus Z [32]

where $\mathbf{q} \sim \eta$ is the momentum transferred from the nucleus. In double ionization, the second electron is moved to a continuum state with momentum $\mathbf{p}_2$ by the shakeoff. The amplitude is

$$F^{++}_{Compt} = \sqrt{2} N(\omega_1) N(\omega_2) \frac{\mathbf{e}_2^* \cdot \mathbf{e}_1}{m} \int d^3 r_1 d^3 r_2 \psi^C_{\mathbf{p}_2}(\mathbf{r}_2) e^{-i\mathbf{q}\cdot\mathbf{r}_1} \Psi(\mathbf{r}_1, \mathbf{r}_2). \quad (9.178)$$

the states with small momentum $p_2 \sim \eta$ determine the cross section σ^{++}_{Compt}. Thus one can expect that at $\omega_1 \gg \eta$, the double-to-single cross section ratio

$$r = \frac{\sigma^{++}_{Compt}}{\sigma_{Compt}}, \quad (9.179)$$

as well as the cross sections themselves reaches a constant value.

Indeed, experiments have shown that for helium, $r = (1.25 \pm 0.30) \times 10^{-2}$ for $\omega_1 = 57$ keV [33] and $r = (0.98 \pm 0.09) \times 10^{-2}$ for $\omega_1 = 97.8$ keV [34]. Since in both single-ionization and double-ionization processes, the electrons interact with the nucleus at distances of order the size of the bound state, the theoretical results are less sensitive to the choice of the function describing the bound state. Calculation with a variational wave function for helium [35] provided $r = 0.8 \times 10^{-2}$. Calculations for heliumlike ions with variational functions [36] and in the perturbative model [37] gave $r = 0.050/Z^2$.

9.3.4 *Distributions in Recoil Momenta*

We have seen that for helium the QFM provides a noticeable contribution to the spectrum of photoelectrons starting from photon energies of about 2 keV. However, it manifests itself only in the vicinity of the center of the energy distribution. This region provides a small contribution to the cross section, while $\omega \ll m \approx 500$ keV. The QFM corrections to the total cross section become noticeable at energies of dozens of keV. For heavier two-electron ions, the corresponding photon energies become larger. As it stands now, experimental data for such energies are not available. However, a clear manifestation of the QFM was observed recently in the experiment carried out by Dörner's group [38] at a much smaller value of the photon energy $\omega = 800$ eV. It was found that the distribution in momenta q transferred to the final-state doubly charged ions in double photoionization of helium has a surplus at small q of order of 1 to 2 atomic units. The experiment was carried out with linearly polarized photons. The recoil momentum $\mathbf{q}$ was measured in the plane perpendicular to the linear polarization vector of the incoming light. This enabled the researchers to exclude the contribution of the dipole terms.

At photon energies $\omega \gtrsim 800$ eV, the distributions $d\sigma^{++}/dq^2 d\varepsilon_i$ for small q can be calculated analytically and can be written as a combination of hypergeometric

functions [39]. Note first that the distributions for small q are dominated by the QFM. Of course, in both SO and FSI mechanisms, there are configurations in which both electrons transfer large momenta $\mathbf{q}_{1,2}$ with $|\mathbf{q}_{1,2}| \gg \mu_b$ to the nucleus, while the total recoil momentum is small, i.e., $|\mathbf{q}_1 + \mathbf{q}_2| \sim \mu_b$. However, since each act of transferring of a large momentum $q_i \gg \mu_b$ leads to an additional small factor, their probabilities are very small. The distribution $d\sigma^{++}/dq^2 d\varepsilon_i$ provided by the SO and the FSI peaks at $q \approx (2m\omega)^{1/2} \gg \mu_b$, becoming very small at $q \sim \mu_b$. Thus we must calculate the QFM contribution.

We calculate the amplitude of the QFM in the lowest order of expansion in powers of q/p_i. This corresponds to expansion of the bound-state wave function in the lowest order in powers of r_{12}/r_i. Recall that r_i stand for the distance between the electron and the nucleus, while r_{12} is the interelectron distance. Since $q \sim \mu_b$, the higher-order terms of the expansion in powers of q/p_i are of the same order as those coming from the interaction between the photoelectrons and the nucleus. However, they are of quite different origin. Thus we include interactions of the electrons with the nucleus exactly, describing the electrons by the nonrelativistic functions of the Coulomb field. The contribution of the FSI between the outgoing electrons is proportional to the squared Sommerfeld parameter $\xi_{ee}^2 = m^2\alpha^2/(\mathbf{p}_1 - \mathbf{p}_2)^2$. In the QFM configuration, $p_1 \approx p_2 \approx (m\varepsilon)^{1/2}$ and $\mathbf{p}_1 \approx -\mathbf{p}_2$. For the photon energy $\omega = 800\,\mathrm{eV}$, the energy carried by the photoelectrons is $\varepsilon \approx 720\,\mathrm{eV}$, and we obtain $\xi_{ee}^2 \lesssim 0.01$. Thus we neglect the interaction between the photoelectrons, presenting the final state function as

$$\Psi_f(\mathbf{r}_1, \mathbf{r}_2) \;=\; \frac{1}{\sqrt{2}}\Big(\psi_1(\mathbf{r}_1)\psi_2(\mathbf{r}_2) + \psi_2(\mathbf{r}_1)\psi_1(\mathbf{r}_2)\Big), \tag{9.180}$$

where ψ_i are the single-particle nonrelativistic Coulomb field functions with asymptotic momenta $\mathbf{p}_i$.

We shall need the functions

$$\psi_i(\mathbf{r}) \;=\; e^{-i\mathbf{p}_i\cdot\mathbf{r}} X_i(\mathbf{r}); \quad i = 1, 2, \tag{9.181}$$

with

$$X_i(\mathbf{r}) \;= N_i X_1 F_1(i\xi_i, 1, ip_i r - i\mathbf{p}_i\mathbf{r}), \tag{9.182}$$

where the normalization factors N_i are defined by (3.20). Recall that $\xi_i = \eta/p_i$ and $\eta = m\alpha Z$. Employing the variables $\mathbf{R}$ and $\boldsymbol{\rho}$ determined by (9.137) and using the notation (9.138), we obtain an expression for the amplitude that is analogous to (9.139), where we did not include interactions of the photoelectrons with the nucleus. We write

$$F^{++} \;=\; T_1 + T_2\,, \tag{9.183}$$

with

$$T_1 = i\frac{2N(\omega)}{\sqrt{2}} \int d^3R d^3\rho e^{-i\mathbf{q}\mathbf{R}+i\mathbf{a}\boldsymbol{\rho}} X_1(\mathbf{R}-\frac{\boldsymbol{\rho}}{2}) X_2\left(\mathbf{R}-\frac{\boldsymbol{\rho}}{2}\right) \frac{\mathbf{e}\cdot\boldsymbol{\nabla}_\rho}{m}\hat{\Psi}\,(\mathbf{R},\boldsymbol{\rho}) + (\mathbf{p}_1 \leftrightarrow \mathbf{p}_2),$$

and

$$T_2 = -i\frac{2N(\omega)}{\sqrt{2}}\int d^3R d^3\rho e^{-i\mathbf{qR}+i\mathbf{a}\rho} X_1\left(\mathbf{R}-\frac{\boldsymbol{\rho}}{2}\right)X_2\left(\mathbf{R}-\frac{\boldsymbol{\rho}}{2}\right)\frac{\mathbf{e}\cdot\boldsymbol{\nabla}_R}{2m}\hat{\Psi}(\mathbf{R},\boldsymbol{\rho})+(\mathbf{p}_1\leftrightarrow\mathbf{p}_2),$$

while $\mathbf{a}$ is defined in (9.142). The integrals corresponding to the amplitudes $T_{1,2}$ are saturated by $R\sim q^{-1}\gg\rho$. Thus we can set $\boldsymbol{\rho}=0$ in the functions X_i. Integrating by parts, we find that $T_2\ll T_1$, and thus putting $F^{++}=T_1$, we obtain

$$F^{++} = \frac{2N(\omega)}{\sqrt{2}}\cdot\frac{\mathbf{e}\cdot\mathbf{a}}{m}\cdot\int d^3R e^{-i\mathbf{qR}}X_1(\mathbf{R})X_2(\mathbf{R})\int d^3\rho e^{i\mathbf{a}\rho}\hat{\Psi}(\mathbf{R},\boldsymbol{\rho})+(\mathbf{p}_1\leftrightarrow\mathbf{p}_2). \tag{9.184}$$

Using (9.141)–(9.144) and employing the second Kato cusp condition (4.85), we obtain

$$F^{++} = -8\pi\alpha\frac{N(\omega)}{\sqrt{2}}\cdot\frac{\mathbf{e}\cdot\mathbf{a}}{a^4}S_1(q)+(\mathbf{p}_1\leftrightarrow\mathbf{p}_2)\,, \tag{9.185}$$

with

$$S_1(q) = \int d^3R e^{-i\mathbf{qR}}X_1(\mathbf{R})X_2(\mathbf{R})\hat{\Psi}(\mathbf{R},0). \tag{9.186}$$

As expected, in the dipole approximation, i.e., putting $\mathbf{k}=0$ in the expression for $\mathbf{a}$, we would obtain $F^{++}=0$. If interactions between the photoelectrons and the nucleus are neglected, then $X_1(\mathbf{R})=X_2(\mathbf{R})=1$ and $S_1(q)=S(q)$ with $S(q)$ defined by (9.146). One can see that (9.185) can be written also as

$$F^{++} = F_0 S_1(q)\,, \tag{9.187}$$

with F_0 the amplitude of the process on the free electrons. Employing (9.153) and integrating over the angles, we obtain

$$\frac{d\sigma^{++}}{dq^2 d\beta} = \frac{2^6}{15}\alpha^3\frac{|S_1(q)|^2}{m^2\omega^2}\,. \tag{9.188}$$

We employ the representation of the ground-state wave function $\Psi(\mathbf{R},0)$ as the sum of two exponential terms $\hat{\Psi}(\mathbf{R},0)=c_1e^{-\lambda_1 R}+c_2e^{-\lambda_2 R}$; see (4.110). Thus

$$|S_1(q)|^2 = N^2(\xi_1)N^2(\xi_2)|\sum_i c_i I(\lambda_i)|^2;\quad I(\lambda_i)=\int d^3R e^{-i\mathbf{qR}}F_1(\mathbf{R})F_2(\mathbf{R})e^{-\lambda_i R}, \tag{9.189}$$

with $F_i(\mathbf{R}) = {}_1F_1(i\xi_i,1,p_iR-i\mathbf{p}_i\mathbf{R})$; see (9.182). One can see that

$$I(\lambda_i) = \frac{-\partial J(\lambda_i)}{\partial\lambda_i};\quad J(\lambda_i)=\int d^3R e^{i\mathbf{qR}}F_1(\mathbf{R})F_2(\mathbf{R})\frac{e^{-\lambda_i R}}{R}. \tag{9.190}$$

Many years ago, Nordsieck calculated the integral $J(\lambda)$ in his studies of bremsstrahlung in the Coulomb field [40]. Employing these results, we obtain

$$I(\lambda) = \frac{8\pi\lambda}{(q^2+\lambda^2)^2}\Theta^{i\xi_1+i\xi_2}(\lambda)T(\lambda)e^{-\pi(\xi_1+\xi_2)/2}. \tag{9.191}$$

Here

$$\Theta(\lambda) = \frac{q^2+\lambda^2}{s(\lambda)u(\lambda)}, \quad s(\lambda) = \sqrt{(p_1+p_2)^2+\lambda^2}, \quad u(\lambda) = \sqrt{(p_1-p_2)^2+\lambda^2},$$

$$T(\lambda) = \left(1-\frac{i(\xi_1+\xi_2)}{2}\right)\Big[(1+g(\lambda))_2F_1(i\xi_1, i\xi_2, 1, g(\lambda)) - \\ - \xi_1\xi_2 g(\lambda)(1-g(\lambda))_2F_1(i\xi_1+1, i\xi_2+1, 2, g(\lambda))\Big],$$

while

$$g(\lambda) = 1 - \frac{q^2+\lambda^2}{u^2(\lambda)}.$$

Note that the dependence of $|S_1|^2$ on the parameters $\pi\xi_i$ is contained in the factors $|N(\xi_i)e^{-\pi\xi_i/2}|^2$. Its expansion does not contain terms linear in $\pi\xi_i$. The contribution to the cross section does not contain the Stobbe factor discussed in Chap. 7.

The cross section $d\sigma^{++}/dq^2d\beta$ is presented in Fig. 9.8 for $\omega = 800\,\text{eV}$. As expected, it obtains the largest values at small $\beta \ll 1$ and in the region of small $q \sim 1$ a.u. It is instructive also to view the energy distribution of the angular correlation. For $\omega \ll \mu_b$ (for helium, this means $\omega \ll 6\,\text{keV}$), we can put $\mathbf{q} = \mathbf{p}_1 + \mathbf{p}_2$, and

$$\frac{d\sigma^{++}}{d\tau d\beta} = 2p_1p_2\frac{d\sigma^{++}}{dq^2d\beta}; \quad \tau = \frac{\mathbf{p}_1\cdot\mathbf{p}_2}{p_1p_2}. \tag{9.192}$$

As expected, the largest values are reached at τ close to -1, corresponding to the electrons ejected in the opposite directions (back to back). To find the distribution in recoil momentum for $\omega \ll \mu_b$, note that since $q \geq |p_1 - p_2|$, we have $\beta \leq q/p$ with $p = (m\varepsilon)^{1/2}$, and

$$\frac{d\sigma^{++}}{dq^2} = \int_0^{q/p} d\beta \frac{d\sigma^{++}}{dq^2d\beta}. \tag{9.193}$$

As expected, the distribution has a local maximum at q about 1 a.u.; see Fig. 9.9.

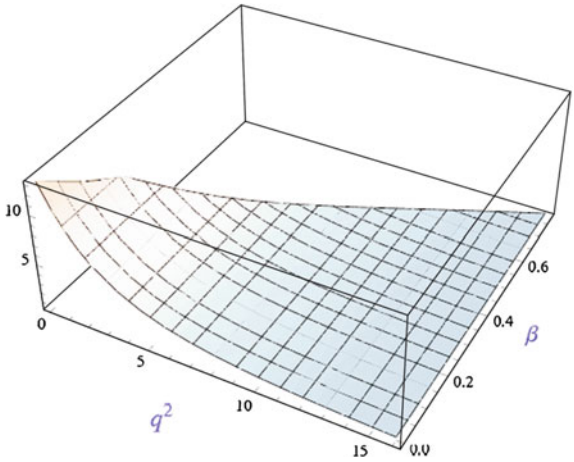

Fig. 9.8 Double differential cross section for the double photoionization of helium at $\omega = 800\,\text{eV}$ [39]

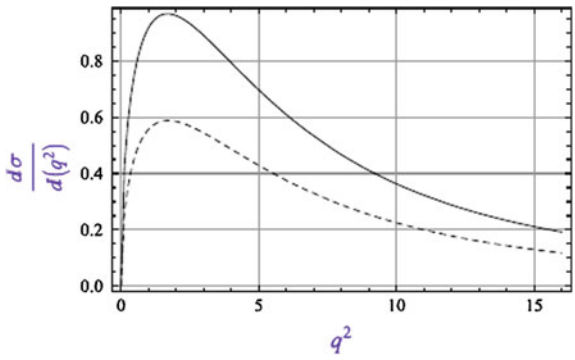

Fig. 9.9 Distribution in recoil momentum for the double photoionization of helium. *Solid line* is for $\omega = 800\,\text{eV}$; *dashed line* is for $\omega = 1\,\text{keV}$ [39]

9.4 Ejection of Relativistic Electrons

9.4.1 Distribution of Photoelectrons

Now we consider the case in which the photon energies are of order the rest energy of the electron $m \approx 511\,\text{keV}$ or strongly exceed this value. At least one of the photoelectrons is a relativistic one. Here we can single out three parts of the spectrum. In each of them, the mechanism of the process is different. Note that in this section, the total energies of the photoelectrons are E_i $(i = 1, 2)$, their kinetic energies are denoted by $\varepsilon_i = E_i - m$, and $\varepsilon = \varepsilon_1 + \varepsilon_2$.

As in the nonrelativistic case, one of the electrons can undergo a single photoionization, with the second electron moved to the continuum due to the sudden change of the Hamiltonian. This shakeoff mechanism (SO) provides mostly the slow secondary electrons with $\varepsilon_2 \sim I_Z$. The SO dominates in this part of the spectrum.

In the nonrelativistic case, the quasifree mechanism (QFM) dominates in the vicinity of the center of the spectrum $\beta \ll 1$. Now the relative size of the region of the QFM domination determined by (9.13) is of order unity.

In the intermediate part of the spectrum where both electrons carry the energies $\varepsilon_i \gg I_Z$ but $\beta < \sqrt{\varepsilon/(\varepsilon + m)}$, the amplitude is enhanced in the kinematic regions where the process goes on through intermediate states close to the mass shell. Double photoionization becomes a two-step process. In one of the channels, the photoelectron created by direct absorption of the photon knocks out the secondary electron in the next step. In the alternative channel, the incoming photon undergoes Compton scattering. In the next step, the scattered photon knocks out the second bound electron. This enables us to obtain relatively simple expressions for the energy distributions of the photoelectrons.

In the edge region, we can neglect the interaction between the photoelectrons. Thus in the expression for the amplitude

$$F^{++} = 2N(\omega)\langle\Psi_f|\gamma|\Psi_i\rangle; \quad \gamma = -e^{i\mathbf{p}_1\cdot\mathbf{r}_1}e_i\gamma^i, \tag{9.194}$$

the photoelectrons can be described by superposition of the single-particle functions of the Coulomb field

$$\Psi_f = \frac{1}{\sqrt{2}}\Big(\psi_{\mathbf{p}_1}(\mathbf{r}_1)\psi_{\mathbf{p}_2}(\mathbf{r}_2) - \psi_{\mathbf{p}_1}(\mathbf{r}_2)\psi_{\mathbf{p}_2}(\mathbf{r}_1)\Big), \tag{9.195}$$

with ψ the single-particle relativistic Coulomb functions. Since $p_2 \sim \mu_b \ll m$, we can describe the secondary electron by a nonrelativistic function with accuracy $\alpha^2 Z^2$.

The first electron transfers a large momentum $\mathbf{q}_1 = \mathbf{k} - \mathbf{p}_1$ to the nucleus ($q_1 = |\mathbf{q}_1| \sim m \gg \mu_b$) in either the initial or final state. It approaches the nucleus at small distances $r_1 \sim 1/q_1 \sim 1/m$. However, the initial-state wave function can be expressed in terms of the nonrelativistic wave function $\Psi(\mathbf{r}_1, \mathbf{r}_2)$ with accuracy $\alpha^2 Z^2$ (see Sect. 2.2.3). The amplitude takes the form $F^{++} = T(\mathbf{p}_1)\Phi(\mathbf{p}_2)$, where $\Phi(\mathbf{p}_2)$ is defined by (9.22). The explicit form of the function $T(\mathbf{p}_1)$ is not important for calculation of the double-to-single cross section ratio, since the amplitude of the single photoionization also contains $T(\mathbf{p}_1)$ as a factor. It is $F^{+} = T(\mathbf{p}_1)\Phi_{1s}$, with Φ_{1s} determined by (9.27). In the single-particle approximation, $T(\mathbf{p}_1)$ is the relativistic amplitude of the photoionization with relative accuracy $\alpha^2 Z^2$; see Sect. 6.3.4.

Hence in the edge region of the spectrum, the ratio F^{++}/F^{+} as well as the distribution $(d\sigma^{++}/d\varepsilon_2)/\sigma^{+}$ is the same as at the nonrelativistic energy transferred to the atom. The angular distribution of the primary electrons is the same as in the single photoionization, while that of the secondary electrons is isotropic. The contribution of the edge region to the double-to-single cross section ratio is given by (9.37). Expressions for asymptotics of the cross section of photoionization accompanied by excitation provided by (9.43) also remain true for $\omega \gtrsim m$.

We turn now to the distributions of photoelectrons in the region of domination of QFM. It is limited by the condition (9.13). The amplitude is expressed by (9.145).

Since the recoil momentum $q \sim \mu_b \ll m$, the function $S(q)$ is given by (9.146), with Ψ the nonrelativistic wave function of the bound state. Now F_0 is the relativistic amplitude of interaction between the photon and the system of two free electrons in the spin–singlet state. It can be written as

$$F_0 = \sqrt{2}N(\omega)(F_a + F_b)\,. \tag{9.196}$$

The two terms correspond to interactions between the electrons in the initial and final states. Introducing the four-vectors $P_a = (2m - E_2, -\mathbf{p}_2)$ and $P_b = (m + \omega, \mathbf{k})$, we can write

$$F_a = \bar{u}_{p_1}\hat{e}G_0(P_a)\gamma^\mu u_{0i}\bar{u}_{p_2}\gamma^\nu u_{0j}D_{\mu\nu}(\varepsilon_2, \mathbf{p}_2) \tag{9.197}$$

and

$$F_b = \bar{u}_{p_1}\gamma^\mu G_0(P_b)\hat{e}u_{0i}\bar{u}_{p_2}\gamma^\nu u_{0j}D_{\mu\nu}(\varepsilon_2, \mathbf{p}_2). \tag{9.198}$$

Here $u_{p_{1,2}}$ and $u_{0i,0j}$ are the Dirac bispinors of the photoelectrons and the electrons at rest, $i, j = 1, 2$ correspond to the two possible projections of the electron spin, G_0 is the propagator of free relativistic electron, and $D_{\mu\nu}$ is the propagator of the photon. The expressions (9.197) and (9.198) are illustrated by Fig. 9.2 with the continuum electrons and the electron in intermediate states described by the relativistic functions of free motion.

Employing the standard QED technique, we obtain the value of $|F_a + F_b|^2$ summed over the polarization of the photoelectrons and averaged over photon polarizations [31]). In actual calculations, it is convenient to employ the Feynman gauge for the propagator $D_{\mu\nu}$. We obtain [31]

$$d\sigma^{++} = \frac{\alpha r_0^2}{16\pi^2}|S(q)|^2 d^3q\,\delta(E_1 + E_2 - \omega - 2m)\frac{W(E_1)d^3p_1}{m^2\omega E_1 E_2}\,, \tag{9.199}$$

with $\mathbf{q} = \mathbf{p}_1 + \mathbf{p}_2 - \mathbf{k}$ and

$$W(E_1) = \left(\frac{\varepsilon_1 - \varepsilon_2}{\varepsilon_1\varepsilon_2}\right)^2\left[m^2 + E_1E_2 - \kappa^2 + \left(\frac{m\omega}{\varepsilon_1\varepsilon_2}\right)^2(2m\omega + m^2 - E_1E_2 + \kappa^2)\right], \tag{9.200}$$

$$\kappa^2 = \frac{\omega^4 - (E_1^2 - E_2^2)^2}{4\omega^2}; \quad \varepsilon_i = E_i - m.$$

The energy–momentum conservation law provides for $\mathbf{q} = 0$:

$$E_2(t_1) = \sqrt{E_1^2 + \omega^2 - 2\omega p_1 t_1}; \quad t_1 = \frac{\mathbf{p}_1 \cdot \mathbf{k}}{p_1 k}\,. \tag{9.201}$$

To obtain the energy distribution, we employ the delta function in (9.199) for integration over t_1. This provides

$$\frac{d\sigma^{++}}{d\beta} = \alpha\pi^2 r_e^2 \frac{\tilde{I}}{2m^2\omega} W(E_1); \quad \beta = \frac{\varepsilon_1 - \varepsilon_2}{\omega}, \tag{9.202}$$

with $\tilde{I}$ determined by (9.166). Direct evaluation leads to

$$\frac{d\sigma^{++}}{d\beta} = \frac{8\pi^2\alpha r_e^2}{m\omega^2} \tilde{I}\mathscr{F}(\beta)\,, \tag{9.203}$$

with

$$\mathscr{F}(\beta) = \left(\frac{\beta}{1-\beta^2}\right)^2 \left[1 + \frac{\beta^2}{\beta_0^2} + \frac{2m}{\omega} + \frac{16m^2}{\omega^2} \cdot \frac{1-\beta^2/\beta_0^2}{(1-\beta^2)^2}\right]. \tag{9.204}$$

Here $\beta_0^2 = \omega/(\omega + m)$ corresponds to the largest values of β for which the process can take place without participation of the nucleus, i.e., with $q = 0$. Examples of the energy distributions are presented in Fig. 9.10. The interval $0 < \beta < 1$ represented in Fig. 9.10 corresponds to the energy of the ejected electron $\omega/2 < \varepsilon_1 < \omega$.

In the nonrelativistic approximation $\omega \ll m$, the distribution becomes zero at $\beta^2 = \beta_0^2$, in agreement with (9.165). One can see that this is not true in the general case. The distribution has a finite value at $\beta^2 = \beta_0^2$, dropping rapidly for $\beta^2 > \beta_0^2$, since here one cannot make the recoil momentum q be as small as the binding momentum μ_b. Note also that the energy distribution vanishes in the center of the spectrum $\beta = 0$.

In the region of QFM dominations the angles between the directions of the momenta of the photoelectrons and that of the photon momentum are unambiguously determined by the photoelectron energies

$$t_1 = \frac{E_1^2 - E_2^2 + \omega^2}{2p_1\omega}; \quad t_2 = \frac{E_2^2 - E_1^2 + \omega^2}{2p_2\omega}\,. \tag{9.205}$$

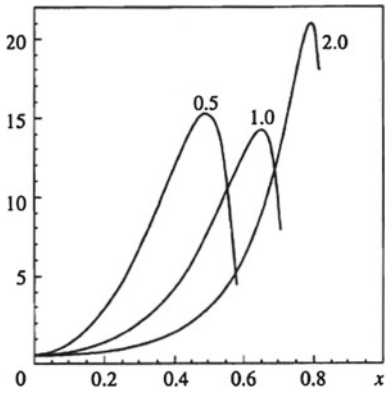

Fig. 9.10 Energy distribution of the electrons in the central region for the double photoionization of helium. The *horizontal* axis is for $x = \beta$. The *vertical* axis is for the function $\mathscr{F}(x)$. The numbers on the *curves* denote the values of the ratio ω/m [31]

This enables us to calculate the angular distributions

$$\frac{d\sigma^{++}}{dt_i} = \frac{d\sigma^{++}}{d\beta}\frac{d\beta}{dt_i}. \tag{9.206}$$

For the faster photoelectron with $E_1 > E_2$,

$$\beta(t_1) = f(t_1); \quad f(t_1) \equiv \frac{-(\omega+2m)\omega(1-t_1^2) + 2mt_1\sqrt{4\omega m + 3\omega^2 + \omega^2 t_1^2}}{(\omega+2m)^2 - \omega^2 t_1^2},$$

while for slower photoelectron, $\beta(t_2) = -f(t_2)$. The angular distributions can be written also as

$$\frac{d\sigma^{++}}{dt_i} = \frac{16\pi^2\alpha r_e^2 \tilde{I}}{m\omega^2}\mathscr{F}_1(t_i); \quad \mathscr{F}_1(t_i) = \frac{p_i}{E-E_i}\frac{\mathscr{F}(\beta(t_i))}{\chi(t_i)}, \tag{9.207}$$

with $E = E_1 + E_2$ and

$$\chi(t_i) = \frac{Ep_i - \omega E_i t_i}{(E-E_i)p_i}. \tag{9.208}$$

Note that for the faster photoelectron,

$$\sqrt{\frac{\omega}{\omega+4m}} \le t_1 \le 1,$$

while for the slower electron,

$$-1 \le t_2 \le \sqrt{\frac{\omega}{\omega+4m}}.$$

The angular distributions are shown in Fig. 9.11.

Note that the QFM provides nonzero values of the distribution $d\sigma^{++}/dt_1$ for the photoelectrons with momenta directed along the momentum of the photon. In single photoionization, we have $d\sigma^{+}/dt_1 = 0$, unless we include the relativistic corrections of order $\alpha^2 Z^2$ to the wave functions.

In the limit $\omega \gg m$, the region of the QFM dominates in the largest part of the energy distribution limited by the condition $0 \le \beta \le \beta_0 = 1 - m/2\omega$, i.e., for both photoelectrons,

$$\varepsilon_i \ge \frac{m}{4} \approx 125\,\text{keV}. \tag{9.209}$$

In the region of QFM domination, we can single out the region $\varepsilon_i \sim m$, where the amplitude reaches its largest values. Here it is determined by the contribution F_a given by (9.197), where $P_a = (2m - E_2, -\mathbf{p}_2)$, and the electron propagator is

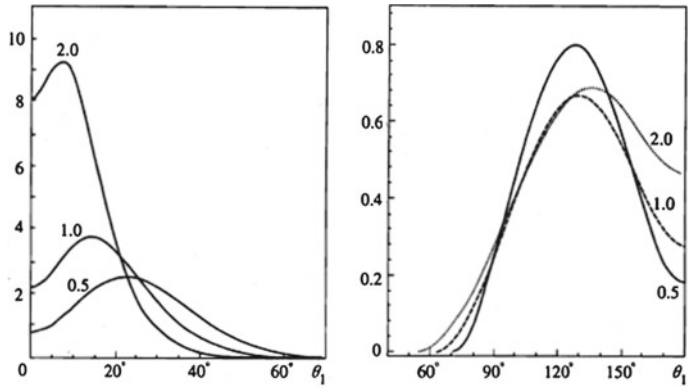

Fig. 9.11 Angular distribution of the electrons for the double photoionization of helium. *Left panel* is for the faster electron. *Right panel* is for the slower electron. The *horizontal* axes are for the angle θ_i. The *vertical* axes are for the function $\mathscr{F}_1(t_i)$. The numbers on the *curves* denote the values of the ratio ω/m [31]

$$G_0(P_a) \;=\; -\frac{\hat{P}_a + m}{4m\varepsilon_2}\,. \tag{9.210}$$

In the contribution F_b, the denominator of the propagator is $2m\omega$, and the amplitude is given by $F_b \sim F_a m/\omega \ll F_a$. The momentum of the faster photoelectron is directed mostly along that of the photon. The energy distribution of the slower photoelectron at $\varepsilon_2 \sim m$ can be obtained from (9.204). In the limit $1-\beta_0^2 \ll 1$, $1-\beta^2 \ll 1$, we obtain $\mathscr{F}(\beta) = \omega^2/(8\varepsilon_2^2)$. Since also

$$\frac{d\sigma^{++}}{d\varepsilon_2} \;=\; \frac{2}{\omega}\frac{d\sigma^{++}}{d\beta}\,,$$

we obtain for $\varepsilon_2 \geq m/4$,

$$\frac{d\sigma^{++}}{d\varepsilon_2} \;=\; \frac{2\pi^2\alpha r_e^2}{\omega m}\frac{\tilde{I}}{\varepsilon_2^2}\,. \tag{9.211}$$

At $\omega \gg m$, this part of the spectrum determines the QFM contribution to the total cross section.

Consider now the intermediate region of the spectrum, where both electrons are fast $\varepsilon_i \gg I_Z$, but their difference is large enough, i.e., $\beta > \sqrt{\omega/(\omega+m)}$, and the QFM does not work. We show that here the energy distribution is determined by two-step mechanisms. Their contributions to the spectrum $d\sigma_1/d\varepsilon_i$ and $d\sigma_2/d\varepsilon_i$ do not interfere.

One of the mechanisms was described in Sect. 4.2 for the nonrelativistic case. In the first step, single photoionization takes place. The real photoelectron passes from the vicinity of the nucleus to the region where the density of the electron cloud reaches

its largest density. Here it knocks out the secondary electron by electron impact. There is such a contribution in the relativistic case as well. The results obtained in Sect. 4.2 with the single-particle functions can be easily generalized to the case of the two-electron functions. The angular correlations peak at $\tau = \varepsilon_1\varepsilon_2/p_1p_2$. The contribution of the discussed mechanism to the spectrum is

$$\frac{d\sigma_1^{++}}{d\varepsilon_i} = s\frac{\sigma^+(\omega)}{\Phi_{1s}^2}\frac{d\sigma_{ee}(\varepsilon)}{d\varepsilon_i}; \quad s = \int d^3r \frac{|\Psi(0,\mathbf{r})|^2}{r^2}, \tag{9.212}$$

where $\varepsilon = \varepsilon_1 + \varepsilon_2$, the last factor is the spectrum of relativistic electron scattering, while s was introduced earlier by (9.125).

In the relativistic case, there is another two-step mechanism. In the first step, the photon undergoes Compton scattering on one of the bound electrons. In the next step, the scattered photon is absorbed by the remaining bound electron, moving it to the continuum. Neglecting the value of the binding energy, we find that the energy of the electron ejected in the second step is $\varepsilon_i = \omega_C$, with ω_C the energy of the scattered photon in the Compton scattering. Similar to (9.212), we can write

$$\frac{d\sigma_2^{++}}{d\varepsilon_i} = \frac{s}{\Phi_{1s}^2}\left(\sigma^+(\varepsilon_i)\frac{d\sigma_C}{d\omega_C}|_{\omega_C=\omega-\varepsilon_i} + \sigma^+(\omega-\varepsilon_i)\frac{d\sigma_C}{d\omega_C}|_{\omega_C=\varepsilon_i}\right), \tag{9.213}$$

where the last factor of the second term in parantheses on the RHS is the energy distribution of the photons in the free Compton scattering.

Finally, the energy distribution of the secondary electrons in the intermediate region is

$$\frac{d\sigma^{++}}{d\varepsilon_i} = \frac{d\sigma_1^{++}}{d\varepsilon_i} + \frac{d\sigma_2^{++}}{d\varepsilon_i}, \tag{9.214}$$

with the two terms on the RHS determined by (9.212) and (9.213). One can see that as in the nonrelativistic case, the contribution of these mechanisms to the cross section is much smaller than that of the QFM.

9.4.2 *Energy Dependence of the Cross Section*

Integration of the RHS of (9.204) provides the contribution of the region of QFM domination to the cross section:

$$\sigma_{QFM}^{++} = \frac{8\pi^2\alpha r_e^2}{m\omega^2}\tilde{I}\cdot V(\omega); \quad V(\omega) = \int_0^{\beta_0} d\beta \mathscr{F}(\beta); \quad \beta_0 = \sqrt{\frac{\omega}{\omega+m}}. \tag{9.215}$$

The integral can be evaluated analytically. It is convenient to represent it in terms of the parameters $y = \omega/m$ and β_0:

$$V(\omega) = A_1 + \frac{A_2}{y} + 16\frac{A_3}{y^2} - 16\frac{A_4}{y^3}; \quad A_1 = \beta_0(y+2) - L, \tag{9.216}$$

$$A_2 = \frac{\beta_0}{2}(3y+5) - \frac{5L}{4}; \quad A_3 = \frac{\beta_0}{4}\Big[(y+1)^2 - \frac{y+1}{2} - \frac{L}{4\beta_0}\Big];$$

$$A_4 = \frac{\beta_0}{6}\Big[(y+1)^3 - \frac{7(y+1)^2}{4} + \frac{3(y+1)}{8} + \frac{3L}{16\beta_0}\Big]; \quad L = \ln\frac{1+\beta_0}{1-\beta_0}.$$

One can see that the contribution of the QFM to the double-to-single cross section ratio is of the same order of magnitude as that of the SO. The contribution of the intermediate part of the spectrum is quenched at least by a factor of order α^2. Thus for the ratio of the cross sections defined by (9.2), we can write for all $\omega \gg I_Z$,

$$R_0(\omega) = C_0 + \frac{4\sqrt{2}}{5Z^2}\mathscr{I}\varphi\Big(\frac{\omega}{m}\Big), \tag{9.217}$$

with $\mathscr{I}$ defined by (9.176). Here the first term is the high-energy limit of the SO contribution. It does not depend on the photon energy; (9.37). The second term is the contribution of QFM. For $\omega \ll m$, we obtain $\varphi(\omega/m) = \omega/m$, while for $\omega \gg m$, we have

$$\varphi(\frac{\omega}{m}) = \frac{5\sqrt{2}}{4}\Big(1 - \frac{m}{\omega}\Big(\ln\frac{4\omega}{m} - \frac{2}{3}\Big)\Big) \approx 1.77\Big(1 - \frac{m}{\omega}\ln\frac{2\omega}{m}\Big). \tag{9.218}$$

In the ultrarelativistic limit $\omega \gg m$, the QFM contribution to the cross section σ^{++}_{QFM} is determined by integration of the distribution (9.211). This provides $\sigma^{++}_{QFM} \sim \omega^{-1}$, and the contribution to the ratio (9.217) does not depend on ω [41]. In the limit $\omega \gg m$, the ratio R_0 reaches a new limiting value,

$$R_0^{ur} = C_0 + \frac{2}{Z^2}\mathscr{I}\,. \tag{9.219}$$

Corrections to the second term are of order $m/\omega \cdot \ln(\omega/m)$. Thus due to the QFM, the asymptotic R_0^{ur} appears to be several times larger than the high-energy nonrelativistic asymptotic C_0:

$$R_0^{ur} = C_0\zeta(Z). \tag{9.220}$$

We traced the Z-dependence of the parameter ζ and obtained $\zeta = 2.83$ for helium. In the limit $Z \gg 1$, when $\mathscr{I} = 1/8$, we obtain $\zeta = 3.78$, in agreement with the perturbative model result [31]. We present ζ for several values of Z in Table 9.5 [42].

Table 9.5 The CFHH values of the parameter $\zeta(Z)$, which expresses the ratio of the ultrarelativistic and high energy nonrelativistic limits of $R_0(\omega)$

Z	$\zeta(Z)$
1	2.27
2	2.83
3	3.08
4	3.17
5	3.28
10	3.52

9.5 Two-Electron Capture with Emission of a Single Photon

9.5.1 Experiment and Theory

Now we consider the process of radiative double-electron capture (RDEC) by nuclei in their scattering on the atoms. The two target electrons are captured to a bound state of the projectile with emission of a single photon. The upper limit for the probability of the RDEC was found for the collisions of argon nuclei with carbon [43] and for those of uranium nuclei with atoms of argon [44]. The process was detected in collisions of the fully stripped ions of oxygen and fluorine with a carbon foil [45, 46]. The most probable channel is the one in which the two electrons are captured independently and thus two photons are emitted. However, the correlated electrons can be captured also with the emission of a single photon. Such a process is a challenge to the theoretical views on charge-transfer reactions and on correlation effects in then atomic system.

In the theoretical treatment of RDEC, we consider the process in the rest frame of the heavy nucleus, following [47]. The target electrons can be considered as free if their atomic velocities are much smaller than that of the projectile. Neglecting interactions between the target electrons, we view the process as the reaction of capture of two electrons from the continuum state of the Coulomb field created by the target nucleus to the bound state, followed by emission of a single photon. This makes the process time-reversed double photoionization. Neglecting the internal motion of the electrons in the target atom, we study the capture of two continuum electrons with equal momenta $\mathbf{p}_1 = \mathbf{p}_2 = \mathbf{p}$. The process is characterized by the kinetic energy per nucleon $\varepsilon_N(MeV/u)$. The corresponding electron kinetic energies are $\varepsilon = \varepsilon_N m/m_N$, where $m_N \approx 940\,\mathrm{MeV}$ is the nucleon mass.

We present the calculations in nonrelativistic approximation. They are true for the energies of the radiated photon $\omega \ll m$ and for relatively light projectile nuclei with $\alpha^2 Z^2 \ll 1$. The probability of double-electron capture to the K shell of a bare ion with emission of a single photon per unit time is

$$dW = \frac{2\pi}{V^2}|F|^2\delta(\varepsilon_1 + \varepsilon_2 - \omega - I^{++})\frac{d^3k}{(2\pi)^3}, \tag{9.221}$$

where $\varepsilon_1 = \varepsilon_2$ are the kinetic energies of the continuum electrons. The RDEC amplitude F can be obtained from that of the double photoionization of the K shell F^{++} by reversing the signs of the momenta of the photon $\mathbf{k} \to -\mathbf{k}$ and of the electrons $\mathbf{p}_i \to -\mathbf{p}_i$ together with the complex conjugation of the polarization vector $\mathbf{e} \to \mathbf{e}^*$. Due to the symmetry with respect to the time reversal, we have $|F|^2 = |F^{++}|^2$. To obtain the effective cross section, one should divide this by the current flux of incident electrons $j = v/V$, with $v = p/m$ the velocity of the electrons before their collisions with the projectile nucleus, while V is the normalization volume

$$d\sigma = \frac{dW}{j} = 2\pi \frac{\omega^2}{vV} |F|^2 \frac{d\Omega}{(2\pi)^3} . \tag{9.222}$$

The cross section depends on V, since we consider the three-body collision problem. In ion–atom collisions, the volume V is a characteristic of the target atom and corresponds to an effective localization volume of the two electrons captured by the nuclei. For each electron, one can define $V = \psi_{\max}^{-2} \int |\psi(\mathbf{r})|^2 d^3r$, where ψ is the single-particle function of a target electron with its largest value ψ_{max}. Employing the hydrogenlike functions, we can estimate for the K electrons

$$V \approx V_0; \quad \frac{1}{V_0} = |\psi(0)|^2 = \frac{\eta^3}{\pi} , \tag{9.223}$$

with $\eta = m\alpha Z_t$, while Z_t is the nuclear charge of the target. For the target electrons in the states with principal quantum numbers $n \geq 2$, we can employ (9.223), replacing η by $m\alpha Z_{eff}/n$, with $Z_{eff} < Z_t$ the effective nuclear charge felt by the electrons. Thus the value of the volume V is much larger than it was for the $1s$ electrons. Hence, we can include only the capture of the K shell target electrons.

For the actual calculations, we employ the perturbative model formulated in Sect. 9.2.2. We use (9.101) for the amplitude, describing the RDEC of two electrons to the K shell of the projectile. The RDEC cross section can be written as [48]

$$\sigma_{KK} = \frac{2^{19} r_e^2}{3\alpha\pi} \frac{Z_t^3}{\lambda Z^5} R(\xi) , \tag{9.224}$$

with Z the charge of the projectile nucleus, $\lambda = V/V_0$. The universal function $R(\xi)$, where $\xi = m\alpha Z/p$, was obtained in [48, 49] for the cross sections σ_{KK} and σ_{KL} of RDEC to the 1^1S_0 and 2^1S_0 states.

The results of measurements and of calculations ($\lambda = 1$) of RDEC cross sections are presented in Table 9.6. The nonrelativistic results for uranium rather estimate the values of the cross sections. However, one can see that the theory is consistent with the upper limits of the cross sections found in experiments with argon and uranium projectiles. The theory underestimates the experimental values obtained in [45, 46], where the RDEC was detected. This leaves much room for improvement of the theoretical approach.

Table 9.6 The RDEC cross sections in $mb/atom$ units measured in [45, 46] and calculated in [48, 49]

Z	$\varepsilon_N, MeV/u$	Z_t	$\sigma_{KK}(exp)$	$\sigma_{KK}(theor)$	$\sigma_{KL}(exp)$	$\sigma_{KL}(theor)$
18	11.4	6	≤ 5.2	3.2		2.2
92	297	18	≤ 10	0.025		6×10^{-4}
8	2.38	6	3200 ± 1900	160	2300 ± 1300	112
9	2.21	6	1900 ± 1200	221	1600 ± 980	194

9.5.2 The High-Energy Case

Now we consider the values of ε_N corresponding to the high but nonrelativistic energies of the captured electrons $I_b \ll \varepsilon_i \ll m$. This corresponds to $\xi_i \ll 1$, for which the cross section drops rapidly. It is unlikely that it will be measured in the nearest future. However, from the point of view of the theory, this case is interesting, since the amplitude is directly related to the ground-state wave function at the double coalescence points $r_1 = 0$, $r_2 = 0$, $r_{12} = 0$ and at the triple coalescence point $r_1 = r_2 = r_{12} = 0$. We assume that the charge of the projectile nucleus is $Z \gg 1$. For such values of Z, we can assume that the binding momentum $\mu_b \approx \eta = m\alpha Z$, and that $I_b = I_Z = m\alpha^2 Z^2/2$.

Interactions of the captured electrons with the target nucleus are described by the parameters $\xi_i = \eta/p_i \ll 1$ and thus can be treated perturbatively. We shall see that to reproduce the main mechanisms of the process, one should include the lowest-order terms describing the interactions of the incoming electrons with the target nucleus and also between themselves.

The initial-state wave function thus can be represented as

$$\Psi_{in} = \Psi_{in}^{(0)} + G_0 V_{eN} \Psi_{in}^{(0)} + G_0 V_{ee} \Psi_{in}^{(0)}, \tag{9.225}$$

where G_0 is the Green function of the two noninteracting electrons, while $\Psi_{in}^{(0)}$ is the symmetrized product of the plane waves. A large momentum $q \gg \eta$ ($q = |\mathbf{q}|$; $\mathbf{q} = \mathbf{p}_1 + \mathbf{p}_2 - \mathbf{k}$) can be transferred to the nucleus by the electrons in both the initial and final states. The two mechanisms provide contributions of the same order of magnitude to the amplitude:

$$F = N(\omega)\langle\Psi|\gamma|\Psi_{in}\rangle; \quad \gamma = \gamma_1 + \gamma_2 . \tag{9.226}$$

We begin with the dipole approximation, i.e., we neglect the terms of order k/p. If all interactions in the initial state are neglected, the amplitude $F^{(0)} = N(\omega)\langle\Psi|\gamma|\Psi_{in}^{(0)}\rangle$ corresponds to the first term on the RHS of (9.225). It can be expressed in terms of the bound-state wave function in momentum space:

$$F^{(0)} = N(\omega)\langle\Psi|\gamma|\Psi_{in}^{(0)}\rangle = 2\sqrt{2}N(\omega)\frac{\mathbf{e}^*\cdot\mathbf{p}}{m}\int d^3r_1 d^3r_2 \Psi(\mathbf{r}_1,\mathbf{r}_2)e^{i\mathbf{p}\cdot\mathbf{r}_1}e^{i\mathbf{p}\cdot\mathbf{r}_2} =$$
$$= 2\sqrt{2}N(\omega)\frac{\mathbf{e}^*\cdot\mathbf{p}}{m}\tilde{\Psi}(\mathbf{p},\mathbf{p}). \tag{9.227}$$

Each of the bound electrons transfers a large momentum p to the nucleus. The integrals are saturated by small $r_1 \sim r_2 \sim 1/p \ll 1/\eta$. Keeping r_1 finite, we can carry out the expansion (9.20) for the function Ψ. Employing the first Kato cusp condition, we find that the linear terms of the expansion provide the contribution

$$F_{lin}^{(0)} = 2M(\omega,\mathbf{p})X(p); \quad X(p) = \int d^3r_1 \Psi(\mathbf{r}_1,\mathbf{r}_2=0)e^{i\mathbf{p}\cdot\mathbf{r}_1}, \tag{9.228}$$

with $M(\omega,\mathbf{p})$ defined by (9.26), where the polarization vector $\mathbf{e}$ should be changed to $\mathbf{e}^*$. However the wave function is not analytic at the tree particle coalescence point $r_1 = r_2 = 0$ and cannot be expanded in a Taylor series. Only the terms linear in $r_{1,2}$ can be singled out; see (4.99). In the amplitude $F^{(eN)} = \langle\Psi|\gamma|G_0V_{eN}\Psi_{in}^{(0)}\rangle$ corresponding to the second term on the RHS of (9.225), we label the electron that emits the photon with 1, and label another incoming electron with 2. The amplitude $F^{(eN)}$ can be written as the sum of two terms describing interactions of electrons 1 and 2 with the nucleus

$$F^{(eN)} = \sqrt{2}\int\frac{d^3f}{(2\pi)^3}\frac{\langle\Psi|\gamma_1|\mathbf{p},\mathbf{f}\rangle\langle\mathbf{f}|V_{eN}|\mathbf{p}\rangle}{\varepsilon_1 - f^2/2m} + \sqrt{2}\int\frac{d^3f}{(2\pi)^3}\frac{\langle\Psi|\gamma_2|\mathbf{p},\mathbf{f}\rangle\langle\mathbf{f}|V_{eN}|\mathbf{p}\rangle}{\varepsilon_2 - f^2/2m}. \tag{9.229}$$

We focus on the contribution $F^{(eN)'}$ of small $f \sim \eta$ and $r_2 \sim 1/\eta$, while $r_1 \sim 1/p \ll \eta$. The first term on the RHS of (9.229) describes the configuration in which electron 1 approaches the nucleus at small distances of order $1/p \ll 1/\eta$ to transfer a large momentum to the nucleus. Electron 2 also transfers a large momentum to the nucleus before being captured by the target. In the second term, electrons 1 and 2 exchange their roles. Direct calculation provides

$$F^{(eN)'} = -2M(\omega,\mathbf{p})X_1(p); \quad X_1(p) = \int\frac{d^3f}{(2\pi)^3}\tilde{\Psi}(\mathbf{p},\mathbf{f}). \tag{9.230}$$

One can see that $X_1 = X$, with X defined by (9.228). Employing (9.228), one finds that $F_{lin}^{(0)} + F^{(eN)'} = 0$.

The amplitude $F^{(ee)} = \langle\Psi|\gamma|G_0V_{ee}\Psi_{in}^{(0)}\rangle$ is expected to be Z times smaller than $F^{(eN)}$, just because the charge of the nucleus is Z times that of the electron. However, it should be included, since the amplitudes $F^{(eN)'}$ and $F^{(0)}$ cancel to a great extent. The main contribution to this amplitude comes from the configuration in which electron 2 transfers its momentum and energy to the first one and is captured by the target at distances of order the size of the bound state $1/\eta$. Electron 1 approaches the nucleus at small distances of order $1/p$:

$$F^{(ee)} = 2\sqrt{2}\int \frac{d^3f}{(2\pi)^3}\cdot\frac{\langle\Psi|\gamma_1|2\mathbf{p}-\mathbf{f},\mathbf{f}\rangle}{2\varepsilon-(2\mathbf{p}-\mathbf{f})^2/2m-f^2/2m}\cdot\frac{4\pi\alpha}{(\mathbf{p}-\mathbf{f})^2}. \tag{9.231}$$

Direct calculation provides

$$F^{(ee)} = -\frac{2}{Z}M(\omega,\mathbf{p})X(2p)\,. \tag{9.232}$$

In the dipole approximation, the leading contribution to the amplitude is $F = F^{(0)} + F^{(eN)'} + F^{(ee)}$ [50]. Thus

$$F = F_1 = 2\sqrt{2}N(\omega)\frac{\mathbf{e}^*\cdot\mathbf{p}}{m}\left[\tilde{\Psi}(\mathbf{p},\mathbf{p}) - Z\frac{8\pi\alpha m}{p^4}X(p) - \frac{8\pi\alpha m}{p^4}X(2p)\right], \tag{9.233}$$

with the function $X(p)$ defined by (9.228). Due to partial cancellation of the first two terms, the Z and p dependence of the amplitude is $F_1 \sim N(\omega)\alpha\eta^4/p^7$.

There is an alternative mechanism of the process that works beyond the dipole approximation. Returning to the amplitudes $F^{(eN)}$, one can see that one of the incoming electrons can transfer a large momentum of about $2\mathbf{p}$ to the nucleus in the first step, moving after this with momentum $\mathbf{p}' = -\mathbf{p}$. Now we have the electrons moving "back to back," and in the second step, they can be captured by the nucleus, transferring to it only a small momentum of order η. The second step is just the time-reversed double photoionization due to the QFM. The amplitude F_2 is determined by the sum of the contributions $F_a^{(eN)}$ and $F_b^{(eN)}$, where the integrals over $\mathbf{f}$ are saturated by $\mathbf{f} = -\mathbf{p} + \mathbf{q}$ with $|\mathbf{q}| \ll p$. Employing the results of Chap. 4, we obtain

$$F_2 = \int \frac{d^3q}{(2\pi)^3}F^*_{QFM}(\mathbf{q})\frac{2m}{p^2-(\mathbf{p}-\mathbf{q}-\mathbf{k})^2}\frac{4\pi\alpha Z}{(2p)^2}. \tag{9.234}$$

The amplitude F^*_{QFM} can be obtained by changing $\mathbf{e}$ to $\mathbf{e}^*$ in the double photoionization amplitude F_{QFM} given by (9.145). Employing (9.145), we obtain

$$F_2 = \int \frac{d^3q}{(2\pi)^3}\frac{S(q)}{p^2-(\mathbf{p}-\mathbf{q}-\mathbf{k})^2}\frac{2\pi\eta}{p^2}F_0^*(\mathbf{p}). \tag{9.235}$$

Here the amplitude for interaction of the photon with two free electrons F_0 is given by (9.147), while the function $S(q)$ is defined by (9.146). Employing (4.105) for the approximate wave function on the electron–electron coalescence line, we obtain for the amplitude of the two-step process

$$F_2 = \frac{\pi N\eta}{p^2}\frac{F_0^*(\mathbf{p})}{\mathbf{p}\cdot\mathbf{k}+2ip\eta}\,, \tag{9.236}$$

with $N \sim \eta^3$ the normalization factor of the wave function on the electron–electron coalescence line.

Comparing the amplitude F_2 of the two-step process and the amplitude F_1 one can see that the two-step process dominates at least for the nonrelativistic electron energies.

References

1. P.K. Kabir, E.E. Salpeter, Phys. Rev. **108**, 1256 (1957)
2. T. Åberg, Phys. Rev. A **2**, 1726 (1970)
3. F.W. Byron, C.J. Joachain, Phys. Rev. **164**, 1 (1967)
4. R. Krivec, M.Y. Amusia, V.B. Mandelzweig, Phys. Rev. A **62**, 064701 (2000)
5. J.C. Levin, G.B. Armen, L.A. Selin, Phys. Rev. Lett. **76**, 1220 (1996)
6. A. Dalgarno, A.L. Stewart, Proc. R. Soc. Lond. Ser. A **76**, 49 (1960)
7. M.Y. Amusia, E.G. Drukarev, V.G. Gorshkov, M.P. Kazachkov, J. Phys. B **8**, 1248 (1975)
8. H.A. Bethe, E.E. Salpeter, *Quantum Mechanics of One- and Two -Electron Atoms* (Dover Publications, NY, 2008)
9. R.C. Forrey, H.R. Sadeghpour, J.D. Baker, J.D. Morgan III, A. Dalgarno, Phys. Rev. A **51**, 2112 (1995)
10. R. Krivec, M.Y. Amusia, V.B. Mandelzweig, Phys. Rev. A **63**, 052708 (2001)
11. M.Y. Amusia, A.I. Mikhailov, JETP **84**, 474 (1997)
12. J.H. McGuire, N. Berrah, R.J. Bartlett, J.A.R. Samson, J.A. Tanis, C.L. Cocke, A.S. Sclachter, J. Phys. B **28**, 913 (1995)
13. E.G. Drukarev, M.B. Trzhaskovskaya, J. Phys. B **31**, 427 (1998)
14. R.A. Bonham, D.A. Kohl, J. Chem. Phys. **45**, 271 (1966)
15. A.I. Mikhailov, I.A. Mikhailov, A.N. Moskalev, A.V. Nefiodov, G. Plunien, G. Soff, Phys. Rev. A **69**, 032703 (2004)
16. S.H. Southworth, E.P. Kanter, B. Krassing, et al., Phys. Rev. A **67**, 062712 (2002)
17. R. Ahopelto, E. Rantavuori, Phys. Scripta **20**, 71 (1979)
18. R. Diamant, S. Huotari, K. Hamalainen et al., Phys. Rev. A **62**, 052519 (2000)
19. E.G. Drukarev, E.Z. Liverts, M.Y. Amusia, R. Krivec, V.B. Mandelzweig, Phys. Rev. A **77**, 012715 (2008)
20. R. Wehlitz et al., J. Phys. B **30**, L51 (1997)
21. A.I. Mikhailov, A.V. Nefiodov, Phys. Rev. A **86**, 013413 (2012)
22. A.Y. Istomin, A.F. Starace, N.L. Manakov, A.V. Meremianin, A.S. Kheifets, I. Bray, Phys. Rev. A **72**, 052708 (2005)
23. E.G. Drukarev, A.I. Mikhailov, V.S. Polikanov, Eur. Phys. J. D **69**, 155 (2015)
24. C. Pan, H.P. Kelly, J. Phys. B **28**, 5001 (1995)
25. E.G. Drukarev, Phys. Rev. A **52**, 3910 (1995)
26. T. Surić, E.G. Drukarev, R.H. Pratt, Phys. Rev. A **67**, 022709 (2003)
27. E.G. Drukarev, Phys. Usp. **50**, 835 (2007)
28. E.Z. Liverts, M.Y. Amusia, E.G. Drukarev, R. Krivec, V.B. Mandelzweig, Phys. Rev. A **71**, 012715 (2005)
29. E.G. Drukarev, Phys. Rev. A **51**, R2684 (1995)
30. A.I. Mikhailov, I.A. Mikhailov, JETP **98**, 248 (2004)
31. A.I. Mikhailov, I.A. Mikhailov, JETP **87**, 833 (1998)
32. R. Krivec, M.Y. Amusia, V.B. Mandelzweig, Phys. Rev. A **64**, 012713 (2001)
33. R. Wehlitz et al., Phys. Rev. A **53**, R3720 (1996)
34. R. Spielberger et al., Phys. Rev. A **59**, 371 (1999)
35. T. Surić, K. Pisk, B.A. Logan, R.H. Pratt, Phys. Rev. Lett. **73**, 790 (1994)
36. T. Surić, K. Pisk, R.H. Pratt, Phys. Lett. A **211**, 289 (1996)
37. A.I. Mikhailov, A.V. Nefiodov, Phys. Rev. A **91**, 013410 (2015)
38. M.S. Schöffler et al., Phys. Rev. Lett. **111**, 0132003 (2013)

39. M.Y. Amusia, E.G. Drukarev, E.Z. Liverts, A.I. Mikhailov, Phys. Rev. A **87**, 043423 (2013)
40. A. Nordsieck, Phys. Rev. **93**, 785 (1954)
41. E.G. Drukarev, F.F. Karpeshin, J. Phys. B. **9**, 399 (1976)
42. M.Y. Amusia, E.G. Drukarev, R. Krivec, V.B. Mandelzweig, Phys. Rev. **66**, 052706 (2002)
43. A. Warczak et al., Nucl. Instr. Meth. Phys. Res. B **98**, 303 (1995)
44. C. Bednarz et al., Nucl. Instr. Meth. Phys. Res. B **205**, 573 (2003)
45. A. Simon, A. Warczak, T. Elkafrawy, J.A. Tanis, Phys. Rev. Lett. **104**, 123001 (2010)
46. T. Elkafrawy, A. Warczak, A. Simon, J.A. Tanis, Phys. Scr. T. **144**, 014024 (2011)
47. V.L. Yakhontov, M.Y. Amusia, Phys. Rev. A **55**, 1952 (1997)
48. A.I. Mikhailov, I.A. Mikhailov, A.V. Nefiodov, G. Plunien, G. Soff, Phys. Lett. A **328**, 350 (2004)
49. A.V. Nefiodov, A.I. Mikhailov, G. Plunien, Phys. Lett. A **346**, 158 (2005)
50. E.G. Drukarev, A.I. Mikhailov, I.A. Mikhailov, W. Scheid, Phys. Rev. A **76**, 062701 (2007)

Chapter 10
Photoionization of Endohedral Atoms

Abstract We study photoionization of fullerenes and of fullerenes with encapsulated atoms. We present the calculation for the photoionization cross section of negative ions C_{60}^-, describing the field of the fullerene shell by the Dirac bubble potential. The investigation of the dependence of the high-energy asymptotics on the shape of the model potential is carried out. We analyze the photoionization of an atom encapsulated into the fullerene. The energy dependence of the cross section may differ fundamentally from that for an isolated atom due to interference of the outgoing electron wave with that reflected by the fullerene shell. We analyze the inelastic processes in the fullerene shell that accompany the photoionization of the encapsulated atom. It appears to be possible to sum the perturbative series for photoelectron interaction with the fullerene shell. The probability of inelastic processes was found to be close to unity in the large interval of the photon energies.

10.1 Photoionization of Fullerenes

10.1.1 Fullerenes

Fullerene is a special kind of molecule containing $N \gg 1$ nuclei of carbon ($Z = 6$) distributed together with $6N$ electrons in a thin layer between two surfaces. Such systems are labeled as C_N. The $2N$ atomic $1s$ electrons are tightly bound to the nuclei. Four $2s2p$ electrons of each carbon atom are collectivized, providing $4N$ valence electrons.

Fullerenes were discovered about thirty years ago [1]. The most studied is the fullerene C_{60}. The nuclei of carbon form 20 hexagons and 12 pentagons. The system has a complicated icosahedral symmetry. However, in applications, the fullerene C_{60} can be assumed to have a spherical shape. The 60 nuclei of carbon are assumed to be located on a sphere of radius R. The empirical value of the radius is $R \approx 6.5r_0$, or $R \approx 6.5$ a.u. The 120 atomic $1s$ electrons are located near their nuclei. The 240 collectivized electrons are located in the layer between spheres of radii R and $R + \Delta$ (sometimes, the radii are denoted by $R - \Delta/2$ and $R + \Delta/2$). The width of the layer is $\Delta \approx 1.5$ a.u.

E.G. Drukarev and A.I. Mikhailov, *High-Energy Atomic Physics*,
Springer Series on Atomic, Optical, and Plasma Physics 93,
DOI 10.1007/978-3-319-32736-5_10

There are a number of other fullerenes C_N, which can be treated approximately as having spherical shape. For all of them,

$$\Delta \ll R\,. \tag{10.1}$$

The charge density inside the layer has been investigated in several papers. It has a sharp maximum in the center of the layer; see a typical shape below in Fig. 10.1.

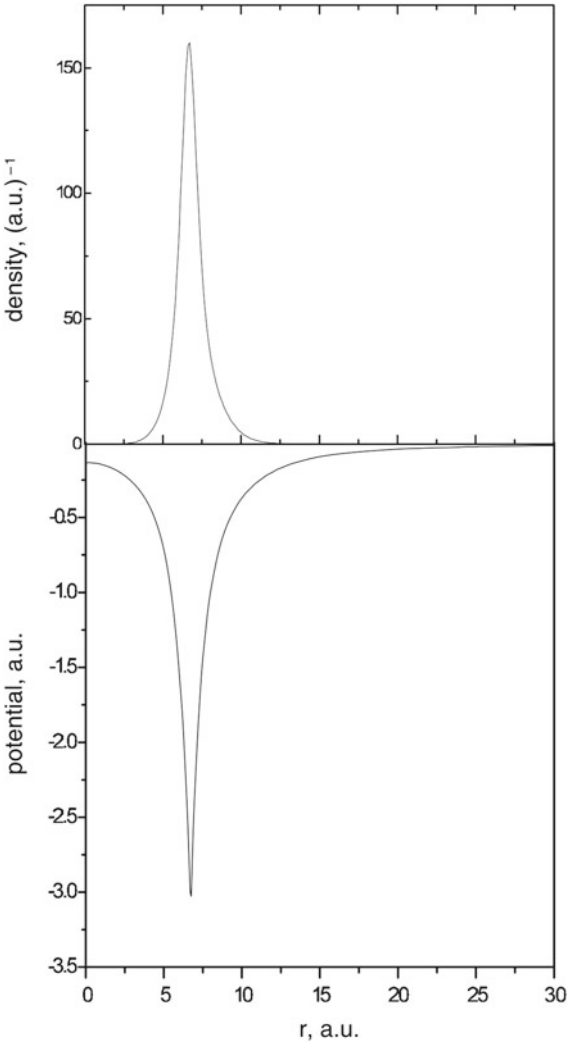

Fig. 10.1 The radial dependence of the electron density (upper panel) and of the potential energy (lower panel) for the fullerene C_{60} obtained in a self-consistent calculation [2]. Reproduced with permission of IOP Publishing

Once the spherical symmetry is accepted, the single-particle states of the electrons can be described by the principal quantum number $n = 1, 2, \ldots$ and the value of the orbital momentum ℓ [3]. The number of the nodes of radial wave functions is $n - 1$. In the fullerene C_{60}, the electron states either have no radial nodes (σ orbitals) or have one node at the spherical surface (π orbitals). In the fullerene C_{20}, 76 out of 80 valence electrons belong either to σ or to π orbitals [2].

The calculations that provide the values of the charge density in the fullerene shell (FS) can give also the shape of the potential $\varphi(r)$ created by the FS. However, in applications it is desirable to have an analytical approximation for $\varphi(r)$.

The FS potential at the space point $\mathbf{r}$ can be presented as the sum of potentials φ_n and φ_e created by the nuclei and the electrons respectively, i.e., $\varphi(r) = \varphi_n(r) + \varphi_e(r)$. The ingredients of $\varphi(r)$ can be represented in terms of the carbon nuclei distribution density ρ_n and the electron distribution density ρ_e

$$\varphi_n(r) \;=\; eZ \int d^3r' \frac{\rho_n(\mathbf{r}')}{|\mathbf{r} - \mathbf{r}'|}; \quad \varphi_e(r) \;=\; -e \int d^3r' \frac{\rho_e(\mathbf{r}')}{|\mathbf{r} - \mathbf{r}'|}\,, \tag{10.2}$$

where $Z = 6$ is the charge of the carbon nucleus. The density of the electron cloud of the FS $\rho_e(\mathbf{r}')$ is normalized as

$$\int d^3r' \rho_e(\mathbf{r}') \;=\; ZN. \tag{10.3}$$

Under the assumption of spherical symmetry, the fixed positions of the carbon nuclei $\mathbf{R}_k$ can be approximated by their uniform distribution over the sphere of radius R:

$$\rho_n(r) \;=\; \frac{N}{4\pi} \frac{\delta(r - R)}{R^2}\,. \tag{10.4}$$

This charge density creates the potential

$$\varphi_n(\mathbf{r}) \;=\; eZN \int \frac{d\Omega}{4\pi} \frac{1}{|\mathbf{r} - \mathbf{R}|}\,, \tag{10.5}$$

where Ω is the solid angle of the vector $\mathbf{R}$. Employing (5.148) we obtain $\varphi_n(r) = eZN/R$ at $r \le R$, while $\varphi_n(r) = eZN/r$ at $r \ge R$.

At $r \to 0$, the total potential reaches a finite value,

$$\varphi(0) \;=\; \frac{eZN}{R} - 4\pi e \int_0^\infty dr' r' \rho_e(\mathbf{r}'). \tag{10.6}$$

The potential $\varphi(r)$ determines the potential energy of the electron in the field of the FS:

$$U(r) \;=\; -e\varphi(r)\,. \tag{10.7}$$

In actual calculations, one usually employs a model potential $U(r)$. The model potential should satisfy the limiting conditions at $r \to 0$ and at $r \to \infty$ presented above. Also, the radial dependence of the charge density is connected with the potential by the Poisson equation $\Delta\varphi = -4\pi e\rho$, which can be written as

$$\frac{1}{r}\frac{d^2[rU(r)]}{dr^2} = 4\pi\alpha\rho(r)\,. \tag{10.8}$$

The shape of the r-dependence of the charge density determined by (10.8) with the model potential $U(r)$ should be consistent with the empirical data.

The simplest model potential is $U(r) = 0$ everywhere outside the FS, while $U(r) = -U_0$ with $U_0 > 0$ inside the FS, i.e., at $R \le r \le R + \Delta$. It can be written as

$$U(r) = -U_0\theta(r-R)\Big(1-\theta(r-R-\Delta)\Big); \quad U_0 > 0. \tag{10.9}$$

It was noted in [4] that this potential does not reproduce the shape of the density dependence on r presented in Fig. 10.1. Indeed, we find from (10.8) that the charge density actually vanishes inside the FS, where $U = \text{const}$. The density is rather concentrated near the walls of the FS, where the potential $U(r)$ suffers the jumps.

A more complicated Dirac bubble potential [5] is

$$U(r) = -U_0 r_0 \delta(r-R); \quad U_0 > 0\,. \tag{10.10}$$

Sometimes, model potentials are determined by analytical functions of r with a peak at $r = R$. The Dirac bubble potential can be viewed as the limiting case of the Lorentz bubble potential. The latter is determined by the analytical formula

$$U(r) = -\frac{U_0}{\pi}\frac{ar_0}{(r-R)^2 + a^2}\,. \tag{10.11}$$

The Dirac bubble potential can be treated as the limiting case of this potential at $a \to 0$. The Gaussian-type potential

$$U(r) = -\frac{U_0}{\pi}\exp\Big(\frac{-(R-r)^2}{s^2}\Big)\,, \tag{10.12}$$

with $s \approx \Delta$ was employed in [6].

The fullerene C_{60} can bind one more electron, creating the negative ion C_{60}^-. The energy of ionization I_{aff} of the additional electron (called also the electron affinity of C_{60}) is known to be about to 2.7 ± 0.1 eV [7]. The value of U_0 is usually chosen to reproduce the value of electron affinity. This provides $U_0 \approx 8$ eV for the "well potential" given by (10.9), while $U_0 \approx 10$ eV for the Dirac bubble potential (10.10).

The solutions of most problems connected with fullerenes require numerical calculations. However, due to the existence of the small parameter Δ/R, some of the effects can be traced analytically, at least in the lowest order in Δ/R. We shall consider the fullerenes that can be treated as having approximately spherical shape.

10.1.2 Photodetachment of C_{60}^-

Photoionization of the neutral fullerene is a much more complicated process than that of an isolated atom. Even in the channel $\gamma + C_{60} \to e^- + C_{60}^+$, the cross section exhibits large peaks corresponding to collective excited states of the ion C_{60}^+ [8, 9]. The double-to-single photoionization ratio in fullerenes appears to be much larger than in the atoms [10]. Thus it is difficult to provide a simple example of analytical calculation in this case. In photoionization of a negative ion C_N^-, one can separate the channel $\gamma + C_N^- \to e^- + C_N$ in which the photon interacts with the additional electron of the fullerene shell while the rest ones in the ground state. Since the additional electron is well separated from the neutral FS, the process can be viewed as a single-particle one. The neutral FS can be treated as a source of an external field.

The existence of the negative ion C_{60}^- was confirmed in experiments long ago. However, there are controversial experimental results on the quantum numbers of the extra electron state. Some experiments provide data consistent with the attachment of the extra electron to the s state (see, e.g., [11]), while others present evidence for a nonzero angular momentum of the observed state [12].

We shall employ the Dirac bubble model for the FS potential, making more general statements at the end. This model allows both the s and p and also the d states for the additional electron. The spectrum of the wave equation with this potential was studied in [13] in connection with the hyperfine splitting of the atomic levels. This was several years before the discovery of fullerenes.

Representing the wave function of the additional electron as $\psi_{n\ell m}(\mathbf{r}) = \chi_{n\ell}(r)\, Y_{\ell m}(\Omega)/r$, we come to the wave equation

$$\left[-\frac{1}{2m}\frac{d^2}{dr^2} + \frac{\ell(\ell+1)}{2r^2} - U_0 r_0 \delta(r-R) \right] \chi_\ell(r) \;=\; \varepsilon_{n\ell}\chi_\ell(r), \tag{10.13}$$

with $\varepsilon_{n\ell}$ the energy of the extra electron. We omit the index n of the function $\chi_{n\ell}(r)$ here and below. Integrating both sides of (10.13) over a small interval near the point $r = R$, we obtain

$$\frac{1}{2m}\int_{R-\delta}^{R+\delta} dr\, \chi_\ell''(r) \;=\; -U_0 r_0 \chi_\ell(R). \tag{10.14}$$

On the other hand, $\int_{R-\delta}^{R+\delta} dr\, \chi_\ell''(r) = \chi_\ell'(R+\delta) - \chi_\ell'(R-\delta)$. Thus the derivative $\chi'(r)$ undergoes a jump at the point $r = R$. The jump of the logarithmic derivative $L(r) = \chi_\ell'(r)/\chi_\ell(r)$ is

$$\Delta L = \lim_{\delta\to 0}\left[\frac{\chi'_\ell(r+\delta)}{\chi_\ell(r)} - \frac{\chi'_\ell(r-\delta)}{\chi_\ell(r)}\right] = -\frac{2U_0}{\alpha}. \tag{10.15}$$

We turn now to the bound-state wave functions. Everywhere except on the sphere $r = R$ (10.13) is just the equation of free motion. Considering first the s states, we obtain $\chi_0(r) = c_1 \exp(-\mu r) + c_2 \exp(\mu r)$, with $c_{1,2}$ certain numerical coefficients that have different values in the regions $r < R$ and $r > R$; $\mu = \sqrt{2mI_{af}}$, while $I_{af} = -\varepsilon_{\ell=0} > 0$ is the electron affinity to the fullerene C_{60}. We must put $c_2 = 0$ for $r > R$, since otherwise, the normalization integral for $|\psi|^2$ would not converge. However, at $r < R$, both of $c_{1,2}$ are nonzero. Since the function $\chi_0(r)$ becomes zero at $r = 0$, we have $c_1 + c_2 = 0$ at $r < R$. Hence there are two independent coefficients. They are determined by the requirement that the function $\chi_0(r)$ is continuous at $r = R$ and by the normalization condition. Finally, for the s states,

$$\chi_0(r) = B_0 \frac{e^{-\mu R}}{\mu R}\sinh(\mu r), \quad r \le R; \tag{10.16}$$

$$\chi_0(r) = B_0 \frac{\sinh(\mu R)}{\mu R} e^{-\mu r} \quad r \ge R.$$

The constant

$$B_0 = \mu^{1/2}\frac{2\mu R}{\left(1-(1+2\mu R)\exp(-2\mu R)\right)^{1/2}}$$

is related to the value of the radial wave function at the origin,

$$\lim_{r\to 0}\frac{\chi_0(r)}{r} = B_0\frac{e^{-\mu R}}{R}, \tag{10.17}$$

with numerical value $B_0 = 3.93 r_0^{-1/2}$.

Carrying out a direct calculation of the discontinuity (jump) of the logarithmic derivative and employing (10.15), we obtain the equation for the energy ε_0 of the s state of the extra electron:

$$U_0 = \frac{\mu\alpha}{2}\frac{e^{\mu R}}{\sinh(\mu R)}. \tag{10.18}$$

This expression can be viewed as representing the electron potential energy in the field of the FS in terms of two observables. The latter are the electron affinity and the radius of the FS. For C_{60}, we have $U_0 = 12\,\text{eV}$.

The solutions of (10.13) for the bound states with any value of the angular momentum ℓ can be written as

$$\chi_\ell(r) = B_\ell\sqrt{\frac{r}{R}} I_{\ell+1/2}(\mu_\ell r) K_{\ell+1/2}(\mu_\ell R), \quad r \le R; \tag{10.19}$$

$$\chi_\ell(r) \;=\; B_\ell\sqrt{\frac{r}{R}}I_{\ell+1/2}(\mu_\ell R)K_{\ell+1/2}(\mu_\ell r), \quad r \;\geq\; R.$$

Here $\mu_\ell = \sqrt{2m|\varepsilon_\ell|}$, $|\varepsilon_\ell|$ is the electron affinity. The functions $I_{\ell+1/2}$ and $K_{\ell+1/2}$, which are the solutions of (10.13), are the modified Bessel functions of the first and third kind, respectively (the latter are known also as the Macdonald functions). They can be represented in terms of elementary functions, e.g.,

$$I_{1/2}(x) \;=\; \lambda(x)\frac{\sinh(x)}{x}; \quad K_{1/2}(x) \;=\; \frac{e^{-x}}{\lambda(x)}; \tag{10.20}$$

$$I_{3/2}(x) \;=\; \lambda(x)\left(-\frac{\sinh(x)}{x^2}+\frac{\cosh(x)}{x}\right); \quad K_{3/2}(x) \;=\; \frac{e^{-x}}{\lambda(x)}\left(1+\frac{1}{x}\right),$$

with $\lambda(x) = \sqrt{2x/\pi}$.

The normalization factors are, e.g., $B_1 = 3.95/r_0^{1/2}$ and $B_2 = 3.86/r_0^{1/2}$. To calculate the jump of the logarithmic derivative at $r = R$, we employ the expression for the Wronskian

$$I'_{\ell+1/2}(x)K_{\ell+1/2}(x) - I_{\ell+1/2}(x)K'_{\ell+1/2}(x) \;=\; \frac{1}{x}\,. \tag{10.21}$$

Using (10.15), we obtain the equality

$$2U_0 R I_{\ell+1/2}(\mu_\ell R)K_{\ell+1/2}(\mu_\ell R) \;=\; \alpha, \tag{10.22}$$

which determines the single-particle spectrum of the extra electron.

The Bargmann condition for the bound states [14],

$$\int dr\frac{r}{r_0}U(r) \;\geq\; \frac{2\ell+1}{2}\,, \tag{10.23}$$

takes the form

$$\ell \;\leq\; U_0 R - \frac{1}{2} \tag{10.24}$$

in the case of the Dirac bubble potential. Thus for the ion C_{60}^-, we have $\ell \leq 2$ [15].

One can see that there is only one state for a given angular momentum ℓ. Indeed, assuming that there are two bound states with the same value of ℓ and different principal quantum numbers n and n', we find that their wave functions are described by (10.19) with different values of $\mu_\ell = \sqrt{2m|\varepsilon_{k\ell}|}$, where $k = n, n'$. These functions should be orthogonal. However, this is impossible, since the functions $I_{\ell+1/2}(x)$ and $K_{\ell+1/2}(x)$ do not change their signs in the interval $0 \leq x < \infty$.

We turn now to the continuum wave functions. The wave function of the continuum state with the kinetic energy ε, angular momentum ℓ, and its projection m can be written as $\psi_{p\ell m}(\mathbf{r}) = \chi_{p\ell}(r)Y_{\ell m}(\Omega)/r$ with $p = (2m\varepsilon)^{1/2}$. The radial function

$\chi_{p\ell}(r)$ satisfies (10.13) with $\varepsilon_{n\ell}$ on its RHS replaced by ε. In the simplest case of $\ell = 0$, we can write $\chi_{p0}(r) = c_1 \sin pr + c_2 \cos pr$, similar to the case of the discrete spectrum. Since $\chi_{p0}(r)$ should vanish at $r = 0$, we obtain $c_2 = 0$ at $r < R$. At $r > R$, both of $c_{1,2}$ are nonzero.

This is true for every value of the orbital momentum ℓ. At $r < R$, the solution of the wave equation is proportional to the regular (finite at the origin) solution of the free wave equation $u_{p\ell}(r) = prj_\ell(pr)$, with $j_\ell(pr)$ the spherical Bessel functions of the first kind. At $r > R$, it is a linear combination of the regular solution and the irregular one $v_{p\ell}(r) = pry_\ell(pr)$, where $y_\ell(pr)$ are the spherical Bessel functions of the second kind, known also as the spherical Neumann functions. The functions $y_\ell(x)$ behave as $x^{-\ell-1}$ at $x \to 0$. In the limit $pr \gg 1$,

$$j_\ell(pr) \sim \frac{\sin(pr - \pi\ell/2)}{pr}; \quad y_\ell(pr) \sim -\frac{\cos(pr - \pi\ell/2)}{pr}. \tag{10.25}$$

Thus in the internal region $r < R$, the wave function is proportional to the regular solution of the free wave equation [15, 16]

$$\chi_\ell(r) = D_\ell(p) u_{p\ell}(r), \quad r \le R. \tag{10.26}$$

In the outer region $r > R$, it is a linear combination of the regular and irregular solutions. Since the asymptotics of the radial wave function at $pr \gg 1$ are $R_\ell(r) \sim \sin(pr - \pi\ell/2 + \delta_\ell)$, we obtain, employing (10.25),

$$\chi_\ell(r) = u_{p\ell}(r) \cos\delta_\ell(p) - v_{p\ell}(r) \sin\delta_\ell(p), \quad r \ge R. \tag{10.27}$$

Proceeding in the same way as in the case of the discrete spectrum, one obtains

$$D_\ell(p) = \cos\delta_\ell(p) \left(1 - \tan\delta_\ell(p) \frac{v_{p\ell}(R)}{u_{p\ell}(R)}\right), \tag{10.28}$$

$$\tan\delta_\ell(p) = \frac{u_{p\ell}^2(R)}{u_{p\ell}(R) v_{p\ell}(R) + p\alpha/2U_0}.$$

Now we are ready to calculate the amplitude of photoionization

$$F(R) = N(\omega) \langle \psi_i | \gamma | \psi_f \rangle,$$

with γ the operator of interaction between the photon and electron. We assume the extra electron to be in the s state. We employ the dipole approximation, and thus only the final-state electron carries the angular momentum $\ell = 1$.

It is reasonable to compare the amplitude $F(R)$ with the amplitude $F_0 = F(R = 0)$ in which the wave functions of the initial and final states are described by the second equality of (10.16) and by (10.27) respectively. The amplitude describing the

photoionization of the negative ion A^- of the atom A in the zero-range potential approach is just F_0. The corresponding cross section is [17]

$$\sigma_0(\omega) \;=\; \frac{8\pi\alpha}{3}\,\frac{I^{1/2}(\omega-I)^{3/2}}{m\omega^3}\,, \tag{10.29}$$

with I the ionization potential of the ion A^-.

The cross section for photoionization of the negative ion of fullerene is

$$\sigma(\omega) \;=\; \sigma_0(\omega)X^2(\omega)\,, \tag{10.30}$$

where

$$X(\omega) \;=\; c\frac{1-e^{-2\mu R}}{R}\,\frac{D_1(p)}{p}\,f(p); \quad c \;=\; \sqrt{\frac{2\pi}{\mu}}N_0 R e^{\mu R}, \tag{10.31}$$

with $p=(2m(\omega-I_{af}))^{1/2}$ the photoelectron momentum, $\mu=(2mI_{aff})^{1/2}$, and $N_0=\psi(\mathbf{r}=0)$, while

$$f(p) \;=\; \cosh(\mu R)\sin pR - \frac{p}{\mu}\cos\mu R + \sin(pR+\delta_1) + \frac{p}{\mu}\cos(\mu R+\delta_1)\,.$$

In the limit $pR\gg 1$, i.e., for the photoelectron energies $\varepsilon\gg 0.3\,\mathrm{eV}$, we can employ the asymptotic expressions for the spherical wave functions $j_1(pR)=-\cos pR/pR$ and $y_1(pR)=-\sin pR/pR$. If $p\alpha\gg 2U_0$, we can neglect the second term of the first equality of (10.28). In this limit, i.e., for the photoelectron energies $\varepsilon\gg I_1(U_0/I_1)^2$ with $I_1=m\alpha^2/2\approx 13.6\,\mathrm{eV}$ (this means $\varepsilon\gg 10\,\mathrm{eV}$ in the case of C_{60}^-), we have $\delta_1=0$ and $D_1=1$. As one can see from (10.27), only the regular part of the photoelectron wave function contributes in this limit. In other words, the photoelectron is described simply by the plane wave. At these energies, the cross section is

$$\sigma(\omega) \;=\; \sigma_0^a(\omega)\Big(\frac{c\sin pR}{pR}\Big)^2, \tag{10.32}$$

with c determined by the second equality of (10.31), while

$$\sigma_0^a(\omega) \;=\; \frac{8\pi\alpha}{3}\,\frac{I_{af}^{1/2}}{m\omega^{3/2}} \tag{10.33}$$

is the high-energy asymptotics of the cross section σ_0 given by (10.29). Note that the Dirac bubble model may appear to be too crude if the electron wavelength $1/p$ much smaller than the thickness Δ of the FS.

Anyway, we shall see in the next section that the asymptotic law

$$\sigma(\omega) \sim \frac{I_{af}^{1/2} \sin^2 pR}{\omega^{5/2}}, \tag{10.34}$$

which follows from (10.32), is true for the model potentials providing the wave function with a discontinuity of the derivative of the wave function at $r = R$.

10.1.3 Asymptotics of the Photoionization Cross Section

We shall demonstrate that the shape of the nonrelativistic asymptotic energy dependence of the cross section of photodetachment from the FS depends on the form of the model potential. We focus on ionization of the ion C_N^-. As we have seen, at large values of the photon energy $\omega \gg U_0$, the photoelectron can be described by a plane wave. The amplitude can be written as

$$F = N(\omega)\frac{\mathbf{ep}}{m}\int d^3r\psi(\mathbf{r})e^{-i\mathbf{pr}}, \tag{10.35}$$

with $\psi(\mathbf{r})$ the single-particle wave function of the additional electron. Recall that the factor $N(\omega) = (4\pi\alpha/2\omega)^{1/2}$ originates from the photon wave function. Assuming the electron to be in the s state, we can write $\psi(\mathbf{r}) = \varphi(r)/\sqrt{4\pi}$, with $\varphi(r)$ the radial part of $\psi(\mathbf{r})$. Thus the amplitude can be represented as

$$F = \sqrt{4\pi}N(\omega)\frac{\mathbf{en}}{m}J(p); \quad J(p) = \int dr \sin(pr)r\varphi(r), \tag{10.36}$$

with $\mathbf{n}$ the unit vector directed along the momentum $\mathbf{p}$. The asymptotic photodetachment cross section is thus

$$\sigma = \frac{8\pi\alpha}{3}\frac{p}{m\omega}|J(p)|^2; \quad p^2 = 2m(\omega - I_{af}). \tag{10.37}$$

We consider first the model potentials providing the wave function $\psi(r)$ with the discontinuity of the first derivative $\varphi'(r)$ at $r = R$, while the function $\varphi(r)$ is continuous at this point. The Dirac bubble potential is one of them. We introduce $R_\pm = R \pm \delta$ and set $J = X_1 + X_2$ with

$$X_1(p) = \int_0^{R_-} dr \sin(pr)r\varphi(r); \quad X_2(p) = \int_{R_+}^{\infty} dr \sin(pr)r\varphi(r); \quad \delta \to 0. \tag{10.38}$$

Integration by parts provides

$$X_1(p) = -\frac{R_-\varphi(R_-)\cos pR_-}{p} + \frac{1}{p}\int_0^{R_-} dr \cos(pr)[r\varphi'(r) + \varphi(r)]. \tag{10.39}$$

After a similar evaluation of the integral $X_2(p)$, we obtain

$$J \;=\; X_3 + X_4\,, \tag{10.40}$$

with

$$X_3 \;=\; \frac{1}{p}\int_0^{R_-} dr\,\cos\,(pr)[r\varphi'(r)+\varphi(r)]; \quad X_4 = \frac{1}{p}\int_{R_+}^{\infty} dr\,\cos\,(pr)[r\varphi'(r)+\varphi(r)]. \tag{10.41}$$

Now integration by parts gives

$$X_3(p) = \frac{[R_-\varphi'(R_-)+\varphi(R_-)]\sin pR_-}{p^2} - \tag{10.42}$$

$$\frac{1}{p^2}\int_0^{R_-} dr\,\sin\,(pr)[r\varphi''(r)+2\varphi'(r)],$$

and after a similar evaluation of X_4, we obtain

$$J(p) \;=\; -\frac{R\lambda_1(R)\sin pR}{p^2} - \frac{1}{p^2}\int_0^{\infty} dr\,\sin\,(pr)[r\varphi''(r)+2\varphi'(r)], \tag{10.43}$$

where $\lambda_n(R) = \lim_{\delta\to 0}[\varphi^{(n)}(R_+) - \varphi^{(n)}(R_-)]$ is the discontinuity of the nth derivative of the radial part of the wave function at $r = R$.

Further sequential integration by parts of the integral on the RHS of (10.42) provides the power series in $\varphi^{(n)}(r)/p^n$ with $r = 0, R \pm \delta$. If these power series converge, the first term on the RHS of (10.42) provides the leading term of the asymptotics of the amplitude. The asymptotic cross section of the photodetachment is thus

$$\sigma \;=\; \frac{4\pi\alpha}{3\sqrt{2}}\frac{R^2\lambda_1^2(R)}{(m\omega)^{5/2}}\sin^2 pR\,. \tag{10.44}$$

Some of the model potentials provide the wave functions with continuous first derivatives of the radial functions. For example, the wave functions corresponding to the well potential (10.9) have a continuous first derivative at $r = R$, while the second derivative $\varphi^{(2)}$ undergoes a jump $\lambda_2(R)$. After two integrations by parts in (10.41), we obtain

$$J(p) \;=\; \frac{2\varphi'(0)+R\lambda_2(R)\cos pR}{p^3} + \frac{1}{p^3}\int_0^{\infty} dr\,\cos(pr)[r\varphi^{(3)}(r)+3\varphi^{(2)}(r)]. \tag{10.45}$$

The first term on the RHS determines the asymptotics of the amplitude under the conditions formulated in the previous paragraph. Thus for the well potential,

$$\sigma = \frac{\sqrt{2}\pi\alpha}{3}\frac{\kappa^2}{(m\omega)^{7/2}}, \tag{10.46}$$

with $\kappa = \varphi'(0) - \lambda_1(R)\cos pR$.

10.2 Photoionization of Caged Atoms

10.2.1 Wave Functions of Caged Atoms

One of the common features of fullerenes is their internal empty space. The system in which an atom A is stuffed into the fullerene C_N is called an endohedral atom and is denoted by $A@C_N$. In this case, the molecule C_N forms the FS, while A is called a caged atom.

For internal shells of a caged atom, the characteristic size r_b is much smaller than the fullerene radius R, i.e.,

$$\frac{r_b}{R} \ll 1; \tag{10.47}$$

the influence of the FS on the electron shell of a caged atom is weak. Hence the wave functions of an isolated atom are often employed for description of a caged atom. However, for the outer electron states of a caged atom, the ratio r_b/R may appear to be not too small. In this case, the electron states of the caged atom are influenced by the FS.

This can be illustrated by analysis of the energy levels of the hydrogen atom stuffed into the fullerene C_{60} carried out in [18]. The wave functions of the discrete spectrum of a caged atom of hydrogen are $\psi_{n\ell m}(\mathbf{r}) = R_{n\ell}(r)Y_{\ell m}(\Omega)$. The Schrödinger equation for the functions $\chi_{\ell m}(r) = rR_{n\ell}(r)$ is

$$\left[-\frac{1}{2m}\frac{d^2}{dr^2} + \frac{\ell(\ell+1)}{2r^2} - \frac{\alpha Z}{r} + U(r)\right]\chi_{n\ell}(r) = \varepsilon_{n\ell}\chi_{n\ell}(r), \tag{10.48}$$

with the potential energy determined by (10.9) was solved numerically. The authors traced the dependence of the binding energies $\varepsilon_{n\ell}$ on the strength of the well potential U_0. It was found that for the $1s$ state with $r_b \sim r_0$, the energy value practically does not change as we vary the value of U_0 between 0 and 15 eV. On the other hand, the binding energy of the $2s$ state with the larger size becomes about half as large as we change U_0 in this interval.

Mixing between atomic and fullerene electron states, called hybridization, can take place also for the outer shells of many-electron atoms [19]. For example, there is strong hybridization of the $5s$ states of Xe and the FS states in the case of the endohedral atom $Xe@C_{60}$ [20]. We limit ourselves to the cases in which the hybridization can be neglected, at least for a qualitative analysis. Thus the wave functions of the atomic bound states are assumed to be the same as those of the isolated atom.

Turning to the photoelectron wave functions, we employ the Dirac bubble model for a description of the FS field. It is convenient to consider the continuum wave functions $\psi_{p\ell m}(\mathbf{r}) = \chi_{p\ell}(r)Y_{\ell m}(\Omega)/r$ with definite values of the modulus of asymptotic momentum $p = (2m\varepsilon)^{1/2}$ and of the orbital angular momentum ℓ with its projection m. The functions $\chi_{p\ell}(r)$ satisfy the wave equation

$$\left[-\frac{1}{2m}\frac{d^2}{dr^2} + \frac{\ell(\ell+1)}{2r^2} + V(r) - U_0 r_0 \delta(r-R) \right] \chi_{p\ell}(r) \;=\; \varepsilon \chi_{p\ell}(r), \quad (10.49)$$

with $V(r)$ the field of the recoil ion. In the previous section, we constructed the continuum functions for the wave equation with the Dirac bubble potential, i.e., for (10.49) with $V(r) = 0$; (10.26) and (10.27). These equations were based on the features of the wave equation in the limiting cases $r \to 0$ and $r \to \infty$, which are common for every central field. Thus they provide also the functions $\chi_{p\ell}(r)$ for the wave equation (10.49). The function $u_{p\ell}(r)$ is the regular (vanishing at the origin) solution of the wave equation for the isolated atom:

$$\left[-\frac{1}{2m}\frac{d^2}{dr^2} + \frac{\ell(\ell+1)}{2r^2} + V(r) \right] u_{p\ell}(r) \;=\; \varepsilon u_{p\ell}(r). \quad (10.50)$$

The function $v_{p\ell}(r)$ is the irregular solution ($v_{p\ell}(r) \to \infty$ for $r \to 0$) of the same equation.

Since the photoionization of the caged atom takes place at distances $r \lesssim r_b \ll R$ from the origin, we need the photoelectron function only in the internal region of the fullerene $r < R$. Here the shape of its r-dependence is the same as that of the regular solution $u_{p\ell}$ for the isolated atom, and $\chi_\ell(r) = D_\ell(p)u_{p\ell}(r)$; see (10.26). Such a form of the wave function can be viewed as a result of the interference between the wave corresponding to the electron ejected from the caged atom and the wave reflected by the attractive fullerene shell [21]. Note that the reflection on the attractive shell (in contrast to that on the repulsive one) does not have a classical analogue.

The coefficient $D_\ell(p)$ and the phase δ_ℓ for the motion in the Dirac bubble potential are given by (10.28). They were obtained by matching the expressions for the wave function at $r = R$ and by employing the expression for the Wronskian $W_{p\ell}(r)$ of (10.49). We can write (10.49) for the solution $u_{p\ell}(r)$. Multiplying both sides by the function $v_{p\ell}(r)$ and subtracting (10.49) for $v_{p\ell}(r)$ multiplied by $u_{p\ell}(r)$, we obtain $u''_{p\ell}(r)v_{p\ell}(r) - u_{p\ell}(r)v''_{p\ell}(r) = 0 = W'_{p\ell}(r)$. Thus $W_{p\ell}(r)$ actually does not depend on r. Calculating it at $r \to \infty$, we find that $W_{p\ell} = u_{p\ell}(r)v'_{p\ell}(r) - u'_{p\ell}(r)v_{p\ell}(r) = p$, i.e., it is the same as that of (10.13). Hence the functions $D_\ell(p)$ and the phase shifts due to the scattering in the FS δ_ℓ are given by (10.28), with $u_{p\ell}(r)$ and $v_{p\ell}(r)$ the regular and irregular solutions of (10.49) [16].

10.2.2 Polarization of the Fullerene Shell

Before interacting with the caged atom, the incoming photon undergoes elastic scattering on the FS. This can be viewed as a modification of the photon wave function. We consider the ionization of the caged atoms in the dipole approximation. In this case, the cross section can be expressed through the dipole polarizability $\alpha_d(\omega)$ introduced in Sect. 7.2. We assume that the photon wavelength greatly exceeds the size of the fullerene, i.e.,

$$\omega R \ll 1 . \tag{10.51}$$

For C_{60}, this means that $\omega \ll 600\,\mathrm{eV}$.

It is convenient to use the length form of the photon–electron interaction in this case. Neglecting the photon interaction with the FS, we can write the amplitude for photoionization of the caged atom as $F_\gamma^{(0)} = ie_i N(\omega)\omega \sum_k \langle \psi_f | r_i^{(k)} | \psi_{in} \rangle$, with $\mathbf{e}$ the polarization vector of the incoming photon. Here $\psi_{in,f}$ denote the initial and final states of the caged atom. The sum is carried out over the electrons of the caged atom.

Photoionization accompanied by elastic scattering on the FS is illustrated by Fig. 10.2.

Employing the results of Sect. 7.2.4, we can write the amplitude for photoionization of the caged atom, which includes the photon scattering on the FS, as

$$F_\gamma = F_\gamma^{(0)} + \langle \psi_f | r_i^{(k)} B_i(\mathbf{r}^{(k)}) | \psi_{in} \rangle, \tag{10.52}$$

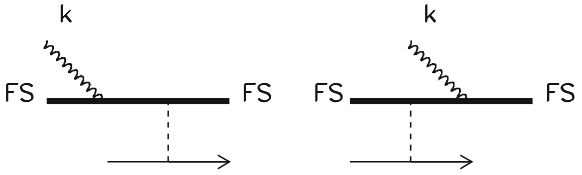

Fig. 10.2 Feynman diagram illustrating the effect of polarization. Before moving the bound electron to the continuum (the continuum electron is labeled by an *arrow*), the photon (the *helical line*) undergoes elastic scattering on the fullerene shell (*bold lines*), labeled FS

with

$$B_i(\mathbf{r}^{(k)}) = e\omega^2 \sum_n \left(\frac{\langle\Psi_0| \sum_s A_i(\mathbf{r}^{(k)}, \mathbf{r}'^{(s)})|\Psi_n\rangle\langle\Psi_n|\mathbf{e}\cdot\mathbf{d}|\Psi_0\rangle}{\omega - \epsilon_{n0} + i\delta} + \right. \tag{10.53}$$

$$\left. \frac{\langle\Psi_0|\mathbf{e}\cdot\mathbf{d}|\Psi_n\rangle\langle|\Psi_n| \sum_s A_i(\mathbf{r}^{(k)}, \mathbf{r}'^{(s)})|\Psi_0\rangle}{-\omega - \epsilon_{n0} + i\delta} \right).$$

Here $\mathbf{r}'(s)$ are the coordinates of the FS electrons. The two terms in parentheses correspond to the two diagrams shown in Fig. 10.2, $\mathbf{d}$ stands for the operator of the dipole momentum. The function $\varphi_i(\mathbf{r}^{(k)})$ describes the amplitude of the second-order process in which one of the photon–electron vertices is replaced by $A_i(\mathbf{r}^{(k)}, \mathbf{r}'^{(s)}) = D_{ij}(\mathbf{r}^{(k)} - \mathbf{r}'^{(s)})r_j^{(s)}$, with $D_{ij}(\mathbf{r}^{(k)} - \mathbf{r}'^{(s)})$ the photon propagator. The latter is shown by the dashed line in Fig. 10.2. It is reasonable to employ the photon propagator in the form given by (2.51), with only the space components D_{ij} having nonzero values. The function $D_{ij}(\mathbf{r} - \mathbf{r}')$ is thus the Fourier transform of the photon propagator $D_{ij}(\mathbf{q})$ determined by (2.51):

$$D_{ij}(\mathbf{x}) = \int \frac{d^3q}{(2\pi)^3} D_{ij}(\mathbf{q}) e^{i\mathbf{q}\mathbf{x}} = \left(\delta_{ij} + \frac{1}{\omega^2}\frac{\partial^2}{\partial x_i \partial x_j}\right)\frac{e^{i\omega x}}{x}. \tag{10.54}$$

In the lowest order of expansion in powers of ωR, we obtain

$$D_{ij}(\mathbf{r}^{(k)} - \mathbf{r}'^{(s)}) = -\frac{\delta_{ij}}{\omega^2|\mathbf{r}^{(k)} - \mathbf{r}'^{(s)}|^3}. \tag{10.55}$$

Note that the integral over r is saturated by the distances of order the size of the bound state of the caged atom, i.e., $r^{(k)} \ll R$. On the other hand, the important values of $r'^{(s)}$ lie in the small interval of order Δ near the value R. Thus we can put $|\mathbf{r}^{(k)} - \mathbf{r}'^{(s)}| = R$ on the RHS of (10.55). This enables us to separate the integrations over r and r' that provide the photoionization amplitude $F_\gamma(\omega)$ and the dipole polarizability $\alpha_d(\omega)$ of the FS respectively. Hence we obtain [22]

$$F_\gamma(\omega) = F_\gamma^{(0)}(\omega)g(\omega); \quad g(\omega) = 1 - \frac{\alpha_d(\omega)}{R^3}, \tag{10.56}$$

In this approach, the factorization (10.56) is demonstrated explicitly. Of course, the same result can be obtained by employing the Coulomb gauge for the propagator. In this case, the main contribution comes from the expansion of the time component D_{00} of the photon propagator $V_{ee} = e^2/|\mathbf{r}^{(k)} - \mathbf{r}'^{((s)}|$ in powers of $r^{(k)}/r'^{(s)}$. The leading contribution is

$$V_{ee} = e^2 \frac{\mathbf{r}^{(k)} \cdot \mathbf{r}'^{(s)}}{R^3}, \tag{10.57}$$

which is the dipole–dipole interaction.

The experimental data on the total cross section $\sigma_{tot}(\omega)$ of the photon absorption by the fullerene C_{60} [22, 23] enable us to find the energy dependence of the polarizability. The optical theorem determines its imaginary part:

$$\mathrm{Im}\,\alpha_d(\omega) \;=\; \frac{\sigma_{tot}(\omega)}{4\pi\omega}\,. \tag{10.58}$$

The real part of $\alpha_d(\omega)$ is determined by the dispersion relation. As one can see from (7.107) and (7.108), the function $\alpha_d(\omega)$ has singularities on the real axis, and the imaginary part $\mathrm{Im}\alpha_d(\omega)$ is an odd function of ω. Thus the dispersion relation can be written as

$$\mathrm{Re}\,\alpha_d(\omega) \;=\; \frac{2}{\pi}\int\limits_{I_0}^{\infty} d\omega' \frac{\omega'\mathrm{Im}\alpha_d(\omega')}{\omega'^2-\omega^2} \;=\; \frac{1}{2\pi^2}\int_{I_0}^{\infty} d\omega' \frac{\sigma_{tot}(\omega')}{\omega'^2-\omega^2}\,. \tag{10.59}$$

Here I_0 is the energy needed for transition of the FS to the lowest excited state of the discrete spectrum. In any case, I_0 is smaller than the FS ionization potential, which is 7.5 eV for C_{60}.

The energy dependence of both the real and imaginary parts of the polarizability as well as that for the total cross section of photoabsorption are shown in Fig. 10.3, where $\alpha_d(\omega)$ is given in units of r_0^3 (or in atomic units). Since $R^3 \approx 300 r_0^3$, one can see that the polarization of the FS strongly influences the amplitude of photoionization of the caged atom. The energy dependence of the imaginary part is similar to that of the total cross section. However, due to the factor $1/\omega$ on the RHS of (10.58), the peculiarities of the cross section at low energy are emphasized in the ω-dependence of $\mathrm{Im}\,\alpha_d(\omega)$. A small peak in the cross section near the threshold transforms to a larger one of $\mathrm{Im}\alpha_d(\omega)$. The peak at $\omega \approx 22$ eV corresponds to the plasmon excitation. The energy dependence of the real part is represented by a rather smooth curve.

In the high-energy limit, i.e., for the photon energies exceeding strongly the FS ionization potential $I \approx 7.5$ eV, the polarization $\alpha_d(\omega)$ decreases as $1/\omega^2$. One can see from Fig. 10.3 that the $\alpha_d(\omega)$ is indeed close to zero for $\omega > 80$ eV. Thus the polarization effects are expected to be negligibly small at these energies.

At very small $\omega < I_0$, the polarizability is real. Due to the interaction with the FS, the strength of the electric field in the electromagnetic wave $E_0(\omega)$ changes to

$$E(\omega) \;=\; E_0(\omega)\Big(1-\frac{\alpha_d(\omega)}{R^3}\Big). \tag{10.60}$$

Note that in electrostatic limit $\omega = 0$, (10.60) can be obtained in the framework of classical electrodynamics. The electric field $E(\omega)$ of the electromagnetic wave shifts the electrons of the FS relative to the positive core. Thus the FS obtains a dipole moment

$$\mathbf{d} \;=\; \int d^3r'\rho(\mathbf{r}')\mathbf{r}'.$$

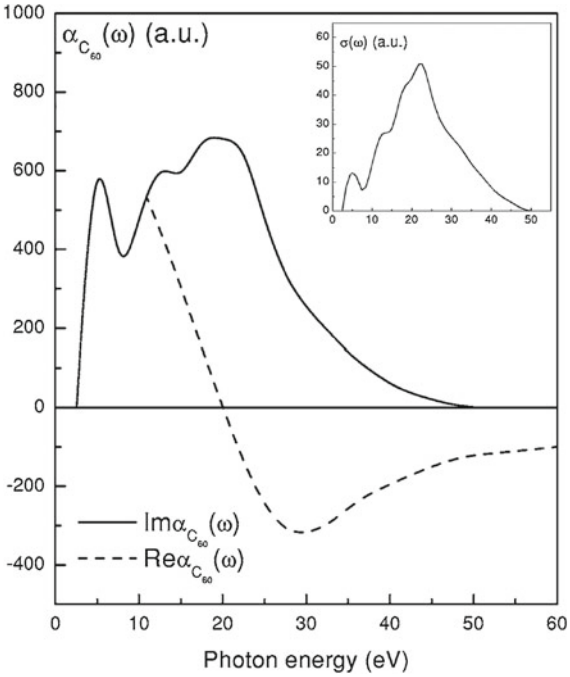

Fig. 10.3 Dependence of the real and imaginary parts of the dipole polarizability $\alpha_d(\omega)$ on the photon energy ω. The *curve* in the *upper right-hand corner* shows the energy dependence of the photoionization cross section for the fullerene C_{60} based on experimental data. Reproduced from [22] with permission of AIP

Here $\rho(\mathbf{r}')$ is the density of the distribution of the electric charge. Since the FS is not charged, $\int d^3r'\rho(\mathbf{r}') = 0$. The FS creates the electric field with the potential

$$\varphi_{FS}(\mathbf{r}) \;=\; \int d^3r' \,\frac{\rho(\mathbf{r}')}{|\mathbf{r}-\mathbf{r}'|}\,.$$

Inside the FS, i.e., at $r < R$,

$$\varphi_{FS}(\mathbf{r}) \;=\; \int d^3r' \frac{\rho(\mathbf{r}')}{r'} + \mathbf{E}_1\cdot\mathbf{r};\quad \mathbf{E}_1 \;=\; \int d^3r' \frac{\rho(\mathbf{r}')}{r'^3}\mathbf{r}' \approx \frac{\mathbf{d}}{R^3}\,.$$

The field $E_{FS}(\omega)$ created by the polarized FS changes the initial electric field $\mathbf{E}_0$ to the effective electric field

$$\mathbf{E} \;=\; \mathbf{E}_0 + \mathbf{E}_{FS}\,, \tag{10.61}$$

with $\mathbf{E}_{FS} = -\nabla\varphi_{FS} = -\mathbf{E}_1$. Thus we arrive at (10.60), with $\alpha_d(\omega)$ defined as the coefficient of proportionality in the equality $\mathbf{d}(\omega) = \alpha_d(\omega)\mathbf{E}_0(\omega)$.

This enables us to test certain assumptions on the macroscopic features of the FS. For example, one can assume that in the static limit $\omega = 0$, the FS is a conductor [24]. This means that the electric field should vanish on the surface of the sphere with $r = R$. In other words, $\alpha_d(0) = R^3$. Note that in assuming the FS to be a conductor, we find that the electric field vanishes inside the FS as well. The FS plays the role of

the Faraday cage. The value $\alpha_d(0) = R^3 \approx 300 r_0^3$ with still smaller values at finite values of ω [24] is unlikely to be consistent with the results presented in Fig. 10.3. Large uncertainties of experimental data for small ω do not allow us to make a more detailed analysis.

10.2.3 Energy Dependence of the Photoionization Cross Section

Now we are ready to calculate the cross section for the single-electron photoionization of the caged atom. We begin with the ionization of the s state. In this case, the photoelectron obtains the angular momentum $\ell = 1$. As we have seen, the process is determined by the distances inside the FS, where the photoelectron wave function is proportional to that for photoionization of the isolated atom; (10.26). Employing also (10.56), we obtain

$$F_{10}(\omega) \;=\; F_{10}^{(0)}(\omega) D_1(\omega) g(\omega)\,, \tag{10.62}$$

where the lower indices label the angular momenta of the final and initial states of the electron. The corresponding cross section is thus

$$\sigma_s(\omega) \;=\; \sigma_s^{(0)}(\omega) \Phi_1(\omega) G(\omega)\,, \tag{10.63}$$

with $\Phi_1(\omega) = D_1^2(\omega)$, while

$$G(\omega) = |g(\omega)|^2 \;=\; |1 - \frac{\alpha_d(\omega)}{R^3}|^2\,. \tag{10.64}$$

If the electron is moved from a bound state with $\ell \neq 0$, the photoelectron can obtain the angular momenta $\ell' = \ell \pm 1$. The photoionization amplitude for the isolated atom is thus a linear combination of the two terms $F_\ell^{(0)}(\omega) = a_{\ell-1,\ell} F_{\ell-1,\ell}^{(0)}(\omega) + a_{\ell+1,\ell} F_{\ell+1,\ell}^{(0)}(\omega)$. Due to the orthogonality of the final-state functions, in these two terms the cross section for ionization of the isolated atom is $\sigma_\ell^{(0)}(\omega) = a_{\ell-1,\ell}^2 \sigma_{\ell-1,\ell}^{(0)}(\omega) + a_{\ell+1,\ell}^2 \sigma_{\ell+1,\ell}^{(0)}(\omega)$. In a similar way, we obtain

$$\sigma_\ell(\omega) \;=\; a_{\ell-1,\ell}^2 \sigma_{\ell-1,\ell}(\omega) + a_{\ell+1,\ell}^2 \sigma_{\ell+1,\ell}(\omega) \tag{10.65}$$

for the cross section of photoionization of the caged atom, with the partial cross sections

$$\sigma_{\ell',\ell} \;=\; \sigma_{\ell',\ell}^{(0)}(\omega) \Phi_{\ell'}(\omega) G(\omega); \quad \ell' \;=\; \ell \pm 1\,. \tag{10.66}$$

Now we apply these equations to analysis of the photoionization of the $4d$ state in the xenon atom encapsulated into the fullerene C_{60} [25]. The ω-dependence of

the cross section for the isolated atom of Xe exhibits a large and broad maximum at ω close to 100 eV; Fig. 10.4. This is known as the giant resonance, which is due to excitation of a collective state [26]. Now we shall see what changes for the photoionization of the endohedral atom $Xe@C_{60}$.

As we have seen, there are two major changes. The outgoing photoelectron wave interferes with the wave that originates from reflection on the FS. We include this effect in the framework of the Dirac bubble model. Here it is described by the factors $\Phi_{\ell\pm1}(\omega)$ in the partial cross sections expressed by (10.66). Also, the incoming photon undergoes interactions with the FS. This is described by the factor $G(\omega)$ on the RHS of (10.66). Here we study the region of relatively large photon energies, where the latter effect is not important (see Fig. 10.3). The partial cross sections of the process on the isolated atom are computed in the framework of RPAE.

The results of calculations carried out in [25] are presented in Fig. 10.4. One can see that the giant resonance curve is transformed into a more complicated one. It has four well-pronounced maxima and three minima. Their origin can be easily understood. The photoelectron can scatter on the FS on its way out of the fullerene. The electron wave ejected from the xenon atom interferes with the scattered one. The constructive interference leads to enhancement of the cross section. The corresponding peaks are called the confinement resonances. The destructive interference provides minima in the energy dependence. At large energies, the interaction of the

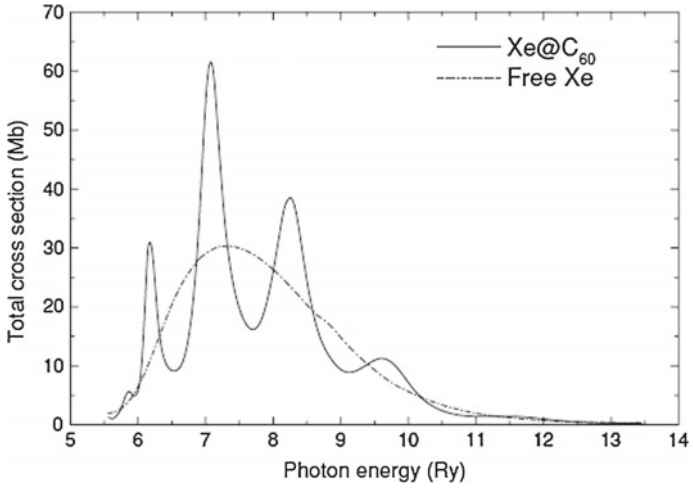

Fig. 10.4 Energy dependence for the cross section of photoionization of the 4*d* state in an isolated atom of Xe (*chain line*) and in the caged atom of Xe in the endohedral atom $Xe@C_{60}$. Reproduced from [25] with permission of IOP Publishing

photoelectron with the FS becomes weaker, and the cross section values become close to those for isolated atoms.

While the shapes of the cross section energy behavior for an isolated atom of Xe and for $Xe@C_{60}$ are quite different, the areas under the curves in the region between 75 eV and 180 eV are very close. They provide about 2/3 of the total contribution to the LHS of the sum rule (7.90).

A more detailed investigation of the photoionization of the Xe atom encapsulated into the fullerene requires a more rigorous technique; see, e.g., [20]. However, the analysis presented above is sufficient to obtain the qualitative picture of the process. The confinement resonance structure of the energy dependence was confirmed experimentally [27].

In this example, the scattering of the photoelectrons on the FS modified the cross section, while the polarization of the FS was not important. At smaller values of the photon energies, both effects contribute. The energy dependence of the angular distributions for photoionization of an isolated neon atom and that of the endohedral atom $Ne@C_{60}$ obtained in the RPAE technique were presented in [28]. The results are shown in Fig. 10.5. The confinement resonances become much more pronounced due to inclusion of the FS polarization by employing (10.64).

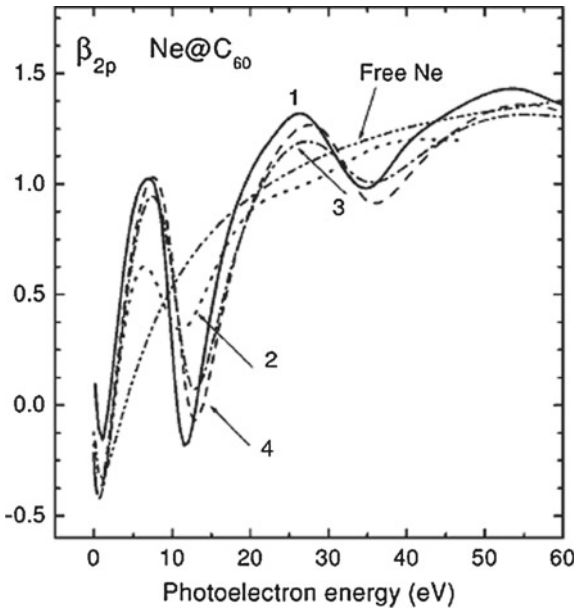

Fig. 10.5 Dipole asymmetry parameter calculated for $2p$ photoionization of isolated neon atom and that of the endohedral atom $Ne@C_{60}$. The *chain line* is for isolated atom. The other lines are for $Ne@C_{60}$ in various approaches. Reproduced from [28] with permission of AIP

10.3 Absorption of Photoelectrons by the Fullerene Shell

10.3.1 Photoelectron Interaction with the Fullerene Shell

In the previous section, we studied the photoionization of the caged atom without fixing the final state of the fullerene shell. In fact, we summed over the available final states. However, the photoelectrons can cause various inelastic processes in the FS. These can be excitation of the collective states of the FS, knockout of one or several electrons, knockout of one or several atoms or ions of carbon, etc. Now we calculate the sum of the cross sections of inelastic processes in the FS during the photoionization of the caged atom.

Because of the lack of detailed information about the FS wave functions, we calculate only the sum of the cross sections of the inelastic processes, also called the cross section of absorption. We shall see that this sum is not sensitive to the details of the FS structure.

We consider the channel in which the photon interaction with the caged atom precedes the transitions in the FS. In another channel of the same process, the photon knocks out an FS electron, and the latter ionizes the caged atom. This mechanism requires a special direction for the momentum of the electron ejected from the FS. The probability is quenched by a small factor of order r_b^2/R^2. Thus we neglect the contribution of this mechanism.

We limit ourselves to the case of nonrelativistic photoelectrons carrying the energy $\varepsilon = p^2/2m$; the photoelectron momentum is $\mathbf{p}$ with $|\mathbf{p}| = p$. The probability that the photoionization of the caged atom is followed by an inelastic process in the FS is expressed by the ratio

$$P_A(\varepsilon) \;=\; \frac{\sigma_A(\varepsilon)}{\sigma^{(isol)}(\varepsilon)}\,, \tag{10.67}$$

with $\sigma^{(isol)}(\varepsilon)$ the cross section for ionization of the isolated atom in which the photoelectron with the energy ε is ejected, while $\sigma_A(\varepsilon)$ is the absorption cross section, i.e., the sum of the cross sections for the processes in which the photoionization of the caged atom is accompanied by an inelastic process in the FS.

We consider the photon energies for which the photoelectron energies ε strongly exceed the energy of its interaction with the FS in the interior of fullerene. We consider only the systems for which the hybridization effects mentioned in Sect. 10.2 can be neglected. In this limit, the amplitude of the process with a transition of the FS to a particular final state x contains the amplitude of photoionization of the isolated atom $F^{(isol)}$ as a factor. Also, the cross section obtains the cross section of the isolated atom $\sigma^{(isol)}$ as a factor. Thus the probability $P_A(\varepsilon)$ does not depend of the parameters of the caged atom.

We calculate the absorption cross section as the difference between the total cross section

$$\sigma_t(\varepsilon) \;=\; \sigma^{(isol)}(\varepsilon)P_t(\varepsilon), \qquad P_t(\varepsilon) \;=\; \sum_x P_x(\varepsilon) \tag{10.68}$$

and the elastic cross section $\sigma_0 = \sigma^{(isol)} P_0$, which describes the process in which the FS state does not change, i.e.,

$$\sigma_A(\varepsilon) = \sigma_t(\varepsilon) - \sigma_0(\varepsilon) \quad P_A(\varepsilon) \;=\; P_t(\varepsilon) - P_0(\varepsilon)\,. \tag{10.69}$$

In the simplest case the FS undergoes ionization with one of its electrons moved to the continuum. This is one of the channels of the double photoionization of the endohedral atom. Recalling the results of Chap. 9, we can discuss three possible mechanisms of the process, i.e., the shakeoff (SO), final-state interactions of the photoelectron (FSI), and the quasifree mechanism (QFM). The QFM requires that two electrons approach each other at small distances. The electrons of the FS are well separated from those of the caged atom. Thus there is no QFM in our case.

The photoionization changes the neutral caged atom to a positive ion. This changes the field felt by the FS electrons. Recall that this is the familiar SO mechanism of excitation. Since the FS electrons are separated from the caged atom by distances of order $R \gg r_b$, the SO amplitude contains the factor r_b/R. Thus the SO probability is proportional to the small factor r_b^2/R^2. Note that the FS reacts to the change of the field as a whole and the probability of the SO does not depend explicitly on the number of electrons in the FS.

The final-state interaction (FSI) between the photoelectron and each of the FS electrons is determined by its Sommerfeld parameter $\xi_{ee} = m\alpha/p$. Here we neglected the momenta of the FS electrons. The FSI cross section is proportional to ξ_{ee}^2. However, we shall see that due to the large number of $N_e \gg 1$ of the FS electrons, the actual FSI parameter is $N_e\xi_{ee}^2$. In the broad interval of energies $N_e\xi_{ee}^2 \gg 1$. At such energies, the FS provides the leading contribution to the absorption cross section σ_A.

We begin with the perturbative calculation. We shall find the ratio (10.67) with taking into account the lowest order terms depending on ξ_{ee}. The detailed calculation for the atoms is given in Chap. 3. The main points remain the same for the case of endohedral atoms.

The leading nonvanishing FSI corrections to the cross section $\sigma_A(\varepsilon)$ are of order ξ_{ee}^2. The amplitude of photoionization of the caged atom accompanied by transition of the FS from the ground state to a final state x can be represented as $F_x = F^{(isol)} T_x$. To include the terms of order ξ_{ee}^2, we calculate $T_x = T_x^{(0)} + T_x^{(1)} + T_x^{(2)}$, with the upper index labeling the number of interactions between the photoelectron and the FS. Denoting the initial (ground) state of the FS by $|\Psi_0\rangle$ and the final state x of the FS by $\langle\Phi_x|$, we can represent the SO amplitude as $T_x^{(0)} = \langle\Phi_x|\Psi_0\rangle$. Note that the SO amplitude is real. The lowest-order FSI amplitude can be written as

$$T_x^{(1)} \;=\; \langle\Phi_x|U_1|\Psi_0\rangle, \quad U_1 \;=\; \sum_k U_1(\mathbf{r}^{(\mathbf{k})})\,, \tag{10.70}$$

where

$$U_1(r^{(k)}) \;=\; \alpha \int \frac{d^3q}{(2\pi)^3} G(\mathbf{q}) g(q) e^{i\mathbf{q}\cdot\mathbf{r}^{(k)}}\,, \tag{10.71}$$

with $G(\mathbf{q}) = 2m[\kappa^2 - [\mathbf{p}+\mathbf{q}]^2 + i0]^{-1}$ the propagator of a free electron, $\kappa^2 = p^2 + \varepsilon_{x0}$. The energy ε_{x0} is transferred by the FSI; $g(q) = 4\pi/(q^2+\lambda^2)$ is the photon propagator ($\lambda \to 0$). Keeping only the terms proportional to the large momentum p in the denominator of the propagator G, we obtain

$$U_1(\mathbf{r}^{(k)}) \;=\; \alpha \int \frac{d^3q}{(2\pi)^3} G_1(\mathbf{q}) g(q) e^{i\mathbf{q}\cdot\mathbf{r}^{(k)}}, \quad G_1 \;=\; \frac{-2m}{2\mathbf{p}\cdot\mathbf{q} - i0}\,. \tag{10.72}$$

Thus in (10.70),

$$U_1 \;=\; i\xi_{ee} \sum_k \ln((r^{(k)} - r_z^{(k)})\lambda), \tag{10.73}$$

where the z-axis is directed along the photoelectron's momentum. In a similar way, one can obtain the second-order amplitude

$$T_x^{(2)} \;=\; \langle \Phi_x | U_2 | \Psi_0 \rangle, \quad U_2 \;=\; \frac{U_1^2}{2}\,, \tag{10.74}$$

which is real.

We demonstrated in Chap. 3 that in the case of photoionization of atoms, the amplitude $T_x^{(1)}$ has a real part that is actually proportional to ξ_{ee}^2. It was due to the terms of order q/p in the expansion of the propagator $G(\mathbf{q})$ in (10.71). The integral over q was saturated by $q \sim 1/r_b$. Now it is saturated by $q \sim 1/R$. This contribution, which provides the real part of $T_x^{(1)}$, is determined by $q \sim 1/R$. The real part of the amplitude obtains the additional small factor r_b^2/R^2, and $\mathrm{Re}T_x^{(1)} \sim \xi_{ee}^2 \cdot r_b^2/R^2 \ll T_x^{(2)}$. Hence it can be neglected. Thus we obtain

$$T_x \;=\; \langle \Phi_x | 1 + U_1 + \frac{U_1^2}{2} | \Psi_0 \rangle\,. \tag{10.75}$$

Now we calculate the total probability P_t. The energies of the final states are limited by the energy conservation law. If the photoelectron energy is large enough, the most important excitations are included, and we can employ the closure condition. Until we have clarified the excitation spectrum of the FS, we must require that the photoelectron energy is much larger than the average energy loss $\langle\varepsilon\rangle$ considered in Sect. 4.2. Following (4.74), we can estimate for the valence FS electrons

$$\langle\varepsilon\rangle = \frac{\xi_{ee}^2 N_1}{4R^2} \ln\frac{\varepsilon}{I_{FS}}\,, \tag{10.76}$$

with I_{FS} the FS ionization potential, $N_1 = 4N$. We obtain $\langle\varepsilon\rangle \approx 45$ eV for the fullerenes C_{60} and C_{20}.

Employing (10.73), we obtain

$$P_t = \sum_x |T_x|^2 = 1; \quad P_0 = \langle\Phi_0|\Psi_0\rangle^2 + \xi_{ee}^2 |\langle\Phi_0|\Lambda|\Psi_0\rangle|^2 - \xi_{ee}^2 \langle\Phi_0|\Psi_0\rangle\langle\Phi_0|\Lambda^2|\Psi_0\rangle, \tag{10.77}$$

with

$$\Lambda \;=\; \sum_k \ln((r^{(k)} - r_z^{(k)})\lambda)\,, \tag{10.78}$$

while $|\Phi_0\rangle$ is the ground state of the FS with the ionized caged atom. Recall that the SO amplitude for every inelastic process in the FS is quenched, e.g., $\langle\Phi_x|\Psi_0\rangle \sim r_b/R \ll 1$ for every excited state x. Since the FS electrons are located in the layer of thickness $\Delta \ll R$, we can put $r^{(k)} = R$ on the RHS of (10.78). By this move, we have neglected the contributions of order $1/R^2$ to the FSI terms. This provides

$$P_0 \;=\; \langle\Phi_0|\Psi_0\rangle^2 + \xi_{ee}^2|\langle\Phi_0|\Lambda_1|\Psi_0\rangle|^2 - \xi_{ee}^2\langle\Phi_0|\Psi_0\rangle\langle\Phi_0|\Lambda_1^2|\Psi_0\rangle\,, \tag{10.79}$$

with

$$\Lambda_1 \;=\; \sum_k \ln(1 - t^{(k)})\,. \tag{10.80}$$

The terms containing the product $R\lambda$ cancel on the RHS of (10.79). Direct calculation gives

$$P_0 \;=\; |T_0^{(0)}|^2 - N_e\xi_{ee}^2, \tag{10.81}$$

with N_e the number of electrons in the FS. This provides

$$P_A(\varepsilon) \;=\; 1 - |T_0^{(0)}|^2 + N_e\xi_{ee}^2\,. \tag{10.82}$$

Neglecting all terms of order $1/R^2$, we put $|T_0^{(0)}|^2 = 1$ and obtain $P_A(\varepsilon) = N_e\xi_{ee}^2$. Note that for C_{60}, the parameter $N_e\xi_{ee}^2$ becomes smaller than unity only for $\varepsilon > 5$ keV. Thus one cannot employ the perturbative approach for $\varepsilon \lesssim 5$ keV. Fortunately, we can sum all the perturbative series for the FSI [29].

One can write the expression for n interactions between the photoelectron and the FS:

$$U_n(\mathbf{r}^{(k)}) \;=\; \alpha \int \frac{d^3q_1}{(2\pi)^3}\cdots\frac{d^3q_n}{(2\pi)^3} G_1(\mathbf{q_1})G_1(\mathbf{q}_1+\mathbf{q}_2)\cdots G_1(\mathbf{q}_1+\mathbf{q}_2+\cdots+\mathbf{q}_n)\times$$
$$g(q_1)\cdots g(q_n)e^{i\mathbf{q}_1\cdot\mathbf{r}^{(k)}}\cdots e^{i\mathbf{q}_n\cdot\mathbf{r}^{(k)}}. \tag{10.83}$$

Recall that the relation $U_2 = U_1^2/2$ was obtained after carrying out the evaluation

$$\frac{1}{\mathbf{pq}_1}\frac{1}{\mathbf{p}(\mathbf{q}_1+\mathbf{q}_2)} = \frac{1}{2}\Big(\frac{1}{\mathbf{pq}_1}+\frac{1}{\mathbf{pq}_2}\Big)\frac{1}{\mathbf{p}(\mathbf{q}_1+\mathbf{q}_2)} = \frac{1}{2}\frac{1}{\mathbf{pq}_1}\frac{1}{\mathbf{pq}_2}\,.$$

see (3.90). It can be generalized for the case of an arbitrary number n. Introducing $a_n = \mathbf{p}\cdot\mathbf{q}_n$ we can write

$$\frac{1}{a_1}\cdot\frac{1}{a_1+a_2}\cdots\frac{1}{a_1+a_2+\ldots a_n} = \frac{1}{n!}\cdot\frac{1}{a_1}\cdot\frac{1}{a_2}\cdots\frac{1}{a_n}\,. \tag{10.84}$$

This equation can be proved by the induction method. Thus for n interactions between the photoelectron and the FS,

$$U_n = \frac{U_1^n}{n!}. \tag{10.85}$$

Hence, for the total amplitude, which includes also the SO (zero order in FSI) term, we obtain

$$T_x = \sum_{n=0} T_x^{(n)} = \langle \Phi_x | e^{U_1} | \Psi_0 \rangle = \langle \Phi_x | e^{i\xi_{ee}\Lambda} | \Psi_0 \rangle, \tag{10.86}$$

with Λ defined by (10.78). Putting $r^{(k)} = R$, we arrive at

$$T_x = \langle \Phi_x | \Pi_k (1 - t^{(k)})^{i\xi_{ee}} | \Psi_0 \rangle; \quad t^{(k)} = \frac{\mathbf{p} \cdot \mathbf{r}^{(k)}}{p r^{(k)}}. \tag{10.87}$$

Here we omitted the constant phase factor $(R\lambda)^{i\xi_{ee}}$. Thus

$$P_A(\varepsilon) = 1 - |\langle \Phi_0 | \Pi_k (1 - t^{(k)})^{i\xi_{ee}} | \Psi_0 \rangle|^2. \tag{10.88}$$

Carrying out the angular integrations, we obtain

$$P_A(\varepsilon) = 1 - \frac{h}{(1 + \xi_{ee}^2)^{N_1}} = 1 - e^{-N_1 \ln(1+\xi_{ee}^2)} h; \quad h = |T_0^{(0)}|^2, \tag{10.89}$$

with N_1 the number of electrons that can participate in the process. At $\varepsilon \leq I_c$, with $I_c \approx 300\,\text{eV}$ the binding energy of the core electrons in the FS, only the valence FS electrons can participate. Thus for the fullerene C_N, we have $N_1 = 4N$. At larger energies, all electrons participate and $N_1 = 6N$.

Neglecting all contributions of order $1/R^2$, we obtain, putting $h = 1$,

$$P_A(\varepsilon) = 1 - e^{-N_1 \ln(1+\xi_{ee}^2)}. \tag{10.90}$$

We return to (10.89). If the photon energy is so large that $N\xi_{ee}^4 \ll 1$ (this means $\varepsilon \gg 300\,\text{eV}$ for C_{60} and $\varepsilon \gg 100\,\text{eV}$ for C_{20}), we can put $\ln(1 + \xi_{ee}^2) = \xi_{ee}^2$ in the exponential factor $e^{-N_1 \ln(1+\xi_{ee}^2)}$. This provides

$$P_A(\varepsilon) = 1 - e^{-N_1 \xi_{ee}^2} h. \tag{10.91}$$

At these energies, all the FS electrons participate, and $N_1 = 360$ for C_{60} and $N_1 = 120$ for C_{20}. At $N_1 \xi_{ee}^2 \ll 1$, we obtain (10.82).

10.3.2 High-Energy Limit

Now we consider the large energies, for which $N_e\xi_{ee}^2 \ll 1$, i.e., $\varepsilon \gg N_e \cdot 13.6\,\mathrm{eV}$. For the fullerene C_{60}, this means that $\varepsilon \gg 5\,\mathrm{keV}$, while for C_{20}, it is $\varepsilon \gg 1.5\,\mathrm{keV}$. At these energies, the FSI can be included in the lowest orders of the perturbative theory. The probability $P_A(\varepsilon)$ is determined by (10.82), and we must calculate the SO amplitude $T_0^{(0)}$.

To estimate the magnitude of the matrix element $\langle\Phi_0|\Psi_0\rangle$, we employ a simple model for the ground states of the FS in endohedral atoms [30]. Since in the SO, the FS reacts as a whole on ionization of the caged atom, we do not need details of the internal structure of the FS.

We assume that the ground states of the FS electrons in the endohedral systems with the caged atom or ion can be described in the framework of the Thomas–Fermi model. The FS electrons are confined inside a sphere of radius R. Thus they occupy the volume $V = 4\pi R^3/3$. The potential energy of the FS electrons $U < 0$ can be obtained from the Thomas–Fermi equation

$$\rho = \frac{(-2mU)^{3/2}}{3\pi^2}, \tag{10.92}$$

with $\rho = N_e/V$. Thus

$$U = -\frac{(3\pi^2\rho)^{2/3}}{2m}. \tag{10.93}$$

Assuming, following [31], that for the fullerene C_{60}, $R = 6.02r_0$, we obtain $U \approx -72\,\mathrm{eV}$.

After the ejection of the photoelectron, the new value of the potential energy is $U' = U + U_h$ with the contribution of the hole in the state n of the caged atom

$$U_h(r) = -e^2 \int d^3r' \frac{\rho_h(\mathbf{r}')}{|\mathbf{r} - \mathbf{r}'|} \approx -\frac{e^2}{r} \approx -\frac{e^2}{R}, \tag{10.94}$$

where ρ_h is the electron density in the state n. The numerical value for C_{60} is $U_h \approx -4.5\,\mathrm{eV}$, and $|U_h| \ll |U|$. Thus U_h can be considered a perturbation. The change of the value of the volume V can be obtained in the lowest order of perturbation theory. We write

$$\rho' = \frac{(-2mU')^{3/2}}{3\pi^2}, \tag{10.95}$$

and the volume of the FS with the caged ion becomes

$$V' = V\left(1 - \frac{3}{2}\frac{U_h}{U}\right) < V. \tag{10.96}$$

Now we must calculate the overlap matrix element $T^{(0)} = \langle \Phi_0 | \Psi_0 \rangle$. A wave function and its lowest-order perturbative correction are known to be orthogonal [32]. Thus the difference of the shapes of the functions Ψ_0 and Φ_0 is a second-order effect. The leading contribution to the deviation of the matrix element $T^{(0)}$ from unity comes from the difference between the volumes V and V'. Since $T^{(0)}$ is determined by integration over the volume V', while the functions Ψ_0 and Φ_0 contain the normalization factors $V^{-1/2}$ and $V'^{-1/2}$ respectively, we obtain

$$\langle \Phi_0 | \Psi_0 \rangle \;=\; 1 - \frac{V'^{1/2}}{V^{1/2}} \;=\; 1 - \frac{3}{4}\frac{U_h}{U}\,. \tag{10.97}$$

Thus for C_{60},

$$1 - \langle \Phi_0 | \Psi_0 \rangle = 0.046, \quad h = \langle \Phi_0 | \Psi_0 \rangle^2 = 0.91. \tag{10.98}$$

The numerical result does not depend strongly on the actual value of R. For example, taking $R = 5.75 r_0$ [33], we obtain

$$1 - \langle \Phi_0 | \Psi_0 \rangle = 0.050, \quad h = \langle \Phi_0 | \Psi_0 \rangle^2 = 0.90. \tag{10.99}$$

For the fullerene C_{20}, we can put, following [2], $R = 3.89 r_0$, providing $\langle \Phi_0 | \Psi_0 \rangle^2 = 0.83$.

Some additional data can be obtained by studying the distributions of the electrons ejected from the FS. The ratio $P_A(\varepsilon)$ can be written as the sum of contributions of the partial waves

$$P_A(\varepsilon) = \sum_{x\ell} |\langle \Phi_{x\ell} | \Psi_0 \rangle|^2 + \xi_{ee}^2 \sum_{x,\ell} |\langle \Phi_{x\ell} | \Lambda | \Psi_0 \rangle|^2 + \xi_{ee}^2 \sum_{x,\ell} \langle \Psi_0 | \Phi_{x\ell} \rangle \langle \Phi_{x\ell} | \Lambda^2 | \Psi_0 \rangle, \tag{10.100}$$

with Λ given by (10.78). The sum is carried out over the excited states $x \neq 0$. As in the previous section, we can put $r^{(k)} = R$, replacing Λ by $\Lambda_1 = \sum_k \ln(1 - t^{(k)})$' see (10.80).

If $\ell = 0$, all three terms on the RHS contribute. However, due to the closure condition, $\sum_{x0} |\langle \Phi_{x0} | \Psi_0 \rangle|^2 = 1 - |\langle \Phi_{00} | \Psi_0 \rangle|^2 \ll 1$. Thus for each excited state $x \neq 0$, we have $|\langle \Phi_{x0} | \Psi_0 \rangle|^2 \ll 1$, and we can neglect the second and third terms on the RHS of (10.100). At $\ell \geq 1$, the first and third terms vanish due to the orthogonality of the angular parts of the wave functions, and only the second term on the RHS survives. Thus we can write

$$P_A(\varepsilon) \;=\; A_0 + \xi_{ee}^2 \sum_{\ell \geq 1} A_\ell\,, \tag{10.101}$$

with

$$A_0 \;=\; \sum_x \langle \Phi_{x0} | \Psi_0 \rangle^2\,, \tag{10.102}$$

while for $\ell \geq 1$,

$$A_\ell \;=\; \sum_x |\langle \Phi_{x\ell}|\Lambda_1|\Psi_0\rangle|^2. \tag{10.103}$$

Thus the contribution to the ratio $P_A(\varepsilon)$, which does not vanish in the limit $\varepsilon \to \infty$, consists of monopole terms. The contribution, which decreases as ε^{-1}, consists of the terms with $\ell \geq 1$. The considered mechanism does not change the projection of the angular momentum m on the direction of the photoelectron's momentum. Thus $\langle \Phi_{n\ell}| = \langle \Phi_{n\ell,m=0}|$ in the equations presented above.

If the photoelectron moves an FS electron from a single-particle s state, we expect the dipole contribution with $\ell = 1$ to dominate in the sum $\sum_{\ell\geq 1} A_\ell$. Indeed, in this case, we obtain, for every s electron of the FS,

$$\langle \Phi_{x\ell}|\Lambda_1|\Psi_0\rangle \;=\; b_\ell d_{x\ell}\,. \tag{10.104}$$

Here

$$d_{x\ell} \;=\; \int_0^\infty dr r^2 \psi_0^r(r)\phi_{x\ell}^r(r), \tag{10.105}$$

with $\psi_0^r(r)$ and $\phi_{x\ell}$ the radial parts of the single-particle functions for the initial- and final-state electrons respectively; b_ℓ are the coefficients of expansion of the function $\ln(1-t)$ in terms of the Legendre polynomials; see (7.173, 7.174). Note that the overlap integral $d_{x\ell}$ is not always small. Employing (7.176) for the coefficients b_ℓ, we obtain for ionization of the s state in the FS

$$P_A(\varepsilon) \;=\; A_0 + \xi_{ee}^2 N_s \sum_{\ell\geq 1} c_\ell |d_{x\ell}|^2, \tag{10.106}$$

with

$$c_\ell \;=\; \frac{2\ell+1}{\ell^2(\ell+1)^2}\,,$$

while N_s is the number of s electrons in the FS. Writing

$$\frac{2\ell+1}{\ell^2(\ell+1)^2} \;=\; \frac{1}{\ell^2} - \frac{1}{(\ell+1)^2}\,,$$

we find that $\sum_{\ell=1} c_\ell = 1$. Since $c_1 = 3/4$, and the overlap integrals $d_{x\ell}$ drop with increasing ℓ, we expect the term with $\ell = 1$ to give the main contribution to the second term on the RHS of (10.106).

10.3.3 Energy Dependence of the Probability of Excitation of the Fullerene Shell

While we did not employ the actual features of the FS excitation spectrum, the equations obtained above are valid for the fullerenes C_{60} and C_{20} at $\varepsilon \gg 45$ eV. However, at least in the case of C_{60}, we can extend our approach to the smaller energies, expecting it to be valid for $\varepsilon \gtrsim 60$ eV [34]. This is because the FS excitation spectrum exhibits a strong peak at $\varepsilon \approx 20$ eV. This is a plasmon excitation in which the 240 valence electrons oscillate relative to the carbon ion core [35]. Also, at $\varepsilon \lesssim 70$ eV the knockout of carbon ions such as C^{2+} is important [36]. These excitations provide a large part of the oscillator strength, leaving little room for the others (see (7.90)).

There is a large discrepancy between the experimental and theoretical results on photoionization of the $4d$ state of the caged atom in the endohedral atom $Xe@C_{60}$ for $\omega \geq 140$ eV [36]. The corresponding photoelectron energies are $\varepsilon \geq 60$ eV. There is the same tendency in photoionization of $Ce@C_{82}^{+}$ [37]. These results can be easily understood. The measurements of the photoionization cross section are based on detection of the outgoing electron with energy $\varepsilon = \omega - I$, with I the ionization potential. There is a large probability for a photoelectron to lose a part of its energy in interaction with the FS. Thus only a small number of the photoelectrons keep this energy and are actually detected.

Now we trace the energy dependence of probability $P_A(\varepsilon)$. If the photoelectron energy is smaller than the ionization potential of the core $1s$ electrons $I_c \approx 315$ eV, the probability $P_A(\varepsilon)$ is determined by (10.89), with N_1 the number of valence electrons, i.e., $N_1 = 240$ for C_{60} and $N_1 = 80$ for C_{20}. At ε close to I_c, we obtain $1 - P_A(\varepsilon) \approx 2 \cdot 10^{-5}$ for C_{60}, while $P_A(\varepsilon) \approx 0.97$ for C_{20}.

At $\varepsilon > I_c$, the core electrons are involved in the process as well. Thus $N_1 = 360$ for C_{60} and $N_1 = 120$ for C_{20}. While the photoelectron energy is of order I_c, the contribution of the core electrons cannot be calculated by employing closure, since some of the excited states cannot be reached due to restrictions imposed by the energy conservation law. However, (10.89), with N_1 the number of valence electrons, provides the upper limit for the value $1 - P_A(\varepsilon)$ at these energies.

At larger energies $\varepsilon \gg I_c$, the probability $P_A(\varepsilon)$ is given by (10.91) with the core electrons included. At $\varepsilon = 2$ keV, we obtain $1 - P_A(\varepsilon) \approx 0.09$ for C_{60}. Hence, $P_A(\varepsilon)$ is very close to unity. At $\varepsilon = 5$ keV, we obtain $P_A(\varepsilon) \approx 0.62$, decreasing as $1/\varepsilon$ at larger energies, following (10.82). For C_{20}, the ratio $P_A(\varepsilon)$ reaches this value at $\varepsilon \approx 8$ keV. The FSI and the SO contributions to $P_A(\varepsilon)$ expressed by (10.82) have the same order of magnitude at $\varepsilon \gtrsim 50$ keV for C_{60}, and at $\varepsilon \gtrsim 8$ keV in the case of C_{20}. The dependence $P_A(\varepsilon)$ for the endohedral atoms $A@C_{60}$ and $A@C_{20}$ is shown in Fig. 10.6.

Thus we have found that in a broad interval of the photon energies, almost each event of photoionization of the caged atom is accompanied by a transition in the fullerene shell. Therefore, the measured cross section of the one-electron photoionization of the caged atom is much smaller than that of an isolated atom. An important

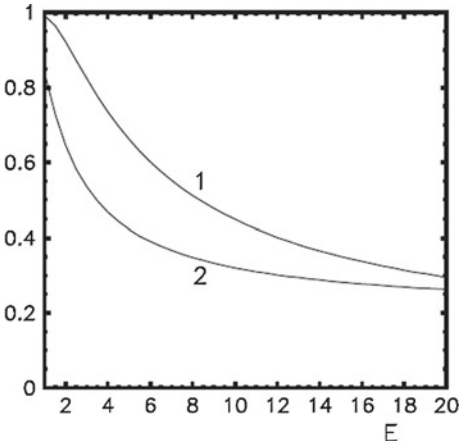

Fig. 10.6 Dependence of the probability P_A on the photoelectron energy. The latter is in keV units. *Curves* 1 and 2 are for the fullerenes C_{60} and C_{20} respectively

outcome of this analysis is that a rigorous treatment of the interaction between a photoelectron and the FS requires an optical potential rather than a simple effective potential.

References

1. H.W. Kroto, J.R. Heath, S.C. O'Brien, R.F. Curl, R.E. Smalley, Nature (London) **318**, 162 (1985)
2. V.K. Ivanov, G.Yu. Kashenock, R.G. Polozkov, A.V. Solov'yov, J. Phys. B **34**, L669 (2001)
3. J.L. Martins, N. Troullier, J.H. Weavier, Chem. Phys. Lett. **180**, 457 (1992)
4. A.S. Baltenkov, S.T. Manson, A.Z. Msezane, J. Phys. B **48**, 185103 (2015)
5. L.L. Lohr, S.M. Blinder, Chem. Phys. Lett. **198**, 100 (1992)
6. E.M. Nascimento, F.V. Prudente, M.N. Guimaraes, A.M. Maniero, J. Phys. B **44**, 5003 (2011)
7. S.H. Yang, C.L. Pettiette, J. Conceicao, O. Cheshnovsky, R.E. Smalley, Chem. Phys. Lett. **139**, 233 (1987)
8. I.V. Hertel, H. Steger, J. de Vries, B. Weisser, C. Menzel, B. Kamke, W. Kamke, Phys. Rev. Lett. **68**, 784 (1992)
9. J. Kou, T. Mori, M. Ono, Y. Haruyama, Y. Kubozono, K. Mitsuke, Chem. Phys. Lett. **374**, 1 (2003)
10. J. Berkowitz, J. Chem. Phys. **111**, 1446 (1999)
11. O. Elhamidi, J. Pommier, R. Abouaf, J. Phys. B **30**, 4633 (1997)
12. T. Jafke, E. Illenberger, M. Lezius, S. Matejcik, D. Smith, T.D. Mark, Chem. Phys. Lett. **226**, 213 (1994)
13. S.M. Blinder, Chem. Phys. Lett. **64**, 485 (1979)
14. V. Bargmann, Proc. Nat. Acad. Sci. USA **38**, 961 (1952)
15. M.Ya. Amusia, A.S. Baltenkov, B.G. Krakov, Phys. Lett. A **243**, 99 (1998)
16. A.S. Baltenkov, J. Phys. B **32**, 2745 (1999)
17. B.H. Armstrong, Phys. Rev. **131**, 1132 (1963)
18. J.P. Connerade, V.K. Dolmatov, P.F. Lakshmi, S.T. Manson, J. Phys. B **32**, L239 (1999)
19. H.S. Chakraborty, M.E. Madjet, J.-M. Rost, S.T. Manson, Phys. Rev. A **79**, 061201 (R) (2009)
20. M.E. Madjet, T. Renger, D.E. Hopper, M.A. McCune, H.S. Chakraborty, J.-M. Rost, S.T. Manson, Phys. Rev. A **81**, 013202 (2010)

21. J.P. Connerade, V.K. Dolmatov, S.T. Manson, J. Phys. B **33**, 2279 (2000)
22. M.Ya. Amusia, A.S. Baltenkov, Phys. Rev. A **73**, 063206 (2006)
23. B.P. Kafle, H. Katayanagy, Md.S.I. Prodhan, H. Yagi, C. Huang, K. Mitsuke, J. Phys. Soc. Jpn **77**, 014302 (2008)
24. J.P. Connerade, A.V. Solov'yov, J. Phys. B **38**, 807 (2005)
25. M.Ya. Amusia, A.S. Baltenkov, L.V. Chernysheva, Z. Felfli, A.Z. Msezane, J. Phys. B **38**, L 169 (2005)
26. M.Ya. Amusia, *Atomic Photoeffect* (Plenum Press, NY and London, 1990)
27. A.L.D. Kilcoyne et al., Phys. Rev. Lett. **105**, 213001 (2010)
28. M.Ya. Amusia, A.S. Baltenkov, V.K. Dolmatov, S.T. Manson, A.Z. Msezane, Phys. Rev. A **70**, 023201 (2004)
29. E.G. Drukarev, M.Ya. Amusia, JETP Lett. **98**, 471 (2013)
30. M.Ya. Amusia, E.G. Drukarev, Phys. Rev. A **89**, 013412 (2014)
31. M.Ya. Amusia, L.V. Chernysheva, V.K. Dolmatov, Phys. Rev. A **84**, 063201 (2011)
32. L.D. Landau, E.M. Lifshits, *Quantum Mechanics. Nonrelativistic Theory* (Pergamon, N.Y., 1977)
33. Y.B. Xu, M.Q. Tan, U. Becker, Phys. Rev. Lett. **76**, 3538 (1996)
34. M.Ya. Amusia, L.V. Chernysheva, E.G. Drukarev, JETP Lett. **100**, 543 (2014)
35. G.F. Bertsch, A. Bulgac, D. Tomanec, Y. Wang, Phys. Rev. Lett. **67**, 2690 (1991)
36. A.L.D. Kilcoyne et al., Phys. Rev. Lett. **105**, 213001 (2010)
37. A. Müller et al., Phys. Rev. Lett. **101**, 133001 (2008)

Chapter 11
Annihilation of Positrons with Atomic Electrons

Abstract We analyze various channels for the annihilation of positrons with atomic electrons. Since in the annihilation process a large energy exceeding 1 MeV is released, relativistic analysis is required even in the case of slow positrons. We study in detail the dominative two-photon annihilation process on the Bethe ridge and outside it. We calculate the characteristics of single-quantum annihilation and annihilation followed by knockout of a bound electron to the continuum. In the latter case, the role of the QFM mechanism described in Chap. 9 is important. We consider also annihilation followed by creation of a $\mu^+\mu^-$ pair and annihilation accompanied by creation of a mesoatom.

11.1 Two-Photon Annihilation

11.1.1 On the Bethe Ridge: Fast Positrons

Annihilation of a positron with a electron bound in an atom can be followed by radiation of two photons. This process, illustrated by Fig. 11.1, has the largest cross section, at least for small Z, among the various channels of annihilation of positrons in their interactions with atomic electrons, since it can take place on the free electrons. The conservation laws for the free process

$$E + m \;=\; \omega_1 + \omega_2; \quad \mathbf{p} \;=\; \mathbf{k}_1 + \mathbf{k}_2\,, \tag{11.1}$$

with E and $\mathbf{p}$ the relativistic energy and three-dimensional momentum of the positron, require that the difference between the energies of the radiated photons be limited by the condition

$$\frac{\omega_1 - \omega_2}{\omega_1 + \omega_2} \;\le\; \sqrt{\frac{E-m}{E+m}}\,. \tag{11.2}$$

Here we have assumed that $\omega_1 \ge \omega_2$.

E.G. Drukarev and A.I. Mikhailov, *High-Energy Atomic Physics*,
Springer Series on Atomic, Optical, and Plasma Physics 93,
DOI 10.1007/978-3-319-32736-5_11

If the condition (11.2) is satisfied and the positron kinetic energy is large enough, i.e., $\xi = \alpha ZE/p \ll 1$, a momentum

$$\mathbf{q} \;=\; \mathbf{k}_1 + \mathbf{k}_2 - \mathbf{p} \tag{11.3}$$

is transferred from the nucleus to the bound electron. Following our general approach, we can write for the amplitude of annihilation with any bound electron at the Bethe ridge ($q \sim \mu_b$)

$$F(E, \omega_1, \mathbf{q}) \;=\; F_0(E, \omega_1) S(q)\,, \tag{11.4}$$

with $S(q)$ defined by (9.146). In this chapter, we describe the electrons by single-particle functions.

The amplitude of the free process F_0 can be expressed in terms of the amplitude F_C of the Compton scattering on the free electron at rest. While dependence of the latter on the energies of the incoming photon and the ejected electron is $F_C(E_C, \omega_{1C})$, we obtain $F_0(E, \omega_1) = F_C(-E_C, -\omega_{1C})$. This is a manifestation of the general principle of the crossing invariance of the amplitudes. The amplitude of the process in which the system of the particles A and B converts to that of the particles C and D and that in which a particle is changed to its antiparticle are described by the same analytical function of kinematic variables.

Employing (2.80), we obtain for the energy distribution

$$\frac{d\sigma}{d\omega_i} \;=\; \frac{d\sigma_0}{d\omega_2} \;=\; \frac{2\pi r_e^2 f_0 m}{p^2}\,, \tag{11.5}$$

with $d\sigma_0/d\omega_i$ the energy distribution for two-photon annihilation on the free electron, while

$$f_0 = \frac{1}{2}\Big[\frac{\omega_1}{\omega_2} + \frac{\omega_2}{\omega_1} + 2\Big(\frac{m}{\omega_1} + \frac{m}{\omega_2}\Big) - \Big(\frac{m}{\omega_1} + \frac{m}{\omega_2}\Big)^2\Big];$$

see (6.168). The angular distribution can be written as

$$\frac{d\sigma}{dt_i} = \frac{d\sigma_0}{dt_i} = \frac{2\pi r_e^2 f_0 \omega_1^2}{p(E+m)}; \quad t_i = \frac{\mathbf{p}\cdot\mathbf{k}_i}{pk_i}\,. \tag{11.6}$$

The total cross section of annihilation is of order r_e^2 for $E - m \sim m$. In the ultra-relativistic limit $E \gg m$, it becomes smaller, i.e., $\sigma \sim r_e^2 m/E$. One can see this by employing (11.5). This equation demonstrates also that in the nonrelativistic limit $p \ll m$ (but still $p \gg \eta$), the energy distribution is larger than at $p \sim m$ ($E - m \sim m$). The increase of the total cross section is not so large, since the interval of photon energy values diminishes, i.e., $|\omega_i - m|/m \lesssim p/m$. Thus in the nonrelativistic case, we obtain $\sigma \sim r_e^2 m/p$. The corrections to these equations are of order $\alpha^2 Z^2$.

The total cross section for the two-quanta annihilation on a free electron is [1]

$$\sigma_0(E) = \frac{\pi r_e^2}{\beta+1}\left[\frac{\beta^2+4\beta+1}{\beta^2-1}\ln\left(\beta+\sqrt{\beta^2-1}\right) - \frac{\beta+3}{\sqrt{\beta^2-1}}\right], \tag{11.7}$$

with $\beta = E/m$. In the ultrarelativistic limit $E \gg m$,

$$\sigma_0(E) = \pi r_e^2 \frac{m}{E}\left(\ln\frac{2E}{m} - 1\right). \tag{11.8}$$

The cross section for annihilation in interaction with an atom containing N electrons is

$$\sigma(E) = N\sigma_0(E). \tag{11.9}$$

In the only experiment on two-quantum annihilation of positrons with atoms [2], the cross section was measured for 300-keV positrons absorbed by atoms of silver ($I_Z = 26\,\text{keV}$). The theoretical results overestimate the measured ones.

In the free process, the values t_i are determined by those of ω_i, i.e.,

$$t_1 = t_{10} = \frac{p^2+\omega_1^2-\omega_2^2}{2p\omega_1}; \quad t_2 = t_{20} = \frac{p^2+\omega_2^2-\omega_1^2}{2p\omega_2}. \tag{11.10}$$

We shall see that after inclusion of the terms of order ξ, the distributions $d\sigma/d\omega_i dt_i$ peak at t_i, which differ from the values defined by (11.10) by values of order $\alpha^2 Z^2$. We calculate the terms $\sim \xi$ for a hydrogenlike atom. We include the terms linear in $\mathbf{q}$ in the amplitude F_0 and the lowest-order correction for interaction between the positron and the nucleus. As in the case of Compton scattering, Coulomb corrections to the propagators provide contributions of order ξ^2. We obtain [3]

$$\frac{d\sigma}{d\omega_1 d\Omega_1 d\Omega_2} = \frac{8r_e^2}{\pi^2}\frac{\eta^5 m\omega_1\omega_2}{pa^4}\left[f_0\cdot\left(1-\frac{2E}{m}L\right) - f_1\frac{\mathbf{q}\cdot\mathbf{k_1}}{m\omega_1} - f_2\frac{\mathbf{q}\cdot\mathbf{k_2}}{m\omega_2}\right]. \tag{11.11}$$

Here $\eta = m\alpha Z$,

$$a = q^2+\eta^2; \quad L = \frac{\eta}{p}\arctan\frac{\eta}{\mathbf{qn}} + \frac{\mathbf{n}\cdot\mathbf{q}}{2p}\frac{q^2+\eta^2}{(\mathbf{n}\cdot\mathbf{q})^2+\eta^2}; \quad \mathbf{n} = \frac{\mathbf{p}}{p}, \tag{11.12}$$

while $f_i = \omega_i \partial f_0/\partial\omega_i$ for $i = 1, 2$, i.e.,

$$f_1 = \frac{1}{2}\left[\frac{\omega_1}{\omega_2} - \frac{\omega_2}{\omega_1} + 2\frac{m}{\omega_1}\left(\frac{m}{\omega_1}+\frac{m}{\omega_2}-1\right)\right]; \quad f_2(\omega_1,\omega_2) = f_1(\omega_1 \leftrightarrow \omega_2).$$

Writing

$$\frac{d\sigma}{d\omega_1 d\Omega_1 d\Omega_2} = \frac{\omega_1^2 d\sigma}{d^3k_1 d\Omega_2} = \frac{\omega_1^2 d\sigma}{d^3q d\Omega_2}$$

and integrating over $\mathbf{q}$, we find that the terms proportional to L, f_1, and f_2 vanish, and we come to the energy distribution $d\sigma/d\omega_2$ in the lowest approximation of the expansion in powers of ξ (11.5). Thus the corrections of order ξ manifest themselves neither in the energy or angular distributions nor in the total cross section.

Integrating the distribution (11.11) over Ω_2, we obtain

$$\frac{d\sigma}{d\omega_1 d\Omega_1} = \frac{8r_e^2}{3\pi}\frac{m\omega_1}{p\omega_2\eta}\frac{f_0(\omega_1,\omega_2)}{(1+x^2)^3}\Big[1+\alpha Z x F(\omega_1,t_1)\Big]. \tag{11.13}$$

Here

$$F(\omega_1,t_1)=\lambda(\omega_1)+\frac{E}{p}\frac{\Phi(x,t)}{f_0};\quad \lambda(\omega_1)=\left(1-\frac{m}{\omega_1}-\frac{m}{\omega_2}\right)\frac{f_1}{f_0}+\frac{f_2}{f_0}-\frac{m}{\omega_2}, \tag{11.14}$$

while

$$x=\frac{q_1-\omega_2}{\eta};\quad \mathbf{q}_1=\mathbf{p}-\mathbf{k}_1;\quad t\equiv\frac{\mathbf{pq}_1}{pq_1}=\frac{p-\omega_1 t_1}{q_1}. \tag{11.15}$$

The function Φ is a rather bulky combination of elementary functions. We do not present it here, referring the interested reader to the paper [3]. We provide only an expression for

$$\Phi(0,t) = \frac{15}{2t^5}\left(-1+\frac{7t^2}{6}+\frac{3t^4}{10}+\frac{2-3t^2+t^6}{4t}\ln\frac{1+t}{1-t}\right), \tag{11.16}$$

which determines the shift of the positions of the peaks of the distribution (11.11) and the shift of the differential cross sections $d\sigma/dt_1$ at fixed ω_1 and $d\sigma/d\omega_1$ at fixed t_1.

In free kinematics, $x=0$, and thus

$$\omega_1=\omega_{10}=\frac{m(E+m)}{E+m-pt_1};\quad \omega_2=\omega_{20}=\frac{m(E+m)}{E+m-pt_2}. \tag{11.17}$$

If we now include the corrections of order ξ, the peak of the distribution (11.13) is reached at

$$x_1=\frac{\alpha Z}{6}\left(\lambda(\omega_1)+\frac{E}{p}\frac{\Phi(0,t_0)}{f_0}\right);\quad t_0=\frac{p-Et_{10}}{E-pt_{10}}, \tag{11.18}$$

with t_{10} the value of t_1 corresponding to the free kinematics determined by (11.10). At a fixed value of ω_1, the peak of the angular distribution is reached at

$$t_1 = t_{10}-\frac{\omega_2\eta}{\omega_1 p}x_1, \tag{11.19}$$

with t_{10} determined by (11.10). The formula for the shift of the position of the energy distribution peak is somewhat more complicated:

$$\omega_1 = \omega_{10} + \frac{\alpha^2 Z^2}{6} \frac{\omega_1 \omega_2}{E+m} \left(\lambda(\omega_1) + \frac{E}{p} \frac{\Phi(0,t_0)}{f_0} + \frac{\omega_2 f_1 - \omega_1 f_2}{f_0 (E+m)} - 2 \right). \quad (11.20)$$

Here t_0 is defined by (11.18), and the RHS should be taken at $\omega_1 = \omega_{10}, \omega_2 = \omega_{20}$ corresponding to the free kinematics. The values of ω_{n0} $(n = 1, 2)$ are given by (11.17). In the nonrelativistic case, (11.17) can be simplified:

$$\omega_1 \;=\; \omega_{10} + \frac{\eta^2}{12p} \left(\Phi(0,t_0) - \frac{3p}{m} + O(\frac{p^2}{m^2}) \right). \quad (11.21)$$

11.1.2 On the Bethe Ridge: Slow Positrons

Now we extend our analysis to the case in which the kinetic energy of the positron is of order the electron binding energy. We must include interaction with the atomic field in the positron wave function. If the ionization potential I_b is not too large, i.e., $I_b \ll m$, the incoming positron can be described by the nonrelativistic function. However, the positron in the intermediate state in Fig. 11.1 carries a large energy and should be described by the relativistic propagator.

Due to the energy conservation law, $\omega_1 + \omega_2 = 2m - I_b \approx 2m$. Introducing $\boldsymbol{\kappa} = \mathbf{k}_1 + \mathbf{k}_2$, we see that on the Bethe ridge, $\kappa \sim \mu_b \ll \omega_1 + \omega_2$. Thus the energies of the radiated photons are close, i.e., $|\omega_1 - \omega_2| \leq \kappa \sim \mu_b$, and

$$\frac{|\omega_1 - \omega_2|}{\omega + \omega_2} \;\lesssim\; \frac{\mu_b}{m} \;\ll\; 1\,. \quad (11.22)$$

Each photon carries the energy $\omega_i \approx m \approx 500\,\mathrm{keV}$. The photons are radiated in nearly opposite directions, with $t_{12} = \mathbf{k}_1 \cdot \mathbf{k}_2 / \omega_1 \omega_2$ close to -1.

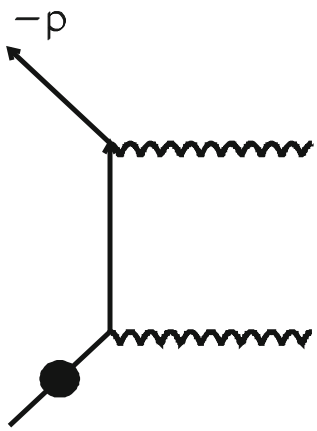

Fig. 11.1 Two-quantum annihilation in the interaction of positrons with atomic electrons. The *solid lines* stand for electrons (positrons). The *arrow* marks the positron, with the direction of the arrow opposite to that of the positron momentum. The *dark blob* labels the bound electron. The *helix lines* are for the photons

We carry out calculations for annihilation with the K-shell electrons, describing them by nonrelativistic Coulomb functions. Due to (11.22), the momenta of the intermediate particles in the Feynman diagrams shown in Fig. 11.1 are large enough ($p_{a,b} \gg \eta$), and with an error of order $\eta/m \sim \alpha Z$ can be described by free relativistic propagators.

To obtain the cross section of the process, we can employ results for differential distributions of the Compton scattering on the K electrons with ejection of slow electrons carried out in Sect. 6.4. The distribution $d\sigma_C/d\omega_2 dt_{12}$ is represented by (6.162). Employing this result, we obtain

$$\frac{d\sigma}{d\omega_1 d\kappa} = r_e^2 \frac{2^7}{3} \frac{m\eta^4 \xi \kappa^3 (p^2 + 3\kappa^2 + \eta^2)}{[(p-\kappa)^2 + \eta^2]^3 [(p+\kappa)^2 + \eta^2]^3} \cdot N(\kappa)(1 + t_{12}^2) \tag{11.23}$$

for $|\omega_1 - m| \lesssim \eta$ and $\kappa \lesssim \eta$. Here

$$N(\kappa) = N_+^2 \exp(2\xi\chi); \quad \chi = \arctan\left(\frac{2\eta p}{\kappa^2 - p^2 + \eta^2}\right), \tag{11.24}$$

with

$$N_+^2(\xi) = \frac{2\pi\xi}{\exp(2\pi\xi) - 1}, \tag{11.25}$$

in the squared normalization factor of the positron wave function. Recall that $\xi = \eta/p = (I_Z/\varepsilon)^{1/2}$.

On the RHS of (11.23), the last factor is the only term depending on ω_1 with $t_{12} = 1 - (4m^2 - \kappa^2)/2\omega_1\omega_2$. Taking into account the identity of two photons, we obtain

$$\frac{d\sigma}{d\kappa} = \frac{1}{2} \int\limits_{m-\kappa/2}^{m+\kappa/2} d\omega_1 \frac{d\sigma}{d\omega_1 d\kappa} = r_e^2 \frac{2^7}{3} \frac{m\eta^4 \xi \kappa^4 (p^2 + 3\kappa^2 + \eta^2)}{[(p-\kappa)^2 + \eta^2]^3 [(p+\kappa)^2 + \eta^2]^3} \cdot N(\kappa). \tag{11.26}$$

This determines the angular distribution

$$\frac{d\sigma}{dt_{12}} = \frac{m^2}{\kappa} \frac{d\sigma}{d\kappa},$$

where the distribution $d\sigma/d\kappa$ is given by (11.26) with $\kappa^2 = 2m^2(1 + t_{12})$. The total cross section can be obtained by integration over κ, and the integral is saturated at $\kappa \sim \eta$. The cross section is of order $r_e^2 \cdot m/p$.

For very slow positrons with $p \ll \eta$, it is reasonable to evaluate

$$\exp(2\xi\chi) = \exp\left(4\eta^2/(\kappa^2 + \eta^2)\right) \tag{11.27}$$

on the RHS of (11.24). In this limit, $\sigma \sim r_e^2 \xi^2 e^{-2\pi\xi}/(\alpha Z)$. The exponential quenching is due to the strong repulsion between the nucleus and the slow positron.

At $\varepsilon \leq I_Z$, annihilation with the electrons of multielectron atoms is more complicated, since the correlation between the positron and atomic electrons should be included. The positron captures one of the atomic electrons, creating a new two-particle bound state, the positronium. In the next step, the positronium decays into two photons if the positronium has spin $S = 0$, or into three photons for $S = 1$. This becomes the dominant annihilation mode [4]. The positron annihilation on molecules is still more complicated, since the vibrational degrees of freedom become involved [5].

11.1.3 Photon Distribution Outside the Bethe Ridge

If the photon energies satisfy the inequality (11.2), we can calculate the angular distribution $d\sigma/dt_1$ for every value of the angle t_1. Recall that if t_1 is close to t_{10} (i.e., their difference is of order αZ), which corresponds to free kinematics and is given by (11.10), the distribution is determined by small recoil momenta $q \sim \eta$. If the values of t_1 are not close to t_{10}, a large recoil momentum $q \gg \mu_b$ should be transferred to the nucleus.

Following the analysis carried out in Chaps. 3 and 5, we can consider the process as consisting of two steps. The first is scattering of the positron on the atom. In this process, a large momentum q is transferred to the atom. As we have seen in previous chapters, since $q \gg \eta$, this momentum should be transferred to the nucleus. After the scattering, the positron carries momentum $\mathbf{p}' = \mathbf{p} + \mathbf{q}'$ with $\mathbf{q}' \approx \mathbf{q}$, i.e., $|\mathbf{q}' - \mathbf{q}| \ll q$. Since the energy is not transferred in this collision, $|\mathbf{p}'| = p' = p$. In the second step, the scattered positron is annihilated with the bound electron. Here two photons are radiated and a small momentum of order μ_b is transferred to the nucleus. The angle between the directions of the momenta $\mathbf{k}_1$ and $\mathbf{p}'$ is determined by free kinematics. Thus for $t' = \mathbf{k}_1\mathbf{p}'/k_1 p'$, we can write

$$t' = t_{10}\,, \tag{11.28}$$

with t_{10} determined by (11.10).

Similar to the case of Compton scattering (8.31), the distribution in photon energy and recoil momentum can be written as

$$\frac{d\sigma}{d\omega_1 d\varphi dq^2} = \frac{\langle\psi_i|r^{-2}|\psi_i\rangle}{4\pi} \cdot \frac{d\sigma_0}{d\omega_1 d\varphi} \cdot \frac{d\sigma_{e^+A}(\varepsilon)}{dq^2}\,. \tag{11.29}$$

Here φ is the angle between the planes determined by the vectors $\mathbf{p}$, $\mathbf{q}$ and $\mathbf{p}'$, $\mathbf{k}_1$; $d\sigma_0/d\omega_1 d\varphi$ is the differential cross section for the positron two-quanta annihilation with the free electron, while $d\sigma_{eA}$ is that for the scattering of the positron on the atom. At $q \gg \eta$, the latter can be treated in the Born approximation. It is dominated

by scattering on the nucleus and can be written similar to (8.32) as

$$\frac{d\sigma_{e^+A}(\varepsilon)}{dq^2} = \frac{d\sigma_{e^+N}(\varepsilon)}{dq^2} = \frac{|V_{e^+N}(q^2)|^2}{2\pi}\frac{E^2}{p^2}\left(1-\frac{q^2}{4E^2}\right), \tag{11.30}$$

with the positron–nucleus interaction $V_{e^+N}(q^2) = 4\pi\alpha Z/q^2$.

The distribution (11.29) can be written in terms of the angular variables of the radiated photon. Writing $q^2 = 2p^2(1-t_p)$ with $t_p = \mathbf{pp}'/p^2$, we represent (11.30) as

$$\frac{d\sigma_{e^+N}(\varepsilon)}{dq^2} = \frac{1}{2p^2}\frac{d\sigma_{e^+N}(\varepsilon)}{dt_p}; \quad \frac{d\sigma_{e^+N}(\varepsilon)}{dt_p} = \frac{4\pi\alpha^2Z^2}{p^2(1-t_p)^2}\frac{E^2}{p^2}\left(1-\frac{p^2(1-t_p)}{2E^2}\right). \tag{11.31}$$

The distribution

$$\frac{d\sigma_{e^+N}(\varepsilon)}{dt_1} = \frac{d\sigma_{e^+N}(\varepsilon)}{dt_p}\frac{dt_p}{dt_1}$$

can be obtained using the relation $t_p = t_1t' + (1-t_1^2)^{1/2}(1-t'^2)^{1/2}\cos\varphi$ and (11.28). Carrying out integration over φ, we obtain

$$\frac{d\sigma}{d\omega_1 dt_1} = \frac{\alpha^2}{2}\frac{\langle\psi_i|r^{-2}|\psi_i\rangle}{p^2}\cdot\frac{E^2}{p^2}\frac{d\sigma_0}{d\omega_1}\cdot\left(\frac{1-t_1t_{10}}{(t_1-t_{10})^2} - \frac{p^2}{2E^2}\frac{1}{|t_1-t_{10}|}\right). \tag{11.32}$$

This expression is true outside the Bethe ridge, i.e., at $|t_1 - t_{10}| \gtrsim \alpha Z$. On the Bethe ridge, $|t_1 - t_{10}| \sim \alpha Z$, and one should use the equations of Sect. 11.1.1.

Another important region outside the Bethe ridge is the one where the energy of one of the photons is much smaller than that of the other one, e.g., $\omega_2 \ll \omega_1$. The distribution of the soft photons is similar to that in Compton scattering; see (8.35):

$$\frac{d\sigma}{d\omega_2 d\Omega_1} = \frac{\alpha}{\pi}\cdot\frac{v^2}{\omega_2}\cdot\int\frac{d\Omega_2}{4\pi}\cdot\frac{1-\tau^2}{(1-v\tau)^2}\cdot\frac{d\sigma_s}{d\Omega_1}; \quad \tau = \frac{\mathbf{p}\cdot\mathbf{k}_2}{p\omega_2}, \tag{11.33}$$

with $\mathbf{v} = \mathbf{p}/E$ the velocity of the positron. Here $d\sigma_s$ is the differential cross section of the process without the soft photon. In other words, σ_s is the cross section of annihilation with all initial energy converted into the energy of a single photon. This process will be analyzed below.

11.2 Annihilation with Radiation of One Photon

11.2.1 Single-Quantum Annihilation

The possibility of single-quantum annihilation of a positron in its interaction with a bound electron was predicted by Fermi and Uhlenbeck in 1933. They carried out the first calculation of the cross section based on the Born approximation and the Coulomb potential. The result is presented, e.g., in the book [1]. The corresponding Feynman diagram is shown in Fig. 11.2. The process in which one of the bound electrons is annihilated while the others do not change their states,

$$e^+ + A \;=\; A^+ + \gamma\,, \tag{11.34}$$

with A and A^+ denoting the atom, and the positive ion is crossing-invariant with respect to the photoionization process

$$\gamma + A \;=\; A^+ + e^-\,.$$

Thus the cross section can be expressed in terms of the photoionization amplitude F_{ph}.

Denoting the four-vector of the photoelectron in the photoionization process by P_{ph}, we can write for the cross section of the single-quantum annihilation

$$d\sigma^+_{ann} \;=\; \frac{1}{v}|F_{ph}(-P_{ph})|^2\frac{\omega^2 d\Omega}{(2\pi)^2};\quad \omega \;=\; E + E_b\,, \tag{11.35}$$

where v is the positron velocity, and E_b is the total energy of the bound electron annihilated in interaction with the positron. The upper index $+$ indicates that we have a single-charged ion A^+ in the final state. The recoil ion obtains large momentum $q \sim m$.

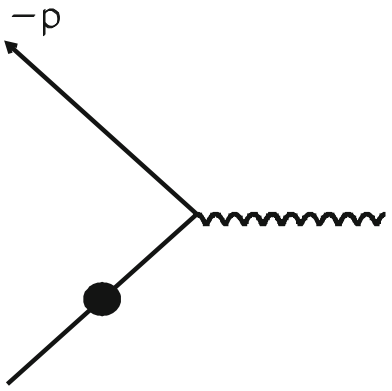

Fig. 11.2 Single-quantum annihilation in interaction of positrons with atomic electrons. The notations are the same as in Fig. 11.1

The theory of the process mirrors that for photoionization. Employing the results of Sect. 6.3, we estimate $\sigma^+_{ann} \sim r_e^2 \alpha^4 Z^5$. In the hydrogenlike approximation, the cross section of annihilation with the K-shell electrons of the atom with nuclear charge Z is

$$\sigma^+_{ann}(E) = \frac{4\pi r_e^2 \alpha^4 Z^5}{(\beta+1)^2\sqrt{\beta^2-1}}\left[\beta^2 + \frac{2}{3}\beta + \frac{4}{3} - \frac{\beta+2}{\sqrt{\beta^2-1}} \ln\left(\beta + \sqrt{\beta^2-1}\right)\right], \tag{11.36}$$

where $\beta = E/m$. This equality is true in the lowest order in $\xi = \alpha Z/v$ [1]. The cross section reaches its largest value at $E \approx 2m$. For annihilation of nonrelativistic positrons with $E - m \ll m$,

$$\sigma^+_{ann}(E) \;=\; \frac{4\pi r_e^2 \alpha^4 Z^5}{3}\frac{p}{m}\,, \tag{11.37}$$

while in the ultrarelativistic limit $E \gg m$,

$$\sigma^+_{ann}(E) \;=\; 4\pi r_e^2 \alpha^4 Z^5 \frac{m}{E}\,. \tag{11.38}$$

These expressions are true in the lowest order in powers of $\xi = \alpha Z/v$. Besides the hydrogenlike calculations, the cross section of annihilation with K and L electrons was obtained for a number of atoms by employing the screened Coulomb functions [6, 7]. Also, the Z-dependence of the angular distribution has been traced experimentally [8].

11.2.2 Annihilation Followed by Ionization

Single-quantum annihilation can be followed by the knockout of a bound electron to the continuum. In the process,

$$e^+ + A \;=\; A^{++} + e^- + \gamma, \tag{11.39}$$

the energy of the positron E, is shared between the electron with energy E_1 and the photon carrying the energy ω. Neglecting the binding energies, we can write

$$E + 2m \;=\; E_1 + \omega\,. \tag{11.40}$$

In this reaction, a three-dimensional momentum

$$\mathbf{q} \;=\; \mathbf{p}_1 + \mathbf{k} - \mathbf{p} \tag{11.41}$$

is transferred from the nucleus. One can see that this reaction is crossing-invariant with respect to the double photoionization considered in Chap. 9.

Here we focus on the case in which the positron annihilates with one of the $1s$ electrons, and the second $1s$ electron is knocked out to the continuum. Let us analyze the contributions of the main mechanisms to the cross section of the process σ_{ann}^{++}.

The annihilation removes one of the bound $1s$ electrons and thus changes the effective charge felt by the second one. This is the familiar shakeoff (SO) mechanism described in Chaps. 3 and 9. The SO determines the spectrum of the electrons at small values of their kinetic energies $\varepsilon_1 = E_1 - m \sim I_b$. Here the energy of the radiated photon is close to its largest value $\omega = E_1 + m - I_b$. It follows from (11.40) that $\varepsilon_1 + \omega \geq 2m$, and we can employ the asymptotic expression (9.37). Thus the contribution of the SO mechanism to the cross section σ_{ann}^{++} of the reaction expressed by (11.39) is

$$\sigma_{ann}^{SO}(E) = \sigma_{ann}^{+}(E) C_0; \quad C_0 = \frac{m}{2\pi^2 \Phi_{1s}^2} \int_0^\infty d\varepsilon_1 p_1 |\Phi(\varepsilon_1)|^2. \tag{11.42}$$

Recall that for helium, $C_0 \approx 0.016$, while the Z-dependence of C_0 is traced in Sect. 9.2.

Before annihilation with the atomic electron, the positron can knock out another electron from a bound state. Note that while single-quantum annihilation with a free electron is not possible, a similar process of interaction of the positron with a system of two free electrons in a spin-singlet state can take place [9]. In such a process, the recoil momentum is $q = 0$. To find the conditions for this quasifree mechanism (QFM), note that in free kinematics, $(\mathbf{p} - \mathbf{k})^2 = p_1^2$, and $E_1 = E_0 - \omega$, with $E_0 = E + 2m$ the largest energy available for the outgoing electron. Since $E_1^2 - p_1^2 = m^2$, we obtain

$$\omega = \frac{2m\omega_0}{E_0 - pt}; \quad t = \frac{\mathbf{p} \cdot \mathbf{k}}{pk}, \tag{11.43}$$

with $\omega_0 = E + m$ the largest energy available for the photon. Thus the limits for the photon energy are

$$\frac{2m\omega_0}{E_0 + p} \leq \omega \leq \frac{2m\omega_0}{E_0 - p}. \tag{11.44}$$

For nonrelativistic positrons with $p \ll m$, the energy of the photon and the kinetic energy of the outgoing electron are $\omega \approx 4m/3$ and $\varepsilon_1 \approx 2m/3$ respectively. They vary in small intervals of order p/m near these values. In the ultrarelativistic limit $E \gg m$, the energy carried by the photon is limited by the condition $m \leq \omega \leq E$.

The QFM amplitude is proportional to that of the process on the free electrons; see (9.145). The energy distribution of the radiated photons in the interval determined by (11.44) is

$$\frac{d\sigma_{ann}^{++}}{d\omega} = \sigma_1 Z^3 W(\omega) \frac{m}{p^2} \mathscr{I}; \quad \sigma_1 = \pi r_e^2 \alpha^4, \tag{11.45}$$

with $\mathscr{I}$ determined by (9.176);

$$W(\omega) = \left(\frac{\varepsilon_1 + \omega_0}{\varepsilon_1 \omega_0}\right)^2 \left[EE_1 - m^2 - \kappa^2 + (\frac{m\omega}{\omega_0 \varepsilon_1})^2 (EE_1 - 2\varepsilon_1 \omega_0 + m^2 + \kappa^2)\right]; \tag{11.46}$$

$$\kappa^2 = \frac{(E^2 - E_1^2)^2 - \omega^4}{4\omega^2}; \quad \omega_0 = \varepsilon_1 + \omega;$$

see (9.200). Introducing the dimensionless parameters $x = \omega/\omega_0$ and $\gamma = m/\omega_0$, we can write (11.45) and (11.46) as

$$\frac{d\sigma_{ann}^{++}}{dx} = \sigma_1 Z^3 W(x) \frac{m}{\varepsilon} \mathscr{I}, \tag{11.47}$$

with

$$W(x) = \gamma \left(\frac{2-x}{1-x}\right)^2 \left[2(x-\gamma) + \left[1 - \left(\frac{\gamma x}{1-x}\right)^2\right]\left[\frac{4(1-x)}{x} - \gamma \frac{(2-x)^2}{x^2}\right]\right]. \tag{11.48}$$

The QFM contribution to the cross section σ_{ann}^{++} is

$$\sigma_{ann}^{QFM}(E) = \sigma_1 Z^3 f(E); \quad f(E) = \mathscr{I} \frac{m}{\varepsilon} \cdot \int_{x_1}^{x_2} dx W(x), \tag{11.49}$$

with the limits of integration

$$x_1 = \frac{2m}{E_0 + p}; \quad x_2 = \frac{2m}{E_0 - p}, \tag{11.50}$$

corresponding to (11.44).

We write $\sigma_{ann}^{+}(E) = \sigma_1 Z^5 \varphi(E)$, with

$$\varphi(E) = \frac{4m^3}{p(E+m)^2}\left(\frac{E^2}{m^2} + \frac{2}{3}\frac{E}{m} + \frac{4}{3} - \frac{E+2m}{p} \ln \frac{E+p}{m}\right),$$

determined by (11.36). We write also $\sigma_{ann}^{QFM}(E) = \sigma_1 Z^3 f(E)$, with $f(E)$ defined by the second equality of (11.49). Similar to the case of double photoionization, the double-to-single ionization ratio can be written as

$$R(E) = \frac{\sigma_{ann}^{++}(E)}{\sigma_{ann}^{+}(E)} = \frac{\sigma_{ann}^{SO}(E) + \sigma_{ann}^{QFM}(E)}{\sigma_{ann}^{+}(E)} = C_0 + \frac{\sigma_{ann}^{QFM}(E)}{\sigma_{ann}^{+}(E)}. \tag{11.51}$$

Here we neglected the terms of order I_b/ε. Employing (11.35) and (11.48), we represent the ratio (11.51) as

$$R(E) = \frac{c+\beta(E)}{Z^2}; \quad \beta(E) = f(E)/\varphi(E). \tag{11.52}$$

Note that the functions $f(E)$ and $\beta(E)$ depend on the quantum number of ionized states through the factor $\mathscr{I}$.

Now we focus on elimination of two $1s$ electrons. We employ the perturbative model developed in Sect. 9.2.2. The amplitude is described by the Feynman diagrams presented in Fig. 11.3. Recall that in this case, the values of the parameters that enter

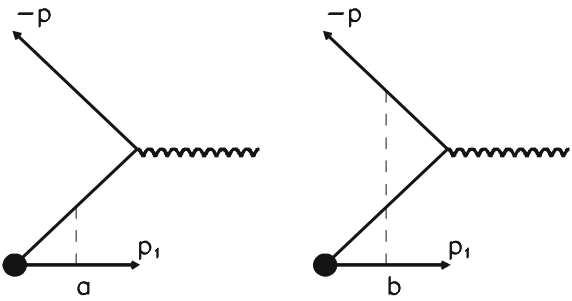

Fig. 11.3 Annihilation of positrons with atomic electrons accompanied by ionization. **a** Corresponds to the shakeoff (SO) mechanism. **b** Illustrates the quasifree mechanism (QFM). The notation is the same as in Fig. 11.1

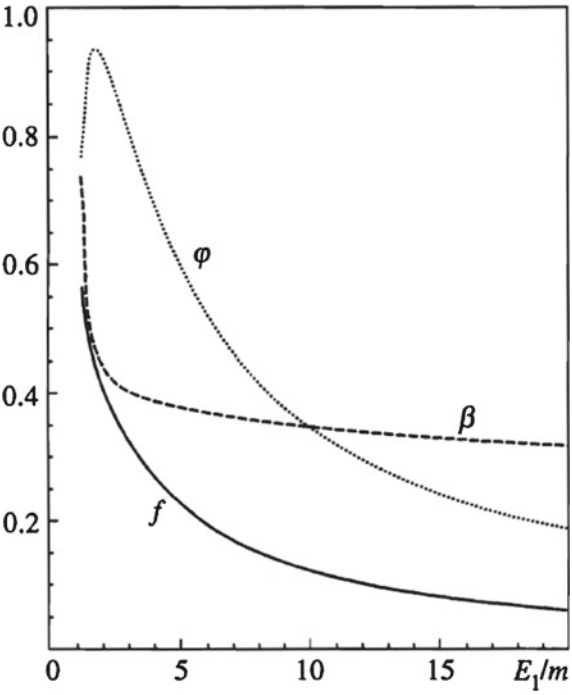

Fig. 11.4 Energy dependence of the cross sections. The horizontal axis is for the positron energy E related to the positron mass m. The *vertical line* is for the functions $f(E)$, $\varphi(E)$, and $\beta(E)$ defined in Sect. 11.1.2. Reproduced from [9]

(11.45), (11.49), and (11.52) are $\mathscr{I} = 1/8$ and $c = 0.09$ respectively. The functions $f(E)$, $\varphi(E)$, and $\beta(E)$ are shown in Fig. 11.4. For nonrelativistic positrons with $\varepsilon \ll m$ (but $\varepsilon = E - m \gg I_Z$), we obtain

$$\beta(E) \;=\; \frac{1}{9} \cdot \frac{m}{E-m}\,. \tag{11.53}$$

Thus at small values of Z and ε, the ratio R can become larger than unity. Hence double ionization can become more probable than a single one. In the ultrarelativistic limit, the two lowest terms of the expansion in powers of m/E provide

$$\beta(E) \;=\; \frac{1}{4}\left[1 + \frac{m}{4E}\left(11\ln\frac{E}{m} + 6\ln 2 - \frac{35}{2}\right)\right]. \tag{11.54}$$

The ultrarelativistic asymptotics for the ratio R corresponds to $\beta = 1/4$ and is:

$$R \;=\; \frac{0.34}{Z^2}. \tag{11.55}$$

Hence it is just the same as for the double-to-single photoionization ratio. However, in contrast to that case, $R(E)$ exceeds its asymptotic value for every value of the positron energy.

11.3 Annihilation Without Radiation

11.3.1 Annihilation with Ionization

The energy released in the annihilation of a positron with a bound electron can be absorbed by another bound electron. The latter moves to the continuum. Thus the final state of the process consists of the ion with two holes in the electron shell and the ejected electron in the continuum. In this process,

$$e^+ + A \;\to\; A^{++} + e^-,$$

illustrated by Fig. 11.5a, the ejected electron obtains the energy

$$E_1 \;=\; E + 2m \tag{11.56}$$

(here we neglected the values of the binding energies). The process cannot take place in a system of free electrons, since it requires a large momentum

$$\mathbf{q} \;=\; \mathbf{p} - \mathbf{p}_1 \tag{11.57}$$

to be transferred to the nucleus. Since $q \geq p_1 - p$, we find, employing (11.56), that $q^2 \geq 4m^2$.

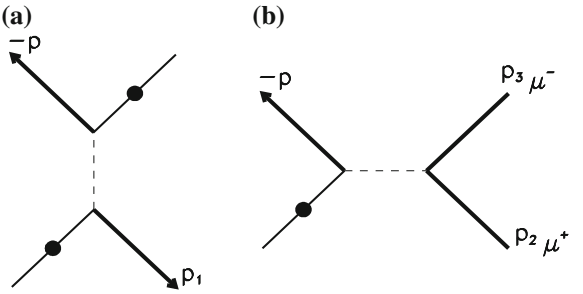

Fig. 11.5 Annihilation of positrons with atomic electrons without radiation. **a** Ionization; **b** Creation of $\mu^+\mu^-$ pairs. The muons are shown by *bold lines*. The other notation is the same as in Fig. 11.1

The amplitude of the process can be written as

$$F = 4\pi\alpha \int d^3r' \bar{\psi}_{-p}(\mathbf{r}')\gamma^\mu \psi_a(\mathbf{r}') \int d^3r D_{\mu\nu}(\boldsymbol{\rho})\bar{\psi}_{p_1}(\mathbf{r})\gamma^\nu \psi_b(\mathbf{r}) - (a \leftrightarrow b). \tag{11.58}$$

Here ψ_{-p} and ψ_{p_1} are the wave functions describing the positron and the ejected electron, $\psi_{a,b}$ are the wave functions of the bound electrons in the states a and b, and $\boldsymbol{\rho} = \mathbf{r} - \mathbf{r}'$. The photon propagator $D_{\mu\nu}$ in the Feynman gauge written in spatial representation is

$$D_{\mu\nu}(\boldsymbol{\rho}) = g_{\mu\nu} \int \frac{d^3f}{(2\pi)^3} \frac{\exp(i\mathbf{f}\boldsymbol{\rho})}{f^2 - \omega^2 - i0}; \quad \omega = E + m. \tag{11.59}$$

Hence, (11.58) can be written as

$$F = 4\pi\alpha \int \frac{d^3f}{(2\pi)^3} \frac{A^\mu(-\mathbf{f}, a)B_\mu(\mathbf{f}, b)}{f^2 - \omega^2 - i0} - (a \leftrightarrow b), \tag{11.60}$$

with

$$A^\mu(-\mathbf{f}, a) = \int d^3r' \bar{\psi}_{-p}(\mathbf{r}')\gamma^\mu \psi_a(\mathbf{r}') \exp(-i\mathbf{f}\mathbf{r}'),$$

$$B_\mu(\mathbf{f}, b) = \int d^3r \bar{\psi}_{p_1}(\mathbf{r})\gamma_\mu \psi_b(\mathbf{r}) \exp(i\mathbf{f}\mathbf{r}).$$

Note that $A^\mu(-\mathbf{f}, a)$ is the matrix element of the single-quantum annihilation of the positron with the bound electron in the state a. Also, $B_\mu(\mathbf{f}, b)$ is the matrix element for photoionization of state b.

As we have seen in Sect. 3.1.2, a large momentum $q \gg \mu_b$ can be transferred to the nucleus by a bound electron or by a positron in the initial state or by a continuum electron in the final state, and the corresponding contributions to the amplitude are of the same order of magnitude. Thus, although the ejected electron carries the kinetic energy $\varepsilon_1 \geq 2m$, its interaction with the recoil ion should be included. On the other

hand, for $\alpha Z \ll 1$, it can be treated perturbatively. The same refers to a description of the positron while its energy is large enough, $\varepsilon_1 \gg I_Z$.

We carry out calculations for the K electrons of the hydrogenlike atom. To obtain the amplitude in the lowest order of the expansion in powers of αZ, we describe all electrons and the positron by the FSM functions; see (6.24) and (6.29) [10]. Note that there were earlier calculations for this process in which the bound electrons were described by the Coulomb functions, while the positron and the ejected electron were described by plane waves. As we said before, such calculations do not include all the terms contributing in the leading order in αZ.

We obtain for the angular distribution

$$\frac{d\sigma}{d\Omega} = \frac{r_e^2(\alpha Z)^8}{4} \frac{N^2(\xi_1)N_+^2(\xi)p_1 m^4}{p\omega^4} T(\theta); \quad \xi = \frac{\alpha Z E}{p}; \quad \xi_1 = \frac{\alpha Z E_1}{p_1}. \tag{11.61}$$

Here N^2 and N_+^2 are the squared normalization factors of the ejected electron and of the positron determined by (3.19) and (11.25); θ is the angle between the directions of the positron and electron momenta $\mathbf{p}$ and $\mathbf{p_1}$. The angular factor

$$T(\theta) = \frac{16m^2}{q^2}\left(1 - \frac{4m^2}{q^2}\right) \tag{11.62}$$

is the same for all Z. It reaches its largest value $T_{\max} = 1$ at $q^2 = 8m^2$, i.e., at

$$\theta = \theta_0 = \arccos\left(1 - \frac{4m^2}{\omega^2}\right)^{1/2}. \tag{11.63}$$

For nonrelativistic positrons $\theta_0 \to \pi/2$. For ultrarelativistic positrons with $E \gg m$, we obtain $\theta_0 \to 0$, i.e., the ejected electron moves in the same direction as the positron. An example of the angular distribution is given in Fig. 11.6.

Integration of the angular distribution (11.61) provides

$$\sigma = 8\pi r_e^2(\alpha Z)^8 \frac{N^2(\xi_1)N_+^2(\xi)m^6}{p^2\omega^4}\left(\ln\frac{p_1 + p}{p_1 - p} - \frac{pp_1}{2\omega^2}\right). \tag{11.64}$$

The cross section obtains its largest values, which are of order $r_e^2(\alpha Z)^8$, at $\varepsilon \sim m$. In the ultrarelativistic region $E \gg m$, it decreases as $r_e^2(\alpha Z)^8 m^6/E^6$. For the nonrelativistic positrons with $\varepsilon, p \ll m$, we obtain, putting $E = m$, $E_1 = 3m$, and $p_1 = 2\sqrt{2}m$,

$$\sigma = \frac{2^{1/2}\pi r_e^2(\alpha Z)^8}{8} \frac{N^2(\xi_1)N_+^2(\xi)m}{p}. \tag{11.65}$$

Note that if the positron energy is so small that $2\pi\xi \gtrsim 1$, the factor $N_+^2(\xi) \sim 2\pi\xi e^{-2\pi\xi}$ provides exponential quenching of the cross section.

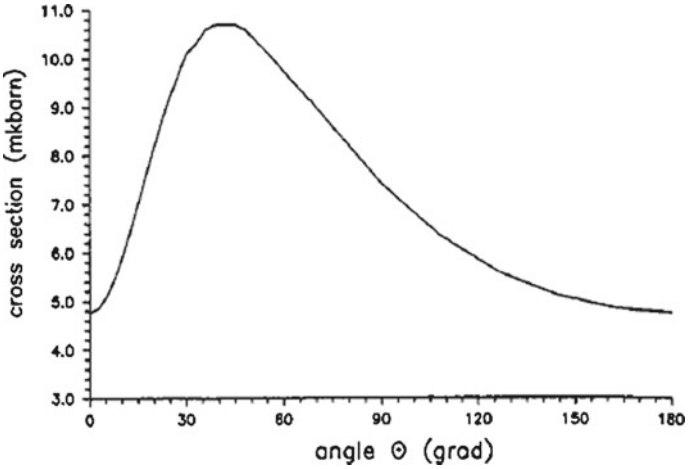

Fig. 11.6 Angular distribution for annihilation with ionization at $E = 2m$. The *horizontal line* is for the angle θ between the directions of the momenta of the incoming positron and the outgoing electron. The *vertical line* is for the differential cross section $d\sigma/d\Omega$ in $\mu b/sterrad$ units. Reproduced from [10]

To obtain more accurate expressions for the cross section, we represent the next-to-leading correction in powers of αZ [11]. We must include the $\alpha^2 Z^2$ terms in the expansion of the wave functions of the bound and continuum electron and that of the positron. Such a term for the $1s$ wave function is determined by (6.53). It is given by the third term on the RHS of (6.48) for the wave function of the ejected electron. Including also a similar correction for the wave function of the positron, we obtain for the angular distribution

$$\frac{d\sigma}{d\Omega} = 4r_e^2(\alpha Z)^8 N^2(\xi_1) N_+^2(\xi) \frac{p_1 m^6}{p\omega^4 q^2} T_1(\theta)\,, \tag{11.66}$$

with

$$T_1(\theta) = 1 - \frac{4m^2}{q^2} + \frac{\pi\eta}{p_1}\left(\frac{8mE_1}{q^2} - \frac{2p_1}{q} - 1\right). \tag{11.67}$$

The total cross section, which includes the lowest αZ correction, is

$$\sigma = 8\pi r_e^2(\alpha Z)^8 \frac{N^2(\xi_1) N_+^2(\xi) m^6}{p^2\omega^4}\left[\ln\frac{p_1+p}{p_1-p} - \frac{pp_1}{2\omega^2} - \frac{\pi\eta}{p_1}\left(\ln\frac{p_1+p}{p_1-p} - \frac{pp_1}{\omega^2}\right)\right]. \tag{11.68}$$

Recall that $m/E_1 < 1/3$.

For example, for $Z = 82$, we find that (11.64) provides $\sigma = 18\mu b$ for the cross section. Inclusion of the lowest-order correction (11.68) changes the value to $\sigma = 15\mu b$.

11.3.2 Annihilation with Creation of $\mu^+\mu^-$ Pairs

If the positron is fast enough, it can annihilate with the bound electron, creating a $\mu^+\mu^-$ pair; see Fig. 11.5b. The process $e^+e^- \to \mu^+\mu^-$ can take place for the free electrons. The threshold positron energy in the rest frame of the electron is

$$\mathscr{E}_0 \;=\; 2m_\mu^2/m \;\approx\; 44\,\mathrm{GeV}, \tag{11.69}$$

with $m_\mu \approx 105\,\mathrm{MeV}$ the muon mass. To obtain the value, we denote the four-momentum of the positron by $p = (E, \mathbf{p})$ and that of the electron at rest by $p' = (m, 0)$; the momenta of μ^+ and μ^- are $p_1 = (E_1, \mathbf{p}_1)$ and $p_2 = (E_2, \mathbf{p}_2)$. The value of the threshold energy can be obtained by squaring the momentum conservation equation $p + p' = p_1 + p_2$ and noting that $(p_1 p_2) \geq m_\mu^2$.

If the electron is in a bound state, the three-dimensional momentum $\mathbf{q} = \mathbf{p} - \mathbf{p}_1 - \mathbf{p}_2$ can be transferred to the nucleus in the process,

$$e^+ + A \;\to\; A^+ + \mu^+ + \mu^-.$$

The energy conservation law is $E + m - I_b = E_1 + E_2$, and the annihilation can take place for $E \geq \mathscr{E}$, where the threshold for creation of free μ^- and μ^+ is [12]

$$\mathscr{E} \;=\; 2m_\mu \;\approx\; 211\,\mathrm{MeV} \tag{11.70}$$

(here we neglected terms of order m/m_μ and I_b/m_μ).

The amplitude of the process can be written as

$$A = \alpha \int d^3r' \bar{\varphi}_{\mathbf{p}_2}(\mathbf{r}')\gamma_\mu \varphi_{-\mathbf{p}_1}(\mathbf{r}') \int d^3r \frac{e^{i\omega R}}{\omega R} \bar{\psi}_{-\mathbf{p}}(\mathbf{r})\gamma^\mu \psi_b(\mathbf{r}); \quad R = |\mathbf{r} - \mathbf{r}'|. \tag{11.71}$$

Here $\omega = E_1 + E_2$ is the total energy of the $\mu^+\mu^-$ pair; $\psi_{-\mathbf{p}}(\mathbf{r})$ and $\psi_b(\mathbf{r})$ are the wave functions of the positron and the bound electrons. The wave functions $\varphi_{-\mathbf{p}_1}$ and $\varphi_{\mathbf{p}_2}$ describe the positive and negative muons carrying momenta $\mathbf{p}_1$ and $\mathbf{p}_2$ respectively. We employ the Feynman gauge for the photon propagator.

The muon wave functions should be calculated in the atomic field with nucleus of finite size. At large $E \gg m_\mu$, the positron can be described by the FSM functions. Recall that the accuracy of the latter can be estimated as $\alpha^2 Z^2/\ell_{eff}$, with ℓ_{eff} the effective value of the orbital moment. Since a large momentum $q \sim m_\mu$ should be transferred to the nucleus, the process takes place at distances $r \sim 1/m_\mu$ from the center of the nucleus. Thus we can estimate $\ell_{eff} = pr \gg 1$.

We shall carry out the calculations in the lowest order of αZ. A large momentum $\mathbf{q} \sim m_\mu$ can be transferred to the nucleus by any of four charged particles. As we know, transfer of large momenta can be treated perturbatively, and we represent the amplitude A as the sum of four terms,

$$A = A_a + A_b + A_c + A_d,$$

corresponding to transfer of the momentum q by the bound electron, by the incoming positron, and by the final-state muons $\mu^{\pm}$ respectively.

We begin with the transfer of the large momentum by the bound electron. At $q \sim m_\mu$, we must take into account the finite size of the nucleus. For the wave function of an electron bound in an atom with a nucleus of finite size, we can write, analogously to (2.94),

$$\psi_b(\mathbf{q}) = -\frac{8\pi\eta}{q^4}\frac{\boldsymbol{\alpha}\mathbf{q}}{2m}\psi_b(r=0)F(q)u_0\,, \tag{11.72}$$

with the nonrelativistic function $\psi_b(r=0)$ on the RHS. In further calculations, we employ the notation $N_b = \psi_b(r=0)$. The charge form factor $F(q)$ is normalized by the condition $F(0)=1$. Describing the continuum particles by plane waves, we write in momentum representation

$$A_a = -(4\pi)^2\alpha^2 Z N_b F(q)\frac{\bar{u}(p_2)\gamma_\mu u(-p_1)\bar{u}(-p)\tilde{q}\gamma^\mu u_0}{q^4 s}, \tag{11.73}$$

with $s=(p_1+p_2)^2=(E_1+E_2)^2-(\mathbf{p}_1+\mathbf{p}_2)^2=(m+E)^2-(\mathbf{p}-\mathbf{q})^2=2mE+2\mathbf{pq}-q^2$ the denominator of the photon propagator. Note that $s \geq 4m_\mu^2$.

Transfer of the momentum q by the incoming positron is determined by the lowest-order correction to the plane wave:

$$A_b = 4\pi\alpha\frac{\bar{u}(p_2)\gamma_\mu u(-p_1)}{s}\int\frac{d^3f}{(2\pi)^3}\frac{\bar{u}(-p)\gamma_0(\hat{k}+m)\gamma^\mu u_0}{k^2-m^2}\cdot\frac{-4\pi\alpha Z F(\mathbf{q}+\mathbf{f})}{(\mathbf{q}+\mathbf{f})^2}\psi(\mathbf{f}); \tag{11.74}$$

$$k = (-E, \mathbf{q}-\mathbf{p}+\mathbf{f})\,.$$

Since the integral over f is saturated by $f \sim \eta \ll q$, we can neglect f everywhere except in the argument of the bound-state wave function. This leads to

$$A_b = (4\pi)^2\alpha^2 Z N_b F(q)\frac{\bar{u}(p_2)\gamma_\mu u(-p_1)\bar{u}(-p)(2E+\tilde{q})\gamma^\mu u_0}{q^2 a s}; \quad a = 2\mathbf{pq}-q^2. \tag{11.75}$$

In a similar way, one can find the contribution of the terms corresponding to the transfer of momentum q by the final-state muons:

$$A_c + A_d = \frac{(4\pi)^2\alpha^2 Z N_b F(q)}{s' q^2}\left[2\left(\frac{E_2}{a_2}-\frac{E_1}{a_1}\right)\bar{u}(p_2)\gamma^\mu u(-p_1) - \frac{\bar{u}(p_2)\gamma^\mu\tilde{q}u(-p_1)}{a_1} - \frac{\bar{u}(p_2)\tilde{q}\gamma^\mu u(-p_1)}{a_2}\right]\bar{u}(-p)\gamma_\mu u_0\,. \tag{11.76}$$

Here $s' = (p + p')^2$; $a_i = 2\mathbf{p}_i\mathbf{q} + q^2$. Since $\psi_b(r = 0) = 0$ for the bound states with $\ell \neq 0$, only the s states contribute to the amplitude.

Note that the denominator of the photon propagator $s' = (p + p')^2 \approx 2mE$ is much smaller than that in the amplitudes A_a and A_b, i.e., $s'/s \sim mE/m_\mu^2$. Considering the energies

$$E \ll \mathscr{E}_0, \tag{11.77}$$

we can put $A = A_c + A_d$ in the main part of the phase volume, since here, $|A_a + A_b| \ll |A_c + A_d|$. Thus the large momentum q is transferred to the nucleus mainly by the final-state muons. In the configuration with $\mathbf{p}_1 = \mathbf{p}_2$ directed along $\mathbf{p}$, the sum of the contributions is $A_c + A_d = 0$. Hence, in the vicinity of this point, all the terms on the RHS of (11.71) are important. Also, at $\mathbf{p}_1 \approx \mathbf{p}_2$, the relative velocity of the outgoing μ^+ and μ^- is small, and they undergo strong attraction; see a similar situation in pair creation by a photon in the field of the nucleus [13].

The differential cross section of the muon pair creation in annihilation with the electrons in the s state can be written as

$$d\sigma \;=\; 2\pi\alpha \frac{N_b^2}{m^2 E} d\sigma_{\gamma\mu^+\mu^-}\,, \tag{11.78}$$

with $\sigma_{\gamma\mu^+\mu^-}$ the cross section for muon pair creation by a photon with energy E and three-momentum $\mathbf{p}$. We consider energies $E \geq 2m_\mu \gg m$, and thus we can put $E^2 = p^2$. In the limit of a point nucleus $F(q) = 1$, the cross section $\sigma_{\gamma\mu^+\mu^-}$ can be evaluated analytically. However, this limit works only for very light atoms, for which the cross section is very small. We carry out analysis that takes into account the finite size of the nucleus.

The differential cross section (11.78) can be written as

$$d\sigma \;=\; \tau(Z) \frac{m_\mu^4}{q^4} \frac{p_1 p_2}{E^2 m_\mu} F^2(q) S(\mathbf{p}_1, \mathbf{p}_2) dE_1 dt_1 dt_2 d\varphi\,. \tag{11.79}$$

Here $t_i = \cos\theta_i$, θ_i are the angles between momenta $\mathbf{p}_i$ and $\mathbf{p}$, φ is the angle between the planes determined by the vectors $\mathbf{p}_1$, $\mathbf{p}$ and $\mathbf{p}_2$, $\mathbf{p}$,

$$S(\mathbf{p}_1, \mathbf{p}_2) = 4m_\mu^2 \Big(\frac{E_2}{a_2} - \frac{E_1}{a_1}\Big)^2 - m_\mu^2 q^2 \Big(\frac{1}{a_2} - \frac{1}{a_1}\Big)^2 + \frac{2}{a_1 a_2}\Big([\mathbf{p_1 q}]^2 + [\mathbf{p_2 q}]^2\Big)^2, \tag{11.80}$$

and

$$\tau(Z) \;=\; 4r_\mu^2 (\alpha Z)^2 \frac{N_b^2}{m^2 m_\mu}; \quad r_\mu \;=\; \frac{\alpha}{m_\mu}\,. \tag{11.81}$$

Note that for the K shell of the hydrogenlike atom with point nucleus, we have $N_b^2 = \eta^3/\pi$, and

$$\tau(Z) \;=\; \frac{4}{\pi} r_\mu^2 (\alpha Z)^5 \frac{m}{m_\mu} \;=\; 0.0114(\alpha Z)^5 \mu b \tag{11.82}$$

provides the scale for the cross section σ. Assuming a uniform distribution in the sphere of radius R for the electric charge of the nucleus, we obtain for the form factor

$$F(q) \;=\; \frac{3(\sin qR - qR\cos qr)}{q^3 R^3}; \quad R \;=\; 1.2 \cdot A^{1/3}\,\mathrm{Fm} \tag{11.83}$$

(recall that $1\mathrm{Fm} = 10^{-13}\,\mathrm{cm}$), with A the number of nucleons in the considered nucleus. Since the nonrelativistic wave functions with $\ell \neq 0$ become zero at the origin, only the s atomic electrons contribute to the process. The K electrons provide the leading contribution.

The final-state muon μ^- can be captured to the atomic bound state. In the process,

$$e^+ + A \;\to\; A^{(\mu)} + \mu^+;$$

$A^{(\mu)}$ denotes the mesoatom, i.e., the atom in which one of the electrons is replaced by the muon μ^-. The amplitude is represented by (11.71) with the wave function $\varphi_{\mathbf{p}_2}(\mathbf{r}')$ of the continuum muon μ^- replaced by its bound-state function in the field of the atom with the nucleus of finite size. The energy conservation law is now $E + m - I_b = E_1 + m_\mu - I_b^{(\mu)}$, with the last term the ionization potential of the mesoatom. The cross section is connected with the cross section $\sigma^b_{\gamma\mu^+\mu^-}$ of the process in which the photon with energy E and three-momentum $\mathbf{p}$ creates a $\mu^+\mu^-$ pair with the negative muon bound in the atom. In the lowest order of the αZ expansion,

$$\sigma = 2\alpha(\alpha Z)^3 \frac{m}{E} \sigma^b_{\gamma\mu^+\mu^-}. \tag{11.84}$$

To calculate the cross section $\sigma^b_{\gamma\mu^+\mu^-}$, one needs the wave function of the bound muon in the field of the finite-size nucleus. It can be found by numerical solution of the Dirac equation. Using the relativistic Coulomb functions for describing the bound electrons and the FSM positron wave functions enables us to trace the nuclear charge dependence of the cross section [14]. At characteristic energy $E = 10m_\mu \approx 1\,\mathrm{GeV}$, it is $\sigma = 10^{-5}\mu b$ for $Z = 60$, yielding $1.5 \cdot 10^{-5}\mu b$ for $Z = 92$.

At $E \gtrsim \mathscr{E}_0$, annihilation on the free electrons becomes possible. In annihilation on a bound electron, a small momentum $q \sim \eta$ is transferred to the nucleus. The total cross section for annihilation on a bound electron is equal to that on a free electron. The latter is [15]

$$\sigma_0 \;=\; \frac{2\pi}{3} r_e^2 \frac{m}{E}\left(1 + \frac{\mathscr{E}_0}{2E}\right)\left(1 - \frac{\mathscr{E}_0}{E}\right)^{1/2}. \tag{11.85}$$

Thus the cross section for annihilation with an atom containing N_e electrons is $\sigma_A = N_e\sigma_0$. In the vicinity of the threshold $E - \mathscr{E}_0 \sim m_\mu\alpha^2$, (11.85) is invalid, since the interaction of the outgoing muons should be taken into account. The RHS of (11.85) obtains a factor that is the wave function of the relative motion of the muons at the origin [13]. Thus at $E \to \mathscr{E}_0$, the cross section has a finite value.

Note that μ^- and μ^+ can form a bound state with binding energy $m_\mu\alpha^2/4 \approx 1.4\,\text{keV}$. The threshold of this channel is smaller than $\mathscr{E}_0$ by that value.

The cross sections σ_0 and σ_A reach their largest values at $E \approx 1.7\mathscr{E}_0$. Here $\sigma_0 \approx r_e^2 m^2/m_\mu^2 \approx 1\mu b$, and thus $\sigma \approx N_e[\mu b]$.

References

1. A.I. Akhiezer, V.B. Berestetskii, *Quantum Electrodynamics* (Pergamon, New York, 1982)
2. T. Nagatomo, Y. Nakayama, K. Morimoto, S. Shimizu, Phys. Rev. Lett. **32**, 1158 (1974)
3. V.G. Gorshkov, A.I. Mikhailov, S.G. Sherman, JETP **72**, 32 (1977)
4. C.M. Surko, G.F. Gribakin, S.J. Buckman, J. Phys. B **38**, R57 (2005)
5. G.F. Gribakin, J.A. Young, C.M. Surko, Rev. Mod. Phys. **28**, 2557 (2010)
6. K.W. Broda, W.R. Johnson, Phys. Rev. A **6**, 1693 (1972)
7. P.M. Bergstrom Jr., L. Kissel, R.H. Pratt, Phys. Rev. A **53**, 2865 (1996)
8. J.C. Palathingal, P. Asoka-Kumar, K.G. Lynn, X.Y. Wu, Phys. Rev. A **51**, 2122 (1995)
9. A.I. Mikhailov, I.A. Mikhailov, JETP **86**, 429 (1998)
10. A.I. Mikhailov, S.G. Porsev, J. Phys. B **25**, 1097 (1992)
11. A.I. Mikhailov, S.G. Porsev, JETP **78**, 441 (1994)
12. A.I. Mikhailov, V.I. Fomichev, Sov. Journ. Nucl. Phys. **38**, 1505 (1983)
13. V.B. Berestetskii, E.M. Lifshits, L.P. Pitaevskii, *Quantum Electrodynamics* (Pergamon, New York, 1982)
14. A.I. Mikhailov, V.I. Fomichev, Sov. Journ. Nucl. Phys. **52**, 126 (1990)
15. V.B. Berestetskii, I. Ya, Pomeranchuk. ZhETF **29**, 864 (1955)

Chapter 12
Nuclear Transitions and the Electron Shell

Abstract We consider the mutual influence of nuclear and electron transitions. We investigate the influence of the electron shell on the energy distribution of electrons ejected in nuclear β decay, employing the approach presented in Chap. 3. We demonstrate how the considered effects manifest themselves in experiments on detection of the neutrino mass. We show how the analysis of interactions between the beta electron and the bound electron in the decay of tritium helped to solve the "heavy neutrino" problem. We present the results for probabilities of creating vacancies in the atomic shell in β^- and β^+ nuclear decay. For the case of nuclear γ decay, we analyzed the calculations of probabilities of internal nuclear conversion. Using the perturbative model developed in Chap. 9, we calculated the probability for ejection of two electrons from the electron shell during the same nuclear γ transition. Employing the results obtained in Chap. 4, we clarify the mechanism and calculate the cross section for the nonresonant photoexcitation of nucleus. We also present analysis of some less-explored influences of the electron shell on the probability of α decay.

12.1 Role of Atomic Electrons in Nuclear Beta Decay

12.1.1 Amplitude of Nuclear Beta Decay

Due to the weak decay of one of the neutrons composing the nucleus,

$$n \;\rightarrow\; p + e^- + \bar{\nu}_e\,,$$

the latter can undergo the transition

$$(A, Z) \;\rightarrow\; (A, Z+1) + e^- + \bar{\nu}_e\,.$$

Here (A, Z) denotes a nucleus containing A nucleons and having charge $|e|Z$. The amplitude of the process can be represented asthe matrix element of the products of

E.G. Drukarev and A.I. Mikhailov, *High-Energy Atomic Physics*,
Springer Series on Atomic, Optical, and Plasma Physics 93,
DOI 10.1007/978-3-319-32736-5_12

the lepton and nucleon weak currents. Each of them is a composition of the vector and axial currents. The lepton current is

$$j_\mu(\mathbf{r}) \;=\; \bar\psi_e(\mathbf{r})\gamma_\mu\psi_\nu(\mathbf{r}) + \bar\psi_e(\mathbf{r})\gamma_\mu\gamma_5\psi_\nu(\mathbf{r}), \tag{12.1}$$

with the two terms on the RHS corresponding to the vector and axial currents. The matrix γ_5 is defined by (2.15). The amplitude of the beta decay can be written as [1]

$$A_\beta \;=\; G_W\langle f|\sum_k t_+^{(k)}(\gamma^{\mu(k)} + g_A\gamma^{\mu(k)}\gamma_5)j_\mu(\mathbf{r_k})|i\rangle\,. \tag{12.2}$$

Here G_W is a constant, $g_A \approx 1.24$; $|i\rangle$ and $\langle f|$ are the initial and final states of the nucleus, and k labels the neutrons. The operator t_+ adds one unit to the projection of isospin, i.e., it transforms the neutron to a proton, $t_+|n\rangle = |p\rangle$. We neglect the higher-order weak interactions and describe the antineutrino by a plane wave. Writing $\psi_e(\mathbf{r}_k) = F(\mathbf{r}_k)\exp(i\mathbf{p}\cdot\mathbf{r}_k)u_e$, with $F(\mathbf{r}_k)$ describing the interaction of the beta electron with the final-state proton, we write

$$j_\mu(\mathbf{r_k}) \;=\; \bar u_e\gamma_\mu(1+\gamma_5)F(\mathbf{r}_k)u_\nu e^{-i\mathbf{p}\cdot\mathbf{r}_k - i\mathbf{p}_\nu\cdot\mathbf{r}_k}\,, \tag{12.3}$$

with $u_{e,\nu}$ the Dirac bispinor of the free motion, $\mathbf{p}$ and $\mathbf{p}_\nu$ the three momenta of the beta electron and antineutrino.

Note that the sizes of the heaviest nuclei are of order $R \lesssim 8\,\mathrm{Fm} \approx (25\,\mathrm{MeV})^{-1}$, see (11.83), while the energy shared by the beta electron and the antineutrino does not exceed several MeV. Thus one can carry out an expansion of the exponential factors on the RHS of (12.3). If the initial and final states have the same parity and their spin difference is $J_i - J_f = 0, \pm 1$, we can neglect the variation of the lepton wave functions inside the nucleus, putting $\exp(-i\mathbf{p}\cdot\mathbf{r}_k) = \exp(-i\mathbf{p}_\nu\cdot\mathbf{r}_k) = 1$. Also, the characteristic kinetic energies of the nucleons composing the nucleus are of order 50 MeV (the rest energy of the nucleon is about 940 MeV), and thus the operators $\gamma^{\mu(k)}$ and $\gamma^{\mu(k)}\gamma_5$ on the RHS of (12.3) can be replaced by their nonrelativistic limits $1\cdot\delta_{\mu 0}$ and $\sigma_i\delta_{\mu i}$ respectively. For such transitions, which are called the "allowed transitions,"

$$A_\beta \;=\; G_W\Big(\langle f|\sum_k t_+^{(k)}|i\rangle j_0 + g_A\sum_k\langle f|\sum_k t_+^{(k)}\sigma_i^{(k)}|i\rangle j_i\Big), \tag{12.4}$$

where $j_\mu = \bar u_e\gamma_\mu(1+\gamma_5)u_\nu\cdot N_0$, with N_0 the electron function on the surface of the daughter nucleus. The first term on the RHS of (12.4) causes the transitions with $J_f = J_i$, and the leptons do not carry the angular momentum. These are the Fermi transitions. The second term leads to transitions with $|J_f - J_i| = 1$. These are the Gamow–Teller transitions. In both cases, the parity of the initial and final states of the nucleus does not change.

In beta decay for which the conditions of Fermi or Gamow–Teller transitions are not satisfied, a nonzero value of the matrix element (12.2) can be obtained

by including the higher-order terms of the expansion of the exponential factor $\exp(-i\mathbf{p}\cdot\mathbf{r}_k - i\mathbf{p}_\nu\cdot\mathbf{r}_k) = 1 + \sum_{n=1}(-i\mathbf{p}_\nu\cdot\mathbf{r}_k - i\mathbf{p}\cdot\mathbf{r}_k)^n/n!$ in (12.3) for the lepton current. The decay is called "L-forbidden" if L is the smallest value of n for which the matrix element (12.2) obtains a nonvanishing value.

12.1.2 Neutrino Mass Measurements

The influence of the electron shell on the spectrum of beta electrons manifests itself brightly in experiments on the measurement of the mass of the electron neutrino. Recall that in 1930 Pauli explained the continuous spectrum of beta electrons assuming that there is a neutral particle that is much lighter than the electron and interacts with the other particles very weakly. The existence of such a particle, which is called a "neutrino," was confirmed experimentally in 1956. Is the neutrino indeed massless, or does it have a small mass? There were numerous attempts to answer this question. The answer is important, e.g., for astrophysical applications.

There are three observed charged leptons, e^-, μ^-, and τ^-. According to the Standard Model of electroweak interactions, each of them has a massless neutral spin-1/2 partner. Thus there should be three types of neutrino, ν_e, ν_μ, and ν_τ. They are indeed observed, and they are much lighter than the corresponding leptons. However, it was found in experiments carried in 1998 [2], and confirmed in later ones (see, e.g., [3]), that $\nu_{e,\mu,\tau}$ are not pure states and can convert into one another. This is called neutrino oscillations. The results are inconsistent with a zero value of neutrino mass. Thus we can conclude that $M_e \neq 0$.

The direct electron neutrino mass search is based on an analysis of the β spectrum in the allowed nuclear decays. In allowed transitions, the nucleon and lepton variables are factorized. The spectrum of beta electrons can be written as

$$\frac{dW}{dE} = C_N f(E)\,, \tag{12.5}$$

with W the probability of the beta decay. The nucleon factor is $C_N = C|\langle f|\sum_k t_+^{(k)}|i\rangle|^2 + g_A^2|\langle f|\sum_k \sigma^{(k)} t_+^{(k)}|i\rangle|^2$; the value of the numerical coefficient C will not be important for us. The dependence on the lepton variables is contained in the function

$$f(E) = F(E, Z+1)pEp_\nu E_\nu\,, \tag{12.6}$$

with E and p the total energy and the modulus of the three-dimensional momentum of the beta electron, while E_ν and p_ν are those of the antineutrino. The function $F(E, Z+1)$, called the Fermi function, is the squared wave function of the beta electron on the surface of the daughter nucleus.

Now we assume that the antineutrino has a nonzero mass M. Due to the CPT invariance, the mass of the electron neutrino also is M. Now we must put

$p_\nu = ((E_0 - E)^2 - M^2)^{1/2}$ on the RHS of (12.6), with E_0 the endpoint of the beta spectrum. One finds that a nonzero value of M would lead to a radical change in the shape of the function $f(E)$ near the endpoint. For $M = 0$, we have $df/dE \to 0$ at $E \to E_0$. If $M \neq 0$, the endpoint shifts to $E_0' = E_0 - M$, and $df/dE \to \infty$ at $E \to E_0'$.

Another important characteristic is the Kurie plot, defined as

$$K(E) = \left(\frac{dW/dE}{C_N F(E, Z+1) pE} \right)^{1/2}, \tag{12.7}$$

taking the form $K(E) = E_0 - E$ if $M = 0$. A nonzero value of M provides deviations from the linear behavior. Considering the region near the endpoint E_0, we define

$$\Delta = E_0 - E. \tag{12.8}$$

In the lowest order of expansion in powers of Δ/E_0, we represent (12.6) in the form

$$f(E) = F(E_0, Z+1) E_0 (E_0^2 - m^2)^{1/2} t(\Delta, M^2); \quad t(\Delta, M^2) = \Delta(\Delta^2 - M^2)^{1/2}, \tag{12.9}$$

and focus on analysis of the functions $t(\Delta, M^2)$ and $K(\Delta, M^2) = \sqrt{t(\Delta, M^2)}$.

In fact, the decay of tritium,

$$^3\mathrm{H} \to ^3\mathrm{He}^+ + e^- + \bar{\nu}_e, \tag{12.10}$$

with the endpoint $\varepsilon = E_0 - m \approx 18.6\,\mathrm{keV}$, has been used in experiments to detect the neutrino mass since the late 1940s. It is the allowed decay with a suitable lifetime of $T_{1/2} = 12.3$ years. In experiments carried out in the 1970s (ITEP, Moscow) and 1980s (INS, Tokyo), researchers employed atoms of tritium implanted into complex organic molecules. In current experiments, molecular tritium is used. We shall carry out our analysis for the general case of allowed beta decay. Since the decaying nucleus can be a part of a complex system, we shall speak about the "parent system" and "daughter system."

The existence of the electron shell surrounding the nucleus modifies the expressions presented above. We begin with an expression for the function $t(\Delta)$. The electron shell is in the ground state $|\Psi_0\rangle$ with (nonrelativistic) energy $\varepsilon_0(Z)$ before decay. It can remain in the ground state $\langle\Phi_0|$, corresponding, however, to the nuclear charge $Z + 1$. Also, it can be in an excited state $\langle\Phi_n|$ $(n \geq 1)$ with energy $\varepsilon_n(Z+1)$ after decay. The probabilities of transitions of the electron shell f_n are normalized by the condition $\Sigma_{n=0} f_n = 1$. If the atomic shell of the daughter system remains in the ground state, it transfers the energy $\varepsilon_0(Z) - \varepsilon_0(Z+1) > 0$ to the beta electron.

If the atomic shell of the daughter system is excited to state $|\Phi_n\rangle$, the energy of the beta electron becomes $E - \varepsilon_{n0}$, with

$$\varepsilon_{n0} \;=\; \varepsilon_n(Z+1) - \varepsilon_0(Z)\,. \tag{12.11}$$

The corresponding endpoints of the beta spectra are $E_0^n = E_0 - \varepsilon_{n0}$.

Thus

$$t(\Delta, M^2) \;=\; \sum_{n=0} f_n \cdot (\Delta - \varepsilon_{n0})\Big((\Delta - \varepsilon_{n0})^2 - M^2)\Big)^{1/2}. \tag{12.12}$$

We define the moments of the distribution of the secondary electrons

$$\langle \varepsilon^k \rangle \;=\; \sum_n f_n \varepsilon_{n0}^k \tag{12.13}$$

and the dispersion

$$\sigma^2 \;=\; \langle \varepsilon^2 \rangle - \langle \varepsilon \rangle^2. \tag{12.14}$$

Assuming M to be very small compared to Δ, we can write

$$t(\Delta, M^2) \;=\; (\Delta - \langle \varepsilon \rangle)^2 - \frac{M^2 - 2\sigma^2}{2}\,. \tag{12.15}$$

For values of Δ much larger than the characteristic values of excitation ε_{0n}, the Kurie plot is

$$K(\Delta, M^2) \;=\; \Delta - \langle \varepsilon \rangle - \frac{M^2 - 2\sigma^2}{4\Delta}\,. \tag{12.16}$$

Thus the electron shell imitates the value of $M^2 = -2\sigma^2$.

The sums on the RHS of (12.13) are limited by the condition $\varepsilon_n(Z+1) - \varepsilon_0(Z) \leq \Delta$. For the excitation energies strongly exceeding the single-particle ground-state energy $\varepsilon \gg I = |\varepsilon_0(Z+1)|$, the probabilities f_ε decrease as $1/\varepsilon^4$ in the SO approximation. Thus the moments $\langle \varepsilon \rangle$ and $\langle \varepsilon^2 \rangle$ are saturated at $\varepsilon_{no} \sim I$. Hence, the parameters $\langle \varepsilon \rangle$ and σ^2 on the RHS of (12.15) and (12.16) do not depend on Δ if $\Delta \gg I$. Indeed, the largest value of Δ is several hundred eV.

For analysis of the experimental data, it is instructive to write (12.15) and (12.16) also in terms of other variables [4]. We introduce

$$\varepsilon_{n0}^*(Z+1) = \varepsilon_n(Z+1) - \varepsilon_0(Z+1) > 0, \tag{12.17}$$

which is the electron excitation energy of the daughter system measured with respect to its ground state. Now $\varepsilon_{n0} = \varepsilon_{n0}^*(Z+1) + \varepsilon_{00}$. The average excitation energy is defined as

$$\langle \varepsilon^* \rangle \;= \langle \varepsilon \rangle - \varepsilon_{00}. \tag{12.18}$$

The shifted endpoint of the beta spectrum is

$$E_0' \;=\; E_0 - \varepsilon_{00}\,. \tag{12.19}$$

Introducing $\Delta' = E_0' - E$, we represent (12.15) and (12.16) as

$$t(\Delta, M^2) \;=\; (\Delta' - \langle\varepsilon^*\rangle)^2 - \frac{M^2 - 2\sigma^2}{2} \tag{12.20}$$

and

$$K(\Delta, M^2) \;=\; \Delta' - \langle\varepsilon^*\rangle - \frac{M^2 - 2\sigma^2}{4\Delta'}\,. \tag{12.21}$$

In the shakeoff (SO) approximation (see Chap. 3), the probabilities of excitation are $f_n \;=\; |\langle\Phi_n|\Psi_0\rangle|^2$. They can be represented as the values of certain operators averaged over the initial state of the electron shell of the decaying system. Employing the closure condition for the states $\langle\Phi_n|$, we obtain

$$\langle\varepsilon\rangle \;=\; \sum_n \langle\Psi_0|\Phi_n\rangle\varepsilon_{n0}\langle\Phi_n|\Psi_0\rangle \;=\; \langle\Psi_0|\Delta H|\Psi_0\rangle, \tag{12.22}$$

where ΔH is the difference between the Hamiltonians of the parent and the daughter systems. Thus

$$\langle\varepsilon\rangle \;=\; -\langle\Psi_0|\sum_k \frac{\alpha}{r_k}|\Psi_0\rangle \;<\; 0\,. \tag{12.23}$$

The negative value of $\langle\varepsilon\rangle$ means that the beta electron gains some energy from the secondary electrons in the SO process. In a similar way, one obtains

$$\langle\varepsilon^2\rangle \;=\; \langle\Psi_0|(\sum_k \frac{\alpha}{r_k})^2|\Psi_0\rangle\,. \tag{12.24}$$

One can calculate the probabilities f_n beyond the SO by employing (3.94) and (4.62). While the SO mechanism makes it possible to excite only the states without a change of orbital momenta, the latter can change due to the FSI. The FSI contributions to the probabilities f_ε for excitation of the bound electrons to the continuum states with energies $\varepsilon \gg I$ decrease as $1/\varepsilon^2$ at $\varepsilon \gg I$; see Sect. 4.2. Thus the expectation value $\langle\varepsilon\rangle$ is determined by all energies $\varepsilon \ll \Delta$, including the region $I \ll \varepsilon \ll \Delta$. The expectation value $\langle\varepsilon^2\rangle$ is determined by the energies $\varepsilon \sim \Delta$. Hence, both $\langle\varepsilon\rangle$ and $\langle\varepsilon^2\rangle$ depend on Δ [5].

At the high-energy endpoint of the tritium decay beta spectrum, the squared Sommerfeld parameter is $\xi_{ee}^2 \approx 7\cdot 10^{-4} \ll 1$. This enables us to include the FSI only in the lowest nonvanishing order. Employing the results of Sect. 4.2.2, we obtain

$$\langle\varepsilon\rangle = \langle\varepsilon\rangle_{SO} + \xi_{ee}^2\frac{\langle r^{-2}\rangle}{2m}\ln\frac{\Delta}{B};\quad \langle r^{-2}\rangle = \langle\Psi_0|\sum_k r_k^{-2}|\Psi_0\rangle \tag{12.25}$$

for the Δ-dependence of the beta electron energy loss. The first term on the RHS is given by (12.23). Determination of the value $B \sim I$ requires a special calculation for the particular system.

For the dispersion, we obtain

$$\sigma^2 \;=\; \sigma_{SO}^2 + \xi_{ee}^2 \frac{\langle r^{-2}\rangle}{2m}\Delta + 0(I_b/\Delta). \tag{12.26}$$

Employing (12.15), we obtain for the Kurie plot, similar to (12.16),

$$K(\Delta, M^2) \;=\; \Delta - \langle\varepsilon\rangle - \frac{M^{*2}}{4\Delta}\,, \tag{12.27}$$

with $\langle\varepsilon\rangle$ determined by (12.25). The "observable" squared neutrino mass is

$$M^{*2} \;=\; M^2 - 2\sigma_{SO}^2 - 2\xi_{ee}^2 \frac{\langle\varepsilon\rangle_{SO}\langle r^{-2}\rangle}{m}\,. \tag{12.28}$$

The deviations from the linear behavior of the Kurie plot manifest themselves in a nonzero value of the second derivative:

$$\frac{d^2K(\Delta, M^2)}{d\Delta^2} \;=\; -\frac{M^2 - 2\sigma^2}{2\Delta^3} + \xi_{ee}^2 \frac{\langle r^{-2}\rangle}{2m\Delta^2}\,. \tag{12.29}$$

Note that the RHS does not contain the parameter B, which enters (12.25).

Here we calculate the characteristics mentioned above for the simplified case of an isolated atom of tritium. There is only one electron in the electron shell. It can be described by the nonrelativistic Coulomb functions with $Z = 1$ in the decaying atom and $Z = 2$ in the daughter atom. We obtain immediately $\varepsilon_{00} = -40.8\,\text{eV}$. Employing (12.23) and (12.24) for the case of a single electron, we find that in the SO approximation,

$$\langle\varepsilon\rangle = -\frac{\nu^2}{m} = -27.2\ \text{eV}; \quad \langle\varepsilon^*\rangle = \frac{\nu^2}{2m} = 13.6\,\text{eV}; \quad \sigma^2 = 4I_1^2 = 740\,\text{eV}^2. \tag{12.30}$$

Recall that $\nu = m\alpha$; $I_1 = \nu^2/2m = -\varepsilon_0(Z = 1) = 13.6\,\text{eV}$.

Now we calculate the occupancies of the final states, taking into account the FSI [6, 7]. Employing (3.94), we have

$$f_n \;=\; \frac{S_n}{S}; \quad S \;=\; \sum_n S_n\,, \tag{12.31}$$

with $S_n = A_n + \xi_{ee}^2 B_n$, where

$$A_n = \langle\varphi_n|\psi_0\rangle^2; \quad B_n = -A_n + D_n; \quad D_n = \langle\varphi_n|\ell|\psi_0\rangle^2 - \langle\psi_0|\varphi_n\rangle\langle\varphi_n|\ell^2|\psi_0\rangle; \tag{12.32}$$

Table 12.1 Occupancies of the final states of He^+ (in percent) at the endpoint of the β electron spectrum in the decay of tritium.

State	Shakeoff	Inclusion of FSI
$1s$	70.23	70.16
$2s$	25.00	25.03
$2p$	0.00	0.04

$$\ell \;=\; \ln\,(r(1-t)\lambda),$$

and $S = 1 - \xi_{ee}^2$. Hence, we can write

$$f_n = \alpha_n + \xi_{ee}^2\beta_n; \quad \alpha_n = A_n; \quad \beta_n = D_n; \quad \sum_n \alpha_n = 1; \quad \sum_n \beta_n = 0. \tag{12.33}$$

Direct calculation provides $\beta_{1s} = -0.98$, $\beta_{2s} = 0.37$, $\beta_{2p} = 0.56$. The modification of the occupancies of the final states due to the FSI near the endpoint of the beta spectrum is presented in Table 12.1. One can see that the FSI diminishes the occupancy of the ground state in favor of that of the L shell.

We turn now to calculation of the average energy loss of the beta electron:

$$\langle\varepsilon\rangle \;=\; \Sigma_n\varepsilon_{n0}S_n \;=\; \langle\varepsilon\rangle_1 + \langle\varepsilon\rangle_2\,. \tag{12.34}$$

Here $\langle\varepsilon\rangle_1$ is the SO contribution, while $\langle\varepsilon\rangle_2$ is that of the FSI and of the interference between the SO and FSI terms. We have seen already that $\langle\varepsilon\rangle_1 = \sum_n \varepsilon_{n0}A_n = -\langle\psi_0|\alpha/r|\psi_0\rangle = -m\alpha^2 = -2I_1$. Employing (12.32), we find that

$$\langle\varepsilon\rangle_2 \;=\; \xi_{ee}^2\left(2I_1 + \sum_n \varepsilon_{n0}D_n\right). \tag{12.35}$$

Now we evaluate

$$\sum_n \varepsilon_{n0}D_n = 2I_1\langle\psi_0|\ell^2|\psi_0\rangle + \alpha\langle\psi_0|\frac{\ell^2}{r}|\psi_0\rangle + \kappa; \quad \kappa = \sum_{\varepsilon_{n0}<\Delta} \varepsilon_n|\langle\varphi_n|\ln(r-r_z)|\psi_0\rangle|^2. \tag{12.36}$$

The first two terms on the RHS of the first equality are obtained by employing closure. They are saturated by the states with $\varepsilon_{n0} \sim I_b$, while κ is saturated by all $\varepsilon_{n0} < \Delta$, and $\kappa \sim \ln\Delta$ at $\Delta \gg I_b$.

The calculations can be simplified by noting that κ can be obtained by employing the plane waves $\varphi_n^{(0)}$ instead of the Coulomb functions φ_n. To prove the statement, note that both φ_n and $\varphi_n^{(0)}$ constitute complete sets of functions

$$\sum_n |\varphi_n\rangle\langle\varphi_n| \;=\; \sum_n |\varphi_n^{(0)}\rangle\langle\varphi_n^{(0)}| \;=\; 1.$$

Writing for the continuum states $|\varphi_n\rangle = |\varphi_n^{(0)}\rangle + |\chi_n\rangle$, we find that

$$\sum_{\varepsilon_{n0}<\Delta} \varepsilon_{n0}\Big[|\varphi_n\rangle\langle\varphi_n| - |\varphi_n^{(0)}\rangle\langle\varphi_n^{(0)}|\Big] \;=\; H_d \sum_{\varepsilon_{n0}>\Delta} \Big[|\varphi_{n0}^{(0)}\rangle\langle\chi_n| + |\chi_n\rangle\langle\varphi_{n0}^{(0)}| + |\chi_n\rangle\langle\chi_n|\Big],$$

with H_d the Hamiltonian of the daughter system. At large ε, the functions χ_n contain an additional factor of order ε^{-1} relative to $\varphi_n^{(0)}$. Hence using the functions $\varphi_n^{(0)}$ instead of φ_n for calculation of κ leads to small errors of order I_1/Δ. We obtain

$$\kappa \;=\; \int \frac{d^3f}{(2\pi)^3} \cdot \frac{f^2}{2m} |\langle\varphi_f^{(0)}| \ln (r - r_z)|\psi_0\rangle|^2. \tag{12.37}$$

Here f is the momentum carried by the electron ejected from the atom; the lower index f labels the continuum electron with momentum f. The upper limit of integration over f is $f_{\max} = \sqrt{2m\Delta} \gg \nu = m\alpha$. Calculating

$$\langle\varphi_f^{(0)}| \ln (r - r_z)|\psi_0\rangle \;=\; \frac{4\pi^{1/2}\nu^{3/2}}{f^2 + \nu^2}\left(\frac{\nu}{f_z^2 + \nu^2} - i\frac{1}{f_z + i\nu}\right), \tag{12.38}$$

with f_z the projection of $\mathbf{f}$ on the direction of the momentum of the beta electron we find

$$\langle\varepsilon\rangle_2 \;=\; 2\xi_{ee}^2 I_1\left(\ln\frac{\Delta}{I_1} + C\right), \tag{12.39}$$

with $C = 7/16 - 2\ln 2 - \pi^2/36 \approx -1.19$, or

$$\langle\varepsilon\rangle_2 \;=\; 2\xi_{ee}^2 I_1 \ln\frac{\Delta}{B}; \quad B \;\approx\; 45\,\text{eV}. \tag{12.40}$$

The current upper limit for the value of the neutrino mass was obtained by the Lobashev Troitsk group [8, 9]:

$$M \;<\; 2.05\,\text{eV}. \tag{12.41}$$

A similar result was obtained by the Mainz group [10]: $M < 2.3\,\text{eV}$. The Karlsruhe Tritium Neutrino Experiment (KATRIN), in which a number of groups collaborated, is planned to reach the sensitivity of $M \sim 0.2\,\text{eV}$.

12.1.3 A Tale of a Heavy Neutrino

Thirty years ago, Simpson [11] reported a surprising result. Tracing the shape of the electron spectrum of tritium beta decay and diminishing the value of the electron kinetic energy $\varepsilon = E - m$, he observed a broad maximum in the interval

$0.75\,\mathrm{keV} < \varepsilon < 1.5\,\mathrm{keV}$. The spectrum curve had a characteristic shape corresponding to the threshold for creation of a particle with mass $M = E_0 - 1.5\,\mathrm{keV} \approx 17\,\mathrm{keV}$. It was called a "heavy neutrino."

The existence of a "heavy neutrino" would require a revision of the Standard Model, which was believed to be the foundation of the theory of electroweak interactions. Astrophysics could not accommodate a stable new particle with a mass of more than a few tens of eV. It would fill the universe, giving it an unacceptably large mass. Thus in accepting the "heavy neutrino," we should assume that there is at least one more unknown scalar particle s that is still lighter, and the "heavy neutrino" decays to an electron neutrino and the scalar s.

The relative magnitude of the surplus observed in [11] was on the order of several units of 10^{-3}. The squared Sommerfeld parameter ξ_{ee}^2 of the interaction between the beta electron and the electron bound in tritium ξ_{ee}^2 ranges between 10^{-2} and $2\cdot 10^{-2}$ in the considered energy interval. Thus it is reasonable to check whether the corrections of order ξ_{ee}^2, often referred to as "screening corrections," are included properly.

Since in this part of the spectrum we have $\xi_{ee}^2 \ll 1$, the screening corrections can be treated perturbatively. The energy is small enough for applying the nonrelativistic equations. The lowest-order correction to the beta spectrum is determined by (3.102). Thus the beta spectrum of the decay of the tritium atom dW/dE and that of the bare tritium nucleus are related as

$$\frac{dW}{dE} = \frac{dW_0}{dE}\Big(1 - \xi_{ee}^2\langle\psi_0|\frac{r_0}{r}|\psi_0\rangle + 0(\xi_{ee}^2\xi^2, \xi_{ee}^4)\Big). \tag{12.42}$$

Here ψ_0 is the wave function of the tritium atom. Note that the interaction of the beta electron with the daughter nucleus is determined by the parameter $\xi = (I_{Z+1}/\varepsilon)^{1/2}$, with $Z = 1$ in our case. The small-distance interactions taking place at $r \lesssim (2m\varepsilon)^{-1/2}$ with $\varepsilon = E - m$ compose the Fermi function (see (12.6)). Interactions with the bound electron take place at much larger distances from the nucleus, $r \sim 1/m\alpha$, i.e., at distances on the order of the size of the atom. Thus the influence of the FSI on the Fermi function manifests itself in the neglected terms of order $\xi_{ee}^2\xi^2$ [12].

In [11], the screening corrections were included in another way. The bound electron was treated as the source of an electrostatic field. It was assumed that the main screening effect is modification of the Fermi function. The latter is formed at small distances of order $1/p$ from the nucleus, where the field of the bound electron is essentially constant. Therefore, interaction with the bound electron adds the value $\langle V\rangle = \langle\varphi_0|\alpha/r|\varphi_0\rangle$ to the potential energy of the beta electron (φ_0 is the ground state of the bound electron in the parent atom). The beta electron energy E is shifted to $E' = E + \langle V\rangle$, and

$$\frac{dW}{dE} = \frac{dW_0}{dE}\frac{p'E'F(E', Z+1)}{pEF(E, Z+1)}. \tag{12.43}$$

In the case of tritium decay, we can neglect effects connected with the finite size of the nucleus. Thus $F(E, Z+1)$ is just the squared nonrelativistic function of the beta electron at the origin:

$$F(E, Z+1) = \frac{2\pi\xi}{1-\exp(-2\pi\xi)}; \quad \xi = \frac{m\alpha \cdot 2}{p}. \tag{12.44}$$

The main effect comes from the shift of the energy in the Fermi function. In the lowest order of expansion in powers of $\langle V\rangle/\varepsilon$,

$$\frac{dW}{dE} = \frac{dW_0}{dE}\Big(1 - \frac{\langle V\rangle}{2\varepsilon}\cdot\frac{2\pi\xi}{\exp(2\pi\xi)-1}\Big). \tag{12.45}$$

Note that although $\xi^2 \lesssim 0.1$, the value of $\pi\xi$ is not small. It is 0.73 at $\varepsilon = 1\,\text{keV}$. Thus we do not carry out expansion in powers of $\pi\xi$. Note that (12.45) is in contrast with the consistent calculation that leads to (12.42). The corrections to the Fermi function should manifest themselves in next-to-leading orders of the perturbation theory. Also, (12.45) contains the value of $\langle V\rangle$ for the daughter atom. In our approach, the screening corrections actually contain the matrix element of the parent atom $\langle\psi|1/r|\psi\rangle$.

Using (12.42) instead of (12.45) for inclusion of the screening corrections, we must change the theoretical results for the Kurie plot by the value

$$\frac{\delta K}{K} = -\frac{1}{2}\Big(-\xi_{ee}^2\langle\psi_0|\frac{r_0}{r}|\psi_0\rangle + \frac{\langle V\rangle}{2\varepsilon}\frac{2\pi\xi}{\exp(2\pi\xi)-1}\Big). \tag{12.46}$$

In Fig. 12.1, we show the experimental and theoretical results after the correction given by (12.46) is included [13]. In the first step, we neglect the influence of the environment on the tritium atom, considering it an isolated one. Employing the nonrelativistic Coulomb functions, we find that the discrepancy at $1\,\text{keV} < \varepsilon < 1.5\,\text{keV}$ is removed.

Now we try to estimate the influence of the environment. In an experiment [11], an atom of tritium was implanted into a silicon crystal. It is known that the value of the squared wave function at the origin $|\psi(0)|^2$ of a muonium atom (the bound state of muon μ^+ and an electron) implanted in Si is quenched more than twice as much as for an isolated atom $|\psi_0(0)|^2$. Indeed, $|\psi(0)|^2 = 0.45|\psi_0(0)|^2$ [14]. The result can be extended to the case of tritium. Assume that $\psi(r)$ has a Coulomb shape with a certain effective value of the nuclear charge Z_{eff}. We know that in the Coulomb field, $|\psi(0)|^2 \sim Z_{eff}^3$, while $\langle\psi|1/r|\psi\rangle \sim Z_{eff}$. Thus for tritium implanted in Si, we have $\langle\psi|r_0/r|\psi\rangle \approx 0.77$. The results based on this estimation are given in Fig. 12.1. They remove the discrepancy between the experimental and theoretical results for $\varepsilon > 700\,\text{eV}$. The discrepancy that remains at $500\,\text{eV} < \varepsilon < 700\,\text{eV}$ is due to the background, which was not subtracted properly during the analysis of the experimental data [15].

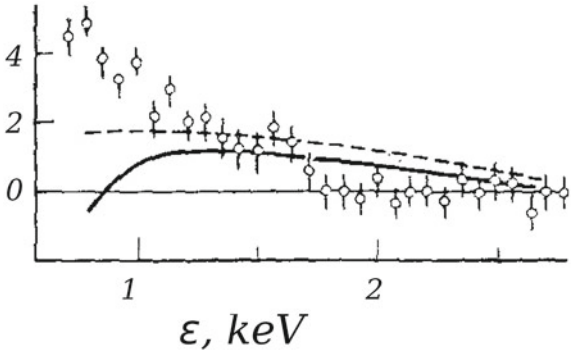

Fig. 12.1 Relative modification of the Kurie plot $\delta K/K$ caused by employing (12.42) multiplied by 10^3. The *horizontal axis* is for the beta electron kinetic energy in keV. The *dots* correspond to the experimental results obtained in [11]. The *solid line* is the theoretical result with the vacuum value of $\langle\psi|r_0/r|\psi\rangle$. The *dashed curve* is for the rough estimation of the influence of the environment on the value of $\langle\psi|r_0/r|\psi\rangle$ described in the text [13]

Thus the proper inclusion of the screening corrections in beta decay of tritium leaves no room for the "heavy neutrino."

In a further development of the story, the lower part of the beta spectrum in decays of heavier nuclei was investigated in the search for the "heavy neutrino." By 1991, three groups reported the observation of an anomaly similar to that in [11]. New experiments with an improved technique (magnetic spectrometer) were carried out. More than ten groups did not see the "heavy neutrino." This stimulated the discussion of the methods applied in the analysis of the experimental data. The details are given in [15]. Finally, all three groups that obtained a positive result removed their statements. By the end of 1993, the community agreed that there is no such thing as the "heavy neutrino."

As D. Morrison wrote, the whole story "raised questions about the Standard Model of particle physics and about cosmological theories, stimulated many theoretical papers and pushed experimental techniques to their limit" [16].

12.1.4 Creation of Vacancies in the Electron K Shell in β^- Decay

Until now, we have analyzed the influence of the electron shell on the spectrum of β electrons. Now we study the rearrangement of the electron shell caused by nuclear β decay. We focus on the case of the best-studied creation of vacancies in the electron K shell. The $1s$ electron can be moved to an excited state of the discrete spectrum or to a continuum state. If the β electron carries the kinetic energy $\varepsilon = E - m \sim I_b$, all interactions in the final state are important, and one should consider the wave

function of $Z+1$ electrons with at least one of them belonging to the continuum and at least one of the others belonging either to the continuum or to an excited state of the discrete spectrum.

For the fast β electrons, one can single out two mechanisms of the process. As we have seen in Chap. 3, the final-state interactions of the beta electron can be treated perturbatively. In the lowest order, we can neglect interactions of the β electrons with the bound ones. The K electron moves to an excited state due to the sudden change of the charge of the nucleus, and the amplitude of the process is $A_n = \mathscr{F} T_n$. Here $\mathscr{F}$ is the amplitude of the β decay of the bare nucleus, while the transitions of the atomic electrons are described by the matrix element $T_n = \langle \Phi_n | \Psi_0 \rangle$. Here Ψ_0 is the ground state of the system consisting of Z electrons in the field of the decaying nucleus with charge Z. The function Φ_n describes the state of these electrons with a hole in the $1s$ state in the field of the nucleus with the charge $Z+1$. The β electron spectrum of the decay during which the vacancy in the $1s$ state of the electron shell is created can be written for $\varepsilon \gg I_b$ as

$$\frac{dW}{d\varepsilon} \;=\; \frac{dW_0}{d\varepsilon} \sum_{n\neq 0} S_n; \quad S_n \;=\; |\langle \Phi_n | \Psi_0 \rangle|^2. \tag{12.47}$$

Here $dW_0/d\varepsilon$ is the spectrum of the beta decay of the bare nucleus. Note that the ground state ($n = 0$) is not included in the sum. To obtain the total probability W, we must integrate each term on the RHS over ε with the upper limit depending on n. However, as we have seen in Chap. 3, the sum over n is saturated by the states with energies $\varepsilon_n \sim I_b$. Thus we can neglect the n-dependence of the upper limit of integration, making the error $I_b/\varepsilon \ll 1$. One can see that $\sum_n S_n = 1$, due to the closure condition for the functions Φ_n, and

$$P \;\equiv\; \frac{W}{W_0} \;=\; 1 - S_0; \qquad S_0 \;=\; \langle \Phi_0 | \Psi_0 \rangle^2. \tag{12.48}$$

For the simplest case of the beta decay of an ion with one $1s$ electron, the states $|\Psi_0\rangle$ and $\langle \Phi_n|$ can be described by the functions ψ_0 and φ_n of the Coulomb field with the charges Z and $Z+1$ respectively. For not very large Z, these can be nonrelativistic functions. Hence, we can calculate the probabilities for transition of the bound electron to any final state. The probability to remain in the $1s$ state is

$$S_0 \;=\; \frac{64 Z^3 (Z+1)^3}{(2Z+1)^6}\,. \tag{12.49}$$

For the beta decay of the tritium atom, $S_0 = 0.70$, and thus the bound electron undergoes transitions with probability $P = 0.30$. The probability that the $1s$ electron moves to the continuum is $P_c = 0.04$, for the case of tritium making about 13% of all transitions. For large $Z \gg 1$, we obtain $S_0 = 1 - 0.75/Z^2 + O(1/Z^3)$, providing $P = 0.75/Z^2$. The role of excitation to continuum states increases, and we obtain $P_c \approx 0.32/Z^2$, which constitutes more than 40% of all transitions.

For two electrons in the $1s$ state, the probability for both of them to remain in the ground state is $P_0 = S_0^2$ in the hydrogenlike approximation. Applying closure for the many-electron atom, we must subtract the probabilities for excitations to the occupied states $P_{exc} > 0$. Thus $P = 1 - S_0^2 - P_{exc}$, and closure can provide the upper limit for the probability P. Say, for $Z \gg 1$, we obtain $P < 1.5/Z^2$ in the hydrogenlike approximation.

The first systematic SO calculations of the probability P based on the closure condition with subtraction of the contribution of the occupied states were carried out by Carlson et al. [17]. Computations carried out later employed more precise wave functions. Rather large deviations between the calculated results and the experimental data in a number of cases [18] stimulated researchers to calculate the contribution of the FSI [19] (the term "direct collisions" is often used in the literature on the subject).

Now we include the FSI corrections to the beta spectrum for $\varepsilon \gg I_b$. We employ the results obtained in Chap. 3. Representing S_n defined by (3.94) as $S_n = A_n + \xi_{ee}^2 B_n$, we obtain

$$\frac{dW}{dE} = \frac{dW_0}{dE}(X_1 + \xi_{ee}^2 X_2); \qquad \xi_{ee} = \frac{\alpha E}{p}, \tag{12.50}$$

with X_1 the SO contribution, while X_2 includes the FSI terms and their interference with the SO terms. Thus

$$X_1 = 1 - A_0 = 1 - |\langle \Phi_0 | \Psi_0 \rangle|^2, \tag{12.51}$$

while $X_2 = \sum_n B_n - B_0$. Employing (3.94) and (3.100), we obtain $X_2 = X_{2a} + X_{2b}$ with

$$X_{2a} = -|\mathrm{Im} T_0^{(0)}|^2 - 2\mathrm{Re} T_0^{(2)} T_0^{(0)}; \quad X_{2b} = 2 \sum_n \mathrm{Re} T_n^{(1)} T_n^{(0)} - 2\mathrm{Re} T_0^{(1)} T_0^{(0)}. \tag{12.52}$$

Neglecting the terms of order $1/Z$ in the FSI contributions, we can put $|\Phi_0\rangle = |\Psi_0\rangle$ in the term X_2. This provides

$$X_{2a} = \langle \Psi_0 | \sum_{k,k1} \ln((r^{(k)} - r_z^{(k)})\lambda) \ln((r^{(k1)} - r_z^{(k1)})\lambda) | \Psi_0 \rangle - | \sum_k \langle \Psi_0 | \ln((r^{(k)} - r_z^{(k)})\lambda)) | \Psi_0 \rangle |^2; \tag{12.53}$$

$$X_{2b} = 0.$$

Since the SO contributions are of order $1/Z^2$, the relative contribution of the FSI is of order I_Z/ε for nonrelativistic $\varepsilon \ll m$. It is of order $\alpha^2 Z^2$ for $\varepsilon \gtrsim m$. Taking into account that there are two electrons in the $1s$ state, we write, in terms of the single-particle functions,

$$X_2 = 2\langle \psi_0 | \ln^2((r - r_z)\lambda | \psi_0 \rangle - 2 |\langle \psi_0 | \ln((r - r_z)\lambda) | \psi_0 \rangle|^2. \tag{12.54}$$

To feel the size of the effect, one can calculate the RHS employing the nonrelativistic Coulomb functions. This provides

$$X_2 \;=\; 2(1+\psi'(3)) \;\approx\; 2.79. \tag{12.55}$$

Here $\psi(x) = d\ln\Gamma(x)/dx$, with $\Gamma(x)$ the Euler gamma function; $\psi'(3) = \pi^2/6 - 5/4$.

To obtain the contribution of the FSI to the probability of creation of a vacancy in the allowed beta transitions, we write, employing (12.5) and (12.6) and assuming the neutrino to be massless,

$$P \;=\; \frac{\int dEpEF(E)\sum_n{}'(E_{0n}-E)^2 S_n}{\int dEpEF(E)(E_0-E)^2} \;=\; P_{SO} + P_{FSI}\,, \tag{12.56}$$

with P_{FSI} consisting of the contribution of the FSI and its interference with the SO. The prime means that the ground state ($n = 0$) is not included in the sum. The sum over n in the numerator is saturated by the states with $\varepsilon_n \sim I_b$, and we can neglect the difference between the high-energy endpoints E_{0n} with an error of order I_b/ε_0.

The case of a very large value of the endpoint energy $\varepsilon_0 = E_0 - m \gg m$ is the simplest for analysis. The probability is determined by large $\varepsilon \gg m$ with accuracy m^3/E_0^3. For these energies of the beta electron, we can put $\xi_{ee}^2 = \alpha^2$, i.e., it does not depend on E. Thus

$$P_{FSI} \;=\; \alpha^2 X_2\,. \tag{12.57}$$

The FSI terms provide corrections of order $\alpha^2 Z^2$ to the contributions of the SO. Thus the calculation of the FSI terms should be carried out together with inclusion of relativistic corrections to the wave functions of the bound electrons at least in the lowest order.

The results for the endpoint energies $\varepsilon_0 \lesssim m$ can be obtained by numerical integration on the RHS of (12.56). The results appear to be several times the expected value $P_{FSI} \approx \xi_{ee}^2(E_0)$. To understand why this happens, consider the simplest form (12.44) for the Fermi function. If $\pi\xi(E_0) \ll 1$, i.e., $\varepsilon_0 \gg 10\cdot I_Z$, we can put $F(E, Z+1) = 1$. Of course, this is possible only for atoms with light nuclei. The integrals on the RHS of (12.56) are dominated by the part of the spectrum with $\pi\xi(E) \ll 1$. If also $\varepsilon_0 \ll m$, i.e., the beta electron can be treated in nonrelativistic approximation, then direct calculations provide

$$P_{FSI} \;=\; 7\xi^2(E_0)X_2 \;=\; 7\frac{I_{Z+1}}{\varepsilon_0}X_2\,. \tag{12.58}$$

For the transitions with smaller endpoint energies with $\pi\xi(E_0) \gtrsim 1$, we can put $F(E, Z+1) = 2\pi\xi(E)$ for the energies with $\pi\xi(E_0) \gtrsim 1$. The integral in the numerator of (12.56) behaves as $\int d\varepsilon/\varepsilon$ for $\pi\xi(E) \lesssim 1$. Thus there is a large contribution from $\varepsilon \sim I_{Z+1}$. At such energies, a perturbative treatment of the beta electron interactions with the electron shell is still possible. However, its interactions

with the daughter nucleus at distances of order the size of the atom determined by the parameter ξ become important. Thus our approach does not work for $\varepsilon \sim I_{Z+1}$. This can be illustrated by the nonrelativistic equation

$$P_{FSI} = 3\xi^2(E_0)\left(X_2 \ln \frac{\varepsilon_0}{I_{Z+1}} - \frac{3}{2}\right), \tag{12.59}$$

while the region $\varepsilon \sim I_{Z+1}$ adds values of order of unity to the expression in parentheses. Thus in this case, our approach gives only a rough estimate but not a quantitative result.

For the L-forbidden transitions,

$$P = \frac{\int dEpEF(E) \sum_n' (E_{0n} - E)^2 g_L(E) S_n}{\int dEpEF(E)(E_0 - E)^2 g_L(E)}, \tag{12.60}$$

with $g_L(E)$ called the shape-factor

$$g_0(E) = 1; \quad g_1(E) = (E_0 - E)^2 + E^2 - m^2. \tag{12.61}$$

One can see that for β decays with $E_0 \gg m$, (12.57) is true for the forbidden transitions as well. For the forbidden transitions, the relative contribution of slow electrons with $\varepsilon \sim I_Z$ is less important than in the allowed ones. In particular, for $L = 1$, we obtain for the decays for $\varepsilon_0 \ll m$ and $\pi\xi(E_0) \sim 1$.

$$P_{FSI} = 4\xi^2(E_0)\left(1 + \frac{3}{2}\frac{\varepsilon_0}{m} \ln \frac{\varepsilon_0}{I_{Z+1}}\right) \tag{12.62}$$

In the nonrelativistic limit with $\varepsilon_0 \ll m$,

$$P_{FSI} = 4\frac{I_{Z+1}}{\varepsilon_0}. \tag{12.63}$$

The results of calculations including the FSI carried out in [19] in the Hartree–Fock approximation are presented in Table 12.2. One can see that they remove or strongly diminish the discrepancy between the experimental data and the SO calculations.

12.1.5 Creation of Vacancies in the Electron K Shell in β^+ Decay

Due to the interplay of nuclear forces, a bound proton can appear to be heavier that a neutron in the same bound state. It can undergo beta decay

$$p \rightarrow n + e^+ + \nu_e\,,$$

Table 12.2 Experimental and theoretical data on creation of vacancies in electronic K shell for allowed and L-forbidden β^- decays

Nucleus	Z	I_K,keV	ε_0, keV	L	$P \times 10^4$ (exp)	$P \times 10^4$ (SO)	$P \times 10^4$ (SO+FSI)
^{35}S	16	2.5	145	0	28 ± 5	17.6	34
^{36}Cl	17	3.2	714	2	22 ± 4	18.8	23.5
^{45}Ca	18	4.5	261	0	24 ± 4	18.8	23.0
^{64}Cu	29	9.7	571	0	12 ± 0.8	10.8	11.3
^{89}Cu	38	17.0	1463	1	8.6 ± 0.7	4.1	6.6
^{90}Y	39	18.0	2273	1	7.4 ± 1.5	4.12	6.1
^{114}In	49	20.2	1989	0	5.4 ± 0.4	2.62	4.7
^{143}Pr	59	43.6	933	1	2.8 ± 0.2	1.46	1.8

For allowed transitions $L = 0$. The experimental data for ^{35}S is from [20]. The data for the other nuclei are from the review paper [18]. The SO results are from [21], except the case ^{64}Cu (there are no data for this decay in [21]) for which it is taken from [17]. The calculations including the FSI were carried out in [19] in the Hartree–Fock approximation

while the nucleus undergoes the transition

$$(A, Z) \;\rightarrow\; (A, Z-1) + e^+ + \nu_e\,.$$

The processes in the electron shell are described by the general expression (3.94). The FSI contribution to the probability is described by the same general equation (12.52) as in the case of β^- decay. However, the real parts of the first-order amplitudes are now

$$\mathrm{Re}T_n^{(1)} = -\frac{\xi_{ee}^2}{2}\frac{m}{E}\langle\Phi_n|\sum_k r_0\Big(\frac{\partial}{\partial r^{(k)}} - \frac{1}{r^{(k)}}\Big)|\Psi_0\rangle - \frac{\xi_{ee}^2}{2}\frac{m^2}{E^2}\langle\Phi_n|\sum_k \frac{r_0}{r^{(k)}}|\Psi_0\rangle\gamma_0, \tag{12.64}$$

with the sign of the first term opposite that for β^- decay. Neglecting the terms of order $1/Z$ in the FSI terms, we find that (12.53) and (12.54), which are true for β^- decay, are true for the β^+ decay as well.

The probabilities for creation of vacancies in the electron K shell during β^+ decay are given by (12.56) and (12.64). The simplest form for the Fermi function is just the squared nonrelativistic positron wave function at the origin in the Coulomb field of the point nucleus with the charge $Z - 1$:

$$F(E, Z-1) \;=\; \frac{2\pi\xi}{exp(2\pi\xi) - 1}; \quad \xi \;=\; \frac{\alpha(Z-1)E}{p}\,. \tag{12.65}$$

Note that the accuracy of our approach for β^+ decay is greater than that for β^- decay for similar values of E_0 and Z. For slow β particles with $\pi\xi(E) \gtrsim 1$, we

obtain $F \sim 2\pi\xi$ for β^- decay and $F \sim 2\pi\xi \exp(-2\pi\xi)$ for β^+ transitions. Thus the contribution of this part of the spectrum is quenched in the latter case.

The results of calculations including the FSI carried out in [19] in the Hartree–Fock approximation for several allowed β^+ decays are presented in Table 12.3. One can see that as in the case of β^- decay, they remove or strongly diminish the discrepancy between the experimental data and the SO calculations.

One more peculiarity of β^+ decay is the annihilation mechanism for creation of a vacancy in the electron shell. The positron emitted in β^+ decay can annihilate with a bound electron. This mechanism is indistinguishable from the electron capture $p + e^- \to n + \nu_e$, in which the proton captures a bound electron, converting to a neutron and a neutrino.

For large positron energies $\varepsilon \gg I_b$, all its interactions with the daughter nucleus take place at its surface and are described by the Fermi function. Interaction with the bound electron takes place at distances of order its classical orbit, transferring a small momentum to the nucleus. Following our general approach, we can write for the contribution of this mechanism to creation of a vacancy in the electron shell

$$\frac{dW}{dE} = \frac{dW_0}{dE} \frac{\langle r^{-2} \rangle}{4\pi} \sigma_{an}^{(0)}(E) . \tag{12.66}$$

Here r^{-2} is averaged over the electron state in which the vacancy is created; $\sigma_{an}^{(0)}(E)$ is the cross section for two-quanta annihilation of the free positron with energy E on the free electron. Note that this expression is true for every channel of annihilation. Two-quanta annihilation is possible if the positron and the bound electron compose the spin-singlet state. For energies $E \gg m$, the cross section of the two-quanta annihilation obtains an additional small factor m/E, and the contribution of the annihilation mechanism becomes negligible relative to the SO and FSI contributions.

Table 12.3 Experimental and theoretical data on creation of vacancies in electronic K shell for β^+ decays

Nucleus	Z	I_K,keV	ε_0, keV	$P \times 10^4$ (exp)	$P \times 10^4$ (SO)	$P \times 10^4$(SO+FSI)
^{58}Co	27	8.3	474	13.8 ± 2.4	6.7	10.0
^{64}Cu	29	9.7	657	13.3 ± 1.1	5.8	9.9
^{65}Zn	30	10.4	325	16.1 ± 3.0	10.8	13.6
^{68}Ga	31	11.1	1880	10.3 ± 1.1	9.7	11.5

The experimental data are from [18]. The SO results are from [22] for Co and Cu, and from [17] for Zn and Ga. The calculations including the FSI were carried out in [19] in the Hartree–Fock approximation

12.2 Interactions of Gamma Quanta with the Electron Shell

12.2.1 Amplitude for Electromagnetic Transition of the Nucleus

Electromagnetic transition of the nucleus between the states ψ_{in} and ψ_f, often called the γ transition, is described by the amplitude

$$F_{em} = -N(\omega)\mathbf{e}\cdot\mathbf{h}, \tag{12.67}$$

where

$$\mathbf{h}(\omega,\mathbf{k}) = \int d^3r\bar{\psi}_f(\mathbf{r})\boldsymbol{\gamma}e^{-i\mathbf{k}\cdot\mathbf{r}}\psi_i(\mathbf{r}); \quad \omega=\varepsilon_f-\varepsilon_i, \tag{12.68}$$

are the spatial components of the conserved four-current h_μ. The conservation of current requires its time component to be

$$h_0(\omega,\mathbf{k}) = \frac{\mathbf{k}\cdot\mathbf{h}(\omega,\mathbf{k})}{\omega}. \tag{12.69}$$

Note that we consider $\omega = k_0$ and $k = |\mathbf{k}|$ as separate variables and do not require that $\omega = k \equiv |\mathbf{k}|$.

The angular momentum of the radiated photon L is limited by the triangle inequality $|J_i - J_f| \le L \le J_i + J_f$, with J_i and J_f the spins of the nucleus in the initial and final states respectively. The angular momentum L is a composition of the photon orbital momentum L' and its spin $S = 1$. Thus $L-1 \le L' \le L+1$. Since the energies of the γ transitions do not exceed several MeV, i.e., the wavelength of the radiated photon is much larger than the size of the nucleus, we can assume that

$$kr \ll 1. \tag{12.70}$$

We carry out calculations in the lowest nonvanishing order in kr, at least in the first steps of our analysis. In this approximation, $L = |J_f - J_i|$.

Now we must consider separately the cases of different spatial parities of the photon states. In electric (EL) transitions, the parities of the initial and final states of the nucleus P_i and P_f satisfy the condition $P_i(-1)^L P_f = 1$. For EL transitions, one can easily calculate the time component h_0 of the current. The operator γ_0 on the RHS of (12.68) can be replaced by its nonrelativistic limit $\gamma_0 = 1$. Due to (12.70), the term with $n = L$ provides the leading contribution in the expansion $e^{-i\mathbf{k}\cdot\mathbf{r}} = \sum(-i\mathbf{k}\cdot\mathbf{r})^n/n!$. Thus we obtain

$$h_0(\omega,\mathbf{k}) = \frac{4\pi}{c_L}k^L Y_{LM}(\mathbf{k}/k)Q^{(E)}_{LM}; \quad Q^{(E)}_{LM} = \int d^3r\bar{\psi}_f(\mathbf{r})r^L Y_{LM}(\mathbf{r}/r)\psi_i(\mathbf{r}), \tag{12.71}$$

with $c_L = (2L+1)!!$. The spatial components of the current h can be obtained by replacing the operators γ_i on the RHS of (12.68) by their nonrelativistic limits $-i\nabla_i/m$. The photon carries the orbital momentum $L' = L-1$ and is described by the spherical vector $\mathbf{Y}_{L,L-1,M}$ with $\mathbf{Y}_{L,L-1,M}(\mathbf{n}) = \sum_\mu C^{LM}_{L-1m,1\mu} Y_{L-1m}(\mathbf{n})\boldsymbol{\chi}_\mu$, where $C^{LM}_{L-1m,1\mu}$ are the Clebsch–Gordan coefficients, while $\boldsymbol{\chi}$ is the photon spin function (see [23] for a more detailed description of the spherical vectors). The term with $n = L-1$ in the expansion of the exponent gives the main contribution. The components of the vector $\mathbf{h}$ are proportional to k^{L-1}. Due to (12.69), they are also proportional to ω. Finally, we obtain

$$\mathbf{h}(\omega,\mathbf{k}) = \frac{4\pi}{c_L}\sqrt{\frac{2L+1}{L}}\omega k^{L-1}\mathbf{Y}_{LL-1M}(\mathbf{k}/k)Q^{(E)}_{LM}. \tag{12.72}$$

In magnetic (ML) transitions, $P_i(-1)^L P_f = -1$. Now in the spatial components of the current, $L' = L$, while $h_0 = 0$. In this case,

$$\mathbf{h}(\omega,\mathbf{k}) = \frac{4\pi}{c_L}\sqrt{\frac{L+1}{L}}k^L\mathbf{Y}_{LLM}(\mathbf{k}/k)Q^{(M)}_{LM};\quad Q^{(M)}_{LM} = \int d^3 r r^L[\mathbf{r}\boldsymbol{\iota}(\mathbf{r})]\cdot\boldsymbol{\nabla}Y_{LM}(\mathbf{r}/r). \tag{12.73}$$

Here $\boldsymbol{\iota}(\mathbf{r}) = \psi_f(\mathbf{r})\boldsymbol{\gamma}\psi_i(\mathbf{r})$, and $\mathbf{Y}_{L,L,M}(\mathbf{n}) = \sum_\mu C^{LM}_{Lm,1\mu}Y_{L,m}(\mathbf{n})\boldsymbol{\chi}_\mu$. These formulas do not cover the case of transitions between the states with $J_i = J_f = 0$, when

$$h_0(\omega,\mathbf{k}) = k^2 Q_0;\quad \mathbf{h}(\omega,\mathbf{k}) = \mathbf{k}\omega Q_0;\quad Q_0 = -\frac{1}{6}\int d^3 r\bar{\psi}_f(\mathbf{r})r^2\psi_i(\mathbf{r}). \tag{12.74}$$

12.2.2 Internal Nuclear Conversion

The energy released in the electromagnetic transition of the nucleus can be totally absorbed by an atomic electron. The latter moves to the continuum. In other words, the energy of the electromagnetic transition of the nucleus converts into the energy of motion of the atomic electron. In terms of single-electron functions, the amplitude of the internal conversion in the nuclear transition with energy ω can be written as

$$F_{conv} = -eN_b\int\frac{d^3q}{(2\pi)^3}h_\mu(\omega,\mathbf{q})D^{\mu\nu}(\omega,\mathbf{q})j_\nu(\omega,-\mathbf{q}),\quad e = -\alpha^{1/2}. \tag{12.75}$$

Here ω is the energy of nuclear transition, N_b is the number of electrons in the bound state b, the nuclear current $h_\mu(q)$ is given by (12.71)–(12.74), while $D^{\mu\nu}(q)$ is the photon propagator. In the electron current

$$j_\nu(\omega, -\mathbf{q}) = \int d^3 r \bar{\psi}_{\mathbf{p}}(\mathbf{r}) \gamma_\nu \psi_b(\mathbf{r}) e^{i\mathbf{q}\cdot\mathbf{r}}, \tag{12.76}$$

$\psi_b(\mathbf{r})$ is the wave function of the bound electron; $\mathbf{p}$ is the asymptotic momentum of the conversion electron. The process is illustrated by Fig. 12.2.

The probability of conversion for electrons in the bound state b is thus

$$dW_b = 2\pi\delta(E_b + \omega - E) N_b |F_{conv}|^2 \frac{pEdEd\Omega}{(2\pi)^3}. \tag{12.77}$$

For *EL* and *ML* transitions, the probability (12.77) is usually compared with the probability of photon radiation in the same transition,

$$dW_{em} = 2\pi |F_{em}|^2 \frac{\omega^2 d\Omega}{(2\pi)^3}, \tag{12.78}$$

with F_{em} determined by (12.67). The ratio

$$\alpha_b(\omega) = \frac{W_b}{W_{em}} \tag{12.79}$$

is called the internal conversion coefficient (ICC) of the state b. The sum over all occupied states constitutes the total ICC $\alpha_T = \sum_b \alpha_b$. In the case of $0 \to 0$ transitions, a single-photon radiation is impossible, and one can discuss only the probability of conversion.

For $\omega \gtrsim m \approx 500\,\text{keV}$ the ICCs are very small, $\alpha_b \ll 1$. However, at $\omega \ll m$, the ICCs become much larger than unity. To understand how this happens, assume that the states b are not too strongly bound, i.e., $I_b = m - E_b \ll m$. Consider the

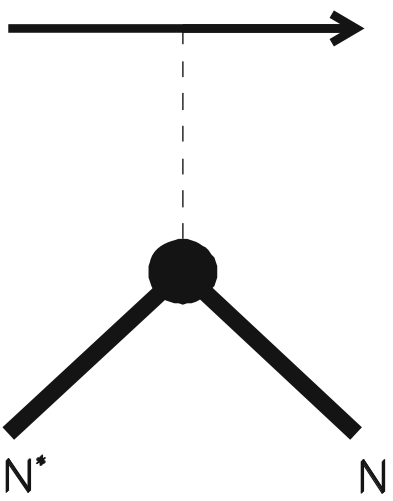

Fig. 12.2 Feynman diagram describing internal nuclear conversion. The *solid lines* stand for electrons. The *bold lines* denote the nucleus. The *dark blob* is for the nuclear transition. Excited and ground-state nuclei are labeled N^* and N. The virtual photon shown by the *dashed line* transfers the energy of the nuclear γ decay

transitions with $\omega \ll m$ but $\omega \gg I_b$. This enables us to describe the outgoing electrons by plane waves and to carry out calculations in the nonrelativistic limit. Employing the Feynman gauge for the photon propagator, one can see that the time components D^{00} provide the leading contribution. In the considered limit, $j_0(\omega, -\mathbf{q}) = \tilde{\psi}_b(\mathbf{p}-\mathbf{q})$, and

$$F_{conv} = e \int \frac{d^3 f}{(2\pi)^3} \frac{4\pi h(\omega, \mathbf{q})}{\omega^2 - q^2} \psi_b(\mathbf{f}); \quad \mathbf{q} = \mathbf{p} - \mathbf{f}; \quad q^2 = |\mathbf{q}|^2. \tag{12.80}$$

Since the bound-state wave function is strongly quenched outside the region $f \sim (2mI_b)^{1/2}$, we can assume that $f \ll p$, putting $\mathbf{q} = \mathbf{p}$ on the RHS of (12.80). Thus

$$F_{conv} = 4\pi e \frac{h_0(\omega, \mathbf{p})}{\omega^2 - p^2} \psi_b(r = 0); \quad p \equiv |\mathbf{p}| \approx (2m\omega)^{1/2}. \tag{12.81}$$

Thus in the internal conversion the virtual photon carries momentum $k \approx p \approx (2m\omega)^{1/2}$. In the radiation process the momentum of the real photon is $k = \omega \ll p$. This explains why the ICCs increase when ω becomes much smaller than m. Combining (12.81), (12.77), and (12.78), we obtain for the ICC in EL transitions at $I_b \ll \omega \ll m$.

$$\alpha_b(\omega) = 2\pi\alpha \frac{|\psi_b(0)|^2}{m^3} \frac{2^{L-1/2} L}{L+1} \left(\frac{m}{\omega}\right)^{L+3/2} \tag{12.82}$$

In the case of the ML transitions, $h_0 = 0$, and only the spatial components of the photon propagator contribute. Calculations similar to those carried out for the EL case provide

$$\alpha_b(\omega) = 2\pi\alpha \frac{\psi_b^2(0)}{m^3} 2^{L+1/2} \left(\frac{m}{\omega}\right)^{L+3/2}. \tag{12.83}$$

Thus for the energies $I_b \ll \omega \ll m$, the ICC for each shell is dominated by contributions of s states. For the states with $\ell \neq 0$, when $\psi_b(0) = 0$, the ICCs are quenched by the powers of I_b/ω. For $\omega \gtrsim m$, we estimate the ICC on the K shell as $\alpha_K \sim \alpha(\alpha Z)^3 \ll 1$ (in the limit $\omega \gg m$, the ICCs for the ML transitions obtain an additional small factor m/ω), with still smaller values for the other shells. However, the ICCs for $\omega \ll m$ are much larger, changing crucially the lifetimes of the excited states of the nuclei. The effect is more pronounced for large values of L. For example, a detailed paper by Raman et al. [24] gives $\alpha_K = 0.09$ for the $M4$ transition with $\omega = 1064\,\text{keV}$ in ^{207}Pb, but $\alpha_K = 2.6$ for the $E3$ transition with $\omega = 128\,\text{keV}$ in ^{134}Cs and $\alpha_K = 1620$ for the $M4$ transition with $\omega = 66\,\text{keV}$ in ^{119}Sn.

There are experimental data for more than 100 values of ICCs (α_K and the sums over all occupied states $\alpha_T = \sum_b \alpha_b$). About 20 of them had a relative accuracy of 2% or better. Also, a number of tables containing theoretical ICC values have been published. In the tables of Band et al. [25], the ICCs were calculated by employing the relativistic Dirac–Fock (DF) method, in which the exchange between the electrons was treated exactly. In tables published earlier, the calculations were based on the rel-

ativistic Hartree–Fock Slater (HFS) approach, in which the nonlocal exchange interaction was approximated by an effective local interaction (see Chap. 7). Employing the DF approach instead of the HFS appeared to be important for reaching consistency with the experimental data. For example, in the $M4$ transition with $\omega = 315\,\text{keV}$ in ^{117}In, the HFS calculation provides $\alpha_T = 1.47$, while the HF result $\alpha_T = 1.43$ is closer to the experimental value $\alpha_T = 1.41$ [24].

The accuracy of computations depends also on the treatment of the wave function of the outgoing electron. Usually, the latter was described as moving in the field of the neutral atom. The vacancy in the atomic shell created by the conversion process was ignored. It was demonstrated in [26] how inclusion of the vacancy improves the agreement between the measured and calculated ICCs. For example, the relative difference between the experimental and theoretical values of α_K in the $M4$ transition with $\omega = 66\,\text{keV}$ in ^{119}Sn makes 5 % without inclusion of the vacancy, dropping to 1% after the vacancy is included.

12.2.3 Two-Electron Processes in the Electron Shell

Two and more bound electrons can change their states during the γ transition of a nucleus. We focus on the case in which two electrons are moved to the continuum. We can single out two mechanisms of the process. In the nuclear mechanism, the nucleus undergoes a two-quantum transition in which each of the quanta knocks out a bound electron to the continuum. In the electron mechanism, the energy of a single-quantum transition is shared between the two knocked-out electrons due to their interactions.

Theoretical investigations of the nuclear mechanism did not provide numerical estimates. Some experiments on detecting the creation of two vacancies in the atomic K shell during γ transitions carried out about 40 years ago gave upper limits for the probability of the effect. They could be treated as upper limits for the nuclear mechanism. However, other experiments provided finite values for the probability of ejection of two electrons from the K shell W_{KK}. Was the result due to the nuclear or electron mechanism? To answer the question, we try to calculate the contribution of the electron mechanism to the creation of two vacancies in the K shell.

The analysis can be simplified for energies strongly exceeding the binding energy I_{1s} of the $1s$ state. At least one of the electrons obtains a large energy $\varepsilon_i \sim \omega \gg I_{1s}$. As in the cases of double photoionization and β decay, we can treat the interaction of the fast electron with the atomic shell (FSI) as a perturbation. The process can take place even if the FSI are neglected. After a γ quantum knocks one of the bound electrons to the continuum, the self-consistent field created by the bound electrons changes. Thus the field "felt" by the second $1s$ electron changes as well, and it can be moved to the continuum. One can see that in this picture, the mechanism that knocks out the second electron is the direct analogue of the shakeoff (SO) in beta decay. However, in the latter case, it was the charge of the nucleus that changed. Now we have the change of some "effective nuclear charge."

This approach was applied in [27, 28], where the $1s$ electrons were described by the screened Coulomb relativistic functions. The screening parameters were obtained from the self-consistent field calculations for the atom and for the ion with vacancies in $1s$ state created by internal conversion. However, as we have seen in Sect. 9.2.2, the correlations beyond the effective field are important for describing such a process.

An alternative approach is based on the perturbative model developed in Sect. 9.2.2 [29]. Quite similar to double photoionization, the energy ε is shared by the outgoing electrons unequally strongly. The electron that interacts with the γ quantum directly carries most of the energy $\varepsilon_1 \approx \omega$, while the secondary electron gets only a small part $\varepsilon_2 \sim I_K$. The model is illustrated by Fig. 12.3. The diagram of Fig. 12.3a describes correlations in the K shell in the initial state. That of Fig. 12.3b illustrates the final-state interactions (FSI) of the outgoing electrons. Neglecting the FSI, we obtain for the ratio of probabilities for knockout of two and one electrons from the K shell during γ decay

$$P_{KK} = \frac{W_{KK}}{W_K} = \frac{0.090}{Z^2}, \tag{12.84}$$

similar to (9.67). Recall that this result is based on calculations with nonrelativistic functions. Thus it contains uncertainties of order $\alpha^2 Z^2$. Also, the derivation of (12.84) employs the total Coulomb propagator, which includes the contribution of the occupied electron states. The latter can be subtracted after explicit calculation (note that only the s states contribute). The procedure diminishes the value of P_{KK}^{SO} by about 10%.

Now we include the final state or direct interactions between the conversion electron and the atomic shell. Since $\omega \gg I_K$, we can use the perturbative approach developed in Chap. 3. Note that the probability for the second electron to move to an excited state of the discrete spectrum is much smaller than the probability of being knocked out to the continuum. At large Z, the characteristic size of an unoccupied state is much larger than that of the $1s$ state. Thus the wave functions ψ_n of the

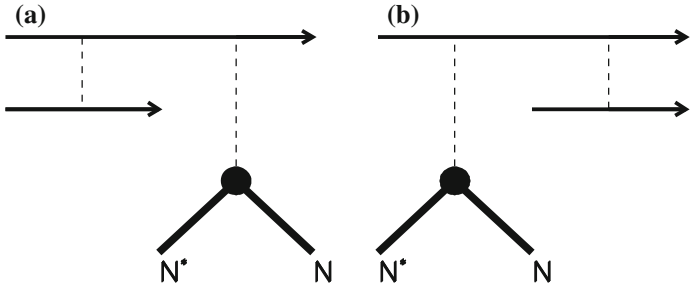

Fig. 12.3 Perturbative model for ejection of two electrons from the atomic shell during the γ transition of the nucleus. The *solid lines* denote the electrons in the Coulomb field of the nucleus. The *arrows* label the ejected electrons. The *dashed lines* denote the virtual photons exchanged between the nucleons and the electrons and between the electrons. Other notation is the same as in Fig. 12.2. **a** The electrons interact only in the initial state. **b** They interact only in the final state

excited states enter the amplitudes $T_n^{(i)}$ $(i = 0, 1, 2)$ on the RHS of (3.94) through their values at the origin. This provides an additional small factor $\psi_n^2(0)/\psi_{1s}^2(0)$ in the corresponding probability. Hence the probability of moving the secondary electron to the continuum can be replaced by the sum of the probabilities of the inelastic processes. This enables us to write $P_{KK} = P_{KK}^a + P_{KK}^b$, where the first term includes electron correlations only in the initial state described by the diagram shown in Fig. 12.3a, while the second term includes the FSI contribution (Fig. 12.3b) and its interference with that of correlations in the initial state. In the lowest order of electron interactions, we obtain

$$P_{KK}^b = \xi_{ee}^2 \Big(\langle \psi_0 | \ln^2((r - r_z))\lambda | \psi_0 \rangle - |\langle \psi_0 | \ln((r - r_z)\lambda) | \psi_0 \rangle|^2 \Big); \quad \xi_{ee}^2 = \frac{\alpha^2 E^2}{E^2 - m^2}, \tag{12.85}$$

with $E \approx m + \omega$ (see (12.54)). Employing (12.55), we arrive at [30]

$$P_{KK} = \frac{0.09}{Z^2} + 1.4\xi_{ee}^2 . \tag{12.86}$$

The experimental and theoretical results for P_{KK} are presented in Table 12.4. One can see that for the lightest nucleus of Fe, the initial-state correlations are as important as the FSI. For heavier nuclei, inclusion of the FSI contribution is decisive.

The process in which one electron is ejected from the K shell and another one from the L shell can be considered in a similar way. We can find the probabilities for simultaneous knockout of the electrons from the $1s$ and $2s$ states W_{1s2s} and from the $1s$ and $2p$ states W_{1s2p}. Similar to (12.84), we define the relative probabilities $P_{1s2s} = W_{1s2s}/W_K$ and $P_{1s2p} = W_{1s2p}/W_K$. They compose the total relative probability of the KL conversion $P_{KL} = P_{1s2s} + P_{1s2p}$. In the perturbative approach with only the initial-state correlations included, we obtain

$$P_{1s2s} = \frac{0.29}{Z^2}; \quad P_{1s2p} = \frac{3.1}{Z^2}; \quad P_{KL} = \frac{3.4}{Z^2}, \tag{12.87}$$

while the FSI contribution is much smaller. Inclusion of screening for the functions of the L-shell electrons [36] increases the value of P_{KL} by 25% for ^{57}Fe and by less than 10% for ^{137}Ba. One can see that the effective field model and the perturbative model provide rather close results in the case of KL conversion (Table 12.5).

12.2.4 Excitation of Nuclear Levels by Electronic Transitions

The excitation of nuclear levels by energy transferred from the excited atomic shell becomes possible if a transition in the atomic shell is close in energy and type to a nuclear transition. Nuclear excitation by electron transition has been observed in a

Table 12.4 Experimental and theoretical data on creation of two vacancies in electronic K shell in γ decays

Nucleus	Z	I_K	ω	$P_{KK} \times 10^5$ (exp)	$P_{KK} \times 10^5$(I)	$P_{KK} \times 10^5$(II)	$P_{KK} \times 10^5$(III)
^{57}Fe	26	6.5	122	12 ± 8 [31]	15	13	25
^{109}Ag	47	25.5	88	25 ± 3 [32]	0.92	4.2	34
^{114}In	49	27.9	192	10.2 ± 0.6 [33]	2.06	3.9	15
^{131}Xe	54	34.5	164	11 ± 2 [34]	1.1	3.2	15
^{137}Ba	56	37.4	662	7.7 ± 4 [35]	3.8	3.0	12

The ionization potential of the $1s$ state I_K and the energy of the nuclear transition are given in keV. The theoretical data obtained in the effective field model [28] are labeled by I. The results obtained in the perturbative model [29] corresponding to (12.84) are labeled by II. The perturbative model results (12.86) which include the FSI [30] are marked as III

Table 12.5 Experimental and theoretical data on creation of vacancies in electronic K and L shells in γ decays of the nuclei

Nucleus	Z	I_K	ω	$P_{KL} \times 10^3$ (exp)	$P_{KL} \times 10^3$(I)	$P_{KL} \times 10^3$(II)
^{57}Fe	26	6.5	136	9.0 ± 4.5 [31]	3.0	5.0 (6.2)
^{97}Tc	43	22.1	96	2.0 ± 0.3 [37]	1.4	1.9
^{137}Ba	56	37.4	662	1.0 ± 0.5 [31]	1.0	1.1 (1.2)
^{137}Ce	58	40.5	255	1.2 ± 0.4 [38]		1.0
^{150}Sm	62	48.5	334	0.38 ± 0.16 [39]	0.86	0.88

The ionization potential of the $1s$ state I_K and the energy of the nuclear transition are given in keV. The label I is for the effective field model results [27]. The results obtained in the perturbative model corresponding to (12.87) are labeled by II. The numbers in brackets are for the results with the screened Coulomb functions for L-shell electrons

number of nuclei (see, e.g., [40]). If the ion has a vacancy in the state a, the amplitude F of nuclear excitation by electron transition (NEET) from occupied electron state b to the vacancy a is given by (12.75) with the function $\bar{\psi}_{\mathbf{p}}(\mathbf{r})$ replaced by $\bar{\psi}_a(\mathbf{r})$ in the current $j_\nu(\omega, -\mathbf{q})$ determined by (12.76). Further evaluation enables us to obtain an expression for the NEET probability [41]:

$$\frac{dW}{d\omega_A} = \frac{|F|^2(\Gamma_a + \Gamma_b)}{(\omega_A - \omega_R)^2 + \Gamma^2/4}\,. \tag{12.88}$$

Here $\omega_A = \varepsilon_b - \varepsilon_a$ is the energy released in the atomic transition, ω_R is the nuclear excitation energy, and $\Gamma = \Gamma_a + \Gamma_b + \Gamma_N$ is the sum of the width of the electron states $\Gamma_a + \Gamma_b$ and that of the nuclear state Γ_N involved in the process.

One of the reasons why the NEET is interesting is that it probes the wave functions of the outer electrons at small distances, of order the size of the inner shells. For $ns_{1/2}$ and $np_{1/2}$ states (beyond the nonrelativistic approximation in the latter case), the wave functions are not quenched in this region and are sensitive to the finite size of the nucleus.

In the inverse NEET (INEET) process, the low-energy nuclear transition can be accompanied by a bound electron transition to an excited state of the discrete spectrum. This can be viewed as a special case of internal conversion.

The electron shell can assist in nonresonant photoexcitation of the nucleus. In this process, excitation of the nuclear state with energy ω_R can be caused by interaction of the atom with a photon carrying the larger energy $\omega > \omega_R$ [42]. To understand how this happens, recall the mechanism of the inverse process in which the electromagnetic transition of the nucleus with energy ω_R is accompanied by knockout of the bound electron and by irradiation of the photon (the internal Compton effect).

It was demonstrated in [43] that the cross section of the internal Compton effect is dominated by the two-step mechanism. In the first step, the nucleus radiates a real photon, which undergoes Compton scattering on the bound electron in the next step. For sufficiently large values of ω_R, we shall obtain a similar picture for nonresonant photoexcitation. In the first step, the photon with energy ω undergoes Compton scattering on a bound electron. In the second step, the scattered photon with energy ω_R excites the nucleus. The probability of the process can be expressed by a simple analytical formula [44].

In nonresonant photoexcitation, the incoming photon carries the three-momentum $\mathbf{k}$ with $k = |\mathbf{k}| = \omega$. The outgoing electron carries momentum $\mathbf{p}$, while the large momentum $\mathbf{q} = \mathbf{k} - \mathbf{p}$ ($q \gg \mu_b$) is transferred to the nucleus. We can single out the act of excitation in which the nucleus absorbs the energy ω_R and the momentum that differs from the large momentum q by small values of order μ_b. In other words, a small momentum $\mathbf{f}$ with $f \sim \mu_b$ is exchanged between the electron and the nucleus with no energy transferred, while in the act of excitation, the electron transfers momentum $\mathbf{q} + \mathbf{f}$ and energy ω_R to the nucleus; see Fig. 12.4. The amplitude of the process can be written in terms of the amplitude F_C for the Compton scattering on the bound electron, in which the radiated photon obtains the energy ω_R. Note that F_C contains the normalization factor $N(\omega_R) = \sqrt{4\pi\alpha/(2\omega_R)}$ of the wave function of the radiated photon. Hence one can write $F_C(\omega, \omega_R; \mathbf{f}) = e^\mu X_\mu(\omega, \omega_R; \mathbf{f})N(\omega_R)$. Here e_μ are the components of the polarization four-vector of the radiated photon. The amplitude of the nuclear nonresonant photoexcitation is thus

$$F_{NR} = \int \frac{d^3f}{(2\pi)^3} X_\mu(\mathbf{f}) D^{\mu\nu}(\omega_R, \mathbf{q}+\mathbf{f}) h_\nu(\omega_R, \mathbf{q}+\mathbf{f}); \quad \mathbf{q} = \mathbf{k} - \mathbf{p}. \tag{12.89}$$

At $\omega, \omega_R \gtrsim m$, the cross section of the process is dominated by large $q \gg \mu_b$. The integral on the RHS of (12.89) is dominated by small $f \sim \mu_b \ll \omega_R$. As we know from Chap. 2, a small momentum $\mathbf{f}$ is transferred to the nucleus mainly by the bound electron. Thus we can neglect $\mathbf{f}$ in the amplitude X_μ and in the hadron current h_ν. Employing the Feynman gauge for the propagator $D^{\mu\nu}$, we obtain

$$F_{NR} = X_\mu(0) h^\mu(\omega_R, \mathbf{q}) \Lambda_\gamma(\omega_R, \mathbf{q}); \quad \Lambda_\gamma(\omega_R, \mathbf{q}) = \int \frac{d^3f}{(2\pi)^3} \tilde{\psi}_b(\mathbf{f}) \frac{4\pi}{\omega_R^2 - (\mathbf{q}+\mathbf{f})^2}. \tag{12.90}$$

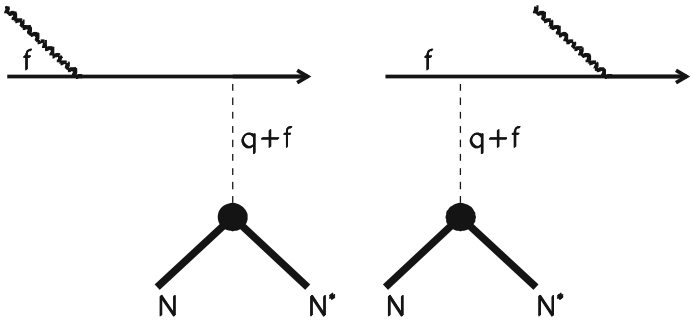

Fig. 12.4 Nonresonant excitation of the nucleus. The *helix line* denotes the incoming photon carrying energy $\omega > \omega_R$. The other notation is the same as in Fig. 12.2

Note that $X_\mu(0)$ corresponds to the Compton scattering on the free electron.

One can see that Λ_γ differs from the function Λ defined by (4.3) only by a constant factor, i.e., $\Lambda_\gamma = 2\pi/m \cdot \Lambda$. Thus we can use the results obtained in Chap. 4. For example, describing the bound $1s$ electron by the nonrelativistic function of the Coulomb field, we obtain, employing (4.14)

$$\Lambda_\gamma \;=\; \frac{-4\pi N_{1s}}{q^2 - (\omega_R + i\eta)^2}; \quad \eta \;=\; m\alpha Z.$$

The probability of nonresonant excitation is determined by the values of q close to ω_R.

Thus we came to the two-step picture of the process. In the first step, Compton scattering on the bound electron takes place with the photon carrying momentum q and energy ω_R in the final state. Only a small momentum $f \sim \mu_b$ is transferred to the nucleus. The process takes place at distances $r \sim 1/\mu_b$, i.e., those of order the size of the bound state. Being approximately on the mass shell ($\omega_R \approx q$), the photon passes distances of order the size of the atom, approaching the nucleus at distances of order $q^{-1} \ll 1/\mu_b$. Here the excitation of the nucleus takes place as the second step. Both Compton scattering and the excitation take place at small time intervals $t \sim \omega^{-1}, \omega_R^{-1}$. The two steps are separated by a time interval $t_1 \sim \mu_b^{-1}$ and $t_1 \gg t$ if $\omega_R \gg \mu_b$.

The mechanism requires that the Compton scattering with the energies of incoming and scattered photons ω and ω_R be possible. The condition (8.12) can be written as

$$\omega\left(1 - \frac{2\omega_R}{m}\right) \;\leq\; \omega_R\,.$$

Thus for $\omega_R > m/2 \approx 250\,\text{keV}$, the described mechanism works at every $\omega > \omega_R$. For $\omega_R < m/2$, we obtain the limitations

$$\omega_R < \omega < \frac{\omega_R}{1 - 2\omega_R/m}\,.$$

Employing (4.50) and (4.53), we obtain for the cross section of the nonresonant photoexcitation

$$\sigma_{NR}(\omega) = \frac{\langle\psi_b|\sum_k (r^{(k)})^{-2}|\psi_b\rangle}{4\pi}\frac{\sigma(\omega_R)}{N^2(\omega_R)}\frac{d\sigma_C(\omega,\omega_2)}{d\omega_2}|_{\omega_2=\omega_R}\,, \tag{12.91}$$

with $\sigma(\omega_R)$ the cross section of the direct photoexcitation, σ_C the cross section of the Compton scattering on the free electron with ω_2 the energy of the scattered photon.

For energies $\omega_R \ll m$, the cross sections for EL excitations at $L > 1$ and for ML excitations are dominated by $q \gg \omega_R$ since the amplitudes are proportional to q^{L-1} and q^L respectively. The cross sections of nonresonant excitations can be estimated as $\sigma_{NR} \sim \alpha^2(m\omega/\omega_R^2)^{L-\lambda}\sigma(\omega_R)$ with $\lambda = 1$ for the EL transitions, while $\lambda = 0$ for the ML transitions.

Nuclear Raman scattering is the alternative mechanism of the process. Here the energy $\omega - \omega_R$ is carried by the outgoing photon. There were numerous attempts to detect the relative process of irradiation of two γ quanta in a single electromagnetic transition. Two-photon emission has been observed for three $0^+ \to 0^+$ transitions when radiation of one photon is impossible (see [45] for references). A number of experiments provided the upper limit $\tau \leq 10^{-6}$ for the double-to-single γ radiation ratio $\tau = W_{\gamma\gamma}/W_\gamma$ instead of the simple QED counting $W_{\gamma\gamma}/W_\gamma \sim \alpha$. Thus there is some additional suppression of nuclear matrix elements that contribute to the two-quantum transitions. There is also additional suppression for the dipole transitions caused by the selection rules for angular momentum.

12.3 Electron Shell in Alpha Decays

12.3.1 Transitions in Internal Shells

Due to the interplay of the nuclear forces, some of the nuclei can undergo α decay. The nucleus containing A nucleons, Z of which are protons, decays as

$$(A, Z) \to (A-4, Z-2) + \alpha,$$

with the α particle being a bound system consisting of two protons and two neutrons (the nucleus of a helium atom). The nuclei (A, Z) and $(A-2, Z-2)$ will be referred to as the parent nucleus and the daughter nucleus respectively. Their masses are m_p and m_d, while m_α is the mass of the α particle. The energy released in the alpha decay of the bare nucleus,

$$Q = m_p - m_d - m_\alpha\,, \tag{12.92}$$

is shared in the asymptotics between the kinetic energies of the alpha particle and the daughter nucleus,

$$Q = \varepsilon_\alpha + \varepsilon_d \,. \tag{12.93}$$

The asymptotic kinetic energies of the alpha particles ε_α vary between 2 and 8 MeV. Thus for estimates, we can assume that the asymptotic velocity of the α particle is $v_\alpha \approx 0.05$.

In the alpha decay of the atom, the daughter atom cannot tie all Z electrons of the parent atom. Since the characteristic energy of the outer electrons is $I_1 = m\alpha^2/2 \approx 13.6\,\text{eV}$, it is energetically profitable that two of them are captured by the alpha particle, forming an atom of helium. Another possibility is the capture of one electron with formation of the ion He^+.

The inelastic transitions of the electron shell proceed at distances of order the size of the bound state. Here the energy of interaction between the alpha particle and the daughter nucleus can be neglected relative to the kinetic energy of the alpha particle. Thus the latter can be considered as traveling with the constant velocity v_α.

Since the velocity of the outer electrons is of order $\alpha \ll v_\alpha$, their knockout to the continuum by the α particle can be calculated by employing the perturbative approach developed in Chap. 3.

The characteristic velocities of the internal shell electrons v are much larger than the velocity of the alpha particle v_α. For the K-shell electrons, we can estimate $v \approx \alpha Z$. Thus we can use the perturbative expansion in powers of v_α^2/v^2. Following [46, 47], we employ the time-dependent perturbation theory. Denote the time by t and assume that the α decay takes place at $t = 0$. At $t < 0$, a bound electron moves in the field of the parent nucleus and that created by the other electrons $U_1(t) = U_p\theta(-t)$. At $t \geq 0$, it moves in the field $U_2(t) = U_{d\alpha}(t)\theta(t)$ of the system consisting of the daughter nucleus and the alpha particle instead of the field of the parent nucleus U_p. We treat the difference $U_2(t) - U_p$ as a perturbation acting at $t > 0$. This can be expressed by introducing $U(t) = U_1(t) + U_2(t)$, which represents the potential energy at every t. The perturbation can be expressed as $\hat{U}(t) = U(t) - U_p$, since $\hat{U}(t) = U_2(t) - U_p$ at $t > 0$ and $\hat{U}(t) = 0$ at $t < 0$.

The amplitude for transition of the bound electron from the state $|b\rangle$ to a state $\langle n|$ can be written as

$$F = \langle n|V|b\rangle F_\alpha; \quad V = -i\int_0^\infty dt e^{i\omega t}\hat{U}(t); \quad \omega = \varepsilon_n - \varepsilon_b \,, \tag{12.94}$$

with F_α the amplitude of the alpha decay. Neglecting the change of the field of the electron cloud and assuming that the alpha particle moves along the z-axis, we can write

$$\hat{U}(t) = U_{d\alpha}(t) = -\frac{e^2 Z_\alpha}{r_\alpha(t)} - \frac{e^2 Z_d}{r_d(t)}. \tag{12.95}$$

In this section, we write the fine structure constant as $e^2 = 1/137$. Recall that $Z_\alpha = 2$ and $Z_d = Z - 2$ are the charges of the alpha particle and the daughter

nucleus. The distances between the bound electron and the alpha particle and between the bound electron and the daughter nucleus are $r_\alpha(t)$ and $r_d(t)$ respectively. Due to conservation of momentum, the daughter nucleus also moves along the z-axis. Hence, the distances are

$$r_\alpha(t) \;=\; \sqrt{\rho^2 + (z + v_\alpha t)^2}; \quad r_d(t) \;=\; \sqrt{\rho^2 + (z + v_d t)^2}\,, \tag{12.96}$$

where $\rho^2 = x^2 + y^2$ does not depend on time; v_d is the velocity of the daughter nucleus. Due to the low kinetic energy of the alpha particles, they can be treated in nonrelativistic approximation. The same refers to the daughter nuclei. The conservation of momentum provides $m_d v_d = -m_\alpha v_\alpha$. Neglecting the very small neutron–proton mass difference (it is to about 1.3 MeV in vacuum), we can write

$$v_d \;=\; -\frac{4}{A-4} v_\alpha\,. \tag{12.97}$$

Integration by parts on the RHS of the second equality of (12.94) provides in the lowest order

$$\langle n|V|b\rangle \;=\; -i\frac{2e^2 v_\alpha \kappa}{\omega^2}\langle n|\frac{z}{r^3}|b\rangle; \quad \kappa \;=\; \frac{A-2Z}{A-4}\,. \tag{12.98}$$

One can write $\langle n|z/r^3|b\rangle = \nabla_z V_C/(e^2 Z)$, where $V_C = -e^2 Z/r$ is the electron potential energy in the Coulomb field of the parent nucleus. Employing (7.71), (7.72), and (7.68), we obtain

$$\langle n|V|b\rangle \;=\; -i\frac{2e^2 v_\alpha \kappa m}{Z}\langle n|z|b\rangle\,. \tag{12.99}$$

Thus the electron transition is determined by the matrix element of the dipole momentum.

The relative probability of ionization of the bound state b is thus

$$P_b \;=\; \frac{W_b}{W_0} \;=\; \frac{8e^4 v_\alpha^2 \kappa^2 m^2}{Z^2}\sum_n |z_{nb}|^2, \tag{12.100}$$

with the sum over all the vacant states, W_0 the probability of α decay of the bare nucleus. Here we included two electrons bound in the state b. The sum is saturated by the states with energies of order the ionization potential I_b. The probabilities for transitions of the bound s states to the continuum states with $\varepsilon_n \gg I_b$ fall off as $\varepsilon_n^{-9/2}$.

The matrix element $\langle n|z|b\rangle$ on the RHS of (12.99) is of order v_b^{-1}, with v_b the characteristic velocity in the bound state. Thus the amplitude is proportional to the ratio v_α/v_b. Further integration by parts in the second equality on the RHS of (12.94) provides the higher-order terms of the expansion in powers of this parameter. On the other hand, for $A \gg 1$, one has $|\kappa| \ll 1$, since the numbers of neutrons and protons do not differ much in heavy nuclei. Hence the dipole terms have an additional small factor, and for $v_\alpha/v_b \gtrsim \kappa$, the next term of the expansion needs to be calculated.

The numerical calculations have been carried out in [47] for the alpha decay of the nucleus ^{210}Po. For the K electrons, $v_\alpha/v_K \approx 0.087$, while $\kappa = 0.20$, and the dipole contribution is expected to dominate. The computation with employing the Coulomb functions provided $P_K = 1.0 \times 10^{-7}$, with the quadrupole terms contributing about 4% of the value. For the L electrons, $v_\alpha/v_L \approx \kappa$, and due to interplay of numerical coefficients, the probability $P_L \approx 10^{-4}$ obtained using the Coulomb functions is dominated by the quadrupole term. However, the accuracy of the Coulomb calculation is obscure.

12.3.2 *Influence of the Electron Shell on the Probability of Alpha Decay*

The possibility of inelastic processes in the electron shell discussed above opens new channels of the reaction. This leads to a small increase in the probability of the process. However, the influence of the elastic scattering on the electron shell appears to be more important. To understand this, recall the main features of alpha decay.

Consider first the decay of the bare nucleus (or the totally ionized atom), tracing the dependence of interaction between the alpha particle and the daughter nucleus on the distance R between them. The products of the decay can be viewed as separate particles at R exceeding the sum of their sizes determined by the second equality of (11.83), i.e., at $R \geq R_1 = 1.2\left((A-4)^{1/3} + 4^{1/3}\right) \sim 10\,\text{Fm}$. At smaller values of R, the nucleons of the system are bound by a strong short-range field $V_N(R)$. Thus the total field V_t is the sum of the field V_N and the Coulomb field

$$V_C(R) = \frac{e^2 Z_\alpha Z_d}{R}, \tag{12.101}$$

i.e., $V_t(R) = V_N(R) + V_C(R)$. At $R \geq R_1$, the strong field can be neglected, while V_C is about 40 MeV at $R = R_1$. The interaction $V_C(R)$ decreases with increasing R. At a certain $R_2 > R_1$, it obtains the value

$$V_C(R_2) = Q, \tag{12.102}$$

with Q the energy released in the decay expressed by (12.92). At $R \geq R_1$, the energy Q is shared between the potential energy of interaction $V_C(R)$ and the kinetic energies of the products of the decay. Thus $Q - V_C(R) = \varepsilon(R) = \varepsilon_\alpha(R) + \varepsilon_d(R)$. The alpha particle carries the kinetic energy $\varepsilon_\alpha = \varepsilon \cdot (A-4)/A$. The kinetic energy of the daughter nucleus, $\varepsilon_d = \varepsilon \cdot 4/A$, is much smaller, since only the heavy nuclei with $A \gg 1$ can undergo α decay. To reach the region where $R > R_1$, the alpha particle should penetrate under the potential barrier V_C. Following the Gamow theory of alpha decay, its probability can be written as

$$W_\alpha \;=\; W_0 P; \quad P \;=\; e^{-2S}, \tag{12.103}$$

with

$$S \;=\; \int_{R_1}^{R_2} dR\sqrt{2m_r(V_C(R)-Q)} \tag{12.104}$$

the action of the alpha particle with the reduced mass

$$m_r \;=\; m_\alpha m_d/(m_\alpha + m_d) \;\approx\; m_\alpha\,. \tag{12.105}$$

The factor P can be evaluated analytically:

$$P \;=\; \exp\frac{-2Z_\alpha Z_d e^2}{v_\alpha(\pi - 2\varphi - \sin 2\varphi)}; \quad \varphi \;=\; \arcsin\left(\frac{QR_1}{e^2 Z_\alpha Z_d}\right)^{1/2}. \tag{12.106}$$

We turn now to the decay of the atom. The energy released in the decay becomes

$$Q_A \;=\; Q + B(Z) - B(Z - Z_\alpha) - B(Z_\alpha); \quad Z_\alpha \;=\; 2, \tag{12.107}$$

with $B(X) < 0$ ($X = Z, Z-2, 2$) the energy of the atomic electrons, X the nuclear charge. The probability of the alpha decay can be written as

$$W_\alpha \;=\; W_0 P_A; \qquad P_A \;=\; e^{-2S_A}, \tag{12.108}$$

with

$$S_A \;=\; \int_{R_1}^{R_{2A}} dR\sqrt{2m_r(V_C(R) + V_e(R) - Q_A)}\,. \tag{12.109}$$

Here $V_e(R)$ is the potential energy of interaction between the alpha particle and the electron cloud. The turning point R_{2A} is determined by the condition $V_C(R_{2A}) + V_e(R_{2A}) - Q_A = 0$. Note that the values of R_2 and R_{2A} are less than one-tenth the size of the K shell. Thus the factors P and P_A are determined by the displacements of the alpha particle, which are very small in the atomic scale.

The difference $Q - Q_A$ behaves as $Z^{4/3}$ at large $Z \gg 1$, since the Thomas–Fermi approach predicts $B(Z) \sim Z^{7/3}$. A typical value is $Q - Q_A \approx 40\,\mathrm{keV}$ in the decay of the nucleus ^{226}Ra ($Z = 88$). In this case, $Q \approx 4.9\,\mathrm{MeV}$, while $(Q - Q_A)/Q \sim 10^{-2}$. However, the deviation of the ratio P_A/P from unity is much smaller, due to cancellation of the leading terms in the difference $Q - Q_A$ and $V_e(R)$.

The interaction of the alpha particle with the electron cloud can be written as

$$V_e(R) \;=\; -e^2 Z_\alpha \sum_{k=1}^{Z} \int dV \frac{\rho(\mathbf{r}_1, \ldots)}{|\mathbf{r_k} - \mathbf{R}|}, \tag{12.110}$$

with the electron density ρ depending on the coordinates of the bound electrons. Since we need this potential at $R \ll r_k$, it is reasonable to write [48]

$$V_e(R) \;=\; V_0 + \delta V_e(R); \quad V_0 \;=\; V_e(R=0); \quad \delta V_e(R=0) \;=\; 0, \qquad (12.111)$$

and $|\delta V_e(R)| \ll |V_0|$.

The cancellation between the contribution V_0 and the leading term of expansion of the difference $Q - Q_A$ in powers of $1/Z$ can be demonstrated by employing the Hellmann–Feynman theorem (HFT). The HFT states that for the solutions of the Schrödinger equation $H(\lambda)\Psi(\lambda) = \varepsilon(\lambda)\Psi(\lambda)$ depending on a parameter λ, one can write $\varepsilon'(\lambda) = \langle\Psi|H'|\Psi\rangle$, with the prime denoting the partial derivative with respect to λ.

This can be demonstrated by straightforward calculation of the derivatives of both sides in the equality $\varepsilon(\lambda) = \langle\Psi(\lambda)|H(\lambda)|\Psi(\lambda)\rangle$. We can write

$$\varepsilon'(\lambda) \;=\; \langle\Psi(\lambda)|H'(\lambda)|\Psi(\lambda)\rangle + \delta\varepsilon,$$

with

$$\delta\varepsilon \;=\; \langle\Psi'(\lambda)|H(\lambda)|\Psi(\lambda)\rangle + \langle\Psi(\lambda)|H(\lambda)|\Psi'(\lambda)\rangle\,.$$

Employing the equation of motion, we obtain

$$\delta\varepsilon \;=\; \varepsilon(\lambda)\Big(\langle\Psi'(\lambda)|\Psi(\lambda)\rangle + \langle\Psi(\lambda)|\Psi'(\lambda)\rangle\Big).$$

The expression in parentheses is

$$\langle\Psi'(\lambda)|\Psi(\lambda)\rangle + \langle\Psi(\lambda)|\Psi'(\lambda)\rangle \;=\; \int dV\Big(\Psi^{*'}(\lambda)\Psi(\lambda) + \Psi^{*}(\lambda)\Psi'(\lambda)\Big) \;=\; J',$$

with $J = \int dV\Psi^*(\lambda)|\Psi(\lambda)$. Since J is just the normalization integral, it does not depend on λ, and $J' = 0$. Hence $\delta\varepsilon = 0$.

Applying the HFT to the Hamiltonian of the parent atom H in which we treat the charge of its nucleus Z as a parameter, we obtain

$$\langle\Psi|H'|\Psi\rangle \;=\; -e^2\sum_{k=1}^{Z}\int dV\,\frac{\rho(\mathbf{r}_1,\dots)}{r_k}\,,$$

with the prime denoting the partial derivative with respect to Z. Thus we can write $\langle\Psi|H'|\Psi\rangle = V_0/Z_\alpha = B'(Z)$, with the latter equality being due to the HFT. On the other hand, we can carry out an expansion of the difference $Q_A - Q$ expressed by (12.107) in powers of $1/Z$. One can see that the leading terms of the expansions of $B(Z)$ and $B(Z - Z_\alpha)$ cancel, and $Q_A - Q = Z_\alpha B'(Z) + \delta_A$, with $|\delta_A| \ll Q - Q_A$. Thus in (12.109),

$$V_e(R) - Q_A \;=\; \Big(V_0 - Z_\alpha B'(Z)\Big) + \delta V_e(R) - \delta_A - Q\,, \tag{12.112}$$

with the term in parentheses becoming zero due to the HFT. Hence every approximate expression for $V_e(R)$ employed for computations should satisfy the condition

$$V_e(0) \;=\; Z_\alpha B'(Z)\,; \quad Z_\alpha = 2. \tag{12.113}$$

Otherwise, they will greatly overestimate the deviations of the ratio P_A/P from unity. Finally, we obtain

$$S_A \;=\; \int_{R_1}^{R_{2A}} dR\sqrt{2m_r(V_C(R) + \delta V_e(R) - \delta_A - Q)}\,. \tag{12.114}$$

The calculations carried out in [49] are based on the adiabatic approximation. The wave function describing the final state of the system $\Psi(\mathbf{R}, \mathbf{r})$ satisfies the wave equation

$$H\Psi \;=\; \varepsilon_f \Psi\,. \tag{12.115}$$

Here $\mathbf{R}$ and $\mathbf{r}$ are the coordinates of the nuclei and electrons respectively. The Hamiltonian can be represented as

$$H \;=\; T_R + V_C(R) + T_r + V_e(\mathbf{R}, \mathbf{r})\,. \tag{12.116}$$

Here T_R is the operator of the kinetic energy of the alpha particle and the daughter nucleus. The operator T_R can be represented as that for the α particle with reduced mass m_r; see (12.105). The potential energy of the alpha particle $V_C(R)$ is determined by (12.101) (we neglected the strong interaction term V_N). The operators T_r and $V_e(\mathbf{R}, \mathbf{r})$ compose the Hamiltonian of the atomic electrons. Their potential energy can be written as

$$V_e(\mathbf{R}, \mathbf{r}) \;=\; V_e^\alpha(\mathbf{R}, \mathbf{r}) + V_e^d(\mathbf{R}, \mathbf{r}). \tag{12.117}$$

The two terms on the RHS describe interactions of the electrons with the alpha particle and with the daughter nucleus:

$$V_e^\alpha(\mathbf{R}, \mathbf{r}) = -\sum_k \frac{e^2 \cdot Z_\alpha}{|\mathbf{r}_k - \mathbf{r}_\alpha|}; \quad V_e^d(\mathbf{R}, \mathbf{r}) = -\sum_k \frac{e^2 \cdot (Z - Z_\alpha)}{|\mathbf{r}_k - \mathbf{r}_d|}; \quad Z_\alpha = 2. \tag{12.118}$$

Here the sum is taken over the electrons of the system. The vectors $\mathbf{r}_\alpha$ and $\mathbf{r}_d$ are the coordinates of the α particle and the daughter nucleus in the frame of reference with the origin in the center of the parent nucleus. They can be expressed in terms of the vector $\mathbf{R} = \mathbf{r}_\alpha - \mathbf{r}_d$, with

$$\mathbf{r}_\alpha \;=\; \frac{m_d}{m_\alpha + m_d}\mathbf{R} \;\approx\; \mathbf{R}; \quad \mathbf{r}_d \;=\; -\frac{m_\alpha}{m_\alpha + m_d}\mathbf{R}\,. \tag{12.119}$$

The final-state energy ε_f on the RHS of (12.115) can be replaced by the initial-state energy

$$\varepsilon_i \;=\; Q + \varepsilon_A(R=0)\,, \tag{12.120}$$

where $\varepsilon_A(R)$ is the energy of the atomic electrons at fixed value of R; $\varepsilon_A(0) = B(Z)$.

Now we look for the solution of (12.115) in the form

$$\Psi(\mathbf{R},\mathbf{r}) \;=\; \varphi(\mathbf{R},\mathbf{r})u(\mathbf{R})\,. \tag{12.121}$$

Here the function $\varphi(\mathbf{R},\mathbf{r})$), in which the vector $\mathbf{R}$ is assumed to be a parameter, is the solution of the wave equation

$$H_e\varphi(\mathbf{R},\mathbf{r})) \;=\; \varepsilon_A(R)\varphi(\mathbf{R},\mathbf{r})\,, \tag{12.122}$$

with the Hamiltonian of the atomic electrons $H_e = T_r + V_e(\mathbf{R},\mathbf{r})$. Substituting (12.122) into the LHS of (12.115), we obtain

$$\varphi(\mathbf{R},\mathbf{r})\Big(T_R + V_C(R) + \varepsilon_A(R)\Big)u(R) + u(R)T_R\varphi(\mathbf{R},\mathbf{r}) - \frac{\nabla_R\varphi(\mathbf{R},\mathbf{r})\cdot\nabla_R u(\mathbf{R})}{2m_r} \;=\; \varepsilon_i\varphi(\mathbf{R},\mathbf{r}))u(\mathbf{R}). \tag{12.123}$$

The two last terms on the LHS contain the derivatives of the wave function $\varphi(\mathbf{R},\mathbf{r})$ with respect to $\mathbf{R}$. The key idea of the adiabatic approximation is that the function φ varies with $\mathbf{R}$ so slowly that these derivatives can be neglected (see, e.g., [50]). Thus (12.115) in the adiabatic approximation can be written as the equation of motion for the α particle (recall that $\mathbf{R} \approx \mathbf{r}_\alpha$):

$$\Big(T_R + V_C(R) + \varepsilon_A(R) - \varepsilon_A(0)\Big)u(\mathbf{R}) \;=\; Qu(\mathbf{R}). \tag{12.124}$$

Note that in decay of the bare nuclei, the alpha particle was described by the equation $(T_R + V_C(R))u(\mathbf{R}) = Qu(\mathbf{R})$. Thus the influence of the electron shell manifests itself in the change of the potential energy of the alpha particle from V_C to $V_C + \varepsilon_A(R) - \varepsilon_A(0)$.

Since the difference $\varepsilon_A(R) - \varepsilon_A(0)$ is expected to be small, we can try to calculate it in the lowest order of perturbation theory. We can write

$$\varepsilon_A(R) - \varepsilon_A(0) = \delta\varepsilon_A(R);\;\; \delta\varepsilon_A(R) = \langle\Psi_i|\delta V_e(\mathbf{R},\mathbf{r})|\Psi_i\rangle;\;\; \delta V_e = V_e(\mathbf{R},\mathbf{r}) - V_e(0,\mathbf{r}), \tag{12.125}$$

with $V_e(\mathbf{R},\mathbf{r})$ determined by (12.117). Here Ψ_i is the wave function of the parent atom. We begin with interactions between the electrons and the alpha particle. Since we consider the diagonal matrix element of the operator V_e^α defined by (12.118), only the monopole term of the expansion in Legendre polynomials contributes. Employing (5.148), we obtain

$$\delta V_e^{\alpha}(\mathbf{R},\mathbf{r}) = -e^2 Z_{\alpha}\left(\frac{1}{R}-\frac{1}{r}\right)\theta(R-r). \tag{12.126}$$

Hence the difference $\delta\varepsilon_A^{\alpha}(R) = \langle\Psi_i|\delta V_e^{\alpha}(\mathbf{R},\mathbf{r})|\Psi_i\rangle$ is determined by the electron distances r, which are much smaller than the size of the bound state. Since the distance between the electron and the daughter nucleus is about $1/A$ times smaller than that between the electron and the alpha particle, the correction $\delta\varepsilon_A^{d}(R) = \langle\Psi_i|\delta V_e^{d}(\mathbf{R},\mathbf{r})|\Psi_i\rangle$ appears to be $1/A$ times smaller than $\delta\varepsilon_A^{\alpha}(R)$. Thus (12.109) can be written as

$$S_A = \int_{R_1}^{R_{2A}} dR\sqrt{2m_r(V_C(R)+\delta\varepsilon_A(R)-Q)}\,, \tag{12.127}$$

with

$$\delta\varepsilon_A(R) = \langle\Psi_i|\delta V_e^{\alpha}(\mathbf{R},\mathbf{r})|\Psi_i\rangle; \quad \delta V_e^{\alpha} = V_e(\mathbf{R},\mathbf{r}) - V_e(0,\mathbf{r}). \tag{12.128}$$

Note that we obtained (12.114) with $\delta_A = 0$.

We found that the difference $\delta\varepsilon_A(R)$ is determined by very small subbarrier electron distances r. They are two orders of magnitude smaller than the size of the atomic K shell. Hence the contribution is determined by the electron states with nonzero values of the wave functions at the origin. In nonrelativistic approximation, these would be only the s states. However, only certain heavy nuclei undergo α decay, and the relativistic effects should be accounted for. With an account of the relativistic effects, the $p_{1/2}$ states also contribute. The computations require taking into account the finite size of the decaying nucleus.

One can see that $\delta\varepsilon_A(R) > 0$. Thus the electron shell makes the Coulomb barrier higher. The probability for the alpha decay of the atom becomes smaller than it was for the bare nucleus. The relative change in the probability $(P_A - P)/P$ is several units of 10^{-3}. In the characteristic case of the alpha decay of ^{226}Ra, one obtains $(P_A - P)/P = -2.3\times 10^{-3}$. The $1s$ electrons provide about 80% of the contribution.

References

1. R.J. Blin-Stoyle, *Fundamental Interactions and the Nucleus* (American Elsivier Publishing Compamy Inc., NY, 1973)
2. Y. Fukuda et al., (Super-Kamiokande collaboration). Phys. Rev. Lett. **81**, 1562 (1998)
3. D.G. Michael et al., (MINOS collaboration). Phys. Rev. Lett. **97**, 191801 (2006)
4. E. Holzschuh, Rep. Prog. Phys. **57**, 1035 (1992)
5. E.G. Drukarev, Phys. Lett. B **262**, 105 (1991)
6. E.G. Drukarev, Sov. J. Nucl. Phys. **50**, 546 (1989)
7. E.G. Drukarev, Phys. Rev. C **54**, 3227 (1996)
8. V.M. Lobashev, Nucl. Phys. A **719**, C153 (2003)
9. V.N. Aseev et al., Phys. Rev. D **84**, 112003 (2011)
10. Ch. Kraus et al., Eur. Phys. J. C **40**, 447 (2005)
11. J.J. Simpson, Phys. Rev. Lett. **54**, 1891 (1985)

12. E.G. Drukarev, M.I. Strikman, Sov. Phys. JETP **64**, 686 (1986)
13. E.G. Drukarev, M.I. Strikman, Sov. J. Nucl. Phys. **50**, 184 (1989)
14. J. Berukole, S.T. Pantelides, Phys. Rev. B **15**, 4935 (1977)
15. A. Franklin, Rev. Mod. Phys. **67**, 457 (1995)
16. D.R.O. Morrison, Nature **366**, 29 (1991)
17. T.A. Carlson, C.W. Nestor Jr., T.C. Tucker, F.B. Malik, Phys. Rev. **169**, 27 (1968)
18. Y. Isozumi, Nucl. Instrum. Methods **A280**, 151 (1989)
19. E.G. Drukarev, M.B. Trzhaskovskaya, Nucl. Phys. A **518**, 513 (1990)
20. D. Ohsawa, R. Katano, Y. Isozumi, Phys. Rev. C **60**, 044604 (1999)
21. Y. Isozumi, T. Mukoyama, S. Shimizu, Nuovo Cimento **41A**, 359 (1971)
22. J. Law, A. Suzuki, Phys. Rev. C **25**, 514 (1982)
23. A.I. Akhiezer, V.B. Berestetskii, *Quantum Electrodynamics* (Pergamon, N.Y., 1982)
24. S. Raman, C.W. Nestor Jr., A. Ichihara, M.B. Trzhaskovskaya, Phys. Rev. C **66**, 044312 (2002)
25. I.M. Band, M.B. Trzhaskovskaya, C.W. Nestor Jr., P. Tikkanen, S. Raman, At. Data Nucl. Data Tables **81**, 1 (2002)
26. N. Nica, J.C. Hardy, V.E. Iacob, M. Bencomo, V. Horvat, H.I. Park, M. Maguire, M.B. Trzhaskovskaya, Phys. Rev. C **89**, 014303 (2014)
27. T. Mukoyama, S. Shimizu, Phys. Rev. C **11**, 1353 (1975)
28. T. Mukoyama, S. Shimizu, Phys. Rev. C **13**, 377 (1976)
29. E.G. Drukarev, Sov. J. Nucl. Phys. **21**, 308 (1975)
30. E.G. Drukarev, Z. Phys. A **359**, 133 (1997)
31. F.T. Porter, M.S. Freedman, F. Wagner, Phys. Rev. C **3**, 2246 (1971)
32. I.N. Vishnevsky et al., Bull. Russ. Acad. Sci. Phys. **63**, 930 (1999)
33. C.W.E. van Eijk, J. Wijnhorst, M.A. Popelier, Phys. Rev. A **24**, 854 (1981)
34. K. Knauf, T. Sommer, H. Kleve-Nebenius, Z. Phys. **197**, 101 (1966)
35. I.N. Vishnevsky et al., Bull. Russ. Acad. Sci. Phys. **71**, 890 (2007)
36. Ch.F. Ficher, At. Data **4**, 305 (1972)
37. A.A. Kluchnikov, A.I. Feoktistov, Bull. Sov. Acad. Sci. Phys. **38**, 1654 (1974)
38. K.P. Artamonova, E.P. Grigoriev, I.I. Gromova, A.B. Zolotavin, V.O. Sergeev, Bull. Sov. Acad. Sci. Phys. **38**, 2047 (1975)
39. P.T. Prokofiev, L.M. Simonova, Sov. J. Nucl. Phys. **21**, 1145 (1975)
40. S. Kishimoto, Y. Yoda, Y. Kobayashi, S. Kitao, R. Haruki, R. Masuda, M. Seto, Phys. Rev. C **74**, 031301 (R) (2006)
41. E.V. Tkalya, Nucl. Phys. A **539**, 209 (1992)
42. A. Ljubicic, Radiat. Phys. Chem. **51**, 341 (1998)
43. E.G. Drukarev, *AIP Conference Proceedings*, vol. 506 (Melville, NY, 2000), p. 496
44. E.G. Drukarev, Sov. J. Nucl. Phys. **17**, 174 (1973)
45. J. Henderson et al., Phys. Rev. C **89**, 064307 (2014)
46. A.B. Migdal, J. Phys. USSR **4**, 449 (1941)
47. J.S. Levinger, Phys. Rev. **90**, 11 (1953)
48. Z. Patryk, H. Geissel, Y.A. Litvinov, A. Musumarra, C. Nociforo, Phys. Rev C. **78**, 054317 (2008)
49. F.F. Karpeshin, Phys. Rev C. **87**, 054319 (2013)
50. L. Schiff, *Quantum Mechanics*, (McGraw Hill, 1968)

Index

E.G. Drukarev and A.I. Mikhailov, *High-Energy Atomic Physics*,
Springer Series on Atomic, Optical, and Plasma Physics 93,
DOI 10.1007/978-3-319-32736-5